Universidade de Aveiro Departamento de Matemática
2012

Patrícia Santos Ribeiro

D-Pavimentações Esféricas Diedrais Triangulares

Universidade de Aveiro Departamento de Matemática
2012

Patrícia Santos Ribeiro

D-Pavimentações Esféricas Diedrais Triangulares

Tese apresentada à Universidade de Aveiro para cumprimento dos requisitos necessários à obtenção do grau de Doutor em Matemática, realizada sob a orientação científica da Doutora Ana Maria Reis d'Azevedo Breda, Professora Associada com Agregação do Departamento de Matemática da Universidade de Aveiro.

Apoio financeiro do Instituto Politécnico de Setúbal no âmbito do Programa de apoio à formação avançada de docentes do Ensino Superior Politécnico (PROTEC) bolsa com referência SFRH/PROTEC/49260/2008.

Dedico este trabalho aos meus filhos e ao Valmi por todo o seu amor.

o júri

presidente

Prof. António Ferreira Pereira de Melo
professor catedrático da Universidade de Aveiro

Profª Doutora Helena Maria Mamede Albuquerque
professora associada com agregação da Faculdade de Ciências e Tecnologia de Ciências da Universidade de Coimbra

Profª Doutora Ana Maria Reis d'Azevedo Breda
professora associada com agregação da Universidade de Aveiro

Profª Doutora Maria do Rosário Machado Lema Sinde Pinto
professora auxiliar da Faculdade de Ciências da Universidade do Porto

Profª Doutora Ana Maria Pereira do Vale
professora auxiliar da Escola de Ciências da Universidade do Minho

Prof. Doutor Domenico Antonino Catalano
professor auxiliar da Universidade de Aveiro

agradecimentos

À minha orientadora Professora Doutora Ana Maria Reis d'Azevedo Breda pela sua capacidade de trabalho e paciência que teve durante todo este tempo para comigo.

Ao Professor Robert Dawson da Universidade Saint Mary, Canadá, pela sua disponibilidade e ajuda na construção das representações 3D em *POV-Ray*.

Ao Departamento de Matemática da ESTSetúbal pelo apoio e confiança que me deram.

Quero também agradecer ao Instituto Politécnico de Setúbal pelo seu apoio financeiro e à Fundação para a Ciência e Tecnologia (FCT) que me deram oportunidade de fazer parte do Programa de apoio à formação avançada de docentes do Ensino Superior Politécnico (PROTEC) com bolsa de referência SFRH/PROTEC/49260/2008.

Por último mas sempre em primeiro lugar no meu coração quero agradecer à minha família, em especial ao Valmi pelo seu apoio incondicional.

palavras-chave Dobragem isométrica, *d*-pavimentação diedral, deformação

resumo

A. Breda, em 1992 classificou todas as *d*-pavimentações esféricas monoedrais bem como as suas propriedades transitivas motivada pelo trabalho de S. A. Robertson. Demonstrou ainda que todas as dobragens isométricas não triviais do plano euclidiano podem ser deformadas na dobragem isométrica *standard.* Contudo, ainda hoje não se sabe a resposta para as dobragens isométricas da esfera S^2.

A. Santos, em 2005 descreveu todas as *d*-pavimentações esféricas diedrais cujos protótipos são um triângulo esférico e um paralelogramo esférico. Definiu ainda uma nova métrica no espaço das *d*-pavimentações esféricas, com o objectivo de tentar estabelecer uma relação entre deformações de dobragens isométricas e deformações de *d*-pavimentações esféricas.

Neste trabalho, descrevemos todas as *d*-pavimentações esféricas diedrais cujos protótipos são um triângulo esférico equilátero e um triângulo esférico isósceles, um triângulo esférico equilátero e um triângulo esférico escaleno e dois triângulos esféricos isósceles não congruentes. Caracterizamos também as suas propriedades transitivas.

No final dos Capítulos 2, 3 e 4 apresentamos deformações ou uma visão das deformações de cada uma das *d*-pavimentações esféricas diedrais encontradas na *d*-pavimentação *standard,* usando a topologia associada à nova métrica definida por A. Santos.

keywords Isometric foldings, dihedral *f*-tilings, deformations

abstract

In 1992, A. Breda classified all monohedral spherical folding tilings (*f*-tilings for short) motivated by S. A. Robertson's work. Proved also that any non-trivial isometric folding of the euclidian space is deformable into the standard one. However, the analogous situation in the sphere S^2 is not yet solved.

In 2005, A. Santos described all dihedral *f*-tilings whose prototiles are a spherical triangle and a spherical parallelogram. He also defined a new metric in the space of the spherical *f*-tilings, with the aim to establish a relation between the deformation of isometric foldings and the deformation of *f*-tilings.

Here, we extend this study and we describe all dihedral *f*-tilings whose prototiles are an equilateral and an isosceles spherical triangle, an equilateral and a scalene spherical triangle and two non-congruent isosceles spherical triangles. We also give their transitive properties.

At the end of Chapters 2, 3 and 4, we give deformations or insights towards deformations of each one of the *f*-tilings produced into the standard *f*-tiling using the topology associated to the new metric introduced by A. Santos.

Contents

Introduction

The theory of isometric foldings (maps that send piecewise geodesic segments into piecewise geodesic segments of the same length) begun with S. A. Robertson in 1977. At this time, it was shown that, for surfaces, the set of singularities of such maps can be regarded as the subjacent graph of a tiling, where

1. all vertices are of even valency and
2. at any vertex, both sums of its alternate angles are always equal to π (angle folding relation).

Motivated by S. A. Robertson's work, A. Breda, in [12] has started the study of spherical f-tilings (edge-to-edge tilings, that satisfy 1. and 2.), where the classification of all monohedral spherical f-tilings (spherical f-tilings where any tile is congruent to one fixed set) and their transitive properties was done.
A. Santos, in [14], with the purpose of extending this study, described all spherical dihedral f-tilings, where the prototiles are a spherical triangle and a spherical parallelogram.
Here, we present a study that resulted in the characterization of classes of dihedral spherical f-tilings, when the prototiles are two non congruent spherical triangles, as well as their transitive properties.

A. Breda, in [12] also proved that any non-trivial isometric folding (isometric folding whose set of singularities is non-empty) of the euclidian plane is deformable into the standard planar folding $f : \mathbb{R}^2 \to \mathbb{R}^2$ defined by $f(x, y) = (x, |y|)$. However, the correspondent situation on the sphere remains an open question.
Related to the problem of the deformation of spherical isometric foldings is the deformation of spherical f-tilings into the standard tiling τ_{stand} (tiling whose underline graph

is a great circle). More precisely, is any spherical f-tiling deformable into the τ_{stand}? And what is the relation between deformation of isometric foldings and deformation of f-tilings?

In what concerns to the second question, some contributions were given by A. Santos in [14], where a new metric was introduced by giving to each face of a spherical f-tiling a convenient orientation. However, the first question persists without answer.

In Chapter 1, we expose basic notions and state some crucial properties of the theory of isometric foldings that can be found in [12] and in [17]. We also state some results, with the aim to establish deformations between spherical f-tilings and τ_{stand}.

In Chapter 2, we study all dihedral f-tilings of the unit sphere S^2, whose prototiles are an equilateral and an isosceles spherical triangle. As a result, we find a two-parameter family and three isolated non-isomorphic dihedral f-tilings that we classify accordingly to their isogonality and isohedrality classes (Section 2.3).

In Chapter 3, we characterize all dihedral f-tilings of S^2, whose prototiles are an equilateral and a scalene spherical triangle, getting three continuous families, four discrete ones and four isolated non-isomorphic dihedral f-tilings. Their transitive properties are given in Section 3.4.

Chapter 4 is dedicated to dihedral f-tilings of S^2, whose prototiles are two non congruent isosceles spherical triangles. In this case, one continuous family, nine discrete families, nine isolated non-isomorphic and seven families of dihedral f-tilings parameterized by two or more parameters arise. We also present their transitive properties in Sections 4.2, 4.4 and 4.6.

It should be pointed out that, a selective elimination of some edges, several of the f-tilings described in Chapters 2, 3 and 4 end up in a monohedral f-tiling or in a dihedral f-tiling whose prototiles are a spherical triangle and a spherical parallelogram and few of them end up in a 3-hedral f-tiling.

At the end of each one of these Chapters, deformations or insights toward deformations of each one of the produced f-tilings into the standard one τ_{stand} are given using the topology induced by the new metric introduced in [14].

We should mention that in the first two Chapters, we have used the software *FreeHand* of Macromedia and in the last one, we have used *POV-Ray* to illustrate the 3D

representations of the dihedral f-tilings described, which explains the diference in the output of the produced images.

Chapter 5 is devoted to the main conclusions of this research work and some research lines to pursue this work are also given.

Chapter 1

Isometric Foldings and Spherical Folding Tilings

The theory of isometric foldings emerged in 1977 by S. A. Robertson [17], as an attempt to formulate the physical action of crumpling a sheet of paper and then crushing it flat against a desk top. For related work, see also [18].

Considering both the paper and the desk top as two dimensional flat Riemannian manifolds, respectively denoted by M and N, the process can be mathematically modeled by a map $f : M \to N$, which sends piecewise geodesic segments to piecewise geodesic segments of the same length.

This concept can be easily adapted to any two Riemannian manifolds of any dimension.

In this Chapter, we expose briefly, the basic notions and state some crucial properties of this theory, that can be found in [12] and [17].

1.1 Isometric Foldings on Riemannian Manifolds

Let M be a smooth ($= C^\infty$) Riemannian manifold and let $I = [a, b] \subset \mathbb{R}$ a closed interval. A map $\gamma : I \to M$ is said to be a **zig-zag** on M, if there exists a subdivision, $a = a_0 < a_1 < \cdots < a_k = b$ of I, such that for all $j = 1, \ldots, k$ the restriction $\gamma_j = \gamma_{|[a_{j-1}, a_j]}$ is a geodesic segment on M parameterized by arc-length. Thus, the

length of γ is

$$L(\gamma) = \sum_{j=1}^{k} L(\gamma_j) = b - a.$$

Definition 1.1 *Let M and N be smooth connected Riemannian manifolds of dimensions, respectively m and n. A map $f : M \to N$ is said to be an **isometric folding** of M into N if, for every zig-zag $\gamma : I \to M$, the induced path $\gamma_* = f \circ \gamma : I \to N$ is a zig-zag on N.*

It follows that $L(\gamma) = L(\gamma_*)$.

We denote by $\mathscr{F}(M, N)$ the set of all isometric foldings from M into N.

It could be shown that:

Proposition 1.1 *1. $\mathscr{F}(M) = \mathscr{F}(M, M)$ is a semigroup with identity element id_M under composition of maps and contains the isometry group $\mathcal{I}(M)$ as a subsemigroup.*

2. For all $x, y \in M$ and $f \in \mathscr{F}(M, N)$

$$d_N(f(x), f(y)) \leq d_M(x, y),$$

where d_M and d_N denote, respectively the induced metrics on M and N by their Riemannian structure.

As a consequence of **2.** in proposition 1.1, any isometric folding from M to N is a continuous map.

An isometric folding need not to be differentiable. The map $f : \mathbb{R}^2 \to \mathbb{R}^2$ given by $f(x, y) = (x, |y|)$ is an isometric folding of the real plane equipped with its standard structure, which is not differentiable at any point of the straight line $y = 0$.

A point $x \in M$ where the isometric folding $f : M \to N$ fails to be differentiable is called a **singularity** of f. We denote by Σf the set of all singularities of f.

The **standard folding**, $f_{stand} : S^2 \to S^2$ defined by

$$f_{stand}(x, y, z) = (x, y, |z|)$$

has as set of singularities

$$\tau_{stand} = \Sigma f_{stand} = \left\{(x, y, z) \in S^2 : z = 0\right\}.$$

$f \in \mathscr{F}(M, N)$ is a **non trivial** isometric folding if $\Sigma f \neq \varnothing$.

Assume now that M and N are complete Riemannian manifolds. Consider the following notations:

1. $S_xM = \{\xi \in T_xM : \|\xi\| = 1\}$, the unit tangent space on $x \in M$;

2. $\gamma_{(x,\xi)}(t) = \exp_x(t\xi)$, $t \in \mathbb{R}$ is the unique geodesic on M through x, such that $\frac{d}{dt}(\exp_x(t\xi))_{|t=0} = \xi$.

Proposition 1.2 *Let $f \in \mathscr{F}(M, N)$ and let U be a convex neighborhood of $x \in M$ such that $f(U)$ is contained in a convex neighborhood of $f(x)$ in N. Let $\xi \in S_xM$ and $t \in \mathbb{R}$ be such that $y = \gamma_{(x,\xi)}(t) \in U$. Then*

$$d_N(f(x), f(y)) < d_M(x, y)$$

if and only if there is a singularity of $\gamma_{*(x,\xi)}$ on $]0, t[$, where $\gamma_{*(x,\xi)}$ denotes the induced path on N.

As a direct consequence one has:

Corollary 1.1 *$f \in \mathscr{F}(M, N)$ is differentiable if and only if f is an isometry.*

A general representation of Σf, for any $f \in \mathscr{F}(M, N)$ was first shown by S. A. Robertson in 1977, [17]. In short:

Theorem 1.1 *Let $f \in \mathscr{F}(M, N)$ be a non trivial isometric folding. Then, there is a decomposition of M into mutually disjoint, connected, totally geodesic submanifolds, which we call **strata**, with the following properties:*

i) $\Sigma f = \bigcup_{k=0}^{m-1} \Sigma_k f$, *where $\Sigma_k f$ (strata of dimension k) is a union of submanifolds of dimension k, $m = \dim M$;*

ii) *For each (stratum) $S \in \Sigma_k f$, $f_{|S}$ is locally an isometric immersion into N;*

iii) *The frontier of each S is a union of strata of lower dimension and in case M is compact this union is finite;*

iv) *The frontier of all strata of dimension k is the union of all sets $\Sigma_j f$, $0 \leq j \leq k-1$.*

If M and N are surfaces, then this characterization is described as follows:

Theorem 1.2 *Let $f \in \mathscr{F}(M, N)$, where M and N are complete Riemannian 2-manifolds. Then, for each $x \in \Sigma f$, the singularities of f near x form the image of an even number of geodesic rays emanating from x and making alternate angles α_1, β_1, α_2, β_2, ..., α_n, β_n, where*

$$\sum_{j=1}^{n} \alpha_j = \sum_{j=1}^{n} \beta_j = \pi. \tag{1.1}$$

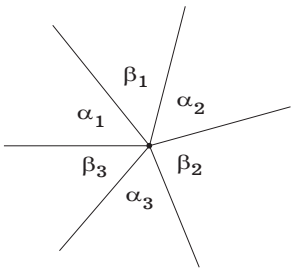

Figure 1.1: The angle folding relation (with $n = 3$).

Thus, the set of singularities of f can be regarded as the subjacent graph of a tiling on M, where all vertices are of even valency and satisfy the **angle folding relation** (1.1).

Recall that, a **tiling** $\tau = \{T_1, T_2, \ldots\}$ is a countable family of closed topological discs, called the tiles of τ, which covers M without gaps or overlaps. More explicitly, the union of all tiles is M and the interior of the sets T_j are pairwise disjoint, see Grumbaum-Shephard [16].

For this reason, the components of $\Sigma_2 f$, $\Sigma_1 f$ and $\Sigma_0 f$ are called, respectively **faces**, **edges** and **vertices**. A **region** and a **side** are defined to be, respectively the closure of a face and the closure of an edge. The border of $\Sigma_2 f$ is the set of all edges - $\Sigma_1 f$ and all vertices - $\Sigma_0 f$.

1.2 Spherical Folding Tilings

In this Section, we will focus our attention on tilings of the 2-dimensional Sphere $S^2 = \{x \in \mathbb{R}^3 \colon \|x\| = 1\}$.

Let τ denote a spherical tiling by convex polygons. Then, τ is said to be an edge-to-edge tiling if for any two tiles, T_1 and T_2 of τ, the intersection $T_1 \cap T_2$ is either empty, a side or a point of T_1 and T_2.

A tiling τ will be called :

i) monohedral if every tile of τ is congruent to one fixed set T, the **prototile** of τ;

ii) dihedral if every tile of τ is congruent to either two fixed sets T_1 and T_2, the prototiles of τ.

iii) n-hedral if every tile of τ is congruent to one of the sets $T_1, T_2, \ldots, T_n$.

Two spherical tilings τ_1 and τ_2 are *isomorphic* (or *congruent*), if there exists a spherical isometry sending τ_1 to τ_2.

In 1996, Y. Ueno and Y. Agaoka in [19] made the classification of all monohedral (edge-to-edge) tilings of the sphere by right triangles (triangles with an angle $\frac{\pi}{2}$). In 2002, the complete classification of all monohedral spherical tilings by triangles, was achieved, along with a complete proof, [21]. Some examples of spherical tilings by congruent quadrangles are given by Y. Ueno and Y. Agaoka in [20]. Dawson and Doyle have also been working on spherical tilings, relaxing the edge to edge condition, [10], [11].

Definition 1.2 *A spherical isometry, σ is a **symmetry** of τ if it maps every tile of τ into a tile of τ. The set of all symmetries of τ is a group under composition of maps, denoted by $G(\tau)$.*

From now on, τ denotes an edge-to-edge spherical tiling by convex polygons.

Looking at the natural action of $G(\tau)$ on τ, we may classify τ according to its transitivity properties. Assigning by V and F the set of, respectively vertices and faces of τ, then τ is

⋆ **k-isogonal**, $k \geq 1$, if this action partitionate V in k classes of transitivity;

⋆ **k-isohedral**, $k \geq 1$, if this action partitioned F in k classes of transitivity.

For a comprehensive study on tilings see Grümbaum and Shephard, [15] and [16].

Definition 1.3 *By a spherical folding tiling or* **spherical f-tiling** *for short, we mean an edge-to-edge tiling of S^2, such that all vertices of are of even valency and satisfy the angle folding relation* (1.1).

Let τ be a spherical f-tiling. Then, τ can be considered as an embedding of some graph Γ on S^2, where the sum of alternate angles around vertices is π.

We shall denote by $\mathscr{T}(S^2)$ the set of all spherical f-tilings.

In [12], A. Breda proved that, if τ is a monohedral spherical f-tiling with even vertex valency, then the prototile of τ must be a triangle (or a spherical moon).

The complete classification of all triangular monohedral spherical f-tilings was given by A. Breda in 1992, [13]. This classification exhibits which triangles can be used as prototiles and determines the number of different ways that a fixed triangle can tile the whole sphere without violating the angle folding relation, (1.1). In Figure 1.2 is illustrated a 3D representation of a representative element of each one of these f-tilings.

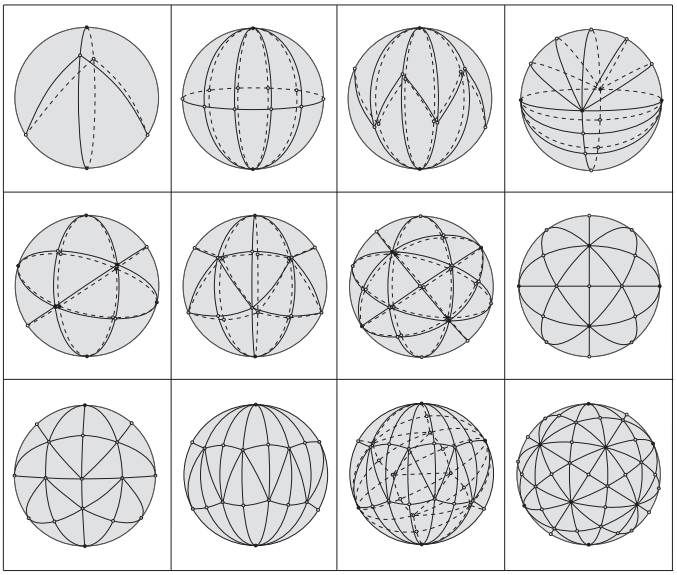

Figure 1.2: Monohedral spherical f-tilings.

In what concerns to dihedral spherical f-tilings two questions arise promptly:

1. Given two convex spherical polygons P_1 and P_2 decide if they can be the prototiles of some dihedral spherical f-tiling;

2. Determine the number of non-isomorphic tilings with prototiles P_1 and P_2 that tile the whole sphere without gaps or overlaps and obeying to the angle folding relation, (1.1).

The study of dihedral spherical f-tilings of the Euclidean sphere S^2 by triangles and r-sided regular polygons was initiated in 2004, where the case $r = 4$ was considered, [7]. The complete classification of all dihedral f-tilings by triangles and parallelograms was made in [14]. In a subsequent paper [1], the same study for $r \geq 5$, was described.

Let Q and T be, respectively a r-sided convex polygon and a s-sided convex polygon of the sphere. We shall denote by $\mathbf{\Omega}(\mathbf{Q}, \mathbf{T})$ the set, up to an isomorphism, of all dihedral spherical f-tilings of S^2 whose prototiles are Q and T.

Given $\tau \in \Omega(Q, T)$, it is possible to establish a relation between the number of r-polygons congruent to Q and the number of s-polygons congruent to T.
Let $M > 0$ and $N > 0$ denote, respectively the number of r-polygons congruent to Q and the number of s-polygons congruent to T and let E and V denote, respectively the number of edges and vertices of τ. Then:

i) $M(r-2) + N(s-2) = 2V - 4$;

ii) $M(r-3) + N(s-3) + E + 6 = 3V$;

iii) there are at least $6 + M(r-3) + N(s-3)$ vertices of valency four.

The proof can be found in [14].

Clearly, we would not expect that any two spherical polygon could be taken as prototiles of a dihedral f-tiling. However, for $r \geq 3$, there exists a dihedral spherical f-tiling with prototiles T and Q, for some spherical triangle T and some r-sided convex polygon Q, see [14].

1.3 Deformations of Spherical f-Tilings *vs* Deformations of Isometric Foldings

We are interested in spherical f-tilings, having always in mind that the set of singularities of spherical isometric foldings are f-tilings.
In this Section, we state some important results given in [14], that will be used in Chapters 2, 3 and 4, with the aim to show that any dihedral f-tiling here characterized is deformable into the standard one, τ_{stand}.

1.3.1 The Concept of Deformation

Proposition 1.3 *Let f and g be isometric foldings of S^2. Then, Σf and Σg are congruent if and only if exists $\varphi, \psi \in Iso(S^2)$, such that $g = \varphi \circ f \circ \psi$.*

Recall that, by $\mathscr{F}(S^2)$ and $\mathscr{T}(S^2)$ we mean, respectively, the set of all isometric foldings of S^2 and the set of all f-tilings of S^2.

Let $f, g \in \mathscr{F}(S^2)$ and let $\tau, \tau' \in \mathscr{T}(S^2)$. The relations $\sim_1$ and $\sim_2$ defined by

- $f \sim_1 g$ if and only if $g = \varphi \circ f \circ \psi$, for some $\varphi, \psi \in Iso(S^2)$;
- $\tau \sim_2 \tau'$ if and only if τ and τ' are congruent

are equivalence relations on $\mathscr{F}(S^2)$ and $\mathscr{T}(S^2)$, respectively.

Definition 1.4 *The map $f \in \mathscr{F}(S^2)$ is **deformable** into $g \in \mathscr{F}(S^2)$ if there exists a map $H : [0,1] \times S^2 \to S^2$, such that*

i) *H is continuous;*

ii) *For each $t \in [0,1]$, H_t defined by $H_t(x) = H(t,x)$, $x \in S^2$ is an isometric folding;*

iii) *$H(0,x) = f(x)$ and $H(1,x) = g(x)$, $\forall x \in S^2$.*

It is a straightforward exercise to show that the relation of deformation is an equivalence relation on $\mathscr{F}(S^2)$.

In a similar way, we define the concept of deformation of spherical f-tilings:

Definition 1.5 *Let τ, $\tau' \in \mathscr{T}(S^2)$. We shall say that τ is **deformable** into τ' if exists a continuous map $\alpha : [0,1] \to \mathscr{T}(S^2)$, such that $\alpha(0) = \tau$ and $\alpha(1) = \tau'$.*

In [12], it was shown that any non-trivial isometric folding of the euclidian plane is deformable into the standard planar folding $f : \mathbb{R}^2 \longrightarrow \mathbb{R}^2$, such that $f(x,y) = (x,|y|)$. A similar statement for the sphere S^2 remains open:

Conjecture: Any non-trivial spherical isometric folding is deformable into f_{stand}. (1.2)

In what follows, we will consider the **compact-open topology** on $\mathscr{F}(S^2)$, in other words, the topology generated by sets of the following form,

$$B(K,U) = \left\{ f \in \mathscr{F}(S^2) : f(K) \subset U \right\},$$

where K is compact in S^2 and U is open in S^2.
Then, f is deformable into g if and only if f and g belong to the same path connected component. Consequently, there is a continuous map $\gamma : [0,1] \to \mathscr{F}(S^2)$ such that $\gamma(0) = f$ and $\gamma(1) = g$.

A natural question is the following: what would be the "good" topology on $\mathscr{T}(S^2)$, such that the deformation of isometric foldings induces a deformation of their associated f-tilings?

1.3.2 A New Metric on f-Tilings

As stated before, the deformation of isometric foldings does not induce a deformation of its associated f-tilings (the set of singularities), in the sense that there is a deformation $H : [0,1] \times S^2 \to S^2$ of f into f', for some $f, f' \in \mathscr{F}(S^2)$, but $\alpha(t) = \Sigma\, H_t$, $t \in [\,0,1\,]$ is not continuous. So, the Hausdorff metric is not enough.

In order to overcome this problem, A. Santos in [14] introduced a new metric in $\mathscr{T}(S^2)$ by giving to each face of a spherical f-tiling a convenient orientation.

Definition 1.6 *Let τ_1, τ_2 be spherical f-tilings. By $\tau_1 \cup \tau_2$, we mean the edge-to-edge polygonal spherical tiling τ, such that its edge-complex is the union of the edge-complexes associated to τ_1 and τ_2. More precisely, $v \in S^2$ is a vertex of τ if and only*

if v is a vertex of τ_1 or v is a vertex of τ_2 or v is the intersection of an edge of τ_1 with an edge of τ_2, if the great circles containing them are distinct. Any geodesic segment joining two of these vertices and contained in an edge of τ_1 or contained in an edge of τ_2 is an edge of τ.

For any face F of $\tau = \tau_1 \cup \tau_2$, exists a face F_1 of τ_1 and a face F_2 of τ_2, such that $F \subset F_1$ and $F \subset F_2$. In Figure 1.3 is illustrated a vertex v, an edge e and the faces of a portion of the tiling $\tau = \tau_1 \cup \tau_2$.

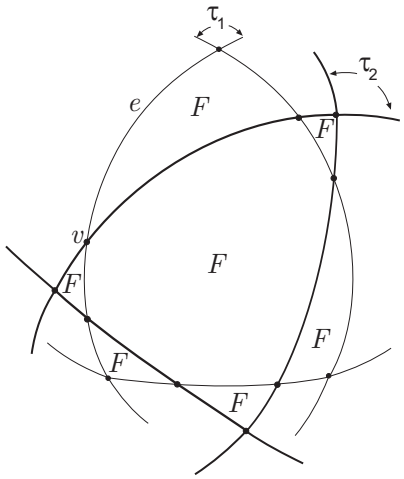

Figure 1.3: The polygonal tiling $\tau = \tau_1 \cup \tau_2$.

Let τ be a spherical f-tiling. Let $\mathcal{F}$ be the set of all faces of τ and let $F \in \mathcal{F}$. Then, there is an unique map $o : \mathcal{F} \to \{+, -\}$, such that $o(F) = +$ and two adjacent faces of $\mathcal{F}$ have opposite signs. The map o is called an orientation of τ.

Definition 1.7 *An oriented spherical f-tiling is a pair (τ, o), where τ is a spherical f-tiling and o is an orientation of τ. For convenience it is denoted by τ^o.*

Each spherical f-tiling τ has two distinct orientations. We denote them, respectively by o and $-o$.

Notation: We shall denote by $\mathscr{T}^{\mathcal{O}}(S^2)$ the set of all oriented spherical f-tilings .

Let $\tau_1^{o_1}$, $\tau_2^{o_2} \in \mathscr{T}^{\mathcal{O}}(S^2)$. A face F of $\tau = \tau_1 \cup \tau_2$ is called *errant* if the faces F_1 of $\tau_1^{o_1}$ and F_2 of $\tau_2^{o_2}$, such that $F_1 \supset F$ and $F_2 \supset F$ have opposite orientations.

Definition 1.8 *Let* $\tau_1^{o_1}$, $\tau_2^{o_2} \in \mathscr{T}^{\mathcal{O}}(S^2)$.

$$c(\tau_1^{o_1}, \tau_2^{o_2}) = \sum_{\substack{F \text{ face of} \\ \tau_1 \cup \tau_2}} \lambda(F)\, Area(F)\,,$$

where $\lambda(F) = 1$ *if* F *is errant and* $\lambda(F) = 0$ *if* F *is non-errant.*

Proposition 1.4 c *is a metric on* $\mathscr{T}^{\mathcal{O}}(S^2)$.

Remark 1.1 *For any* $\tau_1^{o_1}$, $\tau_2^{o_2} \in \mathscr{T}^{\mathcal{O}}(S^2)$, *one has* $c(\tau_1^{o_1}, \tau_2^{o_2}) \leq 4\pi$ *and*

- $c(\tau_1^{o_1}, \tau_2^{o_2}) = c(\tau_1^{-o_1}, \tau_2^{-o_2}) = 4\pi - c(\tau_1^{o_1}, \tau_2^{-o_2}) = 4\pi - c(\tau_1^{-o_1}, \tau_2^{o_2})$;
- $c(\tau_1^{o_1}, \tau_2^{o_2}) = 4\pi$ *if and only if* $\tau_1 = \tau_2$ *and* $o_1 = -o_2$.

Whenever we refer to the space $\mathscr{T}^{\mathcal{O}}(S^2)$ it means that $\mathscr{T}^{\mathcal{O}}(S^2)$ is equipped with the topology induced by the metric c.

Definition 1.9 *Let* $\tau_1^{o_1}$, $\tau_2^{o_2} \in \mathscr{T}^{\mathcal{O}}(S^2)$. *We shall say that* $\tau_1^{o_1}$ *is* ***deformable*** *into* $\tau_2^{o_2}$ *if there is a continuous map* $\alpha : [0,1] \to \mathscr{T}^{\mathcal{O}}(S^2)$, *such that* $\alpha(0) = \tau_1^{o_1}$, $\alpha(1) = \tau_2^{o_2}$.

Orienting positively the north face of τ_{stand} and (consequently) negatively the south face, one gets the oriented standard f-tiling $\tau_{stand}^{\pm}$ and similarly, we define $\tau_{stand}^{\mp}$.

Theorem 1.3 (Deformation movements) *Let* $\tau^o \in \mathscr{T}^{\mathcal{O}}(S^2)$ *and let* A *be a fixed non-empty open set of* S^2. *For each vertex* $v \in \mathscr{V}(\tau^o)$, *let* $\gamma_v : [0,1] \to S^2$ *be a continuous path with* $\gamma_v(0) = v$ *that verifies the following conditions:*

i) *If* $\gamma_v(t_0) = \gamma_{v'}(t_0)$ *for some* $0 \leq t_0 < 1$, *then* $\gamma_v(t) = \gamma_{v'}(t)$, *for all* $t \geq t_0$;

ii) *If* $\gamma_v(t) \neq \gamma_{v'}(t)$, *then* $e(t)$ *is incident to* $\gamma_v(t)$ *and* $\gamma_{v'}(t)$ *if and only if* $e = e(0)$ *is incident to* v *and* v'.

But, if there are n *sides, say* (v_i, e_i, v_i'), $i = 1, \ldots, n$, *such that* $\gamma_{v_i}(t_0) = P$ *and* $\gamma_{v_i'}(t_0) = P'$, *for some* P, $P' \in S^2$ $(P \neq P')$ *and some* $t_0 \in]0,1]$, *then:*

a) *if* n *is odd, the edges* $e_1(t_0), \ldots, e_n(t_0)$ *are identified;*

b) *if* n *is even, the edges* $e_1(t_0), \ldots, e_n(t_0)$ *are eliminated.*

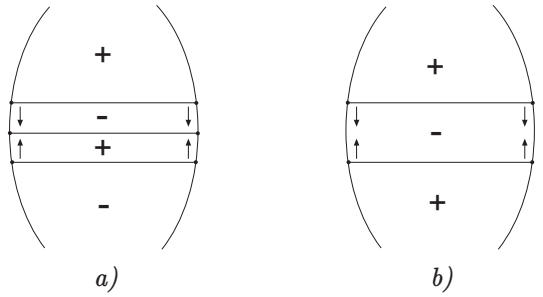

Figure 1.4: The **ii)** condition.

If the above procedure origins, for each $t \in [0,1]$*, an oriented tiling* $\alpha(t) = \tau_t^{o_t}$ *obeying the angle folding relation, such that* $\alpha(t)$ *contains a face* F_t *containing* A *with* $o_t(F_t) = +$ *and* $\alpha(1)$ *has at most two vertices, then* $\alpha(0) = \tau^o$ *is deformable into* $\tau^{\pm}_{stand}$*.*

Proof. (*Sketch of the proof of Theorem 1.3*) The set A permit us to attribute to each face of $\alpha(t)$ the suitable sign. Besides, whenever edges are identified or eliminated, some faces "disappear" and consequently we have to re-label the remaining faces. The **ii)** condition (illustrated in Figure 1.4) assure us that there are not any exchange of signs when re-labeling these faces.

□

Altino Santos in [14] proved that, under certain conditions, given $f \in \mathscr{F}(S^2)$ and $\tau^o \in \mathscr{T}^{\mathcal{O}}(S^2)$, if $\alpha\colon [0,1] \to \mathscr{T}^{\mathcal{O}}(S^2)$ is a deformation of $(\Sigma f)^{o_f}$ into τ^o, then f is deformable into g, for some $g \in \mathscr{F}(S^2)$, such that its induced oriented f-tiling is τ^o or τ^{-o}.

However, this is only possible if the *continuity conjecture* is proven, in other words, for a fixed $t_0 \in [0,1]$ and a certain $\varepsilon_0 > 0$, the map $H\colon [t_0 - \varepsilon_0, t_0 + \varepsilon_0] \times S^2 \to S^2$ defined by $H(t,x) = f_t(x)$ is continuous, where f_t is the unique isometric folding of S^2, such that:

$\Sigma f_t = \tilde{\alpha}(t)$ and $f_{t_{|_A}} = i_{|_A}$, for some non-empty open set $A \subset F$, with $\widetilde{\alpha} = \pi \circ \alpha$ being continuous ($\pi : \mathscr{T}^{\mathcal{O}}(S^2) \to \mathscr{T}(S^2)$, $\pi(\tau^o) = \tau$), i a spherical isometry and F a face of $\tilde{\alpha}(t_0)$.

We are interested in oriented spherical f-tilings which are deformable into the f-

tiling $\tau^{\pm}_{stand}$ and whose associated isometric foldings are deformable into the standard one, f_{stand}.

Next Chapters are dedicated to classify dihedral spherical f-tilings, for certain prototiles and, for each one, we intend to add a convenient orientation and find their deformation into $\tau^{\pm}_{stand}$.

Chapter 2

Dihedral f-Tilings of S^2 by Equilateral and Isosceles Triangles

In this Chapter, we classify all dihedral f-tilings of the unit sphere S^2, in which the prototiles are an equilateral and an isosceles triangle. Proofs of all results can be found in [5].

We recall that, a dihedral f-tiling of the sphere $S^2 = \{ x \in \mathbb{R}^3 : \|x\| = 1 \}$, with prototiles T_1 and T_2 (spherical triangles) is an edge-to-edge polygonal decomposition of the sphere, such that each polygonal face is congruent to either T_1 or T_2 and all vertices satisfy the angle-folding relation meaning, each vertex is of even valency and the sums of alternate angles at each vertex are π.

Two dihedral f-tilings of S^2, τ_1 and τ_2 are isomorphic (or congruent) if and only if there is an isometry ψ of S^2 such that $\psi(\tau_1) = \tau_2$. Next, by "unique f-tiling", we mean unique up to an isomorphism.

$\Omega(T_1, T_2)$ is the set, up to an isomorphism, of all dihedral f-tilings of S^2, whose prototiles are T_1 and T_2.

After some initial assumptions, it is usually possible to deduce the sequence and orientation of most of the tiles. Eventually, either a complete tiling, or an impossible configuration proving that the hypothetical tiling fails to exist is reached. In the diagrams that follows, the order in which deductions are made is indicated by the number of tiles. For $j > 2$, the location of tile j is deduced directly from the locations of tiles $(1, 2, \ldots, j-1)$ and from the assumption that the configuration is part of a

complete representation of a f-tiling, except where otherwise indicated.

Recall that, in dihedral f-tilings, there are at least six vertices of valency four.

From now on, T_1 denotes an equilateral spherical triangle of angle α and side a and T_2 an isosceles spherical triangle of angles β, β, γ, with sides b (opposite to β) and c (opposite to γ).

We begin by pointing out that, any element of $\Omega(T_1, T_2)$ has at least two cells congruent, respectively, to T_1 and T_2, such that they are in adjacent positions in one and only one of the situations illustrated in Figure 2.1.

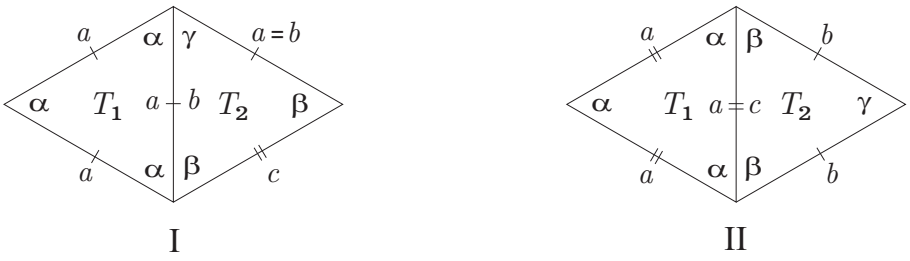

Figure 2.1: Distinct cases of adjacency.

Each type of adjacency can be, respectively analytically described by the following equations:

$$\frac{\cos\alpha\,(1+\cos\alpha)}{\sin^2\alpha} = \frac{\cos\beta(1+\cos\gamma)}{\sin\beta\sin\gamma} \tag{2.1}$$

and

$$\frac{\cos\alpha\,(1+\cos\alpha)}{\sin^2\alpha} = \frac{\cos\gamma+\cos^2\beta}{\sin^2\beta}. \tag{2.2}$$

2.1 Triangular Dihedral f-Tilings with Adjacency of Type I

In this section, we study the set $\Omega(T_1, T_2)$ when T_1 and T_2 are tiles with adjacency of type I (see Figure 2.1) satisfying the equation (2.1).

From the configuration I of Figure 2.1, we are led to the one illustrated in Figure 2.2 concluding that the sum of alternate angles containing α and β is of the form $\alpha+\beta \leq \pi$.

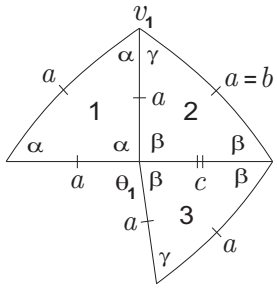

Figure 2.2: Local configuration.

Proposition 2.1 *If T_1 and T_2 are tiles with adjacency of type I such that $\alpha + \beta = \pi$, then $\Omega(T_1, T_2) \neq \varnothing$ if and only if $\alpha + k\gamma = \pi$, for some $k \geq 2$. In this situation, we end up with $\lceil \frac{k}{2} \rceil + 1$ non-isomorphic dihedral f-tilings (Figure 2.5).*

Proof. In the conditions of this Proposition, the union of T_1 and T_2 forms an isosceles triangle of sides a, a, $a + c$ and so $\alpha = \beta = \frac{\pi}{2}$.

The angle labeled θ_1, in Figure 2.2, cannot be γ, otherwise T_2 would be an equilateral triangle congruent to T_1. Taking into account the sides of the two triangles, θ_1 is not equal to β, either. Therefore, $\theta_1 = \alpha$.

We may add some new cells to the local configuration and a decision must be made about the angle $\theta_2 \in \{\alpha, \beta, \gamma\}$ in the new configuration (Figure 2.3-I).

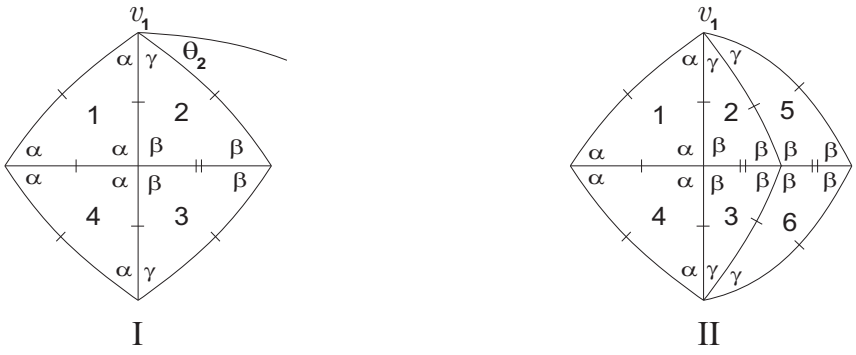

Figure 2.3: Local configurations.

Assuming $\theta_2 = \beta$ or $\theta_2 = \alpha$, we may conclude that v_1 is a vertex of valency four and the other two (alternate) angles around v_1 are respectively γ and β or γ and α. In any case, $\gamma = \frac{\pi}{2}$, leading once more to the contradiction of T_2 being an equilateral triangle

congruent to T_1. Hence, $\theta_2 = \gamma$ and so the local configuration of τ can be expanded a little bit more leading to the following configuration in Figure 2.3-II.

Looking at the sequence of alternate angles around vertex v_1 (Figure 2.3-II), one has $\alpha + \gamma \leq \pi$. However, the assumption that $\alpha + \gamma = \pi$ implies $\gamma = \frac{\pi}{2}$ and, as we have seen before, we end up in a contradiction. Therefore, $\alpha + \gamma < \pi$ and so $\gamma < \frac{\pi}{2}$.

Around vertex v_1, the sum of the alternate angles containing α must be of type $\alpha + k\gamma = \pi$, for some $k \geq 2$. The sides arrangement emanating from this vertex oblige that the other sum of alternate angles is also composed by one angle α and k angles γ, see Figure 2.4.

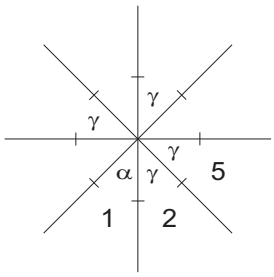

Figure 2.4: Angles arrangement emanating from vertex v_1 with $k = 3$.

There are k possibilities to place angle α around v_1, each one leading to a complete tiling $\tau \in \Omega(T_1, T_2)$, but only $\lceil \frac{k}{2} \rceil$ represent non-isomorphic f-tilings.

These two-parameter family of f-tilings will be denoted by $\mathcal{A}_k^i$, where $k \geq 2$ and $i = 1, \ldots, \lceil \frac{k}{2} \rceil + 1$. It is composed by vertices of valency four whose sums of alternate angles satisfy $\alpha + \beta = \pi$, with $\alpha = \beta = \frac{\pi}{2}$ and vertices of valency $2(1 + k)$ satisfying $\alpha + k\gamma = \pi,\ k \geq 2$.

In Figure 2.5, we present the 2 non-isomorphic tilings $\mathcal{A}_3^i$, $i = 1, 2$ corresponding to $\gamma = \frac{\pi}{6}$.

Observe that for each $k \geq 2$, all the f-tilings $\mathcal{A}_k^i$, $i = 1, \ldots, \lceil \frac{k}{2} \rceil + 1$ can be obtained from a monohedral f-tiling with prototile an isosceles triangle of angles $\frac{\pi}{2}$, $\frac{\pi}{2k}$, $\frac{\pi}{2k}$ by adding edges.

□

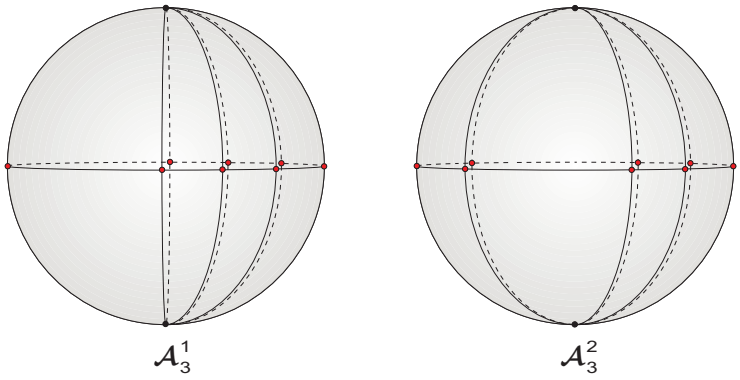

Figure 2.5: 3D representations of the f-tilings $\mathcal{A}_3^1$ and $\mathcal{A}_3^2$.

Proposition 2.2 *If T_1 and T_2 are tiles with adjacency of type I, with $\alpha + \beta < \pi$ (Figure 2.2), then $\Omega(T_1, T_2) = \varnothing$.*

Proof. By the adjacency condition (2.1) and since $\alpha + \beta < \pi$, then $\alpha, \beta < \frac{\pi}{2}$.

Taking into account that vertices of valency four must exist, then $\gamma \geq \frac{\pi}{2}$.

It is a straightforward exercise to show that: given a family of isosceles triangles T_θ (Figure 2.6) of angles $\theta, \varepsilon, \varepsilon$ and sides l_θ, x_0, x_0 where x_0 is a fixed value of $]0, \frac{\pi}{2}[$ and $\theta \in]0, \pi[$, then θ increases if and only if ε decreases.

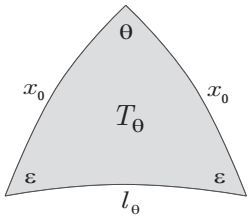

Figure 2.6: A family of isosceles triangle with two fixed sides.

Using this result, we may conclude that $\alpha > \beta$. Summarizing one has,

$$\beta < \alpha < \frac{\pi}{2} \leq \gamma.$$

Let us consider again, the local configuration illustrated in Figure 2.2. Taking into account the order relation between α, β and γ and the possible angles surrounding vertex v_1, the sum of alternate angles containing γ can satisfy neither $2\gamma < \pi$, $\gamma + \alpha < \pi$ nor $\gamma + \beta < \pi$ (observe that $2\gamma + \beta > \gamma + \alpha + \beta > \gamma + 2\beta > \pi$). On the other hand,

if it satisfies $2\gamma = \pi$ or $\gamma + \beta = \pi$, then $\alpha + \rho = \pi$ for some $\rho \in \{\alpha, \beta, \gamma\}$, which is not possible under the angle ordering established above. Hence, $\alpha + \gamma = \pi$.

Starting from the configuration illustrated in Figure 2.2, we may add new cells ending up with the one illustrated in Figure 2.7.

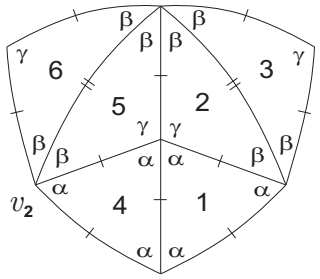

Figure 2.7: Local configuration.

Now, we are able to order all the angles

$$\frac{\pi}{6} < \beta < \frac{\pi}{3} < \alpha < \frac{\pi}{2} < \gamma < \frac{2\pi}{3}.$$

The first observation is that, any vertex surrounded by an angle γ is of valency four and it is surrounded, in cyclic order, by the sequence of angles $(\gamma, \gamma, \alpha, \alpha)$.

The sums of the alternate angles of vertices that do not have angles γ around them must obey to one of the following conditions:

$$4\beta = \pi, \;\; 5\beta = \pi, \;\; \alpha + 2\beta = \pi, \;\; \alpha + 3\beta = \pi \;\; \text{or} \;\; 2\alpha + \beta = \pi.$$

Next, we shall show that all vertices without angles γ around them are of the same type.

Clearly, the sums of the alternate angles surrounding vertex v_2, in Figure 2.7, must satisfy

$$\alpha + 2\beta = \pi, \;\; \alpha + 3\beta = \pi \;\; \text{or} \;\; 2\alpha + \beta = \pi.$$

- If $\alpha + 2\beta = \pi$, then obviously $\alpha + 3\beta \neq \pi$ and $2\alpha + \beta \neq \pi$. We also have $4\beta \neq \pi$ and $5\beta \neq \pi$, otherwise $\alpha = \frac{\pi}{2}$ or $\alpha = \frac{3\pi}{5}$, contradicting the condition $\alpha < \frac{\pi}{2}$.

- If $\alpha + 3\beta = \pi$, then obviously $\alpha + 2\beta \neq \pi$ and also $4\beta \neq \pi$, otherwise $\alpha = \frac{\pi}{4}$, contradicting the condition $\alpha > \frac{\pi}{3}$. In cases $2\alpha + \beta = \pi$ or $5\beta = \pi$, we get $\alpha = \frac{2\pi}{5}$ and $\gamma = \frac{3\pi}{5}$.

- If $2\alpha + \beta = \pi$, then $\alpha + 2\beta \neq \pi$. The case $4\beta = \pi$ leads to $\alpha = \frac{3\pi}{8}$ and $\gamma = \frac{5\pi}{8}$. Finally, in cases $5\beta = \pi$ or $\alpha + 3\beta = \pi$ we get, as before, $\alpha = \frac{2\pi}{5}$ and $\gamma = \frac{3\pi}{5}$.

Summarizing, any local configuration of $\tau \in \Omega(T_1, T_2)$ must contain two triangles in adjacent positions in one of the following situations, Figure 2.8. However, they are not compatible. In fact, the sides signed in those configurations are of different lengths.

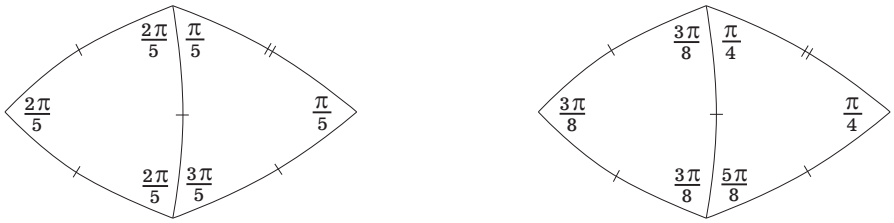

Figure 2.8: Incompatible adjacent triangles.

We have just shown that all vertices surrounded by a set of angles not containing γ are all of the same type.

The configuration illustrated in Figure 2.7 eliminates the cases $4\beta = \pi$, $5\beta = \pi$ and $2\alpha + \beta = \pi$. The remaining cases are

$$\alpha + 2\beta = \pi \text{ and } \alpha + 3\beta = \pi.$$

Considering $\alpha + 2\beta = \pi$, the configuration in Figure 2.9 takes place, leading to a contradiction (observe the angles surrounding vertex v_3).

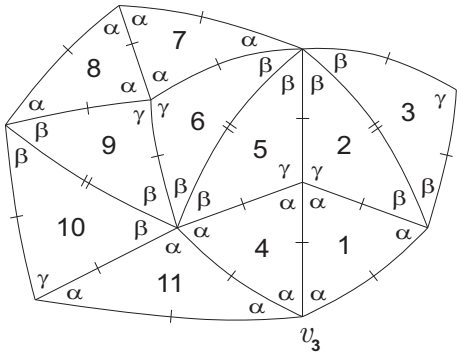

Figure 2.9: Local configuration.

Assuming that $\alpha+3\beta=\pi$ and taking into account the symmetry of the local configuration, we get the one illustrated in Figure 2.10 leading, once again, to a contradiction (observe the angles surrounding vertex v_4).

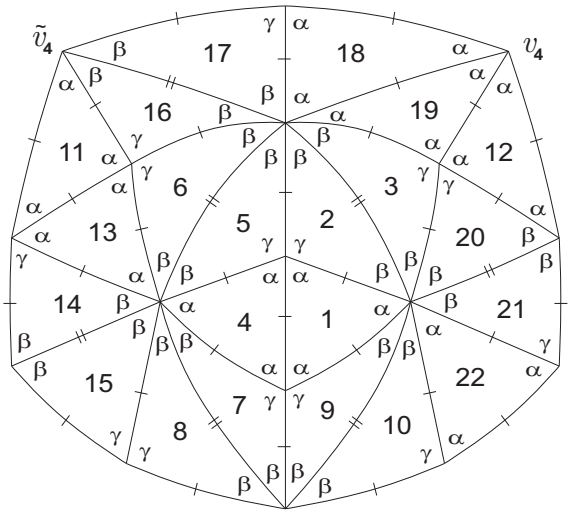

Figure 2.10: Local configuration.

Note: On construction, we assume that tile 13 is an equilateral triangle. If we had considered that it was an isosceles triangle, then we also end up into a contradiction (at vertex $\tilde{v}_4$). □

2.2 Triangular Dihedral f-Tilings with Adjacency of Type II

In this section, we describe the set $\Omega(T_1,T_2)$ where T_1 is an equilateral triangle of angle α and T_2 is an isosceles triangle of angles β, β, γ with adjacency of type II (Figure 2.1-II) and satisfying the equation (2.2). This adjacency condition implies immediately that $\alpha\neq\beta$. Starting a local configuration of $\tau\in\Omega(T_1,T_2)$ with two adjacent cells congruent to T_1 and T_2, respectively (Figure 2.11), a choice for the angle $\theta_3\in\{\beta,\gamma\}$ must be made.

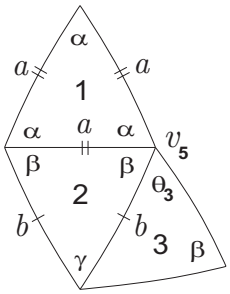

Figure 2.11: Local configuration.

With the above terminology, one has:

Proposition 2.3 *If $\Omega(T_1, T_2) \neq \varnothing$, then $\theta_3 = \beta$ and $\alpha + \beta < \pi$. In this case, we end up with three isolated non-isomorphic dihedral f-tilings (Figure 2.21).*

Proof. Using the labeling of Figure 2.11, it follows that $\theta_3 = \gamma$ or $\theta_3 = \beta$ and $\alpha + \theta_3 = \pi$ or $\alpha + \theta_3 < \pi$. We shall study each case separately.

1. If $\theta_3 = \gamma$ and $\alpha + \gamma = \pi$, then expanding the configuration illustrated in Figure 2.11, yields the configuration in Figure 2.12.

Accordingly, $\beta = \frac{\pi}{2}$ and, by the adjacency condition (2.2), $a = \gamma$. However,

$$\frac{\cos\alpha + \cos^2\alpha}{\sin^2\alpha} = \frac{\cos(\pi-\gamma) + \cos^2(\pi-\gamma)}{\sin^2(\pi-\gamma)} = \cos\gamma,$$

implying that $-1 + \cos\gamma = \sin^2\gamma$, leading to the impossibility $\gamma = 0$.

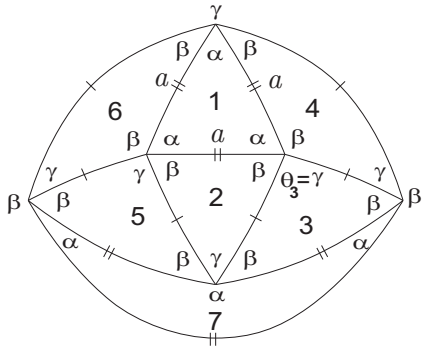

Figure 2.12: Local configuration.

2. If $\theta_3 = \gamma$ and $\alpha + \gamma < \pi$, then one of the sums of alternate angles around vertex v_5 (Figure 2.11) is either of the form $\alpha + \gamma + \lambda = \pi$, where the parameter λ can be a sum of several angles γ ($\lambda = k\gamma$, $k \geq 1$) or a sum of angles where at least one of them is either α or β.

2.1. In the first case, having in mind the adjacency rules for the sides (see Figure 2.13-I), we conclude that there is a contribution of at least two angles β and one angle γ for the other sum of alternate angles (around v_5), leading to a contradiction, since $2\beta + \gamma > \pi$.

2.2. Suppose now, that λ is a sum of angles where at least one of them is α. Then $2\alpha + \gamma \leq \pi$ and hence $\gamma < \frac{\pi}{3} < \alpha < \frac{\pi}{2}$. By the existence of vertices of valency four, we conclude that $\beta \geq \frac{\pi}{2}$ and the angles arrangement around vertex v_5 is of the form illustrated in Figure 2.13-II.

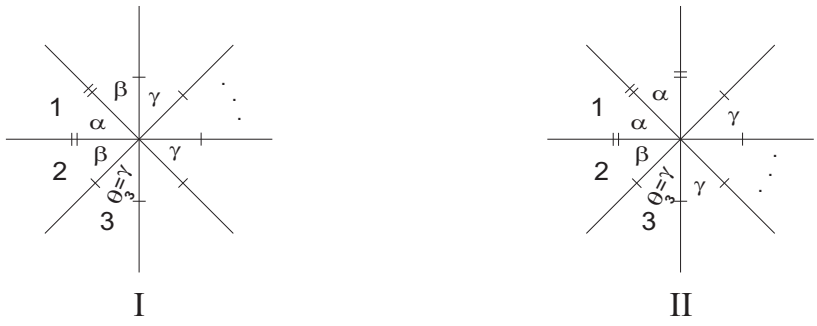

Figure 2.13: Angles arrangement around vertex v_5.

The sum of the alternate angles around v_5 containing β, visible in Figure 2.13-II, is of the form $\beta + k\gamma + \alpha = \pi$, $k \geq 1$. Once again, the adjacency rules for the sides imply that the other sequence of alternate angles cannot have more than one angle α, contradicting our assumption.

2.3. Finally, assume that λ is a sum of angles where at least one of them is β. Therefore, $\alpha + \gamma + \beta \leq \pi$. As $2\beta + \gamma > \pi$, then $\alpha < \beta$. Consequently, $\gamma < \frac{\pi}{3} < \alpha < \beta$, but the existence of vertices of valency four forces $\beta = \frac{\pi}{2}$ (observe that $\alpha + \beta < \pi$, $\alpha + \gamma < \pi$, $\gamma + \beta < \pi$, $2\gamma < \pi$ and if $\alpha = \frac{\pi}{2}$, then $\alpha + \beta + \gamma > \pi$).

Looking at the other sequence of alternate angles around v_5 containing β, we may

have either one angle β and all the other ones γ (see Figure 2.14-I) or one angle β, one angle α and all the other ones γ (see Figure 2.14-II).

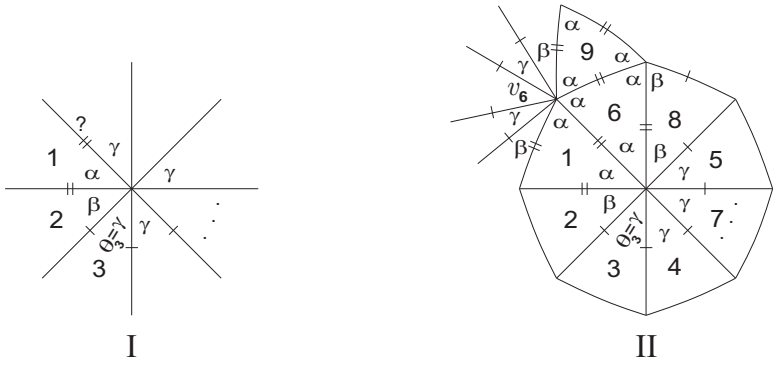

Figure 2.14: Local configurations.

In the first case, the adjacency rules for the sides are violated and in the second case, in spite of being able to add some more cells, one of the sums of alternate angles around vertex v_6 is of the form $2\alpha + s\gamma = \pi$ and the other $\alpha + \beta + (s-1)\gamma + \beta = \pi$, for some $s \geq 1$. But this is impossible, since $\beta = \frac{\pi}{2}$.

3. If $\theta_3 = \beta$ and $\alpha + \beta = \pi$, then $\alpha = \gamma$ (the cells T_1 and T_2 form a spherical lune) and a decision about the angle labeled $\theta_4 \in \{\gamma, \beta\}$, in Figure 2.15-I, must be taken.

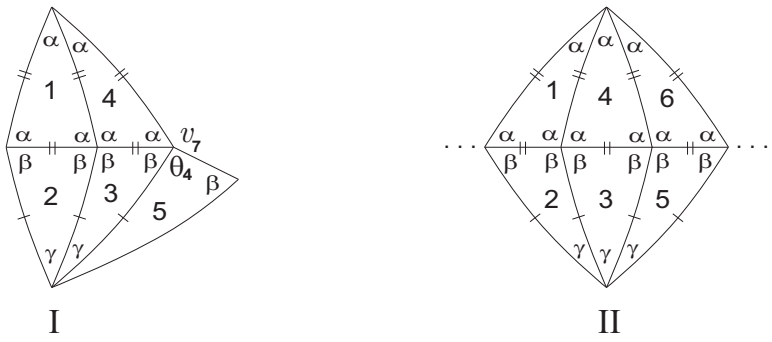

Figure 2.15: Local configurations.

Assuming $\theta_4 = \gamma$, then $\alpha + \gamma < \pi$ (otherwise $\beta = \gamma$) and so $\frac{\pi}{3} < \alpha = \gamma < \frac{\pi}{2}$. As, $\alpha + \beta = \pi$ and $\alpha < \frac{\pi}{2}$, then $\beta > \frac{\pi}{2}$. Consequently, the sum $\alpha + \gamma + \lambda$ violates the angle folding relation, for any $\lambda \in \{\alpha, \beta, \gamma\}$.

Therefore, $\theta_4 = \beta$ and we can extend the configuration illustrated in Figure 2.15-I, obtaining the one given in Figure 2.15-II. From this configuration, we conclude that $\alpha = \gamma = \frac{\pi}{k}$, $k \geq 2$. For $k = 2$, $\alpha = \frac{\pi}{2} = \gamma = \beta$ and for $k > 2$, $\alpha \leq \frac{\pi}{3}$ and so this global planar representation does not give rise to a spherical f-tiling.

4. Finally, we analyze the case $\theta_3 = \beta$ and $\alpha + \beta < \pi$ (see Figure 2.11). Consider the sum of alternate angles containing α and β around vertex v_5. Besides α and β, this sum must contain, at least, one other angle θ_5, with $\theta_5 \in \{\alpha, \beta, \gamma\}$.

4.1. If $\theta_5 = \alpha$, then $2\alpha + \beta \leq \pi$ and so $\beta < \frac{\pi}{3} < \alpha < \frac{\pi}{2} \leq \gamma$.

Expanding the configuration illustrated in Figure 2.11, we get one of the local configurations illustrated in Figure 2.16, where the angle labeled θ_6 must be γ or β.

If $\theta_6 = \gamma$ (Figure 2.16-I), the order relation between the angles α, β and γ obliges $\alpha + \gamma = \pi$ and as $\beta + \gamma < \pi$, vertex v_8 must be of valency greater than four, which is a contradiction, since $\gamma + \beta + \lambda > \pi$, for any $\lambda \in \{\alpha, \beta, \gamma\}$.

The case $\theta_6 = \beta$ (Figure 2.16-II) allows us to conclude that $\gamma = \frac{\pi}{2}$ and consequently $\beta > \frac{\pi}{4}$ (observe that $\gamma + 2\beta > \pi$). Ordering, one has

$$\frac{\pi}{4} < \beta < \frac{\pi}{3} < \alpha < \frac{\pi}{2} = \gamma.$$

It follows that, the sum of alternate angles around v_5 containing α and β is of the form $2\alpha + \beta = \pi$, otherwise $2\alpha + \beta + \lambda \geq 2\alpha + 2\beta > \pi$ for any $\lambda \in \{\alpha, \beta, \gamma\}$. By the order relation between the angles, we may also conclude that the sum of the alternate angles around any vertex is either $2\alpha + \beta = \pi$ or $2\gamma = \pi$.

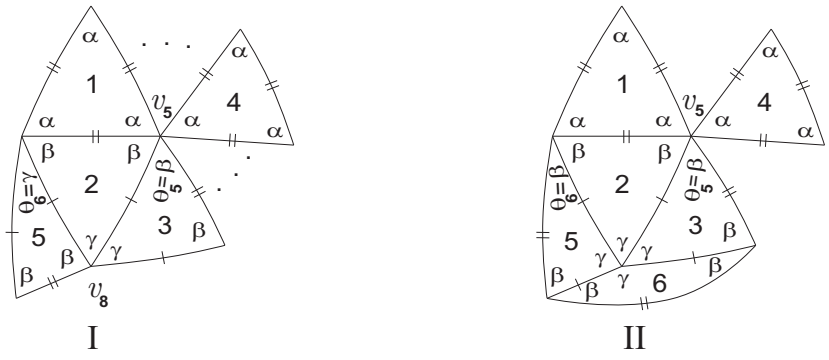

Figure 2.16: Local configurations.

This information permits us to extend the configuration illustrated in Figure 2.16-II getting the one below, Figure 2.17.

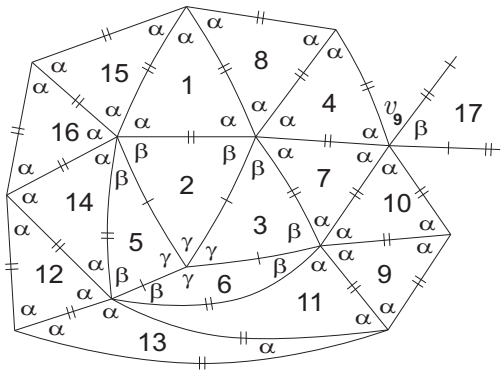

Figure 2.17: Local configuration.

Looking at vertex v_9 (Figure 2.17), a decision about the tile numbered 17 must be made. We have two choices to assign edge length to this tile. However, this choice is irrelevant, since any one of them leads to a tiling $\tau \in \Omega(T_1, T_2)$, as illustrated in Figure 2.18. This f-tiling will be denoted by $\mathcal{A}$.

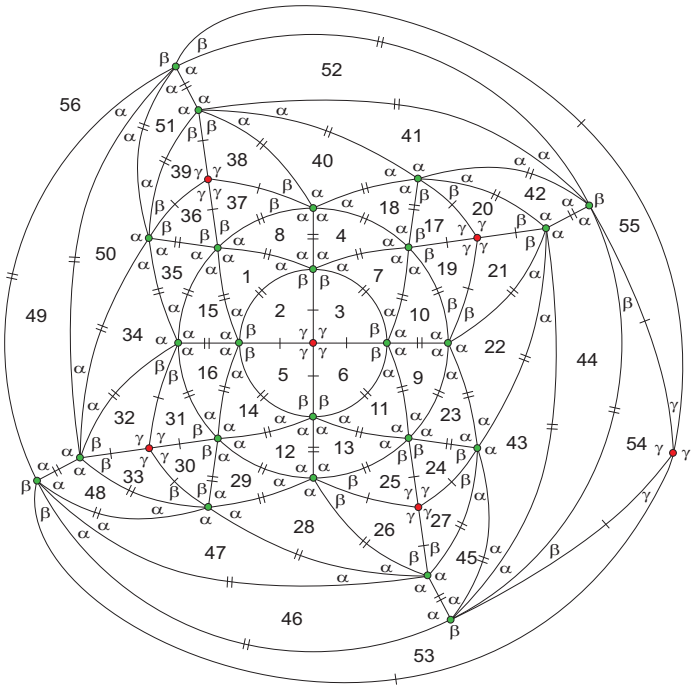

Figure 2.18: Complete planar representation of $\mathcal{A}$.

It is composed by 32 equilateral triangles and 24 isosceles triangles. A 3D repre-

sentation is illustrated in Figure 2.21. Since $\gamma = \frac{\pi}{2}$ and $2\alpha + \beta = \pi$, the adjacency condition (2.2) implies $\alpha \approx 65.188°$ and $\beta \approx 49.624°$.

4.2. Assuming that $\theta_5 = \beta$, then $\alpha + 2\beta \leq \pi$. As $2\beta + \gamma > \pi$, one has $\beta < \frac{\pi}{3} < \alpha < \gamma$.

Accordingly, the sum of the alternate angles around v_5 containing α and β must be of the form $\alpha + p\beta = \pi$, $p \geq 2$ (the other cases were already studied). Extending the configuration illustrated in Figure 2.11, we get the one in Figure 2.19-I and tile 5 must be as shown, leading us to $\gamma = \frac{\pi}{2}$. Now, $\beta > \frac{\pi}{4}$ since $2\beta + \gamma > \pi$. Consequently, $p = 2$ and so $\alpha + 2\beta = \pi$.

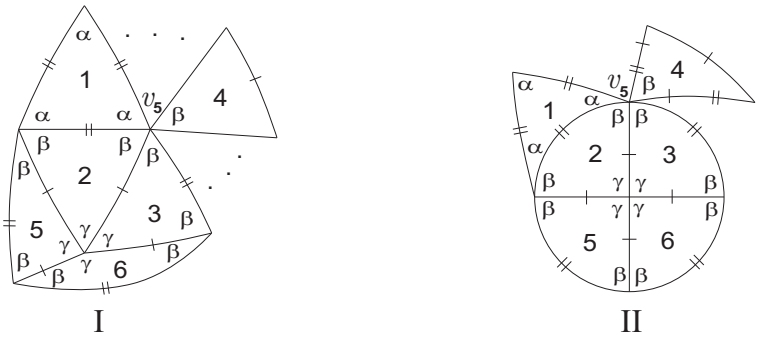

Figure 2.19: Local configurations.

By the adjacency condition (2.2), we have $\alpha \approx 70.529°$ and $\beta \approx 54.735°$.

The local configuration illustrated in Figure 2.19-I can now be extended a little bit more and a resolution about the two possible positions for the sides of the tile 4 must be taken (see Figure 2.19-II). The two choices lead to two extended local configurations of non-isomorphic dihedral f-tilings, as illustrated in Figure 2.20. We shall denote them, respectively by $\mathcal{B}_1$ (Figure 2.20-I) and $\mathcal{B}_2$ (Figure 2.20-II). 3D representations are illustrated in Figure 2.21.

Note: On construction of the configuration in Figure 2.20-II, tile 11 could have been placed in a different way, giving rise to two adjacent angles α and the tiling could still have been completed. However, the resulting tiling would have been equivalent to that in Figure 2.20-I. Later on, the same argument implies the placement of tile 17.

It should be pointing out that the f-tilings $\mathcal{B}_1$ and $\mathcal{B}_2$ can be obtained from a monohedral f-tiling with prototile an equilateral triangle of angles $\frac{\pi}{2}, \frac{\pi}{2}, \frac{\pi}{2}$, adding some

edges.

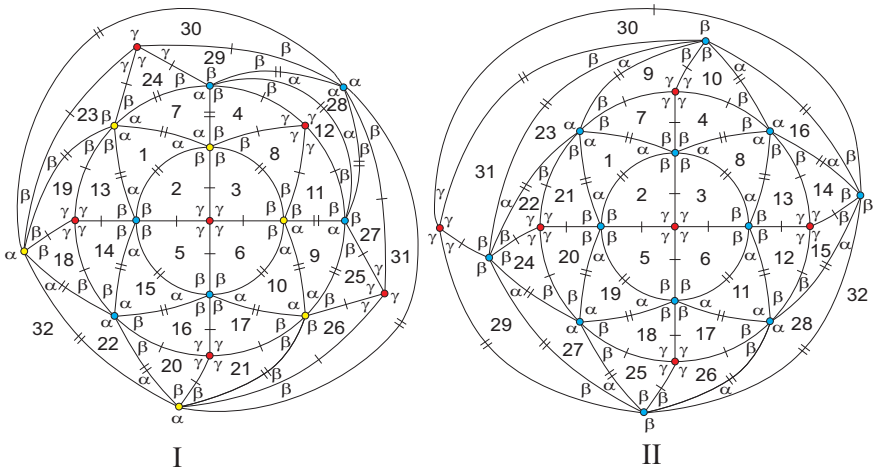

Figure 2.20: Complete planar representations.

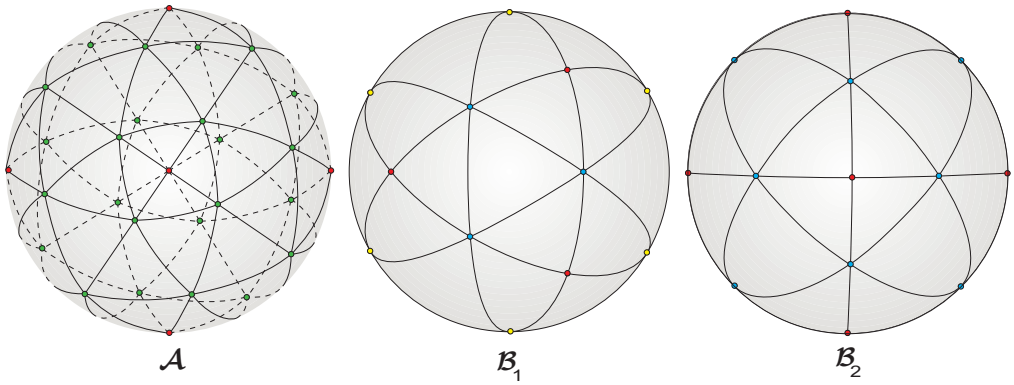

Figure 2.21: 3D representations.

4.3. In case $\theta_5 = \gamma$, then $\alpha + \beta + \gamma \leq \pi$ and so $\beta > \alpha$, since $2\beta + \gamma > \pi$. Consequently, $\gamma < \frac{\pi}{3} < \alpha < \beta$. The existence of vertices of valency four implies that $\beta = \frac{\pi}{2}$ (as seen before in (2.3)) and so the other sequence of alternate angles must have either one angle β and several angles γ or one angle β, one angle α and several angles γ. However, the adjacency rules for the sides eliminates all these hypotheses. Hence, there are no angles γ in the sum of alternate angles containing α and $\theta_5 = \beta$ (Figure 2.11). $\square$

2.3 Isohedrality-Classes and Isogonality-Classes

It is well known that, any spherical isometry is either a reflection, a rotation or a glide-reflection, which consists of reflecting through some spherical great circle (or a plane containing the origin) and then rotating around the line orthogonal to the great circle and containing the origin. On the other hand, if v and v' are vertices of a spherical f-tiling τ, and σ is a symmetry of τ, such that $\sigma(v') = v$, then every symmetry of τ that sends v' into v is a composition of σ with a symmetry of τ fixing v. It is also convenient to state that the isometries that fix v are exactly the rotations around the line containing $\pm v$ and the reflections through the great circles by $\pm v$.

Here, we determine the transitivity classes of isogonality and isohedrality.

In **Table 2.1** it is shown a complete list of all spherical dihedral f-tilings, whose prototiles are an equilateral triangle T_1 of angle α and an isosceles triangle T_2 of angles β, β, γ. We have used the following notation:

- M and N are, respectively, the number of triangles congruent to T_1 and the number of triangles congruent to T_2 used in such dihedral f-tilings;
- The numbers of isohedrality-classes and isogonality-classes are denoted, respectively, by # isoh. and # isog..

f-tiling	α	β	γ	M	N	# isoh.	# isog.
$\mathcal{A}_k^i,\ k \geq 2,\ i = 1 \ldots, \lceil \frac{k}{2} \rceil + 1$	$\frac{\pi}{2}$	$\frac{\pi}{2}$	$\frac{\pi}{2k}$	4	$4k$	$k+1$	$k+2$
$\mathcal{A}$	65.188°	49.624°	$\frac{\pi}{2}$	32	24	2	2
$\mathcal{B}_1$	70.529°	54.735°	$\frac{\pi}{2}$	8	24	5	3
$\mathcal{B}_2$	70.529°	54.735°	$\frac{\pi}{2}$	8	24	2	2

Table 2.1: The Combinatorial Structure of Dihedral f-Tilings of the Sphere by Equilateral and Isosceles Triangles.

2.4 Deformations

In this section, for each obtained dihedral f-tiling, we shall present geometrical sketches of its deformation into the standard folding (up to a rotation) via the paths $\gamma_v(t)$ referred in Theorem 1.3. The arrows indicate the way the vertices move. In order to facilitate the reasoning performed, we attribute to each face a suitable sign and, whenever the f-tiling is symmetric, we label only the angles placed in the semi-space $x \geq 0$.

It should be pointed out that, in each step of the deformation, the angle folding relation and the continuity of the deformation map ϕ must be preserved. The function $\phi : [0,1] \to \mathscr{T}^{\mathcal{O}}(S^2)$ maps each $t \in [0,1]$ into a f-tiling τ_t obeying to a system of parameterized angles leading, generally to a piecewise-defined function.
Recall that $\mathscr{T}^{\mathcal{O}}(S^2)$ is equipped with the metric structure given by (Proposition 1.4)

$$c(\tau_1^{o_1}, \tau_2^{o_2}) = \sum_{\substack{\text{F face of} \\ \tau_1 \cup \tau_2}} \lambda(F)\, Area(F)\,,$$

where $\tau_1^{o_1}$, $\tau_2^{o_2} \in \mathscr{T}^{\mathcal{O}}(S^2)$ and $\lambda(F) = 1$ if F is errant and $\lambda(F) = 0$ if F is non-errant.

Let us begin by showing that:

1. For each $k \geq 2$ and $i = 1 \ldots, \lceil \frac{k}{2} \rceil + 1$, $(\mathcal{A}_k^i)^o$ is deformable into τ^+_{stand}.

   (a) Figure 2.22 gives an idea of how to define a deformable map $\phi : [0,1] \to \mathscr{T}^{\mathcal{O}}(S^2)$ of $(\mathcal{A}_3^1)^o$ into τ^+_{stand}. The angles are $\alpha = \beta = \frac{\pi}{2}$ and $\gamma = \frac{\pi}{6}$.

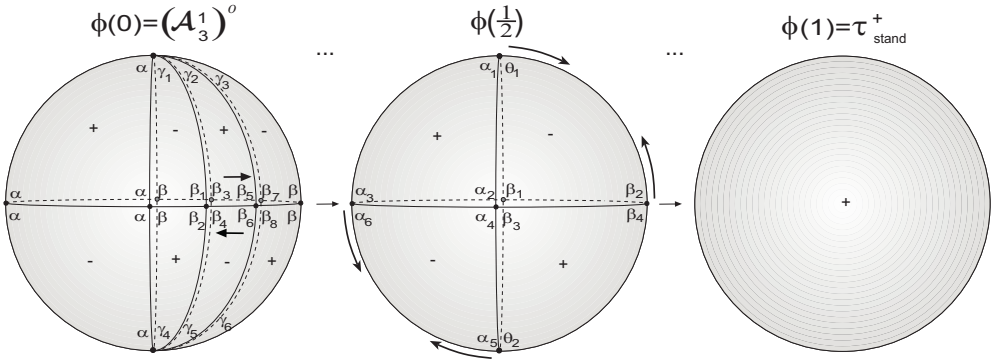

Figure 2.22: Deformation of $(\mathcal{A}_3^1)^o$.

In the first stage of the deformation, that is for each $t \in [0, \frac{1}{2}]$, labeling the angles as shown in Figure 2.22, one has:

- $\widetilde{\gamma}_i(t) = (1-2t)\,\gamma_i,\ i = 2, 5$;
- $\widetilde{\gamma}_i(t) = \gamma_i + t\gamma_2,\ i = 1, 3$ and $\widetilde{\gamma}_j(t) = \gamma_j + t\gamma_5,\ j = 4, 6$;
- $\widetilde{\beta}_i(t) \equiv \beta = \frac{\pi}{2},\ i = 1, 3, 5, 7$;
- $\widetilde{\beta}_i(t) = \pi - \widetilde{\beta}_{i-3}(t),\ i = 4, 8$ and $\widetilde{\beta}_j(t) = \pi - \widetilde{\beta}_{j+1}(t),\ j = 2, 6$.

In the second stage of the deformation, for each $t \in]\frac{1}{2}, 1]$:

- $\widetilde{\beta}_1(t) = (2-2t)\beta_1$ and $\widetilde{\alpha}_4(t) = \pi - \widetilde{\beta}_1(t)$;
- $\widetilde{\alpha}_2(t) = \alpha_2 - \beta_1 + 2t\beta_1$ and $\widetilde{\beta}_3(t) = \pi - \widetilde{\alpha}_2(t)$;
- $\widetilde{\alpha}_1(t) = \widetilde{\theta}_1(t) = \widetilde{\beta}_2(t) = \widetilde{\beta}_4(t) = \widetilde{\alpha}_5(t) = \widetilde{\theta}_2(t) = \widetilde{\alpha}_3(t) = \widetilde{\alpha}_6(t) \equiv \frac{\pi}{2}$.

We shall prove now that ϕ is continuous in $[0, 1]$. Next figure helps us count the errant faces in the first stage of the deformation.

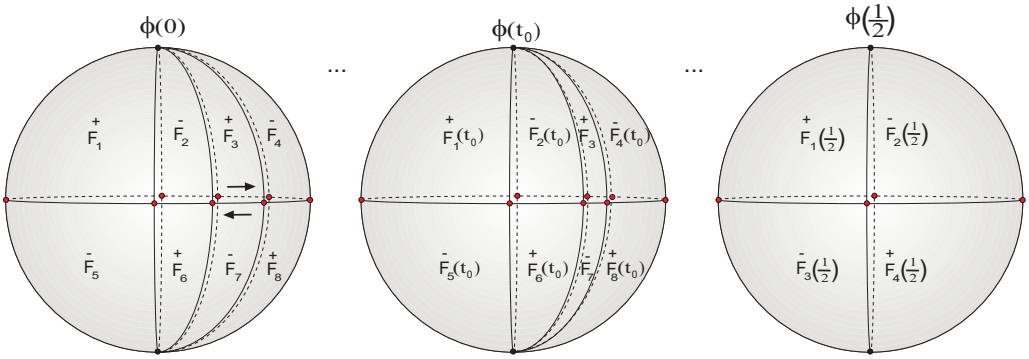

Figure 2.23: First stage of the deformation of $(\mathcal{A}_3^1)^o$.

If $t \in]0, \frac{1}{2}[$:

$$\begin{aligned} c(\tau_t^{o_t}, \tau_0) &= \sum_{\substack{F \text{face of} \\ \tau_t \cup \tau_0}} \lambda(F)\, Area(F) \\ &= 8 \times \left(\frac{\pi}{2} + \frac{\pi}{2} + \frac{\widetilde{\gamma}_2(0) - \widetilde{\gamma}_2(t)}{2} - \pi \right) \\ &= 8 \times \left(\frac{\gamma_2 - (1-2t)\gamma_2}{2} \right). \end{aligned}$$

When $t \to 0^+$, we may conclude that $c(\tau_t^{o_t}, \tau_0) \to 0$ implying that ϕ is continuous at $t = 0$.

Fixing $t_0 \in]0, \frac{1}{2}[$:

$$\begin{aligned} c(\tau_t^{o_t}, \tau_{t_0}) &= \sum_{\substack{F \text{face of} \\ \tau_t \cup \tau_{t_0}}} \lambda(F)\, Area(F) \\ &= 4 \times \left(\frac{\pi}{2} + \frac{\pi}{2} + \widetilde{\gamma}_1(t_0) - \widetilde{\gamma}_1(t) - \pi\right) \\ &+ 4 \times \left(\frac{\pi}{2} + \frac{\pi}{2} + \widetilde{\gamma}_3(t_0) - \widetilde{\gamma}_3(t) - \pi\right) \\ &= 8 \times (t_0 - t)\gamma_2. \end{aligned}$$

When, $t \to t_0$, then $c(\tau_t^{o_t}, \tau_{t_0}) \to 0$ and consequently, ϕ is continuous in $t_0 \in [0, \frac{1}{2}[$.

For each $t \in]0, \frac{1}{2}[$:

$$\begin{aligned} c(\tau_t^{o_t}, \tau_{\frac{1}{2}}) &= \sum_{\substack{F \text{face of} \\ \tau_t \cup \tau_{\frac{1}{2}}}} \lambda(F)\, Area(F) \\ &= 4 \times Area(F_3(t)) \\ &= 4 \times \left(\frac{\pi}{2} + \frac{\pi}{2} + (1 - 2t)\gamma_2 - \pi\right). \end{aligned}$$

Therefore, $c(\tau_t^{o_t}, \tau_{\frac{1}{2}}) \underset{(t \to \frac{1}{2}^-)}{\longrightarrow} 0$.

Figure 2.24 shows the errant faces in the second stage of the deformation.

If $t \in]\frac{1}{2}, 1[$:

$$\begin{aligned} c(\tau_t^{o_t}, \tau_{\frac{1}{2}}) &= \sum_{\substack{F \text{face of} \\ \tau_t \cup \tau_{\frac{1}{2}}}} \lambda(F)\, Area(F) \\ &= 8 \times \left(\frac{\pi}{2} + \frac{\pi}{2} + \frac{\widetilde{\beta}_1\left(\frac{1}{2}\right) - \widetilde{\beta}_1(t)}{2} - \pi\right). \end{aligned}$$

When, $t \to \frac{1}{2}^+$, then $c(\tau_t^{o_t}, \tau_{\frac{1}{2}}) \to 0$. Consequently, we may conclude that ϕ is continuous at $t = \frac{1}{2}$.

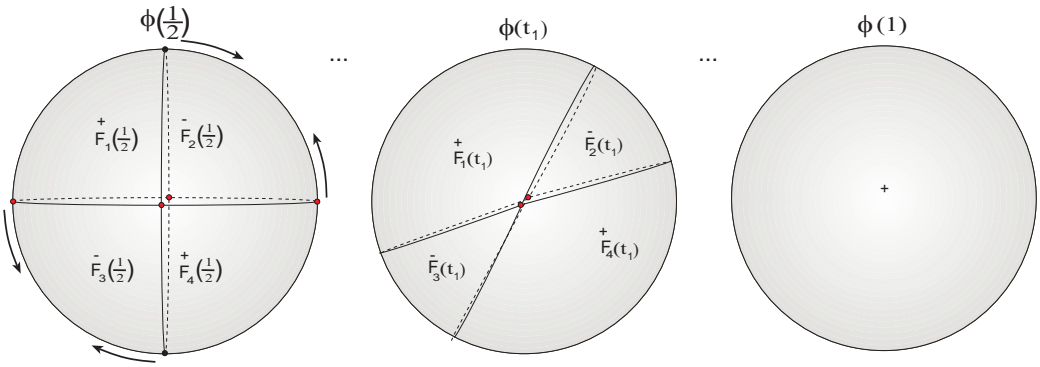

Figure 2.24: Second stage of the deformation of $(\mathcal{A}_3^1)^o$.

For $t_1 \in]\frac{1}{2}, 1[$:

$$\begin{aligned} c(\tau_t^{o_t}, \tau_{t_1}) &= \sum_{\substack{F \text{face of} \\ \tau_t \cup \tau_{t_1}}} \lambda(F)\, Area(F) \\ &= 4 \times \left(\frac{\pi}{2} + \frac{\pi}{2} + \frac{\widetilde{\beta}_1(t_1) - \widetilde{\beta}_1(t)}{2} - \pi \right). \end{aligned}$$

When, $t \to t_1$, then $c(\tau_t^{o_t}, \tau_{t_1}) \to 0$. Therefore, ϕ is continuous at $t = t_1$.

On the other hand, for $t \in]\frac{1}{2}, 1[$:

$$\begin{aligned} c(\tau_t^{o_t}, \tau_{stand}) &= \sum_{\substack{F \text{face of} \\ \tau_t \cup \tau_{stand}}} \lambda(F)\, Area(F) \\ &= 4 \times Area(F_2(t)) \\ &= 4 \times \left(\frac{\pi}{2} + \frac{\pi}{2} + (2 - 2t)\beta_1 - \pi \right). \end{aligned}$$

When $t \to 1^-$, we may conclude that $c(\tau_t^{o_t}, \tau_{stand}) \to 0$ implying that ϕ is continuous at $t = 1$ and so ϕ is continuous in $[0, 1]$. Hence, $(\mathcal{A}_3^1)^o$ is deformable into τ_{stand}^+.

(b) $(\mathcal{A}_3^2)^o$ is also deformable into τ_{stand}^+. Figure 2.25 illustrates the process of deformation, where the angles are $\alpha = \beta = \frac{\pi}{2}$ and $\gamma = \frac{\pi}{6}$.

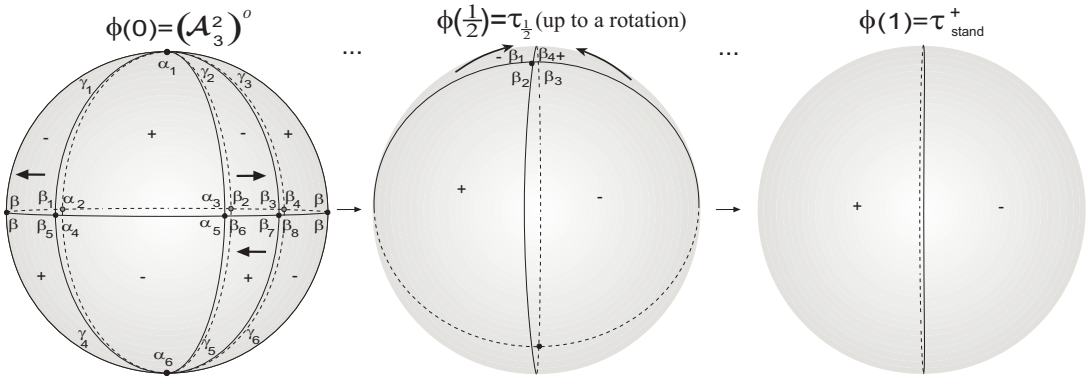

Figure 2.25: Deformation of $(\mathcal{A}_3^2)^o$.

Labeling the angles as illustrated in Figure 2.25, with $t \in [0, \frac{1}{2}]$:

- $\widetilde{\gamma}_i(t) = (1-2t)\gamma_i,\ i = 1, 2, 4, 5;$
- $\widetilde{\alpha}_1(t) = \alpha_1 + t\gamma_2 + 2t\gamma_1$ and $\widetilde{\alpha}_6(t) = \alpha_6 + t\gamma_5 + 2t\gamma_4;$
- $\widetilde{\gamma}_3(t) = \gamma_3 + t\gamma_2$ and $\widetilde{\gamma}_6(t) = \gamma_6 + t\gamma_5;$
- $\widetilde{\alpha}_2(t) = \widetilde{\alpha}_3(t) = \widetilde{\beta}_i(t) \equiv \beta,\ i = 1, \ldots, 8;$
- $\widetilde{\alpha}_4(t) = \pi - \widetilde{\beta}_1(t)$ and $\widetilde{\alpha}_5(t) = \pi - \widetilde{\beta}_2(t)$.

If $t \in]\frac{1}{2}, 1]$:

- $\widetilde{\beta}_i(t) = (2-2t)\beta_i,\ i = 1, 4;$
- $\widetilde{\beta}_2(t) = \pi - \widetilde{\beta}_4(t)$ and $\widetilde{\beta}_3(t) = \pi - \widetilde{\beta}_1(t)$.

Let us show that ϕ is continuous at $t \in [0, 1]$.

For $t \in]0, \frac{1}{2}[$, one has:

$$\begin{aligned} c(\tau^{o_t}, \tau_0) &= \sum_{\substack{F \text{face of} \\ \tau_t \cup \tau_0}} \lambda(F)\, Area(F) \\ &= 12 \times \left(\frac{\pi}{2} + \frac{\pi}{2} + \widetilde{\gamma}_1(0) - \widetilde{\gamma}_1(t) - \pi \right) \\ &= 12 \times (\gamma_1 - (1-2t)\gamma_1). \end{aligned}$$

When, $t \to 0^+$, then $c(\tau^{o_t}, \tau_0) \to 0$, that is ϕ is continuous at $t = 0$.

$$\begin{aligned} c(\tau_t^{o_t}, \tau_{\frac{1}{2}}) &= \sum_{\substack{F\text{face of} \\ \tau_t \cup \tau_{\frac{1}{2}}}} \lambda(F)\, Area(F) \\ &= 4 \times \left(\frac{\pi}{2} + \frac{\pi}{2} + \widetilde{\gamma}_1(t) - \pi\right) + 4 \times \left(\frac{\pi}{2} + \frac{\pi}{2} + \widetilde{\gamma}_2(t) - \pi\right) \\ &= 4(1-2t)\gamma_1 + 4(1-2t)\gamma_2. \end{aligned}$$

As $t \to \frac{1}{2}^-$, we get $c(\tau_t^{o_t}, \tau_{\frac{1}{2}}) \to 0$.

Now, if $t \in]\frac{1}{2}, 1[$:

$$\begin{aligned} c(\tau_t^{o_t}, \tau_{\frac{1}{2}}) &= \sum_{\substack{F\text{face of} \\ \tau_t \cup \tau_{\frac{1}{2}}}} \lambda(F)\, Area(F) \\ &= 4 \times 2 \left(\widetilde{\beta}_1\left(\frac{1}{2}\right) - \widetilde{\beta}_1(t)\right). \end{aligned}$$

Making $t \to \frac{1}{2}^+$, one has $c(\tau_t^{o_t}, \tau_{\frac{1}{2}}) \to 0$.

Finally,

$$\begin{aligned} c(\tau_t^{o_t}, \tau_{stand}) &= \sum_{\substack{F\text{face of} \\ \tau_t \cup \tau_{stand}}} \lambda(F)\, Area(F) \\ &= 2 \times \widetilde{\beta}_1(t). \end{aligned}$$

When, $t \to 1^-$, then $c(\tau^{o_t}, \tau_{stand}) \to 0$, that is ϕ is continuous at $t = 1$. Consequently, ϕ is continuous in $[0, 1]$ and so ϕ is a deformation of $(\mathcal{A}_3^2)^o$ into τ_{stand}^+.

2. The f-tiling $(\mathcal{A})^o$ is deformable into τ_{stand}^+. In what concerns to the steps of the deformation in some dihedral f-tilings, as was in this case, the algebraic view overlaps with the geometric view.

   This f-tiling is composed by vertices of valency four surrounded exclusively by angles γ and vertices of valency six, whose sums of alternate angles satisfy $2\alpha + \beta = \pi$, with $\alpha \approx 65,188°$ and $\beta \approx 49,624°$. In this process of deformation,

areas of the triangles of angles $(\widetilde{\beta}(t), \widetilde{\beta}(t), \widetilde{\gamma}(t))_{t\in[0,\frac{1}{2}]}$ converge to 0 as $t \to \frac{1}{2}^-$ and some of the areas of the equilateral triangles converge to 0 and others to $\frac{\pi}{2}$, as $t \to \frac{1}{2}^-$. Figure 2.26 helps us understand how to define the deformable map $\phi : [0,1] \to \mathscr{T}^{\mathcal{O}}(S^2)$.

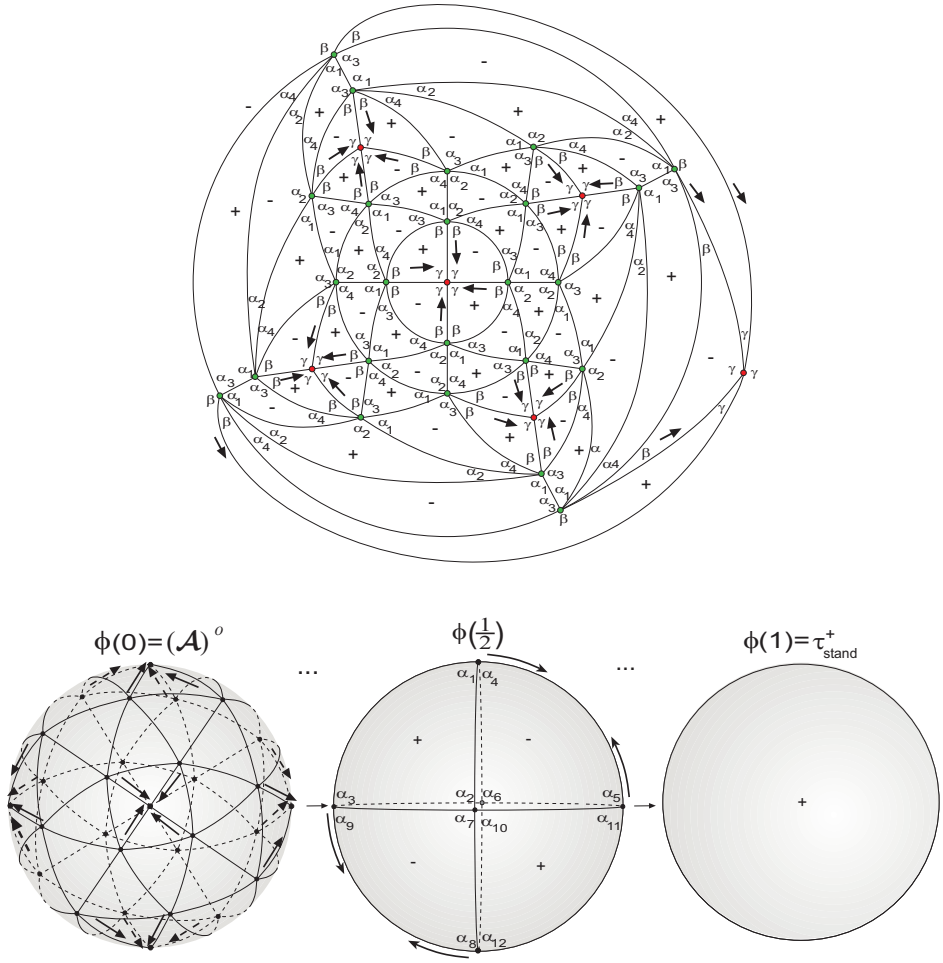

Figure 2.26: Deformation of $(\mathcal{A})^o$.

So, for each $t \in [0, \frac{1}{2}[$,

- $\widetilde{\alpha}_1(t) = (1-2t)\alpha_1$ and $\widetilde{\beta}(t) = \beta + 2t\left(\frac{\pi}{4} - \beta\right)$;
- $\widetilde{\alpha}_2(t) = \alpha_2 + 2t(\frac{\pi}{2} - \alpha_2)$;
- $\widetilde{\alpha}_3(t) = \alpha_3 + 2t(\frac{\pi}{4} - \alpha_3)$ and $\widetilde{\alpha}_4(t) = \alpha_4 + 2t(\frac{3\pi}{4} - \alpha_4)$.

If $t \in]\frac{1}{2}, 1]$,

- $\star$ $\widetilde{\alpha}_6(t) = (2-2t)\alpha_6$ and $\widetilde{\alpha}_7(t) = \pi - \widetilde{\alpha}_6(t)$;
- $\star$ $\widetilde{\alpha}_2(t) = \alpha_2 - \alpha_6 + 2t\alpha_6$ and $\widetilde{\alpha}_{10}(t) = \pi - \widetilde{\alpha}_2(t)$;
- $\star$ $\widetilde{\alpha}_j(t) \equiv \frac{\pi}{2},\ j = 1,3,4,5,8,9,11,12.$

We will show that ϕ is continuous at $t = 0$.

Now, if $t \in]0, \frac{1}{2}[$:

$$\begin{aligned} c(\tau^{o_t}, \tau_0) &= \sum_{\substack{F \text{face of} \\ \tau_t \cup \tau_0}} \lambda(F)\, Area(F) \\ &\leq K_1 \times \left| \left(\frac{\pi}{2} + 2\widetilde{\beta}(0) - \pi \right) - \left(\frac{\pi}{2} + 2\widetilde{\beta}(t) - \pi \right) \right| \\ &+ K_2 \times |(\widetilde{\alpha}_1(0) + \widetilde{\alpha}_3(0) + \widetilde{\alpha}_4(0) - \pi) - (\widetilde{\alpha}_1(t) + \widetilde{\alpha}_3(t) + \widetilde{\alpha}_4(t) - \pi)| + \\ &K_3 \times |(3\widetilde{\alpha}_2(0) - \pi) - (3\widetilde{\alpha}_2(t) - \pi)|\,, \end{aligned}$$

where $K_1 + K_2 + K_3$ is the total number of errant faces (next figure helps us to define the errant faces).

As $t \to 0^+$, then $c(\tau^{o_t}, \tau_0) \to 0$.

Still for $t \in]0, \frac{1}{2}[$:

$$\begin{aligned} c(\tau^{o_t}, \tau_{\frac{1}{2}}) &= \sum_{\substack{F \text{face of} \\ \tau_t \cup \tau_{\frac{1}{2}}}} \lambda(F)\, Area(F) \\ &< 56 \times \left(\frac{\pi}{2} + \widetilde{\beta}_1(t) + \widetilde{\beta}_2(t) - \pi \right) \\ &= 56 \times \left(-\frac{\pi}{2} + (1-2t)\beta_1 + \beta_2 + 2t\left(\frac{\pi}{2} - \beta_2 \right) \right). \end{aligned}$$

If $t \to \frac{1}{2}^-$, then $c(\tau^{o_t}, \tau_{\frac{1}{2}}) \to 0$.

The proof of the continuity at $t = \frac{1}{2}^+$ follows the same reasoning as in 1.

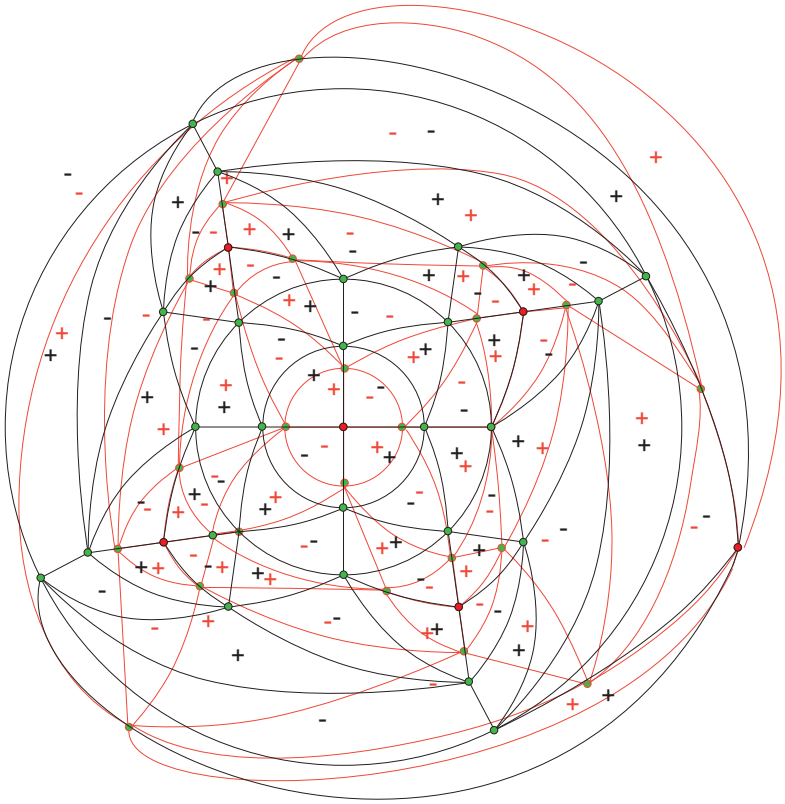

Figure 2.27: Errant faces of $\tau_0 \cup \tau_t$.

3. The f-tiling $(\mathcal{B}_1)^o$ is deformable into τ^+_{stand}. It is composed by vertices of valency four surrounded by angles γ and vertices of valency six, whose sums of alternate angles are of the form $\alpha+2\beta = \pi$, with $\alpha \approx 70,529°$ and $\beta \approx 54,735°$. In this case, in the process of deformation, areas of the triangles of angles $(\widetilde{\beta}(t), \widetilde{\beta}(t), \widetilde{\gamma}(t))_{t\in[0,\frac{1}{2}]}$ converge to zero as $t \to \frac{1}{2}^-$ and the areas of triangles $(\widetilde{\alpha}(t), \widetilde{\alpha}(t), \widetilde{\alpha}(t))$ converge to $\frac{\pi}{2}$, as $t \to \frac{1}{2}^-$, see Figure 2.28.

   So, for each $t \in [0, \frac{1}{2}]$,

   - $\star$ $\widetilde{\beta}_1(t) = (1-2t)\beta_1$;
   - $\star$ $\widetilde{\beta}_2(t) = \beta_2 + 2t(\frac{\pi}{2} - \beta_2)$;
   - $\star$ $\widetilde{\alpha}(t) = \alpha + 2t(\frac{\pi}{2} - \alpha)$.

   For $t \in]\frac{1}{2}, 1]$,

   - $\star$ $\widetilde{\gamma}_i(t) = (2-2t)\gamma_i,\ i = 1, 2$;

⋆ $\widetilde{\gamma}_3(t) = \pi - \widetilde{\gamma}_1(t)$ and $\widetilde{\gamma}_4(t) = \pi - \widetilde{\gamma}_2(t)$;

⋆ $\widetilde{\gamma}_j(t) \equiv \frac{\pi}{2},\ i = 5, 6, 7, 8.$

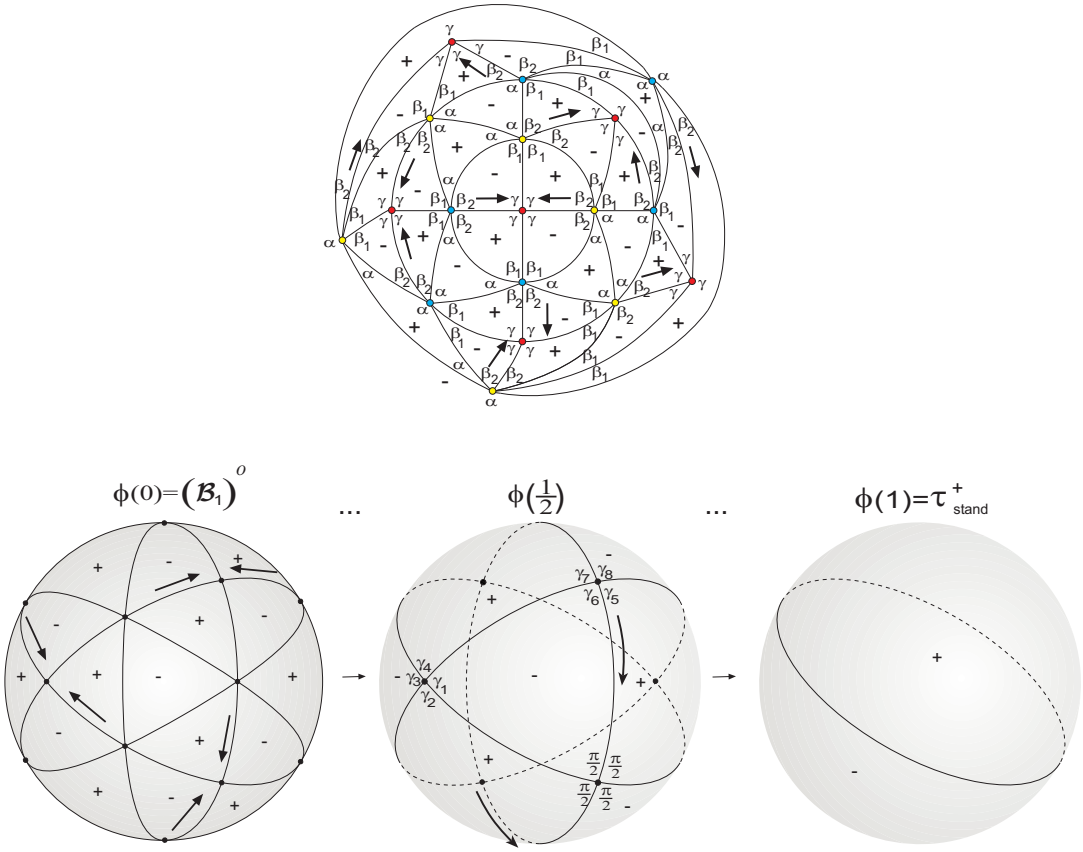

Figure 2.28: Deformation of $(\mathcal{B}_1)^o$.

Let us show that the map $\phi : [0, 1] \to \mathscr{T}^{\mathcal{O}}(S^2)$ defined by $\phi(t) = \tau_t$ is continuous at $t = 0$.

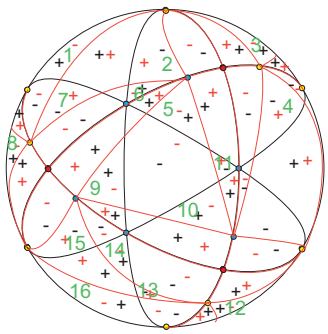

Figure 2.29: Errant faces of $\tau_0 \cup \tau_t$

Consider $t \in]0, \frac{1}{2}[$. Then,

$$\begin{aligned} c(\tau^{o_t}, \tau_0) &= \sum_{\substack{F \text{face of} \\ \tau_t \cup \tau_0}} \lambda(F)\, Area(F) \\ &\leq K_1 \left|(3\widetilde{\alpha}(0) - \pi) - (3\widetilde{\alpha}(t) - \pi)\right| \\ &+ K_2 \left|\left(\frac{\pi}{2} + \widetilde{\beta}_1(0) + \widetilde{\beta}_2(0) - \pi\right) - \left(\frac{\pi}{2} + \widetilde{\beta}_1(t) + \widetilde{\beta}_2(t) - \pi\right)\right| \\ &= K_1 \left|(3\alpha - \pi) - \left[3\left(\alpha + 2t\left(\frac{\pi}{2} - \alpha\right)\right] - \pi\right)\right| \\ &+ K_2 \left|\left(-\frac{\pi}{2} + \beta_1 + \beta_2\right) - \left(-\frac{\pi}{2} + (1-2t)\beta_1 + \beta_2 + 2t\left(\frac{\pi}{2} - \beta_2\right)\right)\right|, \end{aligned}$$

where $K_1 + K_2 = 32$, the total number of errant faces, see Figure 2.29.

When, $t \to 0^+$, we conclude that $c(\tau^{o_t}, \tau_0) \to 0$.

For $t \in]0, \frac{1}{2}[$:

$$\begin{aligned} c(\tau^{o_t}, \tau_{\frac{1}{2}}) &= \sum_{\substack{F \text{face of} \\ \tau_t \cup \tau_{\frac{1}{2}}}} \lambda(F)\, Area(F) \\ &= 24 \times \left(\frac{\pi}{2} + \widetilde{\beta}_1(t) + \widetilde{\beta}_2(t) - \pi\right) \\ &= 24 \times \left(-\frac{\pi}{2} + (1-2t)\beta_1 + \beta_2 + 2t\left(\frac{\pi}{2} - \beta_2\right)\right). \end{aligned}$$

If $t \to \frac{1}{2}^-$, we conclude that $c(\tau^{o_t}, \tau_{\frac{1}{2}}) \to 0$.

The continuity of ϕ at $t = \frac{1}{2}^+$ and $t = 1$ was already proved in 1.

Therefore, ϕ is continuous in $[0, 1]$ and so ϕ is a deformation of $(\mathcal{B}_1)^o$ into τ^+_{stand}.

4. With respect to the f-tiling $(\mathcal{B}_2)^o$, Figure 2.30 illustrates the process of deformation into τ^+_{stand}, where $\phi : [0, 1] \to \mathscr{T}^{\mathcal{O}}(S^2)$ is the map $\phi(t) = \tau_t$. As in $\mathcal{B}_1$, this f-tiling is composed by vertices of valency four surrounded by angles γ and vertices of valency six, whose sums of alternate angles are of the form $\alpha + 2\beta = \pi$, with $\alpha \approx 70,529^\circ$ and $\beta \approx 54,735^\circ$.

   If $t \in [0, \frac{1}{2}]$:

   $\star$ $\widetilde{\beta}_i(t) = (1-2t)\beta_i,\ i = 1, 3;$

- $\widetilde{\alpha}_1(t) = \alpha_1 + 2t\beta_1 + 2t\beta_3$;
- $\widetilde{\alpha}_k(t) = (1-2t)\alpha_k,\ k = 2, 3$;
- $\widetilde{\beta}_k(t) = \beta_k + t\alpha_2,\ k = 2, 5$ and $\widetilde{\beta}_k(t) = \beta_k + t\alpha_3,\ k = 4, 6$.

For $t \in]\frac{1}{2}, 1]$:

- $\widetilde{\gamma}_6(t) = (2-2t)\gamma_6$ and $\widetilde{\gamma}_7(t) = \pi - \widetilde{\gamma}_7(t)$;
- $\widetilde{\gamma}_2(t) = \gamma_2 - \gamma_6 + 2t\gamma_6$ and $\widetilde{\gamma}_{10}(t) = \pi - \widetilde{\gamma}_2(t)$;
- $\widetilde{\gamma}_k(t) \equiv \frac{\pi}{2},\ k = 1, 3, 4, 5, 8, 9, 11, 12$.

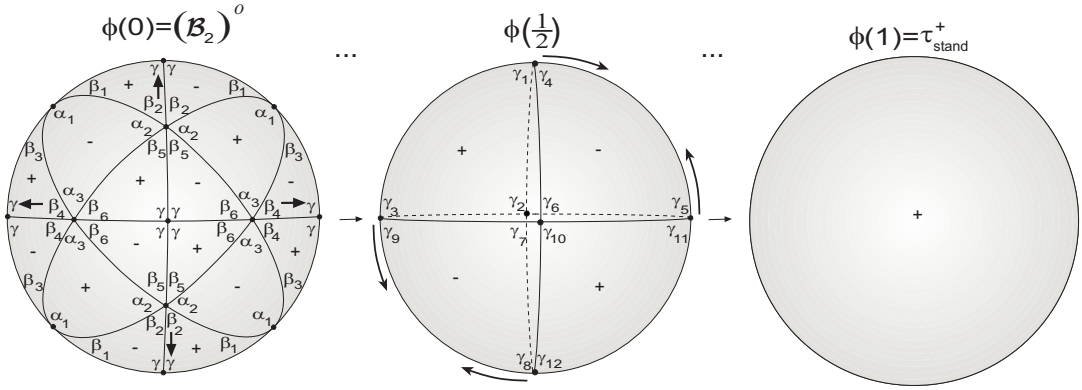

Figure 2.30: Deformation of $(\mathcal{B}_2)^o$.

Let us show that the deformable map $\phi : [0, 1] \to \mathscr{T}^{\mathcal{O}}(S^2)$ is continuous. Next figure gives an idea of the errant faces in the first stage of the deformation.

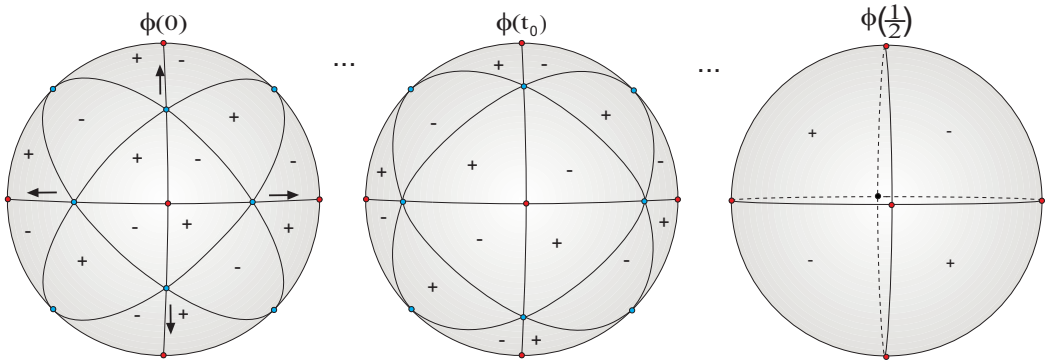

Figure 2.31: First stage of the deformation of $(\mathcal{B}_2)^o$.

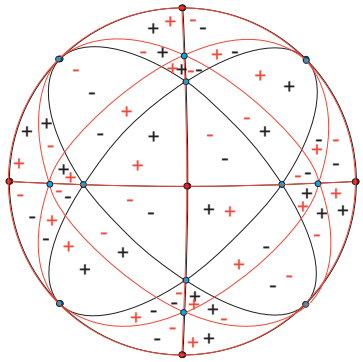

Figure 2.32: Errant faces of $\tau_0 \cup \tau_t$.

For $t \in]0, \frac{1}{2}[$ then,

$$\begin{aligned} c(\tau^{o_t}, \tau_0) &= \sum_{\substack{F \text{face of} \\ \tau_t \cup \tau_0}} \lambda(F)\, Area(F) \\ &\leq 16 \times \left| \left(\frac{\pi}{2} + \widetilde{\beta}_1(0) + \widetilde{\beta}_2(0) - \pi \right) - \left(\frac{\pi}{2} + \widetilde{\beta}_1(t) + \widetilde{\beta}_2(t) - \pi \right) \right| \\ &+ 8 \times \left| \left(\frac{\pi}{2} + \widetilde{\beta}_5(t) + \widetilde{\beta}_6(t) - \pi \right) - \left(\frac{\pi}{2} + \widetilde{\beta}_5(0) + \widetilde{\beta}_6(0) - \pi \right) \right|. \end{aligned}$$

When, $t \to 0^+$, we conclude that $c(\tau^{o_t}, \tau_0) \to 0$.

If $t \in]0, \frac{1}{2}[$, then

$$\begin{aligned} c(\tau^{o_t}, \tau_{\frac{1}{2}}) &= \sum_{\substack{F \text{face of} \\ \tau_t \cup \tau_{\frac{1}{2}}}} \lambda(F)\, Area(F) \\ &= 8 \times (\widetilde{\alpha}_1(t) + \widetilde{\alpha}_2(t) + \widetilde{\alpha}_3(t) - \pi) \\ &= 8 \times (\alpha_1 + 2t\beta_1 + 2t\beta_3 + (1-2t)\alpha_2 + (1-2t)\alpha_3 - \pi)\,. \end{aligned}$$

When, $t \to \frac{1}{2}^-$, then $c(\tau^{o_t}, \tau_{\frac{1}{2}}) \to 0$.

The continuity of ϕ at $t = 1$ and $t = \frac{1}{2}^+$ was already seen in the first f-tiling. Hence, ϕ is continuous in $[0, 1]$ concluding that $(\mathcal{B}_2)^o$ is deformable into τ^+_{stand}.

Chapter 3

Dihedral f-Tilings of the 2-Sphere by Equilateral and Scalene Triangles

Here, we classify the class of dihedral f-tilings of the sphere S^2, whose prototiles are an equilateral spherical triangle and a scalene spherical triangle.

From now on, T_1 denotes an equilateral spherical triangle of angle α and side a and T_2 a scalene spherical triangle of angles δ, γ, β, with the order relation $\delta < \gamma < \beta$ and with sides b (opposite to β), c (opposite to γ) and d (opposite to δ).

We begin by pointing out, that any element of $\Omega(T_1, T_2)$ has at least two cells congruent, respectively, to T_1 and T_2, such that they are in adjacent positions in one and only one of the situations illustrated in Figure 3.1.

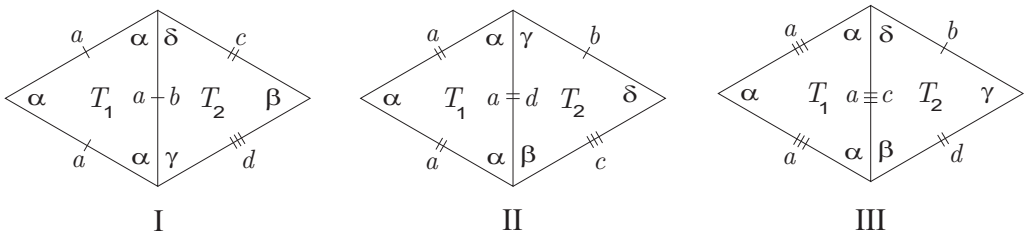

Figure 3.1: Distinct cases of adjacency.

As before and, to facilitate the construction of the dihedral f-tilings, we find useful

to start considering one of its *representations*, beginning with a vertex common to an equilateral triangle and a scalene triangle in adjacent positions. In the diagrams that follows, it is convenient to label the tiles according to the following procedures:

(i) The tiles by which we begin the local configuration of a tiling $\tau \in \Omega(T_1, T_2)$ are labeled, respectively by 1 and 2;

(ii) For $j \geq 2$, the presence of a tile j as shown, can be deduced from the configuration of tiles $(1, 2, \ldots, j-1)$ and from the hypothesis that the configuration is part of a complete local configuration of a f-tiling (except in the cases indicated).

3.1 Triangular Dihedral f-Tilings with Adjacency of Type I

All results in this section were published in a technical report in [6].

Let T_1 and T_2 be tiles with adjacency of type I. The type I edge-adjacency condition can be analytically described by the equation:

$$\frac{\cos\alpha\,(1+\cos\alpha)}{\sin^2\alpha} = \frac{\cos\beta + \cos\delta\cos\gamma}{\sin\delta\sin\gamma}. \tag{3.1}$$

Starting a local configuration of such tiling $\tau \in \Omega(T_1, T_2)$, we are led to the one illustrated in Figure 3.2, where $\theta_1 \in \{\beta, \gamma\}$.

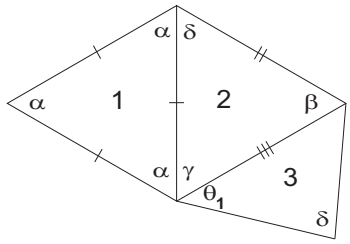

Figure 3.2: Local configuration.

The cases $\theta_1 = \beta$ and $\theta_1 = \gamma$ will be studied separately.

Let us begin by assuming that $\theta_1 = \beta$. Accordingly, $\alpha + \beta \leq \pi$.

Proposition 3.1 *If T_1 and T_2 are tiles with adjacency of type I and $\alpha + \beta \leq \pi$, then $\Omega(T_1, T_2) = \varnothing$.*

Proof. Suppose that $\alpha + \beta = \pi$. The configuration of τ illustrated in Figure 3.2 expands to the following one (Figure 3.3):

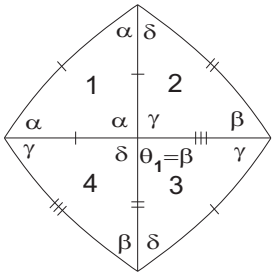

Figure 3.3: Local configuration.

Since $\alpha + \beta = \gamma + \delta = \pi$ and $\beta > \gamma$, then $\alpha < \delta$. Therefore, $\alpha < \delta < \frac{\pi}{2} < \gamma < \beta$ and so $\cos\alpha, \cos\delta > 0$ while $\cos\beta, \cos\gamma < 0$, contradicting the adjacency condition (3.1).

If $\alpha + \beta < \pi$, the edge compatibility around a vertex surrounded by a sequence of angles of type $(\star, \star, ..., \alpha, \gamma, \beta, \star, ...)$ implies that all the angles, in this sequence, different from α and β must have amplitude δ. Consequently, $\alpha + \beta + k\delta = \pi$, for some integer $k \geq 1$.

The configuration shown in Figure 3.2 can be expanded to the one illustrated in Figure 3.4.

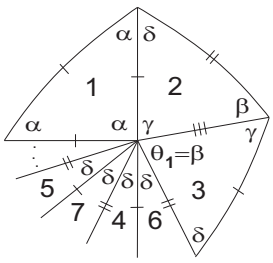

Figure 3.4: Local configuration.

In this situation, we end up with the equation $\alpha + \beta + k\delta = \pi = \gamma + (k+1)\delta$, from which we derive the condition $\alpha + \beta = \gamma + \delta$. Consequently, $\frac{\pi}{3} < \alpha < \delta < \gamma < \beta$, contradicting $\alpha + \beta + k\delta = \pi$, for some integer $k \geq 1$. □

Let us assume now that $\theta_1 = \gamma$, see Figure 3.2.

Proposition 3.2 *If T_1 and T_2 are tiles with adjacency of type I and $\alpha + \gamma \leq \pi$, then $\Omega(T_1, T_2) \neq \varnothing$ if and only if $\beta = \frac{\pi}{2}$ and $\alpha+\gamma+\delta = \pi$ ending up with two non isomorphic dihedral f-tilings denoted by $\mathcal{C}_1^\delta$ and $\mathcal{C}_2^\delta$. 3D representations of representative elements of each family are given in Figures 3.15 and 3.16.*

Proof.

A) If $\alpha + \gamma = \pi$, the configuration in Figure 3.2 extends to the one illustrated in Figure 3.5-I.

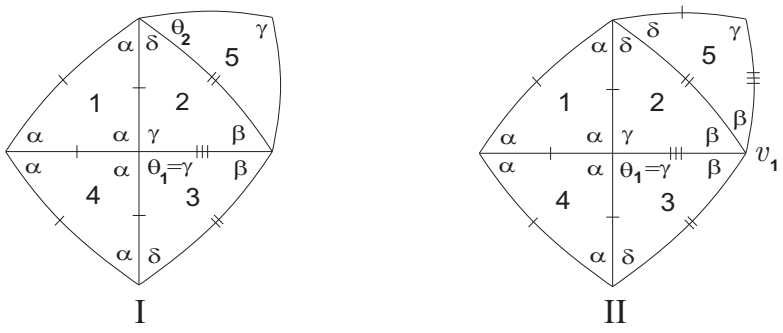

Figure 3.5: Local configurations.

A decision about the angle $\theta_2 \in \{\delta, \beta\}$ must be taken. Taking into account that $\pi = \alpha + \gamma < \alpha + \beta$, then $\theta_2 = \delta$ (Figure 3.5-II).

One of the sums of alternate angles, at vertex v_1 obeys to the condition $2\beta \leq \pi$. Then, $\delta < \gamma < \beta \leq \frac{\pi}{2}$ and consequently $\alpha > \frac{\pi}{2}$, contradicting the adjacency condition (3.1).

B) Consider now that $\alpha + \gamma < \pi$. The angle θ_3 belongs to the set $\{\delta, \beta\}$, see Figure 3.6.

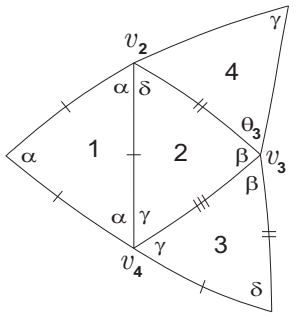

Figure 3.6: Local configuration.

1. Suppose firstly, that $\theta_3 = \delta$.

The sum of alternate angles at vertex v_2 containing α and β satisfies $\alpha + \beta < \pi$ (otherwise it would become $\alpha + \beta = \pi = \delta + \gamma$ implying $\alpha < \delta < \frac{\pi}{2} < \gamma < \beta$ and not satisfying the adjacency condition (3.1)). As $\alpha + \beta < \pi$ and taking into account that $\alpha, \beta > \dfrac{\pi}{3}$ and $\alpha + \beta + \gamma > \pi$, then $\alpha + \beta + k\delta = \pi$, for some $k \geq 1$ (vertex v_2). Now, the sum of alternate angles containing β and δ at vertex v_3 satisfies $\beta + \delta < \pi$. Summarizing, since $\beta + \gamma + \delta > \pi$ and $\alpha + \beta + k\delta = \pi,\ k \geq 1$, then $\delta < \frac{\pi}{3} < \alpha < \gamma < \beta$.

Consequently, the sum of alternate angles, at vertex v_4, containing α and γ must be of the form $\alpha + \gamma + t\delta = \pi$, for some $t > k \geq 1$. The configuration extends to the one in Figure 3.7-I.

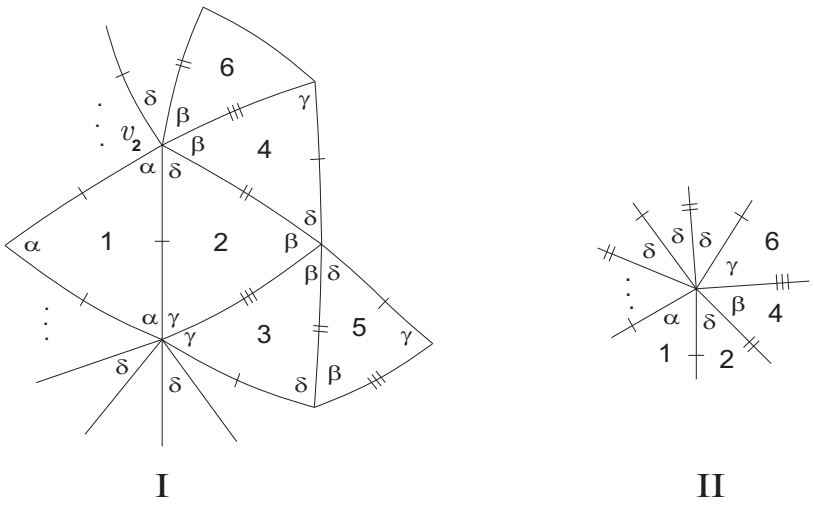

Figure 3.7: Local configuration and angles arrangement around vertex v_2.

Observe that in tile numbered 6, if the angle β was γ, vertex v_2 would be surrounded

by the sequence of angles illustrated in Figure 3.7-II. Both sums of alternate angles would satisfy $\alpha+\beta+k\delta = \pi = \delta+\gamma+k\delta$. Therefore, $\alpha+\beta = \delta+\gamma$, which is impossible since $\delta < \alpha < \gamma < \beta$.

We may add some new cells to the configuration in Figure 3.7-I getting the one illustrated in Figure 3.8, with $\theta_4 \in \{\beta, \gamma\}$.

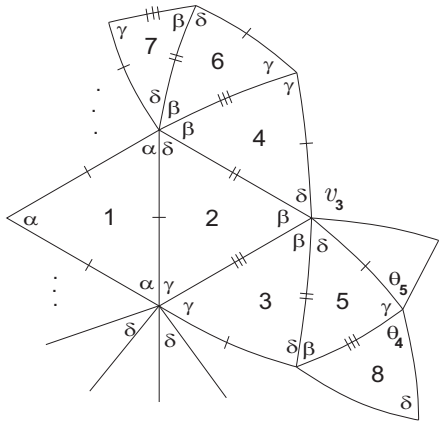

Figure 3.8: Local configuration.

1.1. If $\theta_4 = \beta$, then $\theta_5 = \gamma$. Note that $\theta_5 = \alpha$ leads to the cyclic sequence $(\alpha, \gamma, \beta, ...)$, which is a contradiction (case already studied in the previous proposition). Thus, both sums of the alternate angles at vertex v_3 are of the form $\beta + r\delta = \pi$, for some $r \geq 1$. Consequently, at vertex v_5 (Figure 3.9), we have $\beta + \gamma = \pi = 2\gamma$ getting again a contradiction, since $\gamma < \beta$.

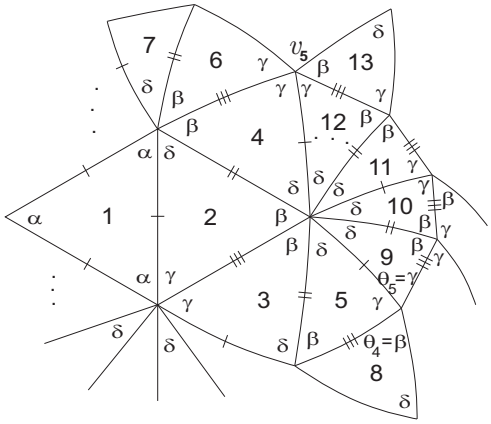

Figure 3.9: Local configuration.

1.2 If $\theta_4 = \gamma$, the configuration in Figure 3.8 gives rise to the one in Figure 3.10-I.

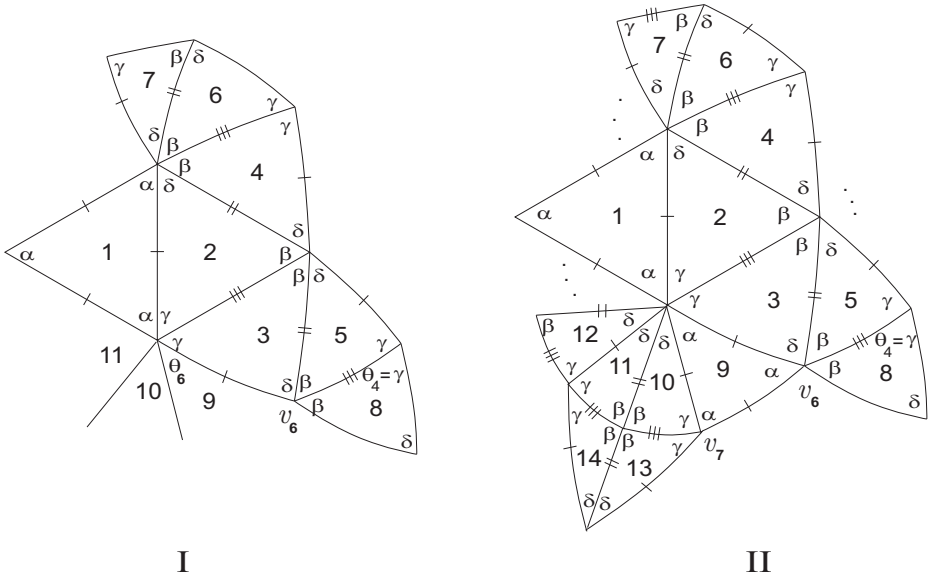

Figure 3.10: Local configurations.

Now, θ_6 is different from δ, otherwise, at vertex v_6 we get the sequence $(\gamma, \delta, \beta, \beta)$ and the sums of the alternate angles would be $\beta + \gamma = \pi = \beta + \delta$, reaching to a contradiction. Due to the compatibility of sides in tiles 10 and 11, θ_6 must be different from γ. Therefore, $\theta_6 = \alpha$ and extending the previous configuration, we conclude that $\beta = \frac{\pi}{2}$ (see Figure 3.10-II).

Consequently, $\gamma + \delta > \frac{\pi}{2}$ and $\gamma < \frac{\pi}{2}$. Accordingly,

$$\delta < \frac{\pi}{3} < \alpha < \gamma < \frac{\pi}{2} = \beta$$

and all the sums of alternate angles containing two angles γ are of the form $2\gamma + \delta = \pi$. Taking into account that, $\beta = \frac{\pi}{2}, 2\gamma + \delta = \pi, \alpha + \gamma + t\delta = \pi$ and $\alpha + \beta + k\delta = \pi$, one has $\alpha + k\delta = \frac{\pi}{2}$ and $(1 - 2t - 2k)\delta = 0$, contradicting the assumption $t > k \geq 1$.

2. Suppose now that $\theta_3 = \beta$ (see Figure 3.6). Then, $\beta = \frac{\pi}{2}$ and $\alpha < \frac{\pi}{2}$ (otherwise the adjacency condition (3.1) is violated, since $\delta < \gamma < \frac{\pi}{2}$). Also $\delta < \alpha$, otherwise $\delta > \frac{\pi}{3}$ and $\alpha + \delta + \rho > \pi$, for any $\rho \in \{\alpha, \delta, \gamma, \beta\}$.

Looking at vertex v_4 in Figure 3.6, the sum of alternate angles containing α and γ satisfies either $\alpha + \gamma + \alpha = \pi$ or $\alpha + \gamma + \gamma = \pi$ or $\alpha + \gamma + t\delta = \pi$, for some $t \geq 1$ (see Figure 3.11).

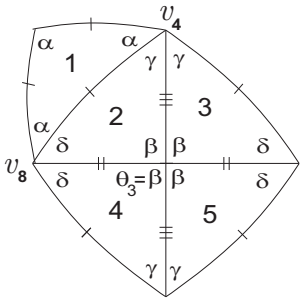

Figure 3.11: Local configuration.

2.1 If $\alpha + \gamma + \alpha = \pi$, then

$$\frac{\pi}{6} < \delta < \gamma < \frac{\pi}{3} < \alpha < \frac{\pi}{2} = \beta.$$

At vertex v_8, in Figure 3.11, the sum of alternate angles containing α and δ must be either of the form

$$2\alpha + \delta = \pi \quad \text{or} \quad \alpha + \delta + \gamma = \pi \quad \text{or} \quad \alpha + 2\delta + \gamma = \pi \quad \text{or} \quad \alpha + 3\delta = \pi.$$

Clearly, the first two cases are impossible. Therefore, $\alpha + 2\delta + \gamma = \pi$ or $\alpha + 3\delta = \pi$. As $\delta + \gamma > \frac{\pi}{2}$ and $\alpha > \gamma$, then $\alpha + 2\delta + \gamma > \pi$ and so $\alpha + 3\delta = \pi$, that is $\delta < \frac{2\pi}{9}$. The sequence of angles around vertex v_8 (of valency eight) is of the form $(\alpha, \alpha, \delta, ..., \delta)$ or $(\alpha, \delta, \delta, \alpha, \delta, ...)$.

Either way, in the expanded configuration, taking into account the edge compatibility, we get a vertex partially surrounded by four consecutive angles γ, as illustrated in Figure 3.12.

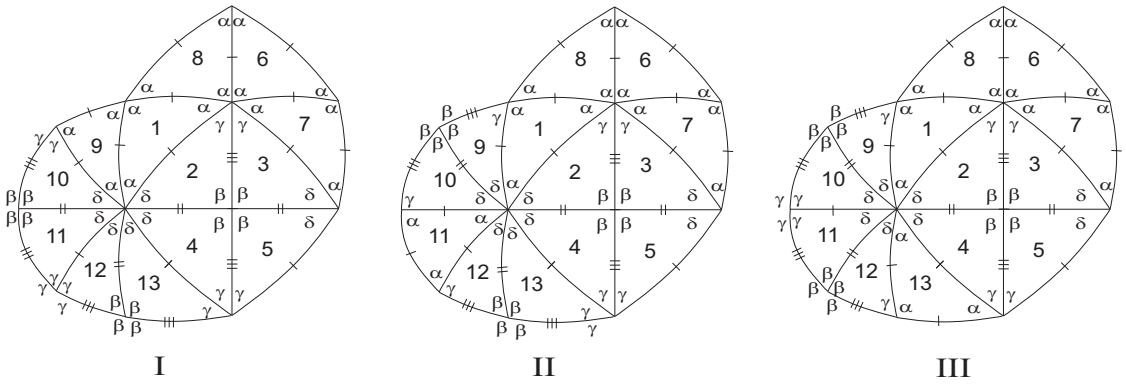

Figure 3.12: Local configurations.

As, $\gamma + \delta > \frac{\pi}{2}$ and $\delta < \gamma < \alpha$ then,

$$2\gamma + \delta < 2\gamma + \gamma < \pi, \qquad 2\gamma + 2\gamma > 2\gamma + 2\delta > \pi,$$
$$2\gamma + \alpha < \gamma + 2\alpha = \pi \text{ and } 3\gamma + \alpha > 3\gamma + \gamma > \pi.$$

Consequently, it is impossible to continue extending the configuration.

2.2 If $\alpha + 2\gamma = \pi$, the order relation between the angles is exactly the same,

$$\frac{\pi}{6} < \delta < \gamma < \frac{\pi}{3} < \alpha.$$

The sum of alternate angles at vertex v_8 containing α and δ must be either

$$\alpha + \delta + \gamma = \pi \text{ or } \alpha + 2\delta + \gamma = \pi \text{ or } \alpha + 3\delta = \pi \text{ or } 2\alpha + \delta = \pi.$$

The first case is incompatible with the assumption $\alpha + 2\gamma = \pi$.
As $\gamma + \delta > \frac{\pi}{2}$ and $\alpha > \gamma$, then $\alpha + 2\delta + \gamma > \pi$ and the second case must be eliminated. The third case should be discarded, using a similar reasoning to the one made in 2.1, under the same assumption.
Suppose now, that $2\alpha + \delta = \pi$. By the adjacency condition (3.1), we get $\gamma \approx 56.489°$, $\alpha \approx 67.022°$ and $\delta \approx 45.956°$.

Starting from configuration in Figure 3.11 we are led, according to the edge position of tile 6, to one of the configurations shown in Figure 3.13.

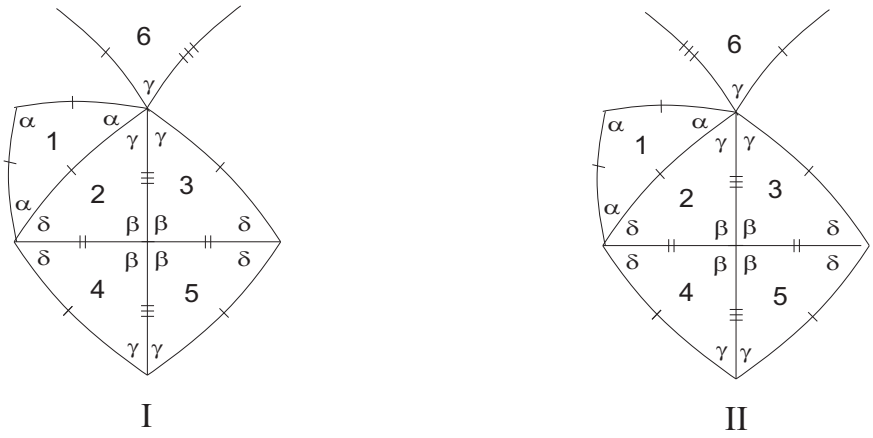

Figure 3.13: Local configurations.

Taking as starting point the configuration I in Figure 3.13, we get the one in Figure 3.14-I, which is impossible to be extended, since both sums of alternate angles at vertex v_9 do not satisfy the angle folding relation (δ is not a submultiple of π and there are no other way to combine δ with any of the other angles).

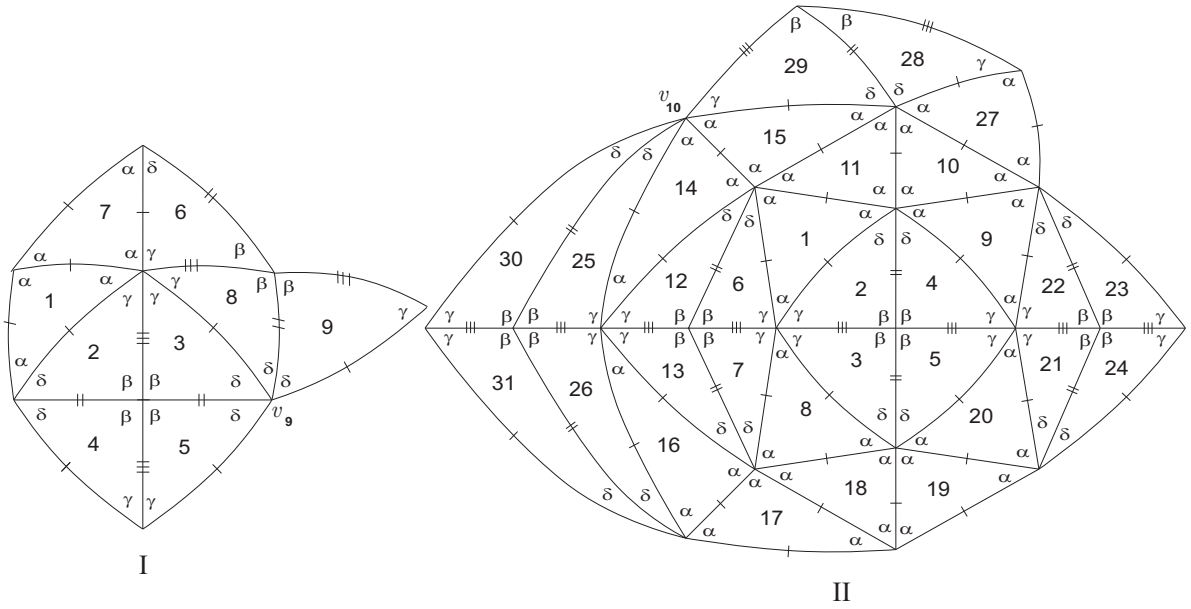

Figure 3.14: Local configurations.

The other possible position for tile 6 gives rise to configuration II. However, the sum of alternate angles containing α, γ and δ, at vertex v_{10}, does not satisfy the angle folding relation, preventing us to continue the expansion of the configuration.

2.3 Assume now that $\alpha + \gamma + t\delta = \pi,\ t \geq 1$. The discussion of the case $t > 2$ follows a similar reasoning to the one done for $t = 2$ and so we will focus our attention in the cases $t = 1$ and $t = 2$.

2.3.1 If $t = 1$, the configuration illustrated in Figure 3.15, having as a starting point the one given in Figure 3.11, corresponds to a particular choice of the position of tiles 6, 11 and 17. It gives rise to a tiling $\tau \in \Omega(T_1, T_2)$ composed by 24 scalene triangles and 8 equilateral triangles and will be denoted by $\mathcal{C}_1^{\delta}$.

The other possible arrangement for the length sides of tile 17 leads us to a complete f-tiling $\tau \in \Omega(T_1, T_2)$. This f-tiling is composed by 24 scalene triangles and 8 equilateral triangles and is denoted by $\mathcal{C}_2^{\delta}$, Figure 3.16.

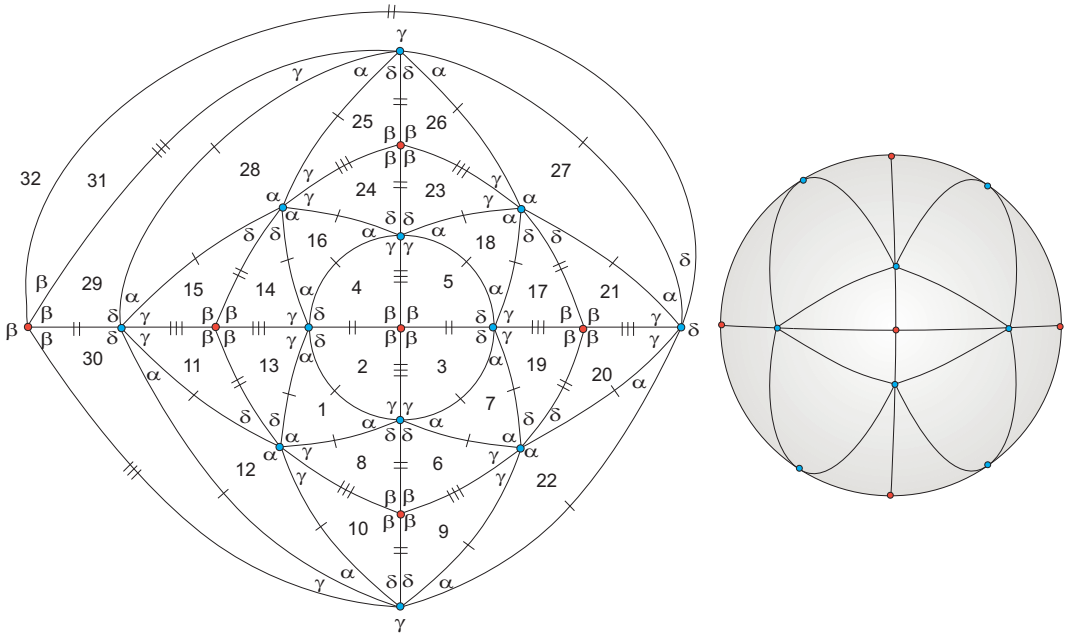

Figure 3.15: 2D and 3D representation of $\mathcal{C}_1^\delta$.

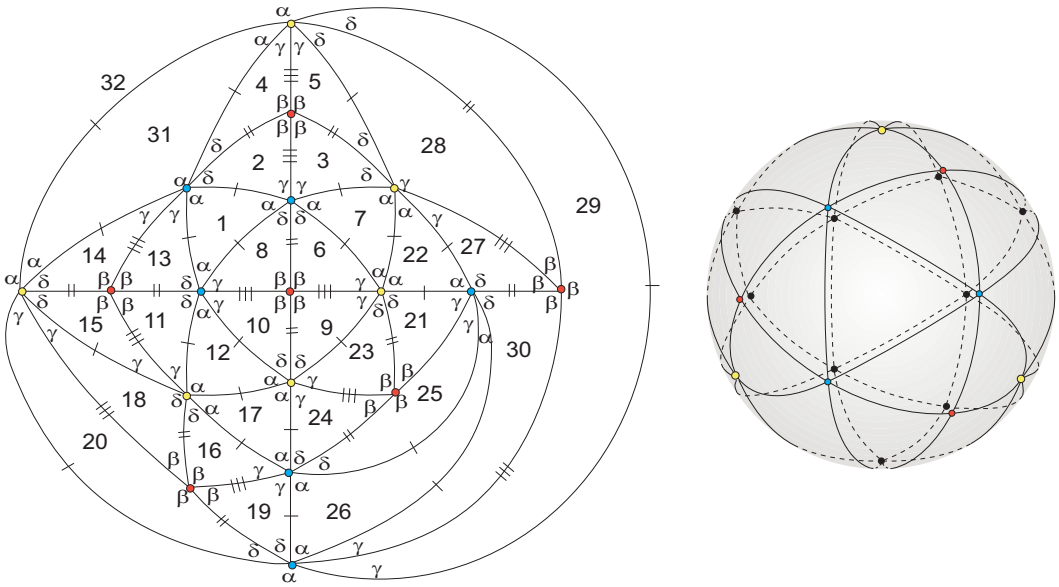

Figure 3.16: 2D and 3D representation of $\mathcal{C}_2^\delta$.

Note that, eliminating some edges in these two f-tilings, we get a monohedral f-tiling, where the prototile is an equilateral triangle.

The other position of tile 11 leads to the configuration shown in Figure 3.17-I.

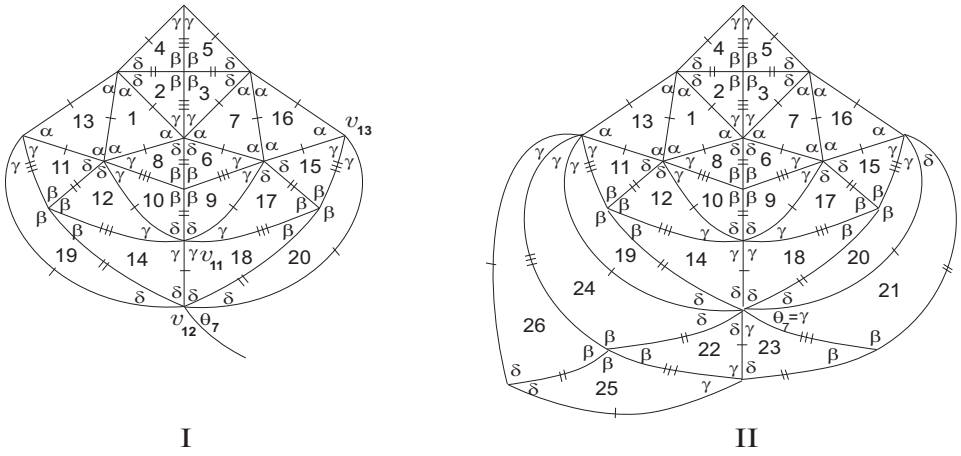

Figure 3.17: Local configurations.

Looking at vertex v_{11}, we conclude that $\gamma + \delta + \gamma = \pi$ (as $2\gamma + \delta + \rho > \pi$, for any $\rho \in \{\alpha, \gamma, \delta, \beta\}$) and so $\alpha = \gamma$. At vertex v_{12}, the angle $\theta_7 \in \{\delta, \gamma, \alpha\}$.

2.3.1.1 If $\theta_7 = \delta$, then at vertex v_{13}, we reach to the condition $2\gamma + \alpha \leq \pi$, which is a contradiction.

2.3.1.2 If $\theta_7 = \gamma$, v_{12} is a vertex of valency greater than six (otherwise $\alpha = \gamma = \delta$). Consequently, one of the sums of alternate angles is of the form $\gamma + q\delta = \pi,\ q \geq 3$. Since, $2\gamma + \delta = \pi$ and $\gamma + q\delta = \pi$, one has $\delta = \frac{\pi}{2q-1}\, \alpha = \gamma = \frac{(q-1)\pi}{2q-1}$. By the adjacency condition (2.1), we get

$$\frac{1 + \cos((q-1)\delta)}{\sin((q-1)\delta)} = \frac{\cos\delta}{\sin\delta},$$

that is, $\sin\delta = \sin((q-2)\delta)$. Therefore, $q = 3$ and as a result $\delta = \frac{\pi}{5},\ \alpha = \gamma = \frac{2\pi}{5}$.

Adding some new cells to the configuration in Figure 3.17-I, we are led to a contradiction, since the vertex surrounded by the sequence of angles $(\gamma, \gamma, \gamma, \gamma, \alpha)$ violates the angle folding relation, see Figure 3.17-II.

2.3.1.3 If $\theta_7 = \alpha$, since $\alpha = \gamma$, we get exactly the same absurd.

The other possibility for the length sides of tile 6 permits to extend a bit more the configuration in Figure 3.11 and a decision on $\theta_8 \in \{\delta, \alpha\}$ must be taken (see

Figure 3.18).

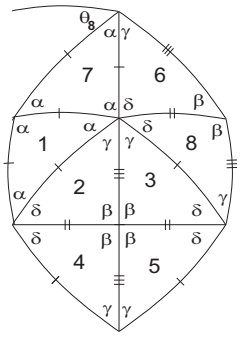

Figure 3.18: Local configuration.

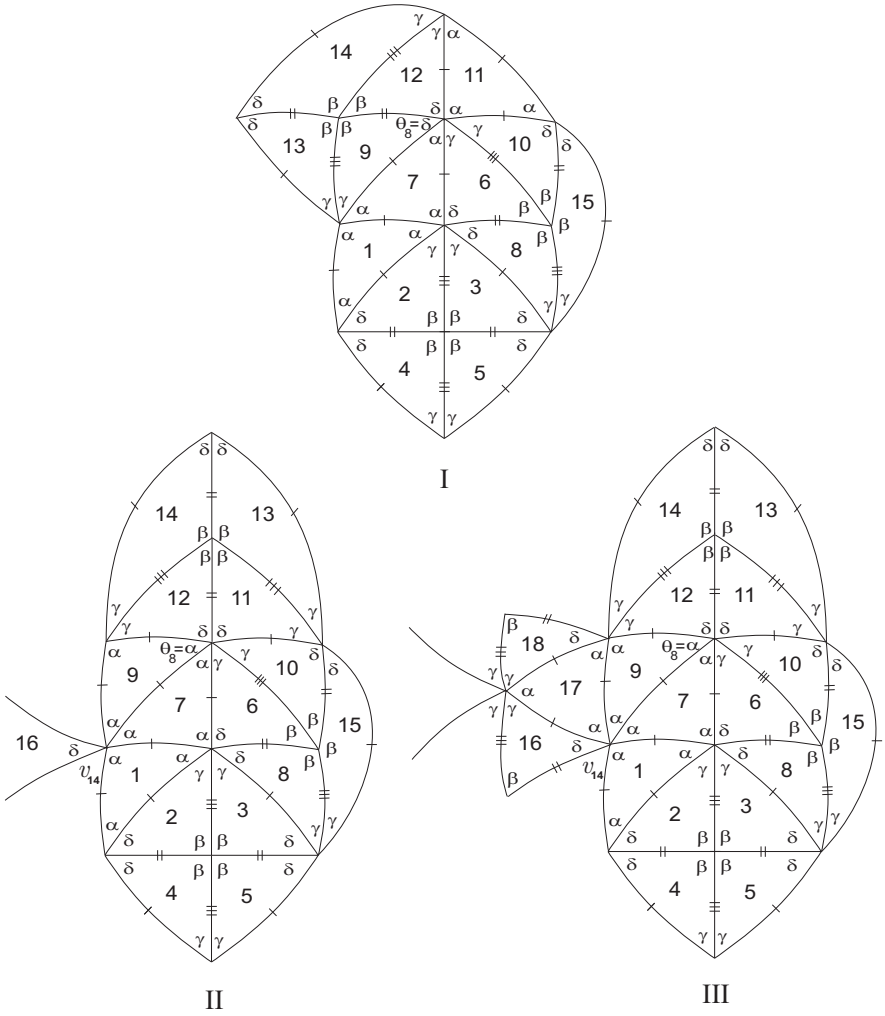

Figure 3.19: Local configurations.

If $\theta_8 = \delta$, the configuration is the one illustrated in Figure 3.19-I. This configuration

expands globally and we get the family of f-tilings $\mathcal{C}_2^{\delta}$ already described.

If $\theta_8 = \alpha$, we get the configuration II illustrated in Figure 3.19-II. Observe that tile 16 obliges that one of the sums of the alternate angles, at vertex v_{14}, is $2\alpha + \delta = \pi$. Adding some new cells to this configuration, we get a vertex partially surrounded by alternate angles $(\gamma, \gamma, \alpha, \gamma, \gamma)$, which is an impossibility (see Figure 3.19-III).

2.3.2 Suppose $t = 2$. Then, $\alpha + \gamma + 2\delta = \pi$ and taking into account that $\gamma + \delta > \frac{\pi}{2}$, one has $\gamma > \alpha$.

2.3.2.1 The configuration in Figure 3.20-I corresponds to a choice for the positions of tiles 6 and 19, with $\theta_9 \in \{\delta, \gamma, \alpha\}$.

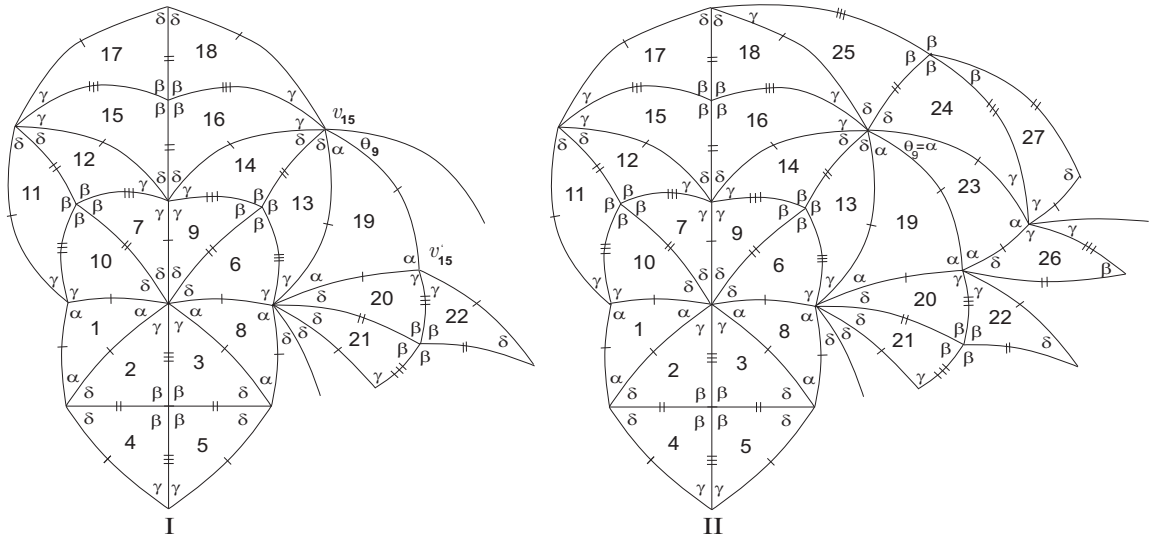

Figure 3.20: Local configurations.

If $\theta_9 = \delta$, then vertex v'_{15} is of valency six whose sums of alternate angles are of the form $2\gamma + \delta = \pi$ and $\alpha + \delta + \gamma = \pi$, contradicting our assumption.

If $\theta_9 = \gamma$, one of the sums of alternate angles, at vertex v_{15}, is $2\gamma + \delta + \mu = \pi$, for $\mu \in \{\alpha, \delta, \gamma, \beta\}$, which is an impossibility. Therefore, $\theta_9 = \alpha$. Adding some new cells to the configuration, we are led to the one in Figure 3.20-II containing a vertex surrounded by the sequence of angles $(\gamma, \gamma, \alpha, \gamma, \gamma, ...)$. Since $\gamma + \alpha + \gamma > \pi$, this configuration does not give rise to a complete f-tiling.

2.3.2.2 If tiles 19 and 21 are, respectively, a scalene triangle and an equilateral triangle, then tile 27 is an equilateral triangle. We are led to a vertex surrounded by the sequence

of angles $(\gamma, \gamma, \alpha, \gamma, \gamma, ...)$ which, as seen before, is a contradiction (see Figure 3.21).

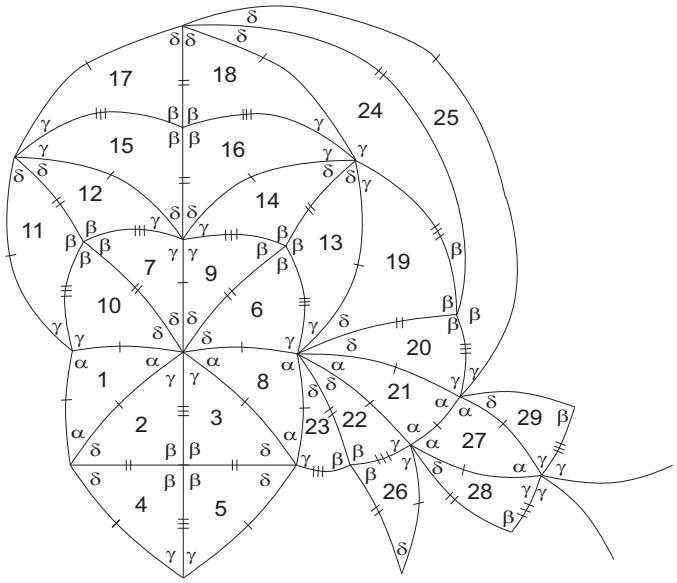

Figure 3.21: Local configuration.

2.3.2.3 If tile 21 is a scalene triangle, adding some tiles to the configuration, we end up to the one illustrated in Figure 3.22. Vertex v_{16} is surrounded, in circular order, by the sequence $(\gamma, \delta, \delta, \delta, \delta, \delta, \delta)$ but $\gamma + 3\delta = \pi$ or $\gamma + 4\delta = \pi$ implies, respectively, the impossibilities $\delta = \frac{\pi}{7}, \gamma = \frac{3\pi}{7}$ or $\alpha = \frac{2\pi}{7}$.

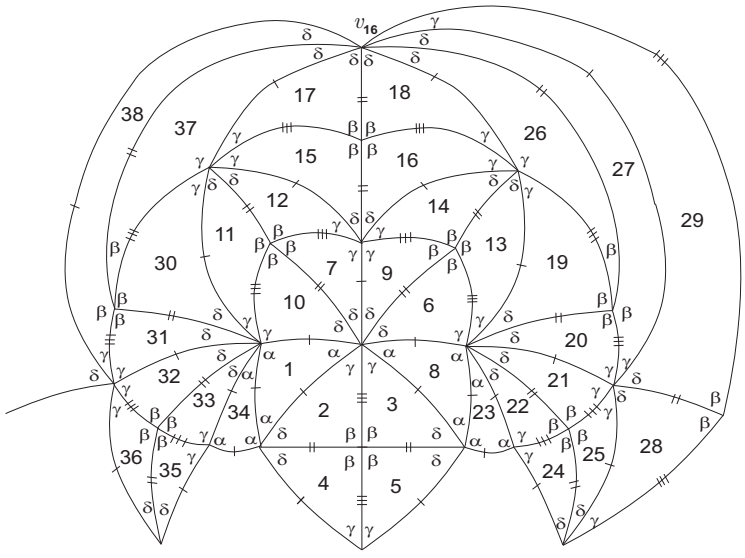

Figure 3.22: Local configuration.

2.3.2.4 Changing the order sides of tile 6 and assuming that tile 9 is a scalene triangle, we end up with the configuration in Figure 3.23, where $\theta_{10} \in \{\alpha, \gamma, \delta\}$.

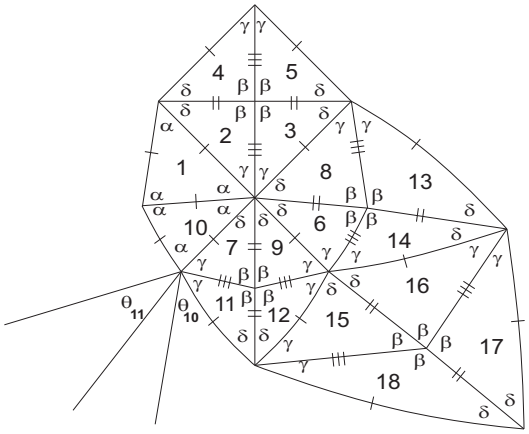

Figure 3.23: Local configuration.

If $\theta_{10} = \alpha$, we are led to a configuration with a vertex partially surrounded by alternate angles $\gamma, \delta, \delta, \delta$, which, as seen before, is an impossibility.

In case $\theta_{10} = \gamma$, then one of the sums of alternate angles at the same vertex does not satisfy $\alpha + \gamma + 2\delta = \pi$. Since $\theta_{10} = \delta$, then $\theta_{11} \in \{\alpha, \delta\}$.
Suppose $\theta_{11} = \alpha$. Therefore, extending the configuration, we end up in a similar impossibility to the one in 2.3.2.2. As, $\theta_{11} = \delta$, the configuration is now the one below (Figure 3.24).
At vertex v_{17}, the sum of the alternate angles containing γ, γ and α does not satisfy the angle folding relation, preventing us to expand the configuration.

2.3.2.5 Finally, if tile 9 is an equilateral triangle, in order to have, at vertices v_{18} and v_{19}, the assumption $\alpha + \gamma + 2\delta = \pi$, then $\theta_{12} = \alpha$ (see Figure 3.25).

Looking at the vertex partially surrounded by angles $(\gamma, \gamma, \alpha, \gamma, \gamma)$, we conclude that this configuration will not expand, since $2\gamma + \alpha > \pi$.

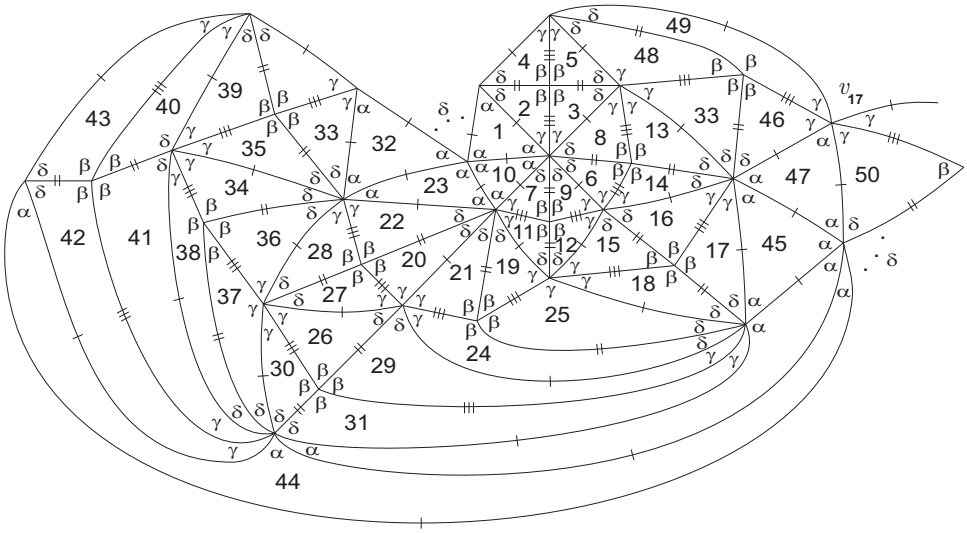

Figure 3.24: Local configuration.

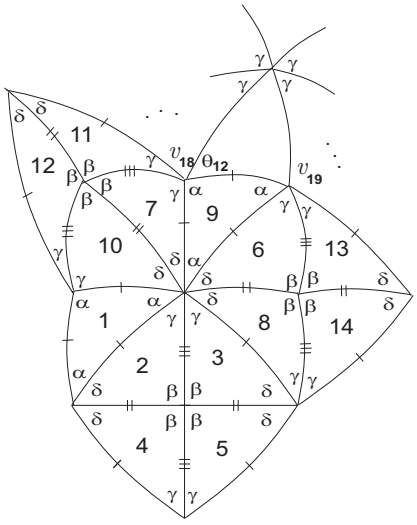

Figure 3.25: Local configuration.

□

Remark: The equation (3.1) with $\beta = \frac{\pi}{2}$ and $\alpha = \pi - (\gamma + \delta)$ is writing in the form

$$\frac{-\cos(\gamma+\delta)}{1+\cos(\gamma+\delta)} = \frac{\cos\gamma\,\cos\delta}{\sin\gamma\,\sin\delta} \tag{3.2}$$

and one of the angles γ or δ is completely determined when the remaining is fixed.

In Chapter 2, it was proved that (3.3) has the solution $\delta = \gamma \approx 54.735^\circ$ (case when the triangle T_2 is isosceles). The graphic illustration in Figure 3.26 shows the variations of γ and $\alpha = \pi - (\gamma + \delta)$, when $\delta \in]0, 54.735^\circ[$. Therefore, the f-tilings $\mathcal{C}_1^\delta$ and $\mathcal{C}_2^\delta$ represented, respectively in Figure 3.15 and Figure 3.16 are continuous families, with $0 < \delta < 54.735^\circ$.

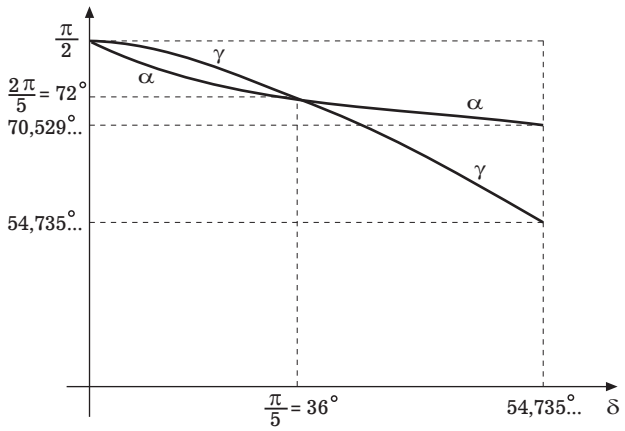

Figure 3.26: α and γ as functions of δ.

3.2 Triangular Dihedral f-Tilings with Adjacency of Type II

Detailed proofs of the results in this section were published in [3].

Here, our interest is focused on spherical triangular dihedral f-tilings whose prototiles are an equilateral triangle and a scalene triangle with adjacency of type II (Figure 3.27).

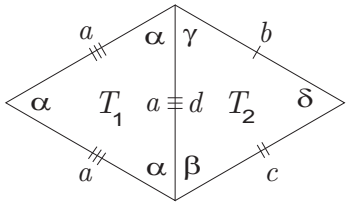

Figure 3.27: Adjacency of type II (performed by the side opposite to δ, in other words, $a = d$).

The type II edge-adjacency condition can be analytically described by the equation

$$\frac{\cos\alpha(1+\cos\alpha)}{\sin^2\alpha} = \frac{\cos\delta + \cos\gamma\cos\beta}{\sin\gamma\sin\beta} \tag{3.3}$$

Starting a local configuration of $\tau \in \Omega(T_1, T_2)$, with two adjacent cells congruent to T_1 and T_2 respectively, see Figure 3.28, a choice for angle $\theta_1 \in \{\gamma, \delta\}$ must be made. We shall consider separately each one of these situations.

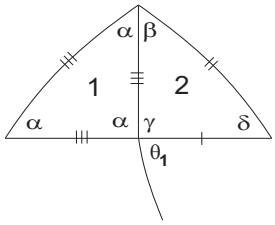

Figure 3.28: Local configuration.

With the above terminology one has:

Proposition 3.3 *If $\theta_1 = \gamma$, then $\Omega(T_1, T_2)$ consists of three discrete families of isolated dihedral f-tilings $(\mathcal{B}^p)_{p\geq 4}$, $(\mathcal{C}^p)_{p\geq 4}$ and $(\mathcal{D}^m)_{m\geq 5}$, such that the sums of alternate angles around vertices are of the form:*

$$\alpha + \beta = \pi,\ 2\alpha + \gamma = \pi \text{ and } p\delta = \pi, \text{ for } \mathcal{B}^p,\ p \geq 4;$$

$$\alpha + \beta = \pi,\ 2\gamma + \alpha = \pi \text{ and } p\delta = \pi, \text{ for } \mathcal{C}^p,\ p \geq 4;$$

$$\alpha + \beta = \pi,\ \alpha + 2\gamma + \delta = \pi \text{ and } m\delta = \pi, \text{ for } \mathcal{D}^m,\ m \geq 5.$$

3D representations of $\mathcal{B}^4, \mathcal{C}^4$ and $\mathcal{D}^5$ are given, respectively, in Figures 3.36,3.39 and 3.46.

Proof. In order to have $\Omega(T_1, T_2) \neq \emptyset$, necessarily $\alpha + \gamma \leq \pi$.

1. Let us assume that $\alpha + \gamma = \pi$.

In this case, $\alpha + \beta > \pi$ and so expanding the configuration illustrated in Figure 3.28, we obtain the following one, implying that $\delta + \beta \leq \pi$.

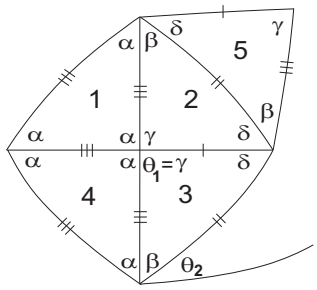

Figure 3.29: Local configuration.

Let us assume that $\beta + \delta = \pi$. As $\alpha + \gamma = \pi$, then by the adjacency condition (3.3), we conclude that $\cot\alpha = -\cot\beta$. Therefore $\alpha < \frac{\pi}{2}$ and so $\gamma > \frac{\pi}{2}$.

The local configuration started in Figure 3.29 can be extended to the one given in Figure 3.30-I. However at vertex v_1, the sum of alternate angles which contains 2γ does not satisfy the angle folding relation and we can not continue the construction of the f-tiling.

In case $\beta + \delta < \pi$, the angle labeled θ_2, in Figure 3.29, is δ (otherwise we would have $\alpha + \beta > \pi$, violating the angle folding relation). Therefore, the configuration gives rise to the one shown in Figure 3.30-II.

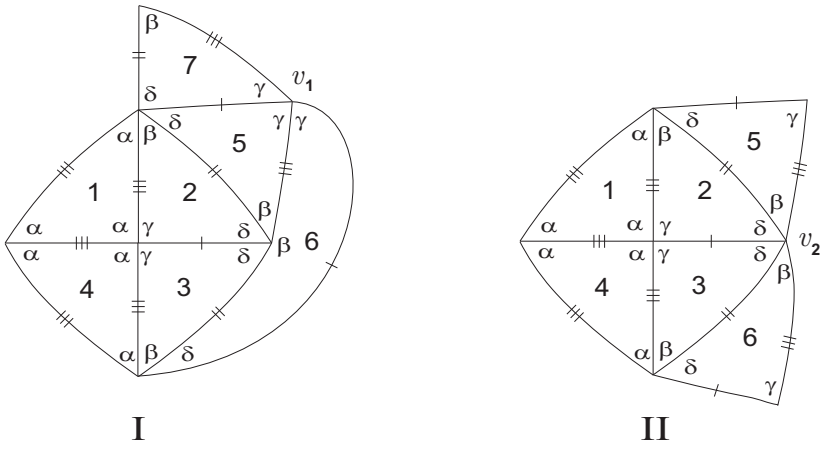

Figure 3.30: Local configurations.

Looking at the angles surrounding vertex v_2, one has $\beta + \delta + \lambda > \pi$, for any $\lambda \in \{\alpha, \gamma, \beta\}$. The angle folding relation is, once again, not satisfied.

2. Now, let us assume that $\alpha + \gamma < \pi$.

Starting from the configuration in Figure 3.28, we end up with the one given in Figure 3.31, with $\theta_3 \in \{\beta, \delta\}$.

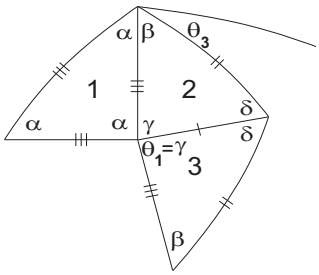

Figure 3.31: Local configuration.

2.1 If $\theta_3 = \beta$ and $\alpha + \beta = \pi$, then $\gamma + \delta > \frac{\pi}{3}$ and by (3.3), we conclude that $\alpha < \frac{\pi}{2} < \beta$.

Now, the sums of the alternate angles containing α and γ must be of the form $\alpha + \gamma + \lambda = \pi$, (Figure 3.32), where the parameter λ is a sum of angles (α, γ, δ). As $\alpha > \frac{\pi}{3}$, the angle α will appear at most once.

2.1.1 Suppose that λ is a sum of angles with one angle α. Then, $2\alpha + \gamma \leq \pi$, but taking into account that $2\alpha + \gamma + \mu > \pi$, for any $\mu \in \{\alpha, \delta, \gamma, \beta\}$, one has $2\alpha + \gamma = \pi$.

Adding some new cells to the configuration illustrated in Figure 3.31, we obtain the

one shown in Figure 3.33.

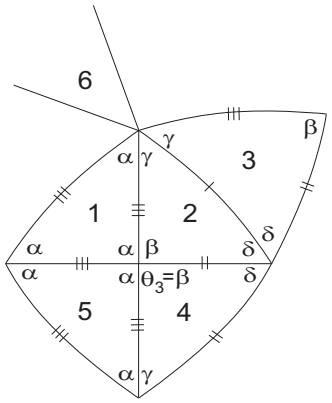

Figure 3.32: Local configuration.

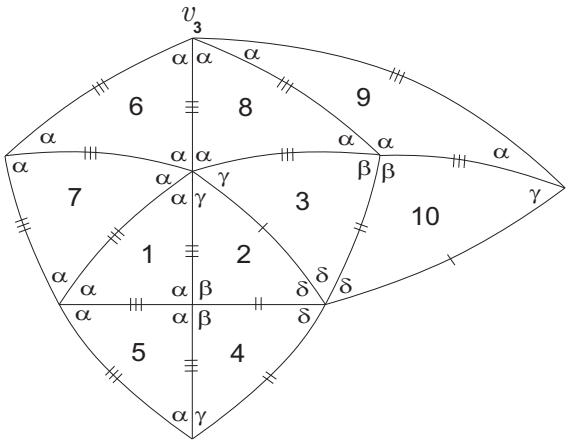

Figure 3.33: Local configuration.

Observe that tile 9 must be an equilateral triangle, otherwise the angle folding relation will not be fulfilled.

One of the sums of alternate angles, at vertex v_3, is either of the form $2\alpha + k\delta = \pi,\ k \geq 1$ or $2\alpha + \gamma = \pi$.

Suppose that $2\alpha + k\delta = \pi$, for some $k \geq 2$. Then, extending the local configuration illustrated in Figure 3.33, we get the one below (Figure 3.34).

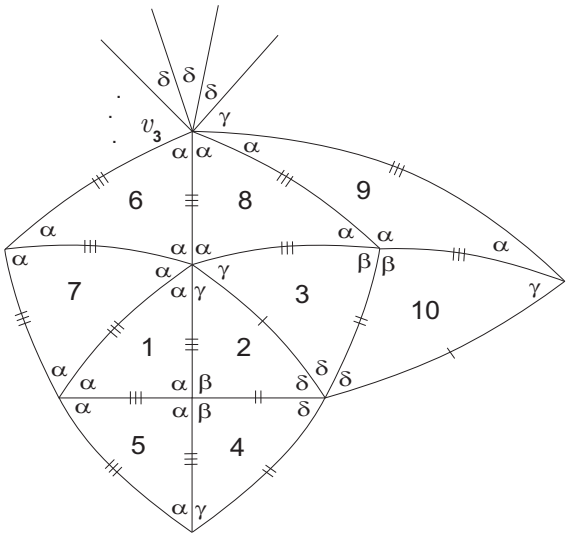

Figure 3.34: Local configuration.

At vertex v_3, we observe that the other sum of alternate angles satisfies $\alpha + \gamma + (k-1)\delta + \beta = \pi$ which is impossible.

Assume now that $2\alpha + \gamma = \pi$. Choosing one of the possible positions for tile 11, the extended local configuration started in Figure 3.33 is the following one.

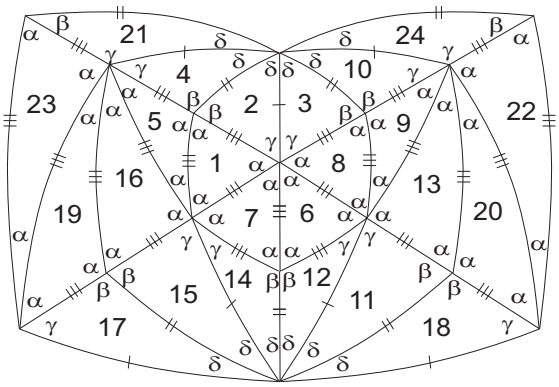

Figure 3.35: Local configuration.

The construction of this configuration follows a symmetric pattern, with three type of vertices: the vertices of valency four whose sums of alternate angles are ruled by the equation $\alpha + \beta = \pi$, the vertices of valency six surrounded by the sequence of angles $(\alpha, \alpha, \alpha, \alpha, \gamma, \gamma)$, and the vertices of valency $2p$ surrounded exclusively by angles δ. The parameter p must be greater or equal to 4, since $\delta = \frac{\pi}{2}$ or $\delta = \frac{\pi}{3}$ contradicts

the adjacency condition (3.3).

For each $p \geq 4$, we get a global f-tiling denoted by $\mathcal{B}^p$ composed by $4p$ equilateral and $4p$ scalene triangles.

In Figure 3.36, we present the case $p = 4$, which is composed by 16 copies of each prototile. The angles are $\delta = \frac{\pi}{4}$, $\alpha = \arccos\left(\frac{-1+\sqrt{1+4\sqrt{2}}}{4}\right)(\alpha \approx 66.7°), \gamma = \pi - 2\alpha\,(\gamma \approx 46.5°)$ and $\beta = \pi - \alpha\,(\beta \approx 113°)$.
The other possible position for tile 11 gives rise to a similar global f-tiling $\mathcal{B}^4$.

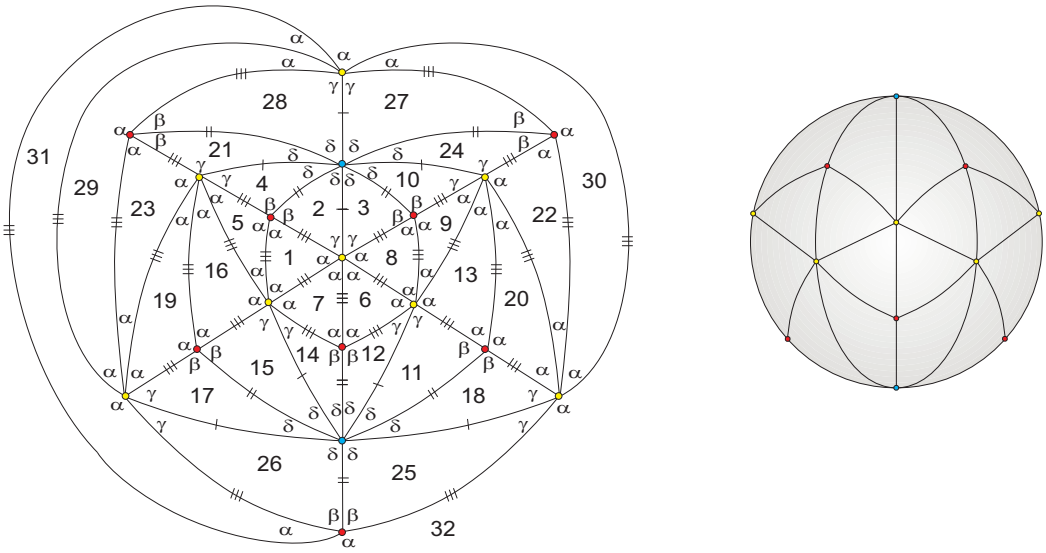

Figure 3.36: Global configuration and 3D representation of $\mathcal{B}^4$.

Observe that, by adding edges, this family of f-tilings can be obtained from the family ${}^{L}\mathcal{R}^{k}_{\gamma}$, where the prototiles are a scalene triangle and a non-equiangular lozenge, see [8] and [14].

2.1.2 Suppose that λ is a sum of angles containing at least one angle γ. Then, $\alpha + 2\gamma \leq \pi$.

2.1.2.1 If $\alpha+2\gamma = \pi$, then $\gamma < \alpha$ and we can extend the local configuration illustrated in Figure 3.31 getting the ones in Figure 3.37.

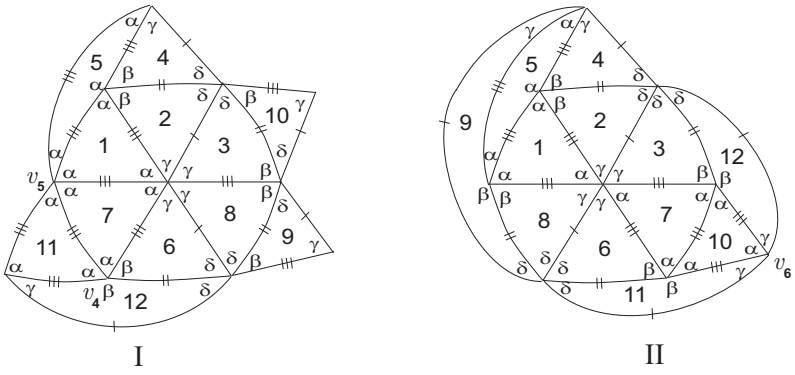

Figure 3.37: Local configurations.

Observe that for tile 6, there are two possibilities for the position of its sides (see Figure 3.37-I and II). In configuration I, tile 11 is necessarily an equilateral triangle (otherwise, one of the sums of alternate angles at vertex v_4 would be $\gamma+\beta=\pi$, so that $\gamma=\alpha>\frac{\pi}{3}$, contradicting $\alpha+2\gamma=\pi$) and so vertex v_5 is surrounded by a sequence of angles containing four adjacent angles α. Accordingly, at this vertex, we should have $2\alpha+k\delta=\pi,\ k\geq 1$ (otherwise $\gamma=\alpha$, contradicting the assumption $\alpha+2\gamma=\pi$). However, the cyclic sequence of angles $(\alpha,\alpha,\alpha,\alpha,\delta,...,\delta)$, around vertex v_5, violates the edge compatibility.

Concerning to the configuration II and, taking into account, that $\alpha+\beta=\pi$, $\alpha+2\gamma=\pi$ $(\gamma<\frac{\pi}{3}<\alpha)$ and $\beta+\gamma+\delta>\pi$ $(\beta>\gamma>\delta)$, we conclude that the sum of alternate angles containing two angles γ, at vertex v_6, must be either $2\gamma+m\delta=\pi,\ m\geq 2$ or $2\gamma+\alpha=\pi$.

2.1.2.1.1 If $2\gamma+m\delta=\pi$ for some $m\geq 2$, the sides arrangement emanating from vertex v_6 require that, the other sum of alternate angles must contain one angle α and $1+m$ angles δ, which is impossible as shown in Figure 3.38.

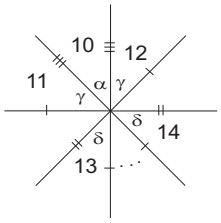

Figure 3.38: Angles arrangement around vertex v_6.

2.1.2.1.2 If $2\gamma+\alpha=\pi$, the configuration in Figure 3.37-II expands globally and in a symmetric way, if and only if $p\delta=\pi$ with $p\geq 4$. Observe that $\delta=\frac{\pi}{2}$ or $\delta=\frac{\pi}{3}$ violates the adjacency condition (3.3).

For each $p\geq 4$, we get a tiling $\tau\in\Omega(T_1,T_2)$ with vertices of vertices of valency four whose sums of alternate angles are of the form $\alpha+\beta=\pi$, valency six, in which both sums of alternate angles satisfy $\alpha+2\gamma=\pi$ and $2p$ surrounded exclusively by angles δ. Each tiling is composed by $2p$ equilateral and $4p$ scalene triangles and is denoted by $\mathcal{C}^p$. Next figure illustrates the case $p=4$, with angles $\delta=\frac{\pi}{4}$, $\gamma=\arccos\left(\frac{-\sqrt{2}+\sqrt{34}}{8}\right)\approx 56.4°$, $\beta=\pi-\alpha\approx 113°$ and $\alpha=\pi-2\gamma\approx 67°$.

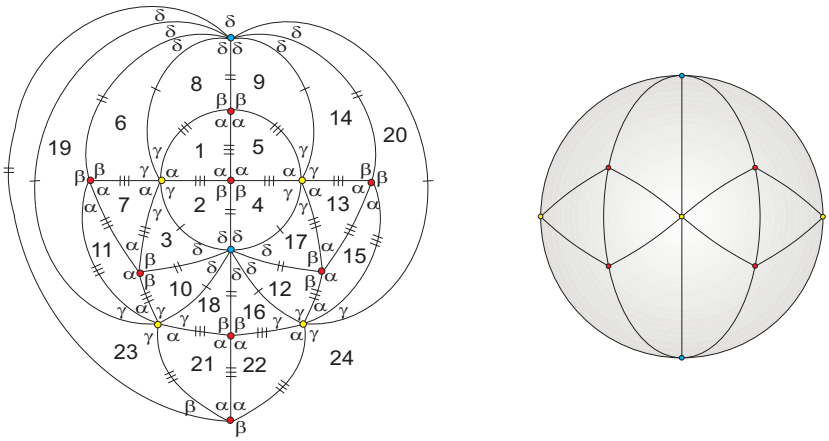

Figure 3.39: 2D and 3D representation of $\mathcal{C}^4$.

In this case, this family of f-tilings $(\mathcal{C}^p)_{p\geq 4}$ can not be obtained neither by any monohedral f-tiling nor by a dihedral f-tiling whose prototiles are a spherical triangle and spherical parallelogram, since either the angle folding relation is violated or vertices of valency four do not occur.

2.1.2.2 If $\alpha+2\gamma<\pi$ $\left(\gamma<\frac{\pi}{3}<\alpha\right)$, then $\alpha+3\gamma=\pi$ or $\alpha+2\gamma+\delta=\pi$, since, from $\alpha+\beta=\pi$ and $\delta+\gamma+\beta>\pi$ $(\beta>\gamma>\delta)$, one has $\gamma+\delta>\alpha>\frac{\pi}{3}$.

2.1.2.2.1 Suppose that $\alpha+3\gamma=\pi$ (Figure 3.31). Then $\gamma<\frac{2\pi}{9}$ and $\beta=3\gamma$. As $\delta+\gamma+\beta>\pi$, we conclude that $\delta>\frac{\pi}{9}$.

Extending the configuration in Figure 3.31, we may add some new cells ending up with the one illustrated in Figure 3.40.

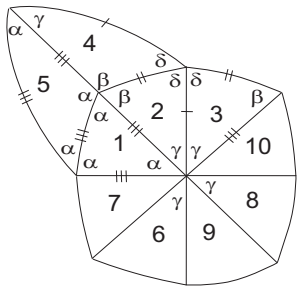

Figure 3.40: Local configuration.

Note that, there are two possible positions for the sides of tile 6. If we make the choice shown in Figure 3.41-I, the angle θ_4, at vertex v_7, is α, γ or β. Whichever we choose, the sum $\beta + \delta + \theta_4 > \pi$ violates the angle folding relation and we cannot continue the expansion of this configuration.

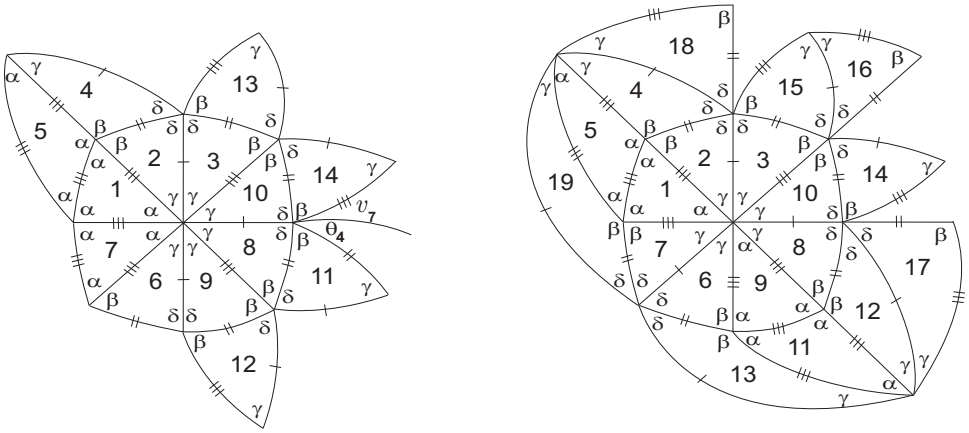

Figure 3.41: Local configurations.

The other choice on the sides of tile 6 forces the configuration illustrated in Figure 3.41-II.

In order to avoid the same situation of incompatibility, tile 8 in Figure 3.41-II is forced to be the one shown.

We conclude that, vertices partially surrounded by alternate angles β and δ must have, at most, four angles δ, since $\beta > \frac{\pi}{2}$ and $\delta > \frac{\pi}{9}$. By the adjacency condition (3.1),

we have

$$\frac{\cos k\delta(1+\cos k\delta)}{\sin^2 k\delta} = \frac{\cos\delta - \cos k\delta\cos\left(\frac{\pi}{3} - k\frac{\delta}{3}\right)}{\sin k\delta\sin\left(\frac{\pi}{3} - k\frac{\delta}{3}\right)}.$$

As $\delta > \frac{\pi}{9}$, then $k = 2$ and $\delta \approx 30.9°$ (for $k = 3, 4$, we get, respectively, $\delta \approx 19.481°, 14.324°$, contradicting $\delta > \frac{\pi}{9}$). Consequently, $\beta \approx 118.2°, \gamma \approx 39.4°$ and $\alpha \approx 61.8°$. The configuration can be extended ending up at a vertex, v_8 whose one of the sums of alternate angles does not satisfy $\beta + 2\delta = \pi$ (see Figure 3.42).

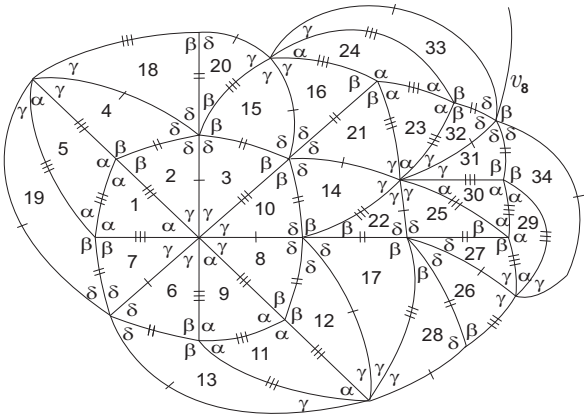

Figure 3.42: Local configuration.

2.1.2.2.2 Suppose now that $\alpha + 2\gamma + \delta = \pi$ (Figure 3.32). Tile 6 can be either a scalene triangle or an equilateral one.

2.1.2.2.2.1 Assume first that tile 6 is a scalene triangle, as illustrated in Figure 3.43.

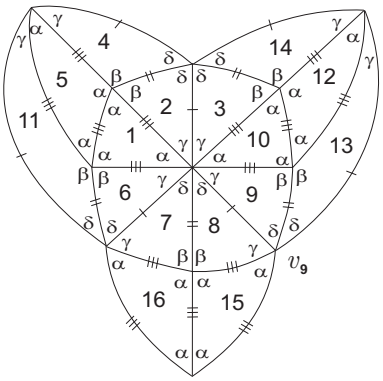

Figure 3.43: Local configuration.

At vertex v_9, the sum of alternate angles containing α and δ is either of the form

$$\alpha + k\delta = \pi \ (k \geq 4), \ \ \alpha + t\delta + \gamma = \pi \ (t \geq 3), \ \ \alpha + \delta + 2\gamma = \pi \ \text{ or } \ 2\alpha + q\delta = \pi \ (q \geq 1).$$

The other sum of alternate angles at vertex v_9 (containing γ and δ) is either of the form

$$\gamma + m\delta = \pi \ (m \geq 4), \ \ \gamma + \alpha + n\delta = \pi \ (n \geq 3), \ \ \alpha + \delta + 2\gamma = \pi \ \text{ or } \ 2\gamma + p\delta = \pi \ (p \geq 1).$$

Taking into account:

- the angular order relation, $\frac{\pi}{3} < \alpha < \frac{\pi}{2}, \ \ \delta < \gamma < \beta, \ \ \gamma > \frac{\pi}{6}, \ \ \beta > \frac{\pi}{2}$,
- $\alpha + \beta = \pi$,
- $\alpha + 2\gamma + \delta = \pi$ and
- the adjacency condition (3.1),

we conclude that the sums of the alternate angles, at vertex v_9, are $\alpha+\gamma+t\delta = \pi, \ t \geq 3$ or $\alpha + 2\gamma + \delta = \pi$, but not both.

2.1.2.2.2.1.1 If $\alpha + \gamma + t\delta = \pi$, for some $t \geq 3$, the possible positions of γ are the ones illustrated in Figures 3.44-I and 3.44-II.

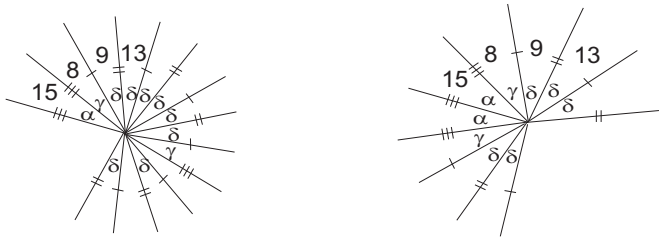

Figure 3.44: Angles arrangement around vertex v_9.

In angular sequence I, the sums of alternate angles satisfy $\alpha + \gamma + t\delta = \pi$ and $\gamma + t\delta + \beta = \pi$, which is impossible, since $\beta + \gamma + \delta > \pi$. Thus, Figure 3.44-II illustrates the way vertex v_9 must be surrounded.

Expanding the configuration in Figure 3.43, we end up with a contradiction at vertex v_{10}, see below (Figure 3.45).

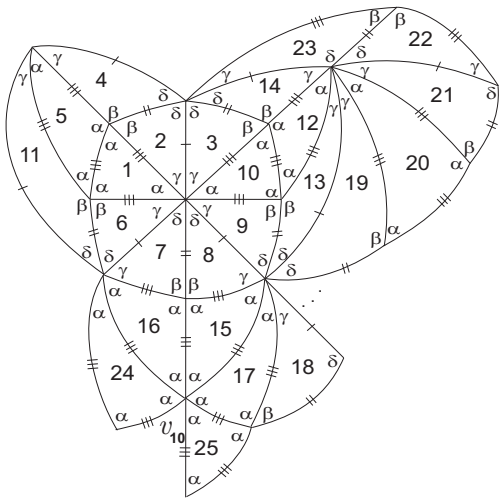

Figure 3.45: Local configuration.

2.1.2.2.2.1.2 Suppose now that, one of the sums of alternate angles, at vertex v_9, is $\alpha + 2\gamma + \delta = \pi$. Extending the configuration in Figure 3.43, we may deduce the existence of vertices surrounded exclusively by angles δ and so $\delta = \frac{\pi}{m}$, for some $m \in \mathbb{N}$. Since $\delta < \gamma < \alpha$, we conclude that $m \geq 5$.

For each $m \geq 5,\ m \in \mathbb{N}$, we obtain an f-tiling denoted by $\mathcal{D}^m$ composed by one class of vertices of valency four whose sums of alternate angles are of the form $\alpha+\beta = \pi$, one of valency eight, in which the sums of alternate angles satisfy $\alpha + 2\gamma + \delta = \pi$ and one of valency $2m$ surrounded exclusively by angles δ. For each m, the f-tiling has $4m$ equilateral triangles and $8m$ scalene triangles. A 3D representation for $m = 5$ is illustrated in Figure 3.46. The angles that compose $\mathcal{D}^5$ are $\alpha \approx 63.442°,\ \beta \approx 116.558°,\ \gamma \approx 40.279°$ and $\delta = \frac{\pi}{5}$.

By elimination of edges, each member of this family does not give rise neither to a monohedral or to a dihedral f-tiling whose prototiles are a spherical triangle and a spherical parallelogram.

2.1.2.2.2.2 Suppose now, that tile 6 (Figure 3.32) is an equilateral triangle. Adding some new cells to the illustrated configuration, we get a vertex, v_{11} surrounded by the sequence of angles $(\alpha, \gamma, \delta, \beta)$, which does not satisfy the angle folding relation (Figure 3.47).

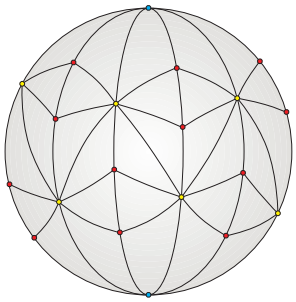

Figure 3.46: 3D representation of $\mathcal{D}^5$

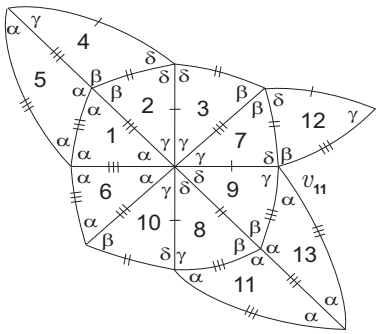

Figure 3.47: Local configuration.

2.1.3 Suppose that λ is a sum of angles containing δ. Then, $\alpha + \gamma + \delta \leq \pi$.

If $\alpha + \gamma + \delta = \pi$, from the configuration in Figure 3.32, tile 6 has two possible positions, see below (Figure 3.48).

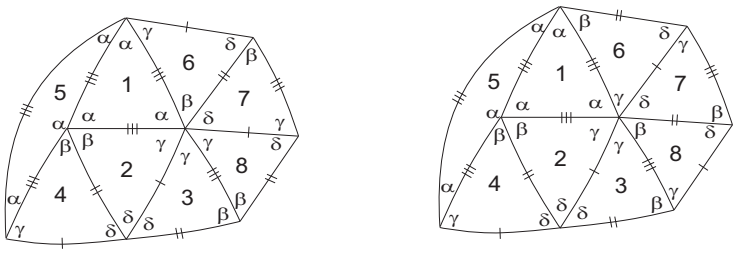

Figure 3.48: Local configurations.

In any of these cases, we get the condition $\beta + 2\gamma = \pi$, which is impossible since $\beta + 2\gamma > \beta + \gamma + \delta > \pi$.

Therefore, $\alpha + \gamma + \delta < \pi$. As the case $\alpha + \gamma + \delta + \gamma = \pi$ was already studied, we assume that $\alpha+\gamma+t\delta = \pi$, for some $t > 2$. Pursuing the extension of the configuration given in Figure 3.32, we end up at a vertex v_{12} surrounded by a cyclic sequence of angles of the form $(\gamma, \gamma, \alpha, \gamma, \delta, \delta, ..., \delta, \beta)$, which is a contradiction since $\beta + \gamma + \delta > \pi$ (see Figure 3.49).

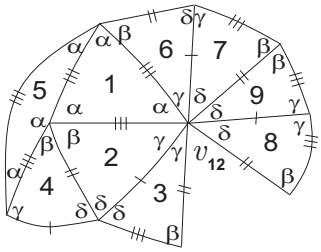

Figure 3.49: Local configuration.

2.2 If $\theta_3 = \beta$ and $\alpha+\beta < \pi$ (Figure 3.31), then $\alpha+\beta+\gamma = \pi$ or $\alpha+\beta+k\delta = \pi,\ k \geq 1$, since $\alpha, \beta > \frac{\pi}{3}$ and $\gamma > \frac{\pi}{6}$.

Suppose that $\alpha + \beta + \gamma = \pi$. Then $\delta > \alpha > \frac{\pi}{3}$, which is an impossibility.

If $\alpha + \beta + k\delta = \pi,\ k \geq 1$, the configuration illustrated in Figure 3.31 can be expanded to the one below (Figure 3.50), according to a choice for the edge position of tile 6. This choice ends up in a contradiction, since $2\beta+\lambda > \pi$, for any $\lambda \in \{\alpha, \delta, \gamma, \beta\}$.

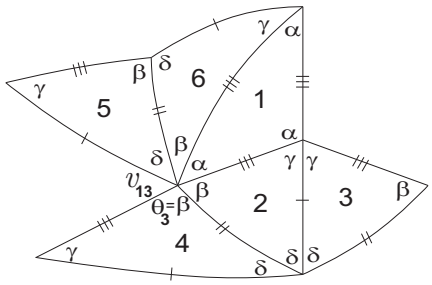

Figure 3.50: Local configuration.

Observe that the other possible position for tile 6 leads us to a sum of alternate angles of the form $\gamma + \beta + \mu = \pi$, for some μ. Nevertheless $\gamma + \beta + \mu > \pi$, for any $\mu \in \{\alpha, \gamma, \delta, \beta\}$.

2.3 If $\theta_3 = \delta$ (Figure 3.31), then $\alpha + \delta < \pi$, since $\alpha + \gamma < \pi$ and $\delta < \gamma$. Consequently, $\beta + \delta \leq \pi$. In case $\beta + \delta = \pi$, then $\beta + \gamma > \pi$ and the configuration in Figure 3.51 exhibits a contradiction at the vertex surrounded by the sequence of angles $(\alpha, \beta, \delta, \gamma)$.

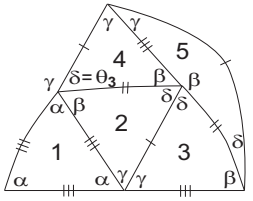

Figure 3.51: Local configuration.

Therefore, $\beta + \delta < \pi$. The configuration is now (Figure 3.52):

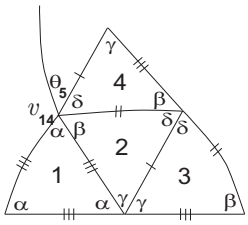

Figure 3.52: Local configuration

A decision about the angle labeled $\theta_5 \in \{\gamma, \delta\}$ must be taken.

2.3.1 Assuming that $\theta_5 = \gamma$, then the sum of alternate angles containing β and γ, at vertex v_{14}, is $\beta + \gamma + \alpha = \pi$ (note that if $\beta + \gamma = \pi$, the other sum of alternate angles would be $\alpha + \delta = \pi$, which is a contradiction). Since $\beta + \gamma + \delta > \pi$, then $\frac{\pi}{3} < \alpha < \delta < \gamma < \beta$, which is an impossibility.

2.3.2 If $\theta_5 = \delta$, then looking at vertex v_{14} in Figure 3.53, the sum of alternate angles containing β must be of the form $\beta + \alpha + n\delta = \pi,\ n \geq 1$.

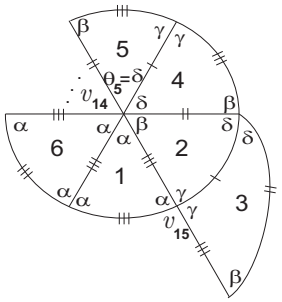

Figure 3.53: Local configuration.

Observe that $\beta \geq \frac{\pi}{2}$, otherwise, $\delta < \gamma < \beta < \frac{\pi}{2}$ and taking into account the adjacency condition (3.1), we would have $\alpha < \frac{\pi}{2}$, which is impossible, since vertices of valency four must occur. In fact, any f-tiling $\tau \in \Omega(T_1, T_2)$ has at least six vertices of valency four as stated in Chapter 1.

2.3.2.1 Considering $\beta = \frac{\pi}{2}$, then $\delta < \gamma < \frac{\pi}{2}$, $\gamma > \frac{\pi}{4}$ and once again, by the adjacency condition (3.1), $\alpha < \frac{\pi}{2}$.

On the other hand, the sequence of alternate angles containing α and γ, at vertex v_{15}, satisfies either $2\alpha + \gamma = \pi$ or $\alpha + 2\gamma = \pi$ or $\alpha + \gamma + t\delta = \pi,\ t \geq 2$.

If $2\alpha+\gamma = \pi$, then $\gamma < \frac{\pi}{3}$ and so $\delta > \frac{\pi}{6}$, contradicting the assumption $\beta+\alpha+n\delta = \pi$, for some $n \geq 1$.

In case $\alpha + 2\gamma = \pi$, the same argument is valid. Therefore, $\alpha + \gamma + t\delta = \pi,\ t \geq 2$ and the configuration illustrated in Figure 3.53 can be extended to the one shown in Figure 3.54-I.

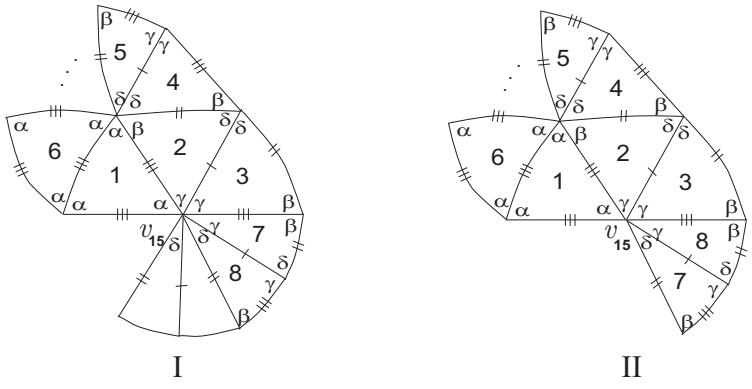

Figure 3.54: Local configurations.

As we also have $\beta+\gamma+\mu>\pi$, for any $\mu\in\{\alpha,\delta,\gamma,\beta\}$, there is only one way to arrange the sides of the tile numbered 7.

Looking at vertex v_{15}, we conclude that the other sequence of alternate angles must have one angle β, which is impossible.

2.3.2.2 Considering now that $\beta>\frac{\pi}{2}$, since $\beta+\delta<\pi$, $\beta+\alpha<\pi$ and $\alpha+\gamma<\pi$, vertices of valency four must be surrounded exclusively by angles γ or by alternate angles β and γ.

In the first case, $\gamma=\frac{\pi}{2}$ and the order relation between the angles is now

$$\beta>\frac{\pi}{2}=\gamma>\alpha>\delta$$

and so $\alpha+\gamma+m\delta=\pi$, for some $m\geq 2$ at vertex v_{15} (see Figure 3.53). However, the edge length compatibility forces the existence of one angle β at vertex v_{15}, which is a contradiction since $\beta+\gamma>\pi$.

Summarizing, we have $\beta+\gamma=\pi$ and $\beta+\alpha+n\delta=\pi$ $(n\geq 1)$. So $\gamma>\alpha>\frac{\pi}{3}$, which means that a sequence of alternate angles at vertex v_{15} is $(\alpha,\gamma,\delta,\ldots,\delta)$. Adding some new cells to the configuration in Figure 3.53, we conclude that there is one angle β surrounding vertex v_{15}, which is an impossibility, since we have $\beta+\gamma+\gamma>\pi$ (see Figure 3.54-II).

□

Proposition 3.4 *If $\theta_1=\delta$ (Figure 3.28), then $\Omega(T_1,T_2)$ is composed by one discrete family of dihedral triangles f-tilings denoted by $(\mathcal{D}^m)_{m\geq 5}$, such that the sums of alternate angles around its vertices are of the form: $\alpha+\beta=\pi$, $\alpha+2\gamma+\delta=\pi$ and $m\delta=\pi$.*

Proof. Assume first that:

1. $\alpha+\theta_1=\pi$ and $\theta_1=\delta$.

If $\alpha\leq\frac{\pi}{2}$, then $\delta\geq\frac{\pi}{2}$ and consequently $\beta>\gamma>\frac{\pi}{2}$, turning impossible any expansion of the configuration shown in Figure 3.28.

Therefore, $\alpha>\frac{\pi}{2}>\delta$ and, by the adjacency condition (3.1), $\gamma<\frac{\pi}{2}<\beta$.

The configuration illustrated in Figure 3.28 can be extended to the following one (Figure 3.55).

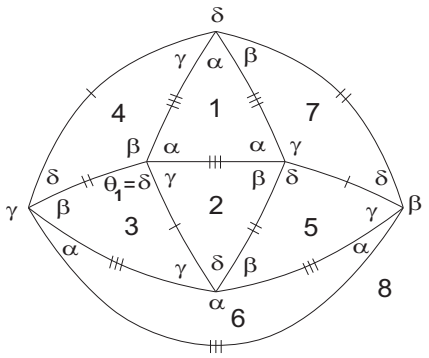

Figure 3.55: Local configuration.

As $\alpha + \delta = \pi = \beta + \gamma$ and $\gamma > \delta$, then $\alpha > \beta$. Accordingly,

$$\alpha > \beta > \frac{\pi}{2} > \gamma > \delta$$

and, by the adjacency condition (3.1), we conclude that $-\cos\alpha - \cos^2\beta < 0$. However, $0 < \cos^2\beta < -\cos\beta < -\cos\alpha$ and consequently $-\cos\alpha - \cos^2\beta > 0$, which is a contradiction. Therefore, the configuration illustrated in Figure 3.55 does not correspond to an f-tiling $\tau \in \Omega(T_1, T_2)$.

2. If $\alpha + \theta_1 < \pi$ and $\theta_1 = \delta$, a decision must be taken about the angle $\theta_6 \in \{\beta, \delta\}$ in Figure 3.56.

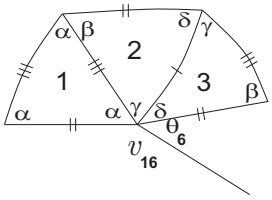

Figure 3.56: Local configuration.

2.1 If $\theta_6 = \beta$, then the sum of alternate angles containing β and γ at vertex v_{16} is $\beta + \gamma + \alpha = \pi$. Since $\beta + \gamma + \delta > \pi$, then $\frac{\pi}{3} < \alpha < \delta < \gamma$, which is an impossibility.

2.2 If $\theta_6 = \delta$, we can add a new cell to the configuration and obtain the one in Figure 3.57.

A decision about the angle $\theta_7 \in \{\delta, \beta\}$ must be taken.

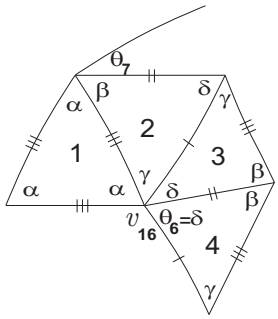

Figure 3.57: Local configuration.

2.2.1 If $\theta_7 = \delta$, the configuration illustrated in Figure 3.57 expands a bit more and gives rise to the one in Figure 3.58.

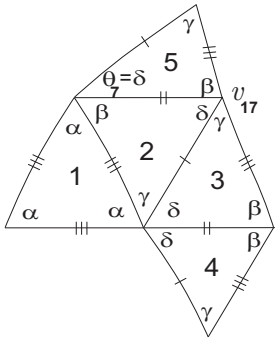

Figure 3.58: Local configuration.

Consider the sum of alternate angles containing β and γ at vertex v_{17}. This sum must be of the form $\beta + \gamma = \pi$. We have at the same vertex, another sum of alternate angles which is $\alpha + \delta = \pi$, contradicting our assumption.

2.2.2 If $\theta_7 = \beta$, then $\alpha + \beta \leq \pi$ and consequently $\gamma + \delta > \frac{\pi}{3}$. We shall consider separately the cases $\alpha + \beta = \pi$ and $\alpha + \beta < \pi$.

2.2.2.1 Let us first analyze the case $\alpha + \beta = \pi$. By the adjacency condition (3.1), we have $\alpha < \frac{\pi}{2} < \beta$.

Consider the sum of alternate angles containing γ and δ at vertex v_{16} (Figure 3.57). Taking into account the relation between the angles and the edge lengths compatibility, it can be seen that this sum is either of the form $\alpha+\gamma+n\delta = \pi,\ n \geq 1$ or $\alpha+2\gamma+\delta = \pi$.

2.2.2.1.1 In the first case, the configuration in Figure 3.57 extends to the following

one (Figure 3.59).

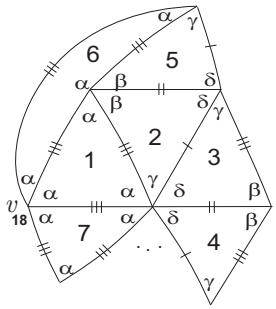

Figure 3.59: Local configuration.

Looking at vertex v_{18}, the sum of alternate angles containing two angles α is satisfies either $2\alpha + \gamma = \pi$ or $2\alpha + p\delta = \pi,\ p \geq 1$.
In case, $2\alpha + \gamma = \pi$ the configuration ends up into the one illustrated in Figure 3.60.

However, the sequence of alternate angles containing γ and β, at vertices v_{19} and $\widetilde{v}_{19}$, must satisfy $\beta + \gamma = \pi$, which is a contradiction, since $\beta + \alpha = \pi$ and $2\alpha + \gamma = \pi$. Observe that, in order to avoid two alternate angles β and due to tile 11, tile 13 must be an equilateral triangle.

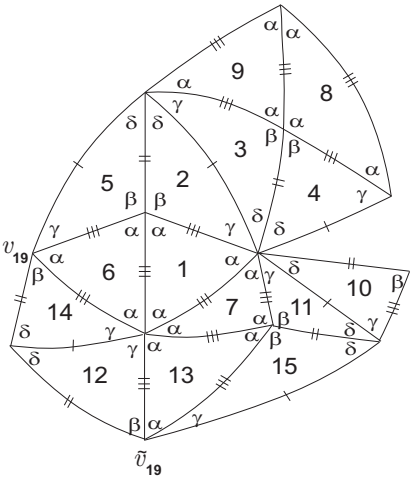

Figure 3.60: Local configuration.

In case $2\alpha + p\delta = \pi,\ p \geq 1$, the sequence of angles at vertex v_{18} must be the one in Figure 3.61 implying that the other sum of alternate angles must contain one angle β, which is an impossibility since $\alpha + \gamma + \beta > \pi$.

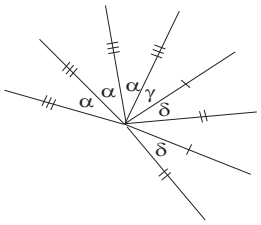

Figure 3.61: Angles arrangement around vertex v_{18}.

2.2.2.1.2 If $\alpha+2\gamma+\delta = \pi$ (vertex v_{16}, Figure 3.57), then the local planar representation extends to one of the configurations illustrated in Figure 3.62, accordingly to the edge position of tile 8.

In the first situation, a vertex partially surrounded by three consecutive angles α takes place. As $\alpha > \gamma$, then $\alpha + m\delta = \pi,\ m \geq 1$ must be one of the sums of alternate angles at this vertex. Taking in account the edge length, there is a contribution of one angle β surrounding such vertex leading us to a contradiction.

In the second case, the local configuration is uniquely extended to a global representation of the f-tilings $\mathcal{D}^m,\ \ m \geq 5$, described before.

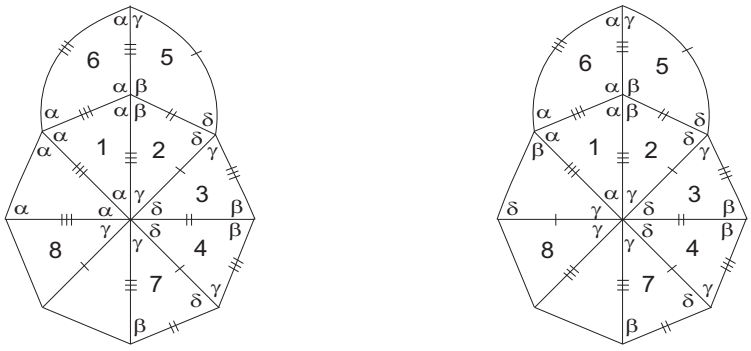

Figure 3.62: Angles arrangement around vertex v_{16}.

2.2.2.2 Consider now that $\alpha + \theta_6 < \pi$, with $\theta_6 = \beta$ (see Figure 3.56).
Then, necessarily $\alpha + \beta + t\delta = \pi,\ t \geq 1$. The configuration in Figure 3.56 ends up, according to a choice of the edge position of tile 7, to the one illustrated below (Figure 3.63). It reveals one sum of alternate angles at vertex v_{20} containing β, γ and δ, which violates the angle folding relation. Observe that the other choice for

the position of tile 7 implies that one of the sums of alternate angles at vertex v_{20} is $2\beta + t\delta = \pi,\ t \geq 1$, which is an impossibility.

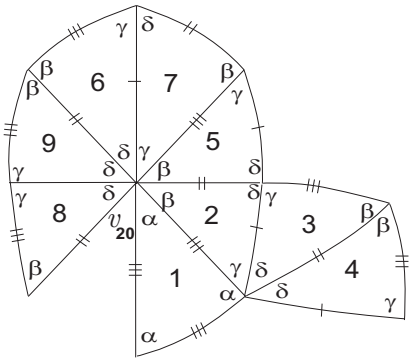

Figure 3.63: Local configuration.

□

3.3 Triangular Dihedral f-Tilings with Adjacency of Type III

Detailed proofs of all results in this section are published in [4].

From now on, we focus our interest in spherical triangular dihedral f-tilings with adjacency of type III.

The type III edge-adjacency condition can be analytically described by the equation

$$\frac{\cos\alpha(1+\cos\alpha)}{\sin^2\alpha} = \frac{\cos\gamma+\cos\delta\cos\beta}{\sin\delta\sin\beta} \tag{3.4}$$

Starting a local configuration of $\tau \in \Omega(T_1, T_2)$ with two adjacent cells congruent to T_1 and T_2 respectively (see Figure 3.116), a choice for angle $x \in \{\gamma, \beta\}$ must be made. We shall consider and study separately each one of the choices $\alpha + x = \pi$ and $\alpha + x < \pi,\ x \in \{\gamma, \beta\}$.

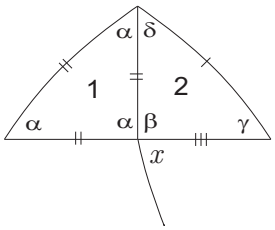

Figure 3.64: Local configuration.

With the above terminology one has:

Proposition 3.5 *If $x = \gamma$ and $\alpha + x = \pi$, then $\Omega(T_1, T_2) \neq \emptyset$ if and only if $\beta + \delta = \pi$. In this case, we get a continuous family of diheral f-tilings denoted by $(\mathcal{E}_\alpha)_{\alpha\in]\frac{\pi}{2},\pi[}$. 3D representation of an element is illustrated in Figure 3.66.*

Proof. Suppose $x = \gamma$ and that $\alpha + x = \pi$. We may add some new cells to the configuration started in Figure 3.116 and get the one illustrated in Figure 3.65, with $\theta_1 \in \{\beta, \gamma\}$.

If $\theta_1 = \beta$, then $\alpha + \theta_1 > \pi$, since $\alpha + \gamma = \pi$ and $\beta > \gamma$, violating the angle folding relation and preventing us to continue the expansion of the configuration.

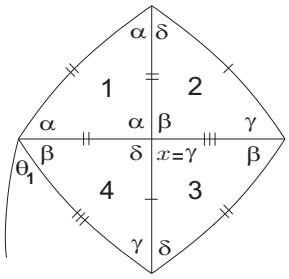

Figure 3.65: Local configuration.

If $\theta_1 = \gamma$, we can add some cells to the configuration in Figure 3.65 getting a complete f-tiling, which is a member of a family of f-tilings denoted by $\mathcal{E}_\alpha$ (see Figure 3.66). This family of tilings is composed by 2 equilateral and 6 scalene triangles and by the adjacency condition (3.4), the condition $\alpha + \gamma = \pi = \beta + \delta$ and the order relation between the angles, we may conclude that $\beta > \alpha > \frac{\pi}{2}$.

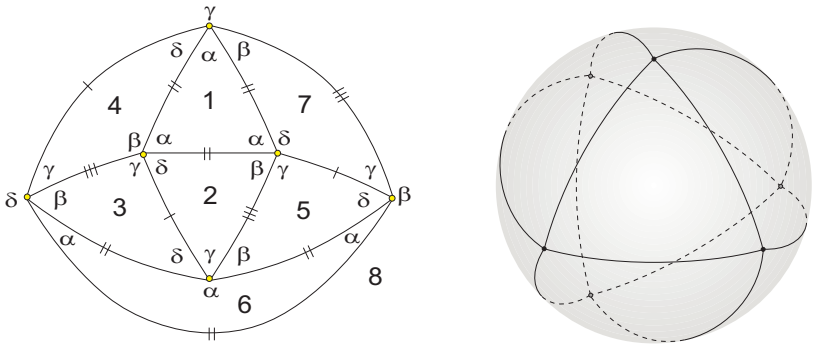

Figure 3.66: 2D and 3D representation of $\mathcal{E}_\alpha$.

This family can not be obtained from any monohedral f-tiling or from any dihedral f-tiling with prototiles a spherical triangle and a parallelogram, since the elimination of edges leads to the absence of vertices of valency four.

□

Proposition 3.6 *If $x = \gamma$ and $\alpha + x < \pi$, then $\Omega(T_1, T_2) \neq \emptyset$ if and only if $\alpha + \gamma + k\delta = \pi$, $\beta + \gamma = \pi$ and $\beta + (k+1)\delta = \pi$, for some $k \geq 1$. In this situation, there is a discrete family of f-tilings denoted by $\left(\mathcal{F}^k\right)_{k\geq 1}$. Configurations for $k = 1$ and $k = 2$ are given*

in Figures 3.74 and 3.77. Also 3D representations are given in the same figures.

Proof. Suppose that $\alpha + x < \pi$, with $x = \gamma$ (see Figure 3.116). We are led to the configuration illustrated in Figure 3.67 and a decision must be taken about the angle labeled $\theta_2 \in \{\gamma, \delta\}$:

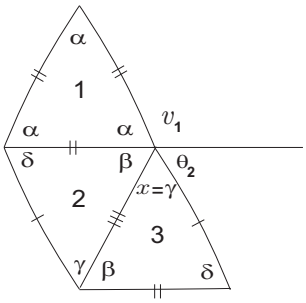

Figure 3.67: Local configuration.

1. If $\theta_2 = \gamma$, then $\beta + \theta_2 < \pi$ and since $\gamma < \beta$, we get $\delta < \gamma < \frac{\pi}{2}$. Consequently $\alpha \geq \frac{\pi}{2}$ or $\beta \geq \frac{\pi}{2}$, since vertices of valency four must exist.

1.1 If $\alpha \geq \frac{\pi}{2}$, from the adjacency condition (3.4), $\beta > \frac{\pi}{2}$ and so the sum $\beta + \theta_2 + \lambda$ violates the angle folding relation for each $\lambda \in \{\alpha, \delta, \gamma, \beta\}$.

1.2 Considering $\beta \geq \frac{\pi}{2}$, in order to satisfy the angle folding relation, the sum of alternate angles containing β and $\theta_2 = \gamma$ (in Figure 3.67) must be of the form $\beta+\gamma+\alpha = \pi$ implying that the other sum is $\alpha + 2\gamma = \pi$, contradicting $\gamma < \beta$.

2. Suppose now that $\theta_2 = \delta$. As $\alpha + \gamma < \pi$, then $\beta + \theta_2 < \pi$ and consequently $\delta < \frac{\pi}{2}$. Additionally, $\gamma < \frac{\pi}{2}$, otherwise $\beta > \gamma \geq \frac{\pi}{2}$, $\alpha \leq \frac{\pi}{2}$ and the adjacency condition (3.4) is not fulfilled. Accordingly, $\delta < \gamma < \frac{\pi}{2}$ and vertices of valency four occur if and only if $\alpha \geq \frac{\pi}{2}$ or $\beta \geq \frac{\pi}{2}$.

2.1 If $\alpha = \frac{\pi}{2}$, by the adjacency condition (3.4), $\beta > \frac{\pi}{2}$. We may add some new cells to the configuration shown in Figure 3.67, obtaining the one illustrated in Figure 3.68

The sum containing alternate angles β and δ must satisfy $\beta + k\delta = \pi$, for some $k > 1$ and taking into account the edge compatibility, we conclude that the other sum satisfies $\alpha + \gamma + (k-1)\delta = \pi$. Therefore, $\beta + \delta = \frac{\pi}{2} + \gamma$ and by the adjacency condition

(3.4),

$$\begin{aligned}\cos\gamma = -\cos\beta\cos\delta &\Leftrightarrow \sin(\beta+\delta) = -\cos\beta\cos\delta\\ &\Leftrightarrow \sin(\pi - k\delta + \delta) = \cos(k\delta)\cos\delta\\ &\Leftrightarrow -\sin(k\delta-\delta) = \cos(k\delta)\cos\delta.\end{aligned}$$

As, $k\delta < \frac{\pi}{2}$, then $\sin(k\delta-\delta) < 0$ and so $k\delta - \delta > \pi$, which is an impossibility.

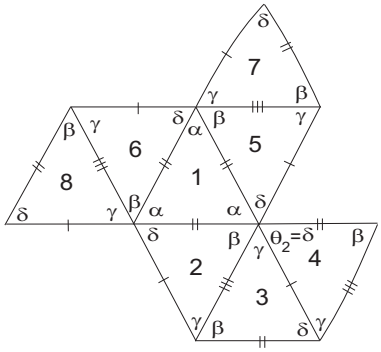

Figure 3.68: Local configuration.

2.2 If $\alpha > \frac{\pi}{2}$, from the adjacency condition (3.4), we conclude that $\delta < \gamma < \dfrac{\pi}{2} < \beta$. Since $\alpha+\gamma < \pi$, $\alpha+\delta < \pi$ and $\beta+\delta < \pi$, vertices of valency four are surrounded by alternate angles β and γ, which violates the adjacency condition.

2.3 If $\beta = \frac{\pi}{2}$, then $\alpha < \dfrac{\pi}{2}$ and vertices of valency four are surrounded exclusively by angles β.

Since $\gamma+\delta > \frac{\pi}{2}$ and $\gamma > \frac{\pi}{4}$, the angular sum containing α and γ must be either of the form $2\alpha+\gamma = \pi$, $\alpha+2\gamma = \pi$ or $\alpha+\gamma+p\delta = \pi$, for some $p \geq 1$. We shall study each case separately.

2.3.1 Vertices of valency six in which, one of the sums of alternate angles is of the form $2\alpha+\gamma = \pi$, are surrounded by the sequence of angles $(\alpha,\alpha,\alpha,\beta,\gamma,\delta)$. By the adjacency condition (3.4), we conclude that $\alpha = \frac{\pi}{3}$ or approximately 128°, which is impossible in both cases.

2.3.2 In case $\alpha+2\gamma = \pi$, the angle arrangement around vertex v_1, in Figure 3.67 (valency six) is impossible, since $\theta_2 = \delta$.

2.3.3 Assume now that $\alpha+\gamma+p\delta=\pi$, for some $p\geq 1$. Extending the configuration in Figure 3.67, we get the one below:

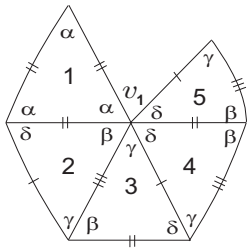

Figure 3.69: Local configuration.

The sum of the alternate angles, at vertex v_1, containing β and δ must satisfy $\beta+t\delta=\pi$, for some $t>1$. By the angles arrangement, we conclude that $\beta+t\delta=\pi=\alpha+\gamma+(t-1)\delta=\pi$ and so $\beta+\delta=\alpha+\gamma$. Consequently, $\delta>\frac{\pi}{12}$ and $\delta=\frac{\pi}{2t}$, $t=2,3,4,5$. By the adjacency condition (3.4), one has

$$-\cos(\gamma+(t-1)\delta)\sin\delta=\cos\gamma\,(1+\cos(\gamma+(t-1)\delta))$$

and for $t=2,3,4,5$ we get, respectively, $\gamma\approx 66.26^\circ$, $\gamma\approx\frac{\pi}{3}$, $\gamma\approx 58^\circ$, $\gamma\approx 57.439^\circ$ and $\alpha\approx 68.74^\circ$, $\alpha\approx\frac{\pi}{3}$, $\alpha\approx 54.5^\circ$, $\alpha\approx 50.56^\circ$. Taking into account that $\alpha>\frac{\pi}{3}$, then $t=2$. However, extending the configuration in Figure 3.69, we are led to a vertex partially surrounded by three consecutive angles γ, whose sum $2\gamma+\mu$ violates the angle folding relation, where μ denotes a sum of angles containing α,δ,γ or β (see Figure 3.70).

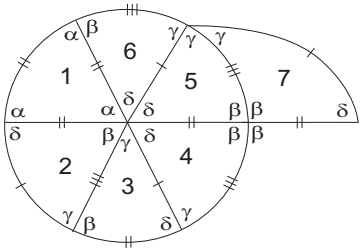

Figure 3.70: Local configuration.

2.4 Consider $\beta>\frac{\pi}{2}$. If $\alpha>\frac{\pi}{2}$, vertices of valency four are surrounded by alternate angles β and γ. But, since $\beta+\delta<\pi$ and $\alpha+\delta<\alpha+\gamma<\pi$, then the sum $\beta+\gamma=\pi$ violates the adjacency condition (3.4). Consequently, $\alpha\leq\frac{\pi}{2}$.

2.4.1 If $\alpha = \frac{\pi}{2}$, then $\beta + \gamma \neq \pi$, otherwise, by the adjacency condition (3.4), $\delta = 0$. The configuration started in Figure 3.67, with $\theta_2 = \delta$, extends to the one shown in the next figure.

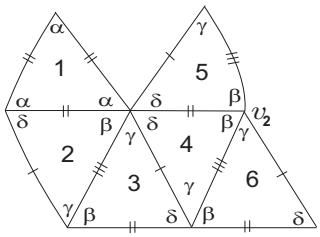

Figure 3.71: Local configuration.

Looking at vertex v_2, we observe that the sum containing the alternate angles β and γ is of the form $\beta + \gamma + \lambda$, which does not satisfy the angle folding relation for any $\lambda \in \{\alpha, \beta, \gamma\}$.

2.4.2 Assume now that $\alpha < \frac{\pi}{2}$. Adding a new cell in the configuration of Figure 3.67, a decision must be taken about the angle $\theta_3 \in \{\alpha, \delta, \beta\}$ as illustrated in Figure 3.72:

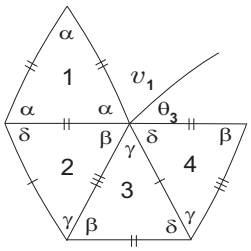

Figure 3.72: Local configuration.

2.4.2.1 Suppose $\theta_3 = \alpha$. Then, $2\alpha + \gamma \leq \pi$ and consequently $\gamma < \frac{\pi}{3}$.
If $2\alpha + \gamma = \pi$, the other sum of alternate angles at vertex v_1 must be of the form $\beta + \delta + \alpha = \pi$ implying that $\alpha + \gamma = \beta + \delta$. Taking into account that $\beta + \gamma + \delta > \pi$, we conclude that $2\gamma + \alpha > \pi$ and consequently $\gamma > \alpha > \frac{\pi}{3}$, contradicting $\gamma < \frac{\pi}{3}$.
If $2\alpha + \gamma < \pi$, we can add some cells to the configuration illustrated in Figure 3.72 and obtain the one in Figure 3.73. Observe that if tile 6 is an equilateral triangle, the sum $\alpha + \delta + \beta$ implies that vertices of valency four must be surrounded by alternate angles β and γ. Consequently $\beta > \frac{2\pi}{3}$, contradicting $\beta + \delta + \alpha \leq \pi$. Furthermore,

in the construction of the configuration, vertex v_3 is of valency four, otherwise this type of vertices would be surrounded by alternate angles β and γ leading to the same contradiction above.

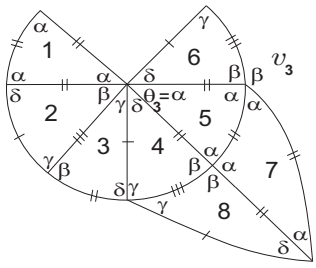

Figure 3.73: Local configuration.

Since $\alpha+\beta=\pi$ and $\beta+\gamma+\delta>\pi$, one has $\gamma+\delta>\alpha>\frac{\pi}{3}$ and $\gamma>\frac{\pi}{6}$. Then, $2\alpha+\gamma+\lambda>\pi$, for any $\lambda\in\{\alpha,\delta,\gamma,\beta\}$, preventing us to continue the construction of the f-tiling.

2.4.2.2 Suppose now that $\theta_3=\delta$. Then, $\alpha+\gamma+\delta\leq\pi$.

If $\alpha+\gamma+\delta=\pi$, the configuration in Figure 3.72 ends up to the one illustrated in Figure 3.74, where we get a complete f-tiling denoted by $\mathcal{F}^1$ which has 2 equilateral and 18 scalene triangles. This f-tiling is composed by vertices of valency four surrounded by angles $(\beta,\beta,\gamma,\gamma)$ and vertices of valency six surrounded by angles $(\alpha,\beta,\gamma,\delta,\delta,\delta)$. From the adjacency condition (3.4), we conclude that $\delta\approx 32.313°$, $\gamma\approx 64.626°$, $\beta\approx 115.374°$ and $\alpha\approx 83.061°$.

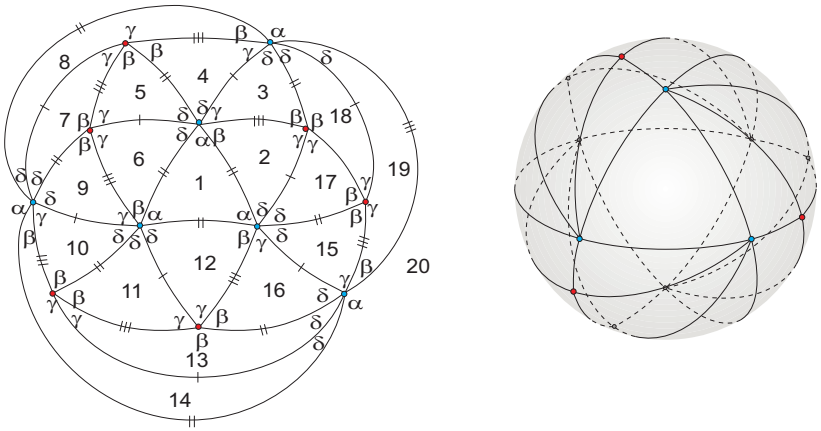

Figure 3.74: 2D and 3D representation of $\mathcal{F}^1$.

Notice that the elimination of some edges leads us to a monohedral f-tiling.

Assume now that $\alpha+\gamma+\delta<\pi$ (see Figure 3.72). Adding new cells to the configuration, we conclude that $\beta+\gamma\leq\pi$, Figure 3.75. In case $\beta+\gamma<\pi$, then $\beta+\alpha=\pi$, since vertices of valency four must exist. Taking into account that $\beta+\gamma+\delta>\pi$, one has $\gamma>\frac{\pi}{6}$ and consequently $\beta+\gamma+\lambda>\pi$, for each $\lambda\in\{\alpha,\gamma,\beta,\delta\}$. Therefore, the configuration cannot be expanded.

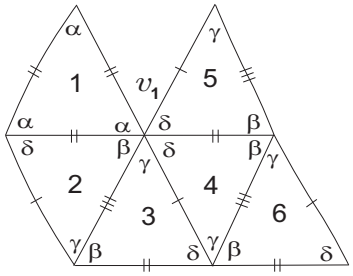

Figure 3.75: Local configuration.

At vertex v_1, the sum of alternate angles containing β and δ satisfies $\beta+k\delta=\pi$ or $\beta+\alpha+t\delta=\pi$, for $k\geq 2$ and $t\geq 1$.

2.4.2.2.1 Assuming that $\beta+k\delta=\pi,\ k\geq 2$, then the other sum of alternate angles at the same vertex satisfies $\alpha+\gamma+(k-1)\delta=\pi$, as shown in Figure 3.76.

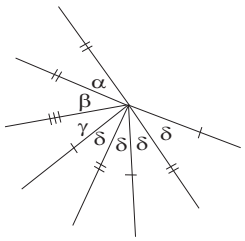

Figure 3.76: Angles arrangement around vertices partially surrounded by alternate β and δ.

We may now expand the configuration in Figure 3.72 getting a complete f-tiling $\tau\in\Omega(T_1,T_2)$. In Figure 3.77, we present a 2D and 3D representation of this tiling with $k=2$, which is denoted by $\mathcal{F}^2$. The corresponding f-tiling is composed by 2 equilateral triangles and 30 scalene triangles, $\delta\approx 19.08°$, $\gamma\approx 57.24°$, $\beta\approx 122.76°$ and $\alpha\approx$

84.6°. Generalizing, for each $k \geq 2$, the corresponding f-tiling, $\mathcal{F}^k$ is composed by 2 equilateral triangles and $6(2k+1)$ scalene triangles. Each member is composed by vertices of valency four whose sums of alternate angles satisfy $\beta + \gamma = \pi$ and vertices of valency of valency $2(2+k)$, in which both sums of alternate angles are of the form $\alpha + \gamma + k\delta = \pi$ and $\beta + (k+1)\delta = \pi$.

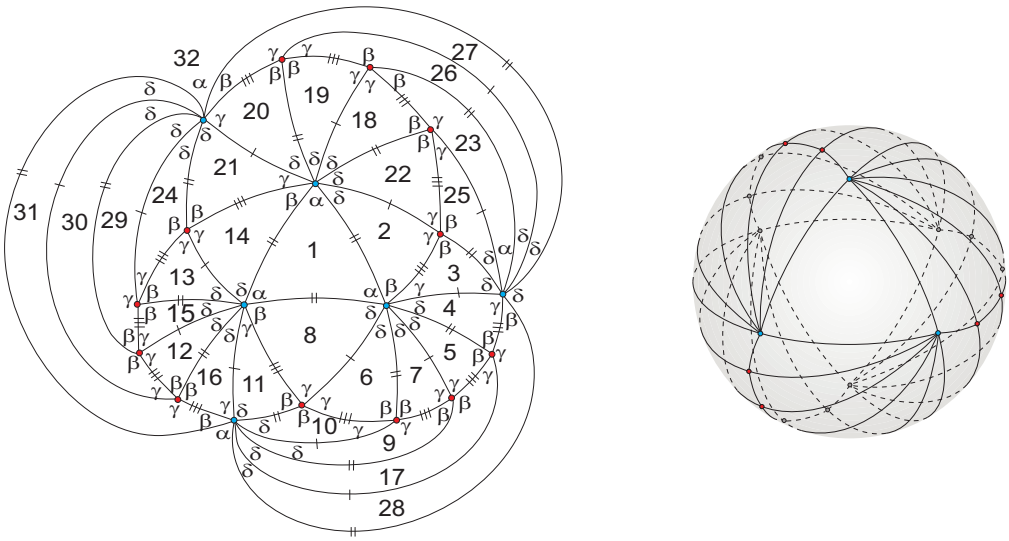

Figure 3.77: 2D and 3D representation of $\mathcal{F}^2$.

2.4.2.2.2 If $\beta + \alpha + t\delta = \pi$, then $t \geq 2$, otherwise $\beta = \gamma$. Taking into account that $\beta + \gamma = \pi$, we get $\gamma > \alpha > \frac{\pi}{3}$ and so vertices partially surrounded by the alternate angles α, γ and δ satisfy $\alpha + \gamma + t\delta = \pi$. Consequently, at vertex v_1, both sums of the alternate angles are of the form $\alpha + \gamma + t\delta = \pi = \beta + \alpha + t\delta$, which is an impossibility, since $\gamma < \beta$.

2.4.2.3 Suppose finally that $\theta_3 = \beta$ (see Figure 3.72). Since vertices of valency four must be surrounded by alternate angles β and α or β and γ, then the sequence of alternate angles around vertex v_1 is impossible. □

Suppose now that $x = \beta$, as shown in Figure 3.78:

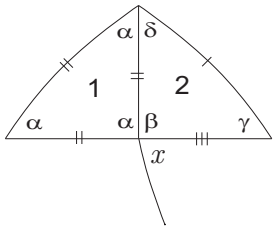

Figure 3.78: Local configuration.

Proposition 3.7 *If $x = \beta$ and $\alpha + x = \pi$, then $\Omega(T_1, T_2)$ is composed of four isolated dihedral triangles f-tilings $\mathcal{D}$, $\mathcal{E}, \mathcal{F}$ and $\mathcal{G}$, such that the sum of alternate angles around vertices are, respectively of the form:*

$$\alpha + \beta = \pi,\ \alpha + 2\delta = \pi \text{ and } \gamma = \frac{\pi}{3},\ \text{for } \mathcal{D};$$
$$\alpha + \beta = \pi,\ 2\alpha + \delta = \pi \text{ and } \gamma = \frac{\pi}{3},\ \text{for } \mathcal{E};$$
$$\alpha + \beta = \pi,\ \alpha + 2\delta + \gamma = \pi \text{ and } \gamma = \frac{\pi}{3},\ \text{for } \mathcal{F};$$
$$\alpha + \beta = \pi,\ \alpha + 2\delta + \gamma = \pi \text{ and } \gamma = \frac{\pi}{4},\ \text{for } \mathcal{G}.$$

3D representations of the f-tilings are illustrated in Figures 3.83, 3.85, 3.88 and 3.90.

Proof. Let us assume that $x = \beta$ and $\alpha + x = \pi$, in Figure 3.78. Then, $\gamma + \delta > \alpha > \frac{\pi}{3}$ and $\gamma > \frac{\pi}{6}$. The configuration started in Figure 3.78 extends to the one illustrated in Figure 3.79.

A decision must be taken about the angle labeled $\theta_1 \in \{\gamma, \delta\}$.

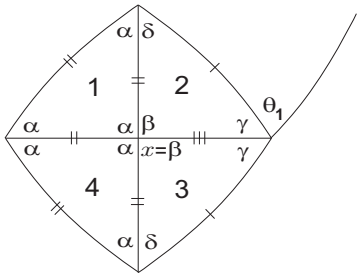

Figure 3.79: Local configuration.

1. Assuming that $\theta_1 = \gamma$, then $\gamma \leq \frac{\pi}{2}$.

If $\gamma = \frac{\pi}{2}$, then $\beta > \frac{\pi}{2}$, $\delta < \frac{\pi}{2}$ and $\alpha < \frac{\pi}{2}$, which is impossible by the adjacency condition (3.4).

Therefore, $\delta < \gamma < \frac{\pi}{2}$ and again, by the adjacency condition, we conclude that $\alpha < \frac{\pi}{2} < \beta$. Since we are assuming that $\theta_1 = \gamma$, the configuration extends a bit more to the one shown in Figure 3.80 and angle θ_2 must be γ, otherwise the sum containing $\theta_2 = \beta$ and γ would be simply $\beta + \gamma$ or $\beta + \gamma + \lambda$.

In the first case, the other sum of alternate angles would satisfy $2\gamma = \pi$, which is impossible and, in the second case, the angle folding relation is violated, for any $\lambda \in \{\alpha, \delta, \gamma, \beta\}$.

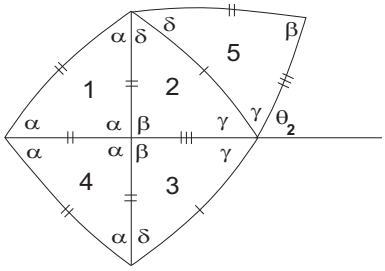

Figure 3.80: Local configuration.

Adding a new cell to the configuration in Figure 3.80, we get the following one, with $\theta_3 \in \{\gamma, \delta\}$:

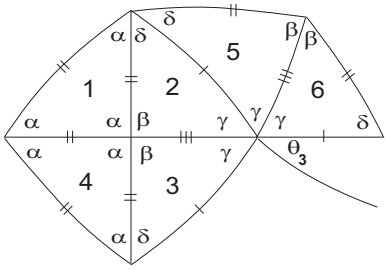

Figure 3.81: Local configuration.

1.1 Suppose firstly that, $\theta_3 = \gamma$ and $\gamma = \frac{\pi}{3}$. We may extend the configuration in Figure 3.81 and a decision must be taken about the angle $\theta_4 \in \{\beta, \alpha\}$, as shown in Figure 3.82.

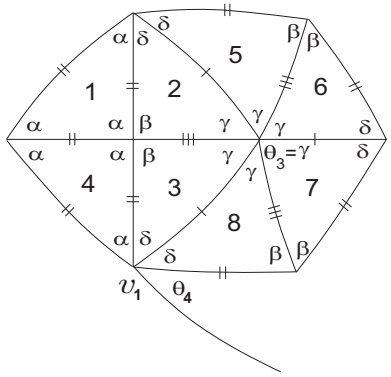

Figure 3.82: Local configuration.

1.1.1 If $\theta_4 = \beta$, then the sum of the alternate angles containing $\theta_4 = \beta$ and δ, at vertex v_1, satisfies $\beta + t\delta = \pi$ and the other satisfies either $\alpha + t\delta = \pi$ or $\alpha + \gamma + (t-1)\delta = \pi$ or $2\alpha + (t-1)\delta = \pi$, for some $t \geq 2$.

In the first case, we get $\alpha = \beta$, which is impossible.

In the second case, by the adjacency condition (3.4), we conclude that

$$\frac{\cos\alpha\,(1+\cos\alpha)}{\sin^2\alpha} = \frac{\frac{1}{2} + \cos\alpha\cos\left(2\alpha + \frac{\pi}{3}\right)}{-\sin\alpha\sin\left(2\alpha + \frac{\pi}{3}\right)}$$

and consequently, $\alpha = \frac{\pi}{3}$, $\alpha \approx 69.156^\circ$ or $\alpha \approx 136^\circ$. Since $\frac{\pi}{3} < \alpha < \frac{\pi}{2}$, then $\alpha \approx 69.156^\circ$, $\beta \approx 110.844^\circ$ and $\delta \approx 18.312^\circ$, which is impossible for any $t \geq 2$.

In the third case, by the adjacency condition (3.4),

$$\frac{\cos\alpha\,(1+\cos\alpha)}{\sin^2\alpha} = \frac{\frac{1}{2} + \cos\alpha\cos(3\alpha)}{-\sin\alpha\sin(3\alpha)},$$

and so $\alpha \approx 72^\circ, \beta \approx 108^\circ$ and $\delta \approx 36^\circ$. Therefore, $t = 2$, but by edge compatibility, we conclude that it is impossible to pursuing the configuration.

1.1.2 Suppose $\theta_4 = \alpha$. The sum of the alternate angles containing $\theta_4 = \alpha$ and δ satisfies either

$$\alpha + t\delta = \pi,\ t \geq 2 \ \text{ or } \ 2\alpha + p\delta = \pi,\ p \geq 1 \ \text{ or } \ \alpha + \gamma + q\delta = \pi,\ q \geq 1.$$

1.1.2.1 In the first case, we have $\alpha = \pi - t\delta$, $\beta = t\delta$ and $\gamma = \frac{\pi}{3}$. For $t = 2$, the configuration extends globally to the one illustrated in Figure 3.83 and is denoted by $\mathcal{D}$.

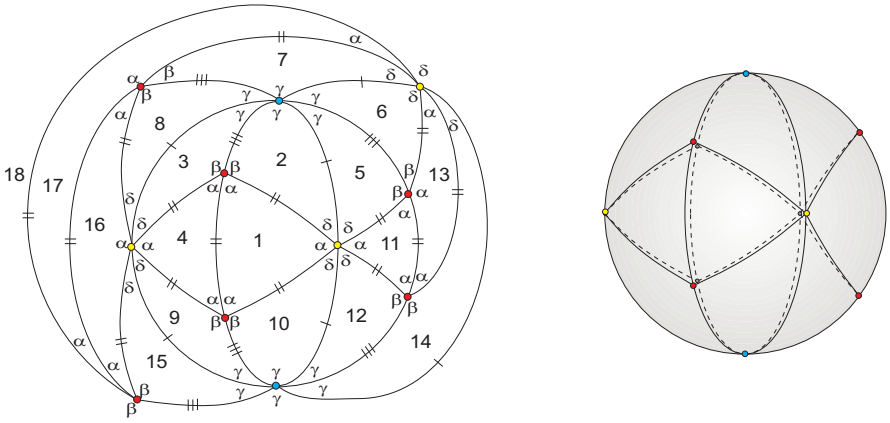

Figure 3.83: 2D and 3D representation of $\mathcal{D}$.

This global f-tiling $\tau \in \Omega(T_1, T_2)$ has 6 equilateral triangles and 12 scalene triangles and it was expanded in an unique way. By the adjacency condition (3.4), we conclude that $\alpha \approx 72,75°,\ \beta \approx 107,25°$ and $\delta \approx 53,63°$.

By the elimination of edges, vertices of valency four cease to occur or the angle folding relation is violated and so this f-tiling does not come from any monohedral or any dihedral f-tiling whose prototiles are a spherical triangle and a parallelogram.

For $t > 2$, the local representation ends up at a vertex v_2 partially surrounded by angles β, β, γ, whose sum $\beta + \gamma$ does not satisfy the angle folding relation.

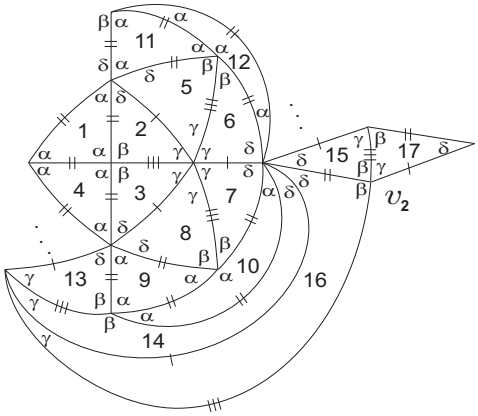

Figure 3.84: Local configuration.

1.1.2.2 In the second case, we have $2\alpha + p\delta = \pi$ and for $p = 1$, we get a complete f-tiling $\tau \in \Omega(T_1, T_2)$, where $\alpha = 72°,\ \delta = 36°$ and $\beta = 108°$. It has 12 equilateral

triangles and 12 scalene triangles and is denoted by $\mathcal{E}$. In Figure 3.85, we present a 2D and 3D representation of this f-tiling. In order to avoid vertices surrounded by the sequence of angles $(\alpha, \alpha, \alpha, \beta, \delta, ...)$, which does not satisfy the angle folding relation, this construction corresponds to a particular choice of the sides of tile 15.

Note that this f-tiling can be obtained from ${}^{L}\mathcal{R}^{3}_{\gamma}$ where the prototiles are a scalene triangle and a non-equiangular Lozenge (see [8] and [14]), by adding some edges.

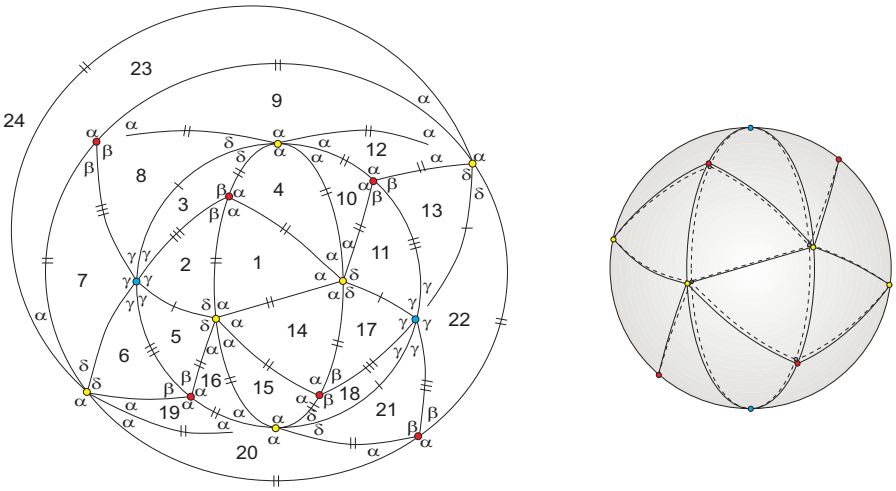

Figure 3.85: 2D and 3D representation of $\mathcal{E}$.

For $p > 1$ and assuming that tile 10 is an equilateral triangle in the positions illustrated below, we always get vertices partially surrounded by alternate angles β and γ (see Figure 3.86-I, II and III), whose sum does not satisfy the angle folding relation. Observe that to avoid vertices partially surrounded by angles β, α, β (whose sum 2β violates the angle folding relation), tile 17 in Figure 3.86-I must be an equilateral triangle and to avoid vertices surrounded by a sequence of angles $(\beta, \alpha, \delta, \delta, ...)$ (which is incompatible with the edge sides), tiles 15 in Figure 3.86-II and 18 in Figure 3.86-III must be the ones illustrated.

The other position for the equilateral triangle in tile 10 is shown in Figure 3.87 and once again, we end up at a vertex partially surrounded by angles β, β, γ or β, γ, γ, whose sum $\beta + \gamma$ does not satisfy the angle folding relation.

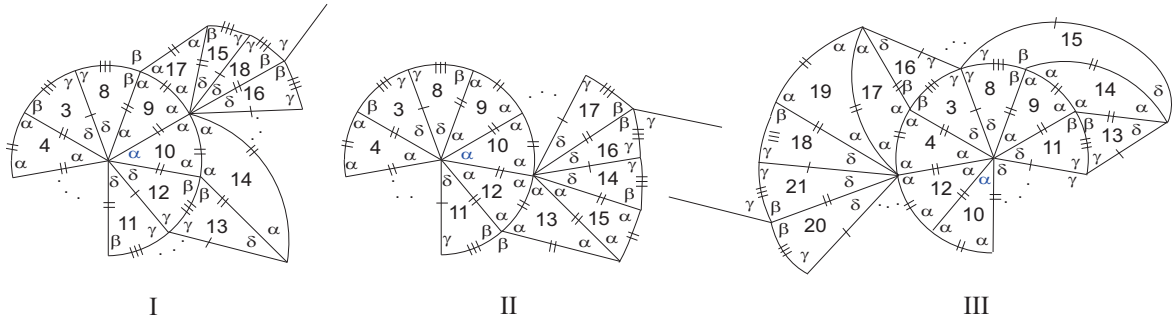

I II III

Figure 3.86: Local configurations.

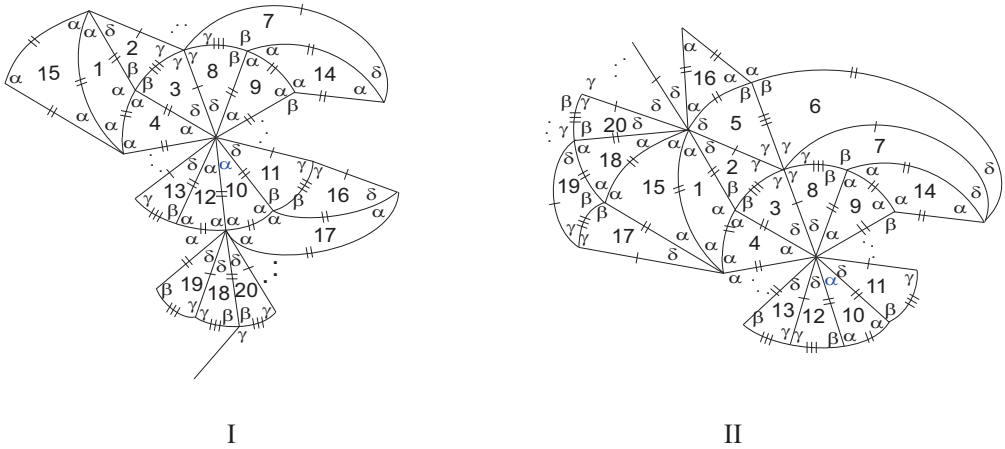

I II

Figure 3.87: Local configurations.

1.1.2.3 In the third case, $\alpha+\gamma+q\delta=\pi$, for $q \geq 1$ and if $q=1$, we get an impossibility due to the edge compatibility of the triangles. For $q=2$, we get $\alpha \approx 70.5°,\ \delta \approx 24.7°$ and $\beta \approx 109.5°$ and we may expand globally the configuration obtaining a complete f-tiling $\tau \in \Omega(T_1, T_2)$, which is denoted by $\mathcal{F}$, see Figure 3.88. It is composed of 12 equilateral triangles and 24 scalene triangles.

The selective elimination of edges in this f-tiling does not give rise neither to a monohedral f-tiling nor a dihedral f-tiling with prototiles a spherical triangle and a spherical parallelogram. Instead, we are led to a 3-hedral f-tiling.

For $q > 2$, we observe that, the angles arrangement at vertices whose sum of alternate angles satisfy $\alpha+\gamma+q\delta=\pi$ has always three consecutive angles δ leading to a vertex partially surrounded by β, β, γ, as illustrated in Figure 3.89, for cases $q=3$ and $q=4$.

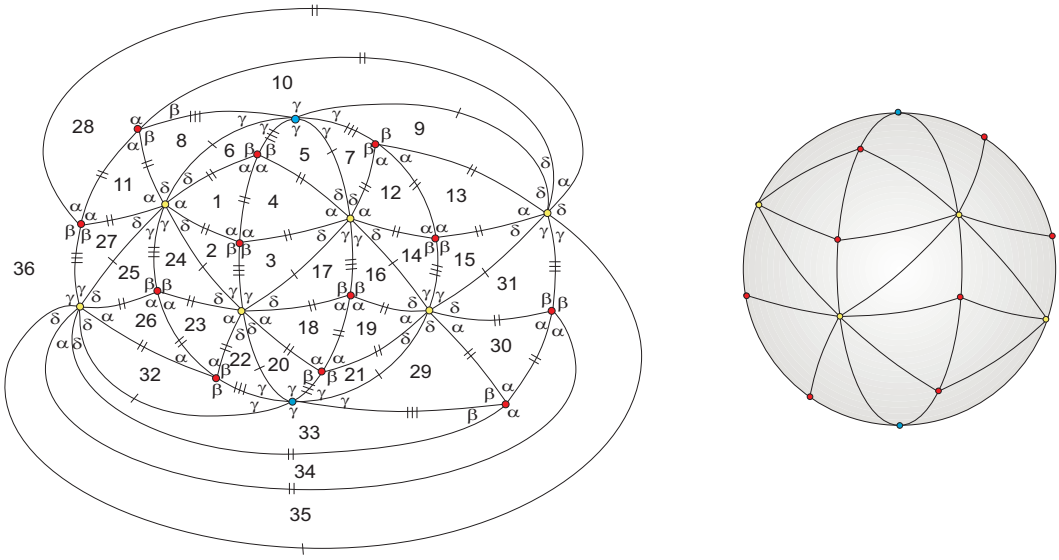

Figure 3.88: 2D and 3D representation of $\mathcal{F}$.

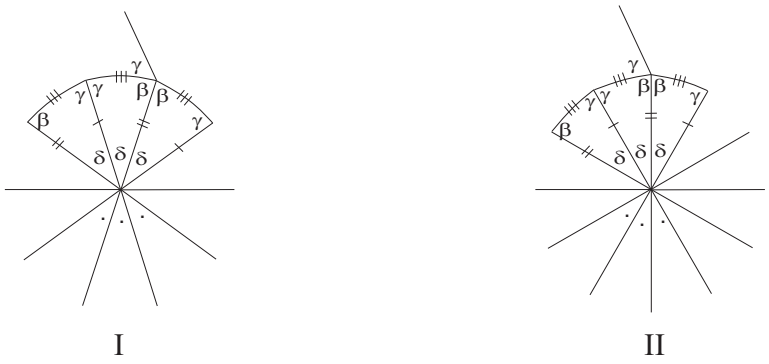

Figure 3.89: Angles arrangement at vertices with the sum $\alpha + q\delta + \gamma = \pi,\ q = 3, 4$.

1.2 Suppose now that $\gamma < \frac{\pi}{3}$, with $\theta_3 = \gamma$ (Figure 3.81). Then, in order to fulfill the angle folding relation, the sum 3γ must contain another parameter ρ being a sum of angles, which does not contain β and α (since the sequence of angles $(\gamma, \gamma, \gamma, \gamma, \gamma, \beta, \alpha, \gamma)$ does not satisfy the angle folding relation). We shall study the cases $\rho = k\gamma,\ k = 1, 2,\ \rho = \gamma + \delta,\ \rho = \delta$ and $\rho = 2\delta$ separately.

1.2.1 Suppose $\rho = \gamma$. If $4\gamma = \pi$, then $\delta > \frac{\pi}{12}$, since $\gamma + \delta > \frac{\pi}{3}$.
The sum of the alternate angles α and δ must satisfy either

- $\alpha + t\delta = \pi,\ t = 2, \ldots, 7$ or

- $2\alpha + p\delta = \pi,\ p = 1, 2, 3$ or
- $\alpha + \delta + 2\gamma = \pi$ or
- $\alpha + k\delta + \gamma = \pi,\ k = 2, 3, 4$ (observe that if $k = 1$, then $\delta > \frac{\beta}{4} = \gamma$).

By the adjacency condition (3.4), the first case is valid for $t = 3, ..., 7$, but expanding the angle arrangement, we always end up at a vertex partially surrounded by angles β, β, γ, whose sum $\beta + \gamma$ does not satisfy the angle folding relation, since $\gamma < \alpha$.

In the second case, we conclude that for $p = 1,\ \delta \approx 46.616°$, which is impossible since $\delta < \gamma$. Therefore, $p = 2, 3$ and once again, the angle arrangement leads us to a vertex partially surrounded by angles β, β, γ (whether $p = 2$ or $p = 3$) and so it is impossible to extend the configuration.

In the third case, the angles arrangement is $(\alpha, \delta, \delta, \beta, \gamma, \gamma, \gamma, \delta)$ and the sum $\delta+\beta+\gamma+\delta$ violates the angle folding relation. It remains the last case and if $\alpha + k\delta + \gamma = \pi,\ k = 2, 3, 4$, we get, respectively, $(\alpha \approx 65.557°,\ \delta \approx 34.721°,\ \beta \approx 114.442°)$ or $(\alpha \approx 63.271°,\ \delta \approx 23.91°,\ \beta \approx 116.728°)$ or $(\alpha \approx 61.432°,\ \delta \approx 18.391°,\ \beta \approx 118.567°)$.
The other sum of alternate angles at vertices partially surrounded by angles α, δ and γ is always (independently of the position of the $k\delta's$) of the form $\alpha + k\delta + \gamma = \pi$ or $\beta + (k + 1)\delta = \pi$.
Taking into account, the angles obtained by the adjacency condition, we conclude that the only possible sum is $\alpha + k\delta + \gamma = \pi,\ k = 2, 3, 4$.
Assuming that $k = 2$, we may expand the configuration in Figure 3.81 and obtain a global f-tiling $\tau \in \Omega(T_1, T_2)$ (see Figure 3.90). Note that in the construction of the f-tiling, we must avoid the appearance of one angle β at vertices that already have two angles β, since it leads to a configuration with a vertex in which one of its sum of alternate angles contains two angles β. This avoidance obliges tile 11 to be an equilateral triangle.
The corresponding f-tiling has 16 equilateral triangles and 32 scalene triangles and is denoted by $\mathcal{G}$ where the angles are $\alpha \approx 65, 56°,\ \beta \approx 114, 44°,\ \delta \approx 37, 72°$ and $\gamma = 45°$.

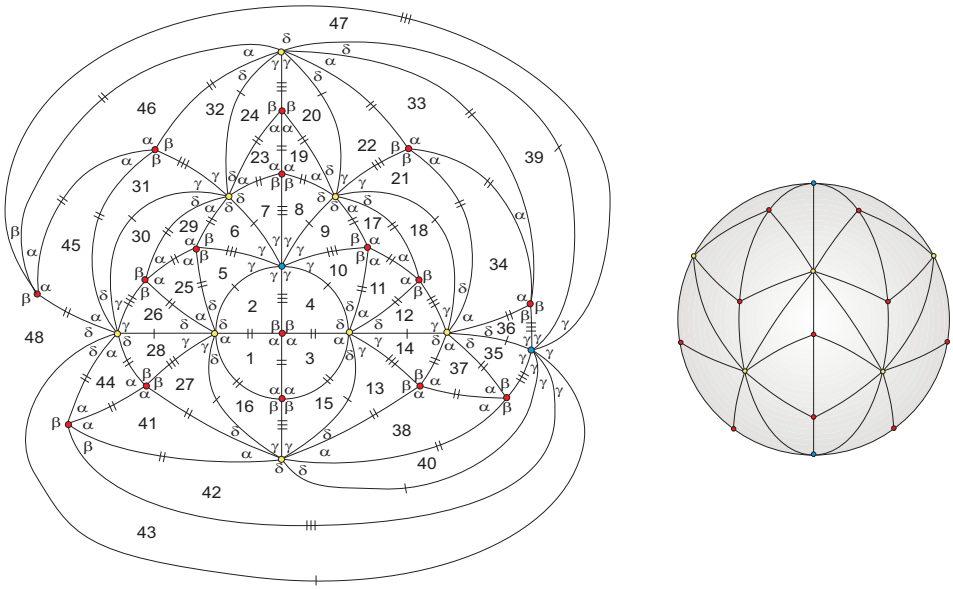

Figure 3.90: 2D and 3D representation of $\mathcal{G}$.

By elimination of some edges, this f-tiling gives rise to a 3-hedral f-tiling.

If $\alpha + k\delta + \gamma = \pi$, for $k = 3$ and $k = 4$, we always end up at a vertex partially surrounded by angles β, β, γ, since the angles arrangement at vertices of valency ten and twelve with this type of alternate sum has always three angles δ in consecutive positions, as in the case 1.1.2.3.

1.2.2 If $5\gamma = \pi$, then $\delta > \frac{2\pi}{15}$ and again, one of the sums of alternate angles, at vertices partially surrounded by α and δ, must satisfy either

- $\alpha + t\delta = \pi,\ t = 2, 3, 4$ or
- $2\alpha + p\delta = \pi,\ p = 1, 2$ or
- $\alpha + \delta + 2\gamma = \pi$ or
- $\alpha + k\delta + \gamma = \pi,\ k = 1, 2, 3.$

1.2.2.1 In the first case, since $\gamma > \delta$, we get $t = 4$ and so $\delta \approx 29.610°$, $\alpha \approx 61.558°$, $\beta \approx 118.442°$. However, expanding the configuration in Figure 3.81, we end up at a vertex surrounded by a sequence of angles of the form $(..., \beta, \beta, \gamma, ...)$ and so the sum $\beta + \gamma + \mu$ violates the angle folding relation, where μ is a sum of angles.

1.2.2.2 In the second case, for $p = 1$, we get $\alpha \approx 64.286°$ and $\delta \approx 51.428°$ which is impossible (since $\delta < \gamma$); for $p = 2$ we get $\alpha \approx 61.306°$, $\delta \approx 28.693°$, $\beta \approx 118.693°$. The configuration extends a bit more and next figure shows the possible positions of the angles arrangement surrounding vertices in which one of sums of alternate angles is $2\alpha + 2\delta$. A contradiction is achieved in the configuration in Figure 3.91-I, II and III, since it always reaches at a vertex partially surrounded by angles β, β, γ or a vertex surrounded by angles β, α, β, whose sum $\beta + \gamma$ or 2β does not satisfy the angle folding relation.

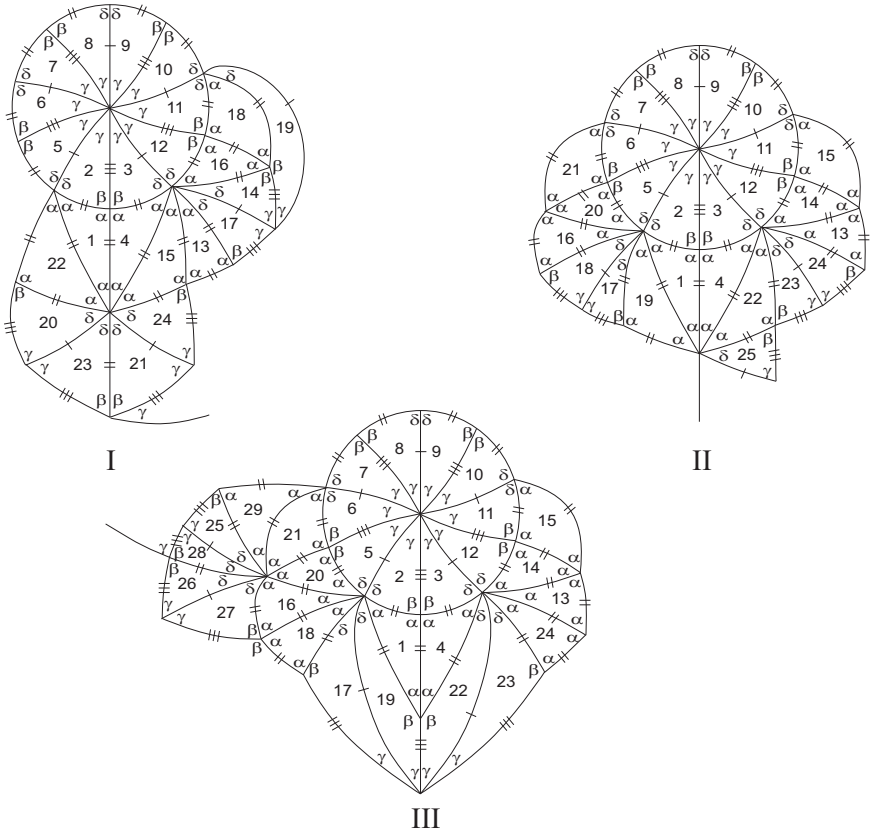

Figure 3.91: Local configurations.

1.2.2.3 If $\alpha + \delta + 2\gamma = \pi$, then, by the adjacency condition (3.4), $\delta \approx 44.1°$, which is impossible.

1.2.2.4 If $\alpha + k\delta + \gamma = \pi$, for $k = 1, 2, 3$, we get, respectively, $\delta \approx 81.188°$ or $\delta \approx 40.278°$ $\delta \approx 27.616°$. Thus, for $k = 1, 2$, $\delta > \gamma$, which is a contradiction. Summarizing, $k = 3$ and $\alpha \approx 61.15°$, $\beta \approx 118.85°$, $\delta \approx 27.616°$. Extending the

configuration in Figure 3.81 and choosing for tile 24 one of its two possible positions, we end up at a vertex surrounded by the sequence of angles $(\beta, \beta, \gamma, ...)$, whose sum is $\beta + \gamma$ or $\beta + \gamma + \mu$, where μ is a sum of angles.

In the first case, we conclude that $\gamma = \alpha$, which is impossible and in the second case, the sum violates the angle folding relation, Figure 3.92-I, II. The other position for tile 24 ends up in a similar impossibility.

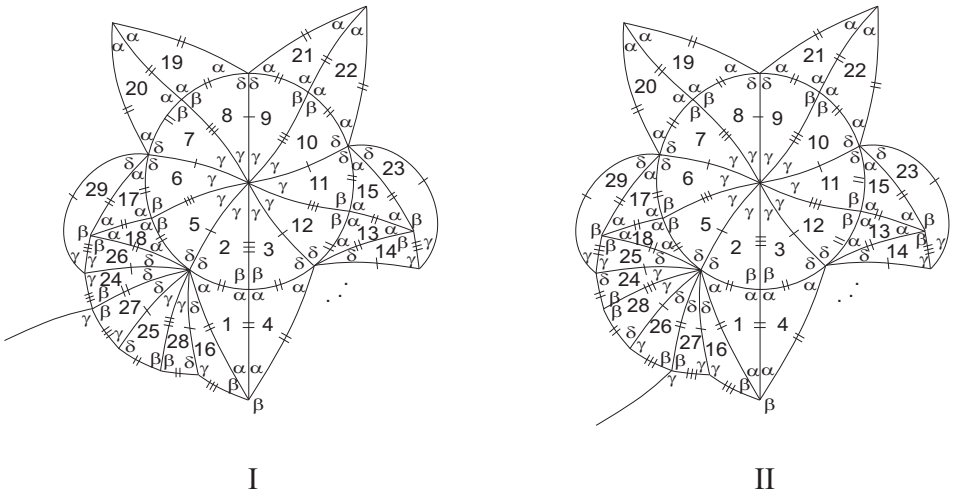

I II

Figure 3.92: Local configurations.

1.2.3 The vertices of valency ten in which one of the sums of alternate angles is $4\gamma + \delta = \pi$ gives rise to another vertex partially surrounded by one alternate angle β and one angle γ, whose sum does not satisfy the angle folding relation, see Figure 3.93-I and II.

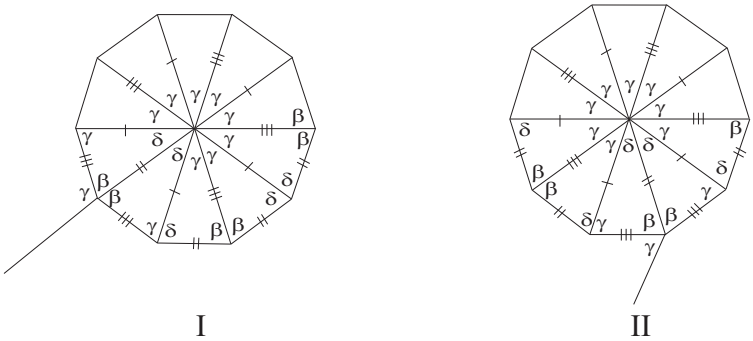

I II

Figure 3.93: Angles arrangement around vertices partially surrounded by four alternate angles γ and one δ.

1.2.4 Suppose $\rho = \delta$. Then, $3\gamma + \delta = \pi$ and the configuration in Figure 3.81 ends up in the one shown in Figure 3.94-I. Once again we get an impossibility at vertex v_3.

1.2.5 If $\rho = 2\delta$, then $3\gamma + 2\delta = \pi$. The configuration ends up in a vertex partially surrounded by angles β and γ, similar to the one in Figure 3.93 and a contradiction is achieved as shown in Figure 3.94-II.

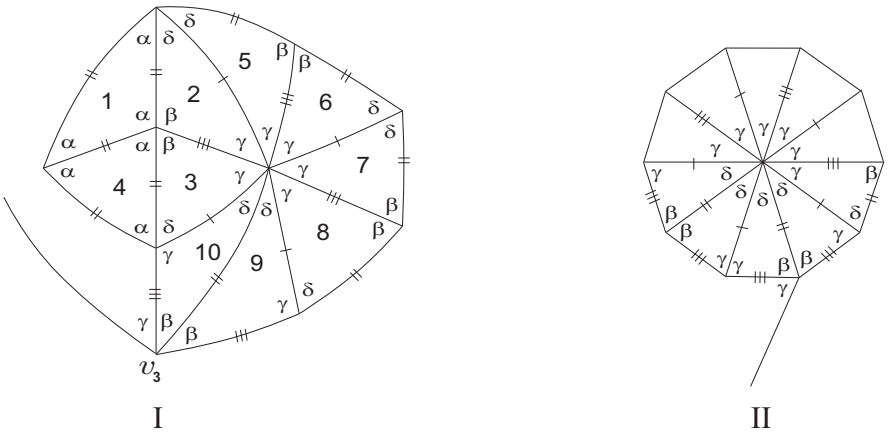

Figure 3.94: Local configurations.

1.3 Suppose now that $\theta_3 = \delta$ (see Figure 3.81). Then, $2\gamma + \delta \leq \pi$ and if $2\gamma + \delta = \pi$, the configuration is given in Figure 3.95.

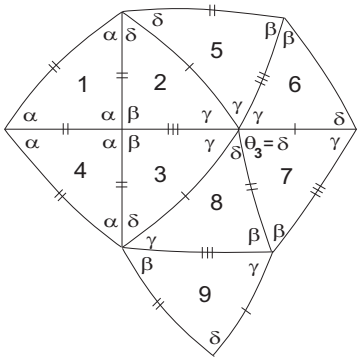

Figure 3.95: Local configuration.

The vertices partially surrounded by angles β and γ must be of valency four, so $\gamma = \alpha$ and consequently by the adjacency condition (3.4), $\alpha = \frac{\pi}{2}$, which is impossible. Therefore, $2\gamma + \delta < \pi$ and a decision must be taken about the angle $\theta_5 \in \{\delta, \alpha\}$ (see Figure 3.96).

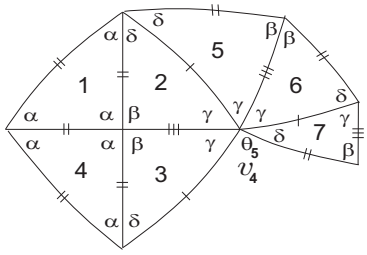

Figure 3.96: Local configuration.

In case $\theta_5 = \delta$, the configuration extends to the one shown in Figure 3.97.

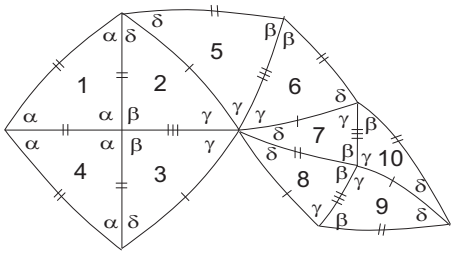

Figure 3.97: Local configuration.

The vertex partially surrounded by angles β and γ must be of valency four and once again $\gamma = \alpha$, which is impossible by the adjacency condition (3.4). Accordingly, $\theta_5 = \alpha$ and since $2\gamma + \alpha < \pi$ (due to edge compatibility), one has $3\gamma + \alpha = \pi$ or $2\gamma + \alpha + \delta = \pi$, taking into account that $\gamma > \frac{\pi}{6}$ and $\gamma + \delta > \alpha$.

If $3\gamma + \alpha = \pi$, then $\delta > \frac{\pi}{9}$ and the other sum of alternate angles at vertex v_4 is of the form $\beta + \delta + 2\gamma = \pi$, which is impossible.

If $2\gamma + \alpha + \delta = \pi$, we may add some new cells to the local configuration illustrated in Figure 3.97 and obtain the one in Figure 3.98.

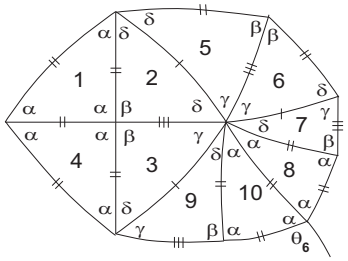

Figure 3.98: Local configuration.

The angle θ_6 must be α or β. In case $\theta_6 = \alpha$, then the sum containing two alternate angles α is either of the form $2\alpha + \gamma = \pi$ or $2\alpha + p\delta = \pi,\ p \geq 1$. However, by the assumption $2\gamma + \alpha + \delta = \pi$, it is impossible that $2\alpha + \gamma = \pi$ (note that $\gamma + \delta > \alpha$). Therefore, $2\alpha + p\delta = \pi$ for some $p \geq 1$. The configuration extends and we obtain the one in Figure 3.99-I.

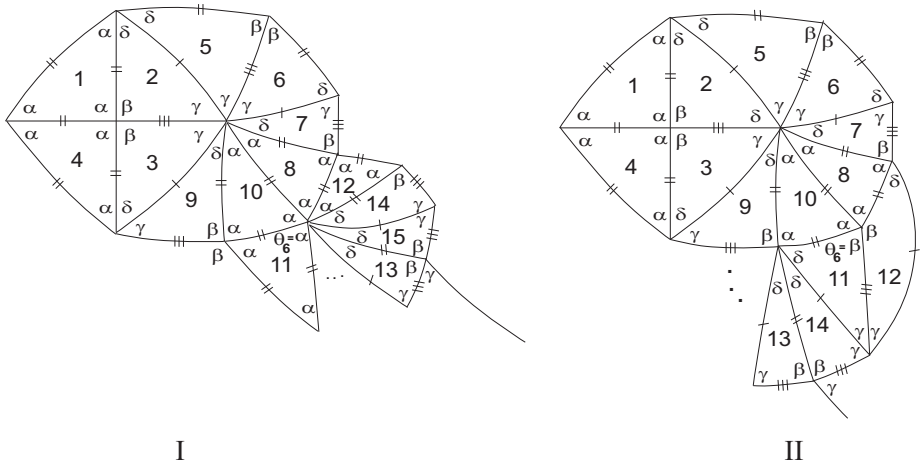

Figure 3.99: Local configurations.

The vertices partially surrounded by alternate angles β and γ, once again are of valency four, which is impossible since $\gamma = \alpha$ does not satisfy the condition $\alpha + \delta + 2\gamma = \pi$.

If $\theta_6 = \beta$, then the configuration extends a bit more, but we end up again at a vertex partially surrounded by alternate angles β and γ, which must be of valency four and consequently $\gamma = \alpha > \frac{\pi}{3}$, contradicting the assumption $2\gamma + \alpha + \delta = \pi$ (Figure 3.99-II).

2. Suppose now that $\theta_1 = \delta$ (see Figure 3.79). If $\gamma + \delta = \pi$, then $\beta > \gamma > \frac{\pi}{2}$ and from the assumption $\alpha + \beta = \pi$, then $\delta, \alpha < \frac{\pi}{2}$. However, the configuration can not be expanded since the sum $\rho + \beta$ (see Figure 3.100) does not satisfy the angle folding relation, for any $\rho \in \{\gamma, \beta\}$.

As $\gamma + \delta < \pi$, then $\delta < \frac{\pi}{2}$. If $\gamma \geq \frac{\pi}{2}$, then $\beta > \frac{\pi}{2}$ and $\alpha < \frac{\pi}{2}$, which is impossible by the adjacency condition (3.4). Therefore, $\gamma < \frac{\pi}{2}$ and also $\alpha < \frac{\pi}{2} < \beta$, by the adjacency condition (3.4).

The configuration started in Figure 3.79 extends to the one in Figure 3.101.

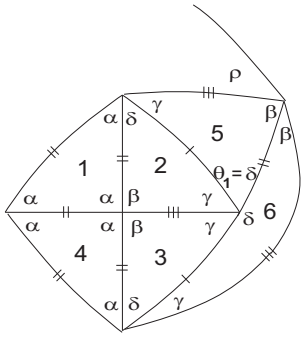

Figure 3.100: Local configuration.

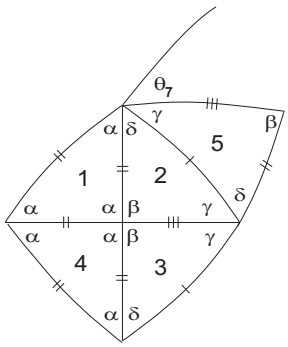

Figure 3.101: Local configuration.

The angle labeled θ_7 is either β or γ.

2.1 Suppose firstly, that θ_7 is β. Therefore, in order to satisfy the angle folding relation, the sum containing alternate angles β and δ is $\beta + r\delta = \pi$, for some $r > 1$. The other sum of alternate angles at the same vertex is $\alpha + \gamma + (r-1)\delta$, as illustrated in Figure 3.102.

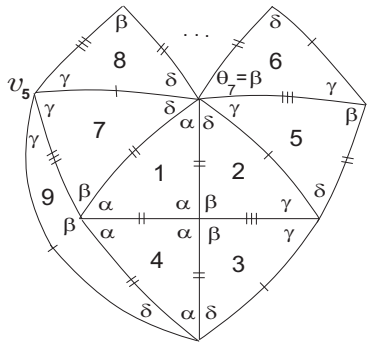

Figure 3.102: Local configuration.

Looking at vertex v_5 surrounded only by angles γ, one of the sums of its alternate angles is of the form $2\gamma+\lambda \leq \pi$, where the parameter λ is a sum of angles not containing any β, due to the angle folding relation.

2.1.1 Suppose that $\lambda = \alpha$. Then, $2\gamma + \alpha \leq \pi$. However, the case $2\gamma + \alpha = \pi$ is impossible, since the other sum of alternate angles is $\beta+\gamma+\delta$, not satisfying the angle folding relation, as illustrated in the Figure 3.103.

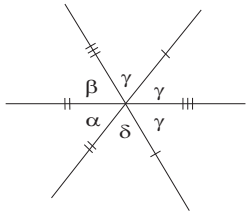

Figure 3.103: Angles arrangement.

As $2\gamma + \alpha < \pi$, then $3\gamma + \alpha = \pi$ or $2\gamma + \alpha + \delta = \pi$.
If $3\gamma + \alpha = \pi$, taking into account that $\alpha + \gamma + (r-1)\delta = \pi$ and $\beta + r\delta = \pi$, we conclude that $\beta + \delta + 2\gamma = \pi$, which is a contradiction.

Also, if $2\gamma + \delta + \alpha = \pi$, for the same reason $\beta + \gamma + 2\delta = \pi$, which is again an impossibility.

2.1.2 Suppose that $\lambda = m\gamma,\ m = 1, 2, 3$.
If $m = 1$, then $3\gamma = \pi$ and the angles arrangement around vertex v_5 is illustrated in the Figure 3.104.

Observing tiles labeled 8, 11 and 12 and the position of the angle β, we can not expand the configuration, since $\beta > \frac{\pi}{2}$.

If $m = 2, 3$, then $4\gamma = \pi$ and $5\gamma = \pi$, but we are led to the same contradiction illustrated in Figure 3.104.

2.1.3 If $\lambda = \gamma + k\delta,\ k = 1, 2$, then $3\gamma + k\delta = \pi$ and the configuration ends up at a vertex partially surrounded by angles γ, δ and β, which is impossible since the sum of the alternate angles β and γ does not satisfy the angle folding relation (see Figure 3.105).

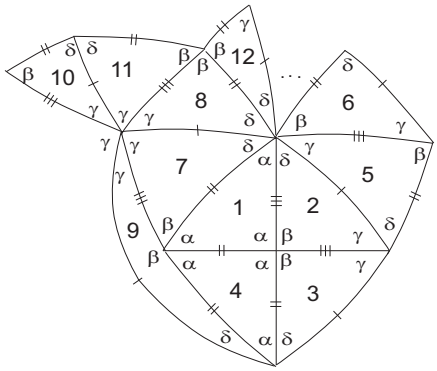

Figure 3.104: Local configuration.

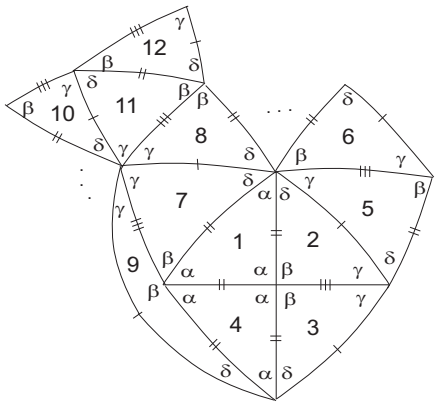

Figure 3.105: Local configuration.

2.1.4 Suppose that $\lambda = \delta$. If the sum $2\gamma + \delta$ satisfies the angle folding relation, then $\gamma > \frac{\pi}{3}$ and the local representation in Figure 3.101 extends to the one illustrated in Figure 3.106-I.

The vertices partially surrounded by alternate angles β and γ must be of valency four, for which $\gamma = \alpha$. From the assumption in 2.1, $r = 2$, in other words, $\beta + 2\delta = \pi = \alpha + \gamma + \delta$. Figure 3.106-II illustrates the expanded configuration and looking at vertex v_6, we conclude that is of valency four, which is impossible since $\delta < \gamma = \alpha$. Therefore, $2\gamma + \delta < \pi$ and so, $2\gamma + k\delta = \pi$, for some $k \geq 2$. However, this case is similar to the case $2\gamma + \delta = \pi$.

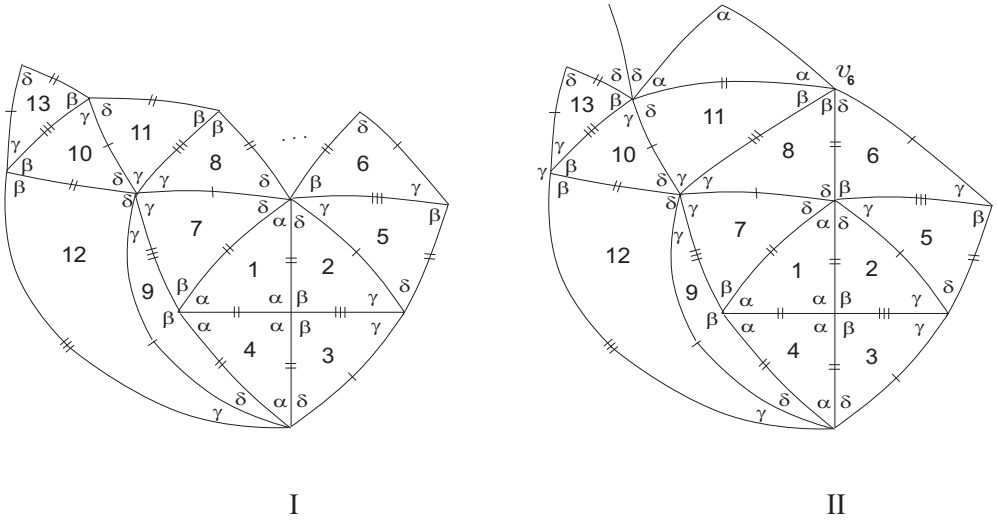

Figure 3.106: Local configurations.

2.2 Suppose that $\theta_7 = \gamma$ (see Figure 3.101). Consequently $\alpha + \gamma + \rho = \pi$, for some ρ different from β.

2.2.1 If $\rho = \alpha$, then we have $2\alpha + \gamma = \pi$, since $\gamma + \delta > \alpha > \frac{\pi}{3}$. However, due to the edge compatibility, it is impossible to arrange the angles in order to satisfy $2\alpha + \gamma = \pi$.

2.2.2 If $\rho = \gamma$, then $\alpha + 2\gamma < \pi$, since $\alpha + 2\gamma = \pi$ implies that the other sum of alternate angles is $\beta + \gamma + \delta = \pi$, which is an impossibility. Taking into account that, $\gamma + \delta > \alpha > \dfrac{\pi}{3}$ and $\gamma > \dfrac{\pi}{6}$, one has either $\alpha + 3\gamma = \pi$ or $\alpha + 2\gamma + \delta = \pi$. Again, by the angle arrangement, the case $\alpha + 3\gamma = \pi$ leads us to the impossible sum $\beta + \delta + 2\gamma = \pi$. Therefore, $\alpha + 2\gamma + \delta = \pi$ and we may add some new cells to the configuration in Figure 3.101. Choosing for tile 7, one of its two possible positions, we end up at the configuration in Figure 3.107.

Looking at vertex labeled v_7, we conclude that it must be of valency four and therefore $\gamma = \alpha > \frac{\pi}{3}$, contradicting the sum $\alpha + 2\gamma + \delta = \pi$.

The other position for tile numbered 7 leads us to a contradiction, (see Figure 3.108) since $\xi = \beta$ or $\zeta = \beta$.

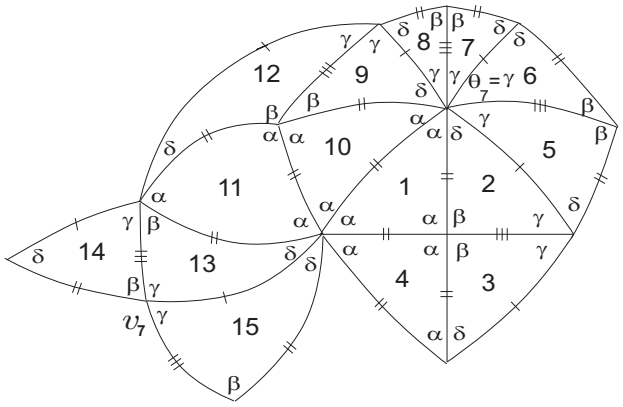

Figure 3.107: Local configuration.

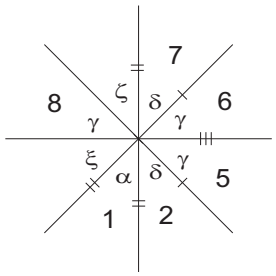

Figure 3.108: Angles arrangement.

2.2.3 If $\rho = \delta$, then $\alpha + \gamma + \delta \leq \pi$. We shall study the cases $\alpha + \gamma + \delta = \pi$ and $\alpha + \gamma + \delta < \pi$ separately.

2.2.3.1 Suppose, firstly, that $\alpha + \gamma + \delta = \pi$. Taking into account that $\gamma + \delta > \alpha$, one has $\gamma > \frac{\pi}{4}$.

The local configuration in Figure 3.101 extends a bit more to the one in Figure 3.109.

In order to satisfy the angle folding relation, the sum of the alternate angles 2α is either of the form $2\alpha + \gamma = \pi$ or $2\alpha + p\delta = \pi$, for some $p \geq 1$.

If $2\alpha + \gamma = \pi$, then $\delta = \alpha > \frac{\pi}{3}$ and consequently $\gamma > \frac{\pi}{3}$ not satisfying $\alpha + \gamma + \delta = \pi$. Therefore, $2\alpha + p\delta = \pi,\ p \geq 1$ and, by the assumption $\alpha + \delta + \gamma = \pi$, we get $\alpha + (p-1)\delta = \gamma$. Consequently, $\gamma \geq \alpha > \frac{\pi}{3}$, implying that the sum of alternate angles at vertices partially surrounded by α and γ must satisfy $\alpha + \gamma + \delta = \pi$. Accordingly, $\alpha + \beta = \pi,\ 2\alpha + p\delta = \pi,\ p \geq 1$ and $\alpha + \gamma + \delta = \pi$. Expanding the configuration and attending to the choice of the edge sides of tile 13, we get the one shown in Figure 3.110.

Looking at vertex v_8, the configuration cannot be extended, since the sum 2β violates the angle folding relation.

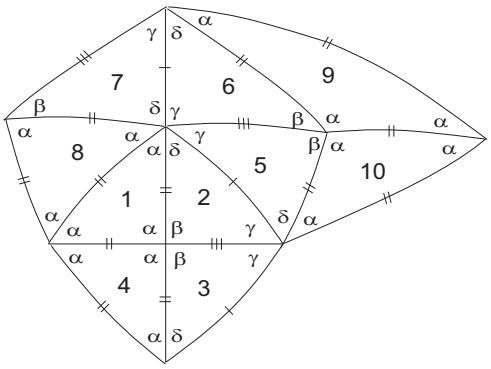

Figure 3.109: Local configuration.

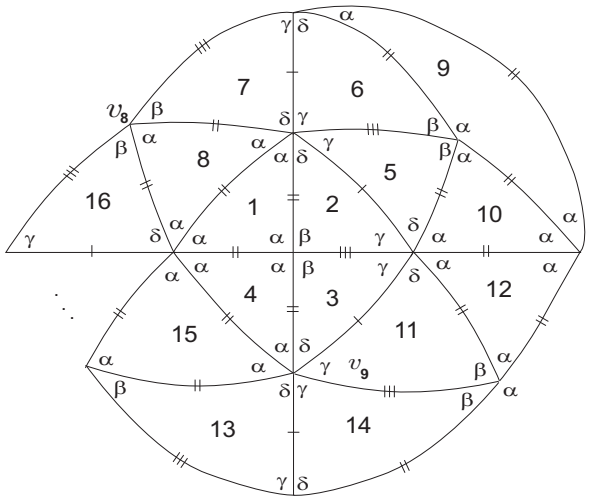

Figure 3.110: Local configuration.

The other position of tile numbered 13 implies that, at vertex v_9, the sequence of angles is $(\alpha, \delta, \gamma, \beta, \delta, \delta)$ (Figure 3.111).

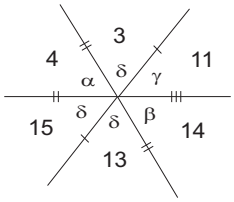

Figure 3.111: Angles arrangement at vertex v_9.

Summarizing,

$$\alpha+\beta=\pi,\ \alpha+\gamma+\delta=\pi,\ \beta+2\delta=\pi \text{ and } 2\alpha+p\delta=\pi,\ p\geq 1,$$

which implies that $\delta > \frac{\pi}{6}$ and $p = 1$. Therefore, $\alpha = \gamma = \frac{2\pi}{5}$, $\delta = \frac{\pi}{5}$ and $\beta = \frac{3\pi}{5}$. The configuration extends to the following one and we are led to vertices partially surrounded by three angles β, whose sum 2β violates the angles folding relation.

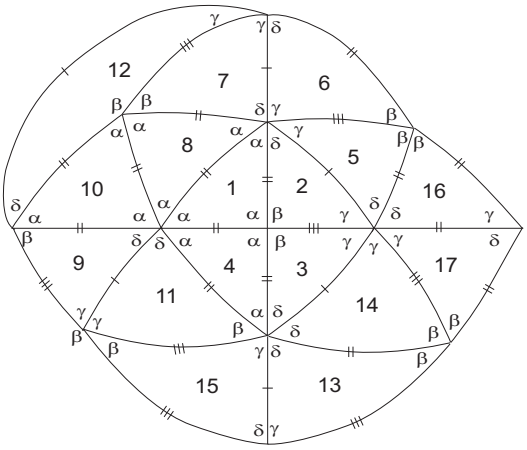

Figure 3.112: Local configuration.

2.2.3.2 Suppose now that $\alpha+\gamma+\delta<\pi$. Then, $\alpha+2\gamma+\delta=\pi$ or $\alpha+\gamma+r\delta=\pi$, for some $r\geq 1$. The first case is similar to the one studied in 2.2.2.
If $\alpha+\gamma+r\delta=\pi,\ r\geq 1$, the configuration in Figure 3.101 can be extended and we get the one in Figure 3.113.

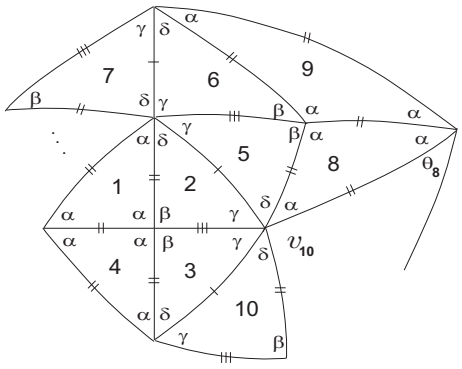

Figure 3.113: Local configuration.

A decision about the angle labeled $\theta_8 \in \{\alpha, \beta\}$ must be taken.

2.2.3.2.1 Assuming that $\theta_8 = \alpha$, the sum containing two alternate angles α must satisfy $2\alpha + p\delta = \pi$, for some $p \geq 1$, otherwise it would satisfy $2\alpha + \gamma = \pi$ and consequently, by the adjacency rules for the sides, the other sum would be $\beta+\alpha+\delta = \pi$, which is impossible. Therefore, the configuration extends a bit more to the one shown in Figure 3.114. Note that to avoid the appearance of one angle β at vertex v_{11}, the sides of tile 12 must be in the position illustrated. Looking at the angle $\omega = \beta$, we conclude that the configuration below can not be extended.

2.2.3.2.2 If $\theta_8 = \beta$, the vertex labeled v_{10} is as illustrated in Figure 3.115 and we conclude that the other sum of alternate angles satisfies $\gamma + (r+1)\delta = \pi$. Consequently $\delta = \alpha < \gamma$, which is impossible.

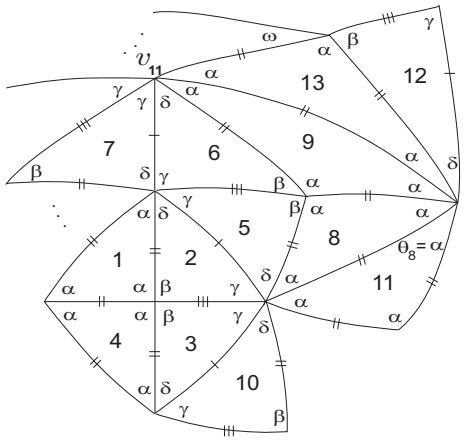

Figure 3.114: Local configuration.

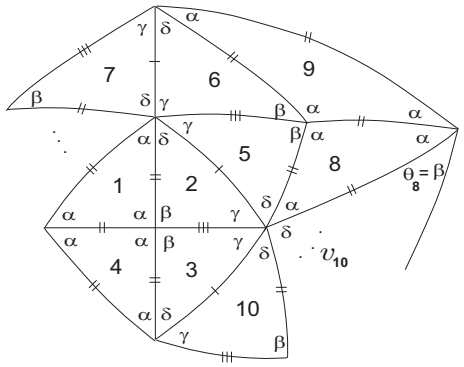

Figure 3.115: Local configuration.

□

Proposition 3.8 *If $x = \beta$ and $\alpha + x < \pi$, then $\Omega(T_1, T_2) = \varnothing$.*

Proof. Suppose that $x = \beta$ (see Figure 3.116) and $\alpha + x < \pi$. Then,

$$\gamma + \delta > \alpha > \frac{\pi}{3},\ \gamma > \frac{\pi}{6}$$

and consequently $\alpha + \beta + \gamma = \pi$ or $\alpha + \beta + t\delta = \pi$, for some $t \geq 1$.

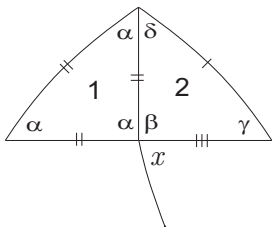

Figure 3.116: Local configuration.

1. Assume that $\alpha + \beta + \gamma = \pi$. The configuration in Figure 3.116 extends to the one illustrated in Figure 3.117 and tile 4 has two possible positions. Either way, the other sum of alternate angles satisfies $2\beta + \delta = \pi$, which is impossible since $\beta + \gamma + \delta > \pi$.

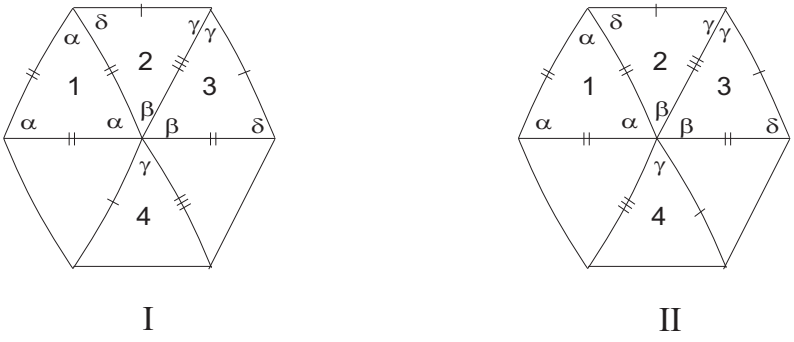

Figure 3.117: Local configurations.

2. If $\alpha + \beta + t\delta = \pi$, for some $t \geq 1$ and since $\beta + \gamma + \delta > \pi$, one has $\gamma > \alpha > \frac{\pi}{3}$.

Assuming that $\gamma \geq \frac{\pi}{2}$, then, $\beta > \frac{\pi}{2}$ and $\alpha < \frac{\pi}{2}$, contradicting the adjacency condition (3.4). Therefore, $\delta < \gamma < \frac{\pi}{2}$, $\alpha < \frac{\pi}{2}$ and consequently $\beta \geq \frac{\pi}{2}$.

2.1 Suppose firstly, that $\beta = \frac{\pi}{2}$. The configuration in Figure 3.116 extends to the one below and a decision must be taken about the angle $\theta_1 \in \{\gamma, \delta\}$.

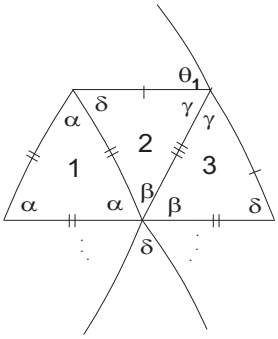

Figure 3.118: Local configuration.

2.1.1 If $\theta_1 = \gamma$, then the sum containing two angles γ is $2\gamma + \delta = \pi$, since $\gamma > \frac{\pi}{3}$ and $\gamma + \delta > \frac{\pi}{2}$. Extending the configuration above, tile 8 has two possible positions as shown in Figure 3.119-I and II.

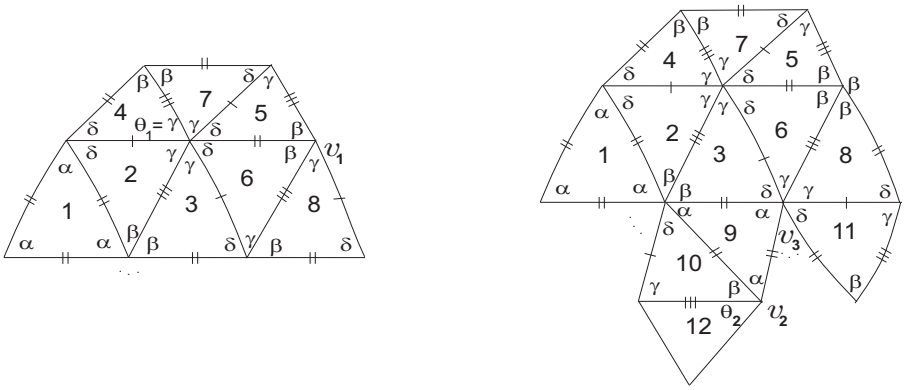

Figure 3.119: Local configurations.

In Figure 3.119-I, the sum of the alternate angles β and γ, at vertex v_1, must satisfy $\beta + \gamma = \pi$, which is impossible since $\beta = \frac{\pi}{2}$ and $\gamma < \beta$.

In Figure 3.119-II, the angle θ_2 in tile 12 must be γ or β.

If $\theta_2 = \gamma$, one of the sums of alternate angles, at vertex v_2, satisfies $\alpha+\gamma+p\delta = \pi$ and the other $\beta+\delta+p\delta = \pi$, for some $p \geq 1$ (see Figure 3.120). From $\alpha+\gamma+p\delta = \beta+\delta+p\delta$, we conclude that $\alpha + \gamma = \beta + \delta$ and since $\gamma > \alpha$, then $\delta > \frac{\pi}{6}$, which contradicts the assumption $\alpha + \beta + t\delta = \pi,\ t \geq 1$. Hence, $\theta_2 = \beta$.

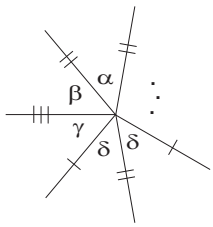

Figure 3.120: Angles arrangement at vertex v_2.

From the conditions, $\alpha + \beta + t\delta = \pi$ and $\alpha + \gamma + p\delta = \pi$, at vertex v_3, we get $\gamma + p\delta = \beta + t\delta$ and since $\gamma + \delta > \frac{\pi}{2}$, then $p < t + 1$. On the other hand, from the same assumptions and since $\gamma < \beta$, we get $t < p$. Therefore, $t < p < t + 1$, which is impossible.

2.1.2 If $\theta_1 = \delta$, the configuration in Figure 3.118 is now,

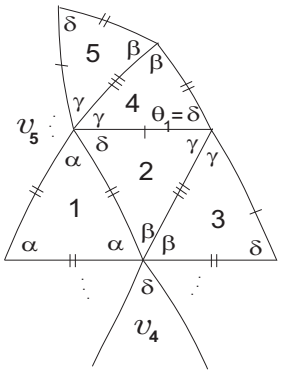

Figure 3.121: Local configuration.

Once again, by the conditions $\alpha + \beta + t\delta = \pi$, at vertex v_4 and $\alpha + \gamma + p\delta = \pi$, at vertex v_5, a contradiction is achieved.

2.2 Assuming that $\beta > \frac{\pi}{2}$ and since $\alpha + \delta < \alpha + \gamma < \alpha + \beta < \pi,\ 2\beta > \pi$ and $\delta < \gamma < \frac{\pi}{2}$, then vertices of valency four must be surrounded by alternate angles γ and β or δ and β.

2.2.1 Extending the same configuration in Figure 3.118 and if the angle labeled θ_1 is γ, then one has $2\gamma + q\delta = \pi$, for some $q \geq 1$ and we get the one illustrated in Figure 3.122.

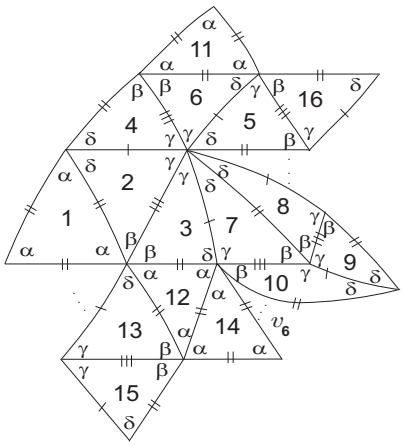

Figure 3.122: Local configuration.

Both sums of the alternate angles at vertex v_6 are $\alpha+\gamma+p\delta = \pi$ and $\alpha+\beta+p\delta = \pi$, which is a contradiction, since $\gamma < \beta$.

2.2.2 Suppose finally that $\theta_1 = \delta$ (see Figure 3.118). The sum containing α and γ must satisfy $\alpha+\gamma+p\delta = \pi$, for some $p \geq 1$ and the configuration is the one illustrated in Figure 3.123.

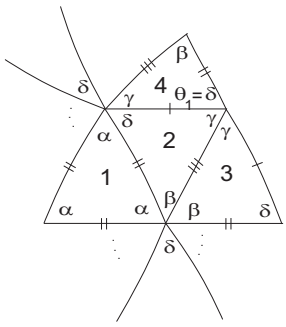

Figure 3.123: Local configuration.

From the sums $\alpha + \gamma + p\delta = \pi$ and $\alpha + \beta + t\delta = \pi$ assumed in 2., we get the same contradiction as in 2.1.1..

□

3.4 Isohedrality-Classes and Isogonality-Classes

Recall that, a spherical isometry σ is a *symmetry* of τ if σ maps every tile of τ into a tile of τ, where τ is a spherical f-tiling.

Furthermore, tiles T and T' of τ are in the same *transitivity class* if exists a symmetry that maps T into T'. If τ contains k transitivity classes of tiles, then τ is said *k-isohedral*. Similarly, if there are k transitivity classes of vertices, then τ is said *k-isogonal*.

Here, we present the transitivity classes of isogonality and isohedrality of the dihedral f-tilings obtained $\mathcal{C}_1^\delta$, $\mathcal{C}_2^\delta$ $(\delta \in]0, \delta_0[)$, $\mathcal{B}^p$, $\mathcal{C}^p$ $(p \geq 4)$, $\mathcal{D}^m$ $(m \geq 5)$, $\mathcal{E}_\alpha$ $(\alpha \in]\frac{\pi}{2}, \pi[)$, $\mathcal{F}^k$ $(k \geq 1)$, $\mathcal{D}$, $\mathcal{E}$, $\mathcal{F}$ and $\mathcal{G}$.

In **Table 3.1** is shown a complete list of all spherical dihedral f-tilings, whose prototiles are an equilateral triangle T_1 of angle α and a scalene triangle T_2 of angles δ, γ, β, $(\delta < \gamma < \beta)$.
We have used the following notation:

- M and N are, respectively, the number of triangles congruent to T_1 and the number of triangles congruent to T_2 used in such dihedral f-tilings;

- The numbers of isohedrality-classes and isogonality-classes for the symmetry group are denoted, respectively, by # isoh. and # isog.;

- The angles δ and γ, in f-tiling $\mathcal{C}_1^\delta$, obey

$$\frac{-\cos(\gamma+\delta)}{1+\cos(\gamma+\delta)} = \frac{\cos\gamma\,\cos\delta}{\sin\gamma\,\sin\delta}.$$

  Besides, $\alpha = \pi - (\gamma + \delta)$;

- $\delta_0 \approx 54.735^\circ$ and $\gamma_0 \approx 70.529^\circ$;

- $\alpha = \alpha_1^p$, $p \geq 4$, in f-tiling $\mathcal{B}^p$, is the solution of

$$\frac{\cos\alpha(1+\cos\alpha)}{\sin^2\alpha} = \frac{\cos\delta + \cos\gamma\cos\beta}{\sin\gamma\sin\beta},$$

  with $p\delta = \pi$, $\beta = \pi - \alpha$ and $\gamma = \pi - 2\alpha$;

- $\alpha = \alpha_2^p, \;\; p \geq 4$, in f-tiling $\mathcal{C}^p$, is the solution of

$$\frac{\cos\alpha(1+\cos\alpha)}{\sin^2\alpha} = \frac{\cos\delta + \cos\gamma\cos\beta}{\sin\gamma\sin\beta},$$

  with $p\delta = \pi$, $\beta = \pi - \alpha$ and $\gamma = \frac{\pi}{2} - \frac{\alpha}{2}$;

- $\alpha = \alpha_3^m, \;\; m \geq 5$, in f-tiling $\mathcal{D}^m$, is the solution of

$$\frac{\cos\alpha(1+\cos\alpha)}{\sin^2\alpha} = \frac{\cos\delta + \cos\gamma\cos\beta}{\sin\gamma\sin\beta},$$

  with $m\delta = \pi$, $\beta = \pi - \alpha$ and $\gamma = \frac{\pi}{2} - \frac{\alpha}{2} - \frac{\pi}{2m}$;

- $\beta = \beta_\alpha$, in f-tiling $\mathcal{E}_\alpha$, is given by

$$\frac{\cos\alpha(1+\cos\alpha)}{\sin^2\alpha} = \frac{\cos\gamma + \cos\delta\cos\beta}{\sin\delta\sin\beta},$$

  with $\gamma = \pi - \alpha$ and $\delta = \pi - \beta$;

- $\delta = \delta_1^k$, in f-tiling $\mathcal{F}^k$, is the solution of

$$\frac{\cos\alpha(1+\cos\alpha)}{\sin^2\alpha} = \frac{\cos\gamma + \cos\delta\cos\beta}{\sin\delta\sin\beta},$$

  with $\alpha = \pi - (2k+1)\delta, \gamma = (k+1)\delta$ and $\beta = \pi - (k+1)\delta$.

f-**tiling**	α	δ	γ	β	M	N	# isoh.	# isog.
$\mathcal{C}_1^\delta$	$]\gamma_0, \frac{\pi}{2}[$	$]0, \delta_0[$	$]\delta_0, \frac{\pi}{2}[$	$\frac{\pi}{2}$	8	24	4	6
$\mathcal{C}_2^\delta$	$]\gamma_0, \frac{\pi}{2}[$	$]0, \delta_0[$	$]\delta_0, \frac{\pi}{2}[$	$\frac{\pi}{2}$	8	24	12	6
$\mathcal{B}^p,\ p \geq 4$	α_1^p	$\frac{\pi}{p}$	$\pi - 2\alpha$	$\pi - \alpha$	$4p$	$4p$	3	3
$\mathcal{C}^p,\ p \geq 4$	α_2^p	$\frac{\pi}{p}$	$\frac{\pi}{2} - \frac{\alpha}{2}$	$\pi - \alpha$	$2p$	$4p$	2	3
$\mathcal{D}^m,\ m \geq 5$	α_3^m	$\frac{\pi}{m}$	$\frac{\pi}{2} - \frac{\alpha}{2} - \frac{\pi}{2m}$	$\pi - \alpha$	$4m$	$8m$	4	3
$\mathcal{E}_\alpha$	$]\frac{\pi}{2}, \pi[$	$\pi - \beta$	$\pi - \alpha$	β_α	2	6	2	1
$\mathcal{F}^k,\ k \geq 1$	$\pi - (2k+1)\delta$	δ_1^k	$(k+1)\delta$	$\pi - (k+1)\delta$	2	$6(2k+1)$	$2k+2$	$k+1$
$\mathcal{D}$	$72.75°$	$53.63°$	$\frac{\pi}{3}$	$107.25°$	6	12	2	3
$\mathcal{E}$	$72°$	$36°$	$\frac{\pi}{3}$	$108°$	12	12	3	3
$\mathcal{F}$	$70.5°$	$24.7°$	$\frac{\pi}{3}$	$109.5°$	12	24	4	3
$\mathcal{G}$	$65.56°$	$34.72°$	$\frac{\pi}{4}$	$114.44°$	16	32	4	3

Table 3.1: Dihedral f-Tilings of the Sphere by Equilateral and Scalene Triangles

3.5 Deformations

Here, we present a deformation into the standard folding (up to a rotation) of the dihedral f-tilings founded in the previous sections. As we made in Chapter 2, we give geometrical sketches of a deformation via the paths $\gamma_v(t)$ referred in Theorem 1.3. Likewise, the arrows indicate the way we should move vertices allowing each f-tiling to be joined to the standard one. In order to facilitate the reasoning, we attribute to each face a suitable sign and, whenever the f-tiling is symmetric, we label only the angles in the semi-space $x \geq 0$.

It should be pointed out that, in each step of the deformation, the angle folding relation and the continuity of the deformation map ϕ must be preserved. The function $\phi : [0,1] \to \mathscr{T}^{\mathcal{O}}(S^2)$ maps each $t \in [0,1]$ into a f-tiling τ_t leading, generally to a piecewise-defined function.
Recall that, the space $\mathscr{T}^{\mathcal{O}}(S^2)$ is equipped with the metric structure given by (Proposition 1.4)

$$c(\tau_1^{o_1}, \tau_2^{o_2}) = \sum_{\substack{\text{F face of} \\ \tau_1 \cup \tau_2}} \lambda(F)\, Area(F)\,,$$

where $\tau_1^{o_1}$, $\tau_2^{o_2} \in \mathscr{T}^{\mathcal{O}}(S^2)$ and $\lambda(F) = 1$ if F is errant and $\lambda(F) = 0$ if F is non-errant.

Let us show that:

1. Each member of the family of f-tilings $(\mathcal{C}_1^{\delta})^o$ is deformable into τ_{stand}^{+}. They are composed by vertices of valency four surrounded exclusively by angles β and vertices of valency six whose both sums of alternate angles satisfy $\alpha + \gamma + \delta = \pi$, with $\alpha \in]70.529°, \frac{\pi}{2}[$, $\gamma \in]54.735°, \frac{\pi}{2}[$ and $\delta \in]0, 54.735°[$. Figure 3.124 shows the process of deformation of a representative member, where $\phi : [0,1] \to \mathscr{T}^{\mathcal{O}}(S^2)$ is the map defined by $\phi(t) = \tau_t$.

   Note that the deformation of this f-tiling is quite similar to the deformation of $(\mathcal{B}_2)^o$ in Chapter 2.

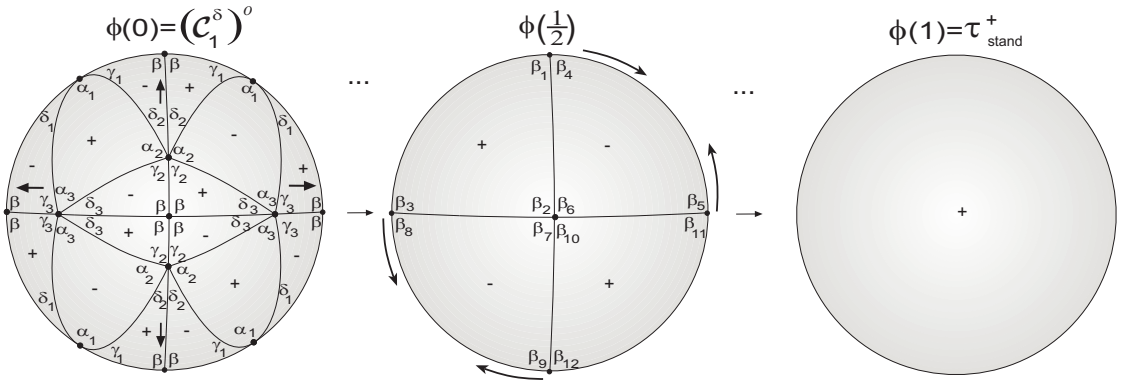

Figure 3.124: Deformation of $\left(\mathcal{C}_1^{\delta}\right)^o$.

For $t \in [0, \frac{1}{2}]$:

- $\star$ $\widetilde{\delta}_1(t) = (1-2t)\delta_1$ and $\widetilde{\gamma}_1(t) = (1-2t)\gamma_1$;
- $\star$ $\widetilde{\alpha}_1(t) = \alpha_1 + 2t\delta_1 + 2t\gamma_1$;
- $\star$ $\widetilde{\alpha}_k(t) = (1-2t)\alpha_k,\ k = 2, 3$;
- $\star$ $\widetilde{\delta}_2(t) = \delta_2 + t\alpha_2$ and $\widetilde{\gamma}_2(t) = \gamma_2 + t\alpha_2$;
- $\star$ $\widetilde{\delta}_3(t) = \delta_3 + t\alpha_3$ and $\widetilde{\gamma}_3(t) = \gamma_3 + t\alpha_3$.

For $t \in]\frac{1}{2}, 1]$:

- $\star$ $\widetilde{\beta}_6(t) = (2-2t)\beta_6$ and $\widetilde{\beta}_7(t) = \pi - \widetilde{\beta}_6(t)$;
- $\star$ $\widetilde{\beta}_2(t) = \beta_2 - \beta_6 + 2t\beta_6$ and $\widetilde{\beta}_{10}(t) = \pi - \widetilde{\beta}_2(t)$;
- $\star$ $\widetilde{\beta}_k(t) \equiv \beta,\ k = 1, 3, 4, 5, 8, 9, 11, 12$.

The continuity of ϕ in $[0, 1]$ can be proved using a reasoning similar to the one done in Chapter 2 for the f-tiling $(\mathcal{B}_2)^o$.

2. Each member of $(\mathcal{C}_2^{\delta})^o$ is deformable into τ_{stand}^-. They are composed by vertices of valency four surrounded exclusively by angles β and vertices of valency six, whose sums of alternate angles satisfy $\alpha+\gamma+\delta = \pi$, with $\delta \in]0, 54.735°[,\ \gamma \in]54.735°, \frac{\pi}{2}[$ and $\alpha \in]70.529°, \frac{\pi}{2}[$. In this case, for the process of deformation, areas of the triangles of angles $(\widetilde{\beta}(t), \widetilde{\gamma}(t), \widetilde{\delta}(t))_{t\in[0,\frac{1}{2}]}$ converge to zero and the areas of triangles

$(\widetilde{\alpha}(t), \widetilde{\alpha}(t), \widetilde{\alpha}(t))_{t\in[0,\frac{1}{2}]}$ converge to $\frac{\pi}{2}$, as $t \to \frac{1}{2}^-$. Figure 3.125 helps us understand this process, where $\phi : [0,1] \to \mathscr{T}^{\mathcal{O}}(S^2)$ is a deformable map defined by $\phi(t) = \tau_t$.

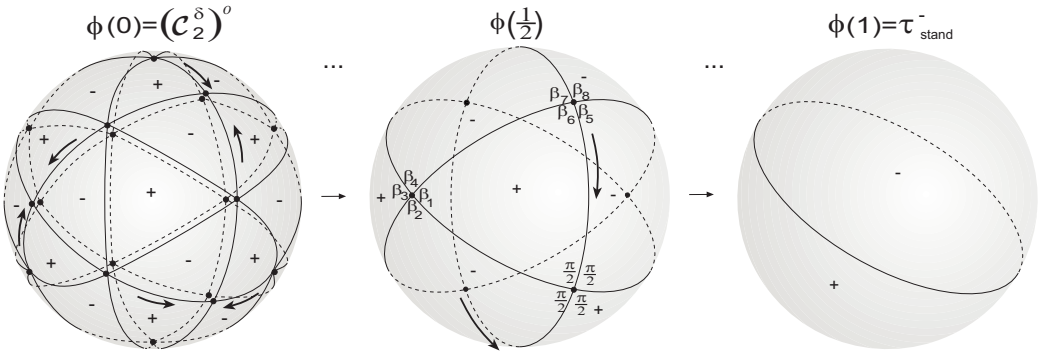

Figure 3.125: Deformation of $(\mathcal{C}_2^{\delta})^o$

For each $t \in [0, \frac{1}{2}]$:

- $\widetilde{\delta}(t) = (1-2t)\delta$;
- $\widetilde{\gamma}(t) = \gamma + 2t(\frac{\pi}{2} - \gamma)$;
- $\widetilde{\alpha}(t) = \pi - \widetilde{\delta}(t) - \widetilde{\gamma}(t)$.

If $t \in]\frac{1}{2}, 1]$;

- $\widetilde{\beta}_i(t) = (2-2t)\beta_i,\ i = 1, 2$;
- $\widetilde{\beta}_j(t) \equiv \frac{\pi}{2},\ j = 5, 6, 7, 8$;
- $\widetilde{\beta}_4(t) = \pi - \widetilde{\beta}_2(t)$ and $\widetilde{\beta}_5(t) = \pi - \widetilde{\gamma}_1(t)$.

The continuity of ϕ at $t = \frac{1}{2}^+$ and $t = 1$ is similar to the one done in Chapter 2 for $\mathcal{B}_1$. So, we will concentrate our attention proving that ϕ is continuous at $t = 0$ and $t = \frac{1}{2}^-$.

Consider $t \in]0, \frac{1}{2}[$. Then,

$$\begin{aligned} c(\tau^{o_t}, \tau_0) &= \sum_{\substack{F \text{face of} \\ \tau_t \cup \tau_0}} \lambda(F)\, Area(F) \\ &\leq K \times \left| \left(\frac{\pi}{2} + \widetilde{\delta}(0) + \widetilde{\gamma}(0) - \pi \right) - \left(\frac{\pi}{2} + \widetilde{\delta}(t) + \widetilde{\gamma}(t) - \pi \right) \right| \\ &+ 12 \times \left| \frac{(3\widetilde{\alpha}(0) - \pi) - (3\widetilde{\alpha}(t) - \pi)}{6} \right| \\ &= K \times \left| \delta + \gamma - \frac{\pi}{2} - (1-2t)\delta - \gamma - 2t\left(\frac{\pi}{2} - \gamma \right) + \frac{\pi}{2} \right| \\ &+ 6 \times \left| 3\alpha - \pi - 3\pi + 3\widetilde{\delta}(t) + 3\widetilde{\gamma}(t) + \pi \right|, \end{aligned}$$

where $K + 12$ is the total number of errant faces, see Figure 3.126.

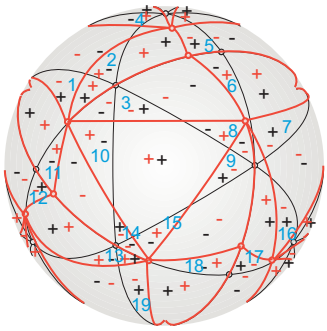

Figure 3.126: Errant faces of $\tau_t \cup \tau_0$.

When, $t \to 0^+$, we conclude that $c(\tau^{o_t}, \tau_0) \to 0$.

For $t \in]0, \frac{1}{2}[$:

$$\begin{aligned} c(\tau^{o_t}, \tau_{\frac{1}{2}}) &= \sum_{\substack{F \text{face of} \\ \tau_t \cup \tau_{\frac{1}{2}}}} \lambda(F)\, Area(F) \\ &= 24 \times \left(\frac{\pi}{2} + \widetilde{\delta}(t) + \widetilde{\gamma}(t) - \pi \right). \end{aligned}$$

When $t \to \frac{1}{2}^-$, we conclude that $c(\tau^{o_t}, \tau_{\frac{1}{2}}) \to 0$.

3. For each $p \geq 4$, $(\mathcal{B}^p)^o$ is deformable into τ^+_{stand}. In the next figure, we present a geometrical sketch of the process of deformation of $\mathcal{B}^4$ and gives us an ideia how

to define the deformable map $\phi : [0,1] \to \mathscr{T}^{\mathcal{O}}(S^2)$. The angles that compose $\mathcal{B}^4$ are $\alpha \approx 66.7°$, $\beta \approx 113°$ $\gamma \approx 46.5°$ and $\delta = \frac{\pi}{4}$.

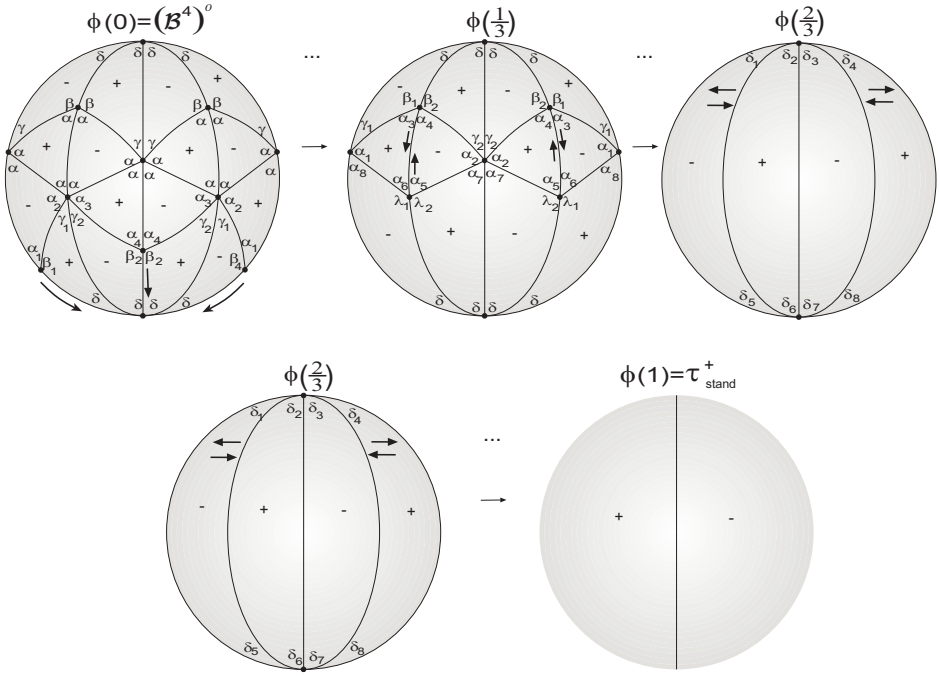

Figure 3.127: Deformation of $(\mathcal{B}^4)^o$.

So, for $t \in [0, \frac{1}{3}]$:

- $\star$ $\widetilde{\gamma}_i(t) = (1-3t)\gamma_i,\ i = 1, 2;$
- $\star$ $\widetilde{\alpha}_i(t) = \alpha_i + 3t\gamma_{i-1},\ i = 2, 3;$
- $\star$ $\widetilde{\alpha}_k(t) = \alpha_k + 3t\left(\frac{\pi}{4} - \alpha_k\right),\ k = 1, 4;$
- $\star$ $\widetilde{\beta}_1(t) = \pi - \widetilde{\alpha}'_1(t)$, where $\widetilde{\alpha}'_1(t) = \alpha'_1 + 3t\left(\frac{\pi}{4} - \alpha'_1\right)$ belongs to the semi-space $x \leq 0$.
- $\star$ $\widetilde{\beta}_2(t) = \pi - \widetilde{\alpha}_4(t).$

If $t \in]\frac{1}{3}, \frac{2}{3}]$:

- $\star$ $\widetilde{\alpha}_i(t) = (2-3t)\alpha_i,\ i = 1, 2;$
- $\star$ $\widetilde{\alpha}_i(t) = 2\alpha_i - \frac{\pi}{2} + t\left(3\frac{\pi}{2} - 3\alpha_i\right),\ i = 3, 4, 5, 6;$
- $\star$ $\widetilde{\beta}_1(t) = \pi - \widetilde{\alpha}_4(t)$ and $\widetilde{\beta}_2(t) = \pi - \widetilde{\alpha}_3(t);$

- $\widetilde{\gamma}_1(t) = \gamma_1 - \frac{\alpha_1}{2} + \frac{3}{2}t\alpha_1$;
- $\widetilde{\alpha}_8(t) = \alpha_8 - \frac{\alpha_1}{2} + \frac{3}{2}t\alpha_1$;
- $\widetilde{\gamma}_2(t) = \gamma_2 - \frac{\alpha_2}{2} + \frac{3}{2}t\alpha_2$;
- $\widetilde{\alpha}_7(t) = \alpha_7 - \frac{\alpha_2}{2} + \frac{3}{2}t\alpha_2$;
- $\widetilde{\lambda}_1(t) = \pi - \widetilde{\alpha}_5(t)$ and $\widetilde{\lambda}_2(t) = \pi - \widetilde{\alpha}_6(t)$.

For $t \in]\frac{2}{3}, 1]$:

- $\widetilde{\delta}_i(t) = 3(1-t)\delta_i,\ i = 1, 4, 5, 8$;
- $\widetilde{\delta}_i(t) = \delta_i + (3t-2)\delta_{i-1},\ i = 2, 6$ and $\widetilde{\delta}_j(t) = \delta_j + (3t-2)\delta_{j+1},\ j = 3, 7$;

We will prove that ϕ is continuous in $[0, 1]$:

If $t \in]0, \frac{1}{3}[$:

$$\begin{aligned} c(\tau_t^{o_t}, \tau_0) &= \sum_{\substack{F \text{face of} \\ \tau_t \cup \tau_0}} \lambda(F)\, Area(F) \\ &= 4 \times \left(\widetilde{\gamma}_1(0) - \widetilde{\gamma}_1(t) + \widetilde{\beta}_1(0) + \widetilde{\alpha}_1(t) - \pi\right) \\ &+ 4 \times \left(\widetilde{\gamma}_2(0) - \widetilde{\gamma}_2(t) + \widetilde{\beta}_2(0) + \widetilde{\alpha}_4(t) - \pi\right) \\ &= 4 \times \left(\gamma_1 - (1-3t)\gamma_1 - \alpha_1' + \alpha_1 + 3t\left(\frac{\pi}{4} - \alpha_1\right)\right) \\ &+ 4 \times \left(\gamma_2 - (1-3t)\gamma_2 - \alpha_5 + \alpha_4 + 3t\left(\frac{\pi}{4} - \alpha_4\right)\right). \end{aligned}$$

As $t \to 0^+$, then, $c(\tau_t^{o_t}, \tau_0) \to 0$.

For $t \in]0, \frac{1}{3}[$:

$$\begin{aligned} c(\tau_t^{o_t}, \tau_{\frac{1}{3}}) &= \sum_{\substack{F \text{face of} \\ \tau_t \cup \tau_{\frac{1}{3}}}} \lambda(F)\, Area(F) \\ &= 4 \times \left(\widetilde{\gamma}_1(t) + \widetilde{\beta}_1(t) + \delta - \pi\right) + 4 \times \left(\widetilde{\gamma}_2(t) + \widetilde{\beta}_2(t) + \delta - \pi\right) \\ &= 8 \times \left((1-3t)\gamma_1 + \pi - \widetilde{\alpha}_1'(t) + \delta - \pi\right) \\ &= 8 \times \left((1-3t)\gamma_1 - \alpha_1' - 3t\left(\frac{\pi}{4} - \alpha_1'\right) + \delta\right). \end{aligned}$$

When, $t \to \frac{1}{3}^{-}$, we may conclude that $c(\tau_t^{o_t}, \tau_{\frac{1}{3}}) \to 0$.

If $t \in]\frac{1}{3}, \frac{2}{3}[$:

$$\begin{aligned} c(\tau_t^{o_t}, \tau_{\frac{1}{3}}) &= \sum_{\substack{F \text{face of} \\ \tau_t \cup \tau_{\frac{1}{3}}}} \lambda(F)\, Area(F) \\ &= 16 \times \left(\frac{\widetilde{\alpha}_1\left(\frac{1}{3}\right) - \widetilde{\alpha}_1(t)}{2} + \widetilde{\alpha}_3(t) + \widetilde{\beta}_1(t) - \pi \right) \\ &= 16 \times \left(\frac{\alpha_1 - (2-3t)\alpha_1}{2} + \frac{3\pi}{2}t - \frac{\pi}{2} + (2-3t)\alpha_3 + \pi - \widetilde{\alpha}_5(t) - \pi \right). \end{aligned}$$

Making $t \to \frac{1}{3}^{+}$, we conclude that $c(\tau_t^{o_t}, \tau_{\frac{1}{3}}) \to 0$ and consequently ϕ is continuous at $t = \frac{1}{3}$.

For $t \in]\frac{1}{3}, \frac{2}{3}[$:

$$\begin{aligned} c(\tau_t^{o_t}, \tau_{\frac{2}{3}}) &= \sum_{\substack{F \text{face of} \\ \tau_t \cup \tau_{\frac{2}{3}}}} \lambda(F)\, Area(F) \\ &= 8 \times (\widetilde{\alpha}_1(t) + \widetilde{\alpha}_3(t) + \widetilde{\alpha}_6(t) - \pi) \\ &= 8 \times \left((2-3t)\alpha_1 + \frac{3\pi}{2}t - \frac{\pi}{2} + (2-3t)\alpha_3 + \frac{3\pi}{2}t - \frac{\pi}{2} + (2-3t)\alpha_6 - \pi \right). \end{aligned}$$

Therefore, $c(\tau_t^{o_t}, \tau_{\frac{2}{3}}) \underset{(t \to \frac{2}{3}^{-})}{\longrightarrow} 0$.

If $t \in]\frac{2}{3}, 1[$:

$$\begin{aligned} c(\tau_t^{o_t}, \tau_{\frac{2}{3}}) &= \sum_{\substack{F \text{face of} \\ \tau_t \cup \tau_{\frac{2}{3}}}} \lambda(F)\, Area(F) \\ &= 4 \times \left(2 \left(\widetilde{\delta}_1\left(\frac{2}{3}\right) - \widetilde{\delta}_1(t) \right) \right) = 8 \times (\delta_1 - 3(1-t)\delta_1). \end{aligned}$$

Making $t \to \frac{2}{3}^{+}$, we get $c(\tau_t^{o_t}, \tau_{\frac{2}{3}}) \to 0$.

Finally,

$$c(\tau_t^{o_t}, \tau_1) = \sum_{\substack{F \text{face of} \\ \tau_t \cup \tau_1}} \lambda(F)\, Area(F)$$
$$= 4 \times \left(2\widetilde{\delta}_1(t)\right) = 8 \times (3(1-t)\delta_1)\,.$$

As $t \to 1^-$, then $c(\tau_t^{o_t}, \tau_1) \to 0$. Consequently, ϕ is continuous in $[0,1]$.

4. For any $p \geq 4$, $(\mathcal{C}^p)^o$ is deformable into τ^+_{stand}. The process is quite similar to the one in $(\mathcal{B}^p)^o$, as illustrated in the next figure for $p = 4$. The angles are $\alpha = 67°,\ \beta = 113°\ \gamma = 56.4°$ and $\delta = \frac{\pi}{4}$.

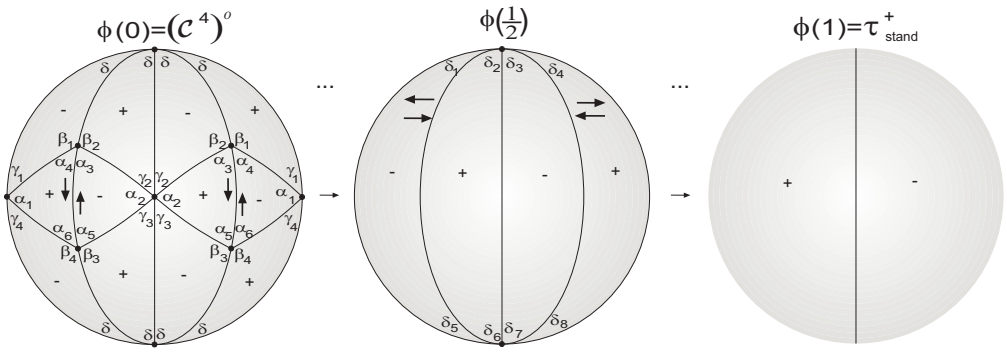

Figure 3.128: Deformation of $(\mathcal{C}^4)^o$.

5. Each element of the family of f-tilings $(\mathcal{D}^m)^o,\ m \geq 5$ is deformable into τ^-_{stand}. Figure 3.132 illustrates the process of deformation, for the member $(\mathcal{D}^5)^o$ and helps us to define the map $\phi : [0,1] \to \mathscr{T}^{\mathcal{O}}(S^2)$. The angles that compose $\mathcal{D}^5$ are $\alpha \approx 63.442°,\ \beta \approx 116.558°,\ \gamma \approx 40.279°$ and $\delta = \frac{\pi}{5}$.

   In the first stage of the deformation (see Figure 3.129), when $t \in [0, \frac{1}{3}]$, one has:

   - $\star\ \widetilde{\alpha}_i(t) = (1-3t)\alpha_i,\ i = 1, 6, 7, 12, 13;$
   - $\star\ \widetilde{\gamma}_i(t) = \gamma_i + 3t\frac{\alpha_1}{2},\ i = 1, 6$ and $\widetilde{\gamma}_i(t) = \gamma_i + 3t\frac{\alpha_6}{2},\ i = 2, 7;$
   - $\star\ \widetilde{\gamma}_i(t) = \gamma_i + 3t\frac{\alpha_7}{2},\ i = 3, 8$ and $\widetilde{\gamma}_i(t) = \gamma_i + 3t\frac{\alpha_{12}}{2},\ i = 4, 9;$
   - $\star\ \widetilde{\gamma}_i(t) = \gamma_i + 3t\frac{\alpha_{13}}{2},\ i = 5, 10;$
   - $\star\ \widetilde{\beta}_k(t) = \beta_k + 3t\left(\frac{\pi}{2} - \beta_k\right),\ k = 1, ..., 10;$

- $\widetilde{\alpha}_k(t) = \pi - \widetilde{\beta}_k(t),\ k = 2, 9,\ \widetilde{\alpha}_3(t) = \pi - \widetilde{\beta}_7(t),\ \widetilde{\alpha}_4(t) = \pi - \widetilde{\beta}_1(t),\ \widetilde{\alpha}_5(t) = \pi - \widetilde{\beta}_6(t),\ \widetilde{\alpha}_8(t) = \pi - \widetilde{\beta}_4(t),\ \widetilde{\alpha}_{10}(t) = \pi - \widetilde{\beta}_8(t),\ \widetilde{\alpha}_{11}(t) = \pi - \widetilde{\beta}_3(t),\ \widetilde{\alpha}_{14}(t) = \pi - \widetilde{\beta}'_5(t)$ and $\widetilde{\alpha}_{15}(t) = \pi - \widetilde{\beta}'_{10}(t)$, where $\widetilde{\beta}'_5(t) = \beta'_5 + 3t\left(\frac{\pi}{2} - \beta'_5\right)$ and $\widetilde{\beta}'_{10}(t) = \beta'_{10} + 3t\left(\frac{\pi}{2} - \beta'_{10}\right)$ belong to the semi-space $x \leq 0$.

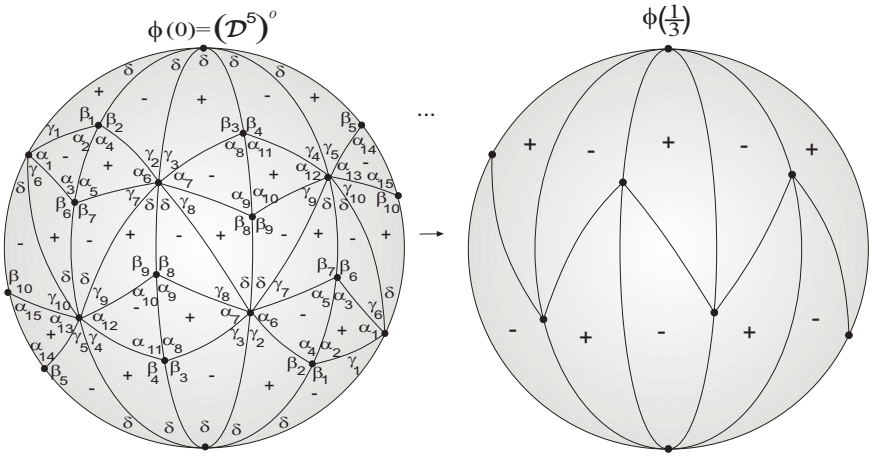

Figure 3.129: First stage of deformation.

In the second stage of the deformation of $(\mathcal{D}^5)^o$, for $t \in]\frac{1}{3}, \frac{2}{3}]$ (see Figure 3.130):

- $\widetilde{\delta}_i(t) = (2 - 3t)\delta_i,\ i = 2, 3, 6, 7, 9;$
- $\widetilde{\theta}_k(t) = \theta_k + (3t - 1)\delta_{k-4},\ k = 6, 7;$
- $\widetilde{\theta}_k(t) = \theta_k + (3t - 1)\delta_{k-2},\ k = 8, 9;$
- $\widetilde{\theta}_5(t) = \theta_5 + (3t - 1)\delta_9;$
- $\widetilde{\theta}_j(t) = 2\theta_j - \frac{4\pi}{5} + 3t\left(\frac{4\pi}{5} - \theta_j\right),\ j = 1, 2, 3, 4, 10;$
- $\widetilde{\delta}_1(t) = \pi - \widetilde{\theta}'_1(t),\ \widetilde{\delta}_4(t) = \pi - \widetilde{\theta}_3(t),\ \widetilde{\delta}_5(t) = \pi - \widetilde{\theta}_2(t),\ \widetilde{\delta}_8(t) = \pi - \widetilde{\theta}_5(t),\ \widetilde{\delta}_{10}(t) = \pi - \widetilde{\theta}'_{10}(t)$, where $\widetilde{\theta}'_k(t) = 2\theta'_k - \frac{4\pi}{5} + 3t\left(\frac{4\pi}{5} - \theta'_k\right),\ k = 1, 10$ belong to the semi-space $x \leq 0$.

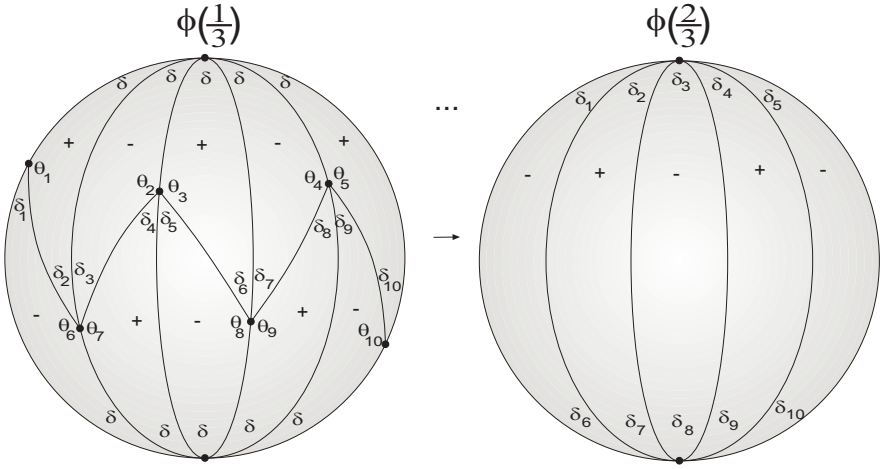

Figure 3.130: Second stage of deformation.

In the last stage of the deformation, when $t \in]\frac{2}{3}, 1]$, then:

- $\widetilde{\delta}_i(t) = 3(1-t)\delta_i,\ i = 2, 4, 7, 9;$
- $\widetilde{\delta}_j(t) = \delta_j - \delta_{j+1} + \frac{3}{2}t\delta_{j+1},\ j = 1, 6,\ \widetilde{\delta}_k(t) = \delta_k - \delta_{k-1} + \frac{3}{2}t\delta_{k-1},\ k = 5, 10$ and $\widetilde{\delta}_l(t) = \delta_l - \delta_{l-1} - \delta_{l+1} + \frac{3}{2}t(\delta_{l-1} + \delta_{l+1}),\ l = 3, 8.$

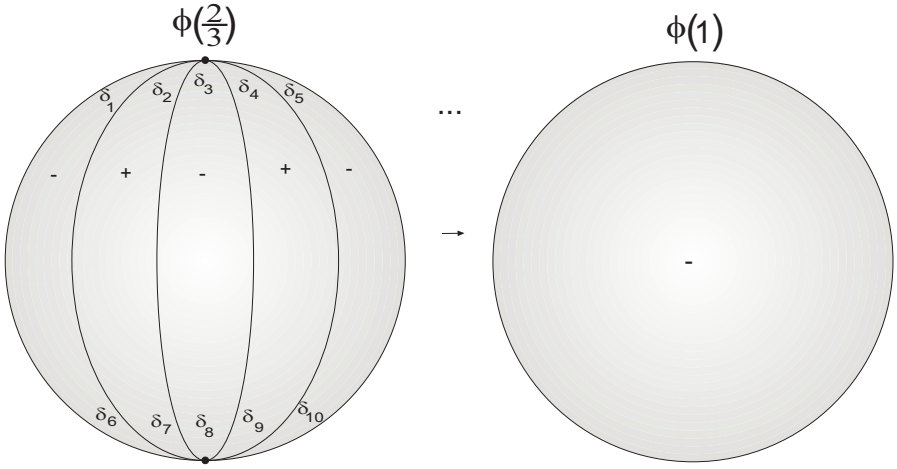

Figure 3.131: Third stage of deformation.

In short:

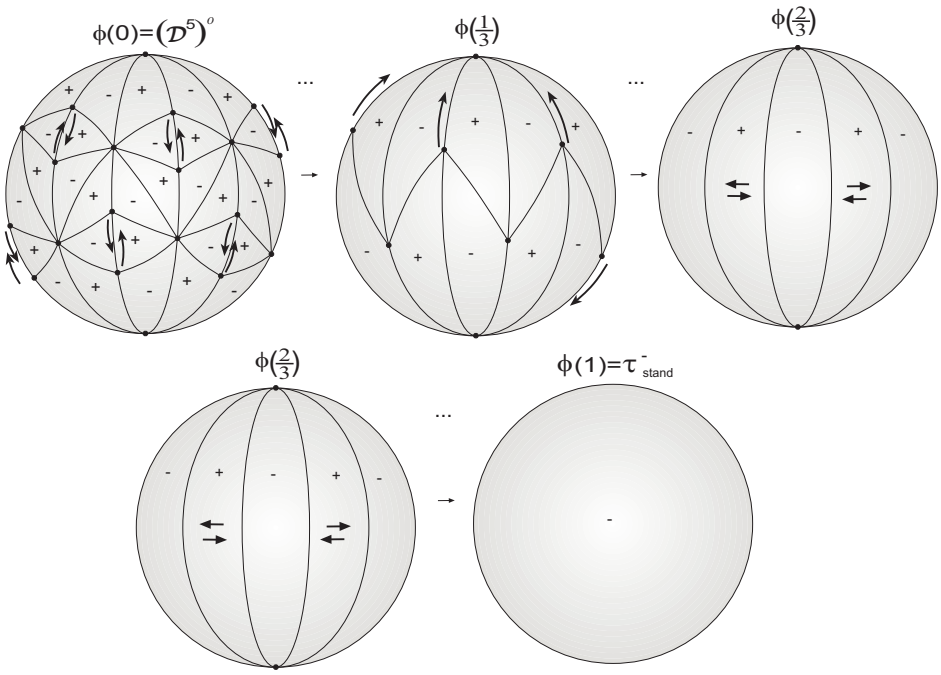

Figure 3.132: Deformation of $(\mathcal{D}^5)^o$.

Let us show that ϕ is continuous in $[0,1]$. We only need to show the continuity for $t = 0^+,\ t = \frac{1}{3}$ and $t = \frac{2}{3}^-$. In fact, for $t \in]0, \frac{1}{3}[$:

$$\begin{aligned} c(\tau_t^{o_t}, \tau_0) &= \sum_{\substack{F \text{face of} \\ \tau_t \cup \tau_0}} \lambda(F)\, Area(F) \\ &= 40 \times \left(\widetilde{\alpha}_1(0) - \widetilde{\alpha}_1(t) + \widetilde{\alpha}_2(0) + \widetilde{\beta}_1(t) - \pi \right) \\ &= 40 \times \left(\alpha_1 - (1-3t)\alpha_1 + \pi - \beta_2 + \beta_1 + 3t \left(\frac{\pi}{2} - \beta_1 \right) - \pi \right). \end{aligned}$$

As, $t \to 0^+$, one has $c(\tau_t^{o_t}, \tau_0) \to 0$.

If $t \in]0, \frac{1}{3}[$:

$$\begin{aligned} c(\tau_t^{o_t}, \tau_{\frac{1}{3}}) &= \sum_{\substack{F\text{face of} \\ \tau_t \cup \tau_{\frac{1}{3}}}} \lambda(F)\, Area(F) \\ &= 20 \times \left(\sum_{i=1}^{3} \widetilde{\alpha}_i(t) - \pi \right) \\ &= 20 \times \left((1-3t)\alpha_1 + \pi - \widetilde{\beta}_2(t) + \pi - \widetilde{\beta}_7(t) - \pi \right). \end{aligned}$$

When, $t \to \frac{1}{3}^{-}$, then $c(\tau_t^{o_t}, \tau_{\frac{1}{3}}) \to 0$.

Now, if $t \in]\frac{1}{3}, \frac{2}{3}[$,

$$\begin{aligned} c(\tau_t^{o_t}, \tau_{\frac{1}{3}}) &= \sum_{\substack{F\text{face of} \\ \tau_t \cup \tau_{\frac{1}{3}}}} \lambda(F)\, Area(F) \\ &= 10 \times \left(\widetilde{\delta}_3\left(\frac{1}{3}\right) - \widetilde{\delta}_3(t) + \widetilde{\theta}_2\left(\frac{1}{3}\right) + \widetilde{\delta}_4(t) - \pi \right) \\ &= 10 \times \left(\delta_3 - (2-3t)\delta_3 + \theta_2 - 2\theta_3 + \frac{4\pi}{5} - 3t\left(\frac{4\pi}{5} - \theta_3\right) \right). \end{aligned}$$

When, $t \to \frac{1}{3}^{+}$, we may conclude that $c(\tau_t^{o_t}, \tau_{\frac{1}{3}}) \to 0$. Therefore, ϕ is continuous at $t = \frac{1}{3}$.

For $t \in]\frac{1}{3}, \frac{2}{3}[$,

$$\begin{aligned} c(\tau_t^{o_t}, \tau_{\frac{2}{3}}) &= \sum_{\substack{F\text{face of} \\ \tau_t \cup \tau_{\frac{2}{3}}}} \lambda(F)\, Area(F) \\ &= 10 \times \left(\widetilde{\theta}_1(t) + \widetilde{\delta}_2(t) + \delta - \pi \right) \\ &= 10 \times \left(2\theta_1 - \frac{4\pi}{5} + 3t\left(\frac{4\pi}{5} - \theta_1\right) + (2-3t)\delta_2 + \delta - \pi \right). \end{aligned}$$

Therefore, $c(\tau_t^{o_t}, \tau_{\frac{2}{3}}) \underset{(t \to \frac{2}{3}^{-})}{\longrightarrow} 0$.

The continuity of ϕ at $t = \frac{2}{3}^{+}$ and $t = 1^{-}$ follows the same steps as in $\mathcal{B}^4$.

6. Each member of the family of f-tilings $(\mathcal{E}_\alpha)^o$, with $\alpha \in]\frac{\pi}{2}, \pi[$ is deformable into τ^-_{stand}. Figure 3.133 illustrates how to define the deformable map $\phi : [0,1] \to \mathscr{T}^{\mathcal{O}}(S^2)$ for a representative member.

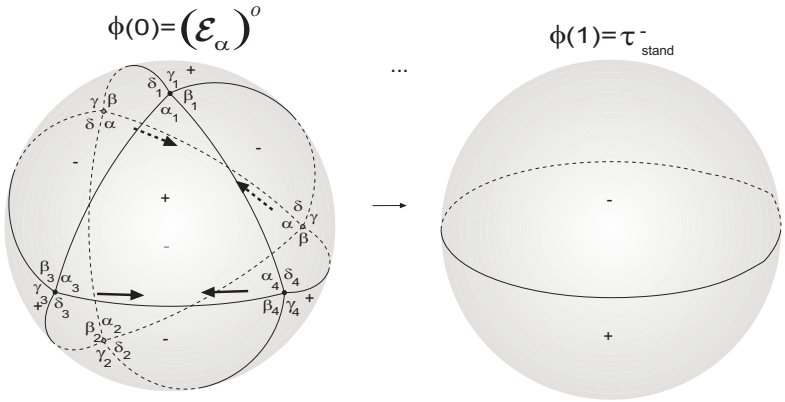

Figure 3.133: Deformation of $(\mathcal{E}_\alpha)^o$.

According to the labeling of the angles shown in Figure 3.133, we have, for $t \in [0,1]$:

- $\widetilde{\alpha}_1(t) = (1-t)\alpha_1$ and $\widetilde{\gamma}_1(t) = \pi - \widetilde{\alpha}_1(t)$;
- $\widetilde{\gamma}_2(t) = (1-t)\gamma_2$ and $\widetilde{\alpha}_2(t) = \pi - \widetilde{\gamma}_2(t)$;
- $\widetilde{\delta}_1(t) = \delta_1 + t\frac{\alpha_1}{2}$ and $\widetilde{\beta}_1(t) = \pi - \widetilde{\delta}_1(t)$;
- $\widetilde{\delta}_2(t) = \delta_2 + t\frac{\gamma_2}{2}$ and $\widetilde{\beta}_2(t) = \pi - \widetilde{\delta}_2(t)$;
- $\widetilde{\alpha}_i(t) = \alpha_i + t(\frac{\pi}{2} - \alpha_i),\ i = 3,4$ and $\widetilde{\gamma}_3(t) = \pi - \widetilde{\alpha}_3(t),\ \widetilde{\gamma}_4(t) = \pi - \widetilde{\alpha}_4(t)$;
- $\widetilde{\delta}_3(t) = \delta_3 + t(\frac{\pi}{2} - \delta_3)$ and $\widetilde{\beta}_3(t) = \pi - \widetilde{\delta}_3(t)$;
- $\widetilde{\beta}_4(t) = \beta_4 + t(\frac{\pi}{2} - \beta_4)$ and $\widetilde{\delta}_4(t) = \pi - \widetilde{\beta}_4(t)$.

We will show that ϕ is continuous at $t = 0$. If $t \in]0,1[$:

$$\begin{aligned}
c(\tau^{o_t},\tau_0) &= \sum_{\substack{F\text{face of}\\ \tau_t\cup\tau_0}} \lambda(F)\,Area(F)\\
&= 4\times((\widetilde{\alpha}_1(0)+\widetilde{\alpha}_3(0)+\widetilde{\alpha}_4(0)-\pi)-(\widetilde{\alpha}_1(t)+\widetilde{\alpha}_3(t)+\widetilde{\alpha}_4(t)-\pi))\\
&+2\times\left((\beta+\gamma_3+\delta_2-\pi)-\left(\beta+\widetilde{\gamma}_3(t)+\widetilde{\delta}_2(t)-\pi\right)\right)\\
&= 4t(\alpha_1-\frac{\pi}{2}+\alpha_3-\frac{\pi}{2}+\alpha_4)+2t\left(\frac{\pi}{2}-\alpha_3-\frac{\gamma_2}{2}\right).
\end{aligned}$$

When, $t\to 0^+$, one has $c(\tau^{o_t},\tau_0)\to 0$.

Now, if $t\in]0,1[$:

$$\begin{aligned}
c(\tau^{o_t},\tau_1) &= \sum_{\substack{F\text{face of}\\ \tau_t\cup\tau_1}} \lambda(F)\,Area(F)\\
&= 2\times(\widetilde{\alpha}_1(t)+\widetilde{\alpha}_3(t)+\widetilde{\alpha}_4(t)-\pi)+2\times(\widetilde{\delta}_3(t)+\widetilde{\beta}_4(t)+\widetilde{\gamma}_2(t)-\pi)\\
&= 2\times\left((1-t)\alpha_1+\alpha_3+t\left(\frac{\pi}{2}-\alpha_3\right)+\alpha_4+t\left(\frac{\pi}{2}-\alpha_4\right)-\pi\right)\\
&+2\times\left(\delta_3+t\left(\frac{\pi}{2}-\delta_3\right)+\beta_4+t\left(\frac{\pi}{2}-\beta_4\right)+(1-t)\gamma_2-\pi\right).
\end{aligned}$$

As $t\to 1^-$, we may conclude that $c(\tau^{o_t},\tau_1)\to 0$ and so ϕ is continuous at $t=1$.

7. For any $k\geq 1$, $(\mathcal{F}^k)^o$ is deformable into τ^+_{stand}. Next figure gives an ideia of how to deform the member $(\mathcal{F}^1)^o$ and how to define the map $\phi:[0,1]\to\mathscr{T}^{\mathcal{O}}(S^2)$. The angles are $\alpha\approx 83.061^\circ$, $\beta\approx 115.374^\circ$, $\gamma\approx 64.626^\circ$ and $\delta\approx 32.313^\circ$.

   For $t\in[0,\frac{1}{2}]$, we have

   - $\widetilde{\delta}_i(t)=(1-2t)\delta_i,\ i=2,5,8;$
   - $\widetilde{\delta}_i(t)=\delta_i+t\delta_2,\ i=1,3;$
   - $\widetilde{\delta}_i(t)=\delta_i+t\delta_5,\ i=4,6;$
   - $\widetilde{\delta}_i(t)=\delta_i+t\delta_8,\ i=7,9;$
   - $\widetilde{\gamma}_k(t)=\gamma_k,\ \widetilde{\beta}_k(t)=\beta_k,\ k=1,2,3,4,5,6.$

   If $t\in]\frac{1}{2},1]$, then

⋆ $\widetilde{\beta}_i(t) = (2-2t)\beta_i$ and $\widetilde{\theta}_i(t) = \pi - \widetilde{\beta}_i(t),\ i = 1, 4;$

⋆ $\widetilde{\alpha}_i(t) = \alpha_i - \beta_i + 2t\beta_i$ and $\widetilde{\gamma}_i(t) = \pi - \widetilde{\alpha}_i(t),\ i = 1, 4;$

⋆ $\widetilde{\alpha}_j(t) = \widetilde{\gamma}_j(t) = \widetilde{\beta}_j(t) = \widetilde{\theta}_j(t) \equiv \frac{\pi}{2},\ j = 2, 3, 5, 6.$

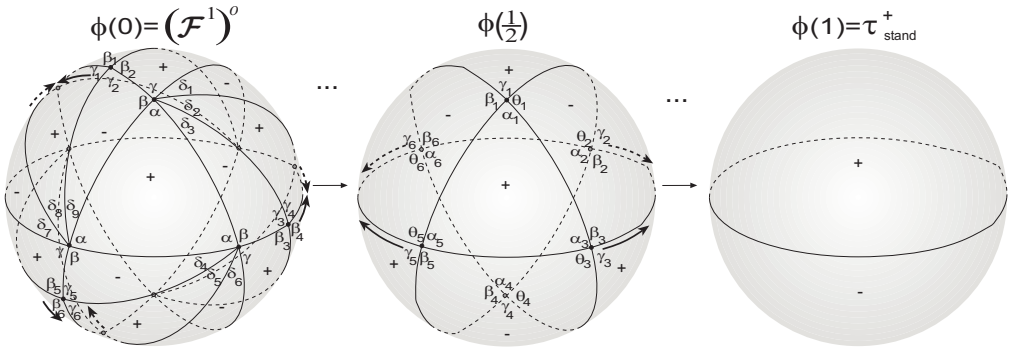

Figure 3.134: Deformation of $(\mathcal{F}^1)^o$.

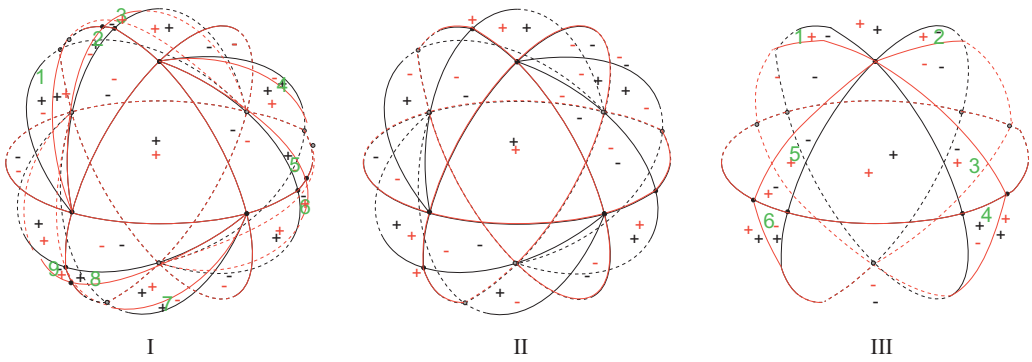

Figure 3.135: Errant faces.

Let us show that ϕ is continuous at $[0, 1]$. For $t \in]0, \frac{1}{2}[$ and observing Figure 3.135-I, one has

$$\begin{aligned}
c(\tau^{o_t},\tau_0) &= \sum_{\substack{F\text{face of}\\ \tau_t\cup\tau_0}} \lambda(F)\,Area(F)\\
&\leq 6\times\left|(\widetilde{\delta}_8(0)+\widetilde{\gamma}_1(0)+\widetilde{\beta}_1(0)-\pi)-(\widetilde{\delta}_8(t)+\widetilde{\gamma}_1(t)+\widetilde{\beta}_1(t)-\pi)\right|\\
&+12\times\left|(\widetilde{\delta}_9(t)+\widetilde{\gamma}_2(t)+\widetilde{\beta}_2(t)-\pi)-(\widetilde{\delta}_9(0)+\widetilde{\gamma}_2(0)+\widetilde{\beta}_2(0)-\pi)\right|\\
&= 6\times|(\delta_8+\gamma_1+\beta_1-\pi)-((1-2t)\delta_8+\gamma_1+\beta_1-\pi)|\\
&+12\times|(\delta_9+t\delta_8+\gamma_2+\beta_2-\pi)-(\delta_9+\gamma_2+\beta_2-\pi)|\,.
\end{aligned}$$

When, $t\to 0^+$, one has $c(\tau^{o_t},\tau_0)\to 0$.

If $t\in]0,\frac{1}{2}[$ (see Figure 3.135-II),

$$\begin{aligned}
c(\tau^{o_t},\tau_{\frac{1}{2}}) &= \sum_{\substack{F\text{face of}\\ \tau_t\cup\tau_{\frac{1}{2}}}} \lambda(F)\,Area(F)\\
&= 6\times\left(\widetilde{\delta}_8(t)+\widetilde{\gamma}_1(t)+\widetilde{\beta}_1(t)-\pi\right)\\
&= 6\times((1-2t)\delta_8+\gamma_1+\beta_1-\pi).
\end{aligned}$$

When, $t\to\frac{1}{2}^-$, one has $c(\tau^{o_t},\tau_{\frac{1}{2}})\to 0$.

For $t\in]\frac{1}{2},1[$ and by Figure 3.135-III,

$$\begin{aligned}
c(\tau^{o_t},\tau_{\frac{1}{2}}) &= \sum_{\substack{F\text{face of}\\ \tau_t\cup\tau_{\frac{1}{2}}}} \lambda(F)\,Area(F)\\
&= 8\times\left(\frac{\widetilde{\theta}_1\left(\frac{1}{2}\right)-\widetilde{\theta}_1(t)}{2}+\widetilde{\beta}_3\left(\frac{1}{2}\right)+\widetilde{\alpha}_3(t)-\pi\right)\\
&= 8\times\left(\frac{\pi-\beta_1-\pi+(2-2t)\beta_1}{2}+\pi-\pi\right).
\end{aligned}$$

When, $t\to\frac{1}{2}^+$, one has $c(\tau^{o_t},\tau_{\frac{1}{2}})\to 0$.

For $t\in]\frac{1}{2},1[$:

$$c(\tau^{o_t}, \tau_1) = \sum_{\substack{F \text{face of} \\ \tau_t \cup \tau_1}} \lambda(F)\, Area(F)$$
$$4 \times \left(\widetilde{\beta}_1(t) + \widetilde{\theta}_5(t) + \widetilde{\gamma}_6(t) - \pi \right)$$
$$= 4 \times \left((2-2t)\beta_1 + \frac{\pi}{2} + \frac{\pi}{2} - \pi \right).$$

As $t \to 1^-$, then $c(\tau^{o_t}, \tau_1) \to 0$. Consequently, ϕ is continuous in $[0,1]$.

8. The f-tiling $(\mathcal{D})^o$ is deformable into τ^-_{stand}, as illustrated in Figure 3.136, where $\phi : [0,1] \to \mathscr{T}^{\mathcal{O}}(S^2)$ is a deformable map. The angles are $\alpha \approx 72.75°$, $\beta \approx 53.63°$, $\gamma = \frac{\pi}{3}$ and $\delta \approx 107.25°$.

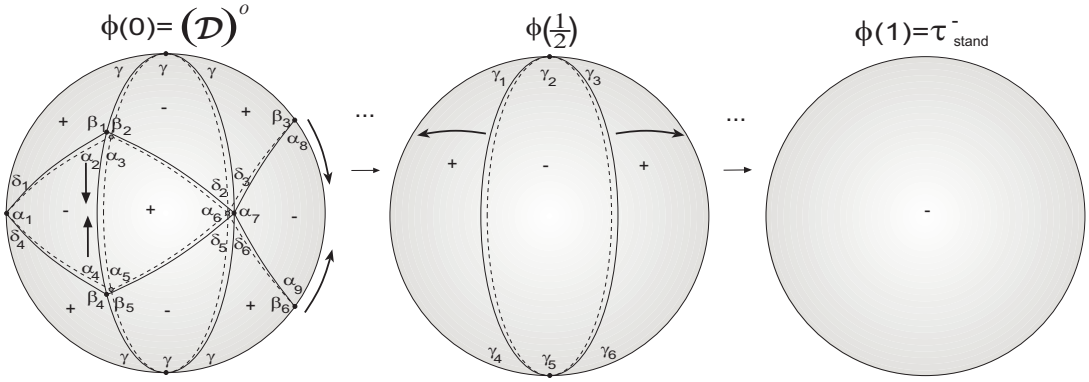

Figure 3.136: Deformation of $(\mathcal{D})^o$.

For $t \in [0, \frac{1}{2}]$:

- ⋆ $\widetilde{\alpha}_i(t) = (1-2t)\alpha_i,\ i = 1, 6, 7$;
- ⋆ $\widetilde{\delta}_1(t) = \delta_1 + t\alpha_1$ and $\widetilde{\delta}_4(t) = \delta_4 + t\alpha_1$;
- ⋆ $\widetilde{\delta}_2(t) = \delta_2 + t\alpha_6$ and $\widetilde{\delta}_5(t) = \delta_5 + t\alpha_6$;
- ⋆ $\widetilde{\delta}_3(t) = \delta_3 + t\alpha_7$ and $\widetilde{\delta}_6(t) = \delta_6 + t\alpha_7$;
- ⋆ $\widetilde{\beta}_j(t) = \beta_j + 2t\left(\frac{\pi}{2} - \beta_j\right), j = 1, 2, 3, 4, 5, 6$;
- ⋆ $\widetilde{\alpha}_2(t) = \pi - \widetilde{\beta}_2(t)$, $\widetilde{\alpha}_3(t) = \pi - \widetilde{\beta}_1(t)$, $\widetilde{\alpha}_4(t) = \pi - \widetilde{\beta}_5(t)$, $\widetilde{\alpha}_5(t) = \pi - \widetilde{\beta}_4(t)$, $\widetilde{\alpha}_8(t) = \pi - \widetilde{\beta}'_3(t)$ and $\widetilde{\alpha}_9(t) = \pi - \widetilde{\beta}'_6(t)$, where $\widetilde{\beta}'_k(t) = \beta'_k + 2t\left(\frac{\pi}{2} - \beta'_k\right)$, $k = 3, 6$ belong to semi-space $x \leq 0$.

If $t \in]\frac{1}{2}, 1]$:

$\star$ $\widetilde{\gamma}_i(t) = (2-2t)\gamma_i,\ i = 1, 3, 4, 6;$

$\star$ $\widetilde{\gamma}_i(t) = \gamma_i - \gamma_{i-1} - \gamma_{i+1} + 2t(\gamma_{i-1} + \gamma_{i+1}),\ i = 2, 5.$

We only need to prove that ϕ is continuous at $t = 0$ and $t = \frac{1}{2}^-$, since the proof for $t = \frac{1}{2}^+$ and $t = 1^-$ is similar to the one done for the f-tiling $\mathcal{B}^4$:

For each $t \in]0, \frac{1}{2}[$,

$$\begin{aligned} c(\tau_t^{o_t}, \tau_0) &= \sum_{\substack{F \text{face of} \\ \tau_t \cup \tau_0}} \lambda(F)\, Area(F) \\ &= 8\left(\widetilde{\beta}_5(t) + \widetilde{\alpha}_5(0) + \widetilde{\alpha}_6(0) - \widetilde{\alpha}_6(t) - \pi\right) \\ &+ 4\left(\widetilde{\alpha}_8(0) + \widetilde{\beta}_3(t) + \widetilde{\alpha}_7(0) - \widetilde{\alpha}_7(t) - \pi\right) \\ &= 8\left(\beta_5 + 2t\left(\frac{\pi}{2} - \beta_5\right) + \pi - \beta + \alpha_6 - (1-2t)\alpha_6 - \pi\right) \\ &+ 4\left(\pi - \beta + \beta_3 + 2t\left(\frac{\pi}{2} - \beta_3\right) + \alpha_7 - (1-2t)\alpha_7 - \pi\right). \end{aligned}$$

When $t \to 0^+$, we conclude that $c(\tau_t^{o_t}, \tau_0) \to 0$.

For each $t \in]0, \frac{1}{2}[$,

$$\begin{aligned} c(\tau_t^{o_t}, \tau_{\frac{1}{2}}) &= \sum_{\substack{F \text{face of} \\ \tau_t \cup \tau_{\frac{1}{2}}}} \lambda(F)\, Area(F) \\ &= 6 \times (\widetilde{\alpha}_1(t) + \widetilde{\alpha}_2(t) + \widetilde{\alpha}_4(t) - \pi) \\ &= 6 \times \left[(1-2t)\alpha_1 + \pi - \widetilde{\beta}_2(t) + \pi - \widetilde{\beta}_5(t) - \pi\right]. \end{aligned}$$

When $t \to \frac{1}{2}^-$, we conclude that $c(\tau_t^{o_t}, \tau_{\frac{1}{2}}) \to 0$.

9. The dihedral f-tiling $(\mathcal{E})^o$ is deformable into τ_{stand}^+. Figure 4.164 shows a geometrical sketch of the deformable of this f-tiling, where $\phi : [0, 1] \to \mathscr{T}^{\mathcal{O}}(S^2)$ is a deformation of $(\mathcal{E})^o$ into τ_{stand}. In this case, $\alpha = 72°$, $\beta = 36°$, $\gamma = \frac{\pi}{3}$ and $\delta = 108°$.

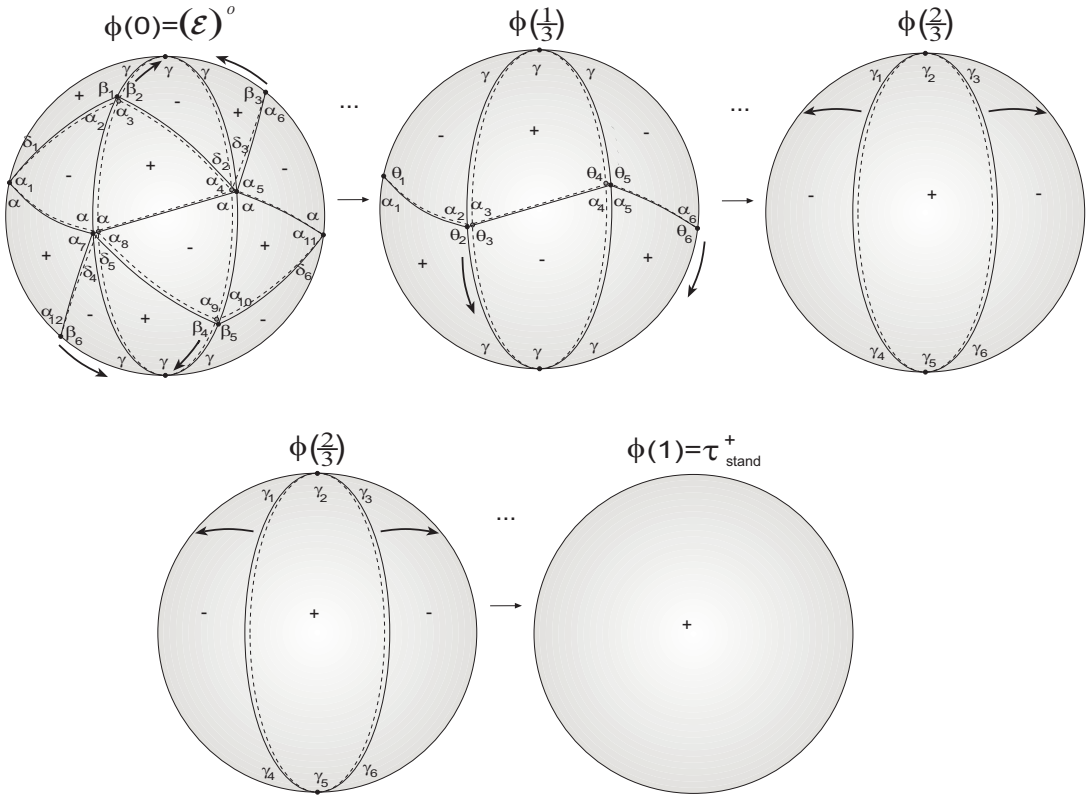

Figure 3.137: Deformation of $(\mathcal{E})^o$.

For $t \in [0, \frac{1}{3}]$:

- $\widetilde{\delta}_i(t) = (1-3t)\delta_i,\ i = 1, \ldots, 6;$
- $\widetilde{\alpha}_1(t) = \alpha_1 + 3t\delta_1,\ \widetilde{\alpha}_4(t) = \alpha_4 + 3t\delta_2,\ \widetilde{\alpha}_5(t) = \alpha_5 + 3t\delta_3,\ \widetilde{\alpha}_7(t) = \alpha_7 + 3t\delta_4,\ \widetilde{\alpha}_8(t) = \alpha_8 + 3t\delta_5$ and $\widetilde{\alpha}_{11}(t) = \alpha_{11} + 3t\delta_6;$
- $\widetilde{\alpha}_k(t) = \alpha_k + 3t\left(\frac{\pi}{3} - \alpha_k\right),\ k = 2, 3, 6, 9, 10, 12;$
- $\widetilde{\beta}_1(t) = \pi - \widetilde{\alpha}_3(t),\ \widetilde{\beta}_2(t) = \pi - \widetilde{\alpha}_2(t),\ \widetilde{\beta}_3(t) = \pi - \widetilde{\alpha}'_6(t),\ \widetilde{\beta}_4(t) = \pi - \widetilde{\alpha}_{10}(t),\ \widetilde{\beta}_5(t) = \pi - \widetilde{\alpha}_9(t)$ and $\widetilde{\beta}_6(t) = \pi - \widetilde{\alpha}'_{12}(t)$, where $\widetilde{\alpha}'_k(t) = \alpha'_k + 3t\left(\frac{\pi}{3} - \alpha'_k\right),\ k = 6, 12$ belong to semi-space $x \leq 0$.

If $t \in]\frac{1}{3}, \frac{2}{3}]$:

- $\widetilde{\alpha}_i(t) = (2-3t)\alpha_i,\ i = 1, 4, 5;$
- $\widetilde{\theta}_i(t) = \pi - \widetilde{\alpha}_i(t),\ i = 1, 6;$
- $\widetilde{\alpha}_k(t) = 2\alpha_k - \frac{\pi}{3} + t(\pi - 3\alpha_k),\ k = 2, 3, 6;$

$\star$ $\widetilde{\theta}_2(t) = \pi - \widetilde{\alpha}_3(t)$, $\widetilde{\theta}_3(t) = \pi - \widetilde{\alpha}_2(t)$ and $\widetilde{\theta}_4(t) = \pi - \widetilde{\alpha}_5(t)$;

$\star$ $\widetilde{\theta}_5(t) = \theta_5 - \alpha_5 + 3t\alpha_5$.

Finally, if $t \in]\frac{2}{3}, 1]$:

$\star$ $\widetilde{\gamma}_i(t) = (3 - 3t)\gamma_i$, $i = 1, 3, 4, 6$;

$\star$ $\widetilde{\gamma}_i(t) = \gamma_i - 2(\gamma_{i-1} + \gamma_{i+1}) + 3t(\gamma_{i-1} + \gamma_{i+1})$, $i = 2, 5$.

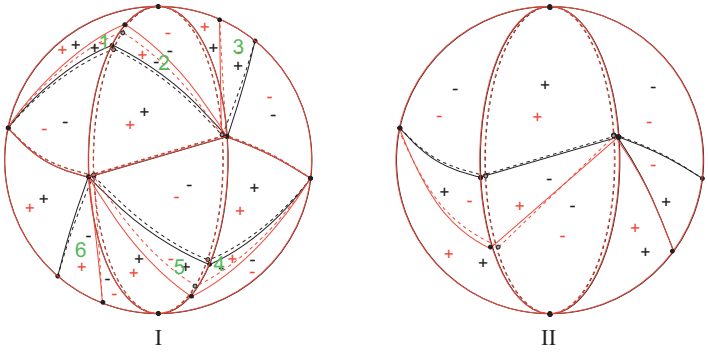

Figure 3.138: Errant faces.

Let us show that ϕ is continuous at $t = 0$ (see Figure 3.138-I):

For each $t \in]0, \frac{1}{3}[$,

$$\begin{aligned} c(\tau_t^{o_t}, \tau_0) &= \sum_{\substack{F \text{face of} \\ \tau_t \cup \tau_0}} \lambda(F)\, Area(F) \\ &= 8 \times \left(\widetilde{\beta}_2(0) + \widetilde{\delta}_2(0) - \widetilde{\delta}_2(t) + \widetilde{\alpha}_2(t) - \pi\right) \\ &+ 4 \times \left(\widetilde{\beta}_3(0) + \widetilde{\alpha}_6(t) + \widetilde{\delta}_3(0) - \widetilde{\delta}_3(t) - \pi\right). \end{aligned}$$

When $t \to 0^+$, then $c(\tau_t^{o_t}, \tau_0) \to 0$.

ϕ is continuous at $t = \frac{1}{3}^-$:

For each $t \in]0, \frac{1}{3}[$,

$$\begin{aligned} c(\tau_t^{o_t}, \tau_{\frac{1}{3}}) &= \sum_{\substack{F \text{face of} \\ \tau_t \cup \tau_{\frac{1}{3}}}} \lambda(F)\, Area(F) \\ &= 2 \times \left(\sum_{k=1}^{6} (\widetilde{\delta}_k(t) + \widetilde{\beta}_k(t)) + 6\gamma - 6\pi \right) \\ &= 12(1-3t)\delta_1 + 12(\pi - \widetilde{\alpha}_2(t)) + 12\gamma - 12\pi. \end{aligned}$$

When $t \to \frac{1}{3}^{-}$, we conclude that $c(\tau_t^{o_t}, \tau_{\frac{1}{3}}) \to 0$.

For each $t \in]\frac{1}{3}, \frac{2}{3}[$, see Figure 3.138-II:

$$\begin{aligned} c(\tau_t^{o_t}, \tau_{\frac{1}{3}}) &= \sum_{\substack{F \text{face of} \\ \tau_t \cup \tau_{\frac{1}{3}}}} \lambda(F)\, Area(F) \\ &= 2 \times \left(\widetilde{\alpha}_1\left(\frac{1}{3}\right) - \widetilde{\alpha}_1(t) + \widetilde{\theta}_2\left(\frac{1}{3}\right) + \widetilde{\alpha}_2(t) - \pi \right) \\ &+ 2 \times \left(\widetilde{\theta}_3\left(\frac{1}{3}\right) + \widetilde{\alpha}_4\left(\frac{1}{3}\right) - \widetilde{\alpha}_4(t) + \widetilde{\alpha}_4(t) - \pi \right) \\ &+ 2 \times \left(\widetilde{\theta}_6\left(\frac{1}{3}\right) + \widetilde{\alpha}_5\left(\frac{1}{3}\right) - \widetilde{\alpha}_5(t) + \widetilde{\alpha}_6(t) - \pi \right). \end{aligned}$$

When $t \to \frac{1}{3}^{+}$, we conclude that $c(\tau_t^{o_t}, \tau_{\frac{1}{3}}) \to 0$ and consequently ϕ is continuous at $t = \frac{1}{3}$.

Now, if $t \in]\frac{1}{3}, \frac{2}{3}[$,

$$\begin{aligned} c(\tau_t^{o_t}, \tau_{\frac{2}{3}}) &= \sum_{\substack{F \text{face of} \\ \tau_t \cup \tau_{\frac{2}{3}}}} \lambda(F)\, Area(F) \\ &= 2(\widetilde{\alpha}_1(t) + \widetilde{\theta}_2(t) + \gamma - \pi) \\ &+ 2(\widetilde{\alpha}_4(t) + \widetilde{\theta}_3(t) + \gamma - \pi) + 2(\widetilde{\alpha}_5(t) + \widetilde{\theta}_6(t) + \gamma - \pi). \end{aligned}$$

When $t \to \frac{2}{3}^{-}$, we conclude that $c(\tau_t^{o_t}, \tau_{\frac{2}{3}}) \to 0$.

The continuity at $t = \frac{2}{3}^{+}$ and $t = 1^{-}$ is trivial.

10. The f-tiling $(\mathcal{F})^o$ is deformable into τ^-_{stand}. Considering $\phi : [0,1] \to \mathscr{T}^{\mathcal{O}}(S^2)$ a deformable map of $(\mathcal{F})^o$ into τ^-_{stand}, next figure gives us an idea of how to define ϕ. The angles that compose $\mathcal{F}$ are $\alpha \approx 70.5°$, $\beta \approx 24.7°$, $\gamma = \frac{\pi}{3}$ and $\delta \approx 109.5°$.

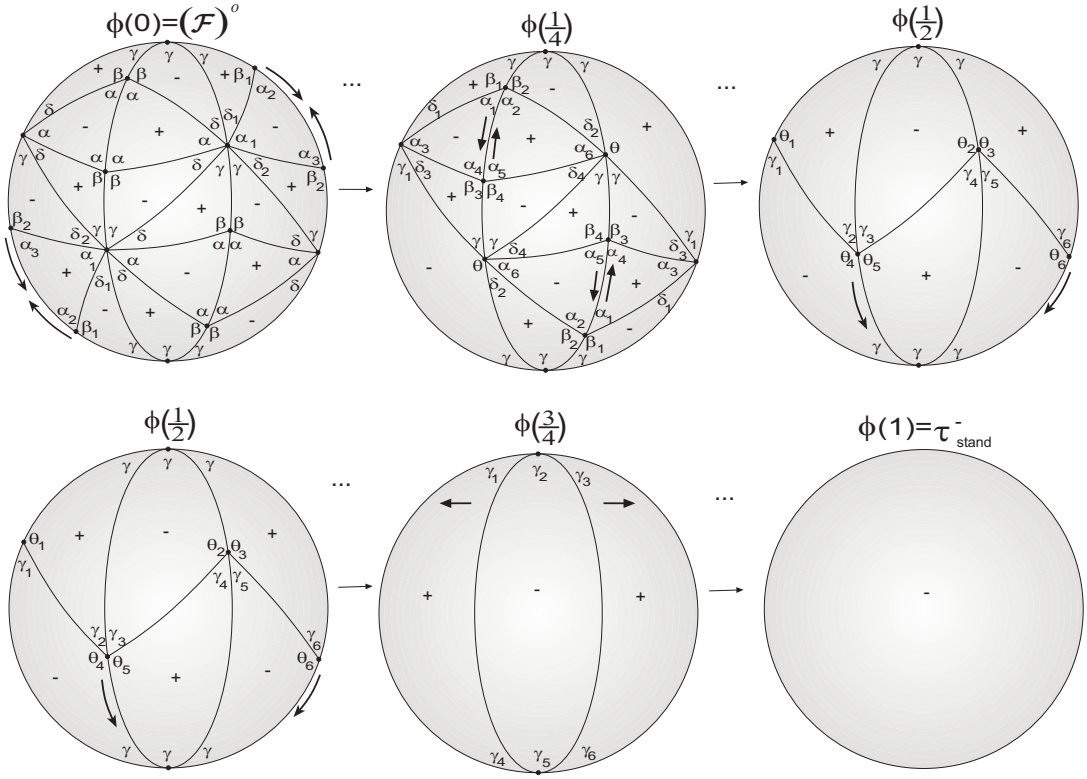

Figure 3.139: Deformation of $(\mathcal{F})^o$.

With $t \in [0, \frac{1}{4}]$:

- $\widetilde{\alpha}_1(t) = (1-4t)\alpha_1$;
- $\widetilde{\delta}_j(t) = \delta_j + 2t\alpha_1,\ j = 1, 2$;
- $\widetilde{\beta}_k(t) = \beta_k + 4t\left(\frac{\pi}{2} - \beta_k\right),\ k = 1, 2$;
- $\widetilde{\alpha}_2(t) = \pi - \widetilde{\beta}'_1(t)$ and $\widetilde{\alpha}_3(t) = \pi - \widetilde{\beta}'_2(t)$, where $\widetilde{\beta}'_k(t) = \beta'_k + 4t\left(\frac{\pi}{2} - \beta'_k\right),\ k = 1, 2$ belong to the semi-space $x \leq 0$.

If $t \in]\frac{1}{4}, \frac{1}{2}]$:

- $\widetilde{\alpha}_i(t) = (2-4t)\alpha_i,\ i = 3, 6$;

- $\widetilde{\delta}_i(t) = \delta_i + (2t - \frac{1}{2})\alpha_3,\ i = 1, 3,\ \widetilde{\delta}_i(t) = \delta_i + (2t - \frac{1}{2})\alpha_6,\ i = 2, 4;$
- $\widetilde{\beta}_k(t) = 2\beta_k - \frac{\pi}{2} + 2t\,(\pi - 2\beta_k)\,,\ k = 1, 2, 3, 4;$
- $\widetilde{\alpha}_1(t) = \pi - \widetilde{\beta}_2(t),\ \widetilde{\alpha}_2(t) = \pi - \widetilde{\beta}_1(t),\ \widetilde{\alpha}_4(t) = \pi - \widetilde{\beta}_4(t)$ and $\widetilde{\alpha}_5(t) = \pi - \widetilde{\beta}_3(t).$

When $t \in]\frac{1}{2}, \frac{3}{4}]$:

- $\widetilde{\gamma}_i(t) = (3 - 4t)\gamma_i,\ i = 1, 4, 5;$
- $\widetilde{\theta}_j(t) = \pi - \widetilde{\gamma}_j(t),\ j = 1, 6;$
- $\widetilde{\theta}_4(t) = \pi - \widetilde{\gamma}_3(t),\ \widetilde{\theta}_5(t) = \pi - \widetilde{\gamma}_2(t)$ and $\widetilde{\theta}_2(t) = \pi - \widetilde{\gamma}_5(t);$
- $\widetilde{\theta}_3(t) = \theta_3 - 2\gamma_5 + 4t\gamma_5;$
- $\widetilde{\gamma}_k(t) = 3\gamma_k - \frac{2\pi}{3} + 4t\left(\frac{\pi}{3} - \gamma_k\right),\ k = 2, 3, 6.$

If $t \in]\frac{3}{4}, 1]$:

- $\widetilde{\gamma}_i(t) = (4 - 4t)\gamma_i,\ i = 1, 3, 4, 6;$
- $\widetilde{\gamma}_i(t) = \gamma_i - 3(\gamma_{i-1} + \gamma_{i+1}) + 4t(\gamma_{i-1} + \gamma_{i+1}),\ i = 2, 5.$

Now, ϕ is continuous at $t = 0$: For $t \in]0, \frac{1}{4}[$,

$$\begin{aligned} c(\tau_t^{o_t}, \tau_0) &= \sum_{\substack{F \text{face of} \\ \tau_t \cup \tau_0}} \lambda(F)\, Area(F) \\ &= 8 \times \left(\widetilde{\alpha}_2(0) + \widetilde{\beta}_1(t) + \frac{\widetilde{\alpha}_1(0) - \widetilde{\alpha}_1(t)}{2} - \pi \right) \\ &= 8 \times \left(\pi - \beta_1 + \beta_1 + 4t\left(\frac{\pi}{2} - \beta_1\right) + \frac{\alpha_1 - (1 - 4t)\alpha_1}{2} - \pi \right). \end{aligned}$$

As $t \to 0^+$, then $c(\tau_t^{o_t}, \tau_0) \to 0$.

If $t \in]0, \frac{1}{4}[$, then:

$$\begin{aligned} c(\tau_t^{o_t}, \tau_{\frac{1}{4}}) &= \sum_{\substack{F \text{face of} \\ \tau_t \cup \tau_{\frac{1}{4}}}} \lambda(F)\, Area(F) \\ &= 4 \times \left(\sum_{k=1}^{3} (\widetilde{\alpha}_k(t)) - \pi \right). \end{aligned}$$

When $t \to \frac{1}{4}^-$, we conclude that $c(\tau_t^{o_t}, \tau_{\frac{1}{4}}) \to 0$.

If $t \in]\frac{1}{4}, \frac{1}{2}[$:

$$\begin{aligned} c(\tau_t^{o_t}, \tau_{\frac{1}{4}}) &= \sum_{\substack{F \text{face of} \\ \tau_t \cup \tau_{\frac{1}{4}}}} \lambda(F)\, Area(F) \\ &= 16 \times \left(\widetilde{\alpha}_2\left(\frac{1}{4}\right) + \widetilde{\beta}_2(t) + \widetilde{\alpha}_6\left(\frac{1}{4}\right) - \widetilde{\alpha}_6(t) - \pi \right) \\ &= 16 \times \left(\pi - \beta_2 + 2\beta_2 - \frac{\pi}{2} + 2t(\pi - 2\beta_2) + \alpha_6 - (2-4t)\alpha_6 - \pi \right). \end{aligned}$$

Then, we conclude that $c(\tau_t^{o_t}, \tau_{\frac{1}{4}}) \to 0$, when $t \to \frac{1}{4}^+$.

For $t \in]\frac{1}{4}, \frac{1}{2}[$, one has:

$$\begin{aligned} c(\tau_t^{o_t}, \tau_{\frac{1}{2}}) &= \sum_{\substack{F \text{face of} \\ \tau_t \cup \tau_{\frac{1}{2}}}} \lambda(F)\, Area(F) \\ &= 8 \times \left(\widetilde{\alpha}_1(t) + \widetilde{\alpha}_3(t) + \widetilde{\alpha}_4(t) - \pi \right). \end{aligned}$$

When $t \to \frac{1}{2}^-$, we conclude that $c(\tau_t^{o_t}, \tau_{\frac{1}{2}}) \to 0$.

If $t \in]\frac{1}{2}, \frac{3}{4}[$:

$$\begin{aligned} c(\tau_t^{o_t}, \tau_{\frac{1}{2}}) &= \sum_{\substack{F \text{face of} \\ \tau_t \cup \tau_{\frac{1}{2}}}} \lambda(F)\, Area(F) \\ &= 6 \times \left(\widetilde{\gamma}_5\left(\frac{1}{2}\right) - \widetilde{\gamma}_5(t) + \widetilde{\theta}_6\left(\frac{1}{2}\right) + \widetilde{\gamma}_6(t) - \pi \right) \\ &= 6 \times \left(\gamma_5 - (3-4t)\gamma_5 + \pi - \gamma_6 + 3\gamma_6 - \frac{2\pi}{3} + 4t\left(\frac{\pi}{3} - \gamma_6\right) - \pi \right). \end{aligned}$$

When $t \to \frac{1}{2}^+$, we conclude that $c(\tau_t^{o_t}, \tau_{\frac{1}{2}}) \to 0$.

For $t \in]\frac{1}{2}, \frac{3}{4}[$, one has:

$$c(\tau_t^{o_t}, \tau_{\frac{3}{4}}) = \sum_{\substack{F\text{face of} \\ \tau_t \cup \tau_{\frac{3}{4}}}} \lambda(F)\, Area(F)$$
$$= 2 \times (\widetilde{\gamma}_1(t) + \widetilde{\theta}_4(t) + \gamma - \pi) + 2(\widetilde{\gamma}_4(t) + \widetilde{\theta}_5(t) + \gamma - \pi)$$
$$+ 2 \times (\widetilde{\gamma}_5(t) + \widetilde{\theta}_6(t) + \gamma - \pi).$$

When $t \to \frac{3}{4}^-$, we conclude that $c(\tau_t^{o_t}, \tau_{\frac{3}{4}}) \to 0$.

Following similar steps to the ones done for $\mathcal{B}^4$, we conclude that ϕ is continuous at $t = \frac{3}{4}^+$ and $t = 1^-$. Consequently, ϕ is a deformable map.

11. The f-tiling $(\mathcal{G})^o$ is deformable into τ_{stand}^-. Consider $\phi : [0,1] \to \mathscr{T}^{\mathcal{O}}(S^2)$ a deformable map. Next figure shows the process of deformation of this f-tiling, where $\alpha \approx 65.56°$, $\beta \approx 34.72°$, $\gamma = \frac{\pi}{4}$ and $\delta \approx 114.44°$.

    If $t \in [0, \frac{1}{3}]$:

    - $\widetilde{\alpha}_i(t) = (1-3t)\alpha_i,\ i = 1, 5, 8, 10;$
    - $\widetilde{\delta}_i(t) = \delta_i + 3t\frac{\alpha_1}{2},\ i = 1, 2$ and $\widetilde{\delta}_j(t) = \delta_j + 3t\frac{\alpha_5}{2},\ j = 3, 4;$
    - $\widetilde{\delta}_i(t) = \delta_i + 3t\frac{\alpha_8}{2},\ i = 5, 6$ and $\widetilde{\delta}_j(t) = \delta_j + 3t\frac{\alpha_{10}}{2},\ j = 7, 8;$
    - $\widetilde{\beta}_k(t) = \beta_k + 3t\left(\frac{\pi}{2} - \beta_k\right),\ k = 1, ..., 7;$
    - $\widetilde{\alpha}_2(t) = \pi - \widetilde{\beta}_2(t),\ \widetilde{\alpha}_3(t) = \pi - \widetilde{\beta}_4(t),\ \widetilde{\alpha}_4(t) = \pi - \widetilde{\beta}_1(t),\ \widetilde{\alpha}_6(t) = \pi - \widetilde{\beta}_3(t),\ \widetilde{\alpha}_7(t) = \pi - \widetilde{\beta}'_5(t),\ \widetilde{\alpha}_9(t) = \pi - \widetilde{\beta}'_7(t),\ \widetilde{\alpha}_{11}(t) = \pi - \widetilde{\beta}_6(t)$ and $\widetilde{\alpha}_{12}(t) = \pi - \widetilde{\beta}_8(t)$, where $\widetilde{\beta}'_5(t) = \beta'_k + 3t\left(\frac{\pi}{2} - \beta'_k\right),\ k = 5, 7$ belong to the semi-space $x \leq 0$.

    Now, if $t \in]\frac{1}{3}, \frac{2}{3}]$, one has:

    - $\widetilde{\gamma}_i(t) = (2-3t)\gamma_i,\ i = 1, 4, 5, 8;$
    - $\widetilde{\lambda}_1(t) = \pi - \widetilde{\gamma}_1(t)$ and $\widetilde{\lambda}_4(t) = \pi - \widetilde{\gamma}_8(t);$
    - $\widetilde{\gamma}_k(t) = 2\gamma_k - \frac{\pi}{4} + 3t\left(\frac{\pi}{4} - \gamma_k\right),\ k = 2, 3, 6, 7;$
    - $\widetilde{\theta}_1(t) = \pi - \widetilde{\gamma}_3(t),\ \widetilde{\theta}_2(t) = \pi - \widetilde{\gamma}_2(t),\ \widetilde{\theta}_3(t) = \pi - \widetilde{\gamma}_7(t)$ and $\widetilde{\theta}_4(t) = \pi - \widetilde{\gamma}_6(t);$

$\star$ $\widetilde{\lambda}_i(t) = \lambda_i - \gamma_{i+2} + 3t\gamma_{i+2},\ i = 2, 3.$

Finally, if $t \in]\frac{2}{3}, 1]$:

$\star$ $\widetilde{\gamma}_i(t) = (3 - 3t)\gamma_i,\ i = 1, 4, 5, 8;$

$\star$ $\widetilde{\gamma}_i(t) = \gamma_i - 2\gamma_{i-1} + 3t\gamma_{i+1},\ i = 2, 6$ and $\widetilde{\gamma}_j(t) = \gamma_j - 2\gamma_{j+1} + 3t\gamma_{j+1},\ j = 3, 7.$

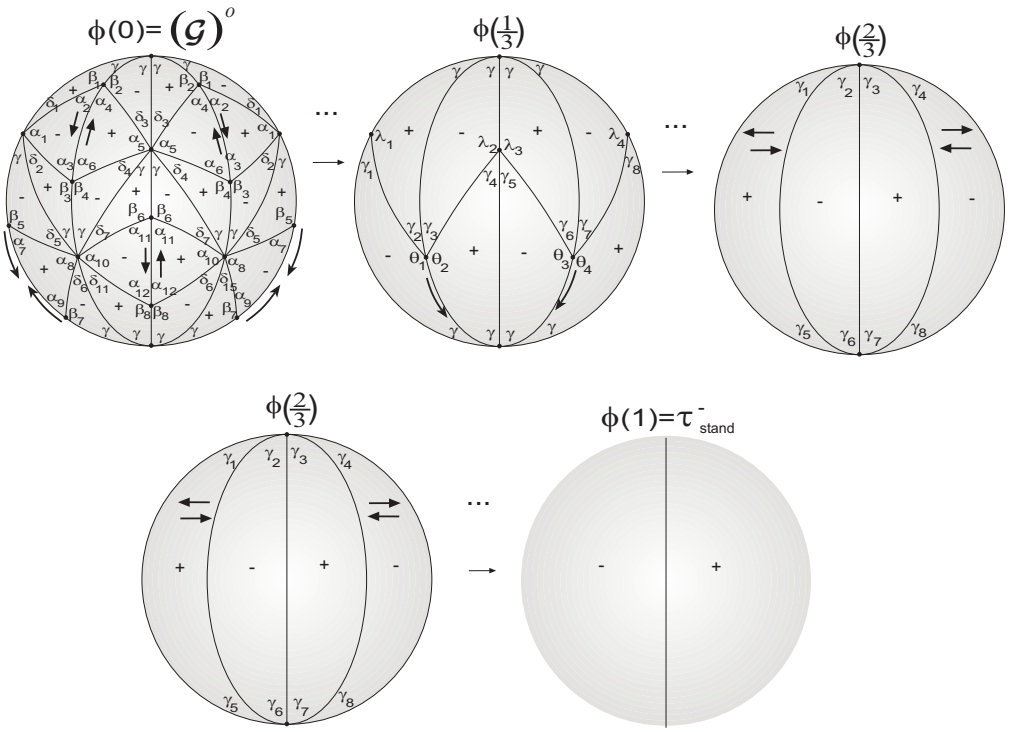

Figure 3.140: Deformation of $(\mathcal{G})^o$.

Let us show that ϕ is continuous. For each $t \in]0, \frac{1}{3}[$:

$$\begin{aligned} c(\tau_t^{o_t}, \tau_0) &= \sum_{\substack{F \text{face of} \\ \tau_t \cup \tau_0}} \lambda(F)\, Area(F) \\ &= 24 \times \left(\widetilde{\alpha}_2(0) + \widetilde{\beta}_1(t) + \frac{\widetilde{\alpha}_1(0) - \widetilde{\alpha}_1(t)}{2} - \pi \right) \\ &= 24 \times \left(\pi - \beta + \beta_1 + 3t\left(\frac{\pi}{2} - \beta_1\right) + \frac{\alpha_1 - (1 - 3t)\alpha_1}{2} - \pi \right). \end{aligned}$$

If $t \to 0^+$, then $c(\tau_t^{o_t}, \tau_0) \to 0$.

Now, for $t \in]0, \frac{1}{3}[$:

$$\begin{aligned} c(\tau_t^{o_t}, \tau_{\frac{1}{3}}) &= \sum_{\substack{F \text{face of} \\ \tau_t \cup \tau_{\frac{1}{3}}}} \lambda(F)\, Area(F) \\ &= 16 \times \left(\sum_{k=1}^{3} (\widetilde{\alpha}_k(t) - \pi) \right) \\ &= 16 \times \left((1-3t)\alpha_1 + \pi - 2\left(\beta_2 + 3t\left(\frac{\pi}{2} - \beta_2\right)\right)\right). \end{aligned}$$

For $t \to \frac{1}{3}^-$, one has $c(\tau_t^{o_t}, \tau_{\frac{1}{3}}) \to 0$.

Now, if $t \in]\frac{1}{3}, \frac{2}{3}[$,

$$\begin{aligned} c(\tau_t^{o_t}, \tau_{\frac{1}{3}}) &= \sum_{\substack{F \text{face of} \\ \tau_t \cup \tau_{\frac{1}{3}}}} \lambda(F)\, Area(F) \\ &= 8 \times \left(\widetilde{\gamma}_1\left(\frac{1}{3}\right) - \widetilde{\gamma}_1(t) + \widetilde{\theta}_1\left(\frac{1}{3}\right) + \widetilde{\gamma}_2(t) - \pi \right) \\ &= 8 \times \left(\gamma_1 - (2-3t)\gamma_1 + \pi - \gamma_3 + 2\gamma_2 - \frac{\pi}{4} + 3t\left(\frac{\pi}{4} - \gamma_2\right) - \pi \right). \end{aligned}$$

When, $t \to \frac{1}{3}^+$, then $c(\tau_t^{o_t}, \tau_{\frac{1}{3}}) \to 0$.

For, $t \in]\frac{1}{3}, \frac{2}{3}[$:

$$\begin{aligned} c(\tau_t^{o_t}, \tau_{\frac{2}{3}}) &= \sum_{\substack{F \text{face of} \\ \tau_t \cup \tau_{\frac{2}{3}}}} \lambda(F)\, Area(F) \\ &= 8 \times \left(\widetilde{\gamma}_1(t) + \widetilde{\theta}_1(t) + \gamma - \pi \right) \\ &= 8 \times \left((2-3t)\gamma_1 + \pi - 2\gamma_3 + \frac{\pi}{4} - 3t\left(\frac{\pi}{4} - \gamma_3\right) + \gamma - \pi \right). \end{aligned}$$

Then, $c(\tau_t^{o_t}, \tau_{\frac{2}{3}}) \to 0$, when$t \to \frac{2}{3}^-$.

The continuity of ϕ at $t = \frac{2}{3}^+$ and $t = 1^-$ is trivial.

Chapter 4

Dihedral f-Tilings of the 2-Sphere by Isosceles Triangles

In this Chapter, we classify all the dihedral f-tilings of the sphere, S^2, whose prototiles are two non-congruent isosceles triangles.

We remind that, in order to facilitate the construction of the f-tilings, we find useful to start by considering a *local representation*, beginning with a common vertex to each one of the isosceles triangles in adjacent positions. In the diagrams that follows, it is convenient to label the tiles according to the following procedures:

(i) The tiles by which we begin the local representation of a tiling $\tau \in \Omega(T_1, T_2)$ are labeled by 1 and 2, respectively;

(ii) For $j \geq 2$, the location of tile j can be deduced from the configuration of tiles $(1, 2, \ldots, j-1)$ and from the hypothesis that the configuration is part of a complete local representation of a f-tiling (except in the cases explicitly indicated).

From Section 4.3 and until the end, we will use the software POV-Ray to give 3D representation of the dihedral f-tilings obtained.

In the following, T_1 denotes an isosceles spherical triangle of angles α, α, β with sides a (opposite to α) and b (opposite to β) and T_2 another isosceles spherical triangle, not congruent to T_1, of angles γ, γ, δ with sides c (opposite to γ) and d (opposite to δ).

In this case, there are three distinct types of adjacency, see Figure 4.1.

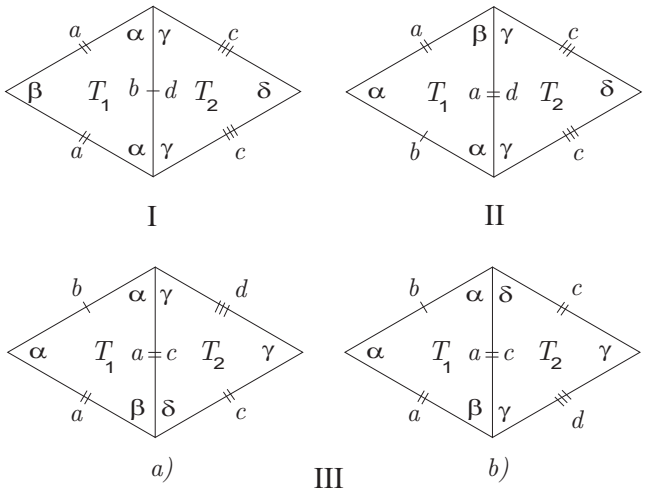

Figure 4.1: Different types of adjacency.

4.1 Triangular Dihedral f-Tilings with Adjacency of Type I

All results of this section and their complete proofs are published in [2].

The type I edge-adjacency condition can be analytically described by the equation,

$$\frac{\cos\beta + \cos^2\alpha}{\sin^2\alpha} = \frac{\cos\delta + \cos^2\gamma}{\sin^2\gamma}. \tag{4.1}$$

Remark 4.1 *Observe that if $\alpha = \gamma$, then $\beta = \delta$, which is an impossibility. Therefore, we shall consider, without loss of generality, $\alpha > \gamma$.*

Let us begin by showing that, it is impossible to have side b equal to side d and side a equal to side c.

In fact, assuming that $b = d$ and $a = c$, which is equivalent to have,

$$\frac{\cos\beta + \cos^2\alpha}{\sin^2\alpha} = \frac{\cos\delta + \cos^2\gamma}{\sin^2\gamma},$$

$$\frac{\cos\alpha(1+\cos\beta)}{\sin\alpha\sin\beta} = \frac{\cos\gamma(1+\cos\delta)}{\sin\gamma\sin\delta} \tag{4.2}$$

and $\sin\alpha = \sin\gamma$ and $\sin\beta = \sin\delta$. However, by the previous remark it is impossible that $\sin\alpha = \sin\gamma$.

As a direct consequence of the type of adjacency I, we get the following result:

Elimination Lemma *In any local configuration of a dihedral f-tiling whose prototiles are isosceles triangles with adjacency of type I, there are no vertices surrounded by sequences of alternate angles containing*:

(a) *p angles β and q angles δ with $p, q \geq 1$ or*

(b) one angle α (resp. γ) *and q angles δ (resp. β), $q \geq 1$ or*

(c) *one angle α (resp. γ), p angles β and q angles δ with $p, q \geq 1$.*

Starting a local configuration of $\tau \in \Omega(T_1, T_2)$ with two adjacent cells congruent to T_1 and T_2 respectively, see Figure 4.2, a choice for angle $\theta_1 \in \{\gamma, \delta\}$ must be made.

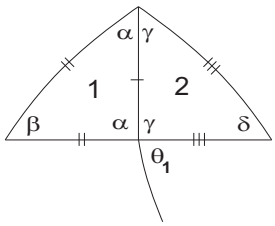

Figure 4.2: Local configuration.

In order to facilitate the construction of the dihedral f-tilings, we distinguish the different order relations between the angles. Therefore, in the first subsection, we shall consider the order relation $\alpha > \beta$ and $\gamma > \delta$, in the second subsection, $\alpha > \beta$ and $\delta > \gamma$, in the third subsection $\beta > \alpha$ and $\gamma > \delta$ and in the fourth subsection $\beta > \alpha$ and $\delta > \gamma$.

4.1.1 $\alpha > \beta$ and $\gamma > \delta$

With the above terminology one has:

Proposition 4.1 *If $\theta_1 = \gamma$, then $\Omega(T_1, T_2) \neq \varnothing$ if and only if $\beta = \delta = \frac{\pi}{k}$, $k \geq 3$, $k \in \mathbb{N}$ and $\alpha + \gamma = \pi$, $\alpha \in]\frac{\pi}{2}, \frac{2\pi}{3}[$. In this case, we get a 2-parameter family of dihedral f-tilings denoted by $(\mathcal{G}_{k,\alpha})_{k\geq 3, \alpha \in]\frac{\pi}{2}, \frac{2\pi}{3}[}$. A 3D representation of a member of this family $\mathcal{G}_{3,\alpha}$ is given in Figure 4.5.*

Proof. In order to have $\Omega(T_1, T_2) \neq \emptyset$, necessarily $\alpha + \theta_1 \leq \pi$.

1. Let us assume that $\alpha + \theta_1 = \pi$, with $\theta_1 = \gamma$. By the adjacency condition (4.1) and having in account that $\alpha > \gamma$, one has

$$\alpha > \frac{\pi}{2} > \gamma > \delta \quad \text{and} \quad \beta = \delta.$$

Expanding the configuration illustrated in Figure 4.2, we obtain the following one, with $\theta_2 \in \{\alpha, \beta\}$.

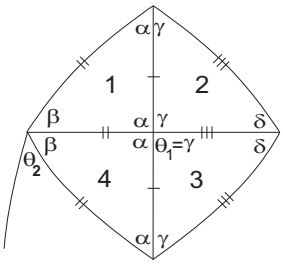

Figure 4.3: Local configuration.

1.1 Suppose firstly, that $\theta_2 = \alpha$. Then, $\alpha + \beta < \pi$, otherwise, from $\alpha + \gamma = \pi$, we get $\beta = \delta = \gamma$, which is impossible. Taking into account the Elimination Lemma, the sum containing the alternate angles θ_2 and β must be of the form $\alpha + k\beta = \pi$, for $k \geq 2$. The configuration extends a bit more, to the one shown in Figure 4.4, but due to the incompatibility of the sides length, it is impossible to pursue the construction of the dihedral f-tiling.

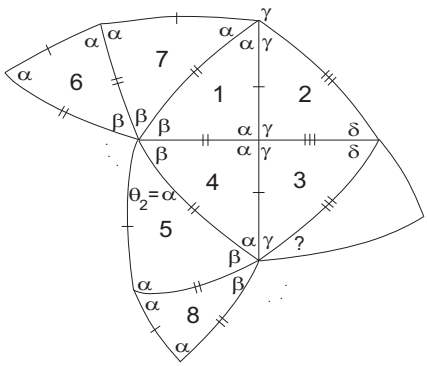

Figure 4.4: Local configuration.

1.2 Assume that $\theta_2 = \beta$.

If β is a submultiple of π, say $\beta = \frac{\pi}{k}$, then $k \geq 3$ and we may expand (in an unique way) the configuration given in Figure 4.3 obtaining a two-parameter family of f-tilings $\tau \in \Omega(T_1, T_2)$ denoted by $(\mathcal{G}_{k,\alpha})_{k\geq 3, \alpha \in]\frac{\pi}{2}, \frac{2\pi}{3}[}$. For each $k \geq 3,\ k \in \mathbb{N}$ and $\alpha \in]\frac{\pi}{2}, \frac{2\pi}{3}[$, $\mathcal{G}_{k,\alpha}$ has $4k$ isosceles triangles ($2k$ of each type). In Figure 4.5, we show a 2D and a $3D$ representation of $\mathcal{G}_{3,\alpha}$.

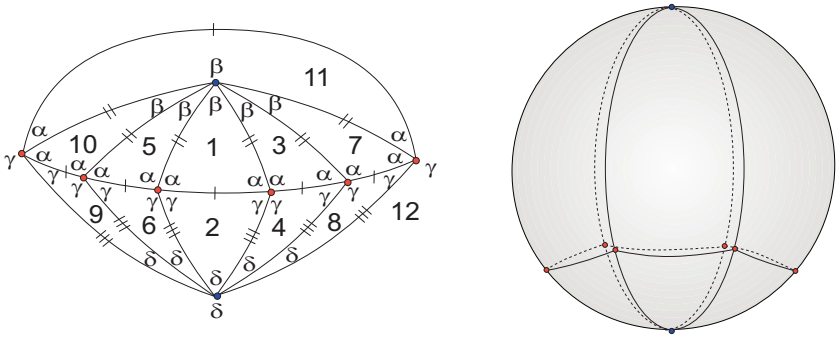

Figure 4.5: 2D and 3D representation of $\mathcal{G}_{3,\alpha}$.

This family does not come from any monohedral or any dihedral f-tiling with prototiles a spherical triangle and a parallelogram, since the elimination of edges leads to the absence of vertices of valency four.

Assuming now, $k\beta \neq \pi,\ k \geq 2$ then, in order to satisfy the angle folding relation, one should have $k\beta + \alpha = \pi$ for $k \geq 2$, by the Elimination Lemma. In this case, the angle α has several possible positions to be placed and we shall study every one of these possibilities.

1.2.1 Assume firstly, that the angle α is placed in tile numbered 6, as in Figure 4.6-I (by a symmetry argument it is not necessary to consider the case in which angle α is placed next to tile 5).

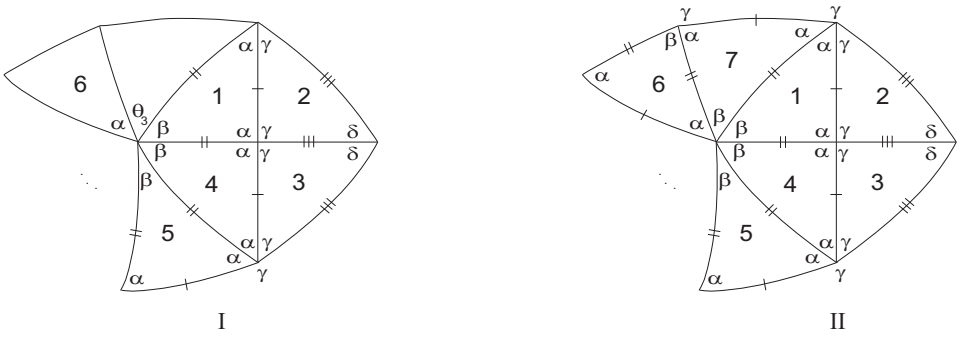

Figure 4.6: Local configuration.

The angle labeled θ_3 is either β or α.
By the Elimination Lemma, the sum of alternate angles containing β and γ does not satisfy the angle folding relation. Therefore, $\theta_3 = \beta$.

Expanding a bit more the configuration in Figure 4.6-I, we get a vertex partially surrounded by alternate angles β and γ, whose sum $\beta + \gamma + \mu$, $\mu \in \{\alpha, \beta, \gamma, \delta\}$ leads to the angle folding relation infringement or it is wiped out by the Elimination Lemma (Figure 4.6-II).

1.2.2 If the angle α is placed in tile labeled 10 (Figure 4.7), the vertices located on the boarder of the configuration, in Figure 4.7, are all of valency four giving rise to a vertex partially surrounded by alternate angles β and γ, which is an impossibility, as we have seen before.

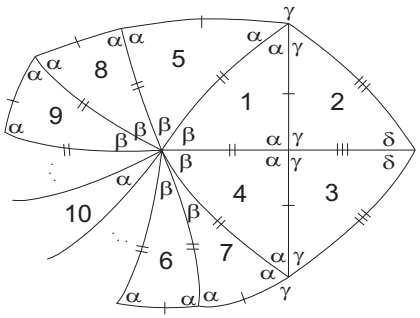

Figure 4.7: Local configuration.

2. Assume that $\alpha + \theta_1 < \pi$, with $\theta_1 = \gamma$ (Figure 4.2). Taking into account that $\alpha > \gamma,\ \alpha > \beta$ and $\gamma > \delta$, then

$$\delta < \gamma < \frac{\pi}{2},\ \alpha + \delta < \pi,\ \beta + \gamma < \pi \text{ and } \beta + \delta < \pi.$$

Since vertices of valency four must exist, then $\alpha \geq \frac{\pi}{2}$.

2.1 Assume that $\alpha = \frac{\pi}{2}$. Then, $\beta < \frac{\pi}{2}$ and vertices of valency four are surrounded exclusively by angles α. Having in account that $\frac{\pi}{2} = \alpha > \gamma >,\ 2\alpha + \beta > \pi$ and $2\gamma + \delta > \pi$, the sum of the alternate angles α and γ satisfies $\alpha + \gamma + k\beta = \pi,\ k \geq 1$. Extending the configuration in Figure 4.2, a decision must be taken about the angle $\theta_4 \in \{\alpha, \gamma\}$, Figure 4.8.

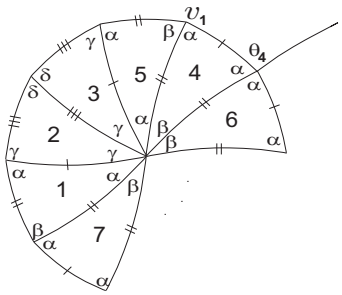

Figure 4.8: Local configuration.

If $\theta_4 = \alpha$, we are led to a vertex partially surrounded by alternate angles α and β, whose sum is either of the form $\alpha + \beta + t\beta = \pi,\ t \geq 1$ or $\alpha + \gamma + k\beta = \pi,\ k \geq 1$, since the other sums are impossible using the Elimination Lemma and the fact that $\alpha > \gamma$. Assuming that $\alpha + \gamma + k\beta = \pi,\ k \geq 1$, the angles arrangement is illustrated in the next figure, where we reach to an incompatibility:

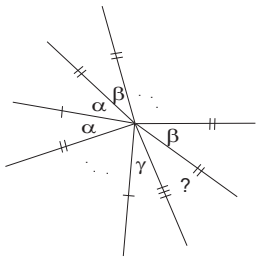

Figure 4.9: Angles arrangement.

Accordingly, vertex v_1 partially surrounded by the angles β, α, α is of valency $2(1+t)$, whose sums of alternate angles satisfy $\alpha + t\beta = \pi,\ t \geq 2$. Expanding the local representation in Figure 4.8, we are led to another incompatibility of the sides length, as shown in Figure 4.10-I.

If $\theta_4 = \gamma$, then the configuration extends a bit more, but we are led to a similar impossibility, Figure 4.10-II.

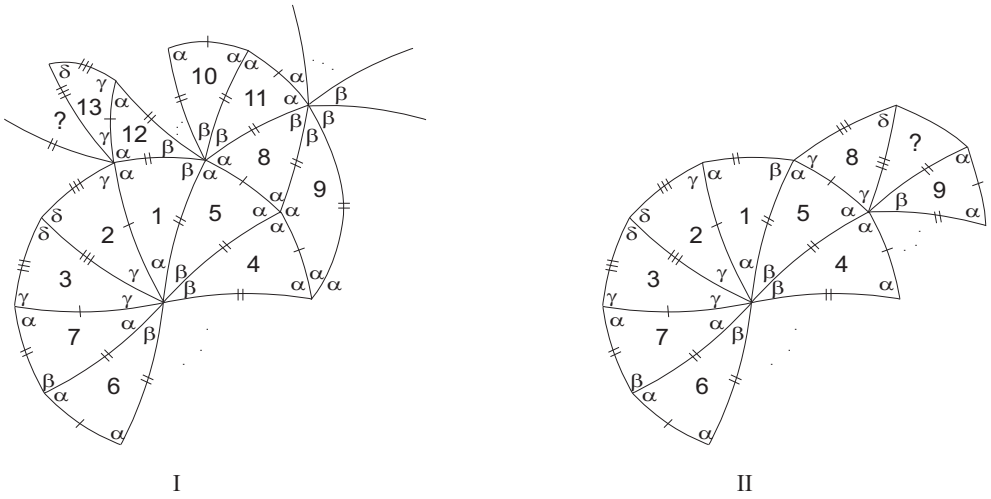

Figure 4.10: Local configurations.

2.2 If $\alpha > \frac{\pi}{2}$, as $\delta < \gamma < \frac{\pi}{2}$, vertices of valency four are surrounded by alternate angles α and β since $\alpha+\delta < \alpha+\gamma < \pi$. Additionally, the sum containing the alternate angles α and γ is of the form $\alpha+\gamma+m\delta = \pi,\ m \geq 1$, which is impossible by the sides length. □

Proposition 4.2 *If $\theta_1 = \delta$ (Figure 4.2) , then $\Omega(T_1, T_2) = \emptyset$.*

Proof. If $\theta_1 = \delta$, then $\alpha + \delta < \pi$ (observe the incompatibility of the sides length if $\alpha + \delta = \pi$). Taking into account the Elimination Lemma, $\alpha > \gamma$ and $2\gamma + \delta > \pi$, the sum containing angles α and δ is $\alpha + \delta + \mu$, which violates the angle folding relation, for any $\mu \in \{\alpha, \beta, \gamma, \delta\}$, preventing us to continue the expansion of the configuration started in Figure 4.2.

□

4.1.2 $\alpha > \beta$ and $\delta > \gamma$

Using the same terminology as in Figure 4.2, we get:

Proposition 4.3 *If $\theta_1 = \gamma$, then $\Omega(T_1, T_2)$ is composed by one parameter continuous family of f-tilings $(\mathcal{H}_\alpha)_{\alpha\in]\frac{\pi}{2},\pi[}$, one discrete family of isolated dihedral f-tilings $\left(\mathcal{I}^k\right)_{k\geq 3, k\in\mathbb{N}}$, and one isolated dihedral f-tiling $\mathcal{H}$ such that the sum of the alternate angles around vertices are respectively of the form:*

$$\alpha + \gamma = \pi,\ \beta = \delta = \frac{\pi}{2} \text{ for } \mathcal{H}_\alpha;$$
$$\alpha + 2\gamma = \pi,\ \delta = \frac{\pi}{2} \text{ and } \beta = \frac{\pi}{k},\ k \geq 3 \text{ for } \mathcal{I}^k;$$
$$2\alpha + \gamma = \pi,\ \alpha = \arccos\frac{\sqrt{6}}{6},\ \delta = \frac{\pi}{2} \text{ and } \beta = \frac{\pi}{3} \text{ for } \mathcal{H}.$$

3D representations of a member of $\mathcal{H}_\alpha$, $\mathcal{I}^3$, and $\mathcal{H}$ are given, respectively in Figures 4.12, 4.17 and 4.18.

Proof. Assume that $\theta_1 = \gamma$, in Figure 4.2. Then, $\alpha + \gamma \leq \pi$.

1. If $\alpha + \gamma = \pi$, then by the adjacency condition (4.1), one has $\beta = \delta$ and since $\delta > \gamma$, then $\beta = \delta > \frac{\pi}{3}$. Adding a new cell to the configuration in Figure 4.2, a decision must be taken about the angle $\theta_5 \in \{\alpha, \beta\}$, as in Figure 4.11.

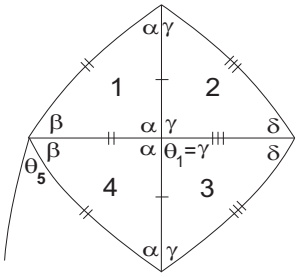

Figure 4.11: Local configuration.

1.1 Suppose firstly that $\theta_5 = \alpha$. Then, $\alpha + \beta < \pi$, otherwise $\beta = \gamma = \delta$, which is an impossibility. As $\alpha + \beta < \pi$ and $\alpha > \beta$, then $\beta < \frac{\pi}{2}$ and consequently $\gamma < \delta = \beta < \frac{\pi}{2} < \alpha$. Therefore, the sum $\alpha + \beta + \mu$ violates the angle folding relation, for any $\mu \in \{\alpha, \beta, \gamma, \delta\}$.

1.2 If $\theta_5 = \beta$, then $\beta \leq \frac{\pi}{2}$.

1.2.1 Suppose that $\beta = \frac{\pi}{2} = \delta$. Then, $\frac{\pi}{4} < \gamma < \frac{\pi}{2}$ and $\alpha > \frac{\pi}{2}$. The configuration expands and we get a continuous family of f-tilings, denoted by $(\mathcal{H}_\alpha)_{\alpha \in]\frac{\pi}{2}, \pi[}$. Figure 4.12 illustrates a representative element and it is composed by 4 isosceles triangles of each prototile.

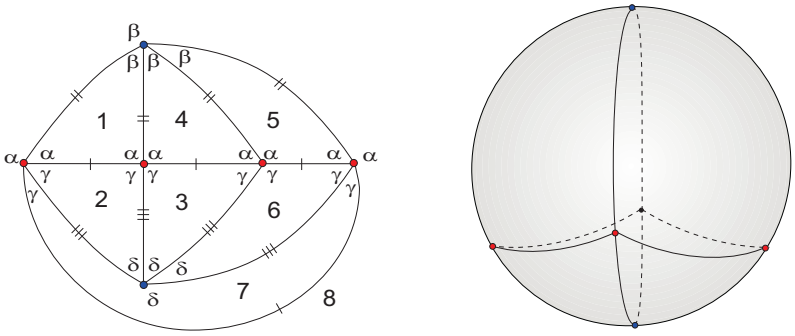

Figure 4.12: 2D and 3D representation of a member of $\mathcal{H}_\alpha$.

This family does not come from any monohedral or any dihedral family of f-tilings whose prototiles are a spherical triangle and a parallelogram.

1.2.2 If $\beta = \delta < \frac{\pi}{2}$, then $\gamma < \frac{\pi}{2} < \alpha$.
Taking into account the order relation between the angles and the Elimination Lemma, the sum $2\beta + \mu$ violates the angle folding relation, for any $\mu \in \{\alpha, \beta, \gamma, \delta\}$.

2. If $\alpha + \gamma < \pi$, a decision about the angle $\theta_6 \in \{\gamma, \delta\}$ must be made.

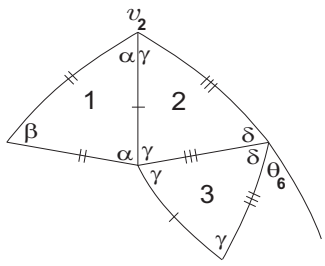

Figure 4.13: Local configuration.

2.1 If $\theta_6 = \gamma$ and $\delta + \theta_6 = \pi$, the configuration ends up at a vertex (v_2 in Figure 4.14) partially surrounded by angles α, γ, δ, whose sum $\alpha+\delta$ must be of the form $\alpha+\delta+k\beta = \pi,\ k \geq 1$, since $\delta + \gamma = \pi,\ \delta > \frac{\pi}{3}$ and $\alpha > \frac{\pi}{3}$. However, it is impossible to arrange the angles in order to satisfy this sum, due to the Elimination Lemma.

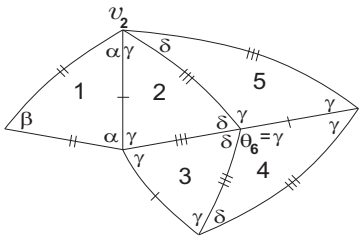

Figure 4.14: Local configuration.

2.2 Suppose that $\theta_6 = \gamma$ and $\delta + \theta_6 < \pi$. Having in account that $\delta > \gamma,\ 2\gamma + \delta > \pi$ and $\alpha > \frac{\pi}{3}$, the sum $\delta + \gamma$ satisfies $\delta + \gamma + k\beta = \pi,\ k \geq 1$. However, it is impossible to arrange the angles in order to satisfy the sum $\delta + \gamma + k\beta = \pi,\ k \geq 1$.

2.3 Assume now that $\theta_6 = \delta$. We shall study the cases $\delta = \frac{\pi}{2}$ and $\delta < \frac{\pi}{2}$ separately.

2.3.1 If $\delta = \frac{\pi}{2}$, then $\frac{\pi}{4} < \gamma < \frac{\pi}{2}$. Since $\alpha > \gamma$, one of the sums of the alternate angles at vertex v_3 in Figure 4.15 is either

- $\alpha + 2\gamma = \pi$ or
- $2\alpha + \gamma = \pi$ or
- $\alpha + \gamma + k\beta = \pi,\ k \geq 1$ or
- $\alpha + 2\gamma + p\beta = \pi,\ p \geq 1$.

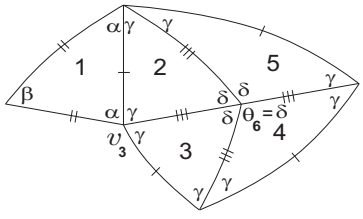

Figure 4.15: Local configuration.

2.3.1.1 If $\alpha+2\gamma=\pi$, at vertex v_3, then $\frac{\pi}{4}<\gamma<\frac{\pi}{3}$. We may expand the configuration in Figure 4.15 and get the one shown in Figure 4.16-I. Note that in the construction of the configuration, vertices surrounded by a sequence of angles containing the subsequence (γ,γ,γ) must be of valency six, with the sum $2\gamma+\alpha=\pi$. Additionally, one of the sums of alternate angles at vertices surrounded by a sequence of angles containing the subsequence (α,γ,γ) is of the form $\alpha+\gamma+k\beta=\pi,\ k\geq 1$ or $\alpha+2\gamma=\pi$.

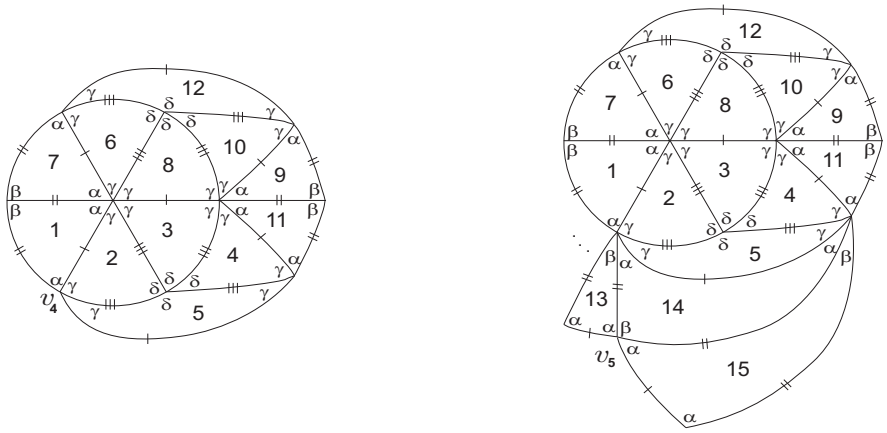

I II

Figure 4.16: Local configuration.

If $\alpha+\gamma+k\beta=\pi,\ k\geq 1$, at vertex v_4, for instance, we extend in an unique way the configuration and we are led to another vertex (v_5) partially surrounded by angles α,β,α, whose sum 2α satisfies $2\alpha+t\gamma=\pi,\ t\geq 1$, Figure 4.16-II. Therefore, from $\alpha+2\gamma=\pi$, we conclude that $t=1$, which is impossible. Accordingly, every vertices partially surrounded by angles α,γ,γ are of valency six, with the sum $\alpha+2\gamma=\pi$ and the configuration expands in an unique and symmetric way. For each $k\geq 3,\ k\in\mathbb{N}$, we get a complete dihedral f-tiling, denoted by $\mathcal{I}^k$ with $4k$ isosceles triangles of angles α,α,β and $8k$ isosceles triangles of angles γ,γ,δ, such that vertices of valency four are surrounded exclusively by angles δ, vertices of valency six are surrounded by alternate angles α,γ,γ and vertices of valency $2k$ are surrounded exclusively by angles β.

Figure 4.17 shows a global representation of $\mathcal{I}^3$. The angles are $\delta=\frac{\pi}{2},\ \beta=\frac{\pi}{3},\gamma=\arctan\left(\sqrt{\frac{5}{3}}\right)\approx 52.239^\circ$ and $\alpha\approx 75.522^\circ$.

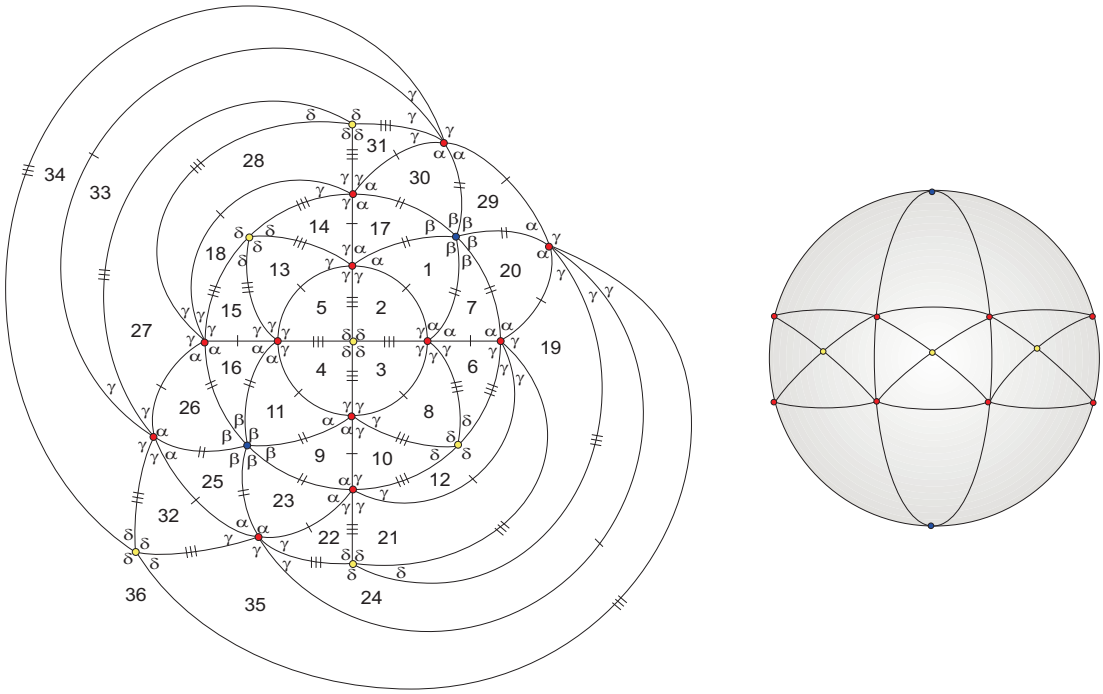

Figure 4.17: 2D and 3D representation of $\mathcal{I}^3$.

Eliminating some edges of each member of this family, we can get ${}^{E}\mathcal{R}^k$, a family of f-tilings whose prototiles are an isosceles triangle and an equiangular parallelogram, which can be found in [7] and [14].

2.3.1.2 If $2\alpha + \gamma = \pi$, at vertex v_3, then

$$\frac{\pi}{4} < \gamma < \beta < \alpha < \frac{\pi}{2} = \delta$$

and all the sums containing angles α and γ must satisfy $2\alpha + \gamma = \pi$, since the other possibilities ($\alpha + 2\gamma = \pi$ and $\alpha + \gamma + \beta = \pi$) imply that $\alpha = \gamma$ and $\alpha = \beta$, which are both impossible. Expanding the configuration, we get a complete f-tiling denoted by $\mathcal{H} \in \Omega(T_1, T_2)$, see Figure 4.18.

$\mathcal{H}$ is composed by 48 isosceles triangles of angles α, α, β and 24 isosceles triangles of angles γ, γ, δ, with $\beta = \frac{\pi}{3},\ \delta = \frac{\pi}{2},\ \alpha = \arccos\frac{\sqrt{6}}{6} \approx 65.905°$ and $\gamma \approx 48.19°$.

Eliminating some edges, we get a monohedral f-tiling, where the prototile is an equilateral triangle of angles $\frac{\pi}{2}, \frac{\pi}{2}, \frac{\pi}{2}$.

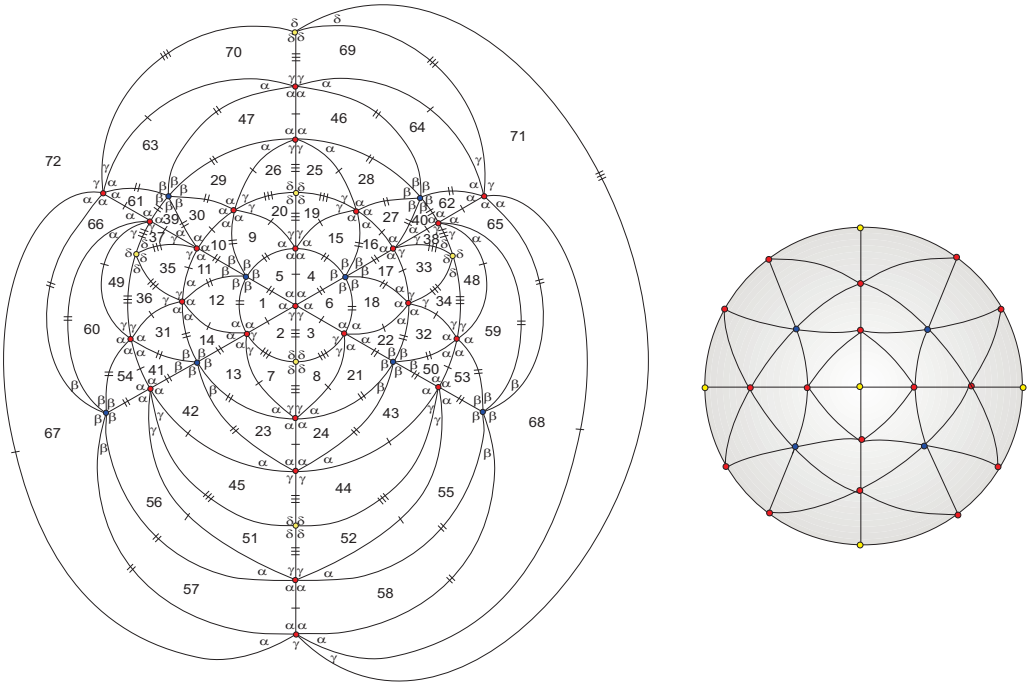

Figure 4.18: 2D and 3D representation of $\mathcal{H}$.

2.3.1.3 Assuming that $\alpha+\gamma+k\beta = \pi,\ k \geq 1$, at vertex v_3, the angle θ_7 (in Figure 4.19-I) is β, since $\theta_7 = \alpha$ implies that $2\alpha + \gamma = \pi$ and so $\frac{\pi}{4} < \gamma < \beta$. Consequently, $k = 1$ and $\alpha = \beta$, which is impossible. Extending the configuration in Figure 4.19-I, with $\theta_7 = \beta$, we end up at a vertex partially surrounded by alternate angles α, γ, γ, whose sum is $\alpha + 2\gamma \leq \pi$ (Figure 4.19-II).

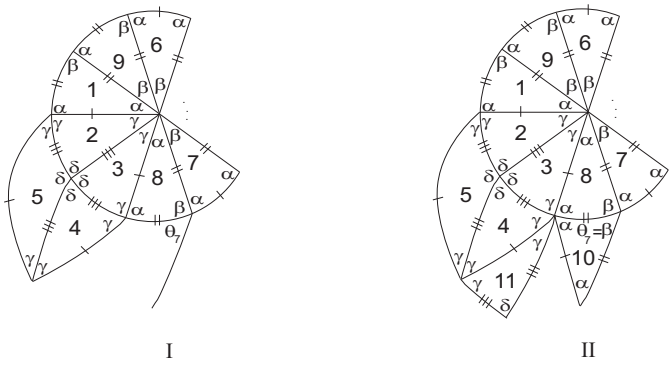

Figure 4.19: Local configurations.

In case $\alpha + 2\gamma = \pi$, we may add some new cells to the configuration above and the sum of the alternate angles at vertex v_6 (see Figure 4.20) is of the form $3\gamma + q\beta = \pi,\ q \geq 1$, which is impossible by the Elimination Lemma. Therefore $\alpha + 2\gamma < \pi$ and it remains the possibility $\alpha + 2\gamma + p\beta = \pi,\ p \geq 1$, which is also an impossibility due to the incompatibility of the edge sides.

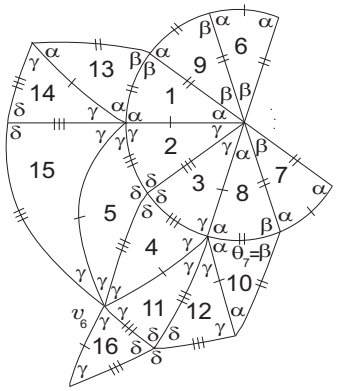

Figure 4.20: Local configuration.

2.3.1.4 If $\alpha + 2\gamma + p\beta = \pi,\ p \geq 1$, at vertex v_3, then $\alpha < \alpha + p\beta < \delta = \frac{\pi}{2}$ and taking into account that $2\gamma + \delta > \pi$ and $2\alpha + \beta > \pi$, then

$$2\gamma \leq 2\gamma + (p-1)\beta < \alpha < \frac{\pi}{2}.$$

Therefore, $\gamma < \frac{\pi}{4}$ (since $2\gamma < \alpha < \frac{\pi}{2}$), contradicting $\delta = \frac{\pi}{2}$ and $2\gamma + \delta > \pi$.

2.3.2 In case $\delta < \frac{\pi}{2}$, then $\frac{\pi}{4} < \gamma < \frac{\pi}{2}$ and so $\alpha \geq \frac{\pi}{2}$ or $\beta \geq \frac{\pi}{2}$. Either way, $\alpha \geq \frac{\pi}{2}$.

The sum of alternate angles α and γ in Figure 4.13 is of the form $\alpha+\gamma+k\beta = \pi,\ k \geq 1$, since the other possibilities ($2\alpha+\gamma = \pi$ or $2\gamma+\alpha = \pi$) contradict the facts $\alpha \geq \frac{\pi}{2}$ and $\alpha > \gamma$. Extending the configuration in Figure 4.13, with $\theta_6 = \delta$, we end up at a vertex whose angles arrangement is impossible, see Figure 4.21-I.

If $\theta_6 = \gamma$ (Figure 4.21-II), then the sum containing the alternate angles δ and α is either of the form $\alpha + \delta + \gamma = \pi$ or $\alpha + \delta + p\beta = \pi,\ p \geq 1$. However, the first case leads to $\alpha < \gamma$, which is a contradiction and the second case is impossible using the Elimination Lemma.

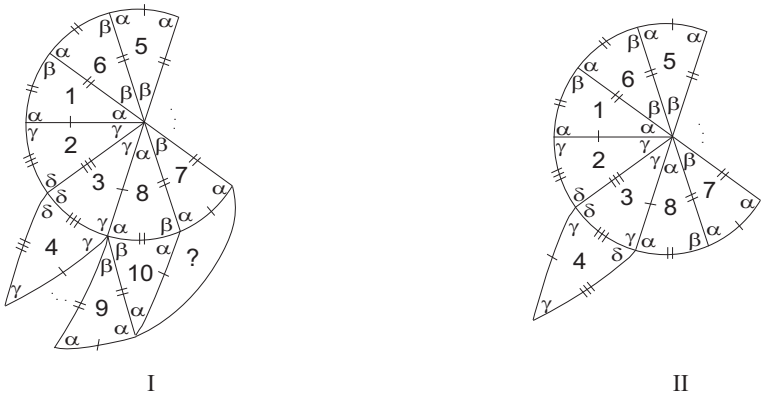

Figure 4.21: Local configuration.

□

Proposition 4.4 *If $\theta_1 = \delta$ (Figure 4.2), then $\Omega(T_1, T_2) = \varnothing$.*

Proof. If $\theta_1 = \delta$, in Figure 4.2, then $\alpha + \delta < \pi$, since $\alpha + \delta = \pi$ implies that vertex is of valency four, which is incompatible with the edge sides.
Taking into account that $\alpha > \frac{\pi}{3}$ and $\delta > \frac{\pi}{3}$, then the sum $\alpha + \delta + \mu$, for some μ is either of the form $\alpha + \delta + \gamma = \pi$ or $\alpha + \delta + \gamma + p\beta = \pi,\ p \geq 1$. Both cases are impossible, since $\alpha > \gamma$ and $2\gamma + \delta > \pi$.

□

4.1.3 $\beta > \alpha$ and $\gamma > \delta$

Suppose now that $\beta > \alpha$ and $\gamma > \delta$. Then, one has $\beta > \alpha > \gamma > \delta$ and also $\beta > \alpha > \gamma > \frac{\pi}{3}$.

Proposition 4.5 *If $\beta > \alpha$ and $\gamma > \delta$, then $\Omega(T_1, T_2) = \varnothing$.*

Proof. Assume that $\beta > \alpha$ and $\gamma > \delta$.

1. If $\theta_1 = \gamma$ in Figure 4.2, then $\alpha + \gamma \leq \pi$. Suppose first that $\alpha + \gamma = \pi$. Then,

$$\delta < \gamma < \frac{\pi}{2} < \alpha < \beta$$

and by the adjacency condition (4.1), we conclude that $\cos\beta = \cos\delta$, which is an impossibility.

If $\alpha+\gamma<\pi$, then in order to satisfy the angle folding relation, the sum containing α and γ is of the form $\alpha+\gamma+k\delta=\pi$, for some $k\geq 1$, since $\beta>\alpha>\gamma>\frac{\pi}{3}$. However, $\alpha+\gamma+k\delta>\gamma+\gamma+k\delta>\pi$, violating the angle folding relation.

2. If $\theta_1=\delta$ (Figure 4.2), then $\alpha+\delta<\pi$ due to the incompatibility of the edge sides. As $\beta>\alpha>\gamma>\delta$ and $2\gamma+\delta>\pi$, then the sum containing α and δ must be of the form $\alpha+k\delta=\pi$, for some $k\geq 1$. However, by the Elimination Lemma, the sequence of alternate angles $(\alpha,\delta,\delta,...,\delta)$ is impossible.

□

4.1.4 $\beta>\alpha$ and $\delta>\gamma$

Assume, finally that $\beta>\alpha$ and $\delta>\gamma$.

Proposition 4.6 *If $\theta_1=\gamma$ (Figure 4.2), then $\Omega(T_1,T_2)=\varnothing$.*

Proof. Assuming that $\theta_1=\gamma$, in Figure 4.2, then $\alpha+\gamma=\pi$ or $\alpha+\gamma<\pi$. We will study both cases separately.

1. If $\alpha+\gamma=\pi$, then $\beta+\delta>\pi$, $\alpha>\frac{\pi}{2}>\gamma$ and by the adjacency condition (4.1), we conclude that $\beta=\delta>\frac{\pi}{2}$. Adding some new cells to the local configuration, we get a vertex surrounded by the sequence α,β,β (see Figure 4.22) and the sum of the alternate angles β and α does not satisfy the angle folding relation, preventing us to continue the expansion of the configuration.

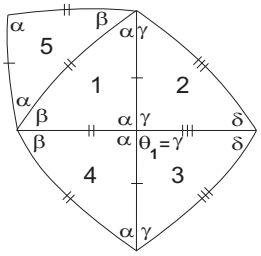

Figure 4.22: Local configuration.

2. Suppose that $\alpha + \gamma < \pi$. A decision about the angle $\theta_8 \in \{\gamma, \delta\}$ must be taken, see Figure 4.23.

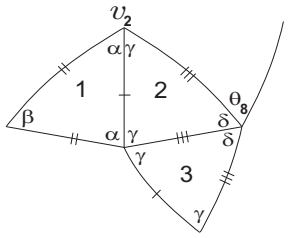

Figure 4.23: Local configuration.

2.1 If $\theta_8 = \gamma$ and $\delta + \gamma = \pi$, then $\delta > \frac{\pi}{2} > \gamma$. By the adjacency condition (4.1), we get $\beta > \frac{\pi}{2}$ and consequently the sum containing α and δ, at vertex v_2, satisfies $\alpha + \delta + k\alpha = \pi,\ k \geq 1$. Since $2\gamma + \delta > \pi$, one has $\alpha + \delta + k\alpha = \pi < 2\gamma + \delta$ and consequently, $2\alpha \leq \alpha + k\alpha < 2\gamma$, which is an impossibility.

2.2 If $\theta_8 = \gamma$ but $\delta + \gamma < \pi$, then $\gamma < \frac{\pi}{2}$ and, in order to satisfy the angle folding relation, one has either $\delta + \gamma + k\alpha = \pi,\ k \geq 1$ or $\delta + \gamma + \beta = \pi$ or $\delta + \gamma + \alpha + \beta = \pi$. In case $\delta + \gamma + k\alpha = \pi,\ k \geq 1$, then $\alpha < \gamma$, which is impossible, since $\alpha > \gamma$.
If $\delta + \gamma + \beta = \pi$ or $\delta + \gamma + \alpha + \beta = \pi$, then $\gamma > \beta > \frac{\pi}{3}$, contradicting the sums.

2.3 If $\theta_8 = \delta$, then $2\delta \leq \pi$.

2.3.1 Assume first that $\delta = \frac{\pi}{2}$. Then, $\frac{\pi}{4} < \gamma < \frac{\pi}{2}$ and, by the adjacency condition (4.1), $\alpha < \frac{\pi}{2}$ and $\beta \neq \frac{\pi}{2}$. The configuration in Figure 4.23 expands to the one shown in Figure 4.24-I, with $\theta_9 \in \{\alpha, \gamma\}$.

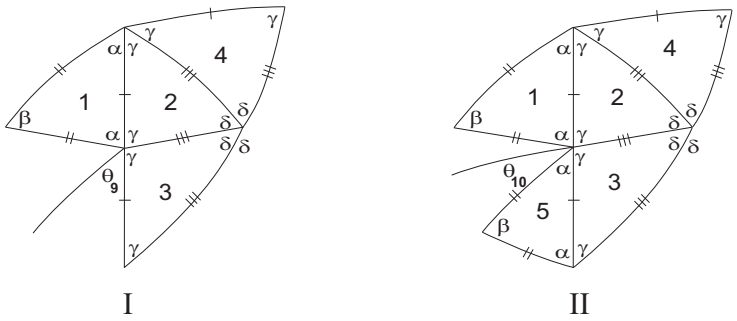

Figure 4.24: Local configurations.

In case $\theta_9 = \alpha$, then angle $\theta_{10} = \beta$ in Figure 4.24-II, otherwise we would have $2\alpha+\gamma = \pi$ and so $\frac{\pi}{3} < \alpha < \frac{3\pi}{8} < \frac{\pi}{2}$. Consequently, from the adjacency condition (4.1), $\beta > \frac{\pi}{2}$ and the configuration leads us to a vertex partially surrounded by angles α, β, β, whose sum $\alpha + \beta + \mu$ violates the angle folding relation for any $\mu \in \{\alpha, \beta, \gamma, \delta\}$. Therefore, $\alpha+\gamma+\beta = \pi$, since the sum $\alpha+\gamma+\beta+\mu$ does not satisfy the angle folding relation, for any $\mu \in \{\alpha, \beta, \gamma, \delta\}$.

The configuration in Figure 4.24-II now takes the form:

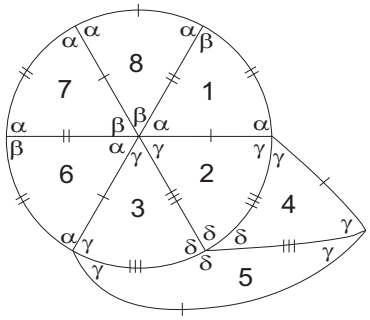

Figure 4.25: Local configuration.

Note that all the sums of alternate angles containing α and γ satisfy $\alpha+\gamma+\beta = \pi$, since the other possibilities ($\alpha + 2\gamma = \pi$ or $2\alpha + \gamma = \pi$) contradict the angle folding relation and the fact that $\alpha < \beta$. So the above configuration is now the one shown below:

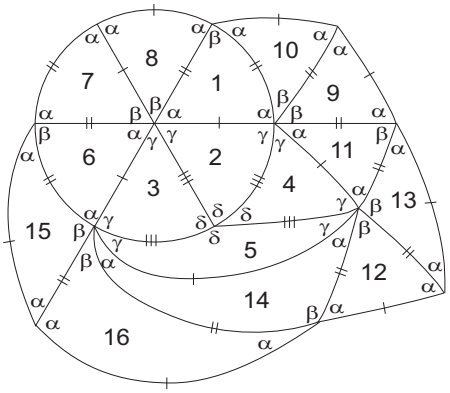

Figure 4.26: Local configuration.

In the above configuration, the sum containing two alternate angles α is either of the form $3\alpha = \pi$ or $2\alpha + \gamma = \pi$, which is impossible, since in the first case, we get the

impossibility $3\alpha = \pi = 2\alpha + \beta$ and in the second case, the contradiction$\alpha = \beta$.

2.3.2 If $\gamma < \delta < \frac{\pi}{2}$, then the sum containing 2δ must satisfy either $2\delta + \gamma = \pi$ or $2\delta + \gamma + s\alpha = \pi,\ s \geq 1$. In both cases, from $2\gamma + \delta > \pi$, we get the contradiction $\delta < \gamma$.

□

Proposition 4.7 *If $\theta_1 = \delta$ (Figure 4.2), then $\Omega(T_1, T_2) = \varnothing$.*

Proof. If $\theta_1 = \delta$, then $\alpha + \delta < \pi$, since the sum $\alpha + \delta = \pi$ is incompatible with the length of the sides. A decision must be taken about the angle $\theta_{11} \in \{\gamma, \delta\}$ in Figure 4.27.

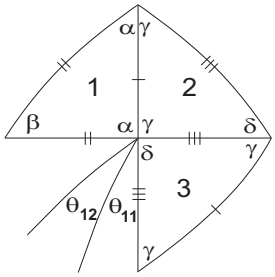

Figure 4.27: Local configuration.

1. If $\theta_{11} = \gamma$, then $\gamma < \frac{\pi}{2}$. The angle labeled θ_{12} is α, otherwise we would have $\alpha + \delta + \gamma \leq \pi$ and from $2\gamma + \delta > \pi$, we conclude that $\alpha < \gamma$, which is an impossibility. Since $\theta_{12} = \alpha$, then $2\alpha + \delta \leq \pi$. But, taking into account that $\alpha > \gamma$ and $2\gamma + \delta > \pi$, then $2\alpha + \delta > \pi$, contradicting $2\alpha + \delta \leq \pi$.

2. If $\theta_{11} = \delta$, then vertex is of valency greater than four, due to the incompatibility of the length of the sides. Accordingly,

$$\alpha + \gamma < \alpha + \delta < \pi,\ \gamma + \delta < \pi,\ \gamma < \frac{\pi}{2}$$

and so, vertices of valency four are surrounded exclusively by angles α or by angles β or by angles δ or by alternate angles α and β. Either way, $\beta \geq \frac{\pi}{2}$ or $\delta = \frac{\pi}{2}$.

2.1 Assuming that $\beta = \frac{\pi}{2}$, then $\frac{\pi}{4} < \alpha < \frac{\pi}{2}$ and consequently, the sum $\alpha + \delta + \mu$ does not satisfy the angle folding relation, for any $\mu \in \{\alpha, \beta, \gamma\, \delta\}$, since $\alpha > \gamma$, $\delta > \gamma$ and $2\gamma + \delta > \pi$.

2.2 If $\beta > \frac{\pi}{2}$, then vertices of valency four are surrounded by alternate angles α and β or exclusively by angles δ. If $\alpha + \beta = \pi$ and having in account that $\alpha + \gamma < \alpha + \delta < \pi$, one has $\gamma < \delta < \beta$. By the order relation between the angles, $\alpha > \gamma$ and $2\gamma + \delta > \pi$, we conclude that the sum containing the alternate angles γ and δ does not satisfy the angle folding relation.

2.3 If $\delta = \frac{\pi}{2}$, then $\frac{\pi}{4} < \gamma < \frac{\pi}{2}$ and by compatibility of the edge sides and having in account that $\alpha > \gamma$ and $2\gamma + \delta > \pi$, the sum containing alternate angles γ and δ violates the angle folding relation.

□

4.2 Isohedrality-Classes and Isogonality-Classes

Recall that, a spherical isometry σ is a *symmetry* of τ if σ maps every tile of τ into a tile of τ, where τ is a spherical f-tiling.

Furthermore, tiles T and T' of τ are in the same *transitivity class* if exists a symmetry that maps T into T'. If τ contains k transitivity classes of tiles, then τ is said *k-isohedral*. Similarly, if there are k transitivity classes of vertices, then τ is said *k-isogonal*.

Here, we present the transitivity classes of isogonality and isohedrality of the spherical f-tilings obtained $\mathcal{G}_{k,\alpha},\ \alpha \in]\frac{\pi}{2}, \frac{2\pi}{3}[,\ \mathcal{H}_{\alpha},\ \frac{\pi}{2} < \alpha < \pi,\ \mathcal{I}^k,\ k \geq 3,\ k \in \mathbb{N}$ and $\mathcal{H}$.

In **Table 4.1** is shown a complete list of all spherical dihedral f-tilings, whose prototiles are an isosceles triangle T_1 of angles α, α, β and another isosceles triangle T_2 of angles γ, γ, δ, with adjacency of type I. We have used the following notation:

- M and N are, respectively, the number of triangles congruent to T_1 and the number of triangles congruent to T_2 used in such dihedral f-tilings;
- The numbers of isohedrality-classes and isogonality-classes for the symmetry group are denoted, respectively, by # isoh. and # isog.;
- $\alpha = \alpha_0^k$, in f-tiling $\mathcal{G}_{k,\alpha}$ is the solution of

$$\frac{\cos\beta + \cos^2\alpha}{\sin^2\alpha} = \frac{\cos\delta + \cos^2\gamma}{\sin^2\gamma}, \tag{4.3}$$

  with $\beta = \delta = \frac{\pi}{k}$ and $\gamma = \pi - \alpha$;
- $\gamma = \gamma_0^k$, in f-tiling $\mathcal{I}^k$, is the solution of

$$\frac{\cos\beta + \cos^2\alpha}{\sin^2\alpha} = \frac{\cos\delta + \cos^2\gamma}{\sin^2\gamma},$$

  with $\alpha = \pi - 2\gamma,\ \delta = \frac{\pi}{2}$ and $\beta = \frac{\pi}{k}$.

f-**tiling**	α	β	γ	δ	M	N	# isoh.	# isog.
$\mathcal{G}_{k,\alpha},\ k \geq 3$	α_0^k	$\frac{\pi}{k}$	$\pi - \alpha$	$\frac{\pi}{k}$	$2k$	$2k$	2	3
$\mathcal{H}_\alpha$	$]\frac{\pi}{2}, \pi[$	$\frac{\pi}{2}$	$\pi - \alpha$	$\frac{\pi}{2}$	4	4	2	3
$\mathcal{I}^k,\ k \geq 3$	$\pi - 2\gamma$	$\frac{\pi}{k}$	γ_0^k	$\frac{\pi}{2}$	$4k$	$8k$	2	3
$\mathcal{H}$	$\arccos \frac{\sqrt{6}}{6}$	$\frac{\pi}{3}$	$\pi - 2\alpha$	$\frac{\pi}{2}$	48	24	2	3

Table 4.1: The Combinatorial Structure of the Dihedral f-Tilings of the Sphere by Isosceles Triangles with Adjacency of type I

4.3 Triangular Dihedral f-Tilings with Adjacency of Type II

Here, we classify all dihedral f-tilings whose prototiles are two non congruent isosceles triangles with adjacency of type II, as illustrated in Figure 4.28.

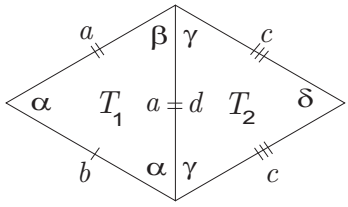

Figure 4.28: Adjacency of type II.

This type of adjacency can be analytically described by the following equation, which is going to be useful in our reasoning:

$$\frac{\cos\alpha(1+\cos\beta)}{\sin\alpha\sin\beta} = \frac{\cos\delta+\cos^2\gamma}{\sin^2\gamma}, \tag{4.4}$$

We start this section by showing that it is impossible to have $a = d$ and $b = c$:

The condition $a = d$ can be described by the adjacency condition (4.4) and $b = c$ can be described by the equation

$$\frac{\cos\beta+\cos^2\alpha}{\sin^2\alpha} = \frac{\cos\gamma(1+\cos\delta)}{\sin\gamma\sin\delta}. \tag{4.5}$$

On the other hand, from the relations

$$\sin\alpha = \sin\delta,\ \sin\beta = \sin\gamma,$$

one has $(\alpha = \delta \vee \alpha = \pi - \delta) \wedge (\beta = \gamma \vee \beta = \pi - \gamma)$ (see Figure 4.29). Next, we shall study all possibilities.

i) Assuming that $\alpha = \delta$ and $\beta = \gamma$ vertices of valency four are surrounded either by angles γ or by angles δ or by alternate angles γ and δ, see Figure 4.29-I.
In the first case, $\gamma = \frac{\pi}{2}$ and by the equation (4.5), we conclude that $\delta = \frac{\pi}{2}$, which is a contradiction.

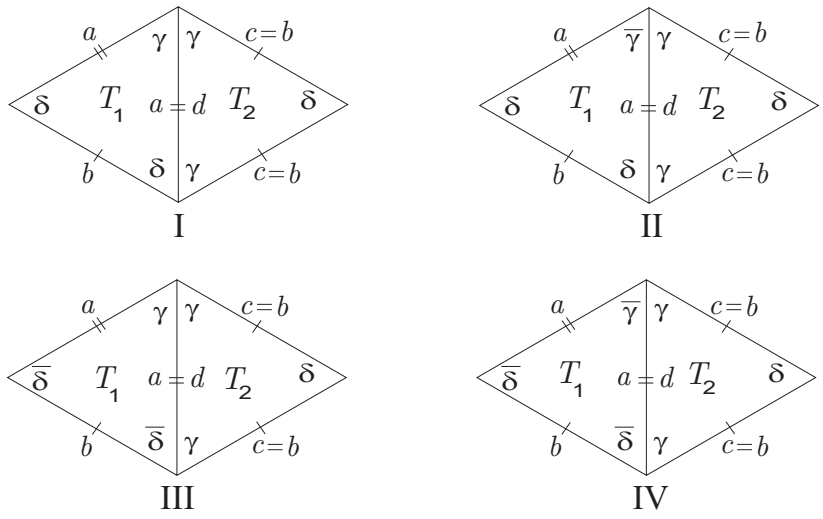

Figure 4.29: Side $a = d$ and $b = c$ with the relations $\sin\alpha = \sin\delta,\ \sin\beta = \sin\gamma$.

In the second case, $\delta = \frac{\pi}{2}$ and by (4.4), we are led to the impossibility $\gamma = \delta$.

Finally, in the third case, $\gamma + \delta = \pi$ and using the adjacency condition (4.4), we are led to $\delta = \frac{\pi}{2} = \gamma$, which is impossible.

ii) If $\alpha = \delta$ and $\beta = \pi - \gamma = \overline{\gamma}$, triangles T_1 and T_2 are shown in Figure 4.29-II. Since, vertices of valency four must occur, then $\gamma = \frac{\pi}{2}$ or $\delta = \frac{\pi}{2}$ or $\gamma + \delta = \pi$ or $\overline{\gamma} + \delta = \pi$.

Using (4.5) for $\gamma = \frac{\pi}{2}$ and using (4.4) for $\delta = \frac{\pi}{2}$, we get the impossibility $\delta = \frac{\pi}{2} = \gamma$.

In case $\gamma + \delta = \pi$ or $\overline{\gamma} + \delta = \pi$, then $\delta = \overline{\gamma}$ or $\delta = \gamma$, which is an impossibility.

iii) Considering $\alpha = \pi - \delta = \overline{\delta}$ and $\beta = \gamma$ (see Figure 4.29-III), then the vertices of valency four are surrounded either by angles γ or angles δ or by alternate angles γ and δ, γ and $\overline{\delta}$ or δ and $\overline{\delta}$.

If $\gamma = \frac{\pi}{2}$, then, by (4.5), we get the contradiction $\delta = \frac{\pi}{2} = \gamma$.

If $\delta = \frac{\pi}{2}$, we may use (4.4) to conclude that $\gamma = \frac{\pi}{2} = \delta$, which is impossible.

If $\gamma + \overline{\delta} = \pi$, then $\gamma = \delta$, an impossibility.

Assume now that vertices of valency four are all surrounded by alternate angles δ and $\overline{\delta}$. Consider $\delta < \gamma$ (the case $\gamma < \delta$ will be studied next). Consequently $\gamma > \frac{\pi}{3}$.

A decision about the angle $\lambda \in \{\gamma, \overline{\delta}\}$ (see next figure) must be taken.

If $\lambda = \gamma$, then $\gamma < \frac{\pi}{2}$, since the case $\gamma = \frac{\pi}{2}$ was already studied. Taking into account that $\gamma > \frac{\pi}{3}$ and $2\gamma + \delta > \pi$, the sum containing the alternate angles γ and λ must be of the form $2\gamma + \overline{\delta} \leq \pi$ and so $2\gamma \leq \delta < \gamma$, a contradiction.

If $\lambda = \overline{\delta}$, then $\gamma + \overline{\delta} < \pi$, otherwise $\gamma = \delta$, an impossibility. As $\gamma + 2\overline{\delta} > \pi$ and $\gamma + \overline{\delta} + \delta > \pi$, then the sum containing the alternate angles γ and $\overline{\delta}$ must satisfy $2\gamma + \overline{\delta} = \pi$. Since, $\gamma + 2\overline{\delta} > \pi$, we conclude that $\delta < \gamma < \overline{\delta}$. Therefore, $\overline{\delta} > \frac{\pi}{2}$ and along with $\gamma > \frac{\pi}{3}$, the condition $2\gamma + \overline{\delta} = \pi$ is violated.

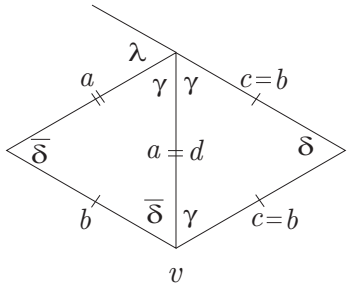

Figure 4.30: Local configuration.

Assume now that $\gamma < \delta$. As $\delta + \overline{\delta} = \pi$, then $\delta < \frac{\pi}{2}$ or $\delta > \frac{\pi}{2}$ (the case $\delta = \frac{\pi}{2}$ was already studied). If $\delta < \frac{\pi}{2} < \overline{\delta}$, then vertex v (Figure 4.30) is of valency $2(1+k)$, $k \geq 2$, whose sums of alternate angles are of the form $\overline{\delta} + k\gamma = \pi$. However, as $\gamma + 2\overline{\delta} > \pi$ and $2\gamma + \delta > \pi$, then $(k-1)\gamma < 2\gamma$ implying that $k = 2$, meaning $\overline{\delta} + 2\gamma = \pi$. Therefore, $\gamma = \frac{\delta}{2}$ and T_2 is an isosceles triangle of angles $(\frac{\delta}{2}, \frac{\delta}{2}, \delta)$ violating the condition $2\delta > \pi$.

Suppose that $\delta > \frac{\pi}{2} > \overline{\delta}$. Vertex v, in Figure 4.30, must be of valency $2(1+k)$, $k \geq 2$ whose sums of alternate angles satisfy $\overline{\delta} + k\gamma = \pi$. By a similar reasoning, we conclude that $k = 2$ and so $\gamma = \frac{\delta}{2}$. Using (4.4) and (4.5), we get $\delta \approx 100°$, $\overline{\delta} \approx 80°$ and $\gamma \approx 50°$. Adding new cells to the local configuration in Figure 4.29-III, tile six has two possible positions, as shown in Figure 4.31.

In the first possibility adding new cells to the configuration, we are led to a contradiction in tile 20, since it must be congruent to T_1 but there is incompatibility with edge sides. In the second possibility for tile 6, a similar contradiction arises at tile 11 preventing us to continue the extension of the configuration.

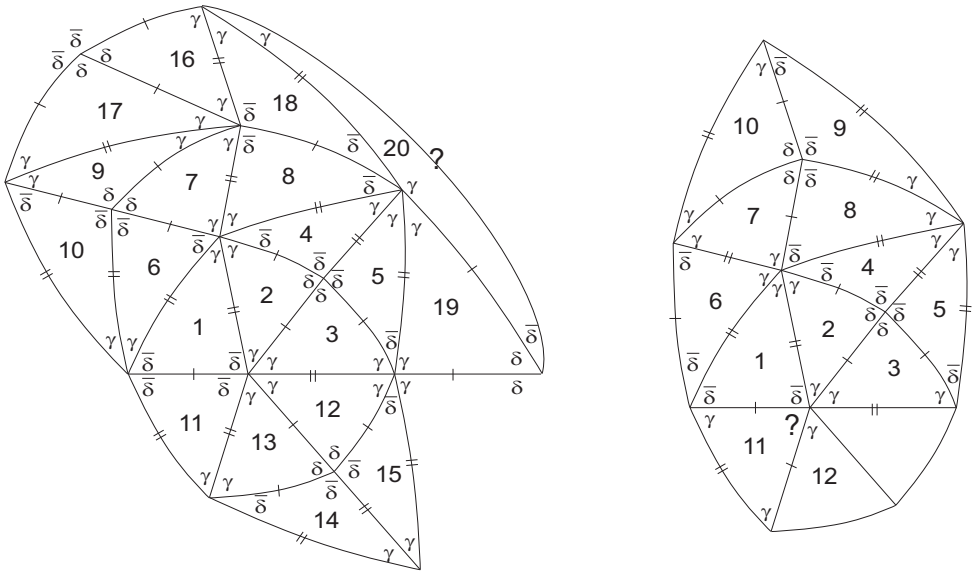

Figure 4.31: Local configuration.

iv) In the last case, $\alpha = \pi - \delta = \overline{\delta}$ and $\beta = \pi - \gamma = \overline{\gamma}$, triangles T_1 and T_2 are the ones shown in Figure 4.29-IV. The union of these triangles forms an isosceles triangle of sides $b,\ b,\ a+b$ and consequently $\delta = \overline{\delta} = \frac{\pi}{2}$. By (4.4), we get $\gamma = \frac{\pi}{2} = \delta$, an absurd.

In order to facilitate the construction of the dihedral f-tilings, we distinguish the possible different order relation between the angles, namely, ($\alpha > \beta$ and $\gamma > \delta$), ($\alpha > \beta$ and $\delta > \gamma$), ($\beta > \alpha$ and $\gamma > \delta$) and finally ($\beta > \alpha$ and $\delta > \gamma$).

If $\tau \in \Omega(T_1, T_2)$ satisfies **adjacency of type II**, then we may start its configuration with two adjacent cells congruent respectively to T_1 and T_2, as shown in Figure 4.32.

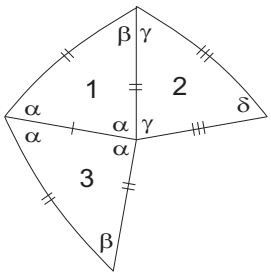

Figure 4.32: Local configuration.

In order to have the angle folding relation fulfilled, the sum containing the alternate angles α and γ must be of the form $\alpha+\gamma \leq \pi$. We shall separate cases $\alpha+\gamma=\pi$ and $\alpha+\gamma<\pi$.

Elimination Lemma-I *If* $\alpha+\gamma=\pi$, *then* $\Omega(T_1,T_2)=\emptyset$.

Proof. By the adjacency condition (4.4), if $\alpha=\frac{\pi}{2}$, then $\gamma=\delta=\frac{\pi}{2}$, which is impossible.

Assume now that $\alpha>\frac{\pi}{2}$. Then, $\gamma<\frac{\pi}{2}<\delta$. Consequently, the configuration illustrated in Figure 4.32 may be extended to the one shown in Figure 4.33-I, leading to a vertex, v_1 partially surrounded by angles $\delta,\gamma,\beta,\gamma,\delta$. As $\delta>\frac{\pi}{2}$, the sum containing the alternate angles δ,β,δ does not satisfy the angle folding relation.

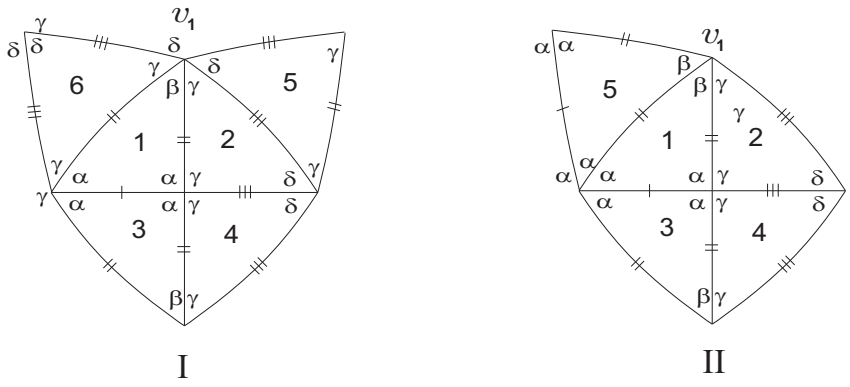

Figure 4.33: Local configurations.

Assuming that $\alpha<\frac{\pi}{2}$, then $\gamma>\frac{\pi}{2}$ and the extended configuration is now the one in Figure 4.33-II. Accordingly, $\alpha\leq\frac{\pi}{3}$ and $\beta<\alpha$, contradicting $2\alpha+\beta>\pi$.

□

Elimination Lemma-II *If* $\alpha>\beta$ *and* $\alpha+\gamma<\pi$, *then* $\Omega(T_1,T_2)=\varnothing$.

Proof. **Suppose first that** $\alpha>\beta$ **and** $\gamma>\delta$.

By the adjacency condition (4.4), if $\alpha\geq\frac{\pi}{2}$, then $\gamma>\delta>\frac{\pi}{2}$ contradicting $\alpha+\gamma<\pi$. Thus, $\beta<\alpha<\frac{\pi}{2}$ and consequently $\delta\geq\frac{\pi}{2}$ or $\gamma\geq\frac{\pi}{2}$. Either way, $\gamma\geq\frac{\pi}{2}$, since $\delta<\gamma$.

Starting from the local configuration in Figure 4.32, since $\alpha,\gamma>\frac{\pi}{3}$, in order to have the sum of the alternate angles containing α, γ and θ_1 (see Figure 4.34-I) obeying to

the angle folding relation, then θ_1 must be β or δ .

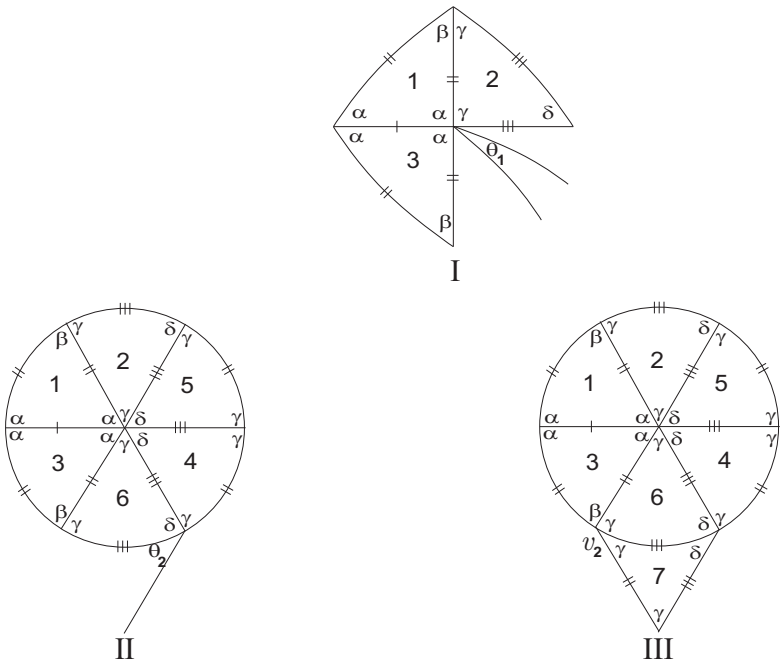

Figure 4.34: Local configurations.

If $\theta_1 = \beta$, then $\alpha+\gamma+\beta \leq \pi$ and from $2\alpha+\beta > \pi$, one has $\frac{\pi}{2} \leq \gamma < \alpha$, contradicting $\alpha + \gamma < \pi$.

If $\theta_1 = \delta$, then $\alpha + \gamma + \delta \leq \pi$. Assuming that $\gamma > \frac{\pi}{2}$, vertices of valency four are surrounded by the sequence of angles $(\gamma, \gamma, \beta, \beta)$. As, $\alpha + \gamma + \delta \leq \pi = \gamma + \beta$, then $\alpha < \beta$, which is an impossibility. Therefore, $\gamma = \frac{\pi}{2}$.

Considering $\alpha + \gamma + \delta = \pi$, we may extend the configuration in Figure 4.34-I getting the one illustrated in Figure 4.34-II, with $\theta_2 = \delta$ (observe that $\theta_2 = \gamma$ implies the impossibility $\beta + \delta = \pi$).

The sum of the alternate angles containing β and γ, at vertex v_2 (see Figure 4.34-III) is either of the form

- $\beta + \gamma + m\beta = \pi,\ m \geq 1$ or
- $\beta + \gamma + n\delta = \pi,\ n \geq 1$ or
- $\beta + \gamma + p\beta + q\delta = \pi,\ p, q \geq 1$.

In the first two cases, we may extend the configuration a little bit more and reach to vertices surrounded, respectively, by angles, $\alpha, \alpha, \alpha, \alpha, \rho$, with $\rho \in \{\alpha, \beta, \gamma\}$ (Figure 4.35-I) or $\gamma, \beta, \gamma, \delta$ (Figure 4.35-II). In the first case, the angle folding relation is not fulfilled. The second case contradicts $\beta, \delta < \frac{\pi}{2}$.

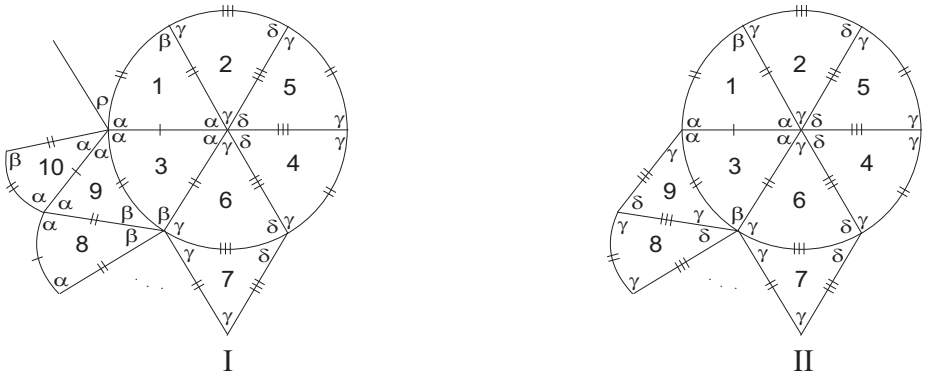

Figure 4.35: Local configurations.

The third case led us, also to an impossibility, since the possible extensions are the ones illustrated in Figure 4.35 and these configurations were already ruled out.

Suppose now that $\alpha + \gamma + \theta_1 < \pi$, with $\theta_1 = \delta$. Taking into account that $\alpha > \frac{\pi}{3}$, $\gamma = \frac{\pi}{2}$ and $2\alpha + \beta > \pi$, then the sum containing the angles α, γ and δ is of the form $\alpha + \gamma + \delta + t\delta = \pi$, for some $t \geq 1$. The configuration in Figure 4.34-I extends to the one below, where a vertex partially surrounded by angles β, γ, γ arises. The sum containing the alternate angles β and γ must satisfy either $\gamma + \beta + m\beta = \pi,\ m \geq 1$ or $\gamma + \beta + n\delta = \pi,\ n \geq 1$ or $\gamma + \beta + p\beta + q\delta = \pi,\ p, q \geq 1$, cases already studied.

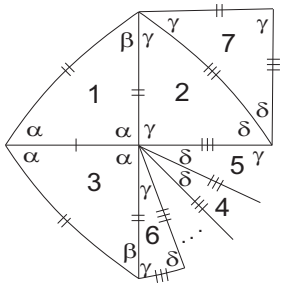

Figure 4.36: Local configuration.

Assume that $\alpha > \beta$ **and** $\delta > \gamma$.

By the adjacency condition (4.4), if $\delta < \frac{\pi}{2}$, then $\beta < \alpha < \frac{\pi}{2}$ and also $\gamma < \frac{\pi}{2}$ preventing the existence of vertices of valency four. Therefore, $\delta \geq \frac{\pi}{2}$.

Looking at the configuration in Figure 4.37, a decision about the angle $\theta_3 \in \{\alpha, \beta, \gamma\}$ must be taken.

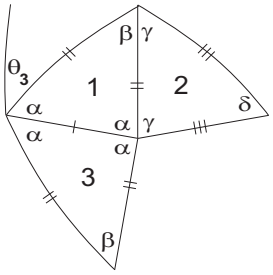

Figure 4.37: Local configuration.

1. Assume first that $\theta_3 = \alpha$. Then, $2\alpha \leq \pi$.

1.1 If $2\alpha = \pi$, then $\beta < \frac{\pi}{2},\ \gamma < \frac{\pi}{2}$ (note that $\alpha + \gamma < \pi$) and $\delta > \frac{\pi}{2}$ (by the adjacency condition (4.4)).
Consequently, the sum of the alternate angles containing α and γ is either of the form

- $\alpha + \gamma + k\gamma = \pi,\ k \geq 1$ or
- $\alpha + \gamma + t\beta = \pi,\ t \geq 1$ or
- $\alpha + \gamma + p\gamma + q\beta = \pi,\ p, q \geq 1$.

The first two cases end up at vertices v_3 and v_4 (see respectively, Figure 4.38-I, II), where v_3 is of valency four surrounded by angles $(\gamma, \delta, \delta, \gamma)$ (implying the contradiction $\delta = \frac{\pi}{2}$) and v_4 is surrounded by a sequence containing (δ, γ, α) violating the angle folding relation.

If $\alpha + \gamma + p\gamma + q\beta = \pi,\ p, q \geq 1$, we are led to similar impossibility as in the two previous cases.

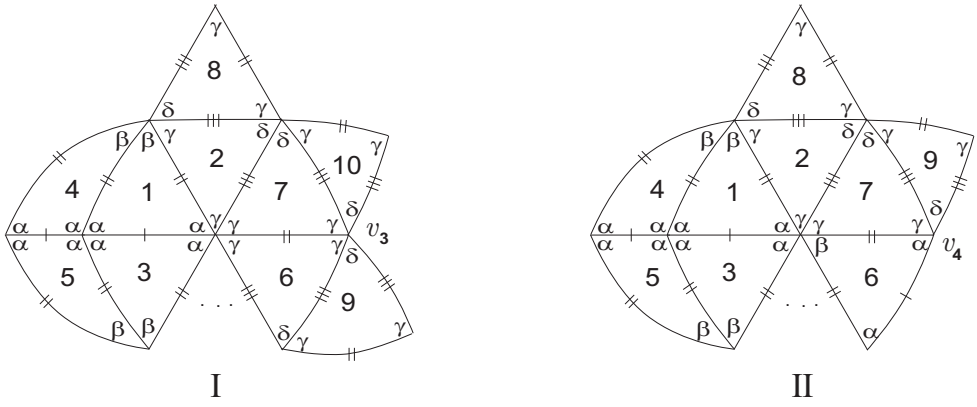

Figure 4.38: Local configurations.

1.2 Suppose now that $2\alpha < \pi$. As $2\alpha + \beta > \pi$, $\alpha > \frac{\pi}{3}$ and $\delta \geq \frac{\pi}{2}$, the sum containing α and θ_3 obeys $2\alpha + k\gamma = \pi$, for some $k \geq 1$. Accordingly,

$$\gamma < \beta < \alpha < \frac{\pi}{2} \leq \delta.$$

Assume firstly, that $\delta = \frac{\pi}{2}$. Then, $\gamma > \frac{\pi}{4}$ and so $k = 1$.
The order relation between the angles is now $\frac{\pi}{4} < \gamma < \beta < \alpha < \frac{\pi}{2} = \delta$. Extending the configuration in Figure 4.37, we get the one illustrated in Figure 4.39-I.

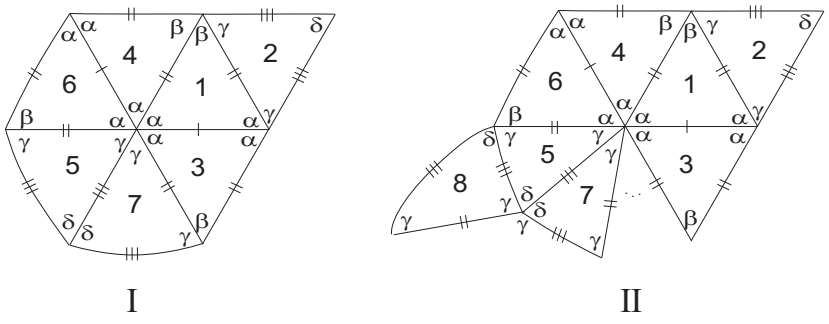

Figure 4.39: Local configurations.

The sum containing the alternate angles β and γ satisfies either $2\beta+\gamma = \pi$ or $2\gamma+\beta = \pi$ or $\beta + \gamma + \alpha = \pi$.
In the first and third cases, the contradiction $\alpha = \beta$ arises. In the second case, we conclude, by the adjacency condition (4.4), that $\alpha \approx 64.085°$ or $\alpha \approx 115.91°$, which are both impossible, since $\beta < \alpha < \frac{\pi}{2}$.

Assume now that $\delta > \frac{\pi}{2}$. The configuration in Figure 4.37 takes the form illustrated in Figure 4.39-II.

The vertex partially surrounded by the angles δ, γ, β is of valency greater than four (otherwise $\beta + \delta = \pi$ and $\gamma = \frac{\pi}{2}$ violating the equality $2\alpha + k\gamma = \pi,\ k \geq 1$). On the other hand, the vertex partially surrounded by the angles γ, δ, δ is also of valency greater than four (otherwise one has the impossibility $\beta + \delta > \gamma + \delta = \pi$, since $\beta > \gamma$). Therefore, the only way to arrange the angles around vertices of valency four is $\delta, \delta, \alpha, \alpha$, which is impossible due to the incompatibility on the edges.

2. Suppose that $\theta_3 = \beta$ (Figure 4.37). Then, $\alpha + \beta \leq \pi$.

2.1 In case $\alpha + \beta = \pi$, then $\gamma < \beta < \frac{\pi}{2} < \alpha$. The extended configuration ends up at a vertex (Figure 4.40-I) partially surrounded by the angles α, α, α, whose sum 2α violates the angle folding relation.

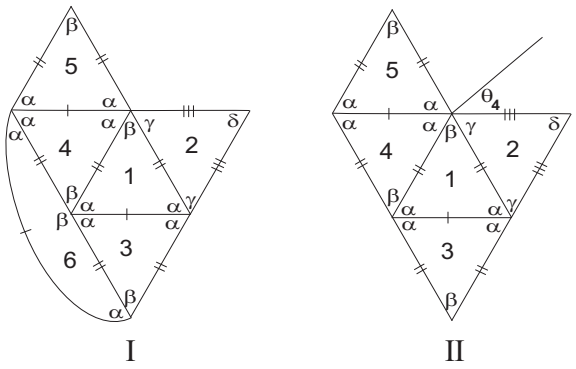

Figure 4.40: Local configurations.

2.2 If $\alpha + \beta < \pi$, then $\beta < \frac{\pi}{2}$ and a decision about the angle $\theta_4 \in \{\gamma, \delta\}$ must be taken, as shown in Figure 4.40-II.

2.2.1 If $\theta_4 = \gamma$, then $\alpha + \beta + \theta_4 \leq \pi$ and $\gamma < \alpha$.

2.2.1.1 Suppose first that $\alpha + \beta + \gamma = \pi$. Extending the configuration in Figure 4.40-II, tile numbered 9 has two possible positions (Figure 4.41-I, II). One of the positions of this tile led us to a vertex that must be of valency four surrounded by the angles $\alpha, \alpha, \delta, \gamma$ (see Figure 4.41-I), implying the contradiction $\gamma = \delta$.

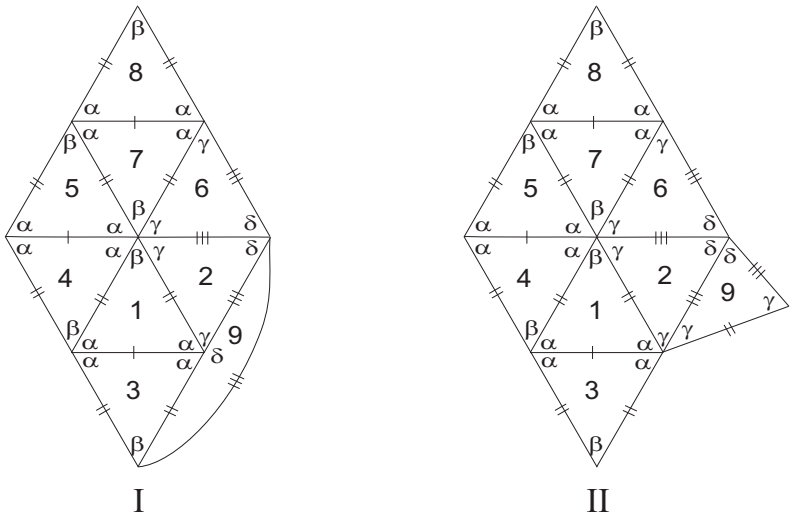

Figure 4.41: Local configurations.

The other possible position for tile 9 gives rise to a vertex partially surrounded by angles δ, δ, δ, which must be of valency four, since $\delta \geq \frac{\pi}{2}$ (see Figure 4.41-II). Therefore, $\delta = \frac{\pi}{2},\ \gamma > \frac{\pi}{4}$ and by (4.4), $\beta < \alpha < \frac{\pi}{2}$.

Consequently, the vertices partially surrounded by alternate angles α and γ are of valency six satisfying either $2\alpha + \gamma = \pi$ or $\alpha + 2\gamma = \pi$ or $\alpha + \gamma + \beta = \pi$.

The first case, implies that $\alpha = \beta$, which is impossible.

In the second case, one has $\gamma = \beta$ and so

$$\frac{\pi}{4} < \gamma = \beta < \alpha < \frac{\pi}{2} = \delta.$$

By the adjacency condition (4.4), we get $\gamma = \beta \approx 52.884^\circ$ and $\alpha \approx 74.232^\circ$. Accordingly, we have three type of vertices: vertices of valency four surrounded exclusively by angles δ and vertices of valency six surrounded by alternate angles α, γ, β and α, γ, γ. Thus, we may extend the configuration in Figure 4.41-II, in an unique way, getting a vertex v_5 (Figure 4.42-I) surrounded by angles $\gamma, \gamma, \gamma, \gamma, \gamma$, whose sum $3\gamma + \mu$ does not satisfy the angle folding relation for any $\mu \in \{\alpha, \beta, \gamma, \delta\}$. Consequently, we can not go on the tiling construction.

It remains the case $\alpha + \gamma + \beta = \pi$. Extending the configuration in Figure 4.41-II, we get a vertex v_6 partially surrounded by angles $\alpha, \alpha, \alpha, \alpha$ (Figure 4.42-II).

As $2\alpha + \beta > \pi,\ \alpha > \frac{\pi}{3},\ \delta = \frac{\pi}{2}$ and $\alpha > \gamma > \frac{\pi}{4}$, the sum 2α must obey to the condition

$2\alpha + \gamma = \pi$. However, from $\alpha + \beta + \gamma = \pi$, a contradiction is achieved.

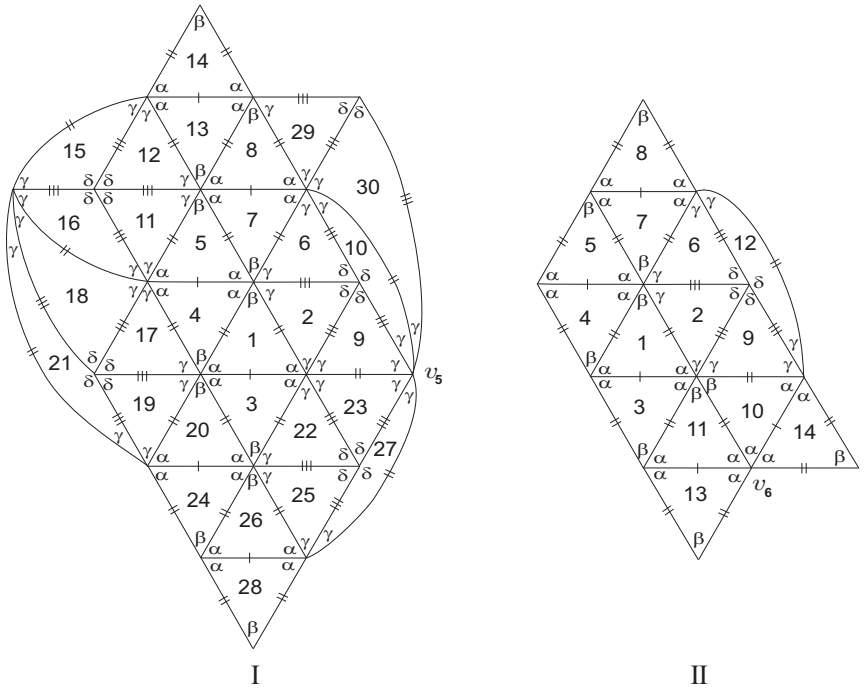

Figure 4.42: Local configurations.

2.2.1.2 Assume that $\alpha + \beta + \theta_4 < \pi$, with $\theta_4 = \gamma$. A decision about the angle $\theta_5 \in \{\gamma, \delta\}$ must be taken in configuration in Figure 4.43-I.

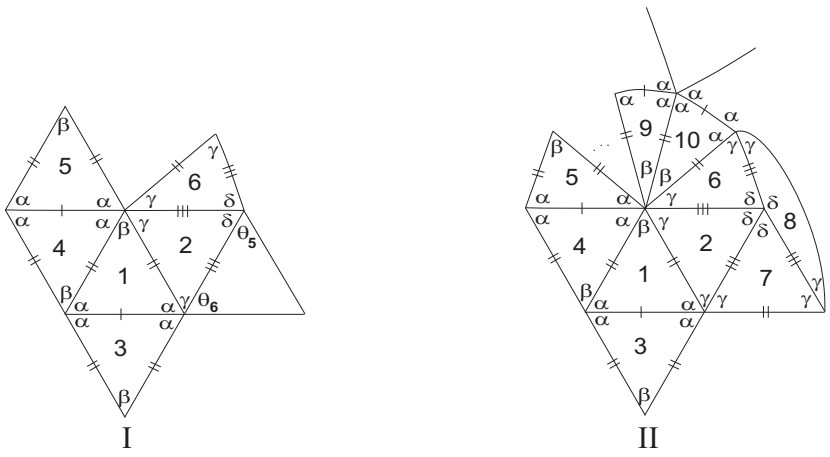

Figure 4.43: Local configurations.

In case $\theta_5 = \gamma$, then $\theta_6 = \delta$ and the sum containing α and δ must satisfy $\alpha+\delta+k\beta = \pi$, $k \geq 1$, since $\alpha > \frac{\pi}{3}$, $\delta \geq \frac{\pi}{2}$, $\gamma < \alpha$ and $2\gamma + \delta > \pi$. However, as $2\alpha + \beta > \pi$, then

$\frac{\pi}{2} \leq \delta < \alpha$ violating the condition $\alpha + \delta + k\beta = \pi$. Thus, $\theta_5 = \delta$ and so $\delta = \frac{\pi}{2}$. Consequently $\frac{\pi}{4} < \gamma < \frac{\pi}{2}$ and from the adjacency condition, one has $\beta < \alpha < \frac{\pi}{2}$. In order to satisfy the angle folding relation, the sum containing the angles α, β and γ must be either of the form $\alpha + 2\gamma + k\beta = \pi,\ k \geq 1$ or $\alpha + \gamma + q\beta = \pi,\ q \geq 2$.
The first case is impossible, since $2\gamma + \delta > \pi$ and $2\alpha + \beta > \pi$ and so $\alpha + \gamma + q\beta = \pi$, for some $q \geq 2$. The configuration can now be extended a bit more getting the one illustrated in Figure 4.43-II.

The vertex partially surrounded by the angles $\alpha, \alpha, \alpha, \alpha$ must be of valency six obeying to $2\alpha + \gamma = \pi$, since $\alpha > \frac{\pi}{3},\ \gamma > \frac{\pi}{4},\ \delta = \frac{\pi}{2}$ and $2\alpha + \beta > \pi$. Hence, $\frac{\pi}{4} < \gamma < \beta$ and consequently from the sum $\alpha + \gamma + q\beta = \pi$, we get the impossibility $q = 1$.

2.2.2 If $\theta_4 = \delta$ (Figure 4.40-II), then $\alpha + \beta + \theta_4 \leq \pi$. As $\delta \geq \frac{\pi}{2}$, we conclude that $\alpha + \beta < \frac{\pi}{2}$, contradicting $2\alpha + \beta > \pi$.

3. Assume finally that $\theta_3 = \gamma$ (Figure 4.44).

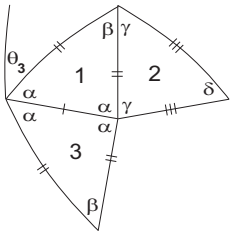

Figure 4.44: Local configuration.

3.1 If $2\gamma = \pi$, then $\delta > \frac{\pi}{2}$ and the extended configuration led us to $\beta + \delta = \pi$. By the adjacency condition (4.4) $\alpha > \frac{\pi}{2}$ violating the condition $\alpha + \gamma < \pi$, see Figure 4.45.

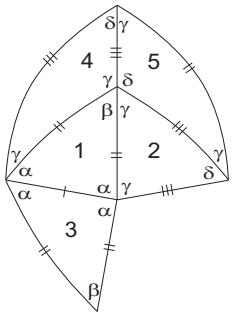

Figure 4.45: Local configuration.

3.2 Suppose now that $2\gamma < \pi$.

The cases the cases $\alpha \geq \frac{\pi}{2}$ and $\alpha < \frac{\pi}{2}$ will be analise separately.

3.2.1 Assume first, that $\alpha \geq \frac{\pi}{2}$. By the adjacency condition (4.4), $\delta > \frac{\pi}{2}$.

In case, $\alpha > \frac{\pi}{2}$, we extend the configuration in Figure 4.37 to the one in Figure 4.46, where tile 7 is congruent to T_1 or to T_2.

If tile 7 is congruent to T_1, then the extended configuration ends up at a vertex partially surrounded by the angles δ, γ, α, whose sum $\delta + \alpha$ violates the angle folding relation (see Figure 4.46-I).

If tile 7 is congruent to T_2, then $\gamma + \delta = \pi$ (Figure 4.46-II) (any other possibility led to the edge incompatibility).

It remains the configuration in Figure 4.46-II, with $\gamma + \delta = \pi$ where the vertex v_7 is partially surrounded by alternate angles δ, β, δ, whose sum 2δ, violates the angle folding relation and so the configuration can not continue.

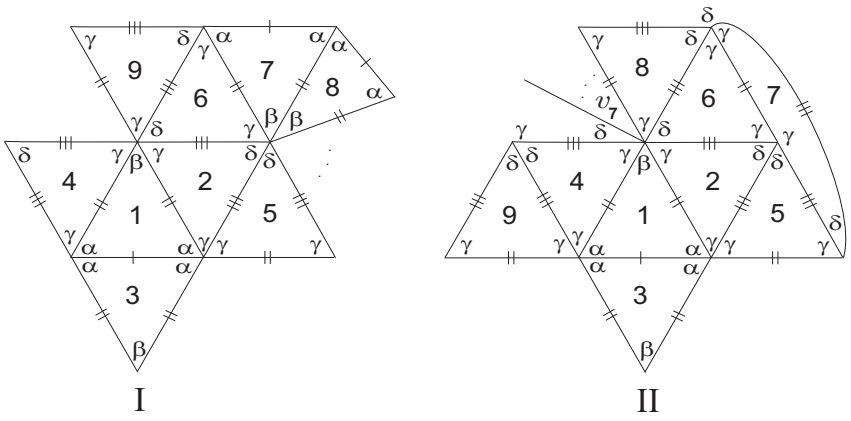

Figure 4.46: Local configurations.

If $\alpha = \frac{\pi}{2}$ then, as seen before, $\delta > \frac{\pi}{2}$.

Extending the configuration in Figure 4.37, we have two possibilities for tile 7 (see Figure 4.47).

In the first case, we get the configuration illustrated in Figure 4.47-I giving rise to a vertex partially surrounded by angles δ, γ, α, whose sum $\delta + \alpha$ does not satisfy the angle folding relation.

In the second case, we are lead to the configuration in Figure 4.47-II. In this con-

figuration, at vertex v_8 we can not add new tiles without violating the angle folding relation or the edge compatibility, preventing us to continue with the expansion of the configuration.

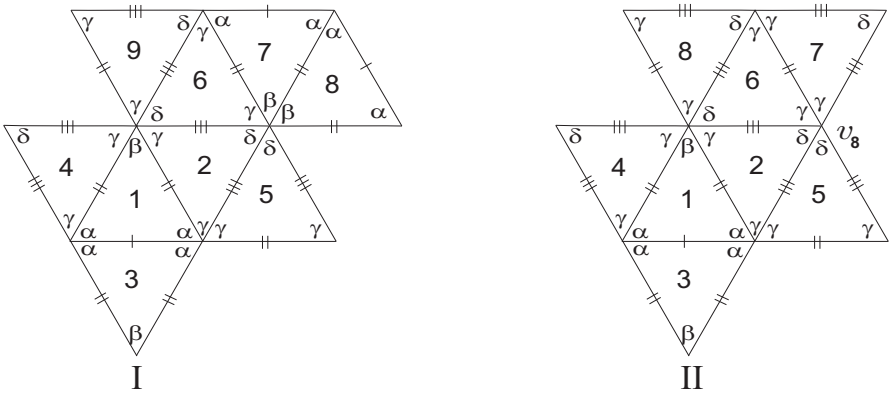

Figure 4.47: Local configurations.

3.2.2 Suppose now that $\alpha < \frac{\pi}{2}$.

If $\delta > \frac{\pi}{2}$, then vertices of valency four are surrounded by alternate angles δ and β or δ and α or δ and γ.

However, by the angles arrangement, the first possibility implies the contradiction $\gamma = \frac{\pi}{2}$.

The second case, violates the edge compatibility and the third case is ruled out by the adjacency condition (4.4), which implies $\alpha > \frac{\pi}{2}$, an impossibility.

If $\delta = \frac{\pi}{2}$, then $\gamma > \frac{\pi}{4}$ and vertices surrounded by alternate angles α and γ must satisfy either

- $\alpha + 2\gamma = \pi$ or
- $2\alpha + \gamma = \pi$ or
- $\alpha + \gamma + k\beta = \pi,\ k \geq 1$ or
- $\alpha + 2\gamma + m\beta = \pi,\ m \geq 1$.

3.2.2.1 Assume that $\alpha + 2\gamma = \pi$. Then,

$$\frac{\pi}{4} < \gamma < \frac{\pi}{3} < \alpha < \frac{\pi}{2} = \delta.$$

The configuration started in Figure 4.37 extends now to the one in Figures 4.48-I and II, according to the two possible positions of tile 5.

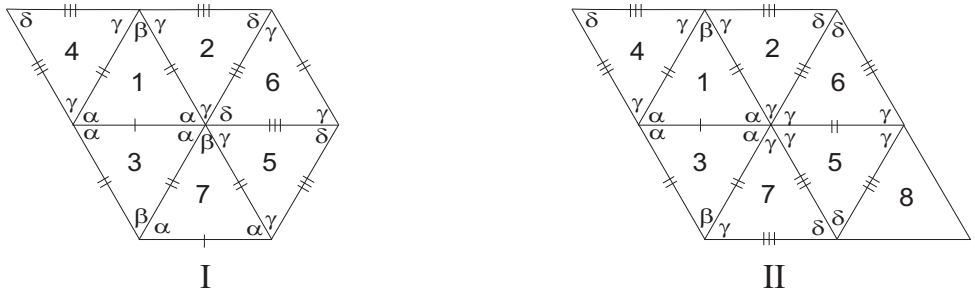

Figure 4.48: Local configuration.

In the first figure, one has $\alpha+2\gamma = \pi = \alpha+\delta+\beta$. Taking into account that $2\alpha+\beta > \pi$, then $\delta < \alpha$, which is a contradiction.

Extending the configuration in Figure 4.48-II, tile 8 can be located in two different positions (see Figure 4.49).

The first possible position led us to a vertex (v_9 in Figure 4.49-I) surrounded by a sequence of angles of the form $\delta, \gamma, \gamma, \gamma, \beta$ whose sums of alternate angles are of the form $\delta + \gamma + t\beta = \pi = 3\gamma + (t-1)\beta,\ t \geq 1$. Consequently, $\delta + \beta = 2\gamma$ and by the adjacency condition (4.4), we conclude that $\gamma \approx 34.824°$, which is impossible.

Analyzing the other position for tile 8, a decision about the angle $\theta_7 \in \{\gamma, \delta\}$ in tile 10 (Figure 4.49-II) must be taken.

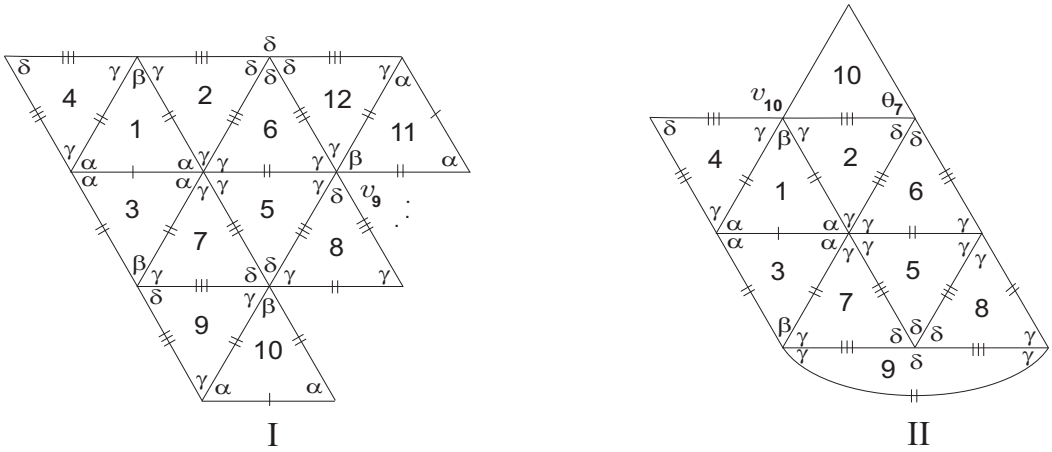

Figure 4.49: Local configurations.

If $\theta_7 = \gamma$, the sums of the alternate angles are of the form $\delta + \gamma + k\beta = \pi = 3\gamma + (k-1)\beta,\ k \geq 1$. As before, an impossibility is achieved using the adjacency condition (4.4).

If $\theta_7 = \delta$, taking into account that $\beta + 2\gamma < \alpha + 2\gamma = \pi$ and the compatibility of the edges, the sum containing the alternate angles β and γ, at vertex v_{10}, must be either of the form

- $2\gamma + m\beta = \pi,\ m \geq 2$ or
- $3\gamma + r\beta = \pi,\ r \geq 1$ or
- $\gamma + \delta + p\beta = \pi, p \geq 1$.

In the first case, we may expand the configuration and get a vertex (v_{11} at Figure 4.50-I) partially surrounded by three angles α. This vertex is of valency six whose both sums of alternate angles satisfy $2\alpha + \gamma = \pi$. Therefore, $\gamma = \alpha = \frac{\pi}{3}$, contradicting the condition $\alpha > \frac{\pi}{3}$.

In the second case, for $r > 1$ the angles arrangement, at vertex v_{10} (Figure 4.50-II) leads to another vertex surrounded by three angles α, whose impossibility is similar to the one studied previously.

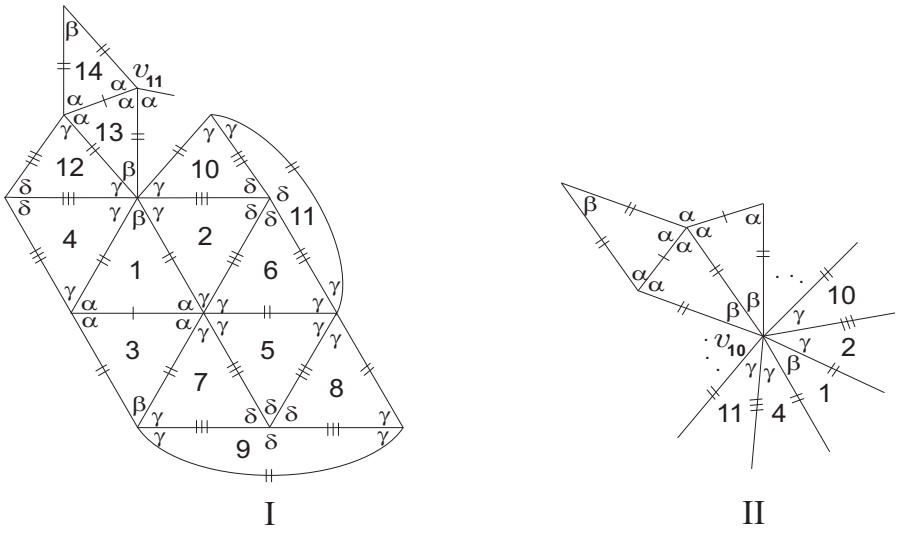

Figure 4.50: Local configuration and angles arrangement at vertex v_{10}.

For $r = 1$, the adjacency condition (4.4) lead us to $\gamma \approx 112.98°$ (impossible) or $\gamma \approx 50.180°$, which implies $\beta \approx 29.46°$ and $\alpha \approx 79.64°$. Proceeding with the extension of

the configuration, we must have in attention that tile numbered 19 has two possible positions, as shown in Figure 4.51-I.

The choice of one of the two possible positions for tile 19 leads to a vertex, v_{12} partially surrounded by three angles α and whose sum $2\alpha + \lambda$ does not satisfy the angle folding relation, for any $\lambda \in \{\alpha, \beta, \gamma, \delta\}$ (see Figure 4.51-II).

The other position for tile 19 gives rise to a vertex, v'_{12} partially surrounded by three angles α and a similar impossibility is achieved, Figure 4.51-III.

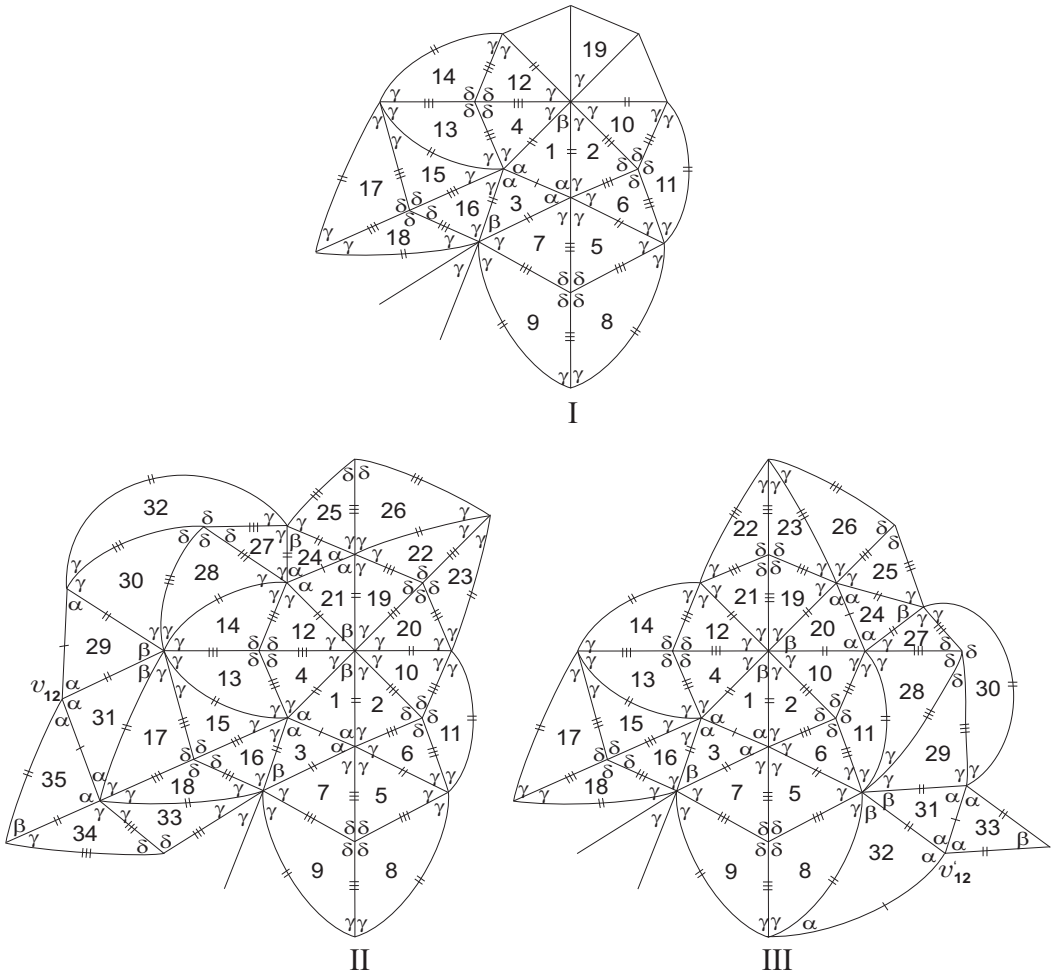

Figure 4.51: Local configurations.

The last case ($\gamma + \delta + p\beta = \pi,\ p \geq 1$) leads us to the sum $3\gamma + (p-1)\beta = \pi$, as illustrated in the next figure.

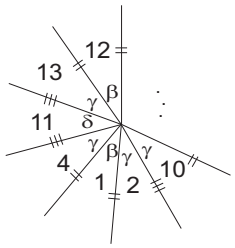

Figure 4.52: Angles arrangement at vertex v_{10}.

Accordingly, $\delta = 2\gamma - \beta$ and $\alpha = \pi - 2\gamma$, implying that $\gamma \approx 34.823°$ violating $\gamma > \frac{\pi}{4}$.

3.2.2.2 Suppose now that $2\alpha + \gamma = \pi$. Ordering,

$$\frac{\pi}{4} < \gamma < \beta < \alpha < \frac{\pi}{2} = \delta.$$

Extending the configuration in Figure 4.37, a decision about the position of tile 8 must be taken (see Figure 4.53-I, II).

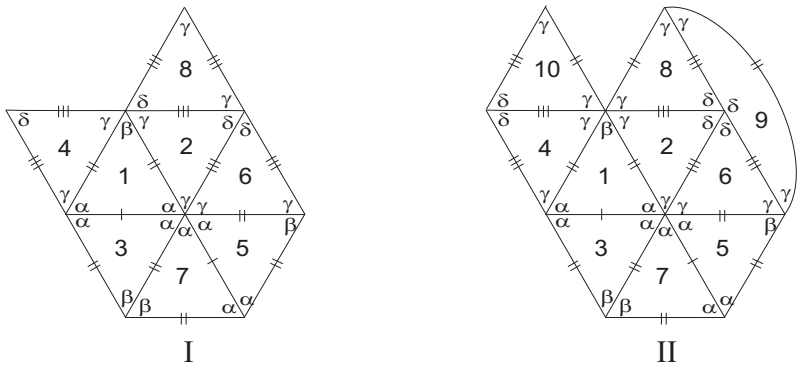

Figure 4.53: Local configurations.

In Figure 4.53-I, at the vertex partially surrounded by angles δ, δ, γ, the sum of alternate angles containing γ and δ violates the angle folding relation, since $\gamma + \delta + \mu > \pi$, for any $\mu \in \{\alpha, \beta, \gamma, \delta\}$ and $\gamma + \delta = \pi$ implies that $\gamma = \delta$, which is impossible.
In Figure 4.53-II, at the vertex partially surrounded by angles $\gamma, \gamma, \beta, \gamma, \gamma$, the sum $\beta + 2\gamma + \lambda$ does not satisfy the angle folding relation, for any $\lambda \in \{\alpha, \beta, \gamma, \delta\}$ and $\beta + 2\gamma = \pi$ implies that $\beta \approx 76.34°$ and $\alpha \approx 64.085°$, which is impossible since $\alpha > \beta$.

3.2.2.3 Assume that $\alpha + \gamma + k\beta = \pi$, for some $k \geq 1$. As $\gamma > \frac{\pi}{4}$, one of the sums of alternate angles at vertices surrounded by the sequence of angles $(\gamma, \beta, \gamma, ...)$ is either

of the form

- $3\gamma = \pi$ and $\gamma + \beta + \delta = \pi$ or
- $2\gamma + p\beta = \pi,\ p \geq 1$ or
- $\alpha + 2\gamma + m\beta = \pi,\ m \geq 1$ or
- $3\gamma + q\beta = \pi,\ q \geq 1$.

In the first case, by the angles arrangement, we get the sequences of angles $(\gamma, \beta, \gamma, \delta, \gamma, \gamma)$ or $(\gamma, \beta, \gamma, \gamma, \gamma, \delta)$. Either way, $\beta = \frac{\pi}{6}$ and from the assumption $\alpha + \gamma + k\beta = \pi$, we conclude that $\alpha = \frac{2\pi}{3} - k\frac{\pi}{6}$, with $k = 1, 2$, contradicting $\frac{\pi}{3} < \alpha < \frac{\pi}{2}$.
In the second case and for $p = 1$, one has $2\gamma + \beta = \pi$ and from $2\alpha + \beta > \pi$, we get $\gamma < \alpha$. On the other hand, from the assumption $\alpha + \gamma + k\beta = \pi$, we conclude that $\alpha + \gamma + \beta \leq \pi = 2\gamma + \beta$, which is an impossibility, since $\alpha > \gamma$. If $p > 1$, then the extended configuration led us to a vertex partially surrounded by three angles α (vertex v_{13} in Figure 4.54-I). This vertex is of valency six whose sums of alternate angles are of the form $2\alpha + \gamma = \pi$. Consequently, $\frac{\pi}{4} < \gamma < \beta$ implying $p = 1$, which is impossible.

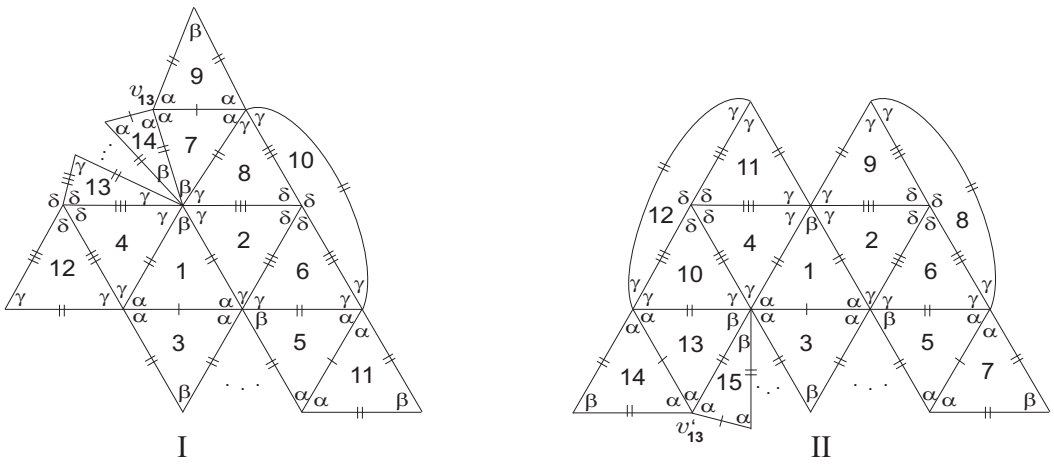

Figure 4.54: Local configurations.

3.2.2.4 Suppose that $\alpha + 2\gamma + m\beta = \pi,\ m \geq 1$. As $2\gamma + \delta > \pi$, then $\alpha + \beta < \delta = \frac{\pi}{2}$ contradicting $2\alpha + \beta > \pi$.

In the fourth case, $3\gamma + q\beta = \pi,\ q \geq 1$. Extending the configuration, we are led to a vertex, v'_{13} (Figure 4.54-II), surrounded by three angles α, whose sum $2\alpha + \lambda$ violates the angle folding relation for any $\lambda \in \{\alpha, \beta, \gamma, \delta\}$ (Figure 4.54-II).

□

Proposition 4.8 *If $\beta > \alpha$, then $\Omega(T_1, T_2)$ is composed by two discrete families of f-tilings denoted by $\left(\mathcal{J}^k\right)_{k\geq 3, k\in\mathbb{N}}$ and $\left(\mathcal{K}^m\right)_{m\geq 4, m\in\mathbb{N}}$ and three (isolated) tilings denoted by $\mathcal{I}$, $\mathcal{J}$ and $\mathcal{K}$ where the sums of alternate angles around vertices are respectively of the form:*

$$\begin{aligned}
\beta + \gamma = \pi,\ 2\alpha + \gamma = \pi \text{ and } \delta = \frac{\pi}{k},\ k \geq 3 \text{ for } \mathcal{J}^k;\\
\alpha = \frac{\pi}{m},\ \beta + \gamma = \pi \text{ and } \alpha + \gamma + \delta = \pi,\ m \geq 4 \text{ for } \mathcal{K}^m;\\
\delta = \frac{\pi}{2},\ \beta + \gamma = \pi \text{ and } \alpha + 2\gamma = \pi \text{ for } \mathcal{I};\\
\delta = \frac{\pi}{2},\ \beta + \gamma = \pi \text{ and } 2\alpha + \gamma = \pi \text{ for } \mathcal{J};\\
\delta = \frac{\pi}{2},\ \alpha = \frac{\pi}{3} \text{ and } \beta + \gamma + \alpha = \pi \text{ for } \mathcal{K}.
\end{aligned}$$

Proof. **Assume that $\beta > \alpha$ and $\gamma > \delta$.**

Using the adjacency condition (4.4), if $\alpha > \frac{\pi}{2}$, then $\beta > \frac{\pi}{2}$ and $\gamma > \delta > \frac{\pi}{2}$ preventing the existence of vertices of valency four, which is an impossibility. Thus, $\alpha \leq \frac{\pi}{2}$.

Starting from the configuration in Figure 4.55, a decision about the angle $\theta_8 \in \{\gamma, \delta\}$ must be made.

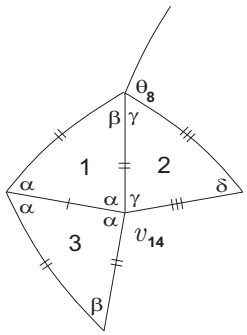

Figure 4.55: Local configuration.

1.1 Suppose firstly that $\theta_8 = \gamma$ and $\beta + \gamma < \pi$. As $\beta, \gamma > \frac{\pi}{3}$, $2\alpha + \beta > \pi$ and $2\gamma + \delta > \pi$, the sum containing the angles β and γ does not satisfy the angle folding relation and the configuration can not be extended.

1.2 Suppose now that $\beta + \gamma = \pi$. Adding some cells to the configuration, we get the one illustrated in Figure 4.56.

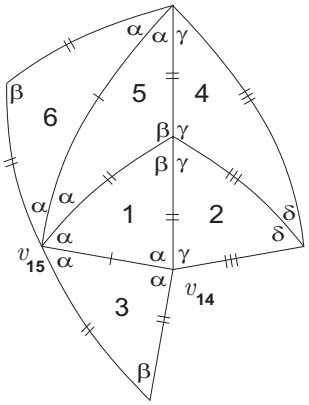

Figure 4.56: Local configuration.

If $\alpha = \frac{\pi}{2}$, then $\beta > \frac{\pi}{2} > \gamma > \delta$, violating the adjacency condition. Therefore, $\alpha < \frac{\pi}{2}$ and since $2\alpha > \gamma$, then $\alpha > \frac{\pi}{6}$.

1.2.1 As $\beta + \gamma = \pi$, assume first that $\beta = \gamma = \frac{\pi}{2}$. Therefore, $\alpha > \frac{\pi}{4}$ and taking into account that $2\gamma + \delta > \pi$, $\gamma < 2\alpha$ and the compatibility of the edges, vertex v_{15} is of valency six surrounded exclusively by angles α. By the adjacency condition (4.4), we get $\delta = \arccos \frac{\sqrt{3}}{3} \approx 54,736°$. Consequently, at vertex v_{14}, the sum $\alpha + \gamma + \mu$ does not satisfy the angle folding relation, for any $\mu \in \{\alpha, \beta, \gamma, \delta\}$.

1.2.2 Assuming that $\beta > \frac{\pi}{2} > \gamma$, the sum containing the alternate angles α and γ, at vertex v_{14}, satisfies either

- $\alpha + 2\gamma = \pi$ or
- $2\alpha + \gamma = \pi$ or $3\alpha + \gamma = \pi$ or
- $\alpha + \gamma + t\delta = \pi,\ t \geq 1$.

1.2.2.1 If $\alpha + 2\gamma = \pi$, then $\alpha < \delta$ and from $\gamma < 2\alpha$, we get $\alpha > \frac{\pi}{5}$. Accordingly, the

order relation between the angles is

$$\frac{\pi}{5} < \alpha < \delta < \gamma < \frac{\pi}{2} < \beta.$$

As a consequence, vertex v_{15} is of valency six or of valency eight surrounded exclusively by angles α (note that the other possibilities namely, $2\alpha + p\delta = \pi,\ p \geq 1$ or $3\alpha + q\delta = \pi,\ q \geq 1$ are incompatible with the edge length and $2\alpha + \gamma = \pi$ or $3\alpha + \gamma = \pi$ imply, respectively, the contradictions $\alpha = \gamma$ and $\gamma = 2\alpha$).

However, the assumption that v_{15} is of valency six led to a contradiction, since $\alpha = \frac{\pi}{3}$ and so $\alpha + 2\gamma > \pi$, absurd.

Assume that v_{15} is of valency eight. Then $\alpha = \frac{\pi}{4},\ \gamma = \frac{3\pi}{8},\ \beta = \frac{5\pi}{8}$ and, by the adjacency condition (4.4), $\delta \approx 64,916°$. Extending the configuration in Figure 4.56, a vertex, v_{16} surrounded by three angles δ arises (see Figure 4.57-I). Since, the sum $2\delta + \mu$ does not satisfy the angle folding relation, for any $\mu \in \{\alpha, \beta, \gamma, \delta\}$, we can not continue pursuing the extension of the configuration.

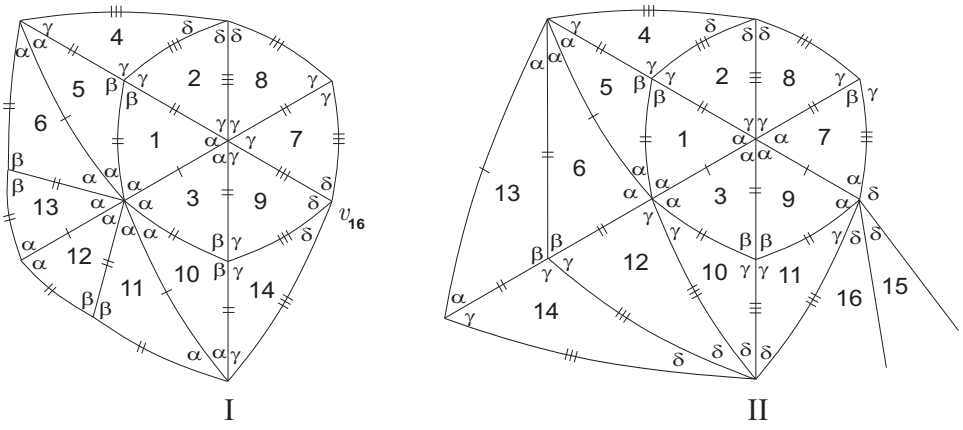

Figure 4.57: Local configurations.

Notice that, in the construction of the configuration in Figure 4.57-I, in spite of tile 7 has two possible positions to be placed, we only present one of them, since the other one would imply a contradiction. In fact, the other possibility would led us to the sums $\alpha + 2\gamma = \pi = \alpha + \beta + \delta$ and by the adjacency condition (4.4), we get $\gamma = \frac{2\pi}{5}$ or $\gamma = \frac{4\pi}{5}$ or $\gamma = \frac{2\pi}{3}$. As $\gamma < \frac{\pi}{2}$ remains $\gamma = \frac{2\pi}{5}$, which implies $\alpha = \frac{\pi}{5}$.

1.2.2.2 If vertex v_{14} satisfies $2\alpha + \gamma = \pi$, then $\frac{\pi}{4} < \alpha < \frac{\pi}{3}$ and consequently vertex v_{15} (and all vertices partially surrounded by two alternate angles α) must be of valency

six obeying to the condition $2\alpha+\gamma=\pi$ (the other possibilities $2\alpha+p\delta=\pi,\ p\geq 1$ or $3\alpha+q\delta=\pi,\ q\geq 1$ are incompatible with the edge length).

On the other hand, vertices surrounded by a sequence of angles containing β must be of valency four satisfying $\beta+\gamma=\pi$ (any other possibilities led to the edge incompatibility or a contradiction arises from the adjacency condition (4.4)).

Besides, vertices partially surrounded by alternate angles α and γ must be of valency six satisfying $2\alpha+\gamma=\pi$ (the other possibility $\alpha+\gamma+t\delta=\pi,\ t\geq 1$ leads us to vertices surrounded by two alternate angles γ, whose sum $2\gamma+\mu$ violates the angle folding relation, for any $\mu\in\{\beta,\gamma,\delta\}$ and $2\gamma+\alpha=\pi$ implies the contradiction $\alpha=\gamma>\frac{\pi}{3}$, as illustrated in Figure 4.57-II).

We may continue expanding the configuration in Figure 4.56 and taking into account the two previous observations, vertices partially surrounded by several angles δ must satisfy $k\delta=\pi,\ k\geq 3$. Consequently, for each $k\geq 3$, the local configuration extends to a complete f-tiling, denoted by $\mathcal{J}^k$. Each member of the discrete family $\mathcal{J}^k$ is composed by vertices of valency four, six and $2k$ whose sums of alternate angles obey, respectively to $\beta+\gamma=\pi$, $2\alpha+\gamma=\pi$ and $k\delta=\pi$. The number of triangular faces of $\mathcal{J}^k$ is $8k$ triangles equally distributed by two classes of congruence.

Next figure shows a 2D and 3D representation of $\mathcal{J}^3$ and it is composed by 12 triangles congruent to T_1 and 12 triangles congruent to T_2, where $\alpha=\arccos\sqrt{\frac{3}{8}}\approx 52,237°,\ \beta\approx 104,474°,\ \gamma\approx 75,526°$ and $\delta=60°$.

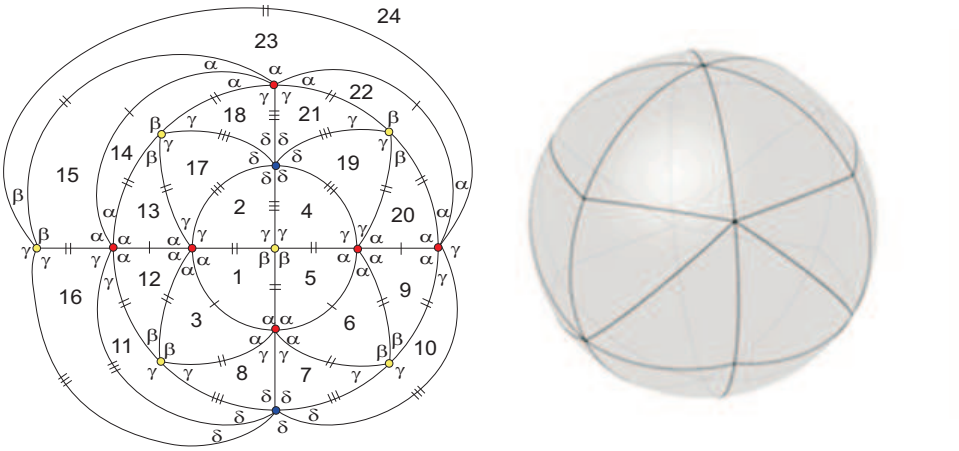

Figure 4.58: 2D and 3D representation of $\mathcal{J}^3$.

This family of tilings can be obtained from the family of dihedral tilings ${}^{E}\mathcal{R}^{k}$ described in [7] and [14], where the prototiles are an isosceles triangle and a spherical square by adding edges.

1.2.2.3 If vertex v_{14} obeys to the condition $3\alpha+\gamma=\pi$, then $\frac{\pi}{5}<\alpha<\frac{\pi}{3}<\gamma$ and as $2\gamma+\delta>\pi$ and $\gamma<2\alpha$, then $\alpha<\delta$. Accordingly, the order relation between the angles is

$$\frac{\pi}{5}<\alpha<\delta<\gamma<\frac{\pi}{2}<\beta.$$

In order to satisfy the angle folding relation and taking into account the compatibility of the edges, vertices partially surrounded by two alternate angles δ are of valency six (obeying to $\delta=\frac{\pi}{3}$ or $2\delta+\gamma=\pi$) or of valency eight (obeying to $\delta=\frac{\pi}{4}$ or $2\delta+\alpha+\gamma=\pi$ or $3\delta+\gamma=\pi$). Next, we shall study each one of these possibilities.

- If $\delta=\frac{\pi}{3}$, by the adjacency condition (4.4), we get $\alpha\approx 38,211^{\circ}$ or $\alpha\approx 94,704^{\circ}$. As $\alpha<\frac{\pi}{2}$, then $\alpha\approx 38,211^{\circ}$ and consequently $\beta\approx 114,62^{\circ}$ and $\gamma\approx 65,38^{\circ}$. However, extending the configuration illustrated in Figure 4.56, we end up at a vertex, v_{17} partially surrounded by the alternate angles $\gamma,\ \alpha,\ \gamma$, whose sum $2\gamma+\alpha+\mu$ violates the angle folding relation, for any $\mu\in\{\alpha,\beta,\gamma,\delta\}$ and so the configuration can not be expanded (see Figure 4.59-I).

  In case $\delta=\frac{\pi}{4}$, then $\alpha\approx 36,712^{\circ},\ \beta\approx 110,136^{\circ}$ and $\gamma\approx 69,864^{\circ}$ but a similar impossibility arises.

- In case $2\delta+\gamma=\pi$, again by the adjacency condition (4.4), one has $\alpha\approx 37,857^{\circ}$ or $\alpha\approx 77,459^{\circ}$ or $\alpha=\frac{2\pi}{3}$. As $\frac{\pi}{5}<\alpha<\frac{\pi}{3}$, then $\alpha\approx 37,857^{\circ},\ \beta\approx 113,571^{\circ},\ \gamma\approx 66,429^{\circ}$ and $\delta\approx 56,785^{\circ}$. Adding some cells to the configuration in Figure 4.56, depending the position of tile 12, we end up at a vertex partially surrounded by angles $\beta,\ \gamma,\ \delta$, whose sum $\beta+\delta+\mu$ violates the angle folding relation, for any $\mu\in\{\alpha,\beta,\gamma,\delta\}$ (Figure 4.59-II) or a vertex surrounded by angles $\alpha,\alpha,\gamma,\delta$, whose sum $\alpha+\delta+\mu$ does not satisfy the angle folding relation, for any $\mu\in\{\alpha,\beta,\gamma,\delta\}$ (Figure 4.59-III).

  If $2\delta+\alpha+\gamma=\pi$ or $3\delta+\gamma=\pi$, an impossibility is achieved ($\alpha=\delta$).

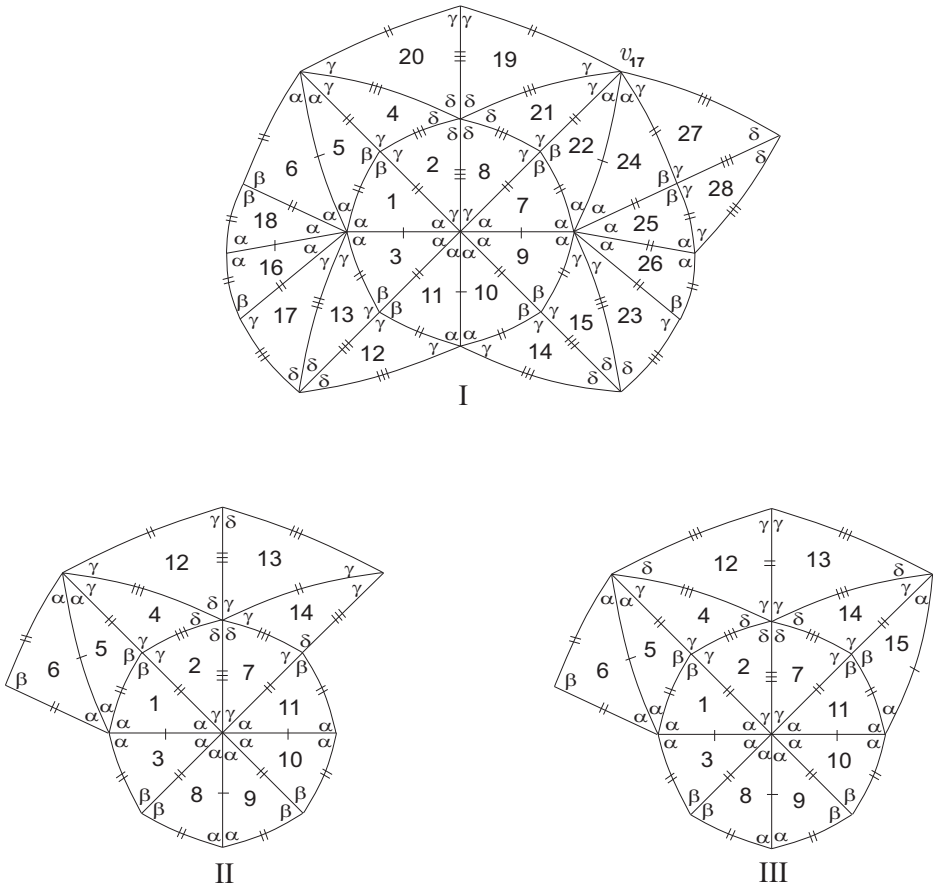

Figure 4.59: Local configurations.

1.2.2.4 Assume that vertex v_{14} satisfies $\alpha + \gamma + t\delta = \pi,\ t \geq 1$. Then, vertex v_{15} (see Figure 4.56) is of valency $2k,\ k = 3, 4, 5$ surrounded exclusively by angles α or of valency six satisfying $2\alpha + \gamma = \pi$ or of valency eight satisfying $3\alpha + \gamma = \pi$. Next, we shall study this five possible cases.

- If $\alpha = \frac{\pi}{k},\ k = 3, 4, 5$, vertices surrounded by the angle β must be of valency four as in case 1.2.2.2.

  Also vertices surrounded by the alternate angles α and γ must satisfy $\alpha+\gamma+t\delta = \pi,\ t \geq 1$ as we will show:

  For $\alpha = \frac{\pi}{3}$, the sum $\alpha + \gamma + \mu$ violates the angle folding relation, for any $\mu \in \{\alpha, \beta, \gamma\}$ preventing the expansion of the configuration.

  For $\alpha = \frac{\pi}{4}$, vertices partially surrounded by alternate angles α and γ may satisfy $2\alpha + \gamma = \pi$ (implying the contradiction $\gamma = \frac{\pi}{2}$) or $\alpha + 2\gamma = \pi$ implying that

$\gamma = \frac{3\pi}{8},\ \beta = \frac{5\pi}{8}$ and $\delta > \beta - \gamma = \frac{\pi}{4}$. Consequently, from $\alpha + \gamma + t\delta = \pi$, we conclude that $t = 1$ and so $\gamma = \delta$, which is impossible.

For $\alpha = \frac{\pi}{5}$, vertices partially surrounded by alternate angles α and γ could satisfy either $2\alpha + \gamma = \pi$ (reaching to the impossibility $\gamma = \frac{3\pi}{5} > \beta = \frac{2\pi}{5}$) or $\alpha + 2\gamma = \pi$ or $3\alpha + \gamma = \pi$. However, these last two possibilities lead to $\gamma = \frac{2\pi}{5},\ \beta = \frac{3\pi}{5}$ and since $\delta > \alpha$, then $t = 1$ implying the impossibility $\delta = \gamma$.

Accordingly, $\beta + \gamma = \pi,\ \alpha + \gamma + t\delta = \pi$ and $\alpha = \frac{\pi}{k},\ k = 3, 4, 5$.

We may add some cells to the configuration in Figure 4.56 but it is impossible to get a complete f-tiling for $t \geq 2$, since by the angle arrangement, it is not possible that vertices partially surrounded by the angles $\gamma, \delta, \delta, \gamma, \alpha, \alpha$ obey to the condition $\alpha + \gamma + t\delta = \pi$ (see Figure 4.60-I for the particular case $\alpha = \frac{\pi}{3}$).

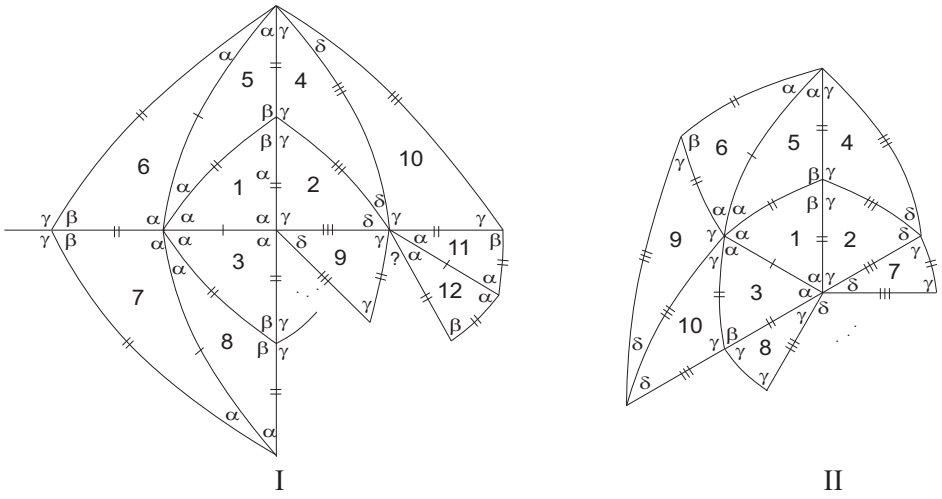

Figure 4.60: Local configurations.

In case, $t = 1$, we get $\beta < 0$ (for $\alpha = \frac{\pi}{3}$), $\beta \approx 56,075°$ or $\beta \approx 115,17°$ (for $\alpha = \frac{\pi}{4}$) and $\beta \approx 40,538°$ (for $\alpha = \frac{\pi}{5}$). Taking into account that $\beta > \frac{\pi}{2}$, it remains the case $\alpha = \frac{\pi}{4}$ with $\beta \approx 115,17°,\ \gamma \approx 64,83°$ and $\delta \approx 70,17°$, contradicting $\gamma > \delta$.

- If $2\alpha + \gamma = \pi$, then we may add some new cells to the configuration in Figure 4.56 and get a vertex, in Figure 4.60-II, partially surrounded by the angles γ, β, γ, whose sum $2\gamma + \mu, \mu \in \{\alpha, \beta, \gamma, \delta\}$ does not verify the angle folding relation or led to the contradiction $\alpha = \gamma > \frac{\pi}{3}$.

- In case, $3\alpha + \gamma = \pi$, then $\alpha > \frac{\pi}{5}$ and $\gamma < \frac{2\pi}{5}$ implying that $\delta > \beta - \gamma > \frac{\pi}{10}$. Consequently, $t = 1, 2, 3, 4$. Using the adjacency condition (4.4) for $t = 1$, we get $\alpha \approx 70, 134°$ or $\alpha \approx 41, 041°$ or $\alpha \approx 114, 39°$. These values for α are impossible, since the first one implies that $\beta \approx 210, 402°$, the second one $\gamma \approx 56, 877°$, contradicting $\gamma > \frac{\pi}{3}$ and the third one is greater than $\frac{\pi}{2}$.

  Using the same adjacency condition for $t = 2$ and $t = 3$, we get values for α, which contradict our assumption. The values for α are: $\alpha = \frac{\pi}{5}, \frac{3\pi}{5}, \frac{\pi}{2}$, for $t = 2$; $\alpha \approx 35, 26°$, for $t = 3$ and $\alpha \approx 35, 12°$, for $t = 4$.

1.2.3 If $\beta + \gamma = \pi$ but $\beta < \frac{\pi}{2} < \gamma$, then $\alpha > \frac{\pi}{4}$. By compatibility of the edges, vertex v_{15} is of valency six surrounded exclusively by angles α. Therefore, $\alpha = \frac{\pi}{3}$. Looking now for vertex v_{14} in Figure 4.56, we conclude that the sum of alternate angles must obey to the condition $\alpha + \gamma + t\delta = \pi,\ t \geq 1$.

As in the case 1.2.2.4, it is impossible to construct a complete f-tiling for $t \geq 2$ and, for $t = 1$, one gets the absurdity $\beta < 0$.

1.3 Assume now that $\theta_8 = \delta$ (see Figure 4.61) and $\beta + \delta < \pi$.

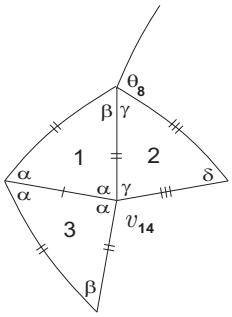

Figure 4.61: Local configuration.

As $\beta, \gamma > \frac{\pi}{3},\ 2\alpha + \beta > \pi$ and $2\gamma + \delta > \pi$, the sum containing β and δ is either of the form

- $\beta + k\delta = \pi,\ k \geq 2$ or
- $2\beta + m\delta = \pi,\ m \geq 1$ or
- $\beta + n\delta + \gamma = \pi,\ n \geq 1$ or

- $\beta + p\delta + \alpha = \pi,\ p \geq 1.$

First and second cases contradict $2\gamma + \delta > \pi$ and $\beta, \gamma > \frac{\pi}{3}$.

In the fourth case, $\beta + p\delta + \alpha = \pi,\ p \geq 1$ implies that the other sum of alternate angles obeys to the condition $\alpha + 2\gamma + (p-1)\delta = \pi$, which is only possible if $p = 1$. Then, $\alpha + 2\gamma = \pi = \beta + \delta + \alpha$ leading to the impossibility $\delta < \alpha < \delta$.

It remains the third case, $\beta + n\delta + \gamma = \pi,\ n \geq 1$. Although the angle γ has several positions to be placed, only one does not violate the conditions $\gamma > \frac{\pi}{3}$ and $2\gamma + \delta > \pi$, as shown in Figure 4.62-I, at vertex v_{18}. Taking into account that $\beta + n\delta + \gamma = \pi,\ n \geq 1,\ \alpha + \gamma < \pi$ and $\alpha + \delta < \pi$, vertices of valency four are surrounded exclusively by angles β or angles γ or angles α or alternate angles α and β. Consequently, $\beta \geq \frac{\pi}{2}$ or $\gamma = \frac{\pi}{2}$.

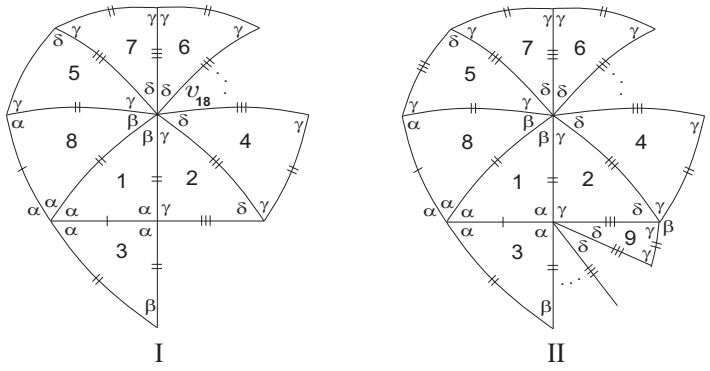

Figure 4.62: Local configurations.

1.3.1 Assuming that $\beta \geq \frac{\pi}{2}$, then $\delta < \gamma < \frac{\pi}{2}$, from $\beta + n\delta + \gamma = \pi$. Therefore, $\beta + \gamma + n\delta > \gamma + \gamma + n\delta > \pi$, which is a contradiction.

1.3.2 If $\gamma = \frac{\pi}{2}$, then $\delta < \frac{\pi}{2}$ and from $\beta + n\delta + \gamma = \pi,\ n \geq 1$, we get $\alpha < \beta < \frac{\pi}{2}$. On the other hand, because $2\alpha + \beta > \pi$, then $\alpha > \frac{\pi}{4}$. Consequently, vertex v_{14} in Figure 4.56 is of valency $2(2+t)$ satisfying $\alpha + \gamma + t\delta = \pi$, for some $t \geq 1$ and the extended configuration ends up at a vertex of valency four surrounded by angles $\gamma, \delta, \gamma, \beta$, which is impossible, since $\beta + \delta < \pi$ (see Figure 4.62-II).

1.4 If $\beta + \delta = \pi$, the angle arrangement obliges $2\gamma = \pi$. Consequently, $\delta < \frac{\pi}{2} < \beta$, since $\delta < \gamma$. Extending the configuration in Figure 4.61, tile numbered 6 has two

possible positions as shown in the next figure.

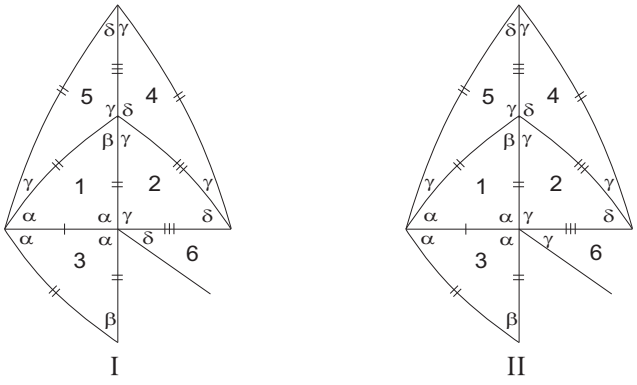

Figure 4.63: Local configurations.

We may continue adding cells to the configuration in Figure 4.63-I in an unique way and we are lead to a vertex partially surrounded by angles β, β, α (note that this vertex is not of valency four, otherwise by the adjacency condition, we would get the impossibility $\alpha = \frac{\pi}{2} = \beta$). However, since $\gamma = \frac{\pi}{2}$, $\beta > \frac{\pi}{2}$, $\beta + \delta = \pi$ and $2\alpha + \beta > \pi$, then $\alpha + \beta + \mu > \pi$, for any $\mu \in \{\alpha, \beta, \gamma, \delta\}$, violating the angle folding relation (Figure 4.64-I).

In configuration 4.63-II, we come up to a vertex partially surrounded by angles $\beta, \alpha, \alpha, \gamma, \delta$, whose sum $\beta + \alpha + \delta$ violates the angle folding relation, as shown in Figure 4.64-II.

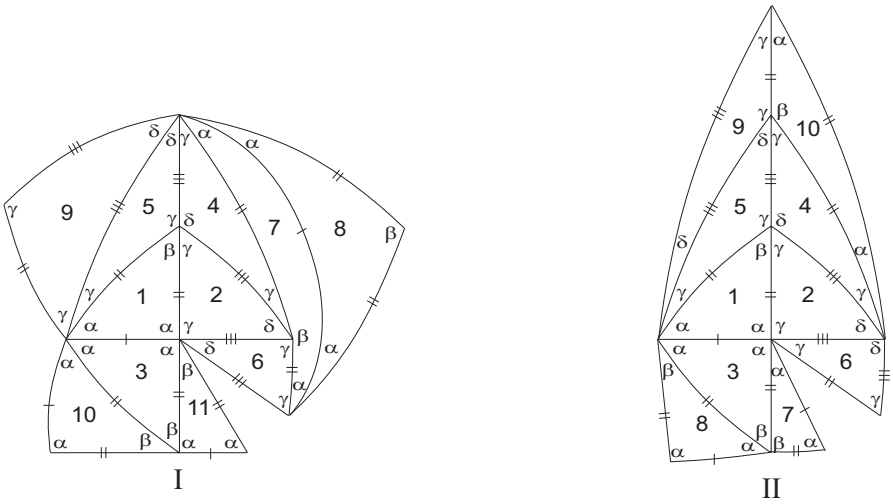

Figure 4.64: Local configurations.

Assume that $\beta > \alpha$ and $\delta > \gamma$.

Starting from the configuration illustrated in Figure 4.61, a decision must be made about the angle $\theta_8 \in \{\gamma, \delta\}$.

1. Suppose firstly that $\theta_8 = \gamma$. We shall study the cases $\beta + \gamma = \pi$ and $\beta + \gamma < \pi$ separately.

1.1 If $\beta + \gamma = \pi$, the extended configuration lead us to a vertex surrounded by three angles α as shown in Figure 4.65-I.

If $\alpha = \frac{\pi}{2}$, then from the adjacency condition, we conclude that $\delta > \frac{\pi}{2}$. As $\beta > \alpha$, then $\beta > \frac{\pi}{2}$ and so $\gamma < \frac{\pi}{2}$. Therefore, at vertex v_{14}, the sum containing the alternate angles α and γ must be of the form $\alpha + t\gamma = \pi,\ t \geq 2$. However, at vertex partially surrounded by three angles δ, the sum 2δ violates the angles folding relation, preventing the extension of the configuration in Figure 4.65-II.

If $\alpha < \frac{\pi}{2}$, as $\gamma < \delta$, by the adjacency condition, $\gamma < \frac{\pi}{2}$ and so $\beta > \frac{\pi}{2}$. Now, for the expansion of the configuration in Figure 4.66, a decision about the angle $\theta_9 \in \{\gamma, \delta\}$ must be taken.

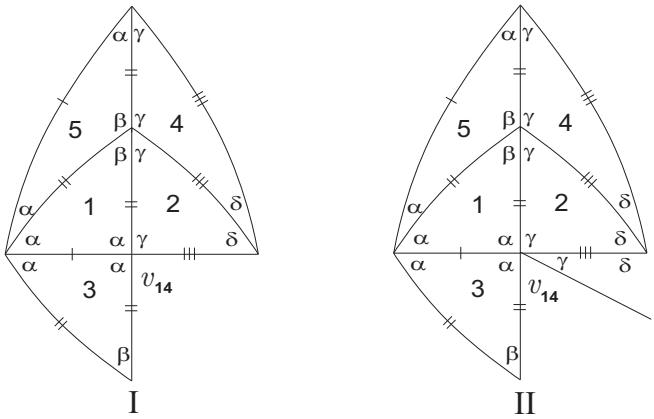

Figure 4.65: Local configurations.

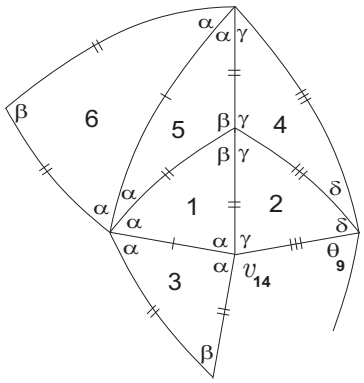

Figure 4.66: Local configuration.

1.1.1 If $\theta_9 = \gamma$, then $\delta + \gamma < \pi = \beta + \gamma$ and so $\delta < \beta$ (observe that $\delta + \gamma = \pi$ implies the contradiction $\cot \alpha = \cot \beta$).
Since the other possibilities violate the angle folding relation, the sum containing the alternate angles δ and γ must obey to $\delta + \gamma + \alpha = \pi$. Accordingly,

$$\alpha < \gamma < \frac{\pi}{2} < \beta,\ \delta < \beta$$

and also $\alpha < \frac{\pi}{3}$ (otherwise, $\delta > \gamma > \alpha \geq \frac{\pi}{3}$ not satisfying the equality $\delta + \gamma + \alpha = \pi$). Extending the configuration in Figure 4.66, we get a family of f-tilings with three types of vertices: vertices of valency four, six and $2m,\ m \geq 4$ surrounded, respectively, by angles $(\beta, \beta, \gamma, \gamma)$, $(\delta, \delta, \gamma, \alpha, \alpha, \gamma)$ and $(\alpha, \alpha, ..., \alpha, \alpha)$ denoted by $\mathcal{K}^m$. The number of triangular faces of each member is $8m$ equally distributed in two classes of congruence. In the next figure, we present 2D and 3D representation of the tiling $\mathcal{K}^4$. In this case, $\alpha = \frac{\pi}{4},\ \gamma \approx 64.83°,\ \delta \approx 70.17°$ and $\beta \approx 115,17°$ and it is composed by 16 triangles congruent to T_1 and 16 triangles congruent to T_2.

Observe that all this family of f-tilings $\mathcal{K}^m,\ m \geq 4$ is obtained from the family of dihedral f-tilings ${}^P\mathcal{R}^k_{\alpha_2}$, where the prototiles are an isosceles triangle and a non-equiangular parallelogram, described in [7] and in [14].

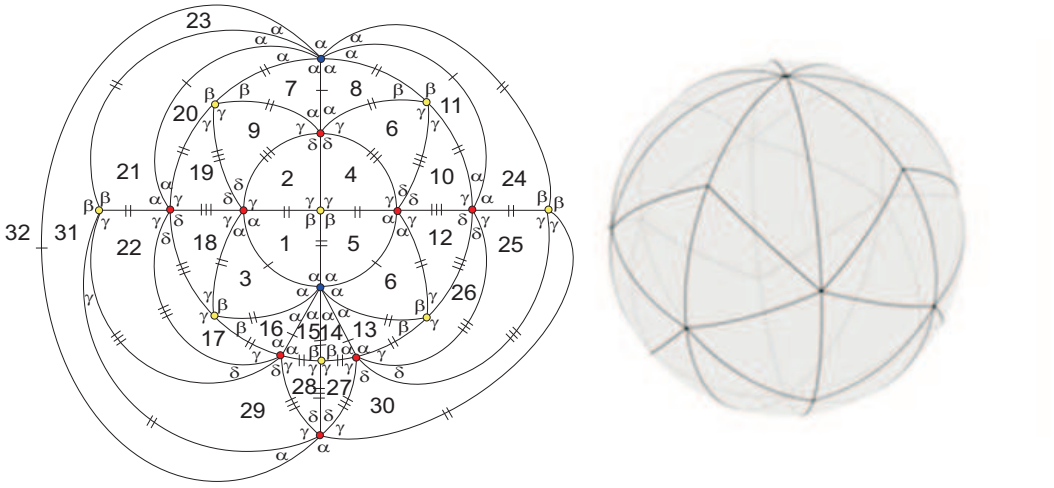

Figure 4.67: 2D and 3D representation of $\mathcal{K}^4$.

1.1.2 If $\theta_9 = \delta$ and $2\delta = \pi$, then $\gamma > \frac{\pi}{4}$. Taking into account that $2\alpha > \pi - \beta = \gamma > \frac{\pi}{4}$ and the compatibility of the edges, we conclude that $\alpha > \frac{\pi}{8}$ and at vertex partially surrounded by four angles α, the sum containing two alternate angles α satisfies either $k\alpha = \pi,\ k = 3, ..., 7$ or $p\alpha + q\gamma = \pi,\ p \geq 2\ q \geq 1,\ p + q \leq 6$.

1.1.2.1 If $k\alpha = \pi,\ k = 3, ..., 7$, we get:

for $k = 3,\ \gamma = 60°,\ \beta = 120°$ or $\gamma \approx 142.533°,\ \beta \approx 37.467°$;

for $k = 4,\ \gamma \approx 54.373°,\ \beta \approx 125.627°$ or $\gamma \approx 154.612°,\ \beta \approx 25.388°$;

for $k = 5,\ \gamma \approx 50.988°,\ \beta \approx 129.012°$ or $\gamma \approx 160.577°,\ \beta \approx 19.423°$;

for $k = 6,\ \gamma \approx 48.534°,\ \beta \approx 131.466°$ or $\gamma \approx 164.193°,\ \beta \approx 15.807°$;

for $k = 7,\ \gamma \approx 46.616°,\ \beta \approx 133.384°$ or $\gamma \approx 166.641°,\ \beta \approx 13.359°$.

It is impossible to continue the extension of the configuration for cases $k = 4, 5, 6, 7$, since, at vertex v_{14}, the sum $\alpha + \gamma + \mu$ violates the angle folding relation, for any $\mu \in \{\alpha, \beta, \gamma, \delta\}$. For the case $k = 3$, one has $\alpha = \gamma = \frac{\pi}{3},\ \beta = \frac{2\pi}{3}$ and consequently vertex v_{14} is of valency six satisfying $2\gamma + \alpha = \pi$. The configuration in Figure 4.66 extends to a global tiling, which is denoted by $\mathcal{I}$. Figure 4.68 presents a 2D and 3D representation of $\mathcal{I}$ and it is composed by 6 copies of T_1 and 12 copies of T_2.

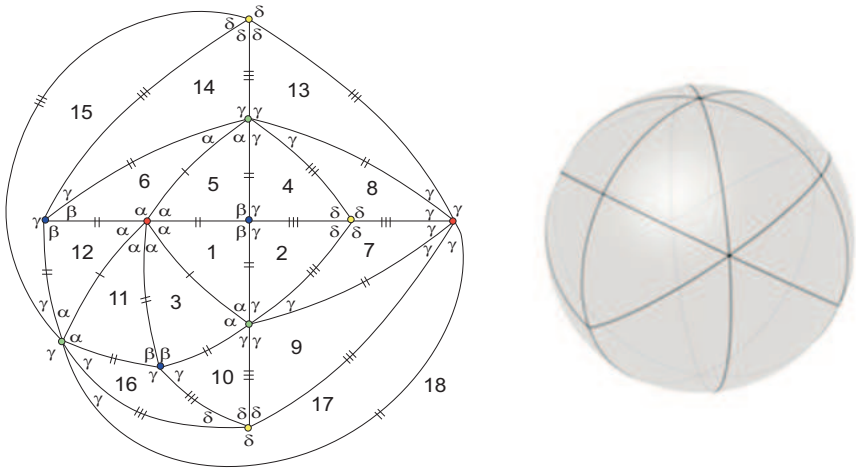

Figure 4.68: 2D and 3D representation of $\mathcal{I}$.

Note that this f-tiling can not be obtained from any dihedral f-tiling, where the prototiles are an isosceles triangle and a parallelogram or a monohedral f-tiling. In fact, whenever some edges are eliminated, the angle folding relation is violated or vertices of valency four don't occur.

1.1.2.2 In the second possibility suppose first that $q = 1$. Then, $p = 2, 3, 4, 5$. For $p = 2,\ 2\alpha + \gamma = \pi,\ \beta + \gamma = \pi,\ \delta = \frac{\pi}{2}$.

We may extend the configuration in Figure 4.66 getting a complete tiling $\tau \in \Omega(T_1, T_2)$ denoted by $\mathcal{J}$, where (by the adjacency condition) $\alpha = \frac{\pi}{3} = \gamma$ and $\beta = \frac{2\pi}{3}$. 2D and 3D representations of $\mathcal{J}$ are illustrated below.

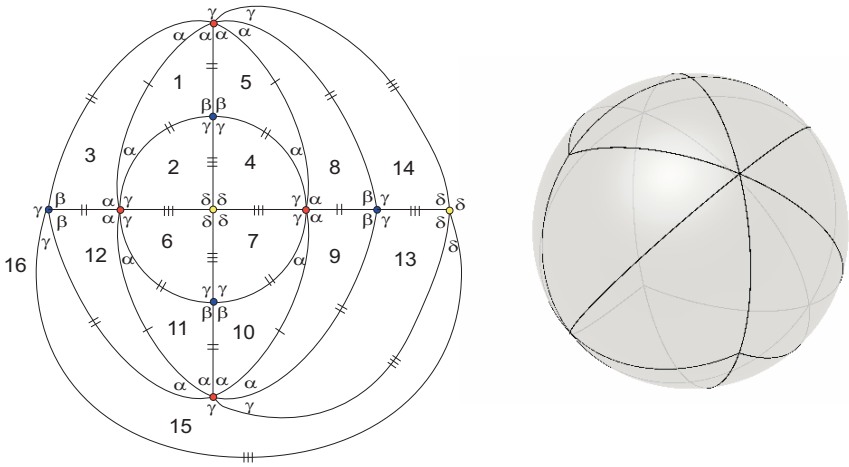

Figure 4.69: 2D and 3D representation of $\mathcal{J}$.

In this case, the tiling $\mathcal{J}$ can be obtained, enhancing some edges, from ${}^{E}\mathcal{R}^2$ described in [7] an in [14].

For $p = 3,\ 3\alpha + \gamma = \pi,\ \beta + \gamma = \pi,\ \delta = \frac{\pi}{2}$. By the adjacency condition (4.4), one has $\alpha = \frac{\pi}{2}$, which is an impossibility.

For $p = 4$, we get $\alpha \approx 32,594°,\ \gamma \approx 49,624°,\ \beta \approx 130,376°$ and for $p = 5$, one has $\alpha \approx 26,597°,\ \gamma \approx 47,015°,\ \beta \approx 132,985°$.

In both cases, vertices partially surrounded by alternate angles α and γ must obey, respectively, to the conditions $p\alpha+\gamma = \pi,\ p = 4, 5$ and so, extending the configuration in Figure 4.66, we end up at a vertex (of valency greater than six) surrounded by angles $\gamma, \alpha, \alpha, \gamma, \gamma$, whose sum $\gamma + \alpha + \gamma + \mu$ does not obey to the angle folding relation, for any $\mu \in \{\alpha, \beta, \gamma, \delta\}$ (see Figure 4.70).

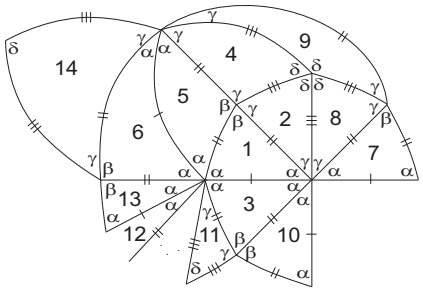

Figure 4.70: Local configuration.

Suppose now that $q = 2$. Then, $2\alpha + 2\gamma = \pi$ or $3\alpha + 2\gamma = \pi$, since $\alpha > \frac{\pi}{8}$ and $\gamma > \frac{\pi}{4}$.

If $2\alpha + 2\gamma = \pi$, by the adjacency condition (4.4), $\alpha \approx 38.173°,\ \gamma \approx 51.827°$ and $\beta \approx 128.173°$. The configuration in Figure 4.66 can be extended to the configuration in Figure 4.71, which shows a vertex, v_{19} partially surrounded by five angles γ, whose sum $3\gamma + \lambda$ violates the angle folding relation, for any $\lambda \in \{\alpha, \beta, \gamma, \delta\}$.

Assuming that $3\alpha+2\gamma = \pi$, by the adjacency condition (4.4), we get $\alpha \approx 28.176°,\ \gamma \approx 47.735°$ and $\beta \approx 132.265°$. The expansion of the configuration in Figure 4.66 must have in consideration that tile numbered 8 has two possible positions to be placed, as shown in Figure 4.72-I, II.

In Figure 4.72-I, we are led to a vertex surrounded by angles $\beta, \gamma, \gamma, \alpha$, that must be of valency four, reaching to the impossibility $\beta = \alpha$.

Figure 4.72-II, corresponds to one of the possible positions for tile labeled 12 and once again, we are led to a vertex surrounded by the same angles reaching to the same impossibility. The other position for tile 12 is illustrated in Figure 4.72-III and the same impossibility is achieved.

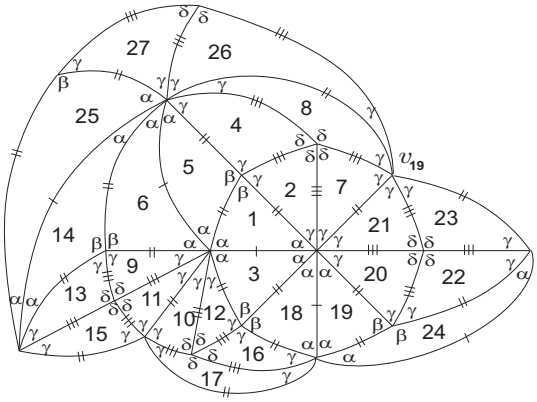

Figure 4.71: Local configuration.

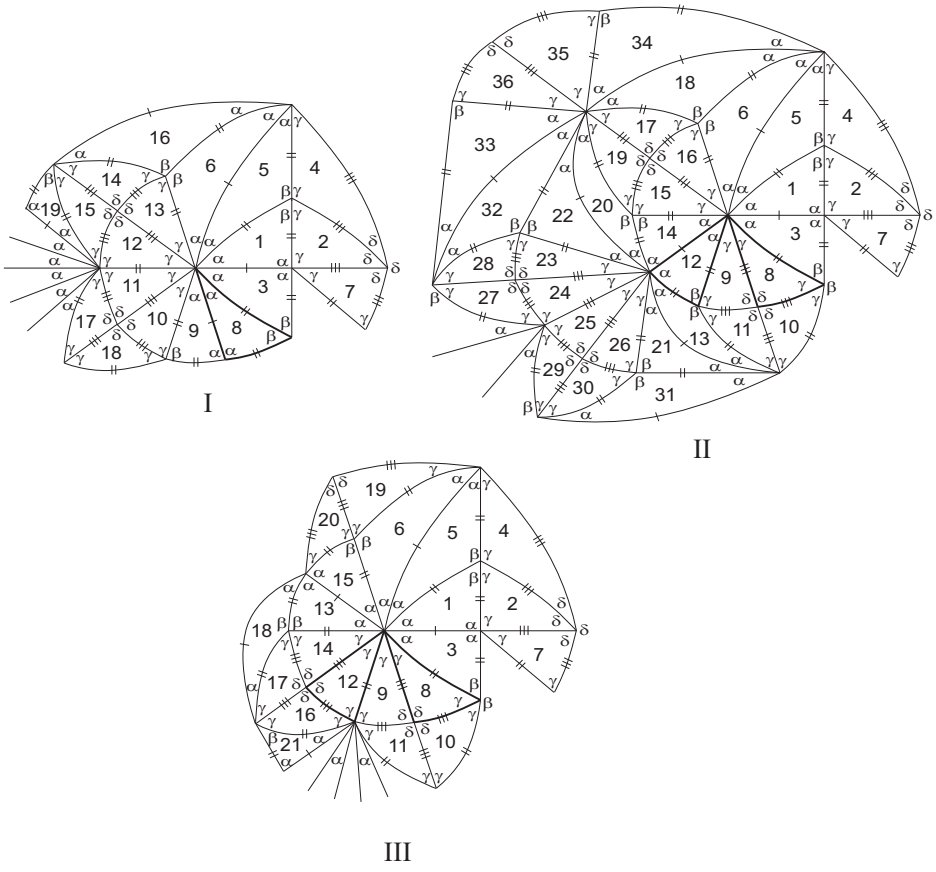

Figure 4.72: Local configurations.

1.1.3 If $\theta_9 = \delta$ but $2\delta < \pi$, it is impossible to expand the configuration in Figure 4.66, since there is always incompatibility of the edges or violation of the angle folding relation at the vertex partially surrounded by three angles δ.

1.2 Suppose that $\beta + \theta_8 < \pi$, for $\theta_8 = \gamma$ (Figure 4.61). In order to satisfy the angle folding relation, the sum containing these two angles is either of the form

- $\beta + \gamma + \beta = \pi$ or
- $\beta + \gamma + n\gamma = \pi,\ n \geq 1$ or
- $\beta + \gamma + \delta = \pi$ or
- $\beta + k\gamma + \alpha = \pi,\ k \geq 1$.

1.2.1 If $\beta + \gamma + \beta = \pi$, then $\gamma < \alpha < \beta < \frac{\pi}{2}$ and $\beta < \delta$. Therefore, $\delta \geq \frac{\pi}{2}$.
Assume first that $\delta = \frac{\pi}{2}$. The configuration in Figure 4.61 may be extended and we get several vertices partially surrounded by four angles α, as shown in the next figure.

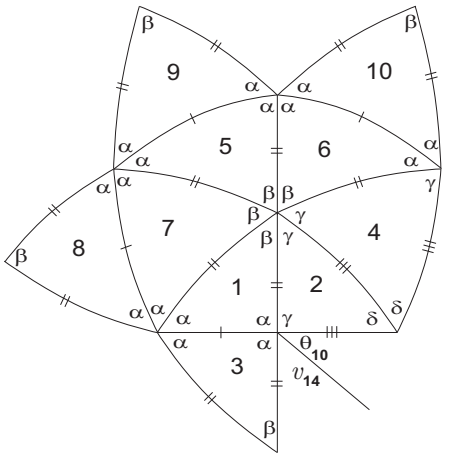

Figure 4.73: Local configuration.

In order to satisfy the angle folding relation, the sum containing two alternate angles α must be $3\alpha = \pi$ or $2\alpha + \gamma = \pi$, since $\alpha > \gamma > \frac{\pi}{4}$.
For $\alpha = \frac{\pi}{3}$, by the adjacency condition (4.4) and $\frac{\pi}{4} < \gamma < \alpha = \frac{\pi}{3} < \beta < \frac{\pi}{2} = \delta$, one has $\beta \approx 66.579^\circ$ and $\gamma \approx 46.842^\circ$. With these values, it is not possible to surround vertex v_{18} without violating the angle folding relation.
If $2\alpha + \gamma = \pi$, then $2\alpha + \gamma = 2\beta + \gamma = \pi$, implying the contradiction $\alpha = \beta$.

Assuming now that $\delta > \frac{\pi}{2}$, then $\theta_{10} = \delta$. Taking into account that $2\gamma+\delta > \pi,\ 2\alpha+\beta > \pi,\ \gamma < \alpha < \beta < \frac{\pi}{2} < \delta$ and the compatibility of the edges, it is impossible to continue the extension of the configuration.

1.2.2 The case $\beta + k\gamma + \alpha = \pi,\ k \geq 1$ will be study, analyzing the cases $k = 1$ and $k > 1$ separately.

If $k = 1$, then $\gamma < \alpha < \frac{\pi}{2}$. Extending the configuration in Figure 4.61, tile numbered 5 has two possible positions, as shown in Figure 4.74-I and II.

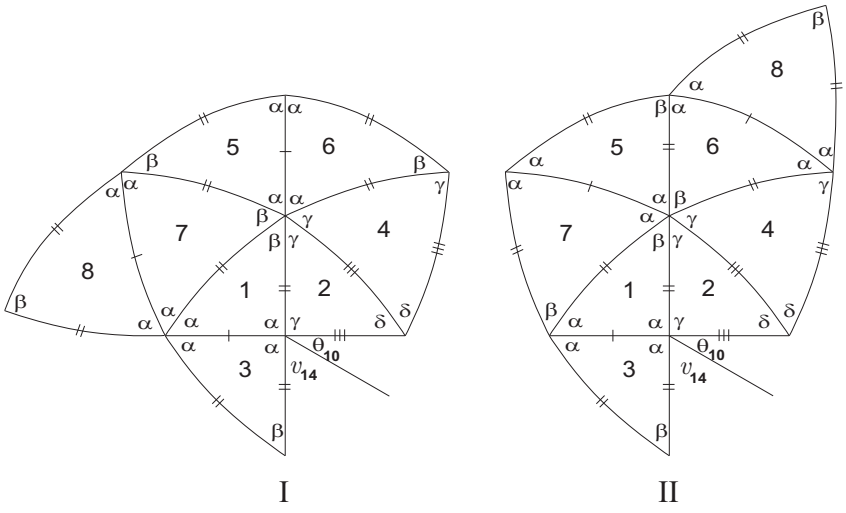

Figure 4.74: Local configurations.

In both configurations, if angle $\theta_{10} = \delta$, then vertex v_{18} must be of valency greater than four. However, as $\gamma < \alpha < \beta,\ \gamma < \delta$ and $2\gamma + \delta > \pi$, then the sum containing the angles α and δ does not satisfy the angle folding relation. Therefore, $\theta_{10} = \gamma$ and $\delta \leq \frac{\pi}{2}$.

In case $\delta = \frac{\pi}{2}$, then $\alpha > \gamma > \frac{\pi}{4}$ and the vertex partially surrounded by four angles α in Figure 4.74-I must be of valency six satisfying $3\alpha = \pi$ (the other possibility, $2\alpha+\gamma = \pi$ contradicts $\beta \neq \alpha$).

By the adjacency condition (4.4), $\beta \approx 71.774°$ and $\gamma \approx 48.226°$. Extending the configuration, we get a complete f-tiling $\tau \in \Omega(T_1, T_2)$, which is denoted by $\mathcal{K}$. It is composed by 48 triangles congruent to T_1 and 24 triangles congruent to T_2 and a 2D and 3D representation of $\mathcal{K}$ are shown in Figure 4.75.

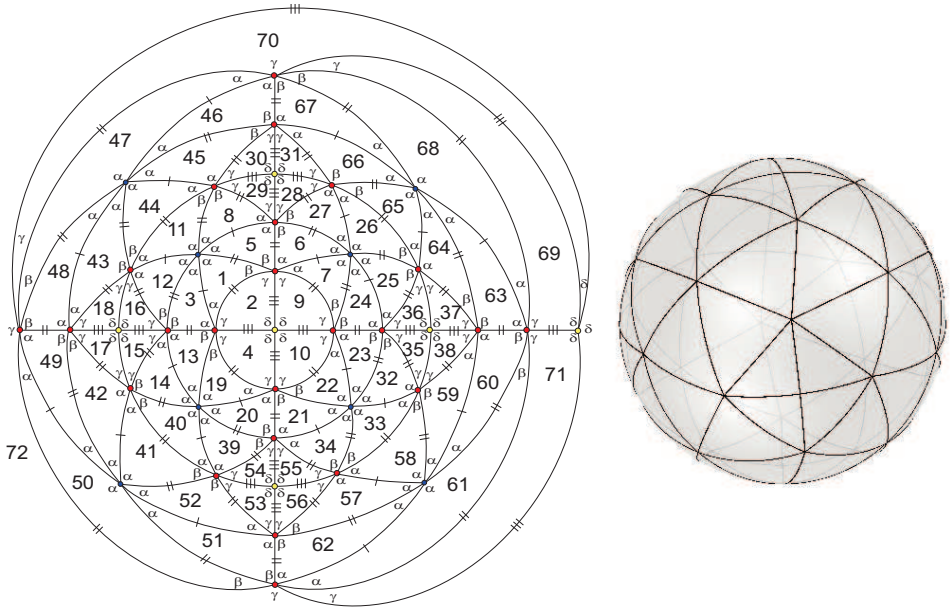

Figure 4.75: 2D and 3D representation of $\mathcal{K}$.

In Figure 4.74-II, with $\theta_{10} = \gamma$ and continue assuming that $\delta = \frac{\pi}{2}$, we may add some cells to the configuration and end up at a vertex partially surrounded by the angles $\alpha, \alpha, \gamma, \gamma, \alpha$, that must be of valency six satisfying $2\alpha+\gamma = \pi$. However, as $\beta+\gamma+\alpha = \pi$, an impossibility is achieved (Figure 4.76).

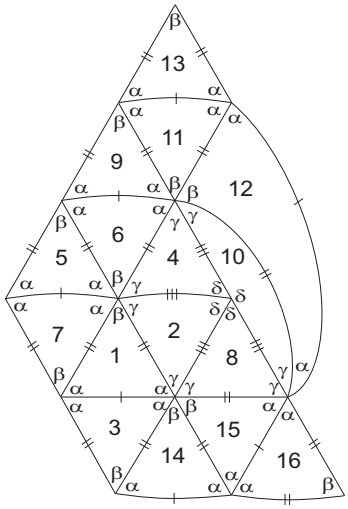

Figure 4.76: Local configuration.

If $\delta < \frac{\pi}{2}$, the sum containing two alternate angles δ violates the angle folding

relation, since $\gamma < \alpha < \beta,\ \gamma < \delta$ and $2\gamma + \delta > \pi$.

Now, if $\beta + k\gamma + \alpha = \pi,\ k \geq 2$, then $\gamma < \alpha < \frac{\pi}{2}$. This condition implies that $\beta \geq \frac{\pi}{2}$ or $\delta \geq \frac{\pi}{2}$ and vertices of valency four are surrounded exclusively by angles β or angles δ or alternate angles δ and γ (note that the other possibilities are incompatible with the edge length).

In the first case, one has $\alpha > \frac{\pi}{4}$ and from $\beta + k\gamma + \alpha = \pi < 2\gamma + \delta$, we conclude that $\delta > \beta + \alpha > \frac{\pi}{2}$. Therefore, adding some cells to the configuration in Figure 4.61, we are lead to a vertex (see Figure 4.77) surrounded by the alternate angles α and δ, which must be of valency greater than four. Nevertheless, the sum $\alpha + \delta + \mu$ violates the angle folding relation, for any $\mu \in \{\alpha, \beta, \gamma, \delta\}$ and we can not continue the expansion of the configuration.

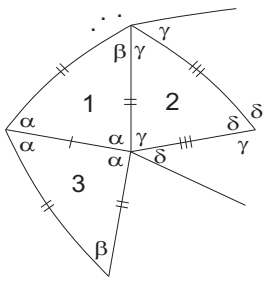

Figure 4.77: Local configuration.

If $\delta = \frac{\pi}{2}$, then $\alpha > \gamma > \frac{\pi}{4}$ and so $k = 1$, impossible.

If $\delta + \gamma = \pi$, then $\delta > \frac{\pi}{2} > \gamma$ and the sum containing the alternate angles α and δ violates the angle folding relation, since $\alpha + \delta > \gamma + \delta = \pi$.

1.2.3 Assuming now that $\beta + \gamma + n\gamma = \pi$, for some $n \geq 1$, then $\gamma < \alpha < \beta < \delta$. Pursuing the configuration in Figure 4.61, tile numbered 5 has two possible positions as illustrated in the next figure.

Looking at the angle $\theta_{11} \in \{\delta, \gamma\}$, if $\theta_{11} = \delta$, then the sum containing the alternate angles α and θ_{11} does not satisfy the angle folding relation, since $\alpha + \delta + \mu > \pi$, for any $\mu \in \{\alpha, \beta, \gamma, \delta\}$. Hence, $\theta_{11} = \gamma$ and $2\delta \leq \pi$.

If $\delta = \frac{\pi}{2}$, then $\alpha > \gamma > \frac{\pi}{4}$ and consequently $n = 1$. Accordingly, $\beta + 2\gamma = \pi$. Thus, vertex v_{14} must be of valency six satisfying $2\alpha + \gamma = \pi$, since the other possibilities

contradict $\alpha \neq \beta$ or $\alpha \neq \gamma$. By the adjacency condition (4.4), one has $\alpha \approx 64.087°, \gamma \approx 51.826°$ and $\beta \approx 76.348°$.

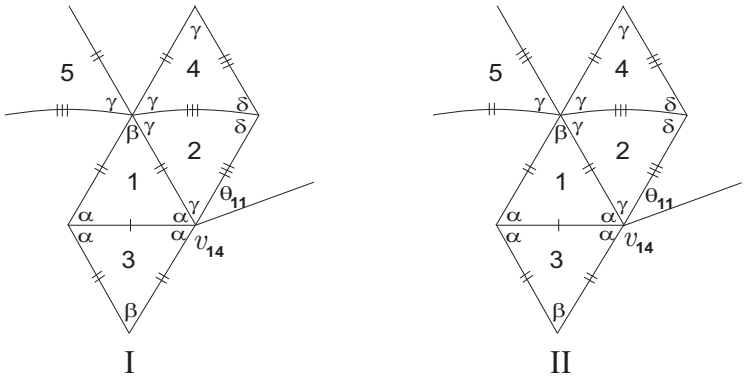

Figure 4.78: Local configurations.

Extending the configuration in Figure 4.78-I, we are led to vertex v_{20} partially surrounded by three angles β, whose sum $2\beta + \lambda$ violates the angle folding relation, for any $\lambda \in \{\alpha, \beta, \gamma, \delta\}$, see Figure 4.79-I.

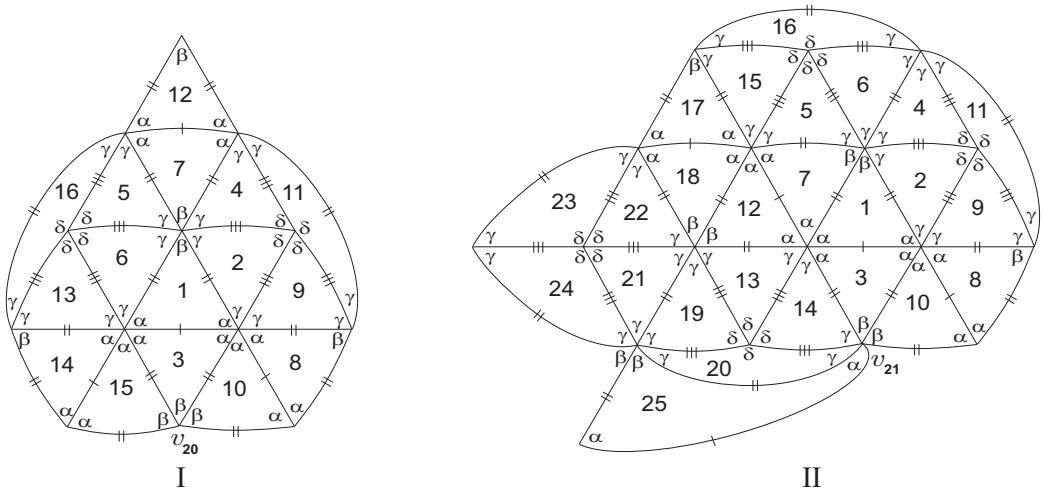

Figure 4.79: Local configurations.

Adding cells to the configuration in Figure 4.78-II, a vertex (v_{21}) surrounded by angles $\alpha, \gamma, \gamma, \beta, \beta$ arises (see Figure 4.79-II). But, the sum $\alpha + \gamma + \beta$ violates the angle folding relation and consequently the extension of the configuration can not be performed.

If $\delta < \frac{\pi}{2}$, then $\alpha > \gamma > \frac{\pi}{4}$ and so $\beta \geq \frac{\pi}{2}$. The sum $2\delta + \lambda$ does not satisfy the angle folding relation, for any $\lambda \in \{\alpha, \beta, \gamma, \delta\}$ and we can not continue pursuing the construction of the configuration.

1.2.4 Assuming that $\beta+\gamma+\delta = \pi$, from $2\gamma+\delta > \pi$ one has $\frac{\pi}{3} < \beta < \gamma$, contradicting the equality $\beta + \gamma + \delta = \pi$.

2. Suppose that $\theta_8 = \delta$ (see Figure 4.80).

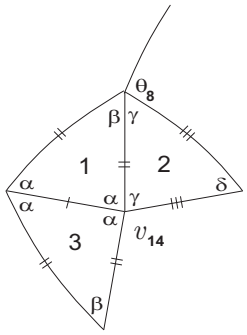

Figure 4.80: Local configuration.

As $\beta, \delta > \frac{\pi}{3}$, $2\alpha + \beta > \pi$ and $2\gamma + \delta > \pi$, then the sum containing β and θ_8 must be of the form $\beta + \delta + \alpha = \pi$ or $\beta + \delta + \gamma = \pi$ or $\beta + \delta = \pi$.
In the first case, one has $\frac{\pi}{3} < \delta < \alpha$, contradicting the equality and in the second case, $\frac{\pi}{3} < \beta < \gamma$ leading to the same contradiction.
Therefore, $\beta + \delta = \pi$ and the angle arrangement implies that $\gamma = \frac{\pi}{2}$. Consequently, $\beta < \frac{\pi}{2} < \delta$ and the order relation between the angles is now

$$\frac{\pi}{6} < \alpha < \beta < \frac{\pi}{2} = \gamma < \delta.$$

The sum containing the alternate angles α and γ, at vertex v_{18}, must obeys to the condition $2\alpha + \gamma = \pi$. Consequently, $\alpha = \frac{\pi}{4}$ and by the adjacency condition (4.4), $\beta \approx 122,94^\circ$ violating $\beta < \frac{\pi}{2}$.

□

4.4 Isohedrality-Classes and Isogonality-Classes

Here, we present the transitivity classes of isogonality and isohedrality of the dihedral f-tilings obtained $\mathcal{J}^k,\ k \geq 3,\ \mathcal{K}^m,\ m \geq 4,\ \mathcal{I},\ \mathcal{J}$ and $\mathcal{K}$.

In **Table 4.2** is shown a complete list of all spherical dihedral f-tilings, whose prototiles are an isosceles triangle T_1 of angles α, α, β and another isosceles triangle T_2 of angles γ, γ, δ. We have used the following notation:

- M and N are, respectively, the number of triangles congruent to T_1 and the number of triangles congruent to T_2 used in such dihedral f-tilings;
- The numbers of isohedrality-classes and isogonality-classes for the symmetry group are denoted, respectively, by # isoh. and # isog.;
- $\alpha = \alpha_0^k$, in f-tiling $\mathcal{J}^k,\ k \geq 3$ is the solution of

$$\frac{\cos\alpha(1+\cos\beta)}{\sin\alpha\sin\beta} = \frac{\cos\delta + \cos^2\gamma}{\sin^2\gamma},$$

  with $\delta = \frac{\pi}{k},\ \beta = 2\alpha$ and $\gamma = \pi - 2\alpha$;

- $\gamma = \gamma_0^k$, in f-tiling $\mathcal{K}^m,\ m \geq 4$, is given by

$$\frac{\cos\alpha(1+\cos\beta)}{\sin\alpha\sin\beta} = \frac{\cos\delta + \cos^2\gamma}{\sin^2\gamma},$$

  with $\alpha = \frac{\pi}{k},\ \beta = \pi - \gamma$ and $\delta = \pi - \alpha - \gamma$;

f-**tiling**	α	β	γ	δ	M	N	# isoh.	# isog.
$\mathcal{J}^k,\ k \geq 3$	α_0^k	2α	$\pi - 2\alpha$	$\frac{\pi}{k}$	$4k$	$4k$	2	3
$\mathcal{K}^m,\ m \geq 4$	$\frac{\pi}{m}$	$\pi - \gamma$	γ_0^m	$\pi - \frac{\pi}{m} - \gamma$	$4m$	$4m$	2	3
$\mathcal{I}$	$\frac{\pi}{3}$	$\frac{2\pi}{3}$	$\frac{\pi}{3}$	$\frac{\pi}{2}$	6	12	3	5
$\mathcal{J}$	$\frac{\pi}{3}$	$\frac{2\pi}{3}$	$\frac{\pi}{3}$	$\frac{\pi}{2}$	8	8	2	3
$\mathcal{K}$	$\frac{\pi}{3}$	71.774°	48.226°	$\frac{\pi}{2}$	48	24	3	5

Table 4.2: The Combinatorial Structure of the Dihedral f-Tilings of the Sphere by Isosceles Triangles with Adjacency of type II

4.5 Triangular Dihedral f-Tilings with Adjacency of Type III

In this Section, we complete the classification of f-tilings by two non congruent isosceles triangles studding the last case of adjacency illustrated in Figure 4.87.

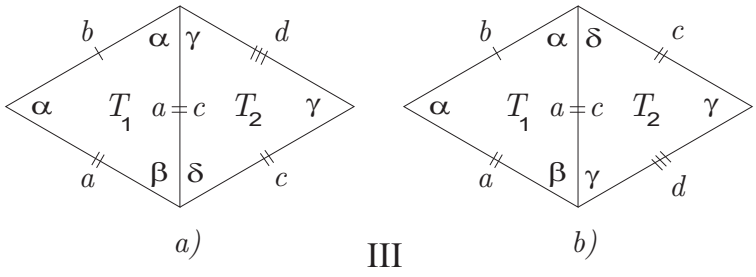

Figure 4.81: Adjacency of type III.

Type III can be described analytically by the following trigonometric equation:

$$\frac{\cos\alpha(1+\cos\beta)}{\sin\alpha\sin\beta} = \frac{\cos\gamma(1+\cos\delta)}{\sin\gamma\sin\delta}. \tag{4.6}$$

Remark 4.2 *In adjacency of type **III**, β and δ must be distinct. In fact, if $\beta = \delta$, then $\alpha = \gamma$, which is an impossibility. From the adjacency condition (4.6), one can conclude that α and γ belong to the same quadrant. These two angles are also distinct, except when $\alpha = \gamma = \frac{\pi}{2}$. Observe that, if $\alpha = \gamma$ and $\alpha, \gamma \neq \frac{\pi}{2}$, then $\frac{1+\cos\beta}{\sin\beta} = \frac{1+\cos\delta}{\sin\delta}$, an impossibility, since the function $f(x) = \frac{1+\cos x}{\sin x}$ is injective, for all $x \in]0, \pi[$. Hence, we will consider, without loss of generality, $\alpha \geq \gamma$.*

We begin by showing that, it is impossible to have side $a = c$ and $b = d$:

Suppose that $a = c,\ b = d$. Besides the adjacency condition (4.6), we now have also

$$\frac{\cos\beta + \cos^2\alpha}{\sin^2\alpha} = \frac{\cos\delta + \cos^2\gamma}{\sin^2\gamma} \tag{4.7}$$

and the relations

$$\sin\alpha = \sin\gamma,\ \sin\beta = \sin\delta$$

implying that $\alpha = \gamma = \frac{\pi}{2}$ and $\beta = \pi - \delta = \overline{\delta}$, by the previous remark.

By (4.7), one has $\delta = \frac{\pi}{2} = \overline{\delta}$ and consequently, T_1 is congruent to T_2, which is impossible.

In what follows, to facilite the construction of dihedral f-tilings, we distinguish the possible different order relation between the angles, namely, ($\alpha > \beta$ and $\gamma > \delta$), ($\alpha > \beta$ and $\delta > \gamma$), ($\beta > \alpha$ and $\gamma > \delta$) and finally ($\beta > \alpha$ and $\delta > \gamma$).

Elimination Lemma *In adjacency of type III a), if* $\beta > \alpha$ *and* $\alpha, \gamma \neq \frac{\pi}{2}$, *then* $\Omega(T_1, T_2) = \varnothing$.

Proof. Assume that the adjacency is of type III a), as described in Figure 4.118.

Suppose that $\beta > \alpha$ and $\gamma > \delta$.

Starting a local configuration of $\tau \in \Omega(T_1, T_2)$ with two adjacent cells congruent to T_1 and T_2 respectively (see Figure 4.82-I) and taking into account the angle folding relation, the order relation between the angles and the fact that $\gamma < \alpha < \frac{\pi}{2}$, the sum $\alpha + \gamma + \mu$ does not satisfy the angle folding relation, for any $\mu \in \{\alpha, \beta, \gamma, \delta\}$ and so the configuration started in Figure 4.82-I can not be extended.

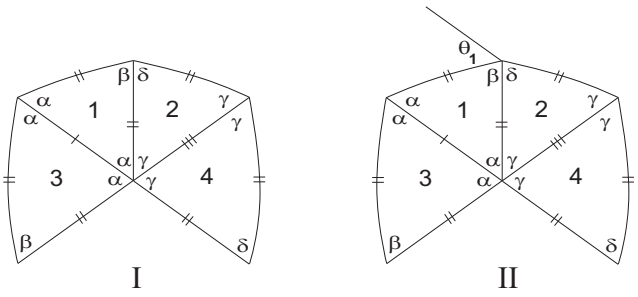

Figure 4.82: Local configuration.

Suppose now that $\beta > \alpha$ and $\delta > \gamma$.

As $\gamma < \alpha < \frac{\pi}{2}$, then $\beta \geq \frac{\pi}{2}$ or $\delta \geq \frac{\pi}{2}$, since vertices of valency four must exist. To continue extending the configuration started in Figure 4.82-I, a decision for the angle $\theta_1 \in \{\alpha, \beta, \gamma, \delta\}$ (Figure 4.82-II) must be taken.

1. Assume first, that $\theta_1 = \alpha$. Then $\alpha + \delta < \pi$, since $\alpha + \delta = \pi$ implies $\beta = \delta$, which is impossible.

We have now to fix $\theta_2 \in \{\gamma, \delta\}$ (see Figure 4.83-I).

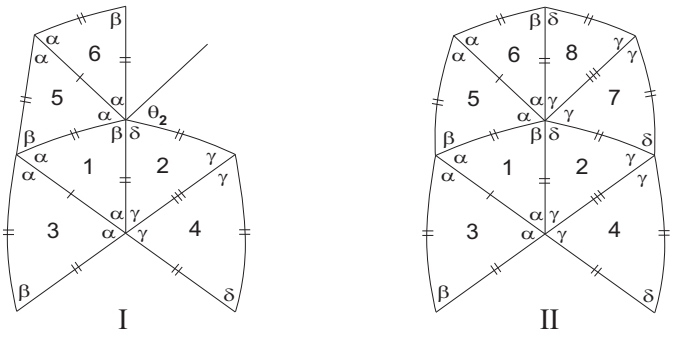

Figure 4.83: Local configurations.

1.1 If $\theta_2 = \gamma$ and $\alpha + \beta + \gamma = \pi$, the angles arrangement leads us to the impossibility $\beta = \delta$ (see Figure 4.83-II).

1.2 If $\theta_2 = \gamma$, but $\alpha + \beta + \gamma < \pi$, in order to satisfy the angle folding relation, the sum containing these three angles must satisfy $\alpha + \beta + k\gamma = \pi,\ k \geq 2$. However, the angle arrangement lead us to $\alpha + \delta + k\gamma = \pi$, contradicting $\delta \neq \beta$.

1.3 Assuming that $\theta_2 = \delta$, one has $\alpha + \beta + \delta \leq \pi$. As $2\gamma + \delta > \pi$ and $\gamma < \alpha$, then $\beta < \alpha$, contradicting $\beta > \alpha$.

2. Assume now, that $\theta_1 = \beta$.

2.1 If $\beta + \delta = \pi$, then $\frac{\pi}{3} < \beta < 2\gamma$ and so $\alpha > \gamma > \frac{\pi}{6}$. Extending the configuration in Figure 4.82-II, we end up at a vertex, v_1 partially surrounded by four angles α, illustrated in Figure 4.84.

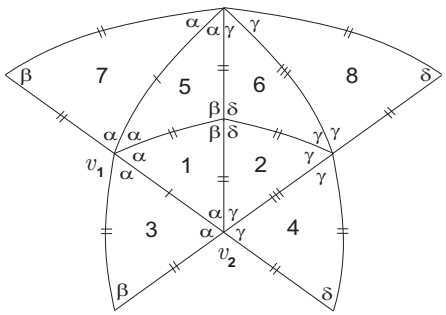

Figure 4.84: Local configuration.

Vertex v_1 must be of valency six, eight or ten surrounded exclusively by angles α or of valency $2(m+n),\ m \geq 2,\ m+n \leq 5$ surrounded by angles α and γ (see Figure 4.85).

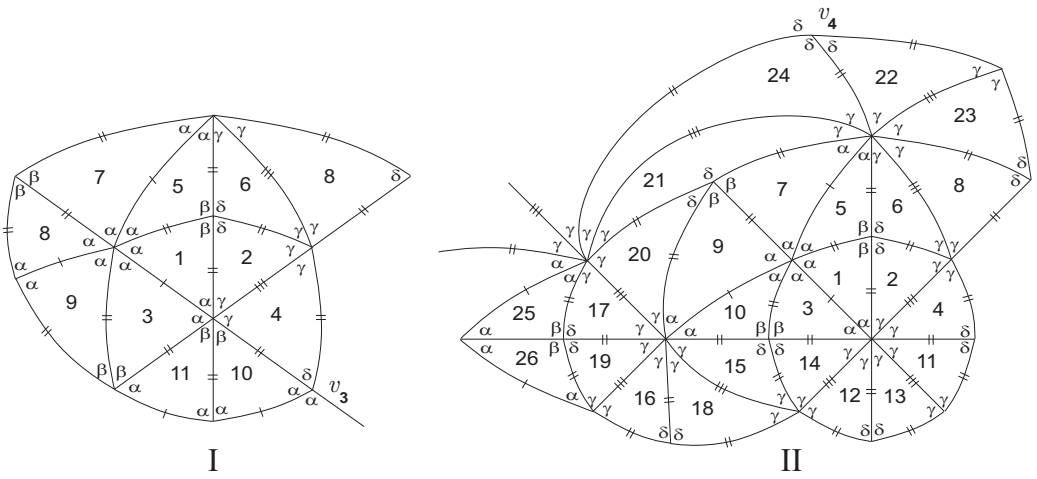

Figure 4.85: Local configurations.

Assume first that v_1 is of valency six surrounded exclusively by angles α. Therefore, $\alpha = \frac{\pi}{3}$ and vertex v_2 must be of valency six obeying either to the condition $2\alpha+\gamma = \pi$ or $\alpha + 2\gamma = \pi$ or $\alpha + \gamma + \beta = \pi$ or of valency eight satisfying $\alpha + 3\gamma = \pi$.
In case, $2\alpha + \gamma = \pi$ or $\alpha + 2\gamma = \pi$, one gets the contradiction $\gamma = \alpha$.
If $\alpha + \gamma + \beta = \pi$, then by (4.6), $\delta \approx 105.286°,\ \beta \approx 74.714°,\ \gamma \approx 45.286°$ and adding some cells to the configuration in Figure 4.84, we end up at a vertex (v_3) of valency greater than four partially surrounded by angles α, α, δ (see Figure 4.85-I). The sum containing the alternate angles α and δ does not satisfy the angle folding relation preventing the extension of the configuration.
If v_2 satisfies $\alpha + 3\gamma = \pi$, then $\gamma = \frac{2\pi}{9} = 40°$ and by the adjacency condition (4.6), $\delta \approx 110.32°$ and $\beta \approx 69.68°$. Extending the configuration in Figure 4.84, we get a vertex, v_4 surrounded by three angles δ, which does not satisfy the angle folding relation, Figure 4.85-II.

Assuming that v_1 is of valency eight surrounded exclusively by angles α, then $\alpha = \frac{\pi}{4}$ and so

$$\frac{\pi}{6} < \gamma < \frac{\pi}{4} = \alpha < \frac{\pi}{3} < \delta < \frac{\pi}{2} < \beta.$$

Vertex v_2 (Figure 4.84) is either of valency six, eight or ten satisfying, respectively

$(2\alpha+\gamma=\pi$ or $\alpha+2\gamma=\pi$ or $\alpha+\gamma+\beta=\pi)$ or $(\alpha+3\gamma=\pi$ or $\alpha+2\gamma+\beta=\pi)$ or $\alpha+4\gamma=\pi$. However, having in consideration the order relation between the angles all these equations have no solution.

If vertex v_1 is of valency ten surrounded exclusively by angles α, then $\alpha=\frac{\pi}{5}$ and

$$\frac{\pi}{6}<\gamma<\frac{\pi}{5}=\alpha<\frac{\pi}{3}<\delta<\frac{2\pi}{5}<\frac{3\pi}{5}<\beta.$$

Looking at vertex v_2, the sum containing the alternate angles must be of the form $p\alpha+m\gamma=\pi,\ p<5$ and $m<6$. Then, $\pi<p\frac{\pi}{5}+m\frac{\pi}{5}$ and so $p+m>5$, contradicting $p<5$ and $m<6$.

Therefore, vertex v_1 is of valency $2(m+n)$ for $m\geq 2,\ n\geq 1,\ m+n\leq 5$ and $m+n\neq 2$ satisfying $m\alpha+n\gamma=\pi$. Since, $2\gamma+\delta>\pi$ and $\beta+\delta=\pi$, one has, for $n\geq 2$, $2\alpha+\beta\leq m\alpha+\beta<(2-n)\gamma+\pi\leq\pi$, which is an impossibility. For $n=1$, one has $(m-1)\alpha+\beta<\pi$, which is also an impossibility for $m\geq 3$.
It remains to analise the case $n=1,\ m=2$, meaning $2\alpha+\gamma=\pi$ and so $\gamma<\frac{\pi}{3}<\alpha$.

Vertex v_2 in Figure 4.84 is of valency six (whose both sums of alternate angles satisfy $2\alpha+\gamma=\pi$) or of valency eight (whose both sums of alternate angles satisfy $\alpha+3\gamma=\pi$). However, the last possibility lead us to the contradiction $\beta<\alpha$, since $2\gamma+\delta>\pi,\ \delta+\beta=\pi$ and $2\alpha+\gamma=\pi$. Consequently, vertex v_2 and all vertices surrounded by alternate angles α and γ obey to the condition $2\alpha+\gamma=\pi$.

On the other hand, looking to the vertex surrounded by four angles γ in Figure 4.84, this must be of valency eight or ten surrounded exclusively by angles γ or of valency six satisfying $2\gamma+\beta=\pi$ or of valency eight satisfying $3\gamma+\alpha=\pi$ or $3\gamma+\beta=\pi$.
Using the adjacency condition (4.6), we observe that the cases $\gamma=\frac{\pi}{4},\frac{\pi}{5}$ must be ruled out, since we get $\beta\approx 65.58^\circ$ and $\alpha=67,5^\circ$, for $\gamma=\frac{\pi}{4}$; and $\beta\approx 51.83^\circ$ and $\alpha=72^\circ$, for $\gamma=\frac{\pi}{5}$, violating, in both cases, the condition $\alpha<\beta$.

In case $2\gamma+\beta=\pi$, since $\beta+\delta=\pi$ and $2\alpha+\gamma=\pi$, then, by the adjacency condition (4.6), we get $\gamma\approx 51.826^\circ,\ \alpha\approx 64.087^\circ,\ \beta\approx 76.348^\circ$ and $\delta\approx 103.652^\circ$. Using this information, we end up with a local configuration, where a vertex partially surrounded by two angles α and one δ appears (see Figure 4.86). The sum $\delta+\alpha+\mu$ violates the angle folding relation, for any $\mu\in\{\alpha,\beta,\gamma,\delta\}$ and so this case must be ruled out.

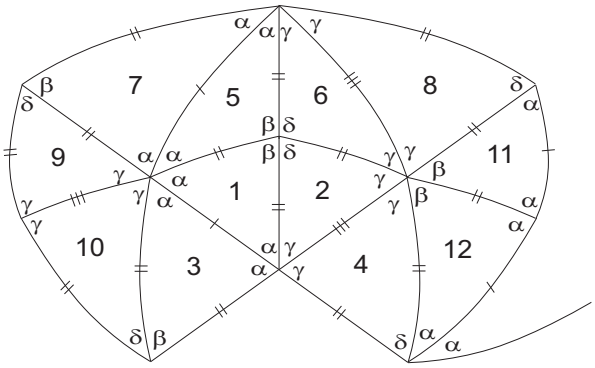

Figure 4.86: Local configuration.

The remaining cases are also impossible, since the conditions $3\gamma+\alpha=\pi,\ 2\alpha+\gamma=\pi,\ \beta+\delta=\pi$ and $2\alpha+\beta>\pi$ imply the contradiction $\alpha>\beta$, as well as the conditions $3\gamma+\beta=\pi,\ 2\alpha+\gamma=\pi,\ \beta+\delta=\pi$ and $2\gamma+\delta>\pi$.

2.2 If $\beta+\delta<\pi$, in order to satisfy the angle folding relation, the sum containing these two angles must be either of the form $\beta+\delta+\alpha=\pi$ or $\beta+\delta+\gamma=\pi$ or $\beta+\delta+\alpha+\gamma=\pi$. In the first case, $\alpha<\frac{\pi}{3}$. On the other hand, as $2\alpha+\beta>\pi$, then $\delta<\alpha$. But $\delta>\frac{\pi}{3}$ from $2\gamma+\delta>\pi$ and $\delta>\gamma$, leading to a contradiction. In a similar way, the remaining cases must be eliminated.

3. If $\theta_1=\gamma$ or δ, in Figure 4.82-II, then $\delta+\theta_1\leq\pi$.

In any case, if the valency of the vertex is four, we reach to the impossibility $\beta=\delta$. If the vertex is of valency greater than four, then the sum containing the alternate angles δ and θ_1 violates the angle folding relation.

□

4.5.1 Adjacency of type III a)

Assume firstly, that triangles T_1 and T_2 satisfy adjacency of type **III a)**, as illustrated in Figure 4.87.

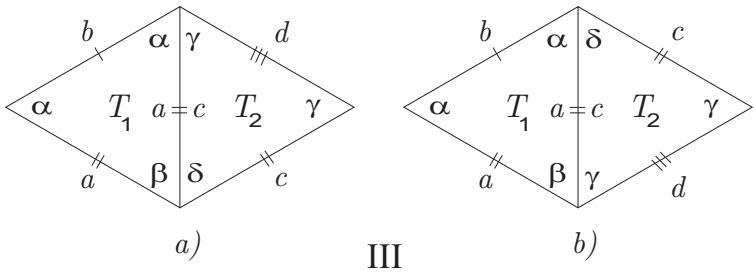

Figure 4.87: Adjacency of type III.

Proposition 4.9 *If $\gamma = \alpha = \frac{\pi}{2}$, then $\Omega(T_1, T_2)$ is composed by the following tilings:*

***for** $\beta > \alpha$ **and** $\gamma > \delta$:*

$\alpha = \gamma = \frac{\pi}{2},\ \beta + k\delta = \pi,\ k \geq 1$ *for* $\mathcal{L}_i^{k,\delta},\ i = 1, \ldots, k$;

***for** $\alpha > \beta$ **and** $\gamma > \delta$:*

$$\alpha = \gamma = \frac{\pi}{2},\ m\beta + n\delta = \pi,\ m + n \neq 2 \text{ for } \mathcal{M}_i^{m,n,\delta},\ i = 1, \ldots, I;$$
$$\alpha = \gamma = \frac{\pi}{2},\ \frac{\pi}{2} + p\beta + q\delta = \pi,\ p, q \geq 1 \text{ for } \mathcal{N}_i^{p,q,\delta},\ i = 1, \ldots, I;$$
$$\alpha = \gamma = \frac{\pi}{2},\ \frac{\pi}{2} + p\beta + q\delta = \pi,\ p, q \geq 1,\ \frac{\pi}{2} + t\beta = \pi,\ p, q \geq 1,\ 1 \leq p < t,\ t \geq 2$$
$$\text{for } \mathcal{O}_i^{p,q,t},\ i = 1, \ldots, I,$$

where I denotes the number of distinct positions to place the angles β and δ, in such a way that the local configuration gives rise to a global f-tiling.

***for** $\alpha > \beta$ **and** $\delta > \gamma$:*

$\alpha = \gamma = \frac{\pi}{2},\ \delta + k\beta = \pi,\ k \geq 2$ *for* $\mathcal{P}_i^{k,\beta},\ i = 1, \ldots, k$.

Proof. Starting a local configuration of $\tau \in \Omega(T_1, T_2)$ with two adjacent cells congruent to T_1 and T_2 and since $\alpha = \gamma = \frac{\pi}{2}$, then vertex v_6 (see Figure 4.88) is of valency four and its both sums of alternate angles are of the form $\alpha + \gamma = \pi$. Observe that if $\beta > \alpha$ and $\delta > \gamma$, then sums of alternate angles containing β and δ do not satisfy

the angle folding relation preventing us to continue the extension of the configuration. To facilite the construction of dihedral f-tilings, we distinguish the possible different order relation between the angles, namely, ($\beta > \alpha$ and $\gamma > \delta$) or ($\alpha > \beta$ and $\gamma > \delta$) or ($\alpha > \beta$ and $\delta > \gamma$).

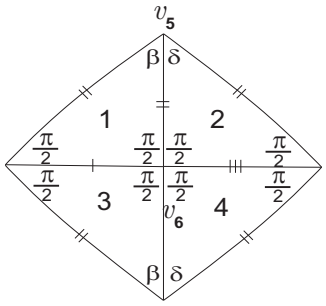

Figure 4.88: Local configuration.

Assume that $\beta > \alpha$ and $\gamma > \delta$.

As $\beta > \alpha = \frac{\pi}{2}$, then sums of alternate angles containing β are of the form $\beta + k\delta = \pi$, for some $k \geq 1$. For each k, we get k two-parameter families of f-tilings denoted by $\mathcal{L}_i^{k,\delta}$, $i = 1, \ldots, k$, with two type of vertices: the ones of valency four surrounded exclusively by $\frac{\pi}{2}$ and the ones of valency $2(1+k)$, whose sums of alternate angles satisfy $\beta + k\delta = \pi$. It is composed by 4 copies of T_1 and $4k$ copies of T_2.

Next two figures show the cases $k = 1$ and $k = 2$.

For $k > 2$, we can get each member of this family by adding some edges to a monohedral f-tiling where the prototile is an isosceles triangle.

Figure 4.89: 3D representation of $\mathcal{L}_1^{1,\delta}$.

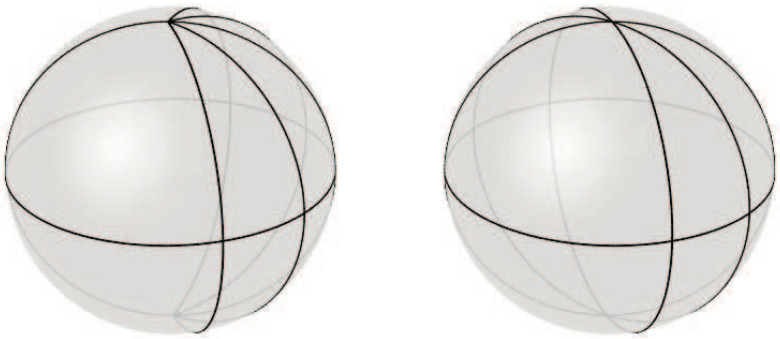

Figure 4.90: 3D representation of $\mathcal{L}_1^{2,\delta}$ and $\mathcal{L}_2^{2,\delta}$.

Suppose that $\alpha > \beta$ and $\gamma > \delta$.

In this case, the sum of alternate angles containing β, at vertex v_5 (see Figure 4.88), must be either of the form

- $k\beta = \pi,\ k \geq 3$ or
- $m\beta + n\delta = \pi,\ m, n \geq 1,\ m + n \neq 2$ or
- $\frac{\pi}{2} + p\beta + q\delta = \pi,\ p, q \geq 1$ or
- $\frac{\pi}{2} + t\beta = \pi,\ t \geq 2$.

Next, we shall study all cases separately.

1. If $k\beta = \pi$, for some $k \geq 3$, the other sum of alternate angles at vertex v_5 satisfy either $k\delta = \pi,\ k \geq 3$ or $a\beta + b\delta = \pi,\ a + b = k$. Both possibilities lead us to a contradiction, since $\beta \neq \delta$.

2. Suppose that $m\beta + n\delta = \pi$, $m, n \geq 1,\ m + n \neq 2$. In the following, we will study the cases $m = n$ and $m \neq n$ separately.

2.1 Suppose that $m = n$ and $m = n = 2$. According to the different possibilities to place the angles β and δ around vertex v_5, we are lead to five non-isomorphic configurations. Each one giving rise to a complete f-tiling denoted by $\mathcal{M}_i^{2,\delta}$, $i = 1, \ldots, 5$ (see Figure 4.91) composed by 8 copies of each prototile.

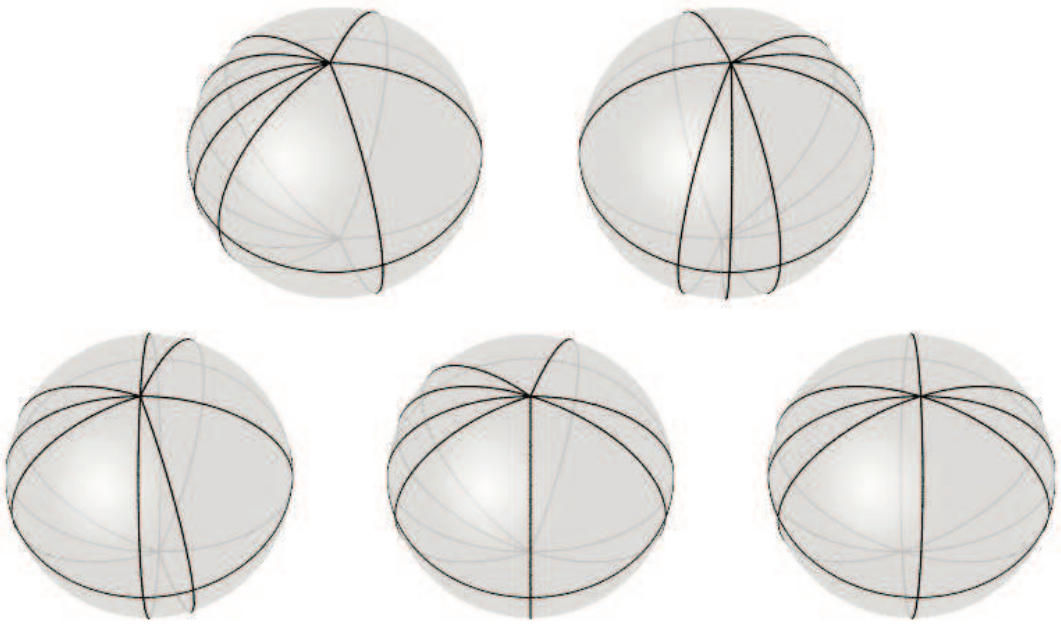

Figure 4.91: 3D representation of $\mathcal{M}_i^{2,\delta}$, $i = 1, \ldots, 5$.

For each $m = n > 2$, we get a continuous family of f-tilings denoted by $\mathcal{M}_i^{m,\delta}$, where i denotes the number of distinct possibilities to locate angles β and δ in order to have $m\beta + m\delta = \pi$. It has two types of vertices: valency four surrounded exclusively by $\frac{\pi}{2}$ and valency $4m$ whose sums of alternate angles satisfy $m\beta + m\delta = \pi$.

2.2 Assume now that $m \neq n$. If $m = 1$ and $n = 2$, we are led to two different configurations, according to the different possibilities to place the angles around vertex v_5. Each one gives rise to a one parameter complete f-tiling denoted by $\mathcal{M}_1^{1,2,\delta}$ and $\mathcal{M}_2^{1,2,\delta}$, as illustrated in Figure 4.92. It is composed by 4 triangles congruent to T_1 and 8 triangles congruent to T_2.

If $m = 1$ and $n > 2$, we get a discrete family of f-tilings denoted $M_i^{1,n,\delta}$, $i = 1, \ldots, n-1$, with 4 copies of T_1 and $4n$ copies of T_2. Starting to generalize, for $m = 2$, one has the family $\mathcal{M}_i^{2,n,\delta}$, where i denotes the number of distinct possibilities to place the angles β and δ, in order to have $2\beta + n\delta = \pi$. If $m > 2$ and $n > 2$, then we have $\mathcal{M}_i^{m,n,\delta}$, $i = 1, \ldots, I$ composed by vertices of valency four surrounded exclusively by $\frac{\pi}{2}$ and vertices of valency $2(m+n)$, whose sums of alternate angles satisfy $m\beta + n\delta = \pi$. It has $4m$ triangles congruent to T_1 and $4n$ triangles congruent to T_2.

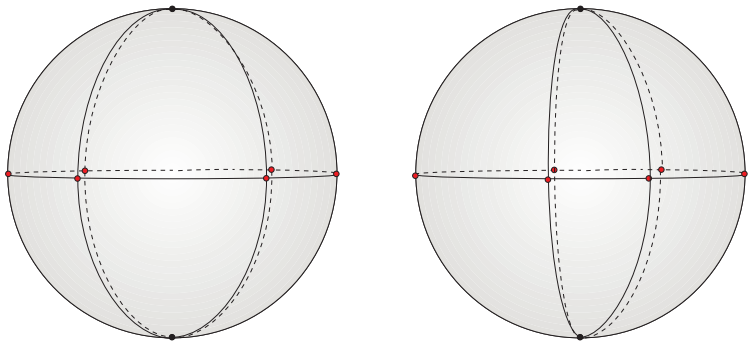

Figure 4.92: 3D representation of $\mathcal{M}_1^{1,2,\delta}$ and $\mathcal{M}_2^{1,2,\delta}$.

3. Suppose that the sum of alternate angles containing β, at vertex v_5 is of the form $\frac{\pi}{2} + p\beta + q\delta = \pi$, $p, q \geq 1$. If $p = q = 1$ and all sums of alternate angles are of the form $\frac{\pi}{2} + \beta + \delta = \pi$, we may add some new cells to the configuration started in Figure 4.88 and get six complete f-tilings, which belong to the one continuous parameter family denoted by $\mathcal{N}_i^{1,\delta}$, $i = 1, \ldots, 6$ (see Figure 4.93). Each tiling of $\mathcal{N}_i^{1,\delta}$ is composed by two classes of congruence equally distributed with two type of vertices: valency four surrounded exclusively by $\frac{\pi}{2}$ and vertices of valency six whose sums of alternate angles satisfy $\frac{\pi}{2} + \beta + \delta = \pi$.

If $p = q > 1$, one has a two-parameter family of f-tilings denoted by $\mathcal{N}_i^{p,\delta}$, $i = 1, \ldots, I$ with two type of vertices: the ones of valency four surrounded by $\frac{\pi}{2}$ and vertices of valency $2(1+2p)$, whose sums of alternate angles satisfy $\frac{\pi}{2} + p\beta + p\delta = \pi$.

Now, if besides the sum $\frac{\pi}{2} + p\beta + p\delta = \pi$, one has also $\frac{\pi}{2} + t\beta = \pi$ with $t \geq 3$ and $p < t$, we get new families of f-tilings denoted by $\mathcal{O}_i^{p,t}$, $i = 1, \ldots, I$. In Figure 4.94, we present a 3D representation of $\mathcal{O}_i^{1,3}$, $i = 1, 2$. They are composed by 4 triangles

congruent to T_1 and 16 triangles congruent to T_2.

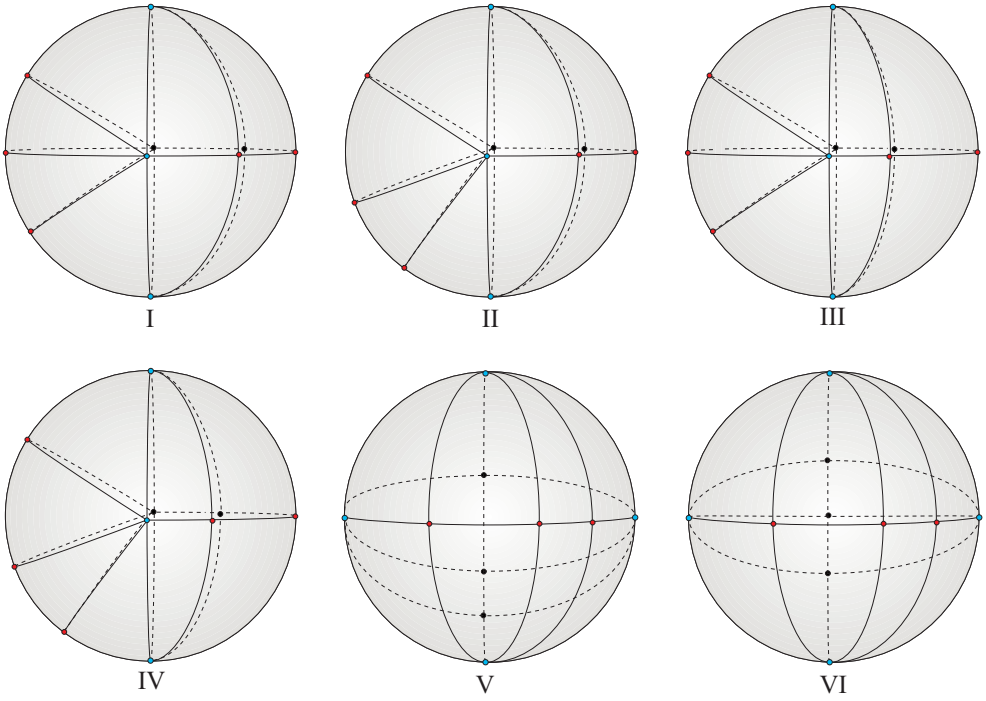

Figure 4.93: 3D representation of $\mathcal{N}_i^{1,\delta}, i = 1, \ldots, 6$.

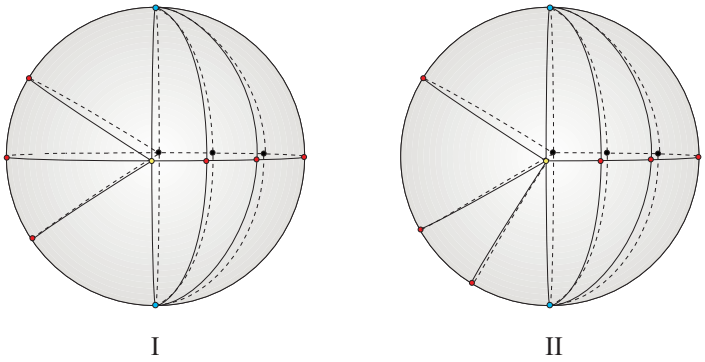

Figure 4.94: 3D representation of $\mathcal{O}_1^{1,3}$ and $\mathcal{O}_2^{1,3}$.

If $p \neq q$ and all vertices of valency four are surrounded exclusively by $\frac{\pi}{2}$ and the sum of alternate angles of vertices of valency $2(1+p+q)$ is of the form $\frac{\pi}{2}+p\beta+q\delta = \pi$, new families of f-tilings denoted by $\mathcal{N}_i^{p,q,\delta}$, $i = 1, \ldots, I$ arise. In Figure 4.95, we present one member of $\mathcal{N}_i^{1,2,\delta}$ composed by 8 copies of T_1 and 16 copies of T_2.

If $p \neq q$ and vertices of valency $2(1+t)$ also occur, with $\frac{\pi}{2} + t\beta = \pi,\ t \geq 2$ and $p < t$, we are led to discrete families of f-tilings denoted by $\mathcal{O}_i^{p,q,t}$.

Figure 4.96 illustrates the case $p = 1,\ q = 2,\ t = 2$, where each member of the family has 12 copies of T_1 and 8 copies of T_2. They are composed by vertices of valency four surrounded exclusively by angles $\frac{\pi}{2}$, vertices of valency six whose sums of alternate angles satisfy $\frac{\pi}{2} + 2\beta = \pi$ and vertices of valency eight whose sums of alternate angles satisfy $\frac{\pi}{2} + \beta + 2\delta = \pi$.

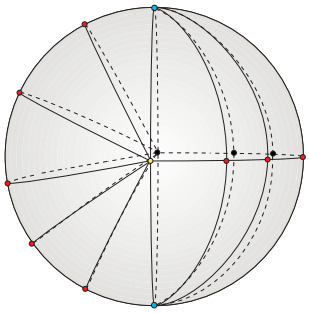

Figure 4.95: 3D representation of one member of $\mathcal{N}_i^{1,2,\delta},\ i = 1, \ldots, I$.

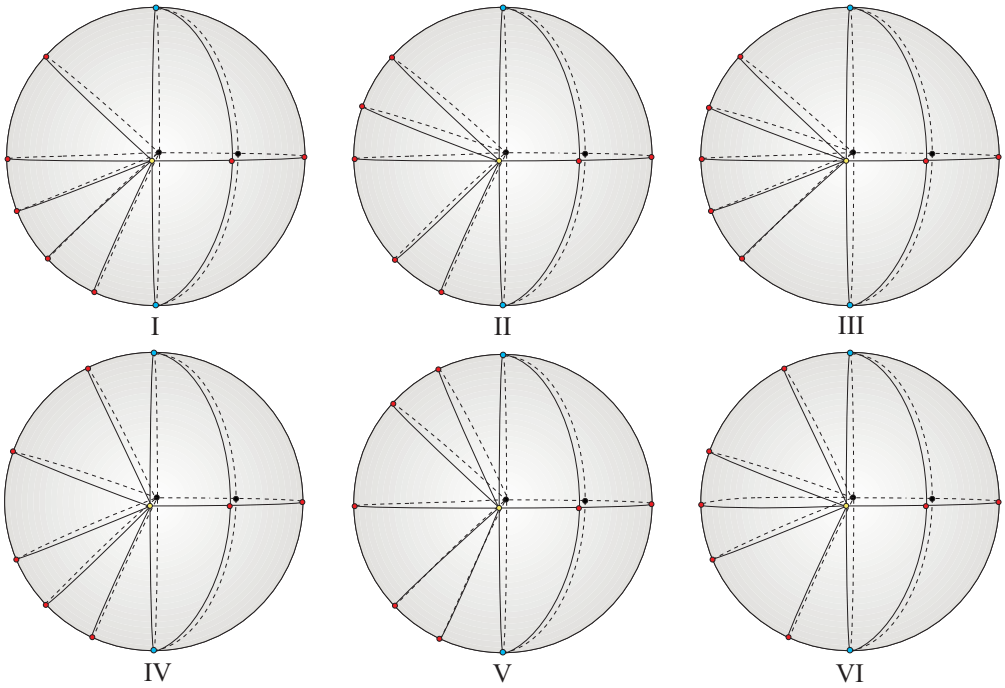

Figure 4.96: 3D representation of $\mathcal{O}_i^{1,2,2},\ i = 1, \ldots, 6$.

It should be mentioned that the families $\mathcal{M}_i^{p,q,\delta}$, $\mathcal{N}_i^{p,q,\delta}$ and $\mathcal{O}_i^{p,q,t}$ can be obtained from a monohedral f-tiling adding some edges.

4. Assuming that $\frac{\pi}{2} + t\beta = \pi,\ t \geq 2$, the angles arrangement at vertex v_5 allows us to conclude that the sum of alternate angles containing δ must be either of the form $\frac{\pi}{2} + t\delta = \pi$ or $\frac{\pi}{2} + a\beta + b\delta = \pi$ where $a + b = t$. Both possibilities lead us to the contradiction $\beta = \delta$ and so we can not continue the extension of the configuration.

Suppose that $\alpha > \beta$ and $\delta > \gamma$.

In this final case, $\delta > \frac{\pi}{2}$ and consequently, the sum of alternate angles containing δ must be of the form $\delta + k\beta = \pi$, for some $k \geq 2$. Switching the roles of angles β and δ, we are led to the family of f-tilings denoted by $\mathcal{P}_i^{k,\beta},\ i = 1, \ldots, k$ similar to $\mathcal{L}_i^{k,\delta}$.

□

Proposition 4.10 *If $\gamma < \alpha$ and $\alpha > \beta$, then $\Omega(T_1, T_2)$ is composed by one discrete family of tilings denoted by $\left(\mathcal{Q}^k\right)_{k\geq 4, k\in\mathbb{N}}$, such that the sums of alternate angles around vertices are of the form $\beta + \delta = \pi,\ 2\alpha + \gamma = \pi$ and $k\gamma = \pi$.*

Proof. Starting a local configuration of $\tau \in \Omega(T_1, T_2)$ with two adjacent cells congruent to T_1 and T_2 respectively (see Figure 4.97-I), vertex v_6 is of valency greater than four, since $\gamma < \alpha$ and α, γ belong to the same quadrant.

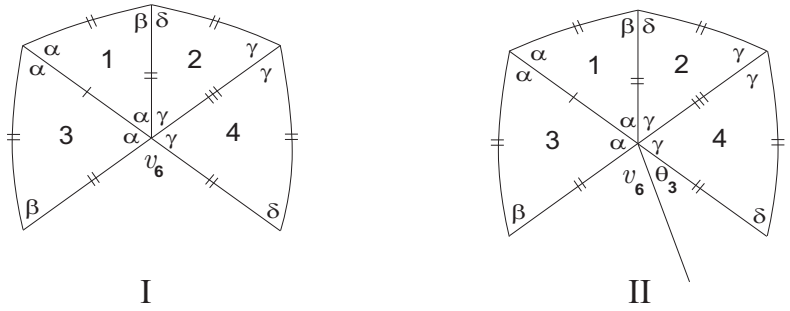

Figure 4.97: Local configurations.

In case $\alpha > \beta$ and $\gamma > \delta$, as $\gamma < \alpha < \frac{\pi}{2}$, we conclude that all angles are lower than $\frac{\pi}{2}$ preventing the existence of vertices of valency four, which is impossible.

Assume that $\alpha > \beta$ and $\delta > \gamma$.

Since $\gamma < \alpha < \frac{\pi}{2}$ and $\beta < \alpha$, then $\delta \geq \frac{\pi}{2}$. We shall study the cases $\delta = \frac{\pi}{2}$ and $\delta > \frac{\pi}{2}$ separately. Starting from the configuration illustrated in Figure 4.97-II, a decision about angle $\theta_3 \in \{\alpha, \beta, \gamma\}$ must be taken (note that if $\theta_3 = \delta$, then $\alpha + \gamma + \theta_3 > 2\gamma + \delta > \pi$, preventing us to continue the extension of the configuration).

A. Suppose firstly, that $\delta = \frac{\pi}{2}$.

1. If $\theta_3 = \alpha$, then vertex v_6 is of valency six satisfying $2\alpha + \gamma = \pi$, since $2\alpha + \gamma + \mu$ does not satisfy the angle folding relation, for any $\mu \in \{\alpha, \beta, \gamma, \delta\}$. Therefore, the order relation between the angles is now

$$\frac{\pi}{4} < \gamma < \beta < \alpha < \frac{\pi}{2} = \delta$$

and so the vertex partially surrounded by angles δ, β and θ_4, shown in Figure 4.98-I, must be of valency four. Observe that for $\theta_4, \mu \in \{\alpha, \beta, \gamma\}$, then $\delta + \theta_4 + \mu > \pi$. Consequently, $\theta_4 = \delta$ and $\beta = \delta$, contradicting the mentioned order relation.

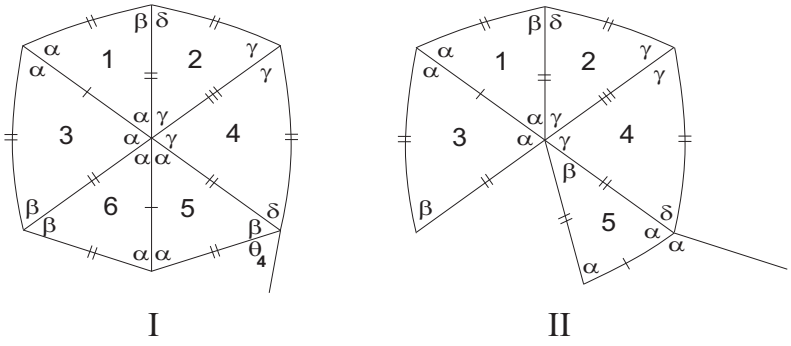

Figure 4.98: Local configurations.

2. Suppose now that $\theta_3 = \beta$, as shown in Figure 4.98-II. In the extended configuration, a vertex (of valency greater than four) surrounded by angles δ, α, α arises, but the sum $\delta + \alpha + \mu$ violates the angle folding relation, for any $\mu \in \{\alpha, \beta, \gamma, \delta\}$.

3. If $\theta_3 = \gamma$, then, $\alpha + 2\gamma \leq \pi$ and so $\frac{\pi}{4} < \gamma < \frac{\pi}{3} < \alpha < \delta = \frac{\pi}{2}$.

3.1 Assuming that $\alpha + 2\gamma = \pi$, a decision about the angle $\theta_5 \in \{\alpha, \beta, \gamma, \delta\}$ must be made, as illustrated in Figure 4.99.

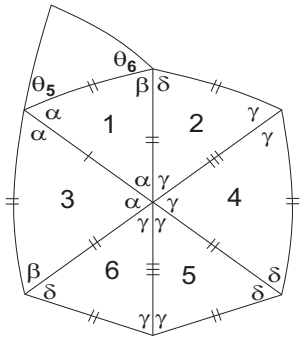

Figure 4.99: Local configuration.

If $\theta_5 = \alpha$, then the vertex partially surrounded by three angles α is of valency six satisfying $2\alpha + \gamma = \pi$ leading to the impossibility $\alpha = \gamma$.

Assuming that $\theta_5 = \beta$, then $\theta_6 = \alpha$ and if $\theta_5 = \delta$, then $\theta_6 = \gamma$. In any case, the sum containing the alternate angles α and δ violates the angle folding relation, since $2\gamma + \delta > \pi,\ 2\alpha + \beta > \pi$ and $\frac{\pi}{4} < \gamma < \frac{\pi}{3} < \alpha < \frac{\pi}{2} = \delta$.

If $\theta_5 = \gamma$, then $\theta_6 = \delta$ and so $\beta = \frac{\pi}{2}$, a contradiction.

3.2 Suppose now that $\alpha + 2\gamma < \pi$. In order to satisfy the angle folding relation and taking into account that $\frac{\pi}{4} < \gamma < \frac{\pi}{3} < \alpha < \frac{\pi}{2} = \delta,\ \beta < \alpha,\ 2\gamma + \delta > \pi$ and $2\alpha + \beta > \pi$, we must have $\alpha + 2\gamma + k\beta = \pi,\ k \geq 1$. Adding some cells to the configuration shown in Figure 4.97-II, we end up at a vertex partially surrounded (see Figure 4.100) by angles α, α and δ, whose sum $\alpha + \delta + \mu$ does not satisfy the angle folding relation, for any $\mu \in \{\alpha, \beta, \gamma, \delta\}$.

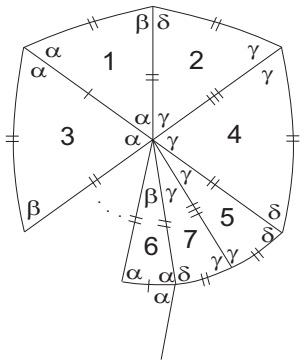

Figure 4.100: Local configuration.

B. Assume that $\delta > \frac{\pi}{2}$.

4. Supposing that $\theta_3 = \alpha$ (see Figure 4.101), then the sum containing the alternate angles α, γ, θ_3 must obey to the condition $2\alpha + t\gamma = \pi,\ t \geq 1$ and so

$$\gamma < \beta < \alpha < \frac{\pi}{2} < \delta.$$

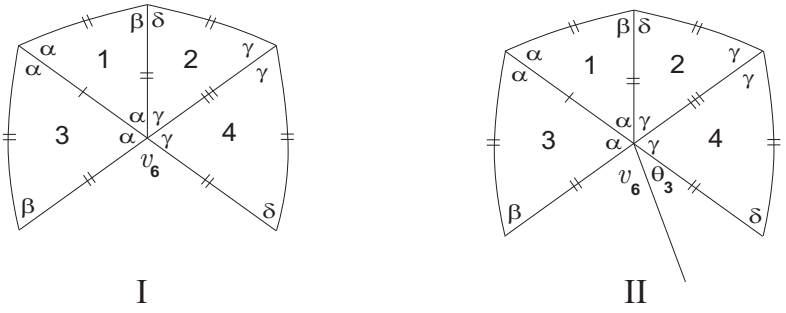

Figure 4.101: Local configurations.

On the other hand, vertex v_7 illustrated in Figure 4.102-I must be of valency four, with $\theta_7 = \beta$.

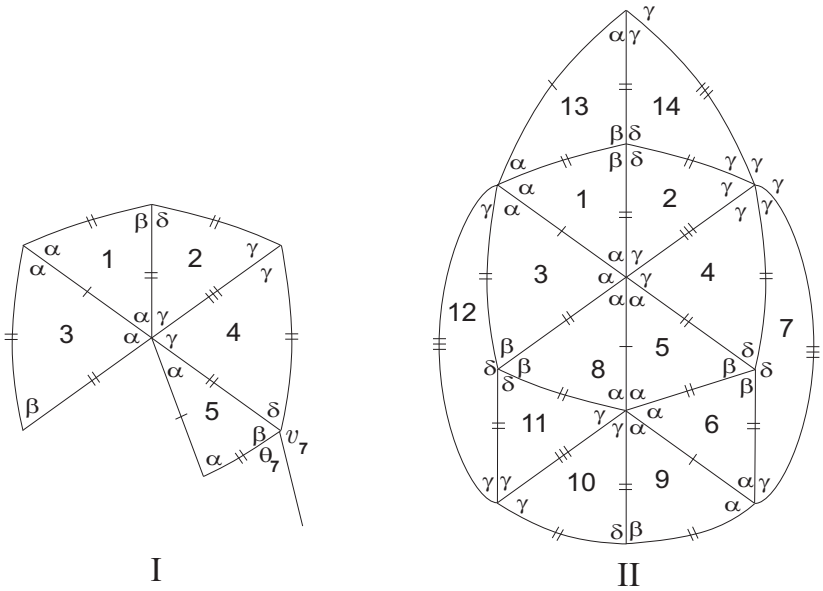

Figure 4.102: Local configurations.

Accordingly, $\delta + \beta = \pi$ and $2\alpha + t\gamma = \pi$, for some $t \geq 1$. As $2\gamma + \delta > \pi$ and $2\alpha + \beta > \pi$, then $\beta < 2\gamma$ and so $2\alpha + 2\gamma > \pi$. Consequently, $t = 1$, in other words, $2\alpha + \gamma = \pi$.

Extending the configuration in Figure 4.102-I, the vertex partially surrounded by six angles γ (Figure 4.102-II) is either

- of valency $2k,\ k \geq 3$ surrounded exclusively by angles γ or
- of valency $2(m+n),\ m \geq 3,\ n \geq 1$ surrounded by $2m$ angles γ and $2n$ angles β or
- of valency $2(p+1)$ whose both sums of alternate angles obey to the condition $p\gamma + \alpha = \pi,\ p \geq 3$ or
- of valency $2(t+q+1),\ t \geq 3,\ q \geq 1$ which both sums of alternate angles satisfy $t\gamma + q\beta + \alpha = \pi$.

When, $\gamma = \frac{\pi}{k}$, we must ruled out $k = 3$, since $k = 3$ implies $\alpha = \gamma$. For each $k \geq 4$, the configuration in Figure 4.102-II extends and we get a global tiling denoted by $\mathcal{Q}^k,\ k \geq 4$. It has $8k$ triangular faces equally distributed and we have three type of vertices valency: four, six and $2k$ whose both sums of alternate angles satisfy respectively, $\delta + \beta = \pi,\ 2\alpha + \gamma = \pi$ and $k\gamma = \pi$. Next figure shows a 2D and 3D representations of $\mathcal{Q}^5$.

This family of tilings may be obtained from the family of dihedral f-tilings ${}^L\mathcal{R}^k, k \geq 4$, with an isosceles triangle and a non-equiangular lozenge as prototiles, described in [8] and in [14].

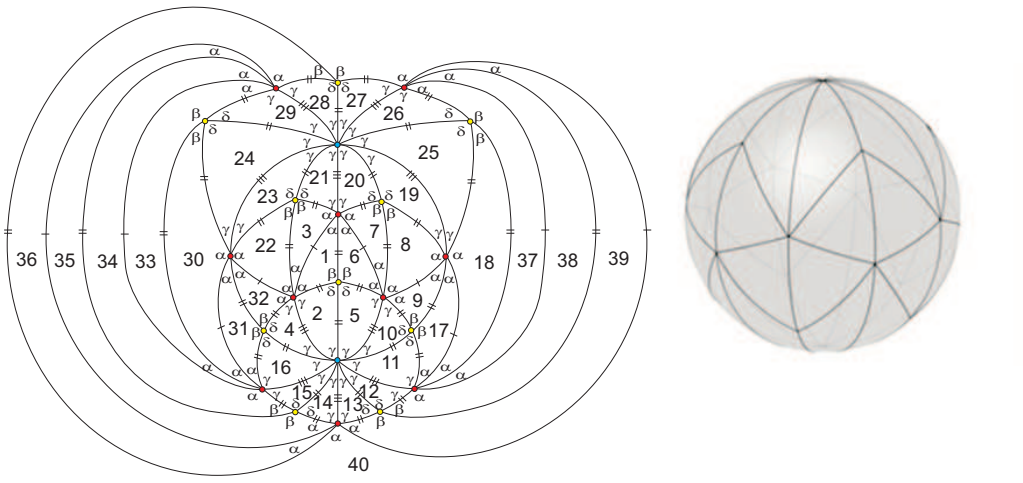

Figure 4.103: 2D and 3D representation of $\mathcal{Q}^5$.

In case $m\gamma + n\beta = \pi$, for some $m \geq 3,\ n \geq 1$, we may add some new cells to the configuration in Figure 4.102-II and end up at a vertex partially surrounded by angles δ, α, α, as illustrated in Figure 4.104-I. Taking into account that $\gamma < \beta < \alpha < \frac{\pi}{2} < \delta,\ \alpha > \frac{\pi}{3},\ 2\alpha + \beta > \pi$ and $2\gamma + \delta > \pi$, the sum containing the alternate angles δ and α violates the angle folding relation, preventing us to continue the extension of the configuration.

If $p\gamma + \alpha = \pi$, for some $p \geq 3$, the configuration extends a bit more and the sum containing the alternate angles δ and μ (see Figure 4.104-II) must be of the form $\delta + \beta = \pi$ or $\delta + \gamma = \pi$, since all the other possibilities violate the angle folding relation or are incompatible with the edge length. However, if $\delta + \beta = \pi$, then $\beta = \frac{\pi}{2}$, a contradiction and if $\delta + \gamma = \pi$, an incompatibility in the edge length arises.

The last case, $t\gamma + q\beta + \alpha = \pi$, for some $t \geq 3$ and $q \geq 1$ is also impossible using a similar reasoning as in the two previous cases.

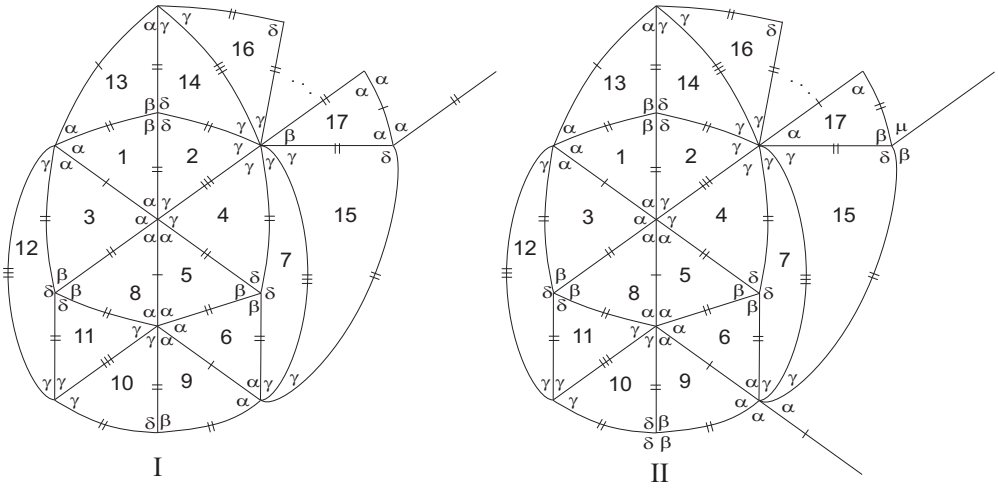

Figure 4.104: Local configurations.

5. Assume that $\theta_3 = \beta$. Then, $\alpha + \gamma + \beta \leq \pi$. The vertex partially surrounded by angles α, α, δ (see Figure 4.105-I for the case $\alpha + \gamma + \beta = \pi$ and Figure 4.105-II for the case $\alpha + \gamma + \beta < \pi$) is of valency four, since $\alpha + \delta + \mu > \pi$, for all $\mu \in \{\alpha, \beta, \gamma, \delta\}$. Therefore, $\alpha + \delta = \pi$, $\frac{\pi}{3} < \alpha < 2\gamma$ and so $\gamma > \frac{\pi}{6}$.

Now, if $\alpha + \gamma + \theta_3 = \pi$, with $\theta_3 = \beta$, then we end up at a vertex (see Figure 4.105-I) partially surrounded by angles $\alpha, \alpha, \alpha, \alpha, \gamma, \gamma$ that must be of valency six, leading to

the contradiction $\beta = \alpha$.

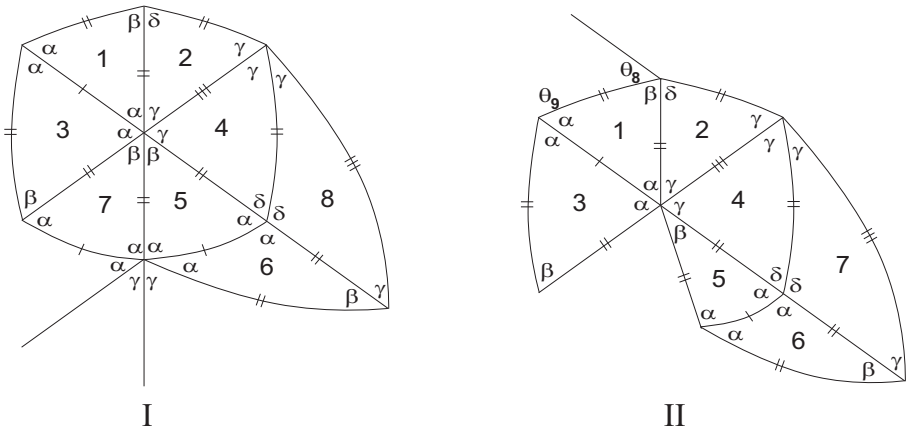

Figure 4.105: Local configurations.

Supposing that $\alpha + \gamma + \theta_3 < \pi$, for $\theta_3 = \beta$, the angle θ_8 in Figure 4.105-II is either β or γ (note that $\theta_8 = \alpha$ forces vertex to be of valency four, which is impossible, since $\beta < \alpha < \frac{\pi}{2}$).

Assuming that $\theta_8 = \beta$, then $\theta_9 = \alpha$ and the sum containing the two alternate angles α must obey to the condition $2\alpha + \gamma = \pi$. Consequently,

$$\frac{\pi}{6} < \gamma < \beta < \alpha < \frac{\pi}{2} < \delta.$$

Thus, the sum containing the alternate angles α, γ and $\theta_3 = \beta$ is either of the form $\alpha + 2\gamma + \beta = \pi$ or $\alpha + \gamma + 2\beta = \pi$.

If $\alpha + 2\gamma + \beta = \pi$, one has $\alpha + \beta < \delta$, from $2\gamma + \delta > \pi$. But $\alpha + \delta = \pi$ and so $2\alpha + \beta < \pi$, which is impossible. Therefore, we must have $\alpha + \gamma + 2\beta = \pi$. The relations known until now are $\alpha + \delta = \pi,\ 2\alpha + \gamma = \pi$ and $\alpha + \gamma + 2\beta = \pi$. By the adjacency condition (4.6), $\beta = 36° = \gamma$ (violating $\gamma < \beta$) or $\beta = 108°$ (violating $\beta < \frac{\pi}{2}$) or $\beta = 60°$ (which implies $\alpha = 120°$, contradicting $\alpha < \frac{\pi}{2}$).

If $\theta_8 = \gamma$, the sum containing the alternate angles γ and δ obeys to the condition $\gamma + \delta + k\beta = \pi,\ k \geq 1$ and so $\beta < \gamma$. In the extended the configuration, we get a vertex surrounded by four angles α (Figure 4.106), but taking into account that $2\alpha + \beta > \pi,\ \beta < \gamma < \alpha < \frac{\pi}{2} < \delta$ and $\alpha > \frac{\pi}{3}$ and so this vertex can not satisfy the angle folding relation and the configuration can not be pursued.

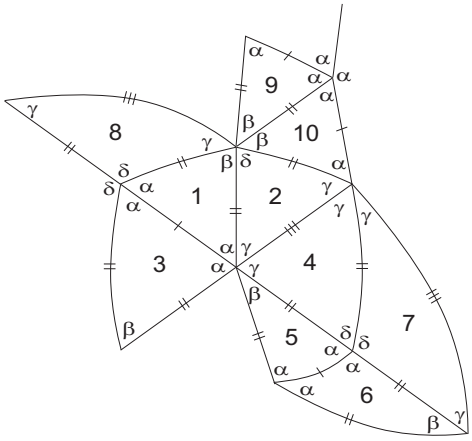

Figure 4.106: Local configuration.

6. Suppose that $\theta_3 = \gamma$. Then $\alpha + 2\gamma \leq \pi$ and so $\gamma < \frac{\pi}{3}$.

6.1 In case, $\alpha + 2\gamma = \pi$, we conclude that $\gamma > \frac{\pi}{4}$.

The configuration started in Figure 4.101-II expands a bit more and a decision about angle $\theta_{10} \in \{\alpha, \beta, \gamma\}$ must be taken, as illustrated in Figure 4.107-I.

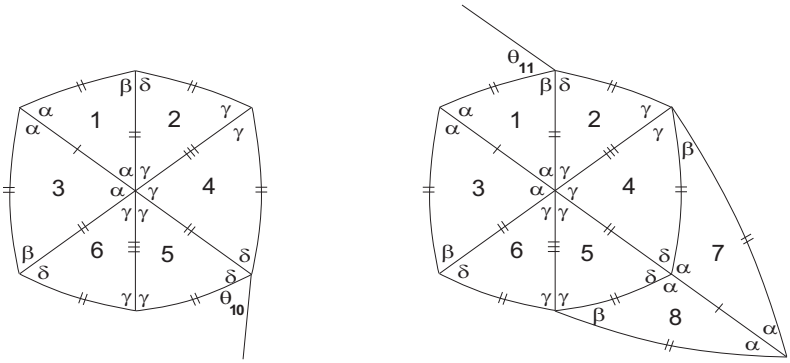

Figure 4.107: Local configurations.

If $\theta_{10} = \alpha$, then the vertex must be of valency four and so $\delta = 2\gamma$. A decision about angle $\theta_{11} \in \{\beta, \gamma\}$ in Figure 4.107-II must be made (if $\theta_{11} = \alpha$, then vertex must be of valency four, which is impossible, since $\beta < \alpha < \frac{\pi}{2}$).

In case $\theta_{11} = \beta$, a vertex partially surrounded by three angles α arises (Figure 4.108-I). This vertex must be of valency six satisfying $2\alpha + \gamma = \pi$. Consequently, from the assumption $\alpha + 2\gamma = \pi$, we get $\alpha = \gamma$, which is an impossibility.

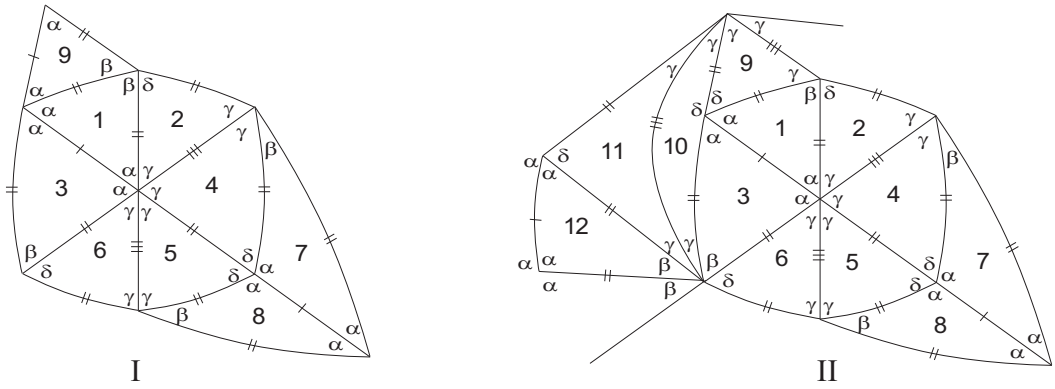

Figure 4.108: Local configurations.

If $\theta_{11} = \gamma$, we may add some new cells to the configuration and end up at a vertex partially surrounded by three angles α (Figure 4.108-II). Again, the sum containing two alternate angles α obeys to the condition $2\alpha+\gamma = \pi$ reaching to the same contradiction.

If $\theta_{10} = \beta$ and $\delta + \beta = \pi$, we may add some new cells to the configuration in Figure 4.107-I. In order to avoid the arising of a vertex partially surrounded by three angles α, leading us to the same contradiction as before, tile 9 must be congruent to T_2, as shown in Figure 4.109. However, the vertex surrounded by angles α, α, δ violates the angle folding relation and the configuration can not be expanded.

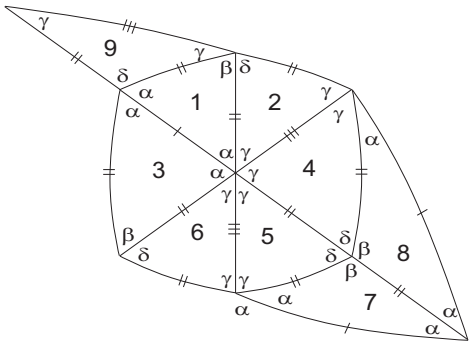

Figure 4.109: Local configuration.

If $\theta_{10} = \beta$ and $\delta + \beta < \pi$, in order to satisfy the angle folding relation, the sum must be either of the form $\delta + m\beta = \pi,\ m \geq 2$ or $\delta + \gamma + t\beta = \pi,\ t \geq 1$.

In the first case, a vertex (Figure 4.110-I) surrounded by four angles α arises but the sum $2\alpha + \mu > \pi$, for $\mu \in \{\alpha, \beta, \delta\}$. The case $2\alpha + \gamma = \pi$ implies $\alpha = \gamma$ (contradiction).

In the second case, to avoid the same impossibilities, tile numbered 9 (Figure 4.110-II) must be congruent to T_2. Extending the configuration, we are led to a vertex surrounded by four angles α ending up to the same impossibilities.

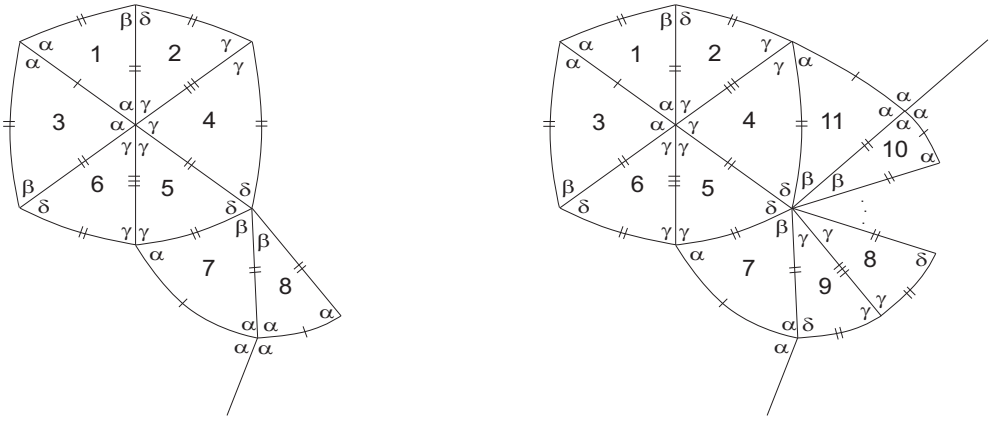

Figure 4.110: Local configurations.

If $\theta_{10} = \gamma$, then the sum containing the alternate angles γ and δ satisfies either $\gamma+\delta = \pi$ or $\gamma + \delta + k\beta = \pi$, for some $k \geq 1$.

In the first case, vertex v_8 (Figure 4.111-I) is of valency four, leading to the impossibility $\beta = \delta$.

In the second case, vertex v_9 (Figure 4.111-II) is of valency four, otherwise the angle folding relation is not fulfilled ($\alpha + \delta + \mu > \pi$, for all $\mu \in \{\alpha, \beta, \gamma, \delta\}$).

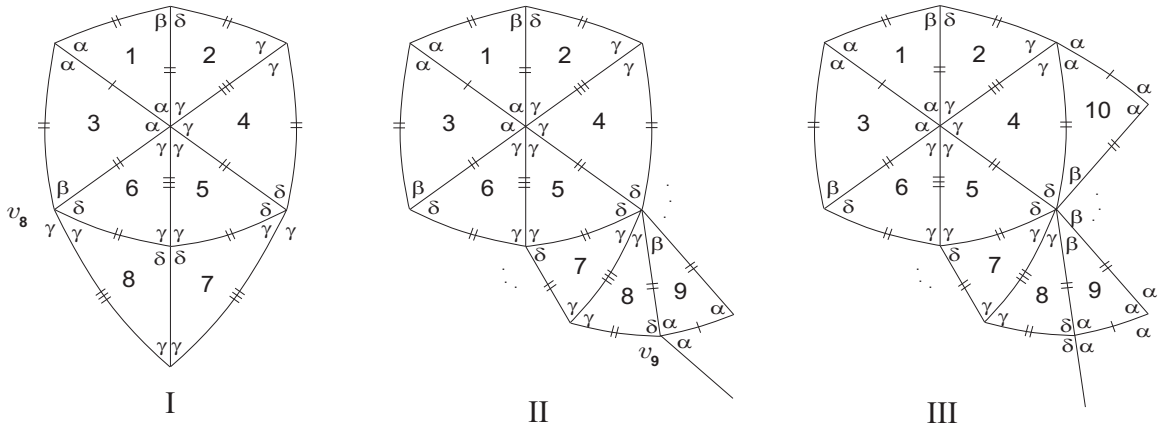

Figure 4.111: Local configurations.

Accordingly, $\alpha+\delta=\pi,\ \alpha+2\gamma=\pi,\ \delta+\gamma+k\beta=\pi,\ k\geq 1$ and consequently

$$\beta<\frac{\pi}{4}<\gamma<\frac{\pi}{3}<\alpha<\frac{\pi}{2}<\delta.$$

Adding some cells to the configuration illustrated in Figure 4.111-II, we end up at a vertex partially surrounded by three angles α (see Figure 4.111). Taking into account the order relation established before and the fact that $2\alpha+\beta>\pi$, this vertex violates the angle folding relation.

6.2 Assuming that $\alpha+2\gamma<\pi$, angle θ_{12} is α,β or γ, see Figure 4.112.

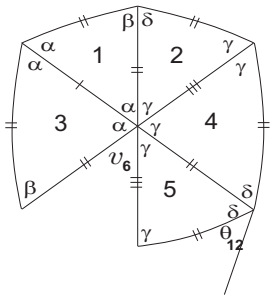

Figure 4.112: Local configuration.

6.2.1 If $\theta_{12}=\alpha$, then $\alpha+\delta=\pi$, since $\delta>\alpha>\gamma,\ 2\gamma+\delta>\pi$ and $2\alpha+\beta>\pi$. Consequently, $\gamma>\frac{\pi}{6}$ and so vertex v_6 is either of valency:

- $2(3+k),\ k\geq 1$ with both sums of alternate angles of the form $\alpha+2\gamma+k\beta=\pi$ or
- eight with both sums of alternate angles of the form $\alpha+3\gamma=\pi$ or
- $2(4+t),\ t\geq 1$ with both sums of alternate angles of the form $\alpha+3\gamma+t\beta=\pi$.

As $2\gamma+\delta>\pi$ and $\alpha+\delta=\pi$, then for the first and third cases, one has $2\alpha+\beta<\pi$, which is an impossibility.

In the second case, since $2\gamma+\delta>\pi,\ \alpha+\delta=\pi$ and $2\alpha+\beta>\pi$, we conclude that $\frac{\pi}{6}<\gamma<\beta$. Accordingly,

$$\frac{\pi}{6}<\gamma<\beta<\alpha<\frac{\pi}{2}<\delta.$$

Adding some new cells to the configuration in Figure 4.112, a decision about the angle $\theta_{13}\in\{\beta,\gamma\}$ (see next figure) must be taken (note that $\theta_{13}\neq\alpha$, otherwise we would have

a vertex of valency four surrounded by angles $\alpha, \alpha, \beta, \delta$ reaching to the contradiction $\beta = \delta > \frac{\pi}{2}$).

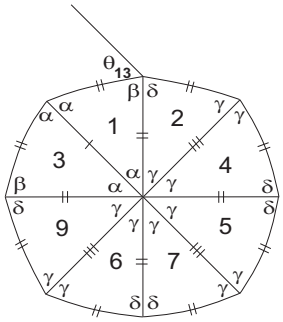

Figure 4.113: Local configuration.

If $\theta_{13} = \beta$, a vertex (Figure 4.114-I) partially surrounded by angles δ, β, δ arises, but the sum 2δ violates the angle folding relation.

If $\theta_{13} = \gamma$, the vertex partially surrounded by angles γ, β, δ is of valency greater than four. However, the sum $\gamma + \delta + \mu$ violates the angle folding relation, for all $\mu \in \{\alpha, \beta, \gamma, \delta\}$ (Figure 4.114-II).

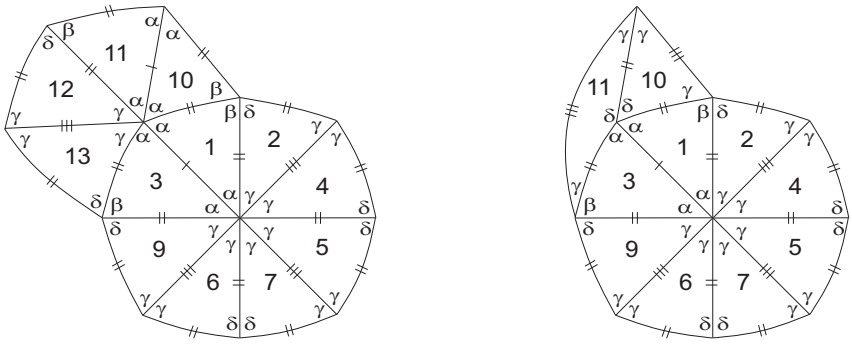

Figure 4.114: Local configurations.

6.2.2 If $\theta_{12} = \beta$ and $\beta + \delta = \pi$, the vertex partially surrounded by four angles α in the extended configuration (Figure 4.115-I) is of valency $2(2 + t)$ and its both sums of alternate angles satisfy $2\alpha + t\gamma = \pi,\ t \geq 1$.

Since $\beta + \delta = \pi$, we conclude $\beta < 2\gamma$. As $2\alpha + \beta > \pi$, then $t = 1$ and so $2\alpha + \gamma = \pi$. On the other hand, the sum containing the alternate angles α, γ, γ must be of the form

$\alpha + t\gamma = \pi,\ t \geq 3$ or $\alpha + m\gamma + n\beta = \pi,\ m \geq 2,\ n \geq 1$.

In the first case, the addition of some cells to the configuration shown in Figure 4.115-I, lead to a vertex, v_{10} surrounded by angles δ, β, δ, violating the angle folding relation, since $\delta > \frac{\pi}{2}$, see Figure 4.115-II.

In the second case, taking into account that $\beta + \delta = \pi$ and $\beta < \alpha$, vertex v_{10} violates the angle folding relation (Figure 4.115-III).

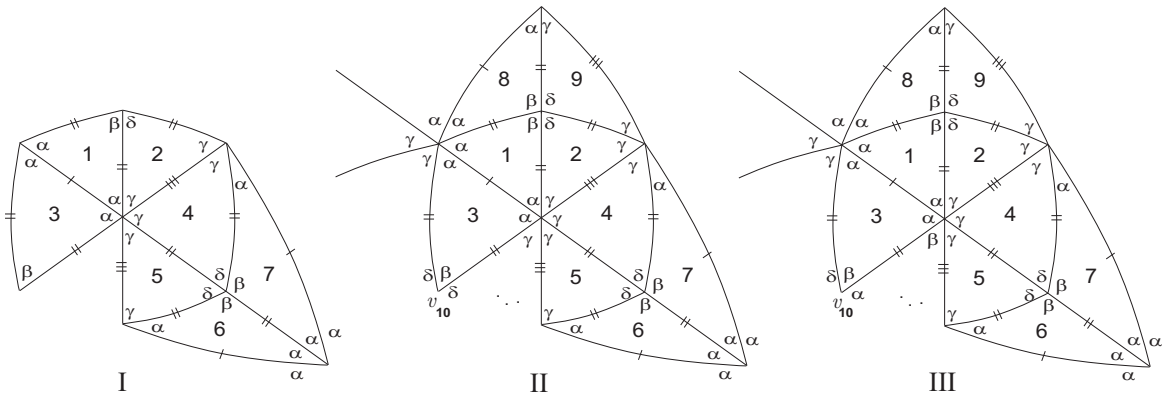

Figure 4.115: Local configurations.

6.2.3 If $\theta_{12} = \beta$ and $\delta + \beta < \pi$, the sum containing these two angles must be of the form $\delta + p\beta = \pi,\ p \geq 2$ or $\delta + \gamma + q\beta = \pi,\ q \geq 1$.

If $\delta + p\beta = \pi,\ p \geq 2$ extending the configuration in Figure 4.112, we end up at a vertex, v_{11}, as shown in Figure 4.116-I, which violates the angles folding relation.

Note that, once again, vertices partially surrounded by two alternate angles α must be of valency six and both sums of its alternate angles satisfy $2\alpha + \gamma = \pi$, since $\beta < 2\gamma$ and $2\alpha + \beta > \pi$.

Assume now that $\delta + \gamma + q\beta = \pi$, for some $q \geq 1$. Then, vertices of valency four are surrounded by alternate angles δ and α. Consequently, $\delta + \alpha = \pi$ and so $\frac{\pi}{3} < \alpha < 2\gamma$. Accordingly, the sum containing the alternate angles α, γ, γ is either

- $\alpha + 3\gamma = \pi$ or
- $\alpha + 2\gamma + k\beta = \pi,\ k \geq 1$ or
- $\alpha + 3\gamma + t\beta = \pi,\ t \geq 1$.

As $2\gamma+\delta > \pi$ and $2\alpha+\beta > \pi$, the second and third cases are impossible, remaining the case $\alpha + 3\gamma = \pi$.

The angle conditions in study are $\delta + \gamma + q\beta = \pi,\ q \geq 1,\ \delta + \alpha = \pi$ and $\alpha + 3\gamma = \pi$ and the configuration is now the one shown in Figure 4.116-II, with $\theta_{14} \in \{\beta, \gamma\}$.

If $\theta_{14} = \beta$, then $\widetilde{\theta}_{14} = \alpha$ and the sum containing two alternate angles α is of the form $2\alpha + \gamma = \pi$, reaching to the impossibility $\alpha = 2\gamma$ (observe that from $\delta + \alpha = \pi$ and $2\gamma + \delta > \pi$, then $\alpha < 2\gamma$).

If $\theta_{14} = \gamma$ then, to avoid the previous contradiction, the angle $\widetilde{\theta}_{14}$ must be δ. However, extending the configuration in Figure 4.116-II, we reach to a vertex partially surrounded by four angles α (Figure 4.116-III), which satisfies $2\alpha + \gamma = \pi$, ending up at the same contradiction.

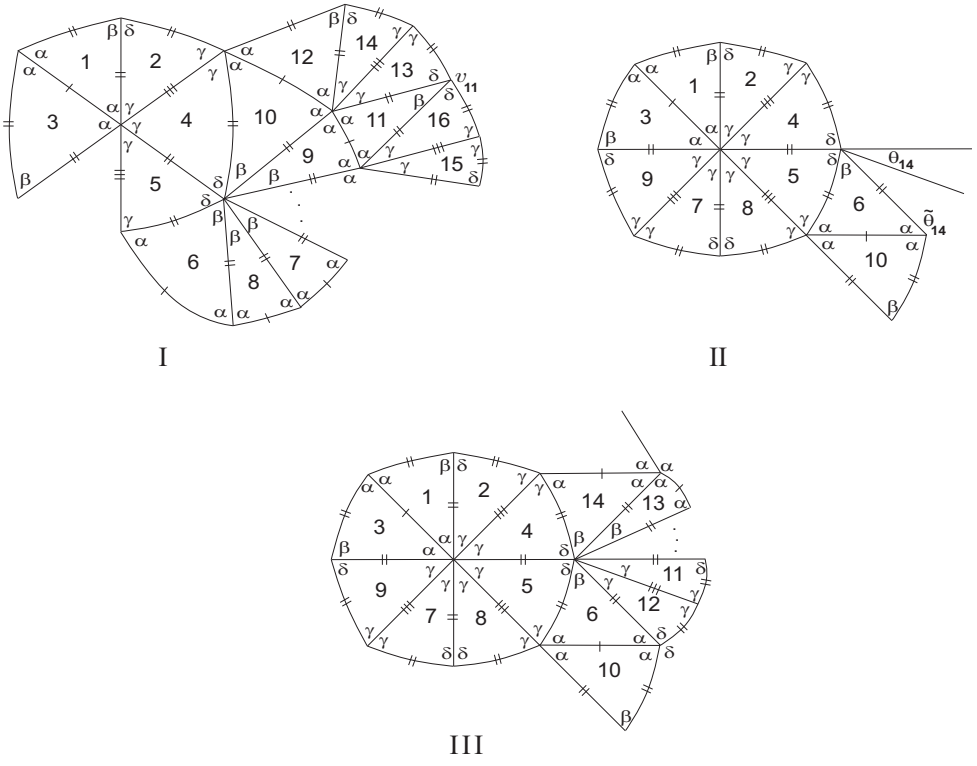

Figure 4.116: Local configurations.

6.2.4 Suppose that $\theta_{12} = \gamma$, in Figure 4.112 and $\gamma + \delta = \pi$. Figure 4.117-I illustrates the configuration after adding some new cells.

Notice that vertex partially surrounded by angles $\beta, \delta, \gamma, \gamma$ violates the angle folding relation, since $\delta + \gamma = \pi$ and $\beta + \gamma < \pi$.

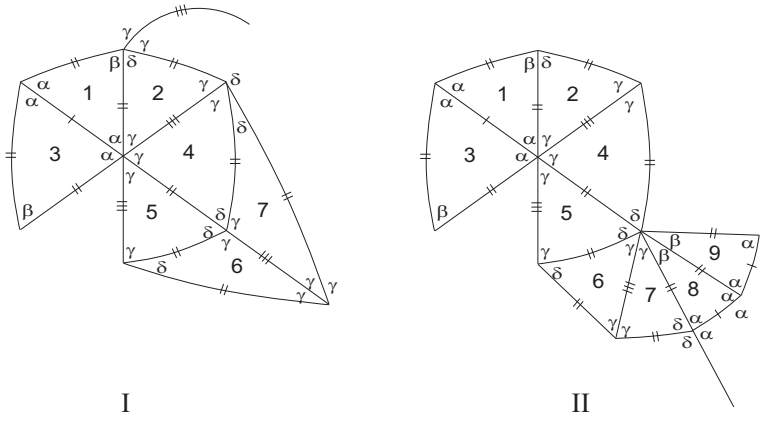

Figure 4.117: Local configurations.

Let us assume now that $\theta_{12} = \gamma$ and $\gamma + \delta < \pi$. The sum containing these two angles must obey to the condition $\delta + \gamma + k\beta = \pi$, for some $k \geq 1$. Therefore, $\beta < \gamma$. Extending the configuration illustrated in Figure 4.112, a vertex partially surrounded by three angles α arises (see Figure 4.117-II). The sum of alternate angles of this vertex violates the angle folding relation, since $2\alpha + \mu > \pi$, for all $\mu \in \{\alpha, \beta, \gamma, \delta\}$ and the configuration can not be pursued.

□

4.5.2 Adjacency of type III b)

Suppose that T_1 and T_2 satisfy adjacency of type **III b)**.

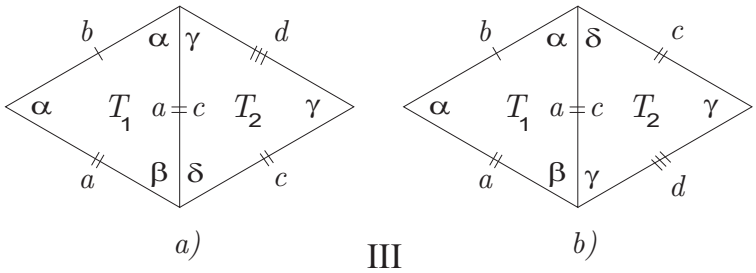

Figure 4.118: Adjacency of type III.

Proposition 4.11 *If* $\gamma = \alpha = \frac{\pi}{2}$, *then* $\Omega(T_1, T_2)$ *is composed by the following* f*-tilings:*

for $\alpha > \beta$ ***and*** $\gamma > \delta$***:***

$$\alpha = \gamma = \frac{\pi}{2},\ \frac{\pi}{2} + k\delta = \pi,\ \textit{and}\ \frac{\pi}{2} + t\beta = \pi,\ k, t \geq 2,\ k \neq t\ \textit{for}\ \mathcal{R}_t^k;$$

$$\alpha = \gamma = \frac{\pi}{2},\ \frac{\pi}{2} + p\beta + q\delta = \pi,\ p, q \geq 1\ \textit{for}\ \mathcal{N}_i^{p,q,\delta},\ i = 1, \ldots, I;$$

$$\alpha = \gamma = \frac{\pi}{2},\ \frac{\pi}{2} + p\beta + q\delta = \pi,\ \frac{\pi}{2} + t\beta = \pi,\ p, q \geq 1,\ 1 \leq p < t$$

$$\textit{for}\ \mathcal{O}_i^{p,q,t},\ i = 1, \ldots, I,$$

where I denotes the number of different positions to place the angles β and δ around vertices, in such a way that the local configuration gives rise to a complete f-tiling.

Proof. If $\tau \in \Omega(T_1, T_2)$ satisfies adjacency of type III b) (see Figure 4.118), then we may start its configuration with two adjacent cells congruent respectively to T_1 and T_2, as shown in Figure 4.119.

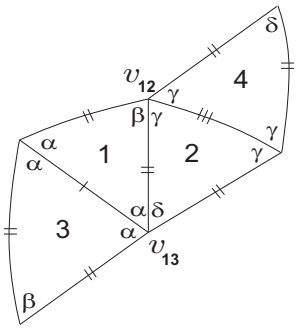

Figure 4.119: Local configuration.

If $\beta > \alpha = \gamma = \frac{\pi}{2}$, then the sum containing the alternate angles β and γ violates the angle folding relation, preventing us to extend the configuration shown before. Therefore, $\beta < \frac{\pi}{2}$. On the other hand, if $\delta > \gamma = \alpha = \frac{\pi}{2}$, the sum containing the alternate angles α and δ does not satisfy the angle folding relation and once again, we can not continue the extension of the configuration before. Accordingly, $\delta, \beta < \frac{\pi}{2}$.

Vertices v_{12} and v_{13} are of valency greater than four.

In order to satisfy the angle folding relation, the sum of alternate angles containing $\frac{\pi}{2}$ and δ is either of the form $\frac{\pi}{2} + k\delta = \pi,\ k \geq 2$ or $\frac{\pi}{2} + m\beta + n\delta = \pi,\ m, n \geq 1$. In any case, angle θ_{15} (see Figure 4.120) is $\frac{\pi}{2}$. At vertex v_{12}, the sum of alternate angles containing β and $\frac{\pi}{2}$ is either of the form $\frac{\pi}{2} + t\beta = \pi,\ t \geq 2$ or $\frac{\pi}{2} + p\beta + q\delta = \pi,\ p, q \geq 1$. In any case, angle θ_{16} is $\frac{\pi}{2}$ (Figure 4.120).

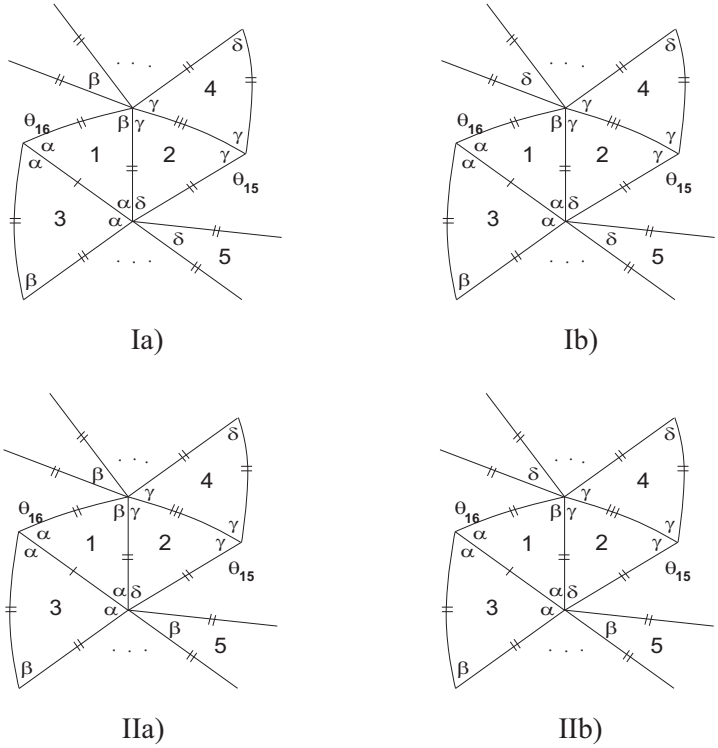

Figure 4.120: Local configurations.

In Figure 4.120-Ia), we have $\frac{\pi}{2} + k\delta = \pi$ and $\frac{\pi}{2} + t\beta = \pi$, where $t \neq k$ and $t, k \geq 2$. For each $t \geq 2$ and $k \geq 2$ with $t \neq k$, we get a complete f-tiling denoted by $\mathcal{R}_k^t$ composed by vertices of valency four surrounded exclusively by $\frac{\pi}{2}$, the ones of valency $2(1+k)$ whose both sums of alternate angles are of the form $\frac{\pi}{2} + k\delta = \pi$ and the ones of valency $2(1+t)$ whose sums of alternate angles satisfy $\frac{\pi}{2} + t\beta = \pi,\ t \geq 2$. It has $4t$ copies of T_1 and $4k$ copies of T_2. In Figure 4.121, we illustrate the case $t = 2$ and $k = 3$.

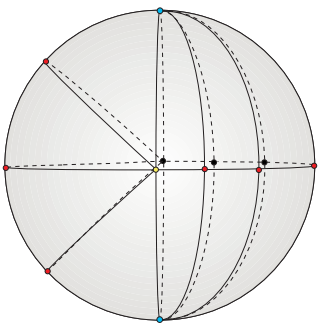

Figure 4.121: 3D representation of $\mathcal{R}_3^2$.

Eliminating some edges in each member of this family, we get a monohedral f-tiling.

In Figure 4.120-Ib), the existence of vertices whose sums of alternate angles are of the form $\frac{\pi}{2}+k\delta=\pi,\ k\geq 2$ and $\frac{\pi}{2}+p\beta+q\delta=\pi,\ p,q\geq 1$ leads to a configuration where two triangles are in a side adjacency of type III a), already studied. Consequently, we get the corresponding families $\mathcal{O}_i^{p,t}$ and $\mathcal{O}_i^{p,q,t}$.

In Figure 4.120-IIa), one has $\frac{\pi}{2}+t\beta=\pi,\ t\geq 2$ and $\frac{\pi}{2}+m\beta+n\delta=\pi,\ m,n\geq 1$. We can reasoning in a similar way as in the previous case, ending up in the same families of f-tilings already referred.

The same reasoning applies to the case shown in Figure 4.120-IIb), where we have $\frac{\pi}{2}+m\beta+n\delta=\pi,\ m,n\geq 1$ ending up with the families denoted by $\mathcal{N}_i^{p,\delta}$ and $\mathcal{N}_i^{p,q,\delta}$ described in adjacency III a).

□

Proposition 4.12 *If $\gamma<\alpha$, then $\Omega(T_1,T_2)$ is composed by the following f-tilings:*
***for** $\beta>\alpha$ **and** $\delta>\gamma$:*

$$\alpha+\delta=\pi,\ \beta+2\gamma=\pi \text{ and } \gamma=\frac{\pi}{k},\ k\geq 4 \text{ for } \mathcal{S}^k;$$
$$\alpha+\delta=\pi,\ \beta+2\gamma=\pi \text{ and } \alpha=\frac{\pi}{k},\ k\geq 3 \text{ for } \mathcal{T}^k;$$
$$\alpha+\delta=\pi,\ \beta+3\gamma=\pi \text{ and } \alpha=\frac{\pi}{k},\ k\geq 3 \text{ for } \mathcal{U}^k;$$
$$\alpha+\delta=\pi,\ \beta+3\gamma=\pi \text{ and } \gamma=\frac{\pi}{k},\ k\geq 5 \text{ for } \mathcal{V}^k;$$
$$\alpha+\delta=\pi,\ 2\beta+\gamma=\pi \text{ and } \alpha=\frac{\pi}{3} \text{ for } \mathcal{L};$$
$$\alpha+\delta=\pi,\ 2\beta+\gamma=\pi,\ \alpha=\frac{\pi}{3} \text{ and } \gamma=\frac{\pi}{5} \text{ for } \mathcal{M};$$
$$\alpha+\delta=\pi,\ \beta+\gamma+\alpha=\pi \text{ and } \gamma=\frac{\pi}{k},\ k\geq 4 \text{ for } \mathcal{X}^k.$$

***for** $\alpha>\beta$ **and** $\delta>\gamma$:*

$$\alpha+\delta=\pi,\ \beta+2\gamma=\pi \text{ and } \gamma=\frac{\pi}{3} \text{ for } \mathcal{N};$$
$$\alpha+\delta=\pi,\ \beta+3\gamma=\pi \text{ and } \gamma=\frac{\pi}{4} \text{ for } \mathcal{O};$$
$$\alpha+\delta=\pi,\ \beta+\gamma+\alpha=\pi \text{ and } \gamma=\frac{\pi}{3} \text{ for } \mathcal{P}.$$

Proof. If $\tau \in \Omega(T_1, T_2)$ satisfies adjacency of type III b) (see Figure 4.118), then we may start its configuration with two adjacent cells congruent respectively to T_1 and T_2, as shown in Figure 4.122.

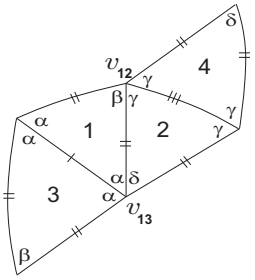

Figure 4.122: Local configuration.

Suppose that $\beta > \alpha$ and $\gamma > \delta$.

In this case, vertex v_{12} is of valency four satisfying $\beta + \gamma = \pi$, since the sum $\beta + \gamma + \mu$, violates the angle folding relation, for any $\mu \in \{\alpha, \beta, \gamma, \delta\}$.

Adding some new cells to the configuration, we are led to a vertex surrounded by four angles α, see Figure 4.123. Taking into account $2\gamma + \delta > \pi,\ 2\alpha + \beta > \pi$, the order relation between the angles and $\alpha > \gamma$, we conclude that the sum of alternate angles containing two α does not satisfy the angle folding relation, preventing us to continue the configuration.

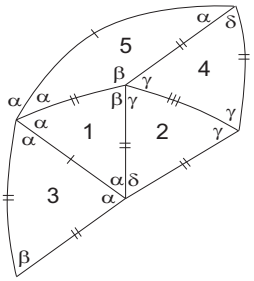

Figure 4.123: Local configuration.

Suppose that $\beta > \alpha$ and $\delta > \gamma$.

As $\beta > \alpha > \gamma,\ 2\gamma + \delta > \pi$ and $\delta > \gamma$, vertex v_{13} should be of valency four surrounded by alternate angles α and δ. Assuming that $\alpha \geq \frac{\pi}{2}$, we get a contradiction immediately, since α and γ belong to the same quadrant. Consequently, $\gamma < \alpha < \frac{\pi}{2} < \delta$.

Remark 4.3 *Vertices in which both sums of its alternate angles satisfy* $p\alpha + q\gamma = \pi$, $p \geq 2$, $q \geq 1$ *lead us to a vertex partially surrounded by the angles* δ *and* β*, which is of valency greater than four (otherwise,* $\delta + \alpha = \beta + \alpha$*, implying the impossibility* $\delta = \beta$*), see Figure 4.124. However, the sum containing the angle* δ *must be of the form* $\delta + \lambda + \mu$*, with* $\lambda \in \{\beta, \gamma\}$*. But for any* $\mu \in \{\alpha, \beta, \gamma, \delta\}$ *the sum violates the angle folding relation.*

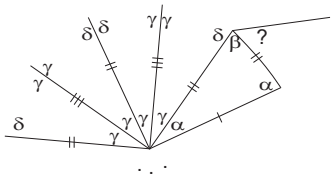

Figure 4.124: Angles arrangement.

Remark 4.4 *Vertices in which both sums of its alternate angles satisfy* $p\gamma + q\alpha = \pi$, $p \geq 2$, $q \geq 1$ *lead us to a vertex partially surrounded by the angles* δ *and* β*, which is of valency greater than four (otherwise,* $\delta + \alpha = \beta + \alpha$*, implying the contradiction* $\delta = \beta$*), see Figure 4.124. However, the sum containing the angle* δ *must be of the form* $\delta + \gamma + \mu$*, which violates the angle folding relation, for any* $\mu \in \{\alpha, \beta, \gamma, \delta\}$*.*

If vertex v_{12} is of valency four, then $\beta + \gamma = \pi$. Extending the configuration started in Figure 4.122, a vertex surrounded exclusively by angles α emerges. Taking into account remark 4.3, this vertex is surrounded only by angles α. By compatibility on the edges, we may extend the configuration and conclude that $\gamma = \alpha$, which is an impossibility. Next figure illustrates the case $k = 3$.

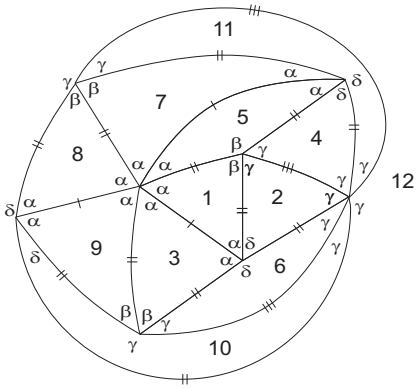

Figure 4.125: Local configuration.

Therefore, vertex v_{12} must be either

- of valency $2(2+t),\ t \geq 2$ whose both sums of alternate angles satisfy $\beta + t\gamma = \pi$ or
- of valency $2(2+m),\ m \geq 1$ whose both sums of alternate angles satisfy $\beta + \alpha + m\gamma = \pi$ or
- of valency $2(2+n),\ n \geq 1$ whose both sums of alternate angles satisfy $2\beta + n\gamma = \pi$.

Let us study each case separately.

1. If $\beta + t\gamma = \pi$, for some $t \geq 2$, then $\beta < \delta$. On the other hand, as $\alpha + \delta = \pi$, then $\alpha < 2\gamma$ and using the fact that $2\alpha + \beta > \pi$, we get $t = 2, 3$.

1.1 In case $t = 2$, the configuration in Figure 4.122 extends to the one in Figure 4.126, with two possible positions for tile 6.

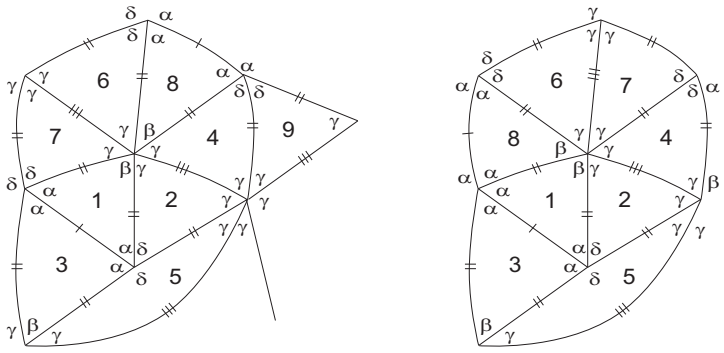

Figure 4.126: Local configurations.

In Figure 4.126-I, a vertex partially surrounded by six consecutive angles γ arises. Hence, either $k\gamma = \pi,\ k \geq 4,\ k \in \mathbb{N}$ (note that $k = 3$ implies the contradiction $\beta = \gamma > \alpha$). For each $k \geq 4$, we may extend the configuration and get a complete f-tiling denoted by $\mathcal{S}^k$ composed by $2k$ copies of T_1 and $4k$ copies of T_2. It has three type of vertices: vertices of valency four (satisfying $\alpha + \delta = \pi$), vertices of valency six (satisfying $\beta + 2\gamma = \pi$) and of valency $2k$ (satisfying $k\gamma = \pi,\ k \geq 4$). Next figure illustrates the case $k = 4$ with $\gamma = \frac{\pi}{4},\ \beta = \frac{\pi}{2},\ \alpha = \frac{\pi}{3}$ and $\delta = \frac{2\pi}{3}$.

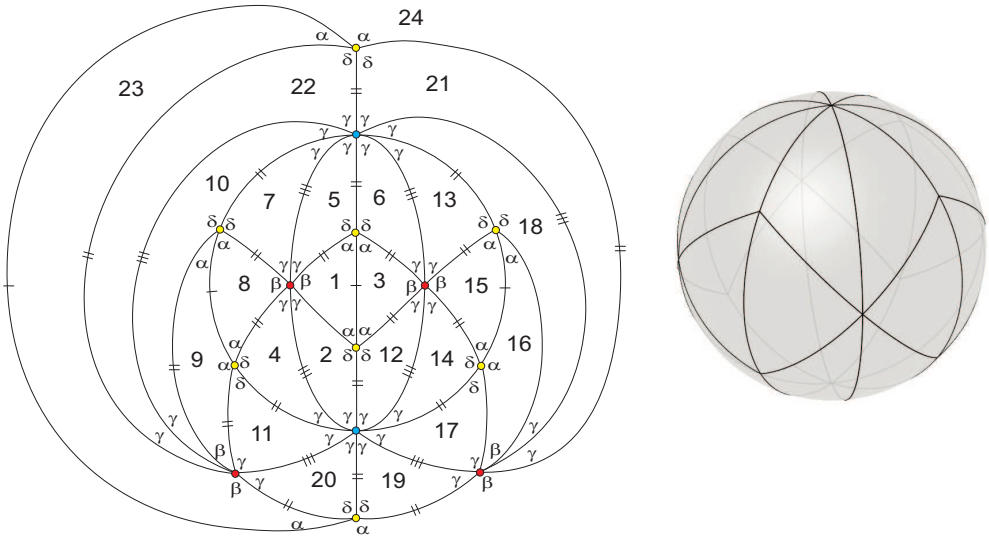

Figure 4.127: 2D and 3D representation of $\mathcal{S}^4$.

This family of f-tilings does not give rise to any monohedral f-tiling or any dihedral f-tiling with prototiles a spherical triangle and a spherical parallelogram, since the elimination of edges leads to the violation of the angle folding relation or to the extinction of vertices of valency four.

Looking at the other position of tile 6 in Figure 4.126-II, a vertex partially surrounded by four angles α arises and taking into account remark 4.3 it must be surrounded exclusively by angles α. Continue spreading the configuration, one has a complete f-tiling denoted by $\mathcal{T}^k$, with three type of vertices: the ones of valency four (satisfying $\alpha + \delta = \pi$), the ones of valency six (satisfying $\beta + 2\gamma = \pi$) and the ones of valency $2k$ (satisfying $k\alpha = \pi$). Next figure shows the case $k = 3$, where it is composed by two classes of congruence equally distributed, with $\alpha = \frac{\pi}{3}$, $\delta = \frac{2\pi}{3}$, $\beta = \frac{\pi}{2}$ and $\gamma = \frac{\pi}{4}$.

Observe that, by the elimination of some edges, we can obtain the f-tiling ${}^L\mathcal{R}^3$ described in [8] and in [14].

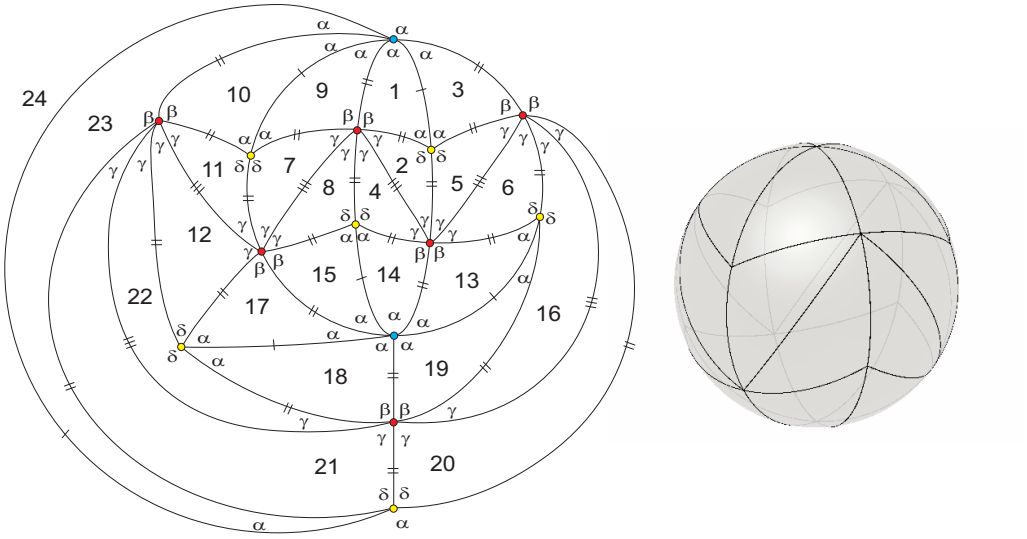

Figure 4.128: 2D and 3D representation of $\mathcal{T}^3$.

1.2 If $t = 3$, tile 6 has two possible positions, as illustrated in Figure 4.129. In Figure 4.129-I, a vertex surrounded exclusively by angles α arises, since the other possibility must be ruled out by remark 4.3.

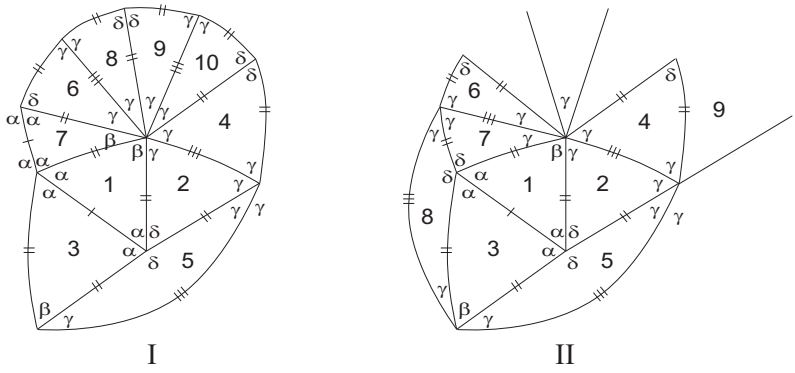

Figure 4.129: Local configurations.

Therefore, $k\alpha = \pi$ and we have a discrete family of f-tilings denotes by $\left(\mathcal{U}^k\right)_{k\geq 3, k\in\mathbb{N}}$. Each member has $8k$ triangles congruent to T_1 and $12k$ triangles congruent to T_2 and the sums of alternate angles around vertices satisfy the following conditions: $k\alpha = \pi$, $\alpha + \delta = \pi$ and $\beta + 3\gamma = \pi$. Next figure presents the member $\mathcal{U}^3$. This tiling has 24 triangles congruent to T_1 and 36 triangles congruent to T_2, with $\alpha = \frac{\pi}{3}$, $\delta = \frac{2\pi}{3}$, $\gamma = \frac{\pi}{5}$ and $\beta = \frac{2\pi}{5}$.

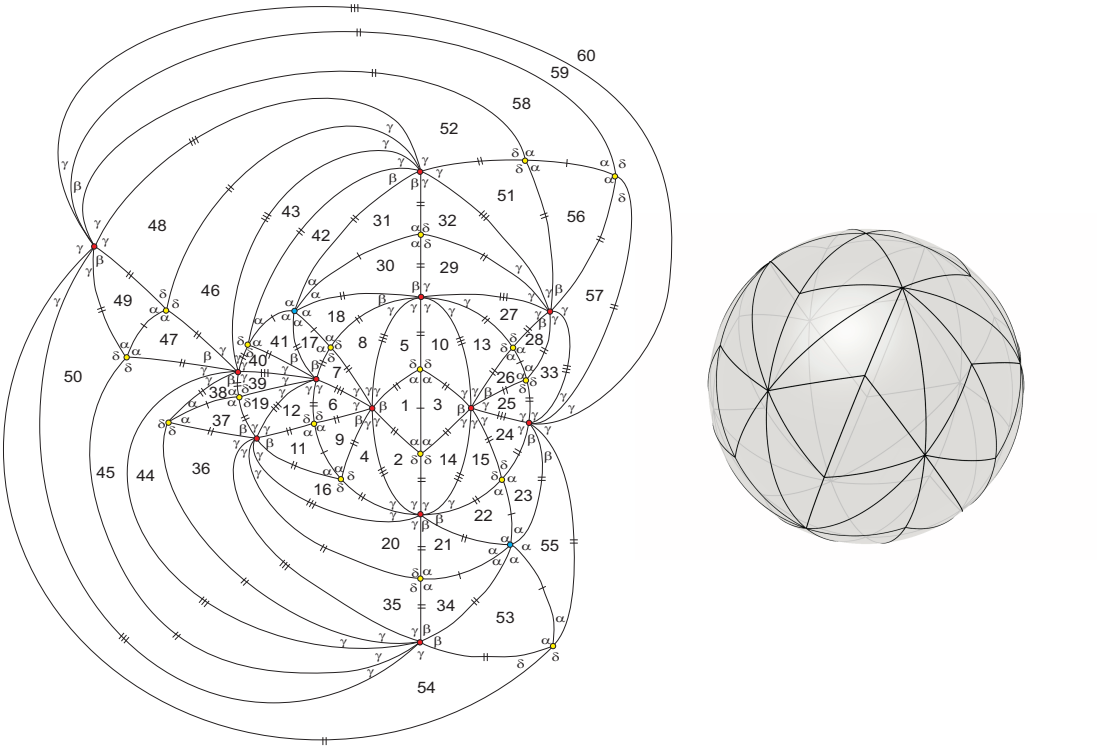

Figure 4.130: 2D and 3D representation of $\mathcal{U}^3$.

Each member of this family does not give rise to any monohedral f-tiling or to any dihedral f-tiling with prototiles a spherical triangle and a spherical parallelogram. Instead, the elimination of edges leads to a 3-hedral f-tiling.

The other possible position for tile 6 (see Figure 4.129-II), allows us to add some new cells to the configuration and the vertex partially surrounded by four consecutive angles γ is either of valency $2k,\ k \geq 5$ surrounded exclusively by angles γ (observe that $k = 4$ implies $\beta = \gamma < \alpha$, which is an impossibility) or of valency eight whose both sums of alternate angles are of the form $\beta + 3\gamma = \pi$.

In case $k\gamma = \pi$, with $k = 5$ and if tile 11 is in a particular position, we may extend the configuration and get a complete f-tiling denoted by $\mathcal{V}^5$ with 60 triangles, see Figure 4.131. It is composed by 20 triangles congruent to T_1 and 40 triangles congruent to T_2, with $\gamma = \frac{\pi}{5},\ \beta = \frac{2\pi}{5},\ \alpha = \frac{\pi}{3}$ and $\delta = \frac{2\pi}{3}$.

If tile 11 is in other position, we get the same f-tiling $\mathcal{V}^5$.

Generalizing, we have one discrete family of f-tilings denoted by $\left(\mathcal{V}^k\right)_{k\geq 5, k\in\mathbb{N}}$, where each member is composed by $4k$ copies of T_1 and $8k$ copies of T_2. The sums of its

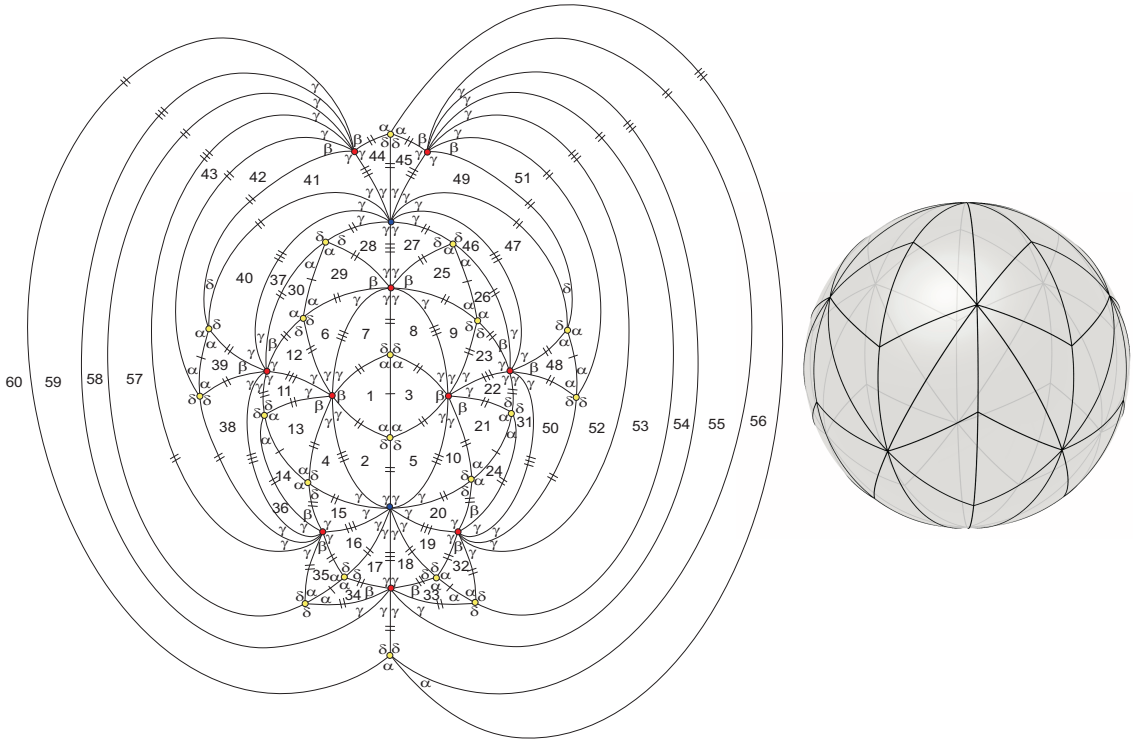

Figure 4.131: 2D and 3D representation of $\mathcal{V}^5$.

alternate angles satisfy: $\alpha+\delta=\pi$, for vertices of valency four, $\beta+3\gamma=\pi$, for vertices of valency eight and $k\gamma=\pi,\ k\geq 5$ for vertices of valency $2k$.

Observe that the elimination of edges does not originate neither a monohedral nor a dihedral f-tiling whose prototiles are a spherical triangle and a parallelogram. Instead, the selective elimination of edges gives rise to a 3-hedral f-tiling.

Assume now that the vertex partially surrounded by four angles γ is of valency eight whose both sums of alternate angles satisfy $\beta+3\gamma=\pi$. If tile 9 is congruent to T_1, we may extend the configuration in Figure 4.129-II, ending up at a vertex surrounded by two angles α. In order to avoid the contradiction described in the previous possibility, this type of vertices are either of valency four surrounded by angles $\alpha,\alpha,\delta,\delta$ or of valency $2m,\ m\geq 3$ surrounded exclusively by α.
In the first case, we may expand the configuration and the vertex surrounded by several angles γ must be surrounded exclusively by γ. Continue expanding the configuration, we are led to the discrete family of f-tilings already mentioned and denoted by $\mathcal{V}^k$, with $k\geq 5$.

In the second case, we are led to the discrete family of f-tilings denoted by $\mathcal{U}^m$, for $m \geq 3$.

If tile 9 is congruent to T_2, the same situation arises, in other words a vertex partially surrounded by two angles α emerges, which must be of valency four surrounded by $\alpha, \alpha, \delta, \delta$ or of valency $2m$ surrounded exclusively by α.
As before, in the first case, we may expand the configuration ending up at the discrete family of f-tilings denoted by $\mathcal{V}^k$.
In the second case, we are led to the discrete family of f-tilings denoted by $\mathcal{U}^m$, with $m \geq 3$.

2. Assuming that $\beta + \alpha + m\gamma = \pi,\ m \geq 1$, then $\beta < \delta$. On the other hand, since $2\gamma > \alpha$, then, $m = 1$ and so $\beta + \alpha + \gamma = \pi$. Adding some cells to the configuration in Figure 4.122, tile 6 has two possible positions, see Figure 4.132 but only one of them (Figure 4.132-II) may be extended, using a similar reasoning as before.

In Figure 4.132-II and taking into account remark 4.4, vertex partially surrounded by four consecutive angles γ is either of valency $2k,\ k \geq 4$ (surrounded exclusively by $2k$ angles γ) or of valency eight (surrounded by six angles γ and two angles β).
From the conditions $\alpha + \delta = \pi$ and $2\gamma + \delta > \pi$, the first possibility is ruled out.

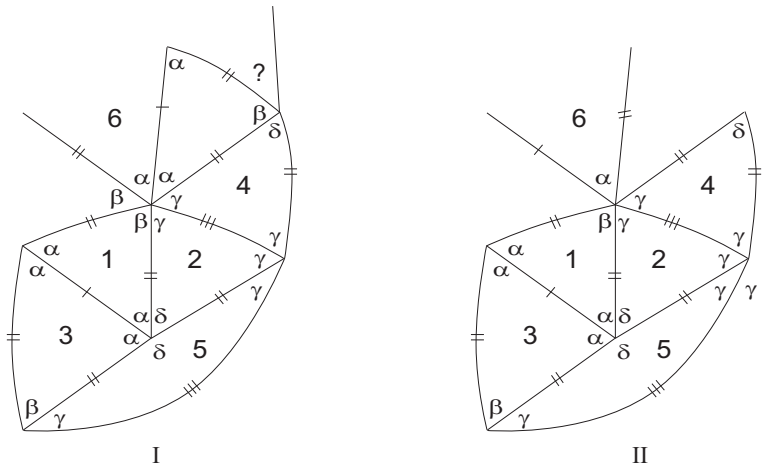

Figure 4.132: Local configurations.

If $k\gamma = \pi,\ k \geq 4$, we get a discrete family of f-tilings denoted by $\left(\mathcal{X}^k\right)_{k\geq 4, k\in\mathbb{N}}$, where each element has $4k$ triangles congruent to T_1 and $4k$ triangles congruent to

T_2. Figure 4.171 shows the 3D representation of the member $\mathcal{X}^4$. The angles are $\gamma = 45°,\ \alpha \approx 53.07°,\ \beta \approx 81.93°$ and $\delta \approx 126.93°$.

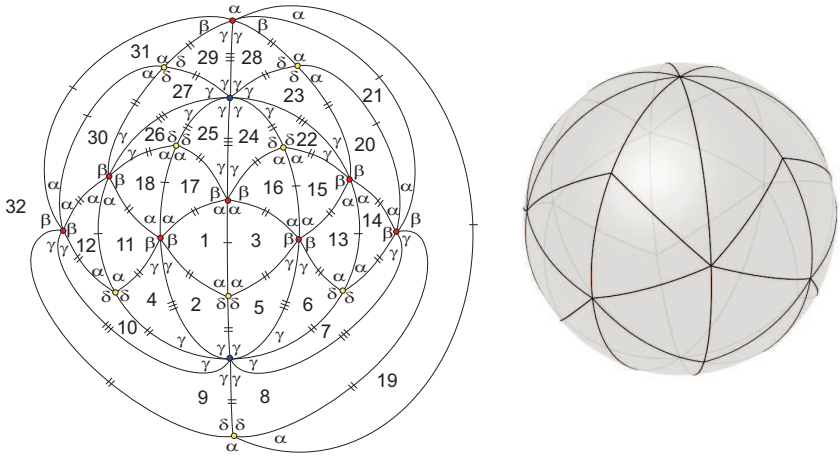

Figure 4.133: 2D and 3D representation of $\mathcal{X}^4$.

Observe that this family of f-tilings can be obtained from ${}^{P}\mathcal{R}^4_{\alpha_2}$ described in [9] and in [14], where the prototiles are a spherical triangle and a parallelogram.

3. If $2\beta + n\gamma = \pi,\ n \geq 1$, then $\beta < \frac{\pi}{2} < \delta$. Moreover, as $2\alpha + \beta > \pi$, then $\alpha > \frac{\pi}{4}$ and since $\alpha < 2\gamma$, we get $\gamma > \frac{\pi}{8}$ implying $n = 1$. Accordingly,

$$\frac{\pi}{8} < \gamma < \alpha < \beta < \frac{\pi}{2} < \delta,\ \alpha > \frac{\pi}{4},\ \alpha + \delta = \pi \text{ and } 2\beta + \gamma = \pi.$$

Adding some new cells to the configuration in Figure 4.122, a vertex partially surrounded by four consecutive angles α arises, see Figure 4.134. By remark 4.3 and remark 4.4, this vertex is of valency six surrounded exclusively by angles.

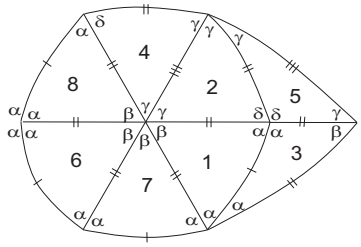

Figure 4.134: Local configuration.

Then, $\delta = \frac{2\pi}{3}$ and by the adjacency condition (4.6), one has $\beta = \frac{2\pi}{5} = 72°$ and $\gamma = \frac{\pi}{5} = 36°$ or $\beta = \frac{4\pi}{5} = 144°$ (which is impossible, since $\beta < 90°$). Observe that all

vertices partially surrounded by several angles α must be of valency six and surrounded exclusively by angles α. Furthermore, vertices surrounded by two or more angles γ are of valency eight whose both sums of alternate angles are of the form $3\gamma + \beta = \pi$ or of valency ten surrounded exclusively by angles γ.

Extending the configuration in Figure 4.122 and assuming that there are no vertices surrounded exclusively by angles γ, we get a global f-tiling $\tau \in \Omega(T_1, T_2)$ denoted by $\mathcal{L}$, see Figure 4.135, which is composed by 36 copies of T_1 and 24 copies of T_2. The angles are $\alpha = \frac{\pi}{3}$, $\delta = \frac{2\pi}{3}$, $\gamma = \frac{\pi}{5}$ and $\beta = \frac{2\pi}{5}$.

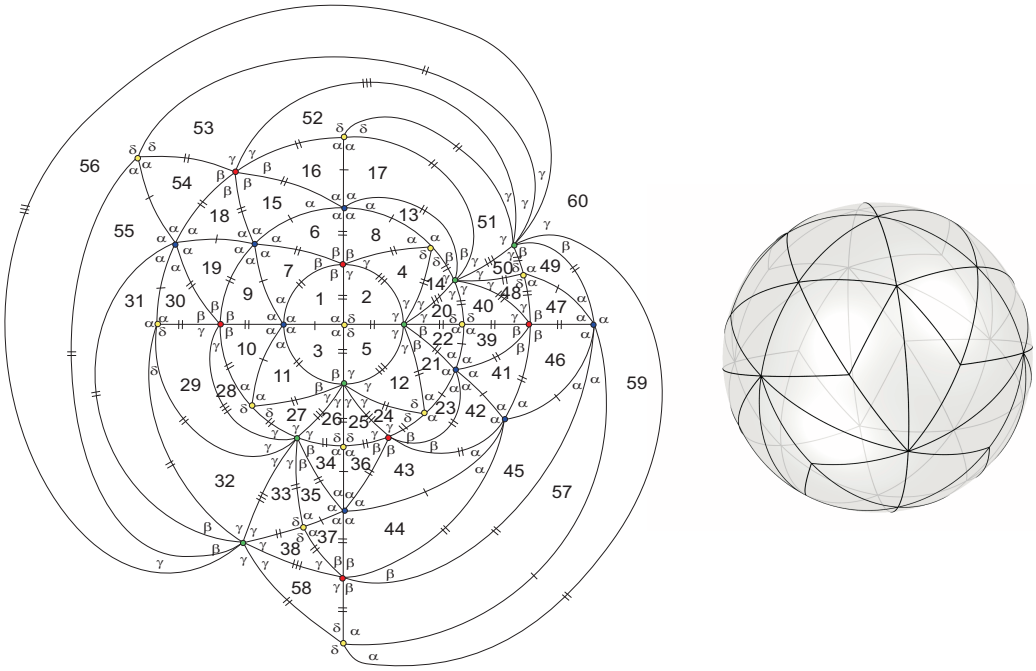

Figure 4.135: 2D and 3D representation of $\mathcal{L}$.

By elimination of some edges, this f-tiling does not give rise to any monoehedral neither dihedral f-tiling whose prototiles are a spherical triangle and a spherical parallelogram.

In case the vertex partially surrounded by tiles 2, 4, 5, 12, 14 in Figure 4.135 is of valency ten (observe that γ must be different from $\frac{\pi}{4}$, otherwise we get the contradiction $\beta = \gamma < \alpha$) surrounded exclusively by angles γ, we get a global f-tiling denoted by $\mathcal{M}$, see Figure 4.136. It is composed by 40 copies of T_1 and 20 copies of T_2 and has four types of vertices: the ones of valency four surrounded by angles $\alpha, \alpha, \delta, \delta$, the ones of valency six surrounded exclusively by angles α or surrounded by four angles β and

two γ and the ones of valency ten surrounded exclusively by angles γ. The values for angles are $\alpha = \frac{\pi}{3},\ \beta = \frac{2\pi}{5},\ \gamma = \frac{\pi}{5}$ and $\delta = \frac{2\pi}{3}$.

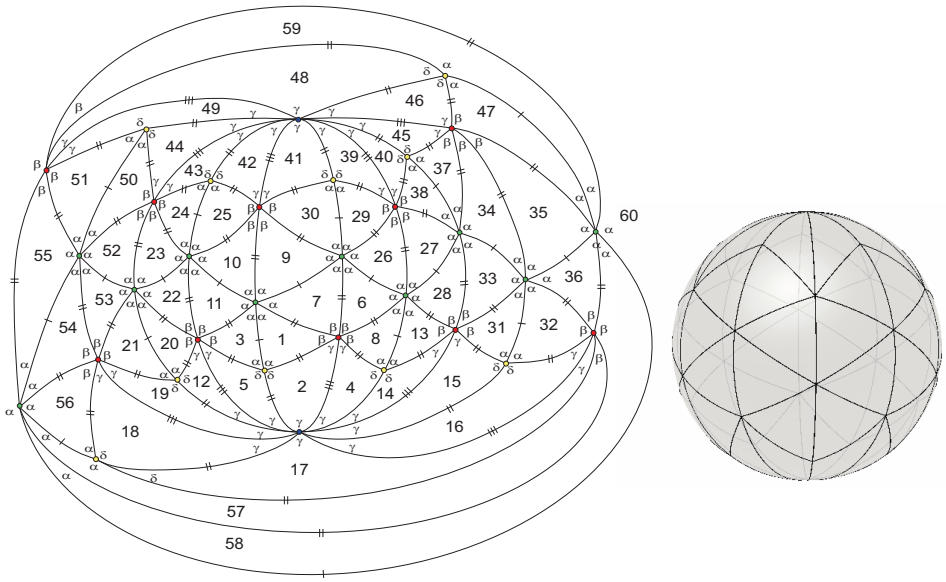

Figure 4.136: 2D and 3D representation of $\mathcal{M}$.

In this case, the selective elimination of edges originates a 3-hedral f-tiling and not any monohedral or dihedral f-tiling with prototiles a spherical triangle and a parallelogram.

Suppose that $\alpha > \beta$ and $\gamma > \delta$.

If $\gamma < \alpha < \frac{\pi}{2}$, then vertices of valency four do not exist, which is an impossibility. Therefore, $\alpha > \gamma > \frac{\pi}{2}$, since $\alpha > \gamma$.

The angle λ shown in Figure 4.137 is either β or δ. Then, $\widetilde{\lambda}$ is, respectively α or γ implying that the sum of alternate angles containing γ and $\widetilde{\lambda}$ is greater than π.

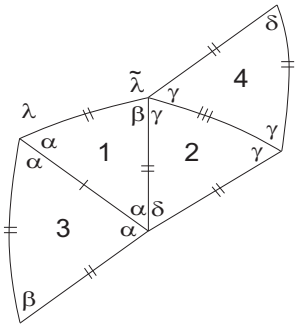

Figure 4.137: Local configuration.

Assume that $\alpha > \beta$ and $\delta > \gamma$.

If $\gamma > \frac{\pi}{2}$, then $\delta > \frac{\pi}{2}$ and the sum $\alpha + \delta$ is greater than π. Therefore, $\gamma < \frac{\pi}{2}$ and since α and γ belong to the same quadrant, one has $\gamma < \alpha < \frac{\pi}{2}$. We have also $\beta < \frac{\pi}{2}$. As vertices of valency four must exist, we conclude that $\delta \geq \frac{\pi}{2}$. Taking into account the order relation between the angles, $2\alpha + \beta > \pi$ and that $2\gamma + \delta > \pi$, then $\alpha + \delta + \mu > \pi$, for any $\mu \in \{\alpha, \beta, \gamma, \delta\}$. Consequently, vertex v_{13} (see Figure 4.122) is of valency four satisfying $\alpha + \delta = \pi$, with $\delta > \frac{\pi}{2}$. On the other hand, since $\alpha > \frac{\pi}{3}$ and $\alpha + \delta = \pi$, then $\gamma > \frac{\pi}{6}$. Accordingly,

$$\frac{\pi}{6} < \gamma < \alpha < \frac{\pi}{2} < \delta \text{ and } \beta < \alpha.$$

In order to satisfy the angle folding relation, one of the sums of the alternate angles around vertex v_{12} is either of the form

- $p\beta + q\gamma = \pi,\ p \geq 1,\ q = 1, 2, 3$ or
- $\alpha + m\beta + \gamma = \pi,\ m \geq 1$ or
- $\delta + r\beta + \gamma = \pi,\ r \geq 1$.

Let us study all cases separately.

- Suppose that $p\beta + q\gamma = \pi$, with $q = 1$. Then, $p \geq 2$. Adding some new cells to the configuration in Figure 4.122, a vertex partially surrounded by four angles α arises. This vertex must be of valency six, whose both sums of alternate angles satisfy $2\alpha + \gamma = \pi$. Therefore,

$$\frac{\pi}{6} < \gamma < \beta < \alpha < \frac{\pi}{2} < \delta$$

and consequently, $p = 3, 4$. Accordingly, either ($\alpha + \delta = \pi,\ \gamma + 3\beta = \pi$ and $2\alpha+\gamma = \pi$) or ($\alpha+\delta = \pi,\ \gamma+4\beta = \pi$ and $2\alpha+\gamma = \pi$). For the first possibility, by the adjacency condition (4.6), one has $\alpha \approx 70,069°,\ \delta \approx 109,931°,\ \beta \approx 46,713°$ and $\gamma \approx 39,862°$. With these values, the sum of alternate angles at vertex partially surrounded by δ, β, γ, see next figure, does not satisfy the angle folding relation, which is impossible.

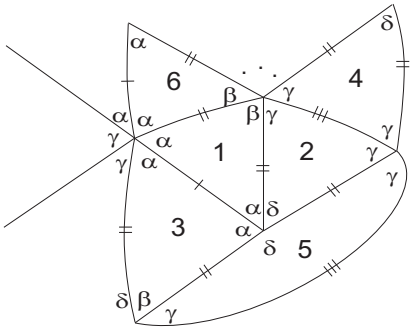

Figure 4.138: Local configuration.

For the second possibility, $\alpha = 72°,\ \delta = 108°$ and $\beta = \gamma = 36°$, which is a contradiction.

If $q = 2$, then $2\gamma + p\beta = \pi$, for $p \geq 1$. Assume first that $p = 1$. Angle γ has two possible positions as shown in Figure 4.139.

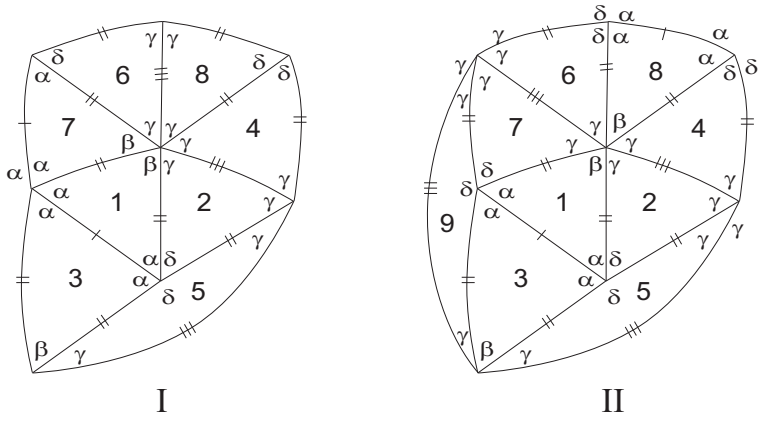

Figure 4.139: Local configurations.

In Figure 4.139-I, we are led to a vertex partially surrounded by two alternate angles α, but the sum $2\alpha + \mu$ violates the angle folding relation, for any $\mu \in$

$\{\alpha, \beta, \gamma, \delta\}$.

In Figure 4.139-II, vertices partially surrounded by five consecutive angles γ are of valency six surrounded exclusively by angles γ (the other possibilities contradict the angle folding relation or the order relation between the angles). As $\gamma = \frac{\pi}{3}$, then $\beta = \gamma$ and the configuration in Figure 4.139-II extends to a complete f-tiling $\tau \in \Omega(T_1, T_2)$, denoted by $\mathcal{N}$, see next figure. This f-tiling is composed by 18 triangles, with $\beta = \gamma = \frac{\pi}{3}$, $\alpha = \arccos\frac{1}{4} \approx 75,522°$ and $\delta \approx 104,478°$.

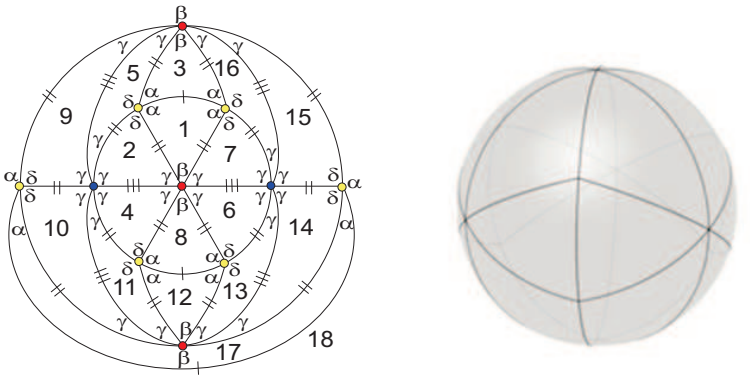

Figure 4.140: 2D and 3D representation of $\mathcal{N}$.

It should be mentioned that this f-tiling can not be obtained from any other f-tiling, since the elimination of edges, lead us to the violation of the angle folding relation or vertices of valency four cease to occur.

For $p = 2$, angle γ has two possible positions to be placed around vertex v_{12} each one giving rise to two another possible local configurations of a f-tiling, see Figure 4.141.

Each one of the configurations led to a vertex partially surrounded by four angles α. Taking into account the angle folding relation and the order relation between the angles, this type of vertices must be of valency six and both sums of its alternate angles are of the form $2\alpha + \gamma = \pi$. Accordingly, we have until now the following conditions: $\alpha + \delta = \pi$, $2\gamma + 2\beta = \pi$ and $2\alpha + \gamma = \pi$. By the adjacency condition (4.6), we get $\alpha \approx 69,647°$, $\beta \approx 49,294°$, $\gamma \approx 40,706°$ and $\delta \approx 110,353°$.

On the other hand, in the expansion of any one of the following configurations,

two types of vertices emerge: vertices surrounded by five angles γ and vertices surrounded by angles $\delta, \beta, \gamma, \gamma$. Taking into account the founded approximate values, there are no way to combining them in order to have the angle folding relation fulfilled.

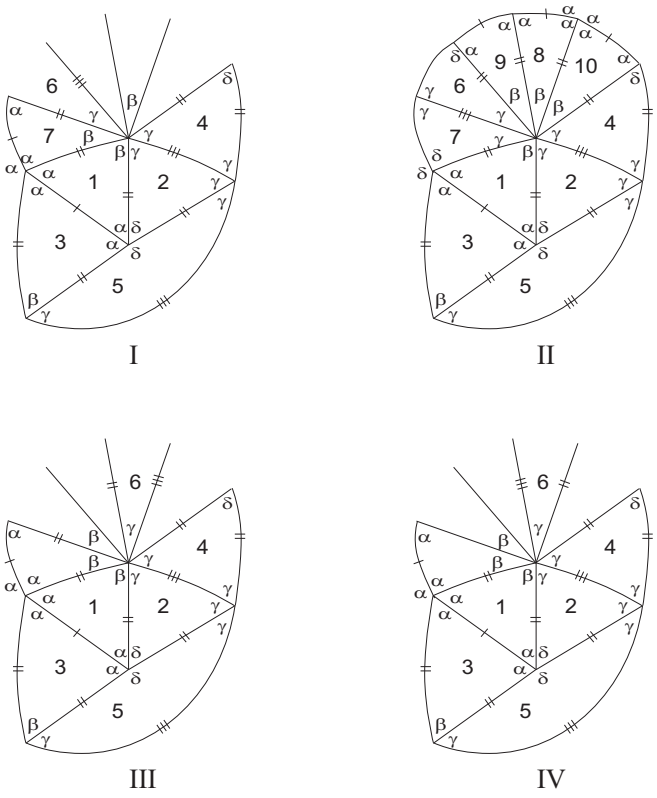

Figure 4.141: Local configurations.

If $p > 2$, angle γ has p possible positions to be placed around vertex v_{12}. Once again, vertices surrounded by four angles α arises satisfying $2\alpha + \gamma = \pi$ implying that $\frac{\pi}{6} < \gamma < \beta$ and so $p = 3$. Therefore, $2\gamma + 3\beta = \pi,\ 2\alpha + \gamma = \pi$ and $\alpha + \delta = \pi$. On the other hand, in the extended configurations, for each position of the angle γ, a vertex partially surrounded by five angles γ emerge. This type of vertices are either of valency six, eight or ten satisfying, respectively $3\gamma = \pi$ or ($4\gamma = \pi$ or $3\gamma + \alpha = \pi$ or $3\gamma + \beta = \pi$) or $5\gamma = \pi$. The values of $\alpha, \beta, \gamma, \delta$ satisfying each one of these possibilities are not possible to be combined in the admissible conditions, in order to validate the angle folding relation.

Suppose now that $q = 3$. Then, $3\gamma + p\beta = \pi$, for $p \geq 1$. Adding some new

cells to the configuration in Figure 4.122 and if tile 6 is a copy of T_1, then a vertex partially surrounded by four angles α arises, see Figure 4.142-I. This type of vertex must be of valency six and the sum of its alternate angles satisfies $2\alpha + \gamma = \pi$. Consequently, we are led to a vertex surrounded by angles δ, β, γ, in which one of its sums of alternate angles does not satisfy the angle folding relation (note that $\delta + \gamma < \pi$ and $\delta + \gamma + \mu > \pi$, for any $\mu \in \{\alpha, \beta, \gamma, \delta\}$) and we can not continue spreading the configuration.

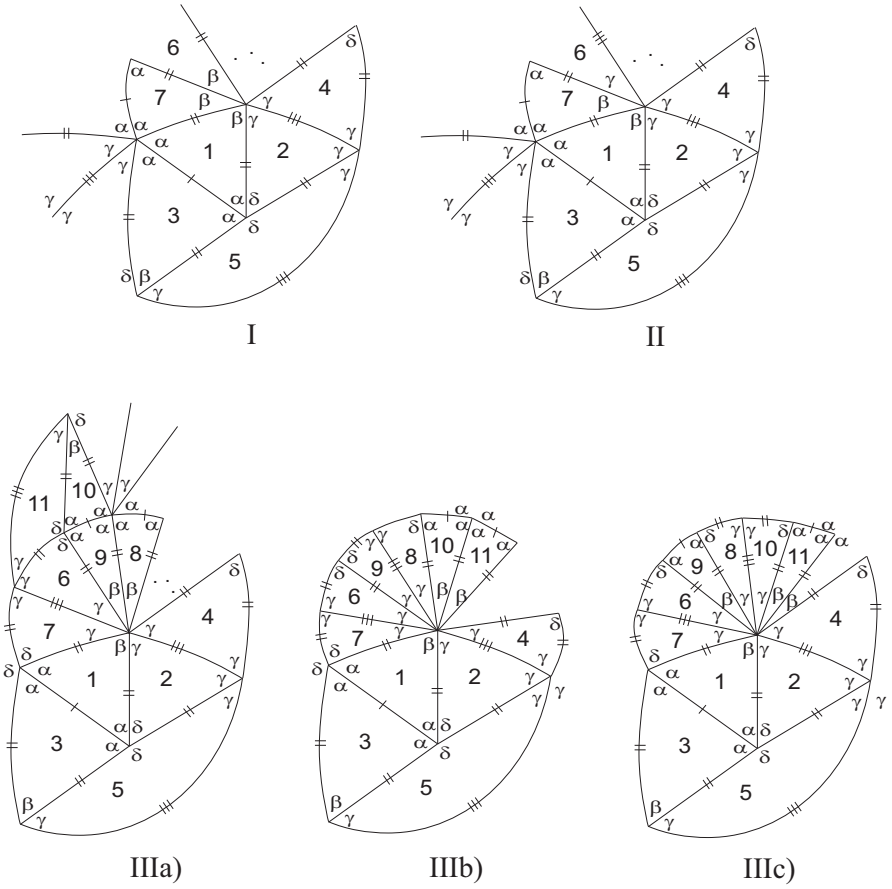

Figure 4.142: Local configurations.

If tile 6 is a copy of T_2 as shown in Figure 4.142-II, III a), b), c) we are led to a similar contradiction as in Figure 4.142-I. In Figures 4.142-III b), c), the six angles γ are already placed implying that the remaining angles must be β. In case $p \geq 2$, we end up at a vertex partially surrounded by three or more consecutive angles α and the same contradiction as before is achieved. For the case $p = 1$, one

has $3\gamma+\beta=\pi$ and we may continue adding cells to the configurations illustrated in Figures 4.142-III b), c).

In Figure 4.142-III b), the vertex partially surrounded by four consecutive angles γ is either of valency $2k$ or of valency eight.
If it is of valency $2k$ surrounded exclusively by angles γ, then $k=4$, since $\beta<\alpha$ and $\alpha<2\gamma$. In this case, we get $\gamma=\beta=\frac{\pi}{4}$, $\alpha\approx 72,965^\circ$ and $\delta\approx 107,031^\circ$ and the complete f-tiling is denoted by $\mathcal{O}$. Figure 4.143 shows a 3D representation.

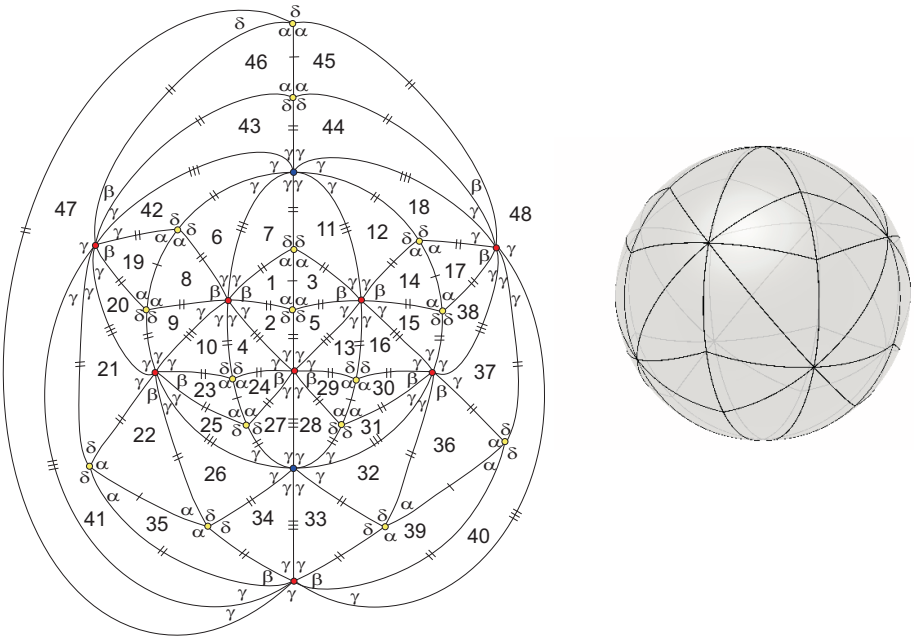

Figure 4.143: 2D and 3D representation of $\mathcal{O}$.

In the same situation, if the vertex partially surrounded by four consecutive angles γ is of valency eight whose both sums of alternate angles are of the form $3\gamma+\beta=\pi$, we are led to a vertex partially surrounded by three consecutive angles α that must be of valency $2m$ and is surrounded only by angles α. In a similar reasoning, as $\beta<\alpha$ and $2\alpha+\beta>\pi$, we are led to the contradiction $m<3$.

Looking at the configuration illustrated in Figure 4.142-III c), if $q=1$ the vertex partially surrounded by four consecutive angles γ is of valency $2k$ surrounded exclusively by angles γ or of valency eight surrounded by two angles β and six

angles γ. As before, we reach to the same conclusions.

- Suppose now that $\alpha + m\beta + \gamma = \pi$, for some $m \geq 1$. According to Figure 4.144, tile 6 is congruent to T_1 with three possible positions.

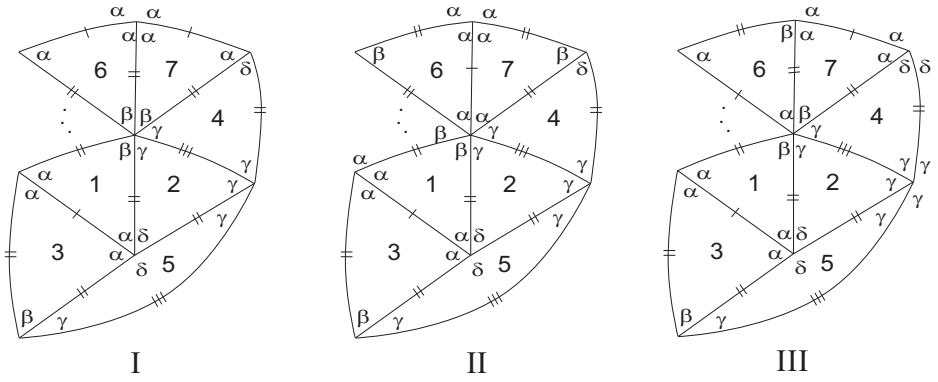

Figure 4.144: Local configurations.

In Figures 4.144-I, II, vertex partially surrounded by four angles α is of valency six and both sums of its alternate angles satisfy $2\alpha+\gamma = \pi$. Consequently, $\frac{\pi}{6} < \gamma < \beta$ and so $m = 1, 2$. However, for $m = 1$, one has the impossibility $\alpha = \beta$, remaining the case $m = 2$. Accordingly, $\alpha + \delta = \pi,\ \alpha + 2\beta + \gamma = \pi$ and $2\alpha + \gamma = \pi$. By the adjacency condition (4.6), $\beta = \frac{\pi}{3}$ (contradicting $\alpha + 2\beta + \gamma = \pi$) or $\beta = \frac{3\pi}{5}$ (an impossibility) or $\beta = \frac{\pi}{5}$. As $\beta = \frac{\pi}{5}$, then $\gamma = \beta$, which is impossible.
In Figure 4.144-III, we will study the cases $m = 1$ and $m > 1$ separately.

In case $m = 1$, we have $\alpha + \beta + \gamma = \pi$ and vertex partially surrounded by several angles γ is of valency six, eight, ten or $2(3 + k),\ k \geq 1$, whose sums of alternate angles satisfy, respectively, $3\gamma = \pi$ or $(4\gamma = \pi,\ 3\gamma + \alpha = \pi)$ or $5\gamma = \pi$ or $3\gamma + k\beta = \pi$.
If $3\gamma = \pi$, by the adjacency condition (4.6), we get $\alpha = 80°,\ \beta = 40°$ and $\delta = 100°$. Local configuration in Figure 4.144-III extends to a complete f-tiling $\tau \in \Omega(T_1, T_2)$ denoted by $\mathcal{P}$, see Figure 4.145. It is composed by 12 copies of each prototile.

This f-tiling can be obtained from ${}^{P}\mathcal{R}^{3}_{\alpha_2}$ described in [9] and in [14], whose prototiles are an isosceles triangle and a parallelogram.

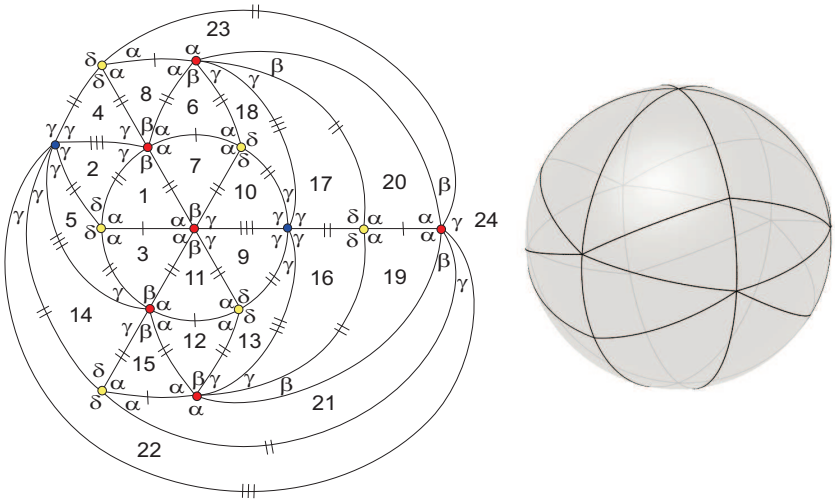

Figure 4.145: 2D and 3D representation of $\mathcal{P}$.

If $4\gamma = \pi$, then, by the adjacency condition (4.6), one has $\alpha \approx 65,948°$, $\delta \approx 114,052°$ and the contradiction $\beta \approx 69,052° > \alpha$.

If $3\gamma + \alpha = \pi$, then $\beta = 2\gamma > \alpha$, which is impossible.

In case $5\gamma = \pi$, using the adjacency condition (4.6), we are led to the impossibility $\alpha \approx 54,865° < \frac{\pi}{3}$.

Finally, if $3\gamma + k\beta = \pi,\ k \geq 1$, then $\alpha + \gamma + \beta = 3\gamma + k\beta$ and since $\alpha < 2\gamma$, we conclude that $k = 0$, a contradiction.

If $m > 1$, we may add come cells to the configuration in Figure 4.144-III and once again, a vertex partially surrounded by several angles α emerges (Figure 4.146).

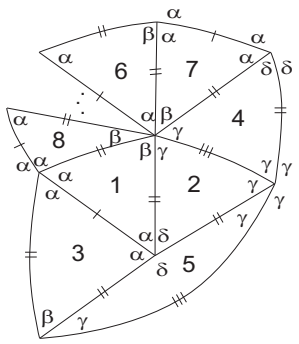

Figure 4.146: Local configuration.

This vertex must be of valency six and both sums of its alternate angles satisfy

$2\alpha + \gamma = \pi$. Therefore, $\gamma < \beta$ implying that $m = 2$. Accordingly, $\alpha + \delta = \pi$, $\alpha + 2\beta + \gamma = \pi$ and $2\alpha + \gamma = \pi$. By the adjacency condition (4.6), we get $\beta = \frac{\pi}{5}$. Therefore, $\alpha = \frac{2\pi}{5}$, $\delta = \frac{3\pi}{5}$ and $\gamma = \beta$, an absurd.

- Assume finally that $\delta + r\beta + \gamma = \pi$, for some $r \geq 1$. We shall study the cases $r = 1$ and $r > 1$ separately.

  Assume firstly that $r = 1$. Then, $\delta + \beta + \gamma = \pi$ and in configuration illustrated in Figure 4.147, tile 7 is congruent to T_1 or T_2 (see Figure 4.147).
  If tile 7 is congruent to T_1 (Figure 4.147-I), we are led to a vertex partially surrounded by four consecutive angles α. As $\frac{\pi}{6} < \gamma < \alpha < \frac{\pi}{2} < \delta$, $\beta < \gamma$, $\alpha > \frac{\pi}{3}$ and $2\alpha + \beta > \pi$, the sum containing two alternate angles α does not satisfy the angle folding relation and so we can not continue the extension of the configuration.

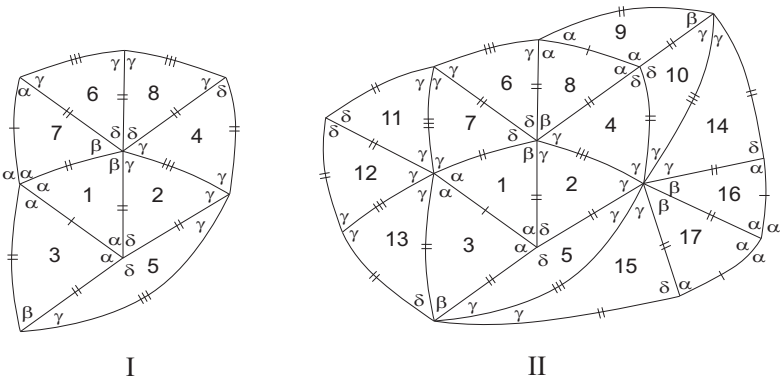

Figure 4.147: Local configurations.

If tile 7 is congruent to T_2 (Figure 4.147-II), in the extended configuration vertices surrounded by angles $\alpha, \alpha, \gamma, \gamma$ (tiles 1,3,7,11) start emerging. Taking into account the order relation between the angles and the conditions on the angles in this subcase, this type of vertex must be of valency six and the sum of its alternate angles satisfy $\alpha + 2\gamma = \pi$. Accordingly, $\alpha + \delta = \pi$, $\delta + \beta + \gamma = \pi$ and $\alpha + 2\gamma = \pi$. By the adjacency condition (4.6), one has $\gamma \approx 50,179°$, $\delta \approx 100,358°$, $\alpha \approx 79,642°$ and $\beta \approx 29,463°$. Consequently, vertex partially surrounded by more than four angles γ is of valency eight and both sums of its alternate angles are of the form $3\gamma + \beta = \pi$. Continue adding cells to the configuration, a vertex surrounded by

four angles α arises. Taking into account, the values already founded, there is no way to combine the angles, in order to fulfilled the angle folding relation.

Suppose now that $r > 1$. The angle δ of the sum containing the alternate angles β and γ, of tiles 1 and 4, has r possible positions to be placed and the other angle δ (around the same vertex) has $r+1$ possible positions to be placed. Anyway, we will end up at a vertex partially surrounded by two consecutive angles β which forces the existence of a vertex surrounded by four consecutive angles α leading to the same contradiction, as in the previous cases.

□

4.6 Isohedrality-Classes and Isogonality-Classes

In this Section, we give the combinatorial structure of the f-tilings described. Next tables show a complete list of all spherical dihedral f-tilings, whose prototiles are two isosceles triangles denoted by T_1 with angles α, α, β and T_2 of angles γ, γ, δ, with adjacency of type III. Angles α, β, γ and δ must satisfy the equation:

$$\frac{\cos\alpha(1+\cos\beta)}{\sin\alpha\sin\beta} = \frac{\cos\gamma(1+\cos\delta)}{\sin\gamma\sin\delta}. \tag{4.8}$$

We have used the following notation:

- M and N are, respectively, the number of triangles congruent to T_1 and the number of triangles congruent to T_2 used in such dihedral f-tilings;
- The numbers of isohedrality-classes and isogonality-classes for the symmetry group are denoted, respectively, by # isoh. and # isog.;
- $\delta = \delta_0^k, \quad k \geq 4$ in $\mathcal{Q}^k$ is the solution of (4.8), with $\gamma = \frac{\pi}{k}$, $\alpha = \frac{\pi}{2} - \frac{\gamma}{2}$ and $\beta = \pi - \delta$;
- $\delta = \delta_1^k, \quad k \geq 4$ in f-tiling $\mathcal{S}^k$ is the solution of (4.8), with $\gamma = \frac{\pi}{k}$, $\beta = \pi - 2\gamma$ and $\alpha = \pi - \delta$;
- $\gamma = \gamma_0^k, \quad k \geq 3$ in f-tiling $\mathcal{T}^k$ is the solution of (4.8), with $\alpha = \frac{\pi}{k}$, $\beta = \pi - 2\gamma$ and $\delta = \pi - \alpha$;
- $\gamma = \gamma_1^k, \quad k \geq 3$ in f-tiling $\mathcal{U}^k$ is the solution of (4.8), with $\alpha = \frac{\pi}{k}$, $\beta = \pi - 3\gamma$ and $\delta = \pi - \alpha$;
- $\delta = \delta_2^k, \quad k \geq 5$ in f-tiling $\mathcal{V}^k$ is the solution of (4.8), with $\gamma = \frac{\pi}{k}$, $\beta = \pi - 3\gamma$ and $\delta = \pi - \alpha$;
- $\beta = \beta_0^k, \quad k \geq 4$ in f-tiling $\mathcal{X}^k$ is the solution of (4.8), with $\gamma = \frac{\pi}{k}$, $\alpha = \pi - \beta - \gamma$ and $\delta = \beta + \gamma$.

f-tiling	α	β	γ	δ	M	N	# isoh.	# isog.
$\mathcal{L}_i^{k,\delta},\ k\geq 1,\ i=1,\ldots,k$	$\frac{\pi}{2}$	$\pi-k\delta$	$\frac{\pi}{2}$	$]0,\frac{\pi}{2}[$	4	$4k$	$k+1$	$k+2$
$\mathcal{M}_i^{n,m,\delta},\ m+n\neq 2,\ i=1,\ldots,I$	$\frac{\pi}{2}$	β_0	$\frac{\pi}{2}$	$\frac{\pi-n\beta}{m}$			*	*
$\mathcal{N}_i^{p,q,\delta},\ p,q\geq 1,\ i=1,\ldots,I$	$\frac{\pi}{2}$	$]0,\frac{\pi}{2}[$	$\frac{\pi}{2}$	$\frac{1}{q}\left(\frac{\pi}{2}-p\beta\right)$			*	*
$\mathcal{O}_i^{p,q,t},\ p,q\geq 1,\ 1\leq p<t,\ i=1,\ldots,I$	$\frac{\pi}{2}$	$\frac{\pi}{2t}$	$\frac{\pi}{2}$	$\frac{1}{q}\left(\frac{\pi}{2}-p\beta\right)$			*	*
$\mathcal{Q}^k,\ k\geq 4$	$\frac{\pi}{2}-\frac{\gamma}{2}$	$\pi-\delta$	$\frac{\pi}{k}$	δ_0^k	$4k$	$4k$	2	3

Table 4.3: Dihedral f-Tilings of the Sphere by Isosceles Triangles with Adjacency of type III a)

* For each fixed value of the parameters m, n, p, q, t and i, we get non-isomorphic tilings with distinct classes of isohedrality and isogonality. The classes of isohedrality and isogonality of the families $\mathcal{M}_i^{n,m,\delta}$, $\mathcal{N}_i^{p,q,\delta}$ and $\mathcal{O}_i^{p,q,t}$ will be specified for representative cases in the next tables.

	$\mathcal{M}_1^{2,\delta}$	$\mathcal{M}_2^{2,\delta}$	$\mathcal{M}_3^{2,\delta}$	$\mathcal{M}_4^{2,\delta}$	$\mathcal{M}_5^{2,\delta}$	$\mathcal{M}_1^{1,2,\delta}$	$\mathcal{M}_2^{1,2,\delta}$
# isohedrality	4	8	4	8	2	2	3
# isogonality	5	9	6	9	4	3	5

Table 4.4: Combinatorial structure of $\mathcal{M}_i^{2,\delta}$ and $\mathcal{M}_i^{1,2,\delta}$.

	$\mathcal{N}_1^{1,\delta}$	$\mathcal{N}_2^{1,\delta}$	$\mathcal{N}_3^{1,\delta}$	$\mathcal{N}_4^{1,\delta}$	$\mathcal{N}_5^{1,\delta}$	$\mathcal{N}_6^{1,\delta}$	$\mathcal{N}_1^{1,2,\delta}$
# isohedrality	4	8	4	8	4	8	12
# isogonality	5	8	6	8	6	5	11

Table 4.5: Combinatorial structure of $\mathcal{N}_i^{1,\delta}$ and $\mathcal{N}_i^{1,2,\delta}$.

	$\mathcal{O}_1^{1,3}$	$\mathcal{O}_2^{1,3}$	$\mathcal{O}_1^{1,2,2}$	$\mathcal{O}_2^{1,2,2}$	$\mathcal{O}_3^{1,2,2}$	$\mathcal{O}_4^{1,2,2\delta}$	$\mathcal{O}_5^{1,2,2}$	$\mathcal{O}_6^{1,2,2}$
# isohedrality	5	10	10	10	5	10	5	5
# isogonality	7	9	10	10	7	10	7	7

Table 4.6: Combinatorial structure of $\mathcal{O}_i^{1,3}$ and $\mathcal{O}_i^{1,2,2}$.

f-**tiling**	α	β	γ	δ	M	N	# isoh.	# isog.
$\mathcal{R}_t^k,\ k,t \geq 2,\ k \neq t$	$\frac{\pi}{2}$	$\frac{\pi}{2t}$	$\frac{\pi}{2}$	$\frac{\pi}{2k}$	$4t$	$4k$	$k+t$	$k+t+1$
$\mathcal{S}^k,\ k \geq 4$	$\pi - \delta$	$\pi - 2\gamma$	$\frac{\pi}{k}$	δ_1^k	$2k$	$4k$	2	3
$\mathcal{T}^k,\ k \geq 3$	$\frac{\pi}{k}$	$\pi - 2\gamma$	γ_0^k	$\pi - \alpha$	$4k$	$4k$	2	3
$\mathcal{U}^k,\ k \geq 3$	$\frac{\pi}{k}$	$\pi - 3\gamma$	γ_1^k	$\pi - \alpha$	$8k$	$12k$	3	5
$\mathcal{V}^k,\ k \geq 5$	$\pi - \delta$	$\pi - 3\gamma$	$\frac{\pi}{k}$	δ_2^k	$4k$	$8k$	3	4
$\mathcal{X}^k,\ k \geq 4$	$\pi - \beta - \gamma$	β_0^k	$\frac{\pi}{k}$	$\beta + \gamma$	$4k$	$4k$	2	3
$\mathcal{L}$	$\frac{\pi}{3}$	$\frac{2\pi}{5}$	$\frac{\pi}{5}$	$\frac{2\pi}{3}$	6	24	5	5
$\mathcal{M}$	$\frac{\pi}{3}$	$\frac{2\pi}{5}$	$\frac{\pi}{5}$	$\frac{2\pi}{3}$	40	20	3	4
$\mathcal{N}$	75.522°	$\frac{\pi}{3}$	$\frac{\pi}{3}$	104.478°	6	12	2	2
$\mathcal{O}$	72.969°	$\frac{\pi}{4}$	$\frac{\pi}{4}$	107.031°	16	32	3	3
$\mathcal{P}$	80°	40°	$\frac{\pi}{3}$	100°	12	12	2	3

Table 4.7: Dihedral f-Tilings of the Sphere by Isosceles Triangles with Adjacency of type III b)

4.7 Deformations

In this Section, we present a deformation into the standard folding (up to a rotation) of the dihedral f-tilings founded in this Chapter. In a similar way, as we made in Chapters 2 and 3, we give a geometrical sketch of a deformation, along with the paths $\gamma_v(t)$ referred in Theorem 1.3. The arrows indicate the way the vertices move. In order to facilitate the reasoning performed, we attribute to each face a suitable sign and, whenever the f-tiling is symmetric, we label only the angles placed in the semi-space $x \geq 0$.

It should be pointed out that, in each step of the deformation, the angle folding relation and the continuity of the deformation map ϕ must be preserved. The function $\phi : [0,1] \to \mathscr{T}^{\mathcal{O}}(S^2)$ maps each $t \in [0,1]$ into a f-tiling τ_t leading, usually to a piecewise-defined function.

Recall that, the space $\mathscr{T}^{\mathcal{O}}(S^2)$ is equipped with the metric structure given by (Proposition 1.4)

$$c(\tau_1^{o_1}, \tau_2^{o_2}) = \sum_{\substack{\text{F face of} \\ \tau_1 \cup \tau_2}} \lambda(F)\, Area(F)\,,$$

where $\tau_1^{o_1}$, $\tau_2^{o_2} \in \mathscr{T}^{\mathcal{O}}(S^2)$ and $\lambda(F) = 1$ if F is errant and $\lambda(F) = 0$ if F is non-errant.

Let us prove that:

1. For each $k \geq 3$ and $\alpha \in]\frac{\pi}{2}, \frac{2\pi}{3}[$, $\mathcal{G}_{k,\alpha}$ is deformable into τ^{-}_{stand}. Let $\phi : [0,1] \to \mathscr{T}^{\mathcal{O}}(S^2)$ be its deformable map. Figure 4.148 gives us an idea of how we can defined ϕ for the member $\mathcal{G}_{3,\alpha}$. The angles are $\beta = \delta = \frac{\pi}{3}$ and $\alpha = \pi - \gamma$, with $\gamma \in]0, \frac{\pi}{2}[$.

   For each $t \in [0, \frac{1}{2}]$:

   - $\star$ $\widetilde{\gamma}_i(t) = (1-2t)\gamma_i,\ i = 1,4,5;$
   - $\star$ $\widetilde{\alpha}_1(t) = \pi - \widetilde{\gamma}_1(t),\ \widetilde{\alpha}_5(t) = \pi - \widetilde{\gamma}_4(t)$ and $\widetilde{\alpha}_4(t) = \pi - \widetilde{\gamma}_5(t);$
   - $\star$ $\widetilde{\alpha}_j(t) = \alpha_j + 2t\left(\frac{\pi}{3} - \alpha_j\right),\ j = 2,3,6;$
   - $\star$ $\widetilde{\gamma}_3(t) = \pi - \widetilde{\alpha}_2(t),\ \widetilde{\gamma}_2(t) = \pi - \widetilde{\alpha}_3(t)$ and $\widetilde{\gamma}_6(t) = \pi - \widetilde{\alpha}_6(t).$

   If $t \in]\frac{1}{2}, 1]$:

⋆ $\widetilde{\beta}_i(t) = 2(1-t)\beta_i$ and $\widetilde{\delta}_i(t) = 2(1-t)\delta_i$ $i = 1, 3$;

⋆ $\widetilde{\beta}_2(t) = \beta_2 + (2t-1)\beta_1 + (2t-1)\beta_3$ and $\widetilde{\delta}_2(t) = \delta_2 + (2t-1)\delta_1 + (2t-1)\delta_3$.

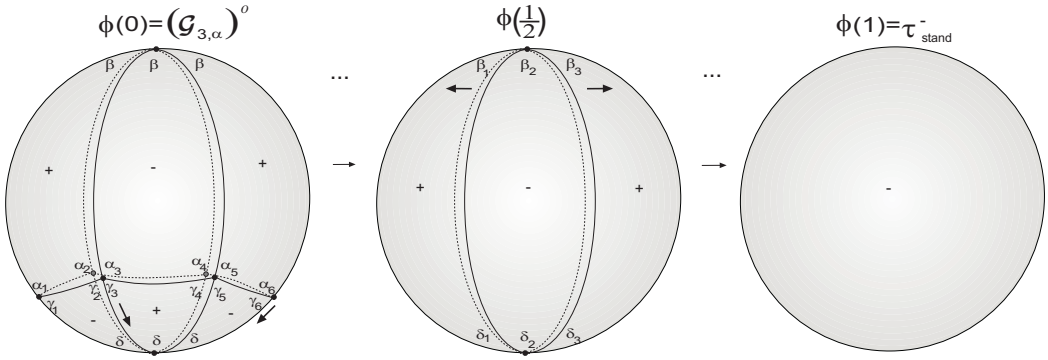

Figure 4.148: Deformation of $(\mathcal{G}_{3,\alpha})^o$.

To prove that ϕ is continuous at $t = 0^-$ and $t = \frac{1}{2}^-$, let us consider $t \in]0, \frac{1}{2}[$:

$$\begin{aligned}
c(\tau_t^{o_t}, \tau_0) &= \sum_{\substack{F \text{face of} \\ \tau_t \cup \tau_0}} \lambda(F)\, Area(F) \\
&= 2 \times (\widetilde{\gamma}_1(0) - \widetilde{\gamma}_1(t) + \widetilde{\alpha}_2(t) + \widetilde{\gamma}_2(0) - \pi) \\
&+ 2 \times (\widetilde{\gamma}_4(0) - \widetilde{\gamma}_4(t) + \widetilde{\gamma}_3(0) + \widetilde{\alpha}_3(t) - \pi) \\
&+ 2 \times (\widetilde{\gamma}_5(0) - \widetilde{\gamma}_5(t) + \widetilde{\alpha}_6(t) + \widetilde{\gamma}_6(0) - \pi) \\
&= 2 \times \left(\gamma_1 - (1-2t)\gamma_1 + \alpha_2 + 2t\left(\frac{\pi}{3} - \alpha_2\right) + \gamma_2 - \pi\right) \\
&+ 2 \times \left(\gamma_4 - (1-2t)\gamma_4 + \gamma_3 + \alpha_3 + 2t\left(\frac{\pi}{3} - \alpha_3\right) - \pi\right) \\
&+ 2 \times \left(\gamma_5 - (1-2t)\gamma_5 + \alpha_6 + 2t\left(\frac{\pi}{3} - \alpha_6\right) + \gamma_6 - \pi\right).
\end{aligned}$$

If $t \to 0^+$, then $c(\tau_t^{o_t}, \tau_0) \to 0$.

$$\begin{aligned}
c(\tau_t^{o_t}, \tau_{\frac{1}{2}}) &= \sum_{\substack{F \text{face of} \\ \tau_t \cup \tau_{\frac{1}{2}}}} \lambda(F)\, Area(F) \\
&= 6 \times (\widetilde{\gamma}_1(t) + \widetilde{\gamma}_2(t) + \delta - \pi) \\
&= 6 \times \left((1-2t)\gamma_1 + \pi - \alpha_3 - 2t\left(\frac{\pi}{3} - \alpha_3\right) + \delta - \pi\right).
\end{aligned}$$

If $t \to \frac{1}{2}^-$, then $c(\tau_t^{o_t}, \tau_{\frac{1}{2}}) \to 0$.

The continuity at $t = \frac{1}{2}^+$ and $t = 1$ is trivial.

2. For each $\alpha \in]\frac{\pi}{2}, \pi[$, $\mathcal{H}_\alpha$ is deformable into τ^+_{stand}. Figure 4.149 shows a geometrical sketch of the process of deformation and how to define $\phi : [0,1] \to \mathscr{T}^{\mathcal{O}}(S^2)$ of a representative member of $\mathcal{H}_\alpha$. The angles are $\beta = \delta = \frac{\pi}{2}$ and $\alpha = \pi - \gamma$, with $\gamma \in]0, \frac{\pi}{2}[$.

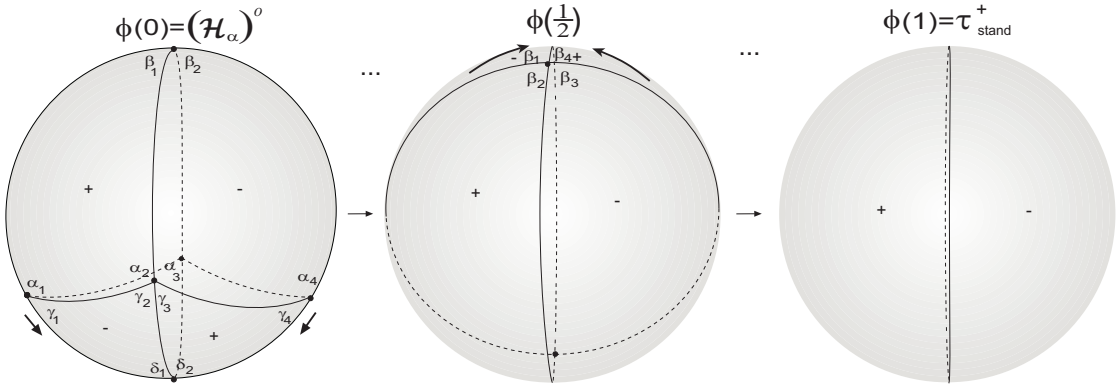

Figure 4.149: Deformation of $(\mathcal{H}_\alpha)^o$.

With $t \in [0, \frac{1}{2}]$:

- $\widetilde{\gamma}_i(t) = (1-2t)\gamma_i,\ i = 2, 3$;
- $\widetilde{\alpha}_2(t) = \pi - \widetilde{\gamma}_3(t)$ and $\widetilde{\alpha}_3(t) = \pi - \widetilde{\gamma}_2(t)$;
- $\widetilde{\alpha}_j(t) = \alpha_j + 2t\left(\frac{\pi}{2} - \alpha_j\right),\ j = 1, 4$;
- $\widetilde{\gamma}_1(t) = \pi - \widetilde{\alpha}_1(t)$ and $\widetilde{\gamma}_4(t) = \pi - \widetilde{\alpha}_4(t)$.

If $t \in]\frac{1}{2}, 1]$:

- $\widetilde{\beta}_i(t) = (2-2t)\beta_i,\ i = 1, 4$;
- $\widetilde{\beta}_2(t) = \pi - \widetilde{\beta}_4(t)$ and $\widetilde{\beta}_3(t) = \pi - \widetilde{\beta}_1(t)$.

To show that ϕ is continuous at $t = 0$, consider $t \in]0, 1[$. Then,

$$
\begin{aligned}
c(\tau_t^{o_t}, \tau_0) &= \sum_{\substack{F \text{face of} \\ \tau_t \cup \tau_0}} \lambda(F)\, Area(F) \\
&= 4 \times (\widetilde{\gamma}_2(0) - \widetilde{\gamma}_2(t) + \widetilde{\gamma}_1(0) + \widetilde{\alpha}_1(t) - \pi) \\
&= 4 \times \left(\gamma_2 - (1-2t)\gamma_2 + \gamma_1 + \alpha_1 + 2t\left(\frac{\pi}{2} - \alpha_1\right) - \pi\right).
\end{aligned}
$$

When, $t \to 0^+$, then $c(\tau_t^{o_t}, \tau_0) \to 0$.

$$
\begin{aligned}
c(\tau_t^{o_t}, \tau_{\frac{1}{2}}) &= \sum_{\substack{F \text{face of} \\ \tau_t \cup \tau_{\frac{1}{2}}}} \lambda(F)\, Area(F) \\
&= 4 \times (\widetilde{\gamma}_1(t) + \widetilde{\gamma}_2(t) + \delta - \pi) \\
&= 4 \times \left(\pi - \alpha_1 - 2t\left(\frac{\pi}{2} - \alpha_1\right) + (1-2t)\gamma_2 + \delta - \pi\right).
\end{aligned}
$$

Making $t \to \frac{1}{2}^-$, one has $c(\tau_t^{o_t}, \tau_{\frac{1}{2}}) \to 0$.

To prove the continuity of ϕ at $t = \frac{1}{2}^+$ and $t = 1^-$, we follow the same reasoning done for $(\mathcal{A}_3^2)^o$ in Chapter 2.

3. For any $k \geq 3$, $\mathcal{I}^k$ is deformable into τ_{stand}^-. Figure 4.150 shows a deformation of the member $\mathcal{I}^3$ into τ_{stand}^-. The angles are $\delta = \frac{\pi}{2}$, $\beta = \frac{\pi}{3}, \gamma = \arctan\left(\sqrt{\frac{5}{3}}\right) \approx 52.239^\circ$ and $\alpha \approx 75.522^\circ$.

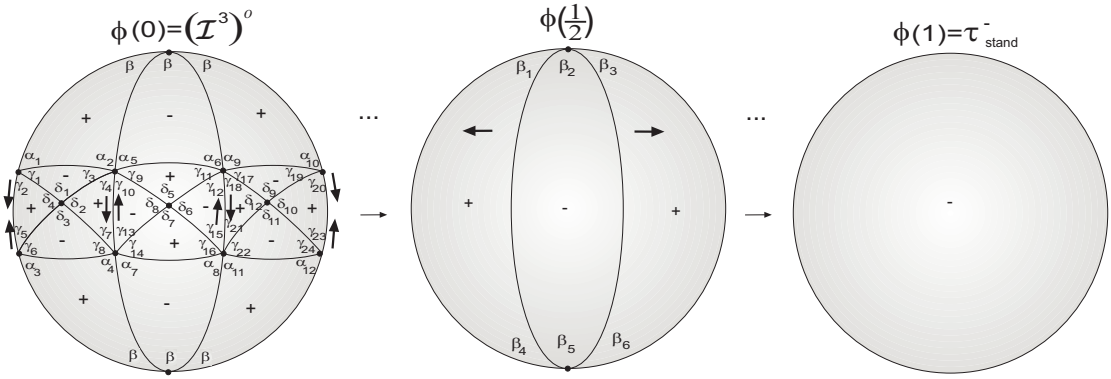

Figure 4.150: Deformation of $(\mathcal{I}^3)^o$.

If $t \in [0, \frac{1}{2}]$:

- $\star\ \widetilde{\delta}_i(t) = (1-2t)\delta_i,\ i = 2, 6, 10;$
- $\star\ \widetilde{\delta}_j(t) = \delta_j + 2t\delta_{j+1},\ j = 1, 5, 9;$
- $\star\ \widetilde{\delta}_k(t) = \pi - \widetilde{\delta}_{k-2}(t),\ k = 3, 4, 7, 8, 11, 12;$
- $\star\ \widetilde{\alpha}_j(t) = \alpha_j + 2t\left(\frac{\pi}{2} - \alpha_j\right),\ j = 1, 2, 3, 4, 5, 6, 7, 8, 9, 10, 11, 12;$
- $\star\ \widetilde{\gamma}_j(t) = (1-2t)\gamma_j,\ j = 1, 3, 6, 7, 8, 9, 11, 14, 16, 17, 19, 22, 24;$
- $\star\ \widetilde{\gamma}_j(t) = \gamma_j + 2t\left(\frac{\pi}{2} - \gamma_j\right),\ j = 2, 4, 5, 7, 10, 12, 13, 15, 18, 20, 21, 23.$

If $t \in]\frac{1}{2}, 1]$:

- $\star\ \widetilde{\beta}_i(t) = (2-2t)\beta_i,\ i = 1, 3, 4, 6;$
- $\star\ \widetilde{\beta}_2(t) = \beta_2 - \beta_1 - \beta_3 + 2t(\beta_1 + \beta_3)$ and $\widetilde{\beta}_5(t) = \beta_5 - \beta_4 - \beta_6 + 2t(\beta_4 + \beta_6).$

Let us show that ϕ is continuous at $t = 0^+$:

For $t \in]0, \frac{1}{2}[$:

$$\begin{aligned} c(\tau_t^{o_t}, \tau_0) &= \sum_{\substack{F \text{face of} \\ \tau_t \cup \tau_0}} \lambda(F)\, Area(F) \\ &\leq 24 \times \left[\left(\widetilde{\gamma}_4(0) + \widetilde{\delta}_2(0) + \widetilde{\gamma}_7(0) - \pi\right) - \left(\widetilde{\delta}_2(t) + \widetilde{\gamma}_4(t) + \widetilde{\gamma}_7(t) - \pi\right)\right]. \end{aligned}$$

When $t \to 0^+$, $c(\tau_t^{o_t}, \tau_0) \to 0$.

Now, if $t \in]0, \frac{1}{2}[$:

$$\begin{aligned} c(\tau_t^{o_t}, \tau_{\frac{1}{2}}) &= \sum_{\substack{F \text{face of} \\ \tau_t \cup \tau_{\frac{1}{2}}}} \lambda(F)\, Area(F) \\ &= 12 \times \left(\widetilde{\gamma}_1(t) + \widetilde{\gamma}_3(t) + \widetilde{\delta}_1(t) - \pi\right) \\ &= 12 \times \left((1-2t)\gamma_1 + (1-2t)\gamma_3 + \delta_1 + 2t\delta_2 - \pi\right). \end{aligned}$$

As $t \to \frac{1}{2}^-$, we conclude that $c(\tau_t^{o_t}, \tau_{\frac{1}{2}}) \to 0$.

The continuity of ϕ at $t = \frac{1}{2}^+$ and $t = 1^-$ is trivial.

4. The f-tiling $\mathcal{H}$ is deformable into τ^{+}_{stand}. Figure 4.155 gives a geometrical sketch of how to define the map $\phi : [0,1] \to \mathscr{T}^{\mathcal{O}}(S^2)$. This f-tiling is composed by vertices of valency four surrounded exclusively by angles δ and vertices of valency six, whose sums of alternate angles satisfy $2\alpha + \gamma = \pi$, with $\alpha \approx 65.905^\circ$ and $\gamma \approx 48.19^\circ$ or surrounded exclusively by angles β.

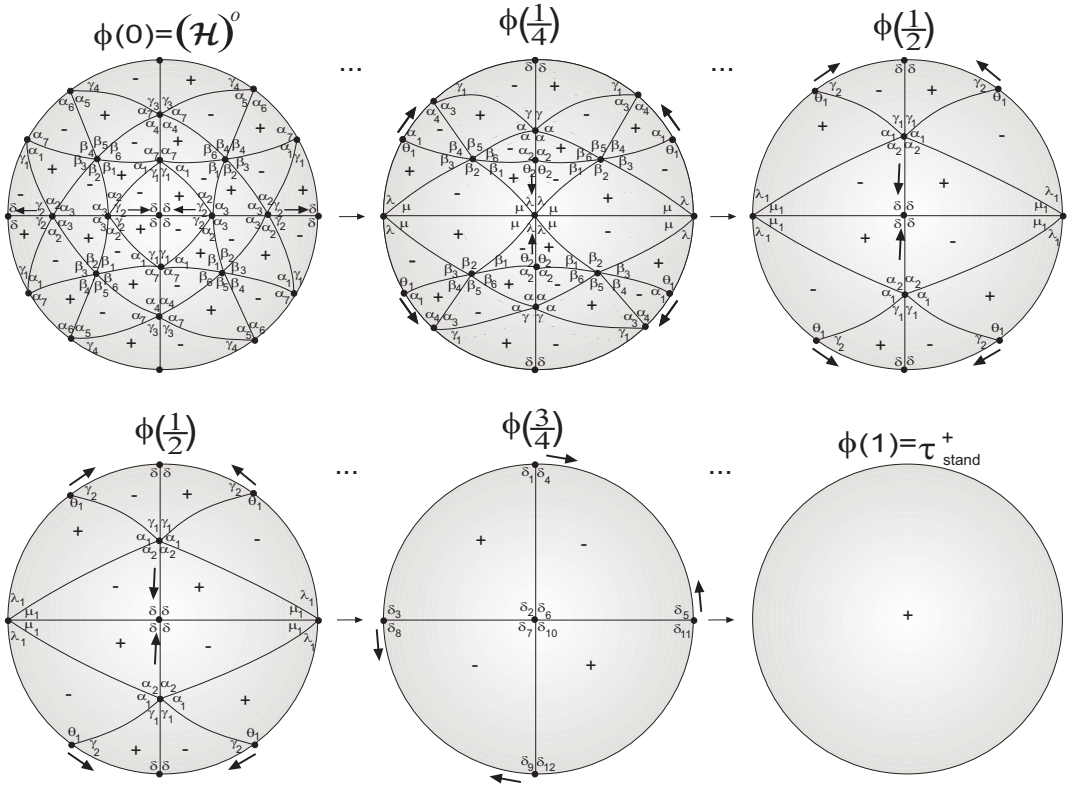

Figure 4.151: Deformation of $(\mathcal{H})^o$.

For $t \in [0, \frac{1}{4}]$:

- $\widetilde{\gamma}_1(t) = (1-4t)\gamma_1$;
- $\widetilde{\gamma}_2(t) = \gamma_2 + 4t\left(\frac{\pi}{2} - \gamma_2\right)$;
- $\widetilde{\gamma}_3(t) = \gamma_3 - 4t\varepsilon$, for some $\varepsilon > 0$;
- $\widetilde{\gamma}_4(t) \equiv \gamma$;
- $\widetilde{\alpha}_1(t) = \alpha_1 + 4t\gamma_1$;
- $\widetilde{\alpha}_2(t) = \widetilde{\alpha}_3(t) = \alpha + 4t\left(\frac{\pi}{4} - \alpha\right)$;

- $\widetilde{\alpha}_4(t) = \alpha + 4t\varepsilon$;
- $\widetilde{\alpha}_5(t) = \alpha - 4t\varepsilon$;
- $\widetilde{\alpha}_6(t) = \alpha + 4t\varepsilon$;
- $\widetilde{\alpha}_7(t) \equiv \alpha$;
- $\widetilde{\beta}_1(t) = \widetilde{\beta}_3(t) = \widetilde{\beta}_4(t) = \widetilde{\beta}_6(t) = \beta - 2t\xi$, for some $\xi > 0$;
- $\widetilde{\beta}_2(t) = \widetilde{\beta}_5(t) = \beta + 4t\xi$.

Taking into account that areas of the triangles must be greater than π, we conclude that, when $t \to \frac{1}{4}^{-}$:

- $Area_(\gamma_1, \gamma_2, \delta) \to 0$;
- $Area_(\alpha_1, \alpha_2, \beta_1) = Area_(\alpha_1, \alpha_2, \beta_3) \to \alpha_1 + \gamma_1 - \frac{\xi}{2} - \frac{5\pi}{12}$ implying that $\xi < 76°$;
- $Area_(\alpha_3, \alpha_3, \beta_2) \to \frac{\pi}{4} + \frac{\pi}{4} + \beta + \xi - \pi$ implying that $\xi > 30°$;
- $Area_(\alpha, \alpha_6, \beta_4) \to \alpha + \alpha_6 + \varepsilon + \beta - \frac{\xi}{2} - \pi$ implying that $\varepsilon > 5°$;
- $Area_(\alpha, \alpha_5, \beta_5) = Area_(\alpha, \alpha_4, \beta_6) \to \alpha + \alpha_5 - \varepsilon + \beta + \xi - \pi$ implying that $\varepsilon < 86°$;
- $Area_(\gamma, \gamma_3, \frac{\pi}{2}) \to \gamma + \gamma_3 - \varepsilon + \frac{\pi}{2} - \pi$ implying that $\varepsilon < 6°$.

Therefore,

$$5° < \varepsilon < 6° \text{ and } 30° < \xi < 76°.$$

For $t \in]\frac{1}{4}, \frac{1}{2}]$:

- $\widetilde{\beta}_i(t) = (2 - 4t)\beta_i,\ i = 1, 4$;
- $\widetilde{\beta}_3(t) = \beta_3 - \beta_4 + 4t\beta_4$ and $\widetilde{\beta}_6(t) = \beta_6 - \beta_1 + 4t\beta_1$;
- $\widetilde{\theta}_1(t) = 2\theta_1 - \alpha_4 + 4t(\alpha_4 - \theta_1)$ and $\widetilde{\theta}_2(t) = 2\theta_2 - 2\mu + 4t(2\mu - \theta_2)$;
- $\widetilde{\alpha}_1(t) = \pi - \widetilde{\theta}_1(t)$ and $\widetilde{\alpha}_2(t) = \pi - \widetilde{\theta}_2(t)$.

If $t \in]\frac{1}{2}, \frac{3}{4}]$:

- $\widetilde{\gamma}_1(t) = (3 - 4t)\gamma_1$ and $\widetilde{\mu}_1(t) = (3 - 4t)\mu_1$;

- $\widetilde{\alpha}_1(t) = 3\alpha_1 - \pi + 4t\left(\frac{\pi}{2} - \alpha_1\right)$ and $\widetilde{\lambda}_1(t) = \lambda_1 - 2\mu_1 + 4t\mu_1$;
- $\widetilde{\theta}_1(t) = 3\theta_1 - \pi + 4t\left(\frac{\pi}{2} - \theta_1\right)$ and $\widetilde{\gamma}_2(t) = \pi - \widetilde{\theta}_1(t)$;
- $\widetilde{\alpha}_2(t) = \pi - \widetilde{\gamma}_1(t) - \widetilde{\alpha}_1(t)$.

If $t \in]\frac{3}{4}, 1]$:

- $\widetilde{\delta}_6(t) = (4 - 4t)\delta_6$ and $\widetilde{\delta}_7(t) = \pi - \widetilde{\delta}_6(t)$;
- $\widetilde{\delta}_2(t) = \delta_2 - 3\delta_6 + 4t\delta_6$ and $\widetilde{\delta}_{10}(t) = \pi - \widetilde{\delta}_2(t)$;
- $\widetilde{\delta}_j(t) \equiv \delta,\ j = 1, 3, 4, 5, 8, 9, 11, 12.$

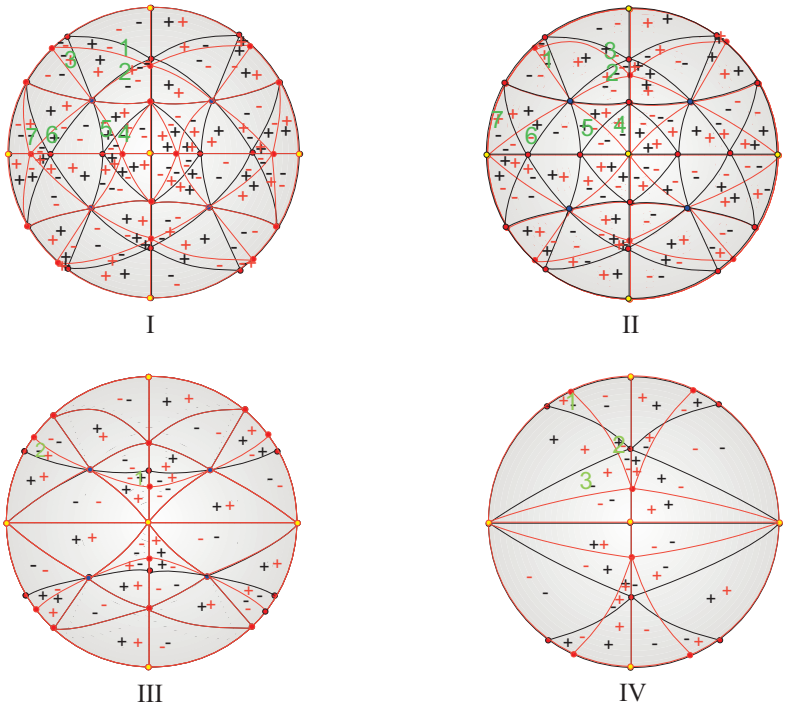

Figure 4.152: Errant faces.

Let us show that ϕ is continuous at $t = 0$ and $t = \frac{1}{4}^-$ (see Figure 4.152-I): for $t \in]0, \frac{1}{4}[$,

$$
\begin{aligned}
c(\tau^{o_t},\tau_0) &= \sum_{\substack{F\text{face of}\\ \tau_t\cup\tau_0}} \lambda(F)\,Area(F)\\
&\le 8\times\left|\left(\frac{\pi}{2}+\widetilde{\gamma}_3(t)+\widetilde{\gamma}(t)-\pi\right)-\left(\frac{\pi}{2}+\widetilde{\gamma}_3(0)+\widetilde{\gamma}(0)-\pi\right)\right|\\
&+16\times\left|\left(\widetilde{\alpha}_4(0)+\widetilde{\alpha}(0)+\widetilde{\beta}_6(0)-\pi\right)-\left(\widetilde{\alpha}_4(t)+\widetilde{\alpha}(t)+\widetilde{\beta}_6(t)-\pi\right)\right|\\
&+16\times\left|\left(\frac{\pi}{2}+\widetilde{\gamma}_1(0)+\widetilde{\gamma}_2(0)-\pi\right)-\left(\frac{\pi}{2}+\widetilde{\gamma}_1(t)+\widetilde{\gamma}_2(t)-\pi\right)\right|\\
&+16\times\left|\left(\widetilde{\alpha}_1(0)+\widetilde{\alpha}_2(0)+\widetilde{\beta}_1(0)-\pi\right)-\left(\widetilde{\alpha}_1(t)+\widetilde{\alpha}_2(t)+\widetilde{\beta}_1(t)-\pi\right)\right|.
\end{aligned}
$$

For $t\to 0^+$, one has $c(\tau^{o_t},\tau_0)\to 0$.

Observing Figure 4.152-II, we have

$$
\begin{aligned}
c(\tau^{o_t},\tau_{\frac{1}{4}}) &= \sum_{\substack{F\text{face of}\\ \tau_t\cup\tau_{\frac{1}{4}}}} \lambda(F)\,Area(F)\\
&\le 16\left[\widetilde{\beta}_5\left(\frac{1}{4}\right)+\widetilde{\alpha}\left(\frac{1}{4}\right)+\widetilde{\alpha}_5\left(\frac{1}{4}\right)-\pi\right]\\
&-16\left(\widetilde{\beta}_5(t)+\widetilde{\alpha}(t)+\widetilde{\alpha}_5(t)-\pi\right)\\
&+16\left[\widetilde{\beta}_1\left(\frac{1}{4}\right)+\widetilde{\alpha}_2\left(\frac{1}{4}\right)+\widetilde{\alpha}_1\left(\frac{1}{4}\right)-\pi\right]\\
&-16\left(\widetilde{\beta}_1(t)+\widetilde{\alpha}_2(t)+\widetilde{\alpha}_1(t)-\pi\right)\\
&+16\left[\widetilde{\beta}_3\left(\frac{1}{4}\right)+\widetilde{\alpha}_1\left(\frac{1}{4}\right)+\widetilde{\alpha}_2\left(\frac{1}{4}\right)-\pi\right]\\
&-16\left(\widetilde{\beta}_3(t)+\widetilde{\alpha}_1(t)+\widetilde{\alpha}_2(t)-\pi\right).
\end{aligned}
$$

Making $t\to\frac{1}{4}^{-}$, we get $c(\tau^{o_t},\tau_{\frac{1}{4}})\to 0$.

Now, if $t\in]\frac{1}{4},\frac{1}{2}[$ (see Figure 4.152-III):

$$
\begin{aligned}
c(\tau^{o_t}, \tau_{\frac{1}{4}}) &= \sum_{\substack{F\text{face of} \\ \tau_t \cup \tau_{\frac{1}{4}}}} \lambda(F)\, Area(F) \\
&= 8 \times \left(\widetilde{\beta}_1\left(\frac{1}{4}\right) + \widetilde{\theta}_2\left(\frac{1}{4}\right) + \lambda - \pi \right) - 8 \times \left(\widetilde{\beta}_1(t) + \widetilde{\theta}_2(t) + \lambda - \pi \right) \\
&+ 8 \times \left(\widetilde{\beta}_4\left(\frac{1}{4}\right) + \widetilde{\alpha}_1\left(\frac{1}{4}\right) + \widetilde{\alpha}_4\left(\frac{1}{4}\right) - \pi \right) \\
&- 8 \times \left(\widetilde{\beta}_4(t) + \widetilde{\alpha}_1(t) + \widetilde{\alpha}_4(t) - \pi \right).
\end{aligned}
$$

Making $t \to \frac{1}{4}^+$, we conclude that $c(\tau^{o_t}, \tau_{\frac{1}{4}}) \to 0$ and so ϕ is continuous at $t = \frac{1}{4}$.

$$
\begin{aligned}
c(\tau^{o_t}, \tau_{\frac{1}{2}}) &= \sum_{\substack{F\text{face of} \\ \tau_t \cup \tau_{\frac{1}{2}}}} \lambda(F)\, Area(F) \\
&= 8 \times \left(\widetilde{\alpha}_1(t) + \alpha_4 + \widetilde{\beta}_4(t) - \pi \right) + 8 \times \left(\widetilde{\beta}_1(t) + \lambda + \widetilde{\theta}_2(t) - \pi \right) \\
&= 8 \times (\pi - 2\theta_1 + \alpha_4 - 4t(\alpha_4 - \theta_1) + \alpha_4 + (2 - 4t)\beta_4 - \pi) \\
&+ 8 \times ((2 - 4t)\beta_1 + +2\theta_2 - 2\mu + 4t(2\mu - \theta_2) + \lambda - \pi).
\end{aligned}
$$

As $t \to \frac{1}{2}^-$, we have $c(\tau^{o_t}, \tau_{\frac{1}{2}}) \to 0$.

For $t \in]\frac{1}{2}, \frac{3}{4}[$ and from Figure 4.152-IV:

$$
\begin{aligned}
c(\tau^{o_t}, \tau_{\frac{1}{2}}) &= \sum_{\substack{F\text{face of} \\ \tau_t \cup \tau_{\frac{1}{2}}}} \lambda(F)\, Area(F) \\
&= 8 \times \left(\frac{\pi}{2} + \widetilde{\gamma}_2\left(\frac{1}{2}\right) + \widetilde{\gamma}_1\left(\frac{1}{2}\right) - \pi \right) - 8 \times \left(\frac{\pi}{2} + \widetilde{\gamma}_2(t) + \widetilde{\gamma}_1(t) - \pi \right) \\
&+ 8 \times \left(\widetilde{\theta}_1\left(\frac{1}{2}\right) + \widetilde{\alpha}_1\left(\frac{1}{2}\right) + \widetilde{\lambda}_1\left(\frac{1}{2}\right) - \pi \right) \\
&- 8 \times \left(\widetilde{\theta}_1(t) + \widetilde{\alpha}_1(t) + \widetilde{\lambda}_1(t) - \pi \right) \\
&+ 8 \times \left(\frac{\pi}{2} + \widetilde{\mu}_1\left(\frac{1}{2}\right) + \widetilde{\alpha}_2\left(\frac{1}{2}\right) - \pi \right) - 8 \times \left(\frac{\pi}{2} + \widetilde{\mu}_1(t) + \widetilde{\alpha}_2(t) - \pi \right).
\end{aligned}
$$

For $t \to \frac{1}{2}^+$, we conclude that $c(\tau^{o_t}, \tau_{\frac{1}{2}}) \to 0$ and consequently, ϕ is continuous at $t = \frac{1}{2}$.

$$
\begin{aligned}
c(\tau^{o_t}, \tau_{\frac{3}{4}}) &= \sum_{\substack{F \text{face of} \\ \tau_t \cup \tau_{\frac{3}{4}}}} \lambda(F)\, Area(F) \\
&= 8 \times \left(\frac{\pi}{2} + \widetilde{\gamma}_2(t) + \widetilde{\gamma}_1(t) - \pi \right) + 8 \times \left(\frac{\pi}{2} + \widetilde{\mu}_1(t) + \widetilde{\alpha}_2(t) - \pi \right) \\
&= 8 \times \left(-\frac{\pi}{2} + \pi - 3\theta_1 + \pi - 4t \left(\frac{\pi}{2} - \theta_1 \right) + (3 - 4t)\gamma_1 \right) \\
&+ 8 \times \left(-\frac{\pi}{2} + (3 - 4t)\mu_1 + \pi - (3 - 4t)\mu_1 - 3\alpha_1 + \pi - 4t \left(\frac{\pi}{2} - \alpha_1 \right) \right).
\end{aligned}
$$

If $t \to \frac{3}{4}^-$, then $c(\tau^{o_t}, \tau_{\frac{3}{4}}) \to 0$.

The continuity at $t = \frac{3}{4}^+$ and $t = 1^-$ is trivial.

5. For each $k \geq 3$, $\mathcal{J}^k$ is deformable into τ^-_{stand}. Figure 4.153 shows a deformation of the member $\mathcal{J}^3$ and gives an idea of how to define the map $\phi : [0, 1] \to \mathscr{T}^{\mathcal{O}}(S^2)$. The angles are $\delta = \frac{\pi}{3}$, $\alpha = \arccos \sqrt{\frac{3}{8}} \approx 52.237°$, $\beta \approx 104.474°$ and $\gamma \approx 75.526°$.

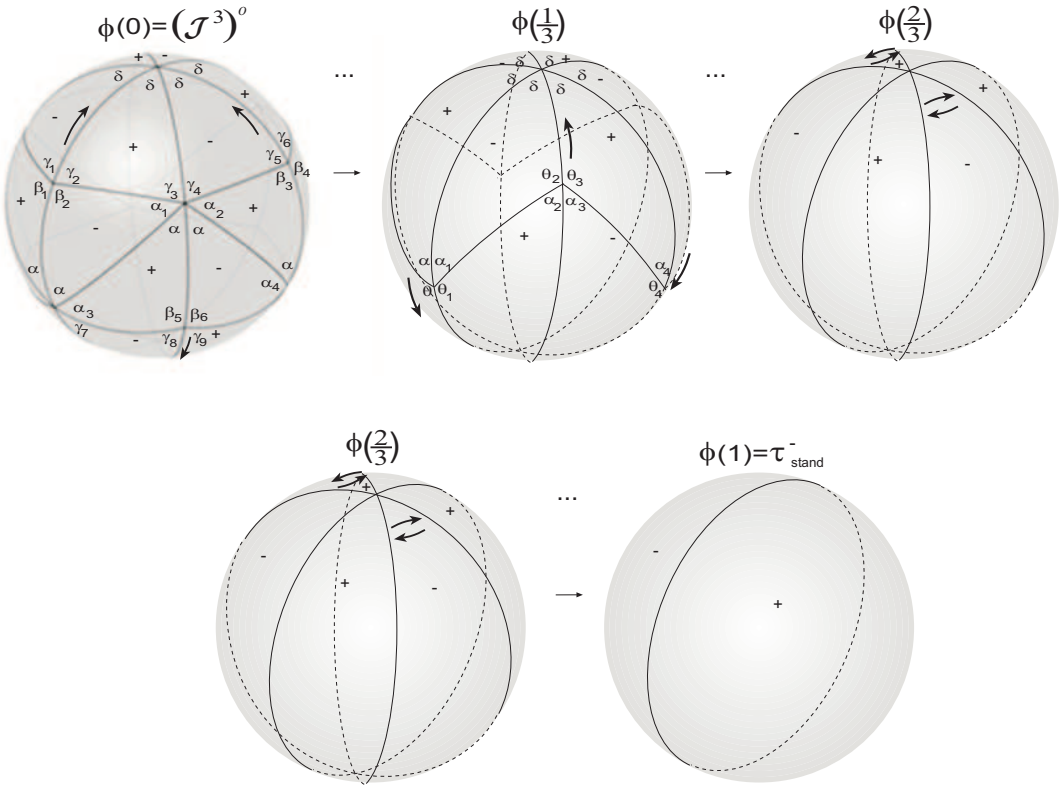

Figure 4.153: Deformation of $(\mathcal{J}^3)^o$.

For $t \in [0, \frac{1}{3}]$:

- $\widetilde{\gamma}_i(t) = (1-3t)\gamma_i,\ i = 3, 4;$
- $\widetilde{\alpha}_i(t) = \alpha_i + 3t\gamma_{i+2},\ i = 1, 2;$
- $\widetilde{\beta}_k(t) = \beta_k + 3t\left(\frac{\pi}{3} - \beta_k\right),\ k = 1, 2, 3, 4;$
- $\widetilde{\gamma}_1(t) = \pi - \widetilde{\beta}_2(t),\ \widetilde{\gamma}_2(t) = \pi - \widetilde{\beta}_1(t),\ \widetilde{\gamma}_5(t) = \pi - \widetilde{\beta}_4(t)$ and $\widetilde{\gamma}_6(t) = \pi - \widetilde{\beta}_3(t).$

For $t \in]\frac{1}{3}, \frac{2}{3}]$:

- $\widetilde{\alpha}_i(t) = (2-3t)\alpha_i,\ i = 1, 4;$
- $\widetilde{\theta}_i(t) = \alpha_i - \theta_i + 3t\theta_i,\ i = 1, 4;$
- $\widetilde{\alpha}_k(t) = 2\alpha_k - \frac{\pi}{3} + 3t\left(\frac{\pi}{3} - \alpha_k\right),\ k = 2, 3;$
- $\widetilde{\theta}_2(t) = \pi - \widetilde{\alpha}_3(t)$ and $\widetilde{\theta}_3(t) = \pi - \widetilde{\alpha}_2(t).$

The paths that define the last stage of deformation are quite similar to the ones done for $\mathcal{B}^4$ in Chapter 3.

To show that ϕ is continuous at $t = 0$, let us consider $t \in]0, \frac{1}{3}[$. Then,

$$\begin{aligned} c(\tau_t^{o_t}, \tau_0) &= \sum_{\substack{F \text{face of} \\ \tau_t \cup \tau_0}} \lambda(F)\, Area(F) \\ &= 12 \times \left(\widetilde{\gamma}_2(0) + \widetilde{\beta}_2(t) + \widetilde{\gamma}_3(0) - \widetilde{\gamma}_3(t) - \pi\right) \\ &= 12 \times \left(\gamma_2 + \beta_2 + 3t\left(\frac{\pi}{3} - \beta_2\right) + \gamma_3 - (1-3t)\gamma_3 - \pi\right). \end{aligned}$$

When, $t \to 0^+$, $c(\tau_t^{o_t}, \tau_0) \to 0$.

For $t \in]0, \frac{1}{3}[$:

$$\begin{aligned} c(\tau_t^{o_t}, \tau_{\frac{1}{3}}) &= \sum_{\substack{F \text{face of} \\ \tau_t \cup \tau_{\frac{1}{3}}}} \lambda(F)\, Area(F) \\ &= 12 \times (\delta + \widetilde{\gamma}_2(t) + \widetilde{\gamma}_3(t) - \pi) \\ &= 12 \times \left(\delta + \pi - \beta_1 + 3t\left(\frac{\pi}{3} - \beta_1\right) + (1-3t)\gamma_3 - \pi\right). \end{aligned}$$

If $t \to \frac{1}{3}^-$, one has $c(\tau_t^{o_t}, \tau_{\frac{1}{3}}) \to 0$.

For $t \in]\frac{1}{3}, \frac{2}{3}[$:

$$\begin{aligned} c(\tau_t^{o_t}, \tau_{\frac{1}{3}}) &= \sum_{\substack{F \text{face of} \\ \tau_t \cup \tau_{\frac{1}{3}}}} \lambda(F)\, Area(F) \\ &= 6 \times \left(\widetilde{\alpha}_1 \left(\frac{1}{3} \right) - \widetilde{\alpha}_1(t) + \widetilde{\theta}_2 \left(\frac{1}{3} \right) + \widetilde{\alpha}_2(t) - \pi \right) \\ &= 6 \times \left(\alpha_1 - (2-3t)\alpha_1 + \pi - \alpha_3 + 2\alpha_2 - \frac{\pi}{3} + 3t \left(\frac{\pi}{3} - \alpha_2 \right) - \pi \right). \end{aligned}$$

If $t \to \frac{1}{3}^+$, one has $c(\tau_t^{o_t}, \tau_{\frac{1}{3}}) \to 0$ and consequently ϕ is continuous at $t = \frac{1}{3}$.

For $t \in]\frac{1}{3}, \frac{2}{3}[$:

$$\begin{aligned} c(\tau_t^{o_t}, \tau_{\frac{2}{3}}) &= \sum_{\substack{F \text{face of} \\ \tau_t \cup \tau_{\frac{2}{3}}}} \lambda(F)\, Area(F) \\ &= 6 \times \left(\widetilde{\alpha}_1(t) + \widetilde{\theta}_2(t) + \delta - \pi \right) \\ &= 6 \times \left((2-3t)\alpha_1 + \pi - 2\alpha_3 + \frac{\pi}{3} - 3t \left(\frac{\pi}{3} - \alpha_3 \right) + \delta - \pi \right). \end{aligned}$$

Consequently, $c(\tau_t^{o_t}, \tau_{\frac{2}{3}}) \to 0$, when $t \to \frac{2}{3}^-$. The continuity at $t = \frac{2}{3}^+$ and $t = 1^-$ is trivial.

6. Any member of the family $\mathcal{K}^m$, with $m \geq 4$ is deformable into τ^+_{stand}. Figure 4.154 shows the process of deformation of the member $\mathcal{K}^4$ and $\phi : [0,1] \to \mathscr{T}^{\mathcal{O}}(S^2)$ is a deformable map. This process is quite similar to the previous one. The angles are $\alpha = \frac{\pi}{4}$, $\gamma \approx 64.83°$, $\delta \approx 70.17°$ and $\beta \approx 115.17°$.

   For $t \in [0, \frac{1}{3}]$:

   - $\widetilde{\alpha}_1(t) = (1-3t)\alpha_1$;
   - $\widetilde{\gamma}_1(t) = \gamma_1 + 3t\alpha_1$;
   - $\widetilde{\beta}(t) = \beta + 3t\left(\frac{\pi}{4} - \beta\right)$;
   - $\widetilde{\gamma}_2(t) = \pi - \widetilde{\beta}(t)$.

For $t \in]\frac{1}{3}, \frac{2}{3}]$:

- $\widetilde{\theta}_1(t) = (2-3t)\theta_1$;
- $\widetilde{\lambda}_1(t) = \lambda_1 - \theta_1 + 3t\theta_1$;
- $\widetilde{\theta}_2(t) = 2\theta_2 - \frac{\pi}{4} + 3t\left(\frac{\pi}{4} - \theta_2\right)$;
- $\widetilde{\lambda}_2(t) = \pi - \widetilde{\theta}_2(t)$.

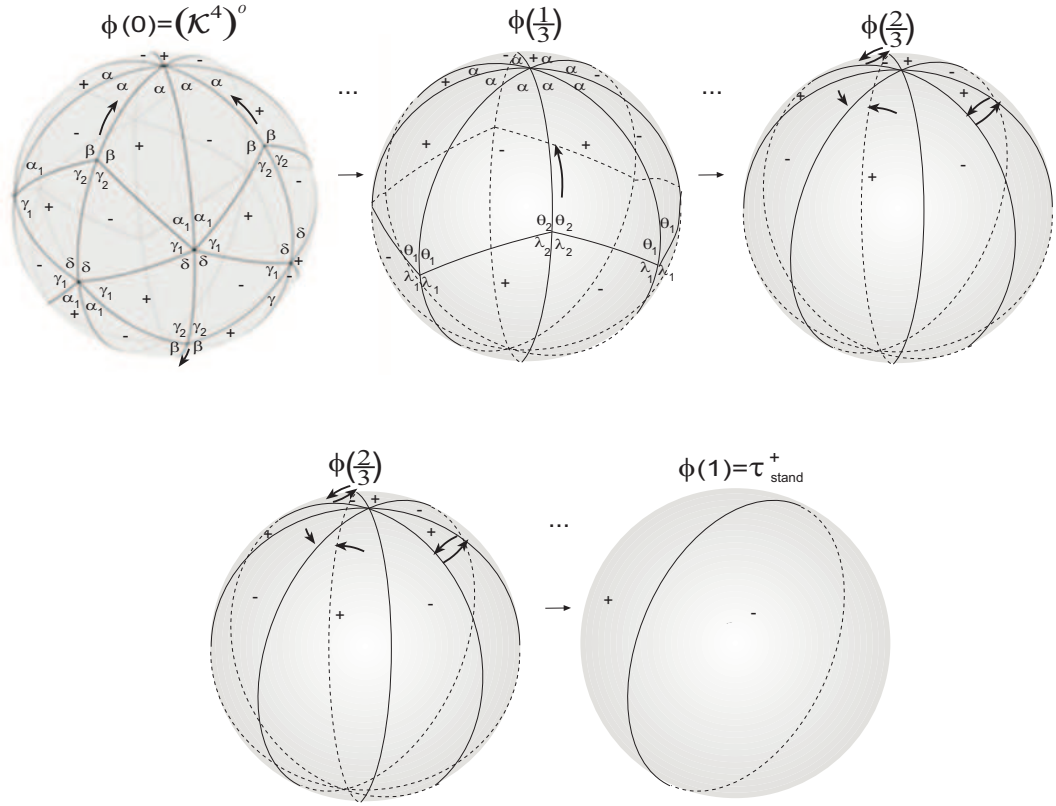

Figure 4.154: Deformation of $(\mathcal{K}^4)^o$.

The paths that define the last stage of deformation are quite similar to the ones done for $\mathcal{B}^4$ in Chapter 3.

The reasoning to prove that ϕ is continuous in $[0,1]$ is quite similar to the previous one.

7. The isolated dihedral f-tiling $\mathcal{I}$ is also deformable into τ^+_{stand}. Next figure helps us to define $\phi : [0,1] \to \mathscr{T}^{\mathcal{O}}(S^2)$. The angles are $\delta = \frac{\pi}{2}$, $\alpha = \gamma = \frac{\pi}{3}$ and $\beta = \frac{2\pi}{3}$.

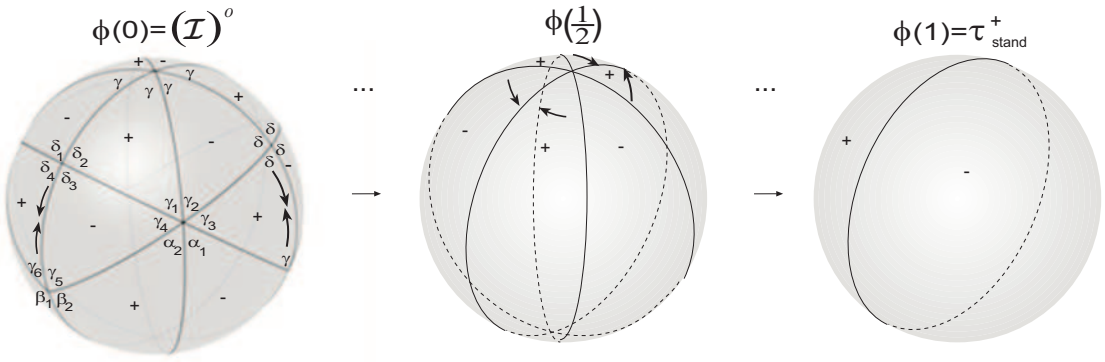

Figure 4.155: Deformation of $(\mathcal{I})^o$.

For $t \in [0, \frac{1}{2}]$:

- $\star$ $\widetilde{\gamma}_i(t) = (1-2t)\gamma_i,\ i = 3, 4;$
- $\star$ $\widetilde{\delta}_i(t) \equiv \delta,\ i = 1, 2, 3, 4;$
- $\star$ $\widetilde{\beta}_i(t) = \beta_i + t(\pi - 2\beta_i),\ i = 1, 2$ and $\widetilde{\gamma}_i(t) = \gamma_i + t(\pi - 2\gamma_i),\ i = 5, 6;$
- $\star$ $\widetilde{\alpha}_1(t) = \alpha_1 + t\gamma_3$ and $\widetilde{\alpha}_2(t) = \alpha_2 + t\gamma_4;$
- $\star$ $\widetilde{\gamma}_1(t) = \gamma_1 + t\gamma_4$ and $\widetilde{\gamma}_2(t) = \gamma_2 + t\gamma_3.$

In the last stage of the deformation, the paths are similar to the ones in Chapter 3 for $\mathcal{B}^4$.

We will prove that ϕ is continuous at $t = 0^-$ and $t = \frac{1}{2}^-$. So, for $t \in]0, \frac{1}{2}[$:

$$\begin{aligned} c(\tau_t^{o_t}, \tau_0) &= \sum_{\substack{F \text{face of} \\ \tau_t \cup \tau_0}} \lambda(F)\, Area(F) \\ &= 8 \times \left(\widetilde{\delta}_3(0) + \widetilde{\delta}_2(t) + \frac{\widetilde{\gamma}_4(0) - \widetilde{\gamma}_4(t)}{2} - \pi \right) \\ &= 8 \times \left(2\delta + \frac{\gamma_4 - (1-2t)\gamma_4}{2} - \pi \right). \end{aligned}$$

When, $t \to 0^+$, we conclude that $c(\tau_t^{o_t}, \tau_0) \to 0$.

Now, assuming that $t \in]0, \frac{1}{2}[$:

$$
\begin{aligned}
c(\tau_t^{ot}, \tau_{\frac{1}{2}}) &= \sum_{\substack{F \text{face of} \\ \tau_t \cup \tau_{\frac{1}{2}}}} \lambda(F)\, Area(F) \\
&= 6 \times \left(\widetilde{\gamma}_4(t) + \widetilde{\delta}_3(t) + \widetilde{\gamma}_5(t) - \pi \right) \\
&= 6 \times \left((1-2t)\gamma_4 + \delta + \gamma_5 + t(\pi - 2\gamma_5) - \pi \right).
\end{aligned}
$$

As $t \to \frac{1}{2}^-$, then $c(\tau_t^{ot}, \tau_{\frac{1}{2}}) \to 0$.

8. Dihedral f-tiling $\mathcal{J}$ is deformable into τ^-_{stand}. Figure 4.156 illustrates the process of deformation of $(\mathcal{J})^o$ into τ^-_{stand} and helps to define $\phi : [0,1] \to \mathscr{T}^{\mathcal{O}}(S^2)$. The angles are $\delta = \frac{\pi}{2}$, $\alpha = \gamma = \frac{\pi}{3}$ and $\beta = \frac{2\pi}{3}$.

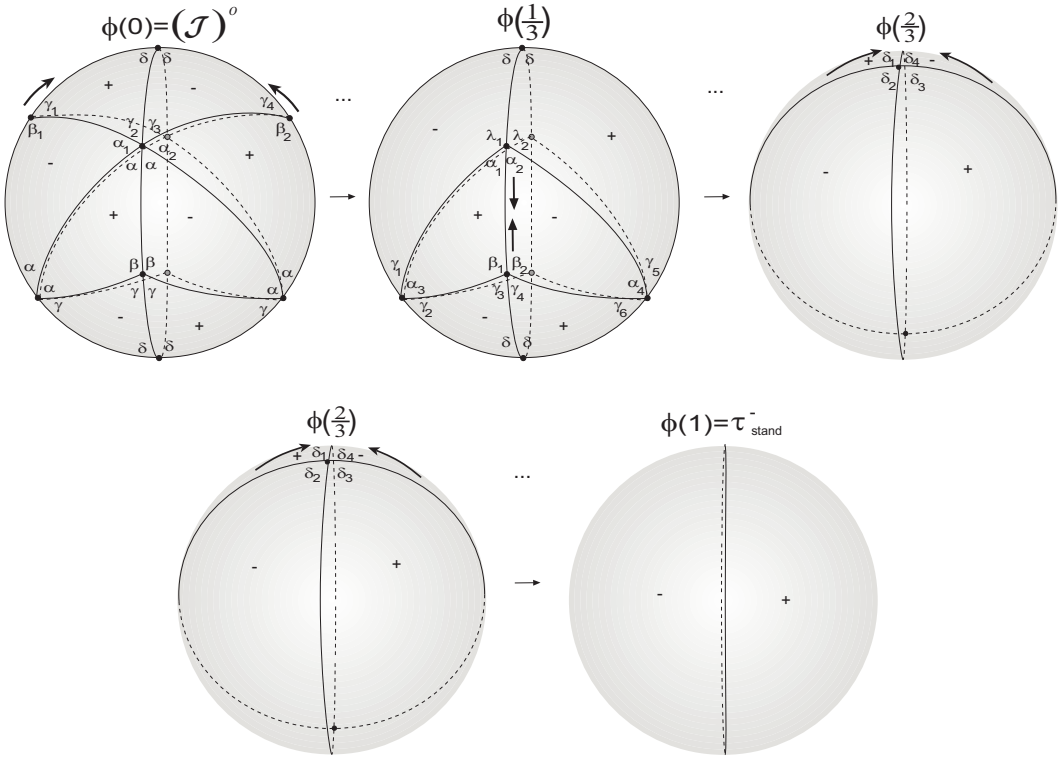

Figure 4.156: Deformation of $(\mathcal{J})^o$.

Then, for $t \in [0, \frac{1}{3}]$, one has:

- $\star$ $\widetilde{\gamma}_i(t) = (1-3t)\gamma_i,\ i = 2, 3$;
- $\star$ $\widetilde{\beta}_i(t) = \beta_i + t(\pi - 3\beta_i),\ i = 1, 2$ and $\widetilde{\gamma}_i(t) = \gamma_i + t(\pi - 3\gamma_i),\ i = 1, 4$;

$\star$ $\widetilde{\alpha}_i(t) = \alpha_i + 3t\gamma_{i+1},\ i = 1, 2.$

If $t \in]\frac{1}{3}, \frac{2}{3}]$:

$\star$ $\widetilde{\alpha}_i(t) = (2 - 3t)\alpha_i,\ i = 3, 4;$

$\star$ $\widetilde{\lambda}_i(t) = 2\lambda_i - \frac{\pi}{2} + 3t\left(\frac{\pi}{2} - \lambda_i\right),\ \widetilde{\alpha}_i(t) = 2\alpha_i - \frac{\pi}{2} + 3t\left(\frac{\pi}{2} - \alpha_i\right),$
$\widetilde{\beta}_i(t) = 2\beta_i - \frac{\pi}{2} + 3t\left(\frac{\pi}{2} - \beta_i\right),\ i = 1, 2$ and $\widetilde{\gamma}_k(t) = 2\gamma_k - \frac{\pi}{2} + 3t\left(\frac{\pi}{2} - \gamma_i\right),\ k = 3, 4;$

$\star$ $\widetilde{\gamma}_1(t) = \gamma_1 - \frac{\alpha_3}{3} + t\alpha_3,\ \widetilde{\gamma}_2(t) = \gamma_2 - \frac{\alpha_3}{3} + t\alpha_3,$
$\widetilde{\gamma}_5(t) = \gamma_5 - \frac{\alpha_4}{3} + t\alpha_4$ and $\widetilde{\gamma}_6(t) = \gamma_6 - \frac{\alpha_4}{3} + t\alpha_4.$

If $t \in]\frac{2}{3}, 1]$:

$\star$ $\widetilde{\delta}_i(t) = (3 - 3t)\delta_i,\ i = 1, 4;$

$\star$ $\widetilde{\delta}_2(t) = \pi - \widetilde{\delta}_4(t)$ and $\widetilde{\delta}_3(t) = \pi - \widetilde{\delta}_1(t).$

ϕ is continuous at $t = 0$: Considering $t \in]0, \frac{1}{2}[$, then,

$$\begin{aligned} c(\tau_t^{o_t}, \tau_0) &= \sum_{\substack{F\text{face of} \\ \tau_t \cup \tau_0}} \lambda(F)\, Area(F) \\ &= 4 \times \left(\widetilde{\gamma}_2(0) - \widetilde{\gamma}_2(t) + \widetilde{\gamma}_1(0) + \widetilde{\beta}_1(t) - \pi\right) \\ &= 4 \times \left(\gamma_2 - (1 - 3t)\gamma_2 + \gamma_1 + \beta_1 + t(\pi - 3\beta_1) - \pi\right). \end{aligned}$$

As $t \to 0^+$, then $c(\tau_t^{o_t}, \tau_0) \to 0$.

If $t \in]0, \frac{1}{3}[$:

$$\begin{aligned} c(\tau_t^{o_t}, \tau_{\frac{1}{3}}) &= \sum_{\substack{F\text{face of} \\ \tau_t \cup \tau_{\frac{1}{3}}}} \lambda(F)\, Area(F) \\ &= 4 \times \left(\widetilde{\gamma}_1(t) + \widetilde{\gamma}_2(t) + \frac{\pi}{2} - \pi\right) \\ &= 4 \times \left(\gamma_2 + t(\pi - 3\gamma_2) + (1 - 3t)\gamma_2 - \frac{\pi}{2}\right). \end{aligned}$$

For $t \to \frac{1}{3}^-$, we conclude that $c(\tau_t^{o_t}, \tau_{\frac{1}{3}}) \to 0$.

If $t \in]\frac{1}{3}, \frac{2}{3}[$, one has

$$\begin{aligned}
c(\tau_t^{o_t}, \tau_{\frac{1}{3}}) &= \sum_{\substack{F \text{face of} \\ \tau_t \cup \tau_{\frac{1}{3}}}} \lambda(F)\, Area(F) \\
&= 4 \times \left(\frac{\widetilde{\alpha}_3\left(\frac{1}{3}\right) - \widetilde{\alpha}_3(t)}{2} + \widetilde{\alpha}_1\left(\frac{1}{3}\right) + \widetilde{\lambda}_1(t) - \pi \right) \\
&+ 4 \times \left(\frac{\widetilde{\alpha}_3\left(\frac{1}{3}\right) - \widetilde{\alpha}_3(t)}{2} + \widetilde{\beta}_1\left(\frac{1}{3}\right) + \widetilde{\gamma}_3(t) - \pi \right) \\
&= 4 \times \left(\frac{\alpha_3 - (2-3t)\alpha_3}{2} + \alpha_1 + 2\lambda_1 - \frac{\pi}{2} + 3t\left(\frac{\pi}{2} - \lambda_1\right) - \pi \right) \\
&+ 4 \times \left(\frac{\alpha_3 - (2-3t)\alpha_3}{2} + \beta_1 + 2\gamma_3 - \frac{\pi}{2} + 3t\left(\frac{\pi}{2} - \gamma_3\right) - \pi \right).
\end{aligned}$$

For $t \to \frac{1}{3}^+$, we get $c(\tau_t^{o_t}, \tau_{\frac{1}{3}}) \to 0$. Therefore, ϕ is continuous at $t = \frac{1}{3}$.

Finally, if $t \in]\frac{2}{3}, 1[$:

$$\begin{aligned}
c(\tau_t^{o_t}, \tau_{\frac{2}{3}}) &= \sum_{\substack{F \text{face of} \\ \tau_t \cup \tau_{\frac{2}{3}}}} \lambda(F)\, Area(F) \\
&= 4 \times \left(\widetilde{\alpha}_1(t) + \widetilde{\alpha}_3(t) + \widetilde{\beta}_1(t) - \pi \right) \\
&= 4 \times [2\alpha_1 - \frac{\pi}{2} + 3t\left(\frac{\pi}{2} - \alpha_1\right) + (2-3t)\alpha_3 \\
&+ 2\beta_1 - \frac{\pi}{2} + 3t\left(\frac{\pi}{2} - \beta_1\right) - \pi].
\end{aligned}$$

Making $t \to \frac{2}{3}^-$, then $c(\tau_t^{o_t}, \tau_{\frac{2}{3}}) \to 0$.

The continuity at $t = \frac{2}{3}^+$ and $t = 1^-$ is trivial.

9. f-tiling $\mathcal{K}$ is deformable into τ_{stand}^+. In this case, the goal is to deform $\mathcal{K}$ in order to achieve the f-tiling $\mathcal{H}$ and consequently follow the same steps as in 4.. The angles are $\alpha = \frac{\pi}{3}$, $\beta \approx 71.774°$, $\gamma \approx 48.226°$ and $\delta = \frac{\pi}{2}$.

   Denoting by $\widehat{\alpha} \approx 65.905°, \widehat{\beta} = \frac{\pi}{3}, \widehat{\gamma} \approx 48.19°$, the angles of the f-tiling $\mathcal{H}$ in 4., for $t \in [0,1]$ we define:

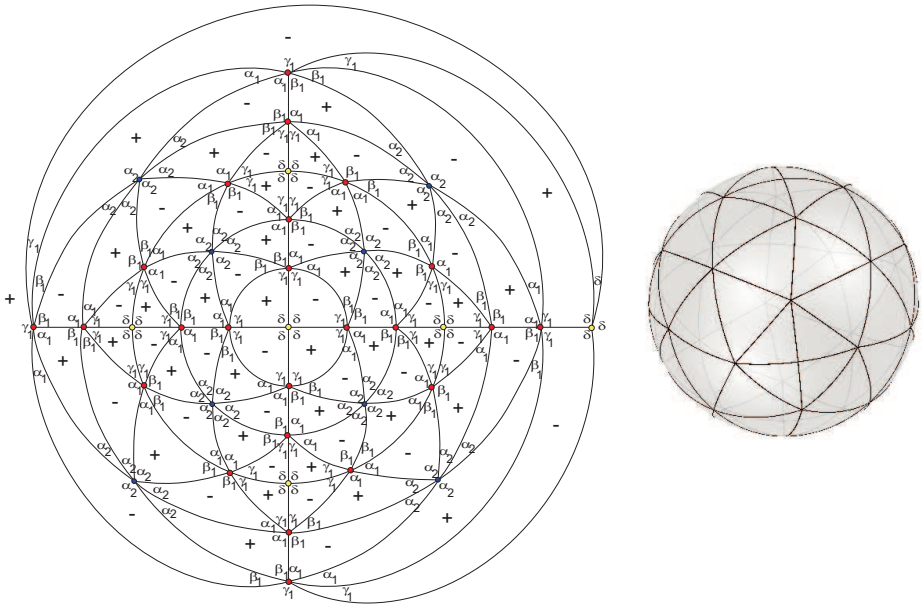

Figure 4.157: Deformation of $(\mathcal{K})^o$.

- $\star\ \widetilde{\alpha}_1(t) = \alpha_1 + t(\widehat{\alpha} - \alpha_1)$;
- $\star\ \widetilde{\alpha}_2(t) = \alpha_2 + t\left(\frac{\pi}{3} - \alpha_2\right)$;
- $\star\ \widetilde{\beta}_1(t) = \beta_1 + t\,(\widehat{\alpha} - \beta_1)$
- $\star\ \widetilde{\gamma}_1(t) = \gamma_1 + t\,(\widehat{\gamma} - \gamma_1)$.

10. For any $i = 1, \ldots, k$ and $k \geq 1$, $\mathcal{L}_i^{k,\delta}$ is deformable into τ_{stand}^+. Next figure shows a sketch of a deformation of $\mathcal{L}_1^{2,\delta}$, with $\phi : [0,1] \to \mathscr{T}^{\mathcal{O}}(S^2)$ be a deformable map. The angles are $\alpha = \gamma = \frac{\pi}{2}$ and $\beta = \pi - 2\delta$.

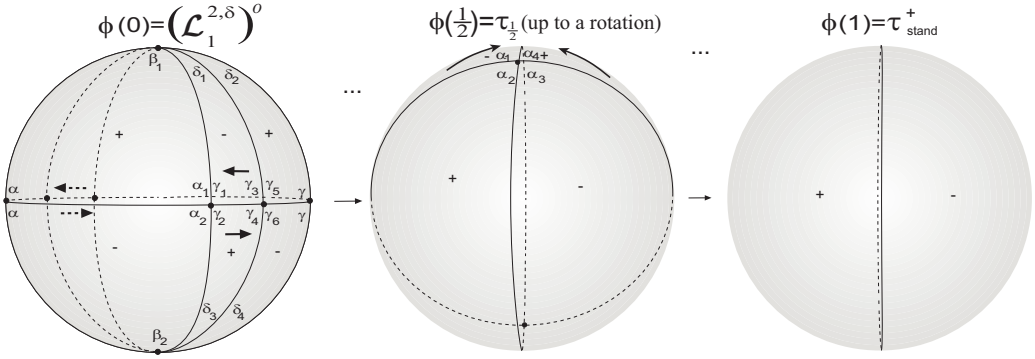

Figure 4.158: Deformation of $(\mathcal{L}_1^{2,\delta})^o$.

For $t \in [0, \frac{1}{2}]$:

- $\widetilde{\delta}_i(t) = (1-2t)\delta_i,\ i = 1, 3;$
- $\widetilde{\beta}_1(t) = \beta_1 + t\delta_1$ and $\widetilde{\delta}_2(t) = \delta_2 + t\delta_1;$
- $\widetilde{\beta}_2(t) = \beta_2 + t\delta_3$ and $\widetilde{\delta}_4(t) = \delta_4 + t\delta_3;$
- $\widetilde{\alpha}_i(t) = \alpha_i + 2t\left(\frac{\pi}{2} - \alpha_i\right),\ i = 1, 2$ and $\widetilde{\gamma}_i(t) = \gamma_i + 2t\left(\frac{\pi}{2} - \gamma_i\right),\ i = 1, \ldots, 6.$

If $t \in]\frac{1}{2}, 1]$:

- $\widetilde{\alpha}_i(t) = (2-2t)\alpha_i,\ i = 1, 4;$
- $\widetilde{\alpha}_2(t) = \pi - \widetilde{\alpha}_4(t)$ and $\widetilde{\alpha}_3(t) = \pi - \widetilde{\alpha}_1(t).$

To show that ϕ is continuous at $t = 0$, we will follow the same reasoning as in Chapter 2. Consider $t \in]0, \frac{1}{2}[$. Then,

$$\begin{aligned} c(\tau_t^{o_t}, \tau_0) &= \sum_{\substack{F\text{face of} \\ \tau_t \cup \tau_0}} \lambda(F)\, Area(F) \\ &= 8 \times \left(\frac{\widetilde{\delta}_1(0) - \widetilde{\delta}_1(t)}{2} + \frac{\pi}{2} + \frac{\pi}{2} - \pi \right) \\ &= 8 \times \left(\frac{\delta_1 - (1-2t)\delta_1}{2} \right). \end{aligned}$$

As $t \to 0^+$, then $c(\tau_t^{o_t}, \tau_0) \to 0$.

For $t \in]0, \frac{1}{2}[$:

$$\begin{aligned} c(\tau_t^{o_t}, \tau_{\frac{1}{2}}) &= \sum_{\substack{F\text{face of} \\ \tau_t \cup \tau_{\frac{1}{2}}}} \lambda(F)\, Area(F) \\ &= 4 \times \left(\widetilde{\delta}_1(t) + \frac{\pi}{2} + \frac{\pi}{2} - \pi \right) \\ &= 4 \times \left((1-2t)\delta_1 \right). \end{aligned}$$

Therefore, $c(\tau_t^{o_t}, \tau_{\frac{1}{2}}) \to 0$, for $t \to \frac{1}{2}^-$. The continuity at $t = \frac{1}{2}^+$ and $t = 1^-$ is trivial.

11. For each $m \geq 2,\ i = 1, \ldots, I$, $\mathcal{M}_i^{m,\delta}$ is deformable into τ_{stand}^+. Figure 4.159 shows a deformation of the member $\mathcal{M}_1^{2,\delta}$ and gives an idea of the deformable map $\phi : [0,1] \to \mathscr{T}^{\mathcal{O}}(S^2)$. The angles are $\alpha = \gamma = \frac{\pi}{2}$ and $\beta = \frac{\pi}{2} - \delta$.

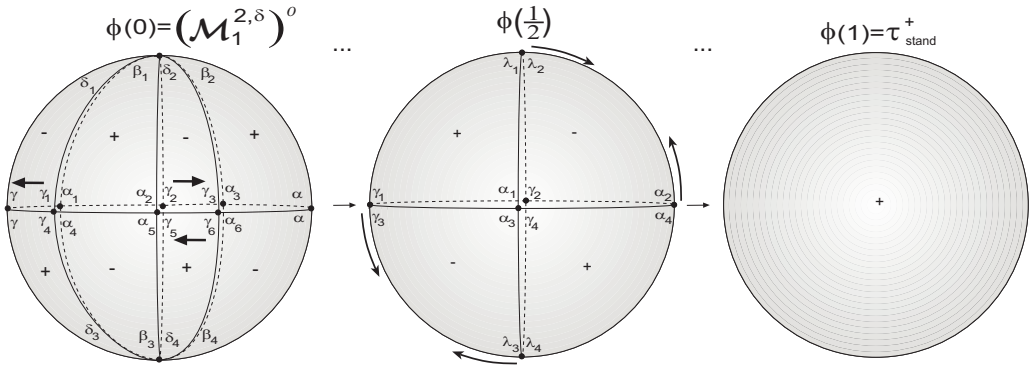

Figure 4.159: Deformation of $(\mathcal{M}_1^{2,\delta})^o$.

If $t \in [0, \frac{1}{2}]$, then:

- $\star\ \widetilde{\delta}_i(t) = (1-2t)\delta_i,\ i = 1,2,3,4;$
- $\star\ \widetilde{\beta}_i(t) = \beta_i + t(\delta_i + \delta_{i+1}),\ i = 1,3$ and $\widetilde{\beta}_i(t) = \beta_i + 2t\delta_i,\ i = 2,4;$
- $\star\ \widetilde{\alpha}_i(t) \equiv \alpha,\ \widetilde{\gamma}_i(t) \equiv \gamma,\ i = 1, \ldots, 6.$

For $t \in]\frac{1}{2}, 1]$, one has:

- $\star\ \widetilde{\gamma}_2(t) = (2-2t)\gamma_2$ and $\widetilde{\alpha}_3(t) = \pi - \widetilde{\gamma}_2(t);$
- $\star\ \widetilde{\alpha}_1(t) = \alpha_1 - \gamma_2 + 2t\gamma_2$ and $\widetilde{\gamma}_4(t) = \pi - \widetilde{\alpha}_1(t);$
- $\star\ \widetilde{\lambda}_i(t) = \widetilde{\gamma}_1(t) = \widetilde{\gamma}_3(t) = \widetilde{\alpha}_2(t) = \widetilde{\alpha}_4(t) \equiv \frac{\pi}{2},\ i = 1,2,3,4.$

To prove that ϕ is continuous in $[0,1]$, the steps are similar to the ones in Chapter 2 for $(\mathcal{A}_3^1)^o$.

12. Likewise, each member of the family $\mathcal{M}_i^{m,n,\delta},\ m,n \geq 1,\ i = 1, \ldots, I$ is deformable into τ_{stand}^+. Next figure shows a deformation of the member $\mathcal{M}_1^{1,2,\delta}$, with $\phi : [0,1] \to \mathscr{T}^{\mathcal{O}}(S^2)$ a deformable map. The angles are $\alpha = \gamma = \frac{\pi}{2}$ and $\beta = \pi - 2\delta$.

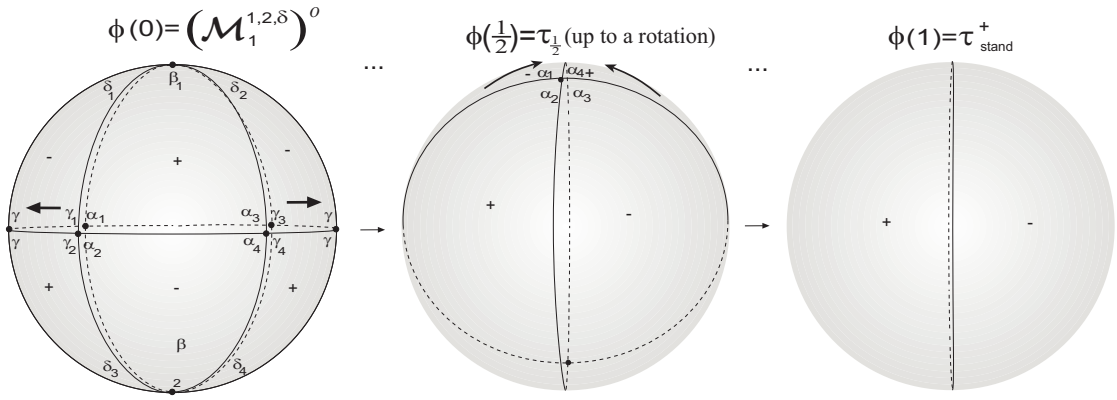

Figure 4.160: Deformation of $(\mathcal{M}_1^{1,2,\delta})^o$.

For $t \in [0, \frac{1}{2}]$:

- $\widetilde{\delta}_i(t) = (1-2t)\delta_i,\ i = 1,2,3,4;$
- $\widetilde{\beta}_1(t) = \beta_1 + t(\delta_1 + \delta_2)$ and $\widetilde{\beta}_2(t) = \beta_2 + t(\delta_3 + \delta_4);$
- $\widetilde{\alpha}_i(t) \equiv \alpha,\ \widetilde{\gamma}_i(t) \equiv \gamma,\ i = 1,2,3,4.$

If $t \in]\frac{1}{2}, 1]$:

- $\widetilde{\alpha}_i(t) = (2-2t)\alpha_i,\ i = 1,4;$
- $\widetilde{\alpha}_2(t) = \pi - \widetilde{\alpha}_4(t)$ and $\widetilde{\alpha}_3(t) = \pi - \widetilde{\alpha}_1(t).$

In the same way, the map ϕ is continuous in $[0,1]$.

13. For any $p \geq 1,\ i = 1, \ldots, I, \mathcal{N}_i^{p,\delta}$ is deformable into τ_{stand}^+. Figure 4.161 illustrates how to deform the member $(\mathcal{N}_1^{1,\delta})^o$ into τ_{stand} and how to define the map ϕ. The angles are $\alpha = \gamma = \frac{\pi}{2}$ and $\beta = \frac{\pi}{2} - \delta$.

    Then, if $t \in [0, \frac{1}{2}]$:

    - $\widetilde{\delta}_i(t) = (1-2t)\delta_i,\ i = 1,2,3,4;$
    - $\widetilde{\beta}_i(t) = \beta_i + 2t\delta_i,\ i = 1,2,3,4;$
    - $\widetilde{\alpha}_i(t) \equiv \gamma$ and $\widetilde{\gamma}_i(t) \equiv \gamma,\ i = 1,2,3,4.$

    For $t \in]\frac{1}{2}, 1]$:

$\star$ $\widetilde{\alpha}_2(t) = (2-2t)\alpha_2$ and $\widetilde{\lambda}_3(t) = \pi - \widetilde{\alpha}_2(t)$;

$\star$ $\widetilde{\lambda}_1(t) = \lambda_1 - \alpha_2 + 2t\alpha_2$ and $\widetilde{\alpha}_4(t) = \pi - \widetilde{\lambda}_1(t)$;

$\star$ $\widetilde{\gamma}_i(t) = \widetilde{\alpha}_1(t) = \widetilde{\alpha}_3(t) = \widetilde{\lambda}_2(t) = \widetilde{\lambda}_4(t) \equiv \frac{\pi}{2},\ i = 1,2,3,4.$

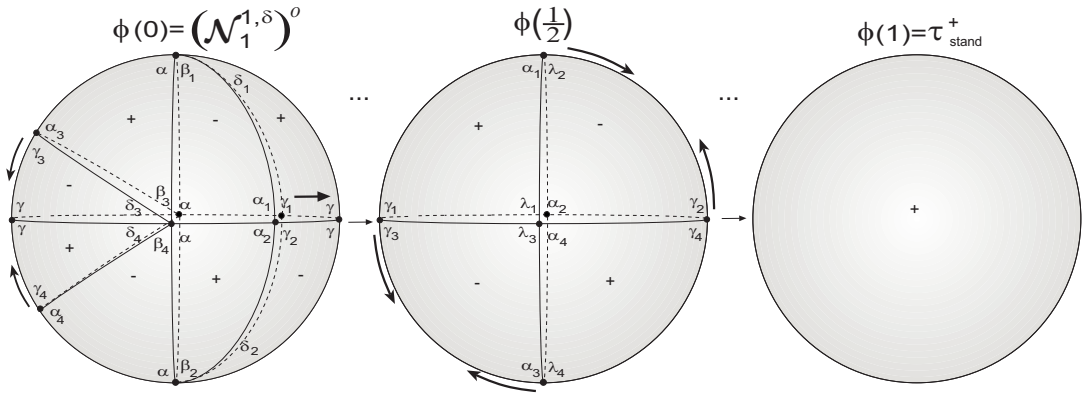

Figure 4.161: Deformation of $(\mathcal{N}_1^{1,\delta})^o$.

We only need to show that ϕ is continuous at $t = 0$ and $t = \frac{1}{2}^-$. Let us consider $t \in]0, \frac{1}{2}[$. Then,

$$\begin{aligned} c(\tau_t^{o_t}, \tau_0) &= \sum_{\substack{F \text{face of} \\ \tau_t \cup \tau_0}} \lambda(F)\, Area(F) \\ &= 4 \times \left(\widetilde{\delta}_1(0) - \widetilde{\delta}_1(t) + \widetilde{\gamma}_1(0) + \widetilde{\alpha}_1(t) - \pi\right) \\ &+ 4 \times \left(\widetilde{\delta}_3(0) - \widetilde{\delta}_3(t) + \widetilde{\gamma}_3(0) + \widetilde{\alpha}_3(t) - \pi\right) \\ &= 4 \times (\delta_1 - (1-2t)\delta_1 + 2\gamma - \pi) + 4 \times (\delta_3 - (1-2t)\delta_3 + 2\gamma - \pi)\,. \end{aligned}$$

For $t \to 0^+$, $c(\tau_t^{o_t}, \tau_0) \to 0$.

Now, if $t \in]0, \frac{1}{2}[$:

$$\begin{aligned} c(\tau_t^{o_t}, \tau_{\frac{1}{2}}) &= \sum_{\substack{F \text{face of} \\ \tau_t \cup \tau_{\frac{1}{2}}}} \lambda(F)\, Area(F) \\ &= 4 \times \left(\widetilde{\delta}_3(t) + \widetilde{\gamma}_3(t) + \gamma - \pi\right) + 4 \times \left(\widetilde{\delta}_1(t) + \widetilde{\gamma}_1(t) + \gamma - \pi\right) \\ &= 8 \times ((1-2t)\delta_3 + 2\gamma - \pi)\,. \end{aligned}$$

As $t \to \frac{1}{2}^-$, then $c(\tau_t^{ot}, \tau_{\frac{1}{2}}) \to 0$.

14. Any member of the family $\mathcal{O}_i^{p,t},\ p \geq 1,\ i = 1, \ldots, I$ is deformable into τ_{stand}^+. Next figure shows a deformation of $(\mathcal{O}_2^{1,3})^o$ into τ_{stand}^+, with $\phi : [0,1] \to \mathscr{T}^{\mathcal{O}}(S^2)$ a deformable map. The angles are $\alpha = \gamma = \frac{\pi}{2},\ \beta = \frac{\pi}{6}$ and $\delta = \frac{\pi}{3}$.

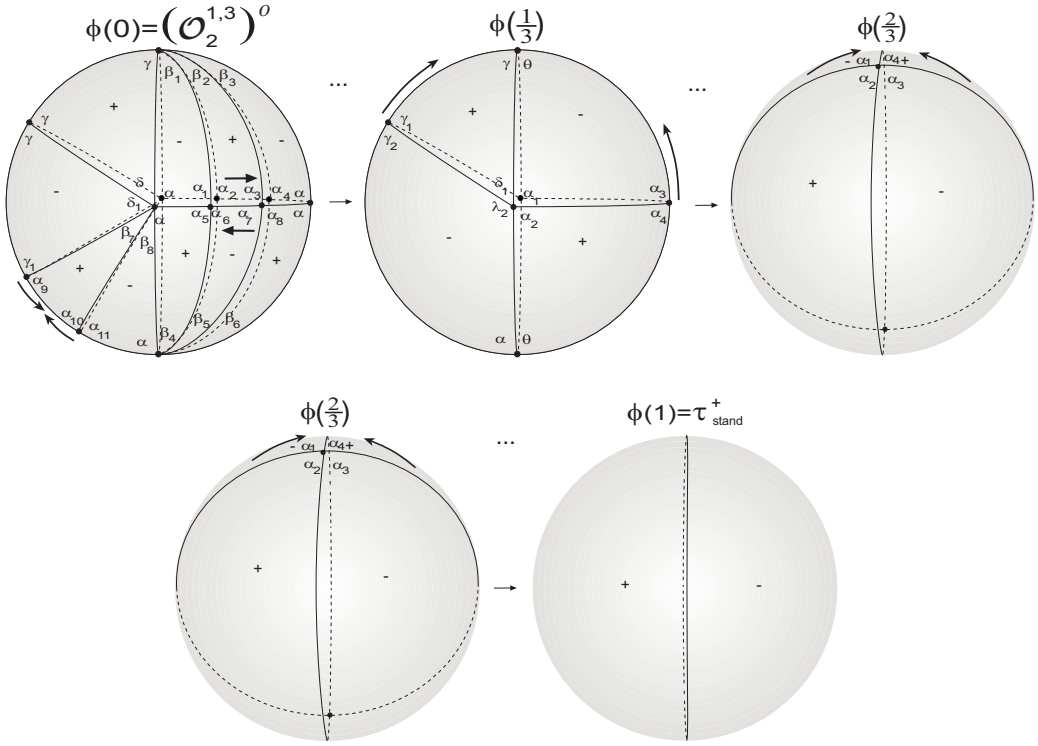

Figure 4.162: Deformation of $(\mathcal{O}_2^{1,3})^o$.

In the first stage of the deformation, $t \in [0, \frac{1}{3}]$, we have:

- $\widetilde{\beta}_i(t) = (1 - 3t)\beta_i,\ i = 2, 5, 7;$
- $\widetilde{\beta}_i(t) = \beta_i + \frac{3}{2}t\beta_2,\ i = 1, 3,\ \widetilde{\beta}_i(t) = \beta_i + \frac{3}{2}t\beta_5,\ i = 4, 6,\ \widetilde{\delta}_1(t) = \delta_1 + \frac{3}{2}t\beta_7$ and $\widetilde{\beta}_8(t) = \beta_8 + \frac{3}{2}t\beta_7;$
- $\widetilde{\alpha}_i(t) \equiv \alpha,\ i = 1, \ldots, 11$ and $\widetilde{\gamma}_1(t) \equiv \gamma.$

In the second stage, $t \in]\frac{1}{3}, \frac{2}{3}]$:

- $\widetilde{\delta}_1(t) = (2 - 3t)\delta_1,\ \widetilde{\alpha}_1(t) = (2 - 3t)\alpha_1;$
- $\widetilde{\alpha}_2(t) = \pi - \widetilde{\delta}_1(t)$ and $\widetilde{\lambda}_2(t) = \pi - \widetilde{\alpha}_1(t);$

$\star$ $\widetilde{\gamma}_i(t) \equiv \gamma,\ i = 1, 2$ and $\widetilde{\alpha}_k(t) \equiv \theta,\ k = 3, 4.$

In the third stage of the deformation, $t \in]\frac{2}{3}, 1]$:

$\star$ $\widetilde{\alpha}_i(t) = (3 - 3t)\alpha_i,\ i = 1, 4;$

$\star$ $\widetilde{\alpha}_2(t) = \pi - \widetilde{\alpha}_4(t)$ and $\widetilde{\alpha}_3(t) = \pi - \widetilde{\alpha}_1(t).$

Let us show that ϕ is continuous at $t = 0$: For $t \in]0, \frac{1}{3}[$, then

$$\begin{aligned} c(\tau_t^{o_t}, \tau_0) &= \sum_{\substack{F \text{face of} \\ \tau_t \cup \tau_0}} \lambda(F)\, Area(F) \\ &= 4 \times \left(\widetilde{\alpha}_9(0) + \widetilde{\gamma}_1(t) + \frac{\widetilde{\beta}_7(0) - \widetilde{\beta}_7(t)}{2} - \pi \right) \\ &+ 8 \times \left(\widetilde{\alpha}_2(0) + \widetilde{\alpha}_1(t) + \frac{\widetilde{\beta}_2(0) - \widetilde{\beta}_2(t)}{2} - \pi \right) \\ &= 4 \times \left(\gamma + \gamma + \frac{\beta_7 - (1 - 3t)\beta_7}{2} - \pi \right) \\ &+ 8 \times \left(\gamma + \gamma + \frac{\beta_2 - (1 - 3t)\beta_2}{2} - \pi \right). \end{aligned}$$

For $t \to 0^+$, one has $c(\tau_t^{o_t}, \tau_0) \to 0$.

Consider now that $t \in]0, \frac{1}{3}[$. Then,

$$\begin{aligned} c(\tau_t^{o_t}, \tau_{\frac{1}{3}}) &= \sum_{\substack{F \text{face of} \\ \tau_t \cup \tau_{\frac{1}{3}}}} \lambda(F)\, Area(F) \\ &= 2 \times \left(\widetilde{\beta}_7(t) + \widetilde{\alpha}_9(t) + \widetilde{\alpha}_{10}(t) - \pi \right) \\ &+ 4 \times \left(\widetilde{\beta}_2(t) + \widetilde{\alpha}_2(t) + \widetilde{\alpha}_3(t) - \pi \right) \\ &= 2 \times ((1 - 3t)\beta_7 + 2\gamma - \pi) + 4 \times ((1 - 3t)\beta_2 + 2\gamma - \pi). \end{aligned}$$

For $t \to \frac{1}{3}^-$, we get $c(\tau_t^{o_t}, \tau_{\frac{1}{3}}) \to 0$.

If $t \in]\frac{1}{3}, \frac{2}{3}[$:

$$
\begin{aligned}
c(\tau_t^{o_t}, \tau_{\frac{1}{3}}) &= \sum_{\substack{F\text{face of} \\ \tau_t \cup \tau_{\frac{1}{3}}}} \lambda(F)\, Area(F) \\
&= 2 \times \left(\widetilde{\gamma}_1 \left(\frac{1}{3} \right) + \widetilde{\gamma}_2(t) + \widetilde{\delta}_1 \left(\frac{1}{3} \right) - \widetilde{\delta}_1(t) - \pi \right) \\
&+ 2 \times \left(\widetilde{\alpha}_3 \left(\frac{1}{3} \right) + \widetilde{\alpha}_4(t) + \widetilde{\alpha}_1 \left(\frac{1}{3} \right) - \widetilde{\alpha}_1(t) - \pi \right) \\
&= 2 \times (2\gamma + \delta_1 - (2-3t)\delta_1 - \pi) + 2 \times (2\theta + \alpha_1 - (2-3t)\alpha_1 - \pi)\,.
\end{aligned}
$$

For $t \to \frac{1}{3}^+$, we conclude that $c(\tau_t^{o_t}, \tau_{\frac{1}{3}}) \to 0$.

Assuming that $t \in]\frac{1}{3}, \frac{2}{3}[$,

$$
\begin{aligned}
c(\tau_t^{o_t}, \tau_{\frac{2}{3}}) &= \sum_{\substack{F\text{face of} \\ \tau_t \cup \tau_{\frac{2}{3}}}} \lambda(F)\, Area(F) \\
&= 2 \times \left(\widetilde{\delta}_1(t) + \widetilde{\gamma}_1(t) + \gamma - \pi \right) + 2 \times (\widetilde{\alpha}_1(t) + \widetilde{\alpha}_3(t) + \theta - \pi) \\
&= 2 \times ((2-3t)\delta_1 + 2\gamma + (2-3t)\alpha_1 + 2\theta - 2\pi)\,.
\end{aligned}
$$

As $t \to \frac{2}{3}^-$, then $c(\tau_t^{o_t}, \tau_{\frac{2}{3}}) \to 0$.

The continuity of ϕ at $t = \frac{2}{3}^+$ and $t = 1^-$ is trivial.

15. Any member of the family $\mathcal{N}_i^{p,q,\delta},\ p, q \geq 1,\ i = 1, \ldots, I$ is deformable into τ_{stand}^-. Next figure shows a deformation of $(\mathcal{N}_1^{1,2,\delta})^o$ into τ_{stand}^-. The angles are $\alpha = \gamma = \frac{\pi}{2}$ and $\beta = \frac{\pi}{2} - 2\delta$.

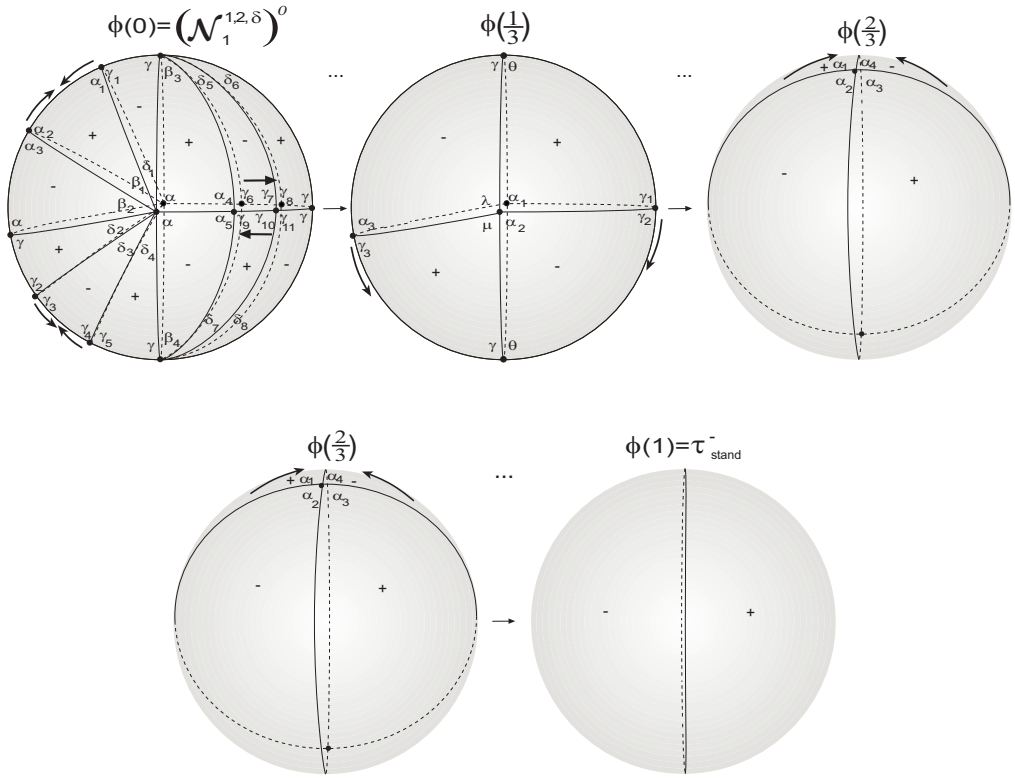

Figure 4.163: Deformation of $(\mathcal{N}_1^{1,2,\delta})^o$.

For $t \in [0, \frac{1}{3}]$:

- $\widetilde{\beta}_1(t) = (1-3t)\beta_1$ and $\widetilde{\delta}_i(t) = (1-3t)\delta_i,\ i = 3, 5, 7$;
- $\widetilde{\delta}_1(t) = \delta_1 + \frac{3}{2}t\beta_1$ and $\widetilde{\delta}_4(t) = \delta_4 + \frac{3}{2}t\delta_3$;
- $\widetilde{\beta}_2(t) = \beta_2 + \frac{3}{2}t\beta_1$ and $\widetilde{\delta}_2(t) = \delta_2 + \frac{3}{2}t\delta_3$;
- $\widetilde{\beta}_3(t) = \beta_3 + \frac{3}{2}t\delta_5$ and $\widetilde{\beta}_4(t) = \beta_4 + \frac{3}{2}t\delta_7$;
- $\widetilde{\delta}_i(t) = \delta_i + \frac{3}{2}t\delta_{i-1},\ i = 6, 8$;
- $\widetilde{\alpha}_i(t) \equiv \alpha,\ i = 1, 2, 3, 4, 5$ and $\widetilde{\gamma}_i(t) \equiv \alpha,\ i = 1, \ldots, 11$.

If $t \in]\frac{1}{3}, \frac{2}{3}]$:

- $\widetilde{\alpha}_2(t) = (2-3t)\alpha_2$ and $\widetilde{\mu}(t) = (2-3t)\mu$;
- $\widetilde{\lambda}(t) = \pi - \widetilde{\alpha}_2(t)$ and $\widetilde{\alpha}_1(t) = \pi - \widetilde{\mu}(t)$;
- $\widetilde{\alpha}_3(t) \equiv \theta,\ \widetilde{\gamma}_1(t) \equiv \gamma$ and $\widetilde{\gamma}_i(t) \equiv \gamma,\ i = 2, 3$.

If $t \in]\frac{2}{3}, 1]$:

- $\star$ $\widetilde{\alpha}_i(t) = (3-3t)\alpha_i,\ i = 1, 4$;
- $\star$ $\widetilde{\alpha}_2(t) = \pi - \widetilde{\alpha}_4(t)$ and $\widetilde{\alpha}_3(t) = \pi - \widetilde{\alpha}_1(t)$.

To prove that ϕ is continuous in $[0, 1]$, we follow the same reasoning done for the deformation of $\mathcal{O}_i^{p,t},\ p \geq 1,\ i = 1, \ldots, I$.

16. For each $t \geq 2,\ p, q \geq 1,\ i = 1, \ldots, I$, $\mathcal{O}_i^{p,q,t}$ is deformable into τ_{stand}^+. Next figure shows a deformation of $(\mathcal{O}_1^{1,2,2})^o$ into τ_{stand}^+, with $\alpha = \gamma = \frac{\pi}{2},\ \beta = \frac{\pi}{4}$ and $\delta = \frac{\pi}{8}$.

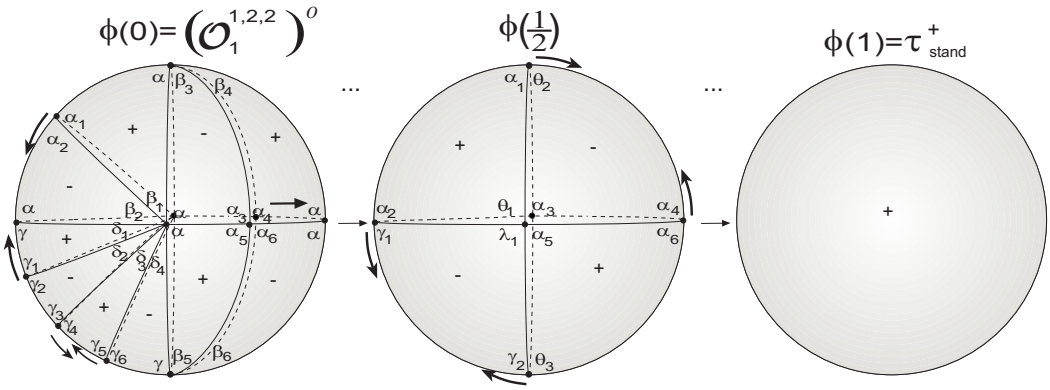

Figure 4.164: Deformation of $(\mathcal{O}_1^{1,2,2})^o$.

For $t \in [0, \frac{1}{2}]$:

- $\star$ $\widetilde{\beta}_i(t) = (1-2t)\beta_i,\ i = 2, 4, 6$ and $\widetilde{\delta}_i(t) = (1-2t)\delta_i,\ i = 1, 3$;
- $\star$ $\widetilde{\beta}_i(t) = \beta_i + 2t\beta_{i+1},\ i = 1, 3, 5$;
- $\star$ $\widetilde{\delta}_2(t) = \delta_2 + 2t\delta_1 + t\delta_3$ and $\widetilde{\delta}_4(t) = \delta_4 + t\delta_3$;
- $\star$ $\widetilde{\alpha}_i(t) \equiv \alpha,\ i = 1, \ldots, 6$ and $\widetilde{\gamma}_i(t) \equiv \alpha,\ i = 1, \ldots, 6$.

If $t \in]\frac{1}{2}, 1]$:

- $\star$ $\widetilde{\alpha}_3(t) = (2-2t)\alpha_3$ and $\widetilde{\lambda}_1(t) = \pi - \widetilde{\alpha}_3(t)$;
- $\star$ $\widetilde{\theta}_1(t) = \theta_1 - \alpha_3 + 2t\alpha_3$ and $\widetilde{\alpha}_5(t) = \pi - \widetilde{\theta}_1(t)$;
- $\star$ $\widetilde{\alpha}_i(t) \equiv \alpha,\ i = 1, 2, 4, 6,\ \widetilde{\gamma}_j(t) \equiv \alpha,\ j = 1, 2$ and $\widetilde{\theta}_k(t) \equiv \alpha,\ k = 2, 3$.

To prove the continuity of ϕ continuous in $[0,1]$, we follow a similar reasoning to the one done for the deformation of $\mathcal{N}_i^{p,\delta},\ p \geq 1,\ i = 1,\ldots,I$.

17. For any $k \geq 4$, $\mathcal{Q}^k$ is deformable into τ_{stand}^-. Next figure gives us a geometrical sketch of a deformation of the member $\mathcal{Q}^4$, where the angles are $\gamma = \frac{\pi}{4},\ \alpha = \frac{3\pi}{8},\ \beta \approx 65.53°$ and $\delta \approx 114.47°$.

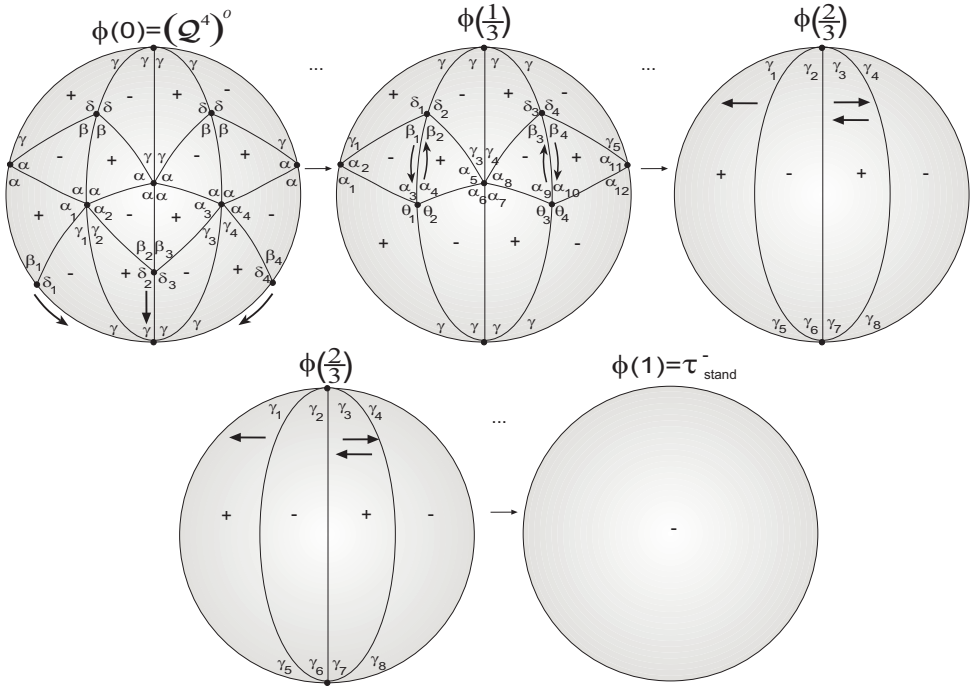

Figure 4.165: Deformation of $(\mathcal{Q}^4)^o$.

For $t \in [0, \frac{1}{3}]$:

- $\star\ \widetilde{\gamma}_i(t) = (1-3t)\gamma_i,\ i = 1,2,3,4;$
- $\star\ \widetilde{\beta}_i(t) = \beta_i + 3t\left(\frac{\pi}{4} - \beta_i\right)$ and $\widetilde{\delta}_i(t) = \delta_i + 3t\left(\frac{\pi}{4} - \delta_i\right),\ i = 1,2,3,4;$
- $\star\ \widetilde{\alpha}_i(t) = \alpha_i + 3t\gamma_i,\ i = 1,2,3,4.$

If $t \in]\frac{1}{3}, \frac{2}{3}]$:

- $\star\ \widetilde{\alpha}_i(t) = (2-3t)\alpha_i,\ i = 2,5,8,11;$
- $\star\ \widetilde{\delta}_i(t) = \frac{3\pi}{2}t - \frac{\pi}{2} + (2-3t)\delta_i,\ \widetilde{\beta}_i(t) = \frac{3\pi}{2}t - \frac{\pi}{2} + (2-3t)\beta_i,\ \widetilde{\theta}_i(t) = \frac{3\pi}{2}t - \frac{\pi}{2} + (2-3t)\theta_i,\ i = 1,2,3,4$ and $\widetilde{\alpha}_k(t) = \frac{3\pi}{2}t - \frac{\pi}{2} + (2-3t)\alpha_k,\ k = 3,4,9,10;$

$\star$ $\widetilde{\alpha}_i(t) = \alpha_i + \frac{\alpha_{i+1}}{2}(3t-1),\ i = 1, 7$ and $\widetilde{\alpha}_j(t) = \alpha_j + \frac{\alpha_{j-1}}{2}(3t-1),\ j = 6, 12.$

For $t \in]\frac{2}{3}, 1]$:

$\star$ $\widetilde{\gamma}_i(t) = 3(1-t)\gamma_i,\ i = 1, 3, 5, 7;$

$\star$ $\widetilde{\gamma}_j(t) = \gamma_j - 2\gamma_{j-1} - \gamma_{j+1} + 3t\left(\gamma_{j-1} + \frac{\gamma_{j+1}}{2}\right),\ j = 2, 6$ and $\widetilde{\gamma}_k(t) = \gamma_k + (3t-2)\gamma_{k-1},\ k = 4, 8.$

The steps to prove that ϕ is continuous in $[0, 1]$ are the same done for $\mathcal{B}^4$ in Chapter 3.

18. Any member of the family $\mathcal{R}^k_t,\ k \neq t,\ k, t > 2$ is deformable into τ^+_{stand}. Next figure shows a sketch of a deformation of $\mathcal{R}^2_3$ into τ^+_{stand}, where $\alpha = \gamma = \frac{\pi}{2},\ \beta = \frac{\pi}{4}$ and $\delta = \frac{\pi}{6}$.

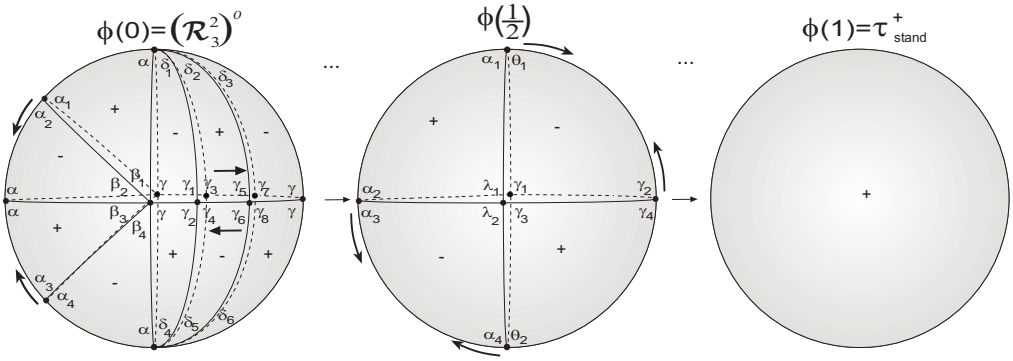

Figure 4.166: Deformation of $(\mathcal{R}^2_3)^o$.

For $t \in [0, \frac{1}{2}]$:

$\star$ $\widetilde{\beta}_i(t) = (1-2t)\beta_i,\ i = 2, 3$ and $\widetilde{\delta}_j(t) = (1-2t)\delta_j,\ j = 2, 5;$

$\star$ $\widetilde{\beta}_1(t) = \beta_1 + t\beta_2,\ \widetilde{\beta}_4(t) = \beta_4 + t\beta_3,\ \widetilde{\delta}_j(t) = \delta_j + t\delta_2,\ j = 1, 3$ and $\widetilde{\delta}_k(t) = \delta_k + t\delta_5,\ k = 4, 6;$

$\star$ $\widetilde{\alpha}_i(t) \equiv \alpha,\ i = 1, 2, 3, 4$ and $\widetilde{\gamma}_j(t) \equiv \gamma,\ j = 1, \ldots, 8.$

If $t \in]\frac{1}{2}, 1]$:

$\star$ $\widetilde{\gamma}_1(t) = (2-2t)\gamma_1$ and $\widetilde{\lambda}_2(t) = \pi - \widetilde{\gamma}_1(t);$

$\star$ $\widetilde{\lambda}_1(t) = \lambda_1 - \gamma_1 + 2t\gamma_1$ and $\widetilde{\gamma}_3(t) = \pi - \widetilde{\lambda}_1(t)$;

$\star$ $\widetilde{\alpha}_i(t) = \widetilde{\theta}_1(t) = \widetilde{\theta}_2(t) = \widetilde{\gamma}_2(t) = \widetilde{\gamma}_4(t) \equiv \frac{\pi}{2},\ i = 1, 2, 3, 4.$

The reasoning to prove the continuity of ϕ in $[0, 1]$ is similar to the one done for $\mathcal{N}_1^{1,\delta}$.

19. Each member of the family of dihedral f-tilings $\mathcal{S}^k,\ \geq 4$ is deformable into τ^+_{stand}. Figure 4.167 shows the process of deformation of the member $\mathcal{S}^4$, with $\gamma = \frac{\pi}{4},\ \beta = \frac{\pi}{2},\ \alpha = \frac{\pi}{3}$ and $\delta = \frac{2\pi}{3}$.

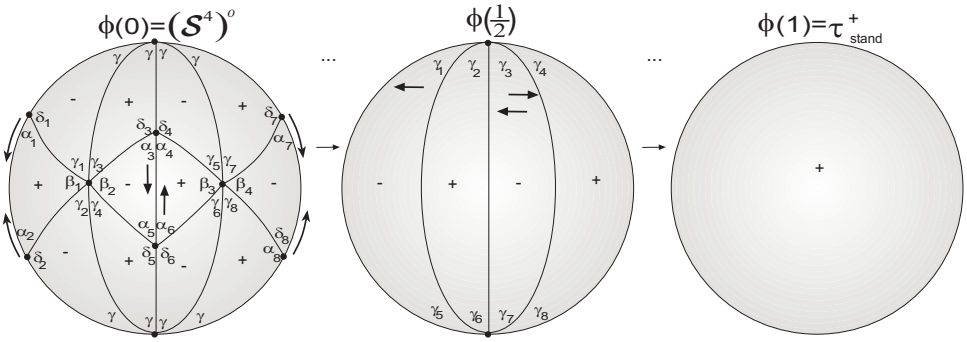

Figure 4.167: Deformation of $(\mathcal{S}^4)^o$.

For $t \in [0, \frac{1}{2}]$:

$\star$ $\widetilde{\beta}_i(t) = (1 - 2t)\beta_i,\ i = 1, 2, 3, 4;$

$\star$ $\widetilde{\alpha}_i(t) = \alpha_i + 2t\left(\frac{\pi}{2} - \alpha_i\right)$ and $\widetilde{\delta}_i(t) = \delta_i + 2t\left(\frac{\pi}{2} - \delta_i\right),\ i = 1, \ldots, 8;$

$\star$ $\widetilde{\gamma}_i(t) = \gamma_i + t\beta_1,\ i = 1, 2,\ \widetilde{\gamma}_j(t) = \gamma_j + t\beta_2,\ j = 3, 4,\ \widetilde{\gamma}_k(t) = \gamma_k + t\beta_3,\ k = 5, 6,$ and $\widetilde{\gamma}_l(t) = \gamma_l + t\beta_4,\ l = 7, 8.$

If $t \in]\frac{1}{2}, 1]$:

$\star$ $\widetilde{\gamma}_i(t) = 2(1 - t)\gamma_i,\ i = 1, 3, 5, 7;$

$\star$ $\widetilde{\gamma}_j(t) = \gamma_j - 2\gamma_{j-1} - \gamma_{j+1} + 3t\left(\gamma_{j-1} + \frac{\gamma_{j+1}}{2}\right),\ j = 2, 6$ and $\widetilde{\gamma}_k(t) = \gamma_k + (2t - 1)\gamma_{k-1},\ k = 4, 8.$

We only need to prove that ϕ is continuous at $t = 0^+$ and $t = \frac{1}{2}^-$.

If $t \in]0, \frac{1}{2}[$:

$$\begin{aligned} c(\tau_t^{o_t}, \tau_0) &= \sum_{\substack{F \text{face of} \\ \tau_t \cup \tau_0}} \lambda(F)\, Area(F) \\ &= 8 \times \left(\widetilde{\alpha}_1(0) + \widetilde{\delta}_1(t) + \frac{\widetilde{\beta}_1(0) - \widetilde{\beta}_1(t)}{2} - \pi \right) \\ &+ 8 \times \left(\widetilde{\alpha}_3(0) + \widetilde{\delta}_3(t) + \frac{\widetilde{\beta}_2(0) - \widetilde{\beta}_2(t)}{2} - \pi \right) \\ &8 \times \left(2\alpha_1 + 2\delta_1 + \frac{\beta_1 - (1-2t)\beta_1}{2} + \frac{\beta_2 - (1-2t)\beta_2}{2} - 2\pi \right). \end{aligned}$$

As $t \to 0^+$, then $c(\tau_t^{o_t}, \tau_0) \to 0$.

Now, for $t \in]0, \frac{1}{2}[$:

$$\begin{aligned} c(\tau_t^{o_t}, \tau_{\frac{1}{2}}) &= \sum_{\substack{F \text{face of} \\ \tau_t \cup \tau_{\frac{1}{2}}}} \lambda(F)\, Area(F) \\ &= 4 \times \left(\widetilde{\beta}_1(t) + \widetilde{\alpha}_1(t) + \widetilde{\alpha}_2(t) - \pi \right) + 4 \times \left(\widetilde{\beta}_2(t) + \widetilde{\alpha}_3(t) + \widetilde{\alpha}_5(t) - \pi \right) \\ &= 4 \times \left(2(1-2t)\beta_1 + 4 \left(\alpha_1 + 2t \left(\frac{\pi}{2} - \alpha_1 \right) \right) - 2\pi \right). \end{aligned}$$

Since $t \to \frac{1}{2}^-$, then $c(\tau_t^{o_t}, \tau_{\frac{1}{2}}) \to 0$.

20. Any representant of the family of dihedral f-tilings denoted by $\mathcal{T}^k,\ k \geq 3$ is deformable into τ_{stand}^+. Figure 4.168 illustrates the deformation of $\mathcal{T}^3$ into τ_{stand}^+. The angles are $\alpha = \frac{\pi}{3},\ \delta = \frac{2\pi}{3},\ \beta = \frac{\pi}{2}$ and $\gamma = \frac{\pi}{4}$.

    If $t \in [0, \frac{1}{3}]$:

    - $\widetilde{\beta}_i(t) = (1-3t)\beta_i,\ i = 1, 2, 3, 4, 5, 6;$
    - $\widetilde{\delta}_i(t) = \delta_i + t\,(\pi - 3\delta_i)\,,\ i = 1, 2, 3, 4, 5, 6;$
    - $\widetilde{\alpha}_1(t) = \pi - \widetilde{\delta}'_1(t),\ \widetilde{\alpha}_j(t) = \pi - \widetilde{\delta}_{j-1}(t),\ j = 3, 5$ and $\widetilde{\alpha}_k(t) = \pi - \widetilde{\delta}_{k+1}(t),\ k = 2, 4$, where $\widetilde{\delta}'_1(t) = \delta'_1 + t\,(\pi - 3\delta'_1)$ belongs to the semi-space $x \leq 0$.

    If $t \in]\frac{1}{3}, \frac{2}{3}]$:

$\star$ $\widetilde{\lambda}_i(t) = (2-3t)\lambda_i,\ i = 2, 3, 6;$

$\star$ $\widetilde{\lambda}_i(t) = 2\lambda_i - \frac{\pi}{3} + t\,(\pi - 3\lambda_i)\,,\ i = 1, 4, 5;$

$\star$ $\widetilde{\theta}_1(t) = \pi - \widetilde{\lambda}'_1(t),\ \widetilde{\theta}_4(t) = \pi - \widetilde{\lambda}_5(t)$ and $\widetilde{\theta}_5(t) = \pi - \widetilde{\lambda}_4(t)$, where $\widetilde{\lambda}'_1(t) = 2\lambda'_1 - \frac{\pi}{3} + t\,(\pi - 3\lambda'_1)$ belongs to the semi-space $x \leq 0$.

If $t \in]\frac{2}{3}, 1]$:

$\star$ $\widetilde{\alpha}_i(t) = (3-3t)\alpha_i,\ i = 1, 3, 4, 6;$

$\star$ $\widetilde{\alpha}_j(t) = \alpha_j - 2\alpha_{j-1} - 2\alpha_{j+1} + 3t(\alpha_{j-1} + \alpha_{j+1}),\ j = 2, 5.$

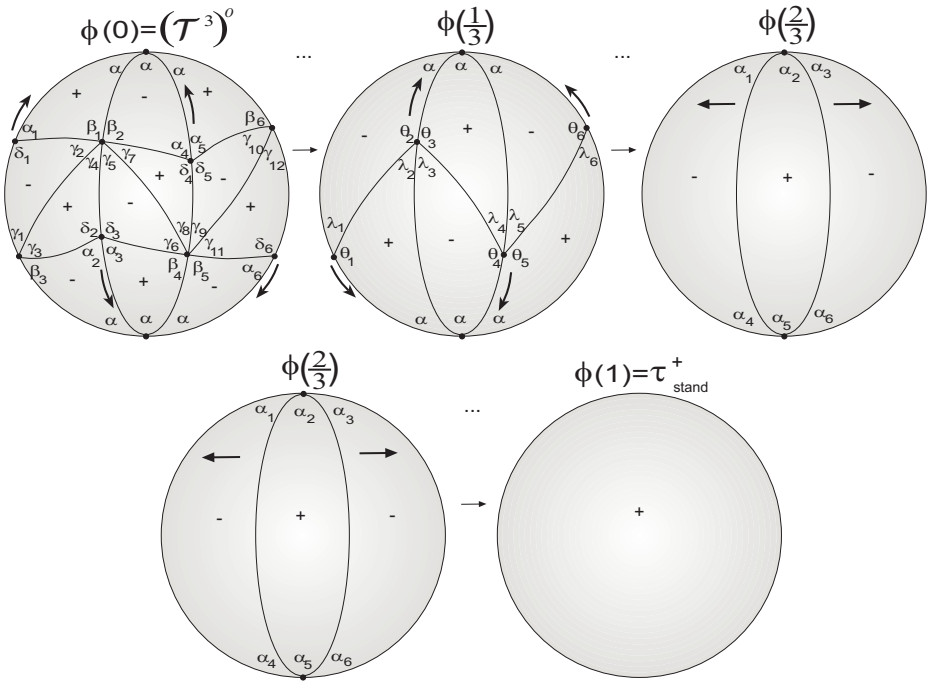

Figure 4.168: Deformation of $(\mathcal{T}^3)^o$.

We only need to prove that ϕ is continuous at $t = 0^-$, $t = \frac{1}{3}$ and $t = \frac{2}{3}^-$.

Considering $t \in]0, \frac{1}{3}[$, one has:

$$\begin{aligned} c(\tau_t^{o_t}, \tau_0) &= \sum_{\substack{F \text{face of} \\ \tau_t \cup \tau_0}} \lambda(F)\, Area(F) \\ &= 4 \times \left(\widetilde{\alpha}_1(0) + \widetilde{\delta}_1(t) + \widetilde{\beta}_1(0) - \widetilde{\beta}_1(t) - \pi \right) \\ &+ 8 \times \left(\widetilde{\alpha}_4(0) + \widetilde{\delta}_4(t) + \widetilde{\beta}_2(0) - \widetilde{\beta}_2(t) - \pi \right) \\ &= 4 \times (\alpha_1 + \delta_1 + t\,(\pi - 3\delta_1) + \beta_1 - (1-3t)\beta_1 - \pi) \\ &+ 8 \times (\alpha_4 + \delta_4 + t\,(\pi - 3\delta_4) + \beta_2 - (1-3t)\beta_2 - \pi)\,. \end{aligned}$$

For $t \to 0^+$, then $c(\tau_t^{o_t}, \tau_0) \to 0$.

Now, if $t \in]0, \frac{1}{3}[$:

$$\begin{aligned} c(\tau_t^{o_t}, \tau_{\frac{1}{3}}) &= \sum_{\substack{F \text{face of} \\ \tau_t \cup \tau_{\frac{1}{3}}}} \lambda(F)\, Area(F) \\ &= 12 \times \left(\widetilde{\alpha}_1(t) + \widetilde{\beta}_1(t) + \alpha - \pi \right) \\ &= 12 \times \left(\pi - \widetilde{\delta}_1'(t) + (1-3t)\beta_1 + \alpha - \pi \right). \end{aligned}$$

For $t \to \frac{1}{3}^-$, we get $c(\tau_t^{o_t}, \tau_{\frac{1}{2}}) \to 0$.

Assuming now that $t \in]\frac{1}{3}, \frac{2}{3}[$:

$$\begin{aligned} c(\tau_t^{o_t}, \tau_{\frac{1}{3}}) &= \sum_{\substack{F \text{face of} \\ \tau_t \cup \tau_{\frac{1}{3}}}} \lambda(F)\, Area(F) \\ &= 12 \times \left(\widetilde{\theta}_1 \left(\frac{1}{3} \right) + \widetilde{\lambda}_1(t) + \widetilde{\lambda}_2 \left(\frac{1}{3} \right) - \widetilde{\lambda}_2(t) - \pi \right) \\ &= 12 \times \left(\theta_1 + 2\lambda_1 - \frac{\pi}{3} + t\,(\pi - 3\lambda_1) + \lambda_2 - (2-3t)\lambda_2 - \pi \right). \end{aligned}$$

As $t \to \frac{1}{3}^+$, then $c(\tau_t^{o_t}, \tau_{\frac{1}{3}}) \to 0$.

If $t \in]\frac{1}{3}, \frac{2}{3}[$:

$$
\begin{aligned}
c(\tau_t^{o_t}, \tau_{\frac{2}{3}}) &= \sum_{\substack{F \text{face of} \\ \tau_t \cup \tau_{\frac{2}{3}}}} \lambda(F)\, Area(F) \\
&= 6 \times \left(\widetilde{\theta}_1(t) + \widetilde{\lambda}_2(t) + \alpha - \pi \right) \\
&= 6 \times \left(\pi - 2\lambda_1 + \frac{\pi}{3} - t\,(\pi - 3\lambda_1) + (2 - 3t)\lambda_2 + \alpha - \pi \right).
\end{aligned}
$$

When, $t \to \frac{2}{3}^{-}$, one has $c(\tau_t^{o_t}, \tau_{\frac{2}{3}}) \to 0$.

21. All member of the family of dihedral f-tilings denoted by $\mathcal{U}^k,\ k \geq 3$ are deformable into τ^{-}_{stand}. Figure 4.169 illustrates the process of deformation of $\mathcal{U}^3$ into τ^{-}_{stand}, with $\phi : [0,1] \to \mathscr{T}^{\mathcal{O}}(S^2)$ be a deformable map. The angles are $\alpha = \frac{\pi}{3},\ \delta = \frac{2\pi}{3},\ \beta = \frac{2\pi}{5}$ and $\gamma = \frac{\pi}{5}$.

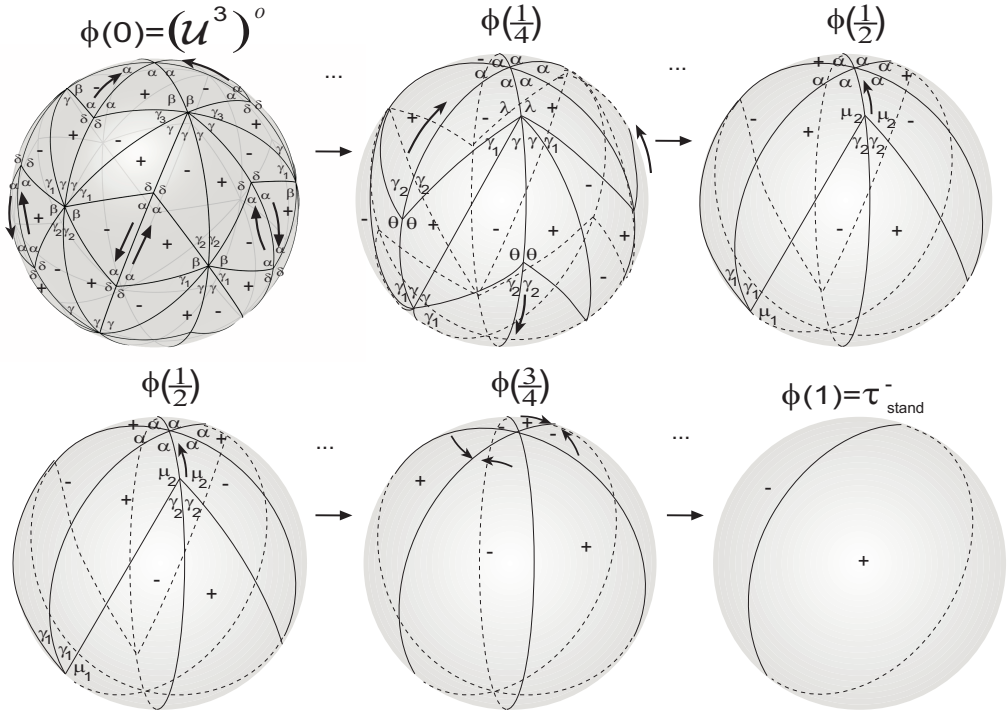

Figure 4.169: Deformation of $(\mathcal{U}^3)^o$.

The process of deformation consists in eliminate all vertices of valency four. In other words, for $t \in [0, \frac{1}{4}]$:

- $\widetilde{\beta}(t) = (1 - 4t)\beta$;

- $\star$ $\widetilde{\delta}(t) \equiv \alpha$;
- $\star$ $\widetilde{\alpha}(t) = \pi - \widetilde{\delta}(t)$;
- $\star$ $\widetilde{\gamma}_i(t) = \gamma_i + 2t\beta,\ i = 1, 2$;
- $\star$ $\widetilde{\gamma}_3(t) = \gamma_3 + 4t\beta$.

If $t \in]\frac{1}{4}, \frac{1}{2}]$:

- $\star$ $\widetilde{\lambda}(t) = (2 - 4t)\lambda$;
- $\star$ $\widetilde{\gamma}_1(t) = \gamma_1 - \lambda + 4t\lambda$;
- $\star$ $\widetilde{\theta}(t) = 2\theta - \alpha + 4t(\alpha - \theta)$ and $\widetilde{\gamma}_2(t) = \pi - \widetilde{\theta}(t)$.

For $t \in]\frac{1}{2}, \frac{3}{4}]$:

- $\star$ $\widetilde{\gamma}_1(t) = (3 - 4t)\gamma_1$ and $\widetilde{\mu}_1(t) = \pi - \widetilde{\gamma}_1(t)$;
- $\star$ $\widetilde{\gamma}_2(t) = 3\gamma_2 - 2\alpha + 4t(\alpha - \gamma_2)$ and $\widetilde{\mu}_2(t) = \pi - \widetilde{\gamma}_2(t)$.

The paths that define the last stage of deformation are quite similar to the ones done for $\mathcal{B}^4$ in Chapter 3.

Let us show that ϕ is continuous at $t = 0$: For $t \in]0, \frac{1}{4}[$,

$$\begin{aligned} c(\tau_t^{o_t}, \tau_0) &= \sum_{\substack{F \text{face of} \\ \tau_t \cup \tau_0}} \lambda(F)\, Area(F) \\ &= 6 \times \left(\widetilde{\alpha}(0) + \widetilde{\delta}(t) + \widetilde{\beta}(0) - \widetilde{\beta}(t) - \pi \right) \\ &\quad + 24 \times \left(\widetilde{\alpha}(t) + \widetilde{\delta}(t) + \frac{\widetilde{\beta}(0) - \widetilde{\beta}(t)}{2} - \pi \right). \end{aligned}$$

For $t \to 0^+$, then $c(\tau_t^{o_t}, \tau_0) \to 0$.

For $t \in]0, \frac{1}{4}[$:

$$\begin{aligned} c(\tau_t^{o_t}, \tau_{\frac{1}{4}}) &= \sum_{\substack{F\text{face of} \\ \tau_t \cup \tau_{\frac{1}{4}}}} \lambda(F)\, Area(F) \\ &= 24 \times \left(\widetilde{\beta}(t) + \widetilde{\alpha}(t) + \alpha - \pi \right) \\ &= 24 \times \left((1-4t)\beta + \pi - \alpha + \alpha - \pi \right). \end{aligned}$$

Making $t \to \frac{1}{4}^{-}$, one has $c(\tau_t^{o_t}, \tau_{\frac{1}{4}}) \to 0$.

Now, considering $t \in]\frac{1}{4}, \frac{1}{2}[$:

$$\begin{aligned} c(\tau_t^{o_t}, \tau_{\frac{1}{4}}) &= \sum_{\substack{F\text{face of} \\ \tau_t \cup \tau_{\frac{1}{4}}}} \lambda(F)\, Area(F) \\ &= 12 \times \left(\widetilde{\lambda}\left(\frac{1}{4}\right) - \widetilde{\lambda}(t) + \widetilde{\gamma}_2\left(\frac{1}{4}\right) + \widetilde{\theta}(t) - \pi \right) \\ &= 12 \times \left(\lambda - (2-4t)\lambda + \pi - \theta + 2\theta - \alpha + 4t(\alpha - \theta) - \pi \right). \end{aligned}$$

For $t \to \frac{1}{4}^{+}$, then $c(\tau_t^{o_t}, \tau_{\frac{1}{4}}) \to 0$ concluding that ϕ is continuous at $t = \frac{1}{4}$.

If $t \in]\frac{1}{4}, \frac{1}{2}[$:

$$\begin{aligned} c(\tau_t^{o_t}, \tau_{\frac{1}{2}}) &= \sum_{\substack{F\text{face of} \\ \tau_t \cup \tau_{\frac{1}{2}}}} \lambda(F)\, Area(F) \\ &= 12 \times \left(\widetilde{\lambda}(t) + \alpha + \widetilde{\gamma}_2(t) - \pi \right) \\ &= 12 \times \left((2-4t)\lambda + \alpha + \pi - 2\theta + \alpha - 4t(\alpha - \theta) - \pi \right). \end{aligned}$$

Making $t \to \frac{1}{2}^{-}$, one has $c(\tau_t^{o_t}, \tau_{\frac{1}{2}}) \to 0$.

If $t \in]\frac{1}{2}, \frac{3}{4}[$:

$$\begin{aligned} c(\tau_t^{o_t}, \tau_{\frac{1}{2}}) &= \sum_{\substack{F \text{face of} \\ \tau_t \cup \tau_{\frac{1}{2}}}} \lambda(F)\, Area(F) \\ &= 6 \times \left(\widetilde{\gamma}_1 \left(\frac{1}{2} \right) - \widetilde{\gamma}_1(t) + \widetilde{\mu}_2 \left(\frac{1}{2} \right) + \widetilde{\gamma}_2(t) - \pi \right) \\ &= 6 \times \left(\gamma_1 - (3-4t)\gamma_1 + \pi - \gamma_2 + 3\gamma_2 - 2\alpha + 4t(\alpha - \gamma_2) - \pi \right). \end{aligned}$$

As $t \to \frac{1}{2}^+$, then $c(\tau_t^{o_t}, \tau_{\frac{1}{2}}) \to 0$ and so ϕ is continuous at $t = \frac{1}{2}$.

$$\begin{aligned} c(\tau_t^{o_t}, \tau_{\frac{3}{4}}) &= \sum_{\substack{F \text{face of} \\ \tau_t \cup \tau_{\frac{3}{4}}}} \lambda(F)\, Area(F) \\ &= 6 \times (\widetilde{\gamma}_1(t) + \widetilde{\mu}_2(t) + \alpha - \pi) \\ &= 6 \times \left((3-4t)\gamma_1 + \pi - \alpha + \alpha - \pi \right). \end{aligned}$$

For $t \to \frac{3}{4}^-$, then $c(\tau_t^{o_t}, \tau_{\frac{3}{4}}) \to 0$.

The continuity of ϕ at $t = \frac{3}{4}^+$ and $t = 1$ is trivial. Hence, ϕ is continuous in $[0, 1]$.

22. For all $k \geq 5$, $\mathcal{V}^k,\ k \geq 5$ is deformable into τ_{stand}^-. Figure 4.170 shows a deformation of $\mathcal{V}^5$ into τ_{stand}^-, with $\alpha = \frac{\pi}{3},\ \delta = \frac{2\pi}{3},\ \beta = \frac{2\pi}{5}$ and $\gamma = \frac{\pi}{5}$.

For $t \in [0, \frac{1}{3}]$:

- $\star\ \widetilde{\beta}(t) = (1-3t)\beta$;
- $\star\ \widetilde{\gamma}_i(t) = \gamma_i + \frac{3}{2}t\beta,\ i = 1, 2$;
- $\star\ \widetilde{\alpha}_1(t) = \alpha_1 + 3t(\delta_2 - \alpha_1)$ and $\widetilde{\delta}_1(t) = \pi - \widetilde{\alpha}_1(t)$;
- $\star\ \widetilde{\alpha}_2(t) \equiv \alpha$ and $\widetilde{\delta}_1(t) = \pi - \widetilde{\alpha}_2(t)$.

If $t \in]\frac{1}{3}, \frac{2}{3}]$:

- $\star\ \widetilde{\gamma}_1(t) = (2-3t)\gamma_1$ and $\widetilde{\theta}_1(t) = \pi - \widetilde{\gamma}_1(t)$;
- $\star\ \widetilde{\gamma}_2(t) = 2\gamma_2 - \gamma + 3t(\gamma - \gamma_2)$ and $\widetilde{\theta}_2(t) = \pi - \widetilde{\gamma}_2(t)$.

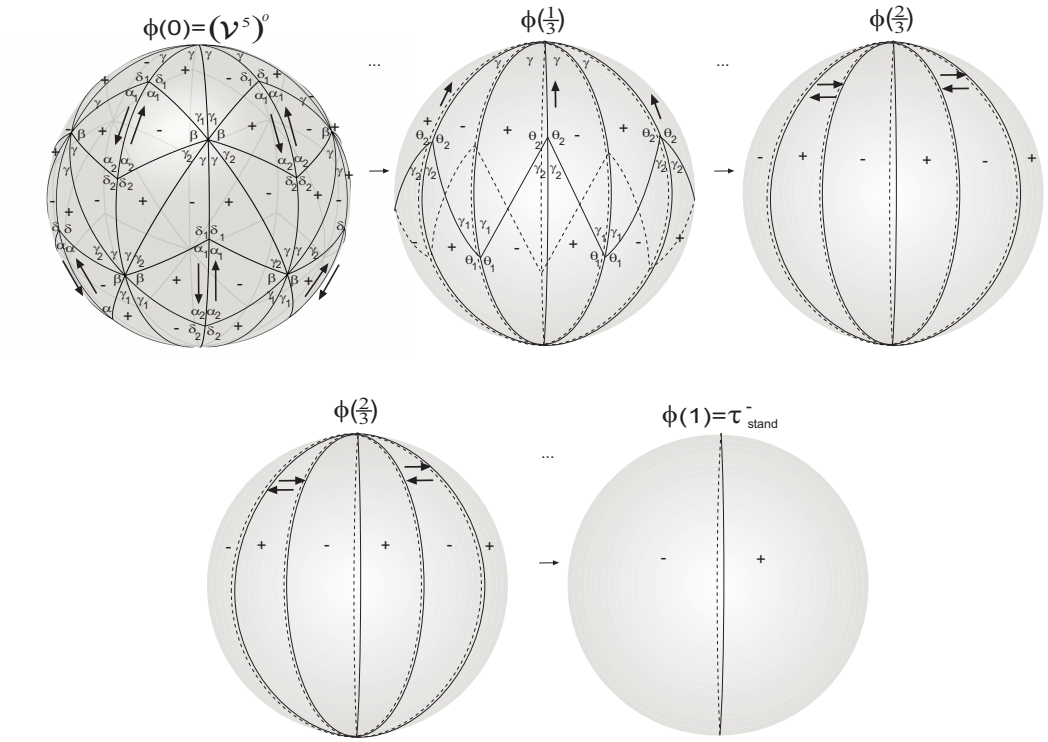

Figure 4.170: Deformation of $(\mathcal{V}^5)^o$.

The paths that define the last stage of the deformation can be defined as in Chapter 3 for the f-tiling $\mathcal{B}^4$.

Now, we will show that ϕ is continuous at $t = 0$:

Considering $t \in]0, \frac{1}{3}[$, then

$$\begin{aligned} c(\tau_t^{o_t}, \tau_0) &= \sum_{\substack{F \text{face of} \\ \tau_t \cup \tau_0}} \lambda(F)\, Area(F) \\ &= 40 \times \left(\frac{\widetilde{\beta}(0) - \widetilde{\beta}(t)}{2} + \widetilde{\alpha}_1(0) + \widetilde{\delta}_1(t) - \pi \right) \\ &= 40 \times \left(\frac{\beta - (1-3t)\beta}{2} + \alpha_1 + \delta_1 - \pi \right). \end{aligned}$$

As $t \to 0^+$, then $c(\tau_t^{o_t}, \tau_0) \to 0$.

For $t \in]0, \frac{1}{3}[$:

$$\begin{aligned} c(\tau_t^{o_t}, \tau_{\frac{1}{3}}) &= \sum_{\substack{F\text{face of} \\ \tau_t \cup \tau_{\frac{1}{3}}}} \lambda(F)\, Area(F) \\ &= 20 \times \left(\widetilde{\alpha}_1(t) + \widetilde{\beta}(t) + \widetilde{\alpha}_2(t) - \pi \right) \\ &= 20 \times \left(\alpha_1 + 3t(\delta_2 - \alpha_1) + (1-3t)\beta + \alpha - \pi \right). \end{aligned}$$

Making $t \to \frac{1}{3}^{-}$, one has $c(\tau_t^{o_t}, \tau_{\frac{1}{3}}) \to 0$.

If $t \in]\frac{1}{3}, \frac{2}{3}[$, then

$$\begin{aligned} c(\tau_t^{o_t}, \tau_{\frac{1}{3}}) &= \sum_{\substack{F\text{face of} \\ \tau_t \cup \tau_{\frac{1}{3}}}} \lambda(F)\, Area(F) \\ &= 10 \times \left(\widetilde{\gamma}_1 \left(\frac{1}{3} \right) - \widetilde{\gamma}_1(t) + \widetilde{\theta}_2 \left(\frac{1}{3} \right) + \widetilde{\gamma}_2(t) - \pi \right) \\ &= 10 \times \left(\gamma_1 - (2-3t)\gamma_1 + \theta_2 + 2\gamma_2 - \gamma + 3t(\gamma - \gamma_2) - \pi \right). \end{aligned}$$

For $t \to \frac{1}{3}^{+}$, we get $c(\tau_t^{o_t}, \tau_{\frac{1}{3}}) \to 0$ and so ϕ is continuous at $t = \frac{1}{3}$.

$$\begin{aligned} c(\tau_t^{o_t}, \tau_{\frac{2}{3}}) &= \sum_{\substack{F\text{face of} \\ \tau_t \cup \tau_{\frac{2}{3}}}} \lambda(F)\, Area(F) \\ &= 10 \times \left(\gamma + \widetilde{\gamma}_1(t) + \widetilde{\theta}_2(t) - \pi \right) \\ &= 10 \times \left(\gamma + (2-3t)\gamma_1 + \pi - 2\gamma_2 + \gamma - 3t(\gamma - \gamma_2) - \pi \right). \end{aligned}$$

For $t \to \frac{2}{3}^{-}$, we have $c(\tau_t^{o_t}, \tau_{\frac{2}{3}}) \to 0$

The steps to prove that ϕ is continuous at $t = \frac{2}{3}^{+}$ and $t = 1^{-}$ are similar to the ones in Chapter 3 for $\mathcal{B}^4$.

23. For each $k \geq 4$, $\mathcal{X}^k$ is deformable into τ_{stand}^{-}. Figure 4.171 shows the process of deformation of the member $\mathcal{X}^4$, where $\gamma = \frac{\pi}{4}$, $\alpha \approx 53.07°$, $\beta \approx 81.93°$ and $\delta \approx 126.93°$.

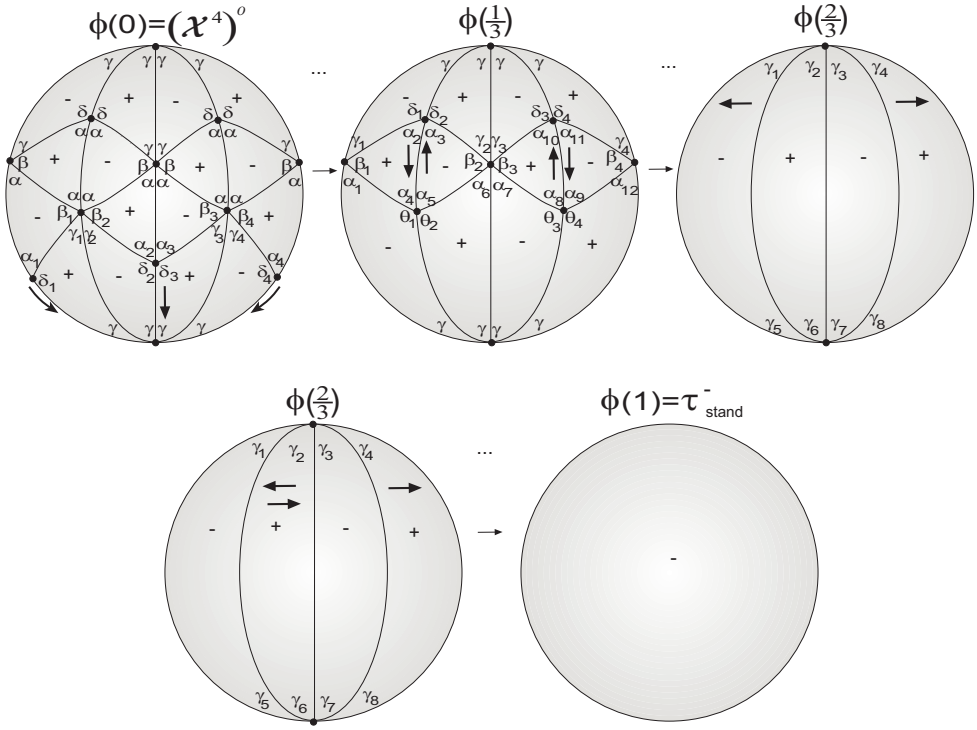

Figure 4.171: Deformation of $(\mathcal{X}^4)^o$.

For $t \in [0, \frac{1}{3}]$:

- $\star$ $\widetilde{\gamma}_i(t) = (1-3t)\gamma_i,\ i = 1,2,3,4;$
- $\star$ $\widetilde{\beta}_i(t) = \beta_i + 3t\gamma_i,\ i = 1,2,3,4;$
- $\star$ $\widetilde{\alpha}_i(t) = \alpha_i + 3t\left(\frac{\pi}{4} - \alpha_i\right),\ i = 1,2,3,4;$
- $\star$ $\widetilde{\delta}_1(t) = \pi - \widetilde{\alpha}'_1(t)$ and $\widetilde{\delta}_4(t) = \pi - \widetilde{\alpha}'_4(t)$, where $\widetilde{\alpha}'_1(t) = \alpha'_1 + 3t\left(\frac{\pi}{4} - \alpha'_1\right)$ and $\widetilde{\alpha}'_4(t) = \alpha'_4 + 3t\left(\frac{\pi}{4} - \alpha'_4\right)$;
- $\star$ $\widetilde{\delta}_2(t) = \pi - \widetilde{\alpha}_3(t)$ and $\widetilde{\delta}_3(t) = \pi - \widetilde{\alpha}_2(t)$.

If $t \in]\frac{1}{3}, \frac{2}{3}]$:

- $\star$ $\widetilde{\beta}_i(t) = (2-3t)\beta_i,\ i = 1,2,3,4;$
- $\star$ $\widetilde{\gamma}_i(t) = \gamma_i + \frac{\beta_i}{2}(3t-1),\ i = 1,2,3,4;$
- $\star$ $\widetilde{\alpha}_1(t) = \alpha_1 + \frac{\beta_1}{2}(3t-1),\ \widetilde{\alpha}_6(t) = \alpha_6 + \frac{\beta_2}{2}(3t-1),\ \widetilde{\alpha}_7(t) = \alpha_7 + \frac{\beta_3}{2}(3t-1)$ and $\widetilde{\alpha}_{12}(t) = \alpha_{12} + \frac{\beta_4}{2}(3t-1);$

- ⋆ $\widetilde{\delta}_i(t) = \frac{3\pi}{2}t - \frac{\pi}{2} + (2-3t)\delta_i$ and $\widetilde{\theta}_i(t) = \frac{3\pi}{2}t - \frac{\pi}{2} + (2-3t)\theta_i,\ i = 1,2,3,4;$
- ⋆ $\widetilde{\alpha}_i(t) = \frac{3\pi}{2}t - \frac{\pi}{2} + (2-3t)\alpha_i,\ i = 2,3,4,5,8,9,10,11.$

As before, the paths that define the last stage of deformation are similar to the ones done for $\mathcal{B}^4$ in Chapter 3.

Following the same steps as in Chapter 3 for $\mathcal{B}^4$, we prove that ϕ is continuous in $[0,1]$.

24. The dihedral f-tiling $\mathcal{L}$ is deformable into τ^-_{stand}. Next figure gives an idea of its deformation where the angles are $\alpha = \frac{\pi}{3},\ \delta = \frac{2\pi}{3},\ \gamma = \frac{\pi}{5}$ and $\beta = \frac{2\pi}{5}$.

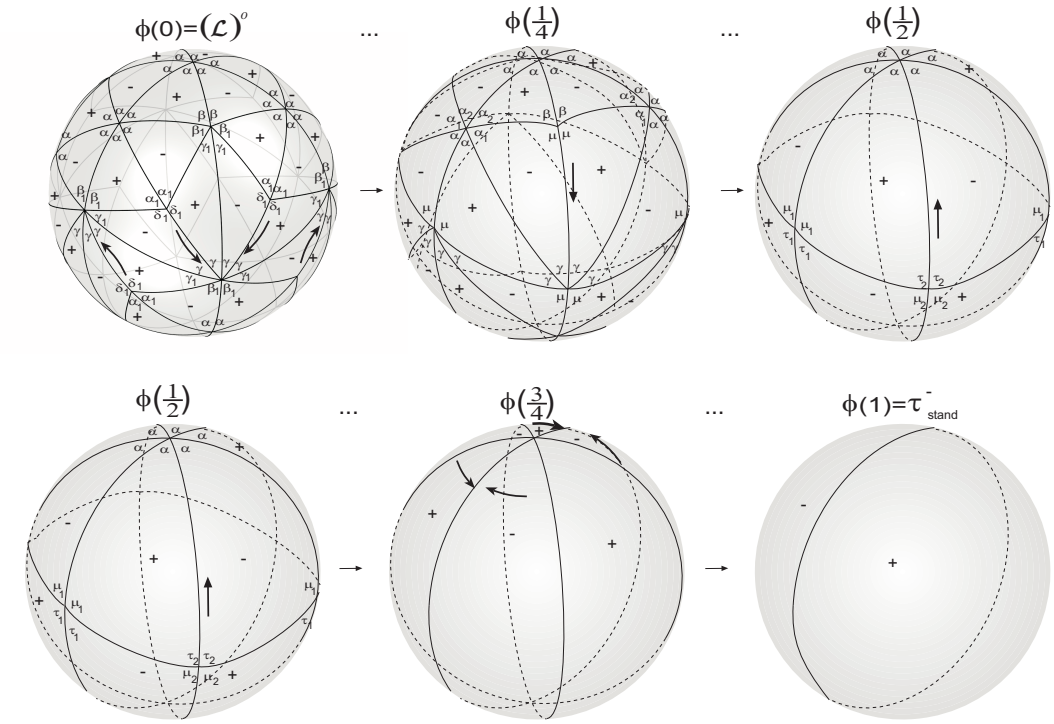

Figure 4.172: Deformation of $(\mathcal{L})^o$.

For $t \in [0, \frac{1}{4}]$:

- ⋆ $\widetilde{\gamma}_1(t) = (1-4t)\gamma_1;$
- ⋆ $\widetilde{\beta}_1(t) = \beta_1 + 4t\gamma_1;$
- ⋆ $\widetilde{\alpha}_1(t) = \alpha_1 + 4t(\gamma - \alpha_1)$ and $\widetilde{\delta}_1(t) = \pi - \widetilde{\alpha}_1(t).$

If $t \in]\frac{1}{4}, \frac{1}{2}]$:

- $\widetilde{\alpha}_1(t) = (2-4t)\alpha_1$;
- $\widetilde{\alpha}_2(t) = \alpha_2 - \alpha_1 + 4t\alpha_1$;
- $\widetilde{\mu}(t) \equiv \mu$ and $\widetilde{\beta}(t) = \pi - \widetilde{\mu}(t)$.

For $t \in]\frac{1}{2}, \frac{3}{4}]$:

- $\widetilde{\mu}_1(t) = (3-4t)\mu_1$ and $\widetilde{\tau}_1(t) = \pi - \widetilde{\mu}_1(t)$;
- $\widetilde{\mu}_2(t) = 3\mu_2 - 2\alpha + 4t(\alpha - \mu_2)$ and $\widetilde{\tau}_2(t) = \pi - \widetilde{\mu}_2(t)$.

For $t \in]\frac{3}{4}, 1]$, we may define the paths as was done for $\mathcal{B}^4$ in Chapter 3.

Let us show that ϕ is continuous at $t = 0$:

For each $t \in]0, \frac{1}{2}[$, one has

$$\begin{aligned} c(\tau_t^{o_t}, \tau_0) &= \sum_{\substack{F \text{face of} \\ \tau_t \cup \tau_0}} \lambda(F)\, Area(F) \\ &= 24 \times \left(\widetilde{\gamma}_1(0) - \widetilde{\gamma}_1(t) + \widetilde{\delta}_1(t) + \widetilde{\alpha}_1(t) - \pi \right) \\ &= 24 \times \left(\gamma_1 - (1-4t)\gamma_1 + \pi - \alpha_1 - 4t(\gamma - \alpha_1) + \alpha_1 + 4t(\gamma - \alpha_1) - \pi \right). \end{aligned}$$

Making $t \to 0^+$, we conclude that $c(\tau_t^{o_t}, \tau_0) \to 0$.

Now,

$$\begin{aligned} c(\tau_t^{o_t}, \tau_{\frac{1}{4}}) &= \sum_{\substack{F \text{face of} \\ \tau_t \cup \tau_{\frac{1}{4}}}} \lambda(F)\, Area(F) \\ &= 20 \times \left(\widetilde{\gamma}_1(t) + \widetilde{\delta}_1(t) + \gamma - \pi \right) \\ &= 20 \times \left((1-4t)\gamma_1 + \pi - \alpha_1 - 4t(\gamma - \alpha_1) + \gamma - \pi \right). \end{aligned}$$

If $t \to \frac{1}{4}^-$, then $c(\tau_t^{o_t}, \tau_{\frac{1}{4}}) \to 0$.

Considering $t \in]\frac{1}{4}, \frac{1}{2}[$:

$$
\begin{aligned}
c(\tau_t^{o_t}, \tau_{\frac{1}{4}}) &= \sum_{\substack{F \text{face of} \\ \tau_t \cup \tau_{\frac{1}{4}}}} \lambda(F)\, Area(F) \\
&= 12 \times \left(\widetilde{\alpha}_1 \left(\frac{1}{4} \right) - \widetilde{\alpha}_1(t) + \widetilde{\mu}(t) + \widetilde{\beta}(t) - \pi \right) \\
&= 12 \times \left(\alpha_1 - (2 - 4t)\alpha_1 + \mu + \pi - \mu - \pi \right).
\end{aligned}
$$

If $t \to \frac{1}{4}^+$, then $c(\tau_t^{o_t}, \tau_{\frac{1}{4}}) \to 0$ and so ϕ is continuous at $t = \frac{1}{4}$.

To prove that ϕ is continuous at $t = \frac{1}{2}$ and $t = \frac{3}{4}^-$, we follow a similar reasoning to the one done for $\mathcal{B}^4$ in Chapter 3.

25. The dihedral f-tiling $(\mathcal{M})^o$ is deformable into τ^+_{stand}. Next figure helps us to define the deformable map ϕ, with $\gamma = \frac{\pi}{5}$, $\alpha = \frac{\pi}{3}$, $\beta = \frac{2\pi}{5}$ and $\delta = \frac{2\pi}{3}$. The process of deformation consists in eliminating vertices of valency four.

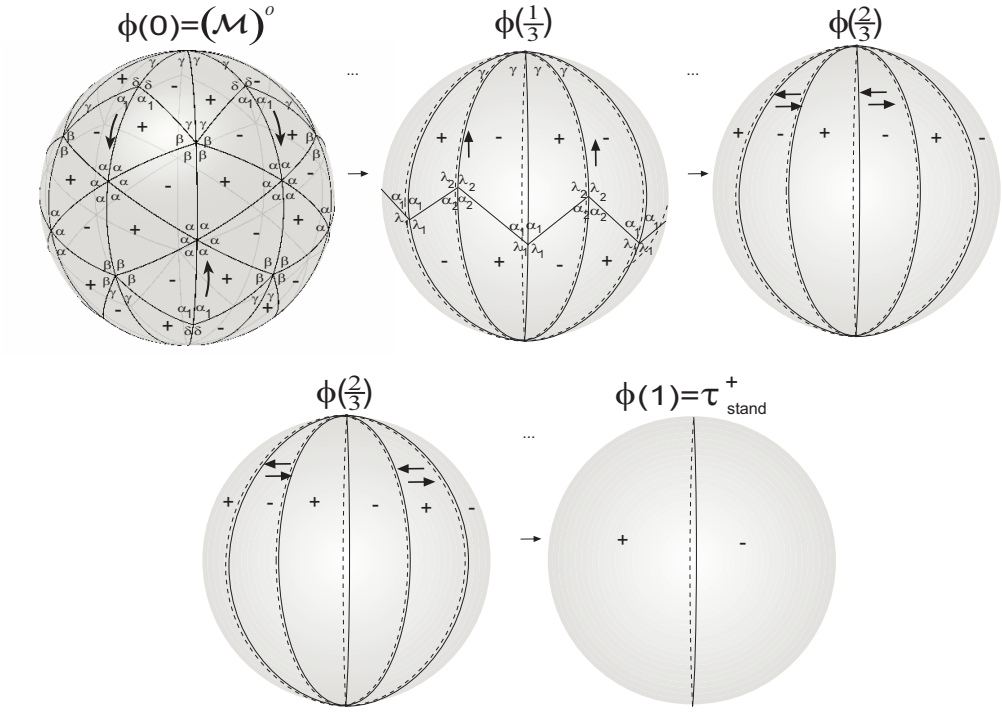

Figure 4.173: Deformation of $(\mathcal{M})^o$.

Hence, for $t \in [0, \frac{1}{3}]$:

$\star$ $\widetilde{\beta}(t) = (1 - 3t)\beta$;

- $\widetilde{\gamma}(t) = \gamma + 3t\beta$;
- $\widetilde{\delta}(t) = \delta + 3t(\alpha - \delta)$ and $\widetilde{\alpha}_1(t) = \pi - \widetilde{\delta}(t)$.

For $t \in]\frac{1}{3}, \frac{2}{3}]$:

- $\widetilde{\alpha}_1(t) = (2 - 3t)\alpha_1$;
- $\widetilde{\lambda}_1(t) = \pi - \widetilde{\alpha}_1(t)$;
- $\widetilde{\alpha}_2(t) = 2\alpha_2 - \gamma + 3t(\gamma - \alpha_2)$ and $\widetilde{\lambda}_2(t) = \pi - \widetilde{\alpha}_2(t)$.

The paths in the final stage of the deformation may be defined as in $\mathcal{B}^4$ in Chapter 3.

Now, we will show that ϕ is continuous at $t = 0$:

Considering $t \in]0, \frac{1}{3}[$, then

$$\begin{aligned} c(\tau_t^{o_t}, \tau_0) &= \sum_{\substack{F \text{face of} \\ \tau_t \cup \tau_0}} \lambda(F)\, Area(F) \\ &= 20 \times \left(\widetilde{\beta}(0) - \widetilde{\beta}(t) + \widetilde{\alpha}_1(0) + \widetilde{\delta}(t) - \pi \right) \\ &= 20 \times \left(\beta - (1 - 3t)\beta + \alpha_1 + \delta + 3t(\alpha - \delta) - \pi \right). \end{aligned}$$

As $t \to 0^+$, then $c(\tau_t^{o_t}, \tau_0) \to 0$.

If $t \in]0, \frac{1}{3}[$, then

$$\begin{aligned} c(\tau_t^{o_t}, \tau_{\frac{1}{3}}) &= \sum_{\substack{F \text{face of} \\ \tau_t \cup \tau_{\frac{1}{3}}}} \lambda(F)\, Area(F) \\ &= 20 \times \left(\widetilde{\alpha}_1(t) + \widetilde{\beta}(t) + \alpha - \pi \right) \\ &= 20 \times \left(\pi - \delta - 3t(\alpha - \delta) + (1 - 3t)\beta + \alpha - \pi \right). \end{aligned}$$

Making $t \to \frac{1}{3}^-$, we get $c(\tau_t^{o_t}, \tau_{\frac{1}{3}}) \to 0$.

If $t \in]\frac{1}{3}, \frac{2}{3}[$:

$$c(\tau_t^{o_t}, \tau_{\frac{1}{3}}) = \sum_{\substack{F\text{face of} \\ \tau_t \cup \tau_{\frac{1}{3}}}} \lambda(F)\, Area(F)$$
$$= 10 \times \left(\widetilde{\alpha}_1 \left(\frac{1}{3} \right) - \widetilde{\alpha}_1(t) + \widetilde{\lambda}_2(t) + \widetilde{\alpha}_2(t) - \pi \right).$$

For $t \to \frac{1}{3}^+$, one has $c(\tau_t^{o_t}, \tau_{\frac{1}{3}}) \to 0$ concluding that ϕ is continuous at $t = \frac{1}{3}$.

$$c(\tau_t^{o_t}, \tau_{\frac{2}{3}}) = \sum_{\substack{F\text{face of} \\ \tau_t \cup \tau_{\frac{2}{3}}}} \lambda(F)\, Area(F)$$
$$= 10 \times \left(\widetilde{\alpha}_1(t) + \widetilde{\lambda}_2(t) + \gamma - \pi \right)$$
$$= 10 \times \left((2 - 3t)\alpha_1 + \pi - \gamma + \gamma - \pi \right).$$

For $t \to \frac{2}{3}^-$, we get $c(\tau_t^{o_t}, \tau_{\frac{2}{3}}) \to 0$.

The continuity at $t = \frac{2}{3}^+$ and $t = 1^-$ is trivial.

26. The dihedral f-tiling $(\mathcal{N})^o$ is deformable into τ^+_{stand}. In Figure 4.174, we can see the process of deformation of $(\mathcal{N})^o$ into τ^+_{stand}. The angles are $\beta = \gamma = \frac{\pi}{3}$, $\alpha \approx 75.522°$ and $\delta \approx 104.478°$.

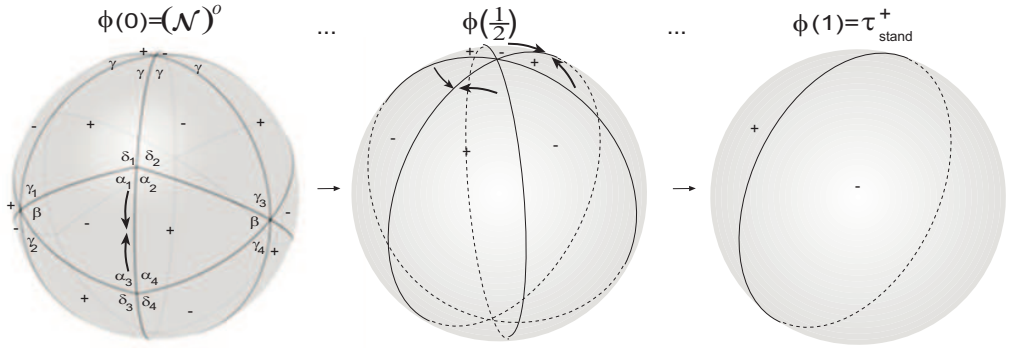

Figure 4.174: Deformation of $(\mathcal{N})^o$.

For $t \in [0, \frac{1}{2}]$:

⋆ $\widetilde{\beta}(t) = (1 - 2t)\beta$;

- $\star$ $\widetilde{\gamma}_i(t) = \gamma_i + t\beta,\ i = 1, 2$ and $\widetilde{\gamma}_j(t) = \gamma_j + t\beta,\ j = 3, 4$;
- $\star$ $\widetilde{\alpha}_i(t) = \alpha_i + 2t\left(\frac{\pi}{2} - \alpha_i\right)$ and $\widetilde{\delta}_i(t) = \pi - \widetilde{\alpha}_{i+1},\ i = 1, 3$ and $\widetilde{\delta}_i(t) = \pi - \widetilde{\alpha}_{i-1},\ i = 2, 4$.

For $t \in]\frac{1}{2}, 1]$, we define the paths as was done for $\mathcal{B}^4$ in Chapter 3.

The process to prove that ϕ is continuous in $[0, 1]$ is the same to the one done for the deformation of $\mathcal{I}$.

27. The dihedral f-tiling $(\mathcal{O})^o$ is deformable into τ^+_{stand}. Figure 4.175 shows the process of deformation and the angles are $\beta = \gamma = \frac{\pi}{4},\ \alpha \approx 72.965°$ and $\delta \approx 107.031°$.

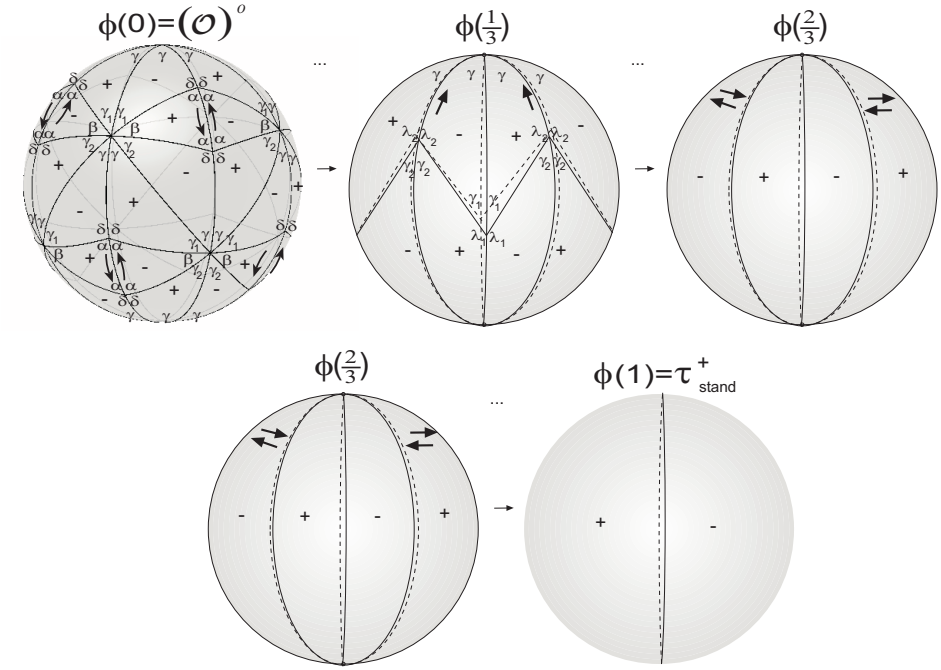

Figure 4.175: Deformation of $(\mathcal{O})^o$.

For $t \in [0, \frac{1}{3}]$:

- $\star$ $\widetilde{\beta}(t) = (1 - 3t)\beta$;
- $\star$ $\widetilde{\gamma}_i(t) = \gamma_i + \frac{3}{2}t\beta,\ i = 1, 2$;
- $\star$ $\widetilde{\alpha}(t) \equiv \frac{\pi}{2}$ and $\widetilde{\delta}(t) \equiv \frac{\pi}{2}$.

If $t \in]\frac{1}{3}, \frac{2}{3}]$:

- $\widetilde{\gamma}_1(t) = (2-3t)\gamma_1$ and $\widetilde{\lambda}_1(t) = \pi - \widetilde{\gamma}_1(t)$;
- $\widetilde{\gamma}_2(t) = 2\gamma_2 - \gamma + 3t(\gamma - \gamma_2)$ and $\widetilde{\lambda}_2(t) = \pi - \widetilde{\gamma}_2(t)$.

The paths for the final stage of the deformation follow the same reasoning as in f-tiling $\mathcal{B}^4$ in Chapter 3.

The reasoning to prove that ϕ is continuous is similar to the one done for $\mathcal{V}^5$.

28. The isolated dihedral f-tiling $(\mathcal{P})^o$ is also deformable into τ^+_{stand}. Considering $\phi : [0,1] \to \mathscr{T}^{\mathcal{O}}(S^2)$ as a deformable map, next figure illustrates the process and gives an idea of how to define ϕ. The angles are $\gamma = \frac{\pi}{3}$, $\alpha = 80°$, $\beta = 40°$ and $\delta = 100°$.

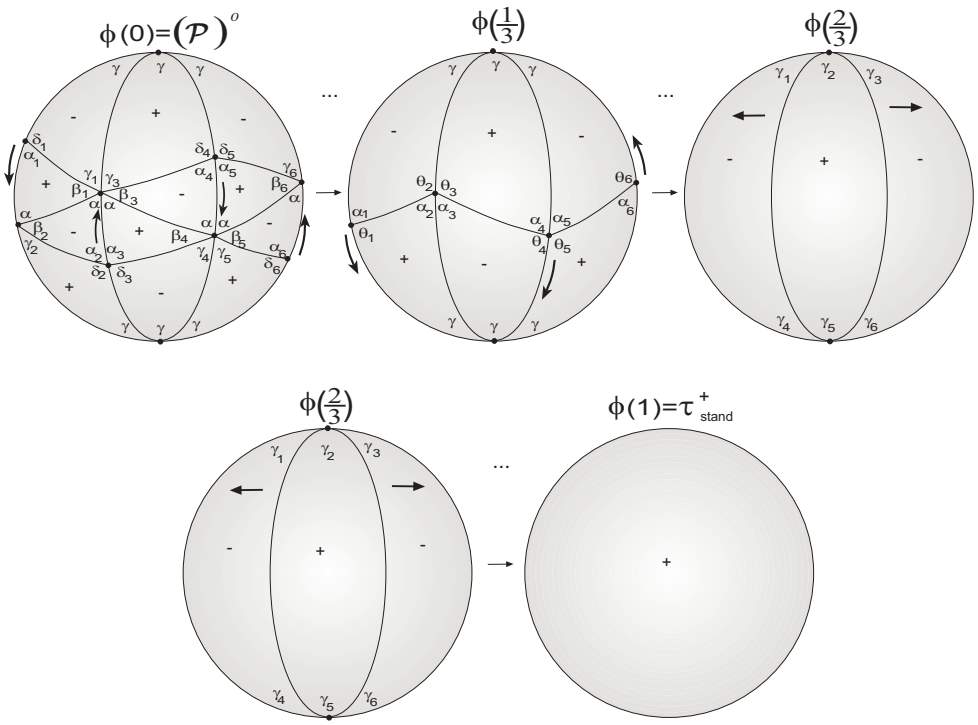

Figure 4.176: Deformation of $(\mathcal{P})^o$.

If $t \in [0, \frac{1}{3}]$:

- $\widetilde{\beta}_i(t) = (1-3t)\beta_i,\ i = 1, \ldots, 6$;
- $\widetilde{\alpha}_j(t) = \alpha_j + 3t(\beta + \gamma - \alpha_j),\ j = 1, \ldots, 6$;

$\star$ $\widetilde{\delta}_j(t) = \pi - \widetilde{\alpha}_j(t),\ j = 1, 6,\ \widetilde{\delta}_k(t) = \pi - \widetilde{\alpha}_{k+1}(t),\ k = 2, 4$ and $\widetilde{\delta}_k(t) = \pi - \widetilde{\alpha}_{k-1}(t),\ k = 3, 5.$

For $t \in]\frac{1}{3}, \frac{2}{3}]$:

$\star$ $\widetilde{\alpha}_i(t) = (2 - 3t)\alpha_i,\ i = 2, 3, 5, 6;$

$\star$ $\widetilde{\theta}_j(t) = \theta_j + t(\pi - 3\theta_j),\ j = 1, 4, 5, 6;$

$\star$ $\widetilde{\alpha}_1(t) = \pi - \widetilde{\theta}'_1(t)$ and $\widetilde{\alpha}_4(t) = \pi - \widetilde{\theta}_5(t).$

For $t \in]\frac{2}{3}, 1]$, the paths can be defined as was done for $\mathcal{B}^4$ in Chapter 3.

We only will prove that ϕ is continuous at $t = 0$ and $t = \frac{1}{3}^-$.

Let us show that ϕ is continuous at $t = 0^-$ and for that consider $t \in]0, \frac{1}{3}[$. Then,

$$\begin{aligned} c(\tau_t^{o_t}, \tau_0) &= \sum_{\substack{F \text{face of} \\ \tau_t \cup \tau_0}} \lambda(F)\, Area(F) \\ &= 4 \times \left(\widetilde{\alpha}_1(0) + \widetilde{\delta}_1(t) + \widetilde{\beta}_1(0) - \widetilde{\beta}_1(t) - \pi\right) \\ &+ 8 \times \left(\widetilde{\alpha}_2(0) + \widetilde{\delta}_2(t) + \widetilde{\beta}_2(0) - \widetilde{\beta}_2(t) - \pi\right) \\ &= 4 \times (\alpha_1 + \pi - \alpha_1 - 3t(\beta + \gamma - \alpha_1) + \beta_1 - (1 - 3t)\beta_1 - \pi) \\ &+ 8 \times (\alpha_2 + \pi - \alpha_3 - 3t(\beta + \gamma - \alpha_3) + \beta_2 - (1 - 3t)\beta_2 - \pi)\,. \end{aligned}$$

For $t \to 0^-$, we get $c(\tau_t^{o_t}, \tau_0) \to 0$.

If $t \in]0, \frac{1}{3}[$:

$$\begin{aligned} c(\tau_t^{o_t}, \tau_{\frac{1}{3}}) &= \sum_{\substack{F \text{face of} \\ \tau_t \cup \tau_{\frac{1}{3}}}} \lambda(F)\, Area(F) \\ &= 12 \times \left(\widetilde{\alpha}_1(t) + \widetilde{\beta}_1(t) + \alpha - \pi\right) \\ &= 12 \times (\alpha_1 + 3t(\beta + \gamma - \alpha_1) + (1 - 3t)\beta_1 + \alpha - \pi)\,. \end{aligned}$$

For $t \to \frac{1}{3}^-$, then $c(\tau_t^{o_t}, \tau_{\frac{1}{3}}) \to 0$.

Chapter 5

Conclusions and future work

In Chapter 1, we exposed basic notions and stated some crucial properties and results within the theory of isometric foldings that can be found in [12], [17] and [14] and which constitute the theoretical framework for the development of the work presented here.

The classification of all dihedral f-tilings of S^2 whose prototiles are an equilateral and an isosceles spherical triangle was obtained in Chapter 2, where we got a two parameter discrete family of dihedral f-tilings and three isolated f-tilings. The combinatorial structure and their transitive properties are exposed in Section 2.3.

Next table gives us 3D representation of a representative element of each dihedral f-tiling obtained in this Chapter.

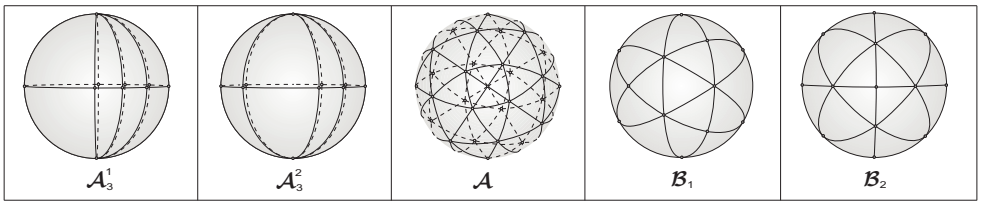

Figure 5.1: 3D representations of dihedral f-tilings of the sphere by an equilateral and an isosceles triangle.

In Chapter 3, the prototiles considered are an equilateral and a scalene spherical triangle. The performed study led to three one parameter continuous families, four one parameter discrete families and four isolated non-isomorphic dihedral f-tilings. The combinatorial structure and their transitive properties are exposed in Section 3.4.

Table 5.2 summarizes all dihedral f-tilings described in this Chapter.

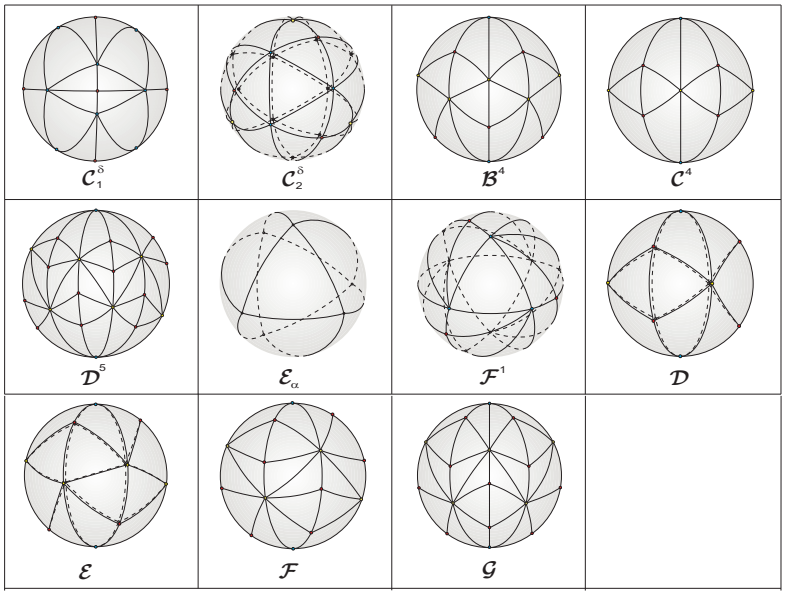

Figure 5.2: 3D representations of dihedral f-tilings of the sphere by an equilateral and a scalene triangle.

In Chapter 4, the considered prototiles are now two non-congruent isosceles spherical triangles ending up in a one continuous parameter family; nine one parameter discrete families, nine non-isomorphic isolated and seven families of dihedral f-tilings parameterized by two or more parameters (discrete/continuous).

The combinatorial structure and their transitive properties are exposed in Sections 4.2, 4.4 and 4.6.

Tables 5.3, 5.4, 5.5 and 5.6 illustrate 3D representation of a representative element of each dihedral f-tiling founded in this Chapter.

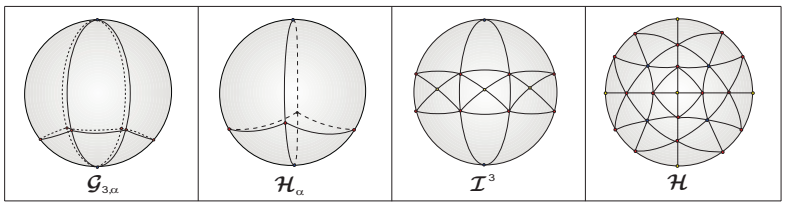

Figure 5.3: 3D representations of dihedral f-tilings of the sphere by two non congruent isosceles triangles with adjacency of type I.

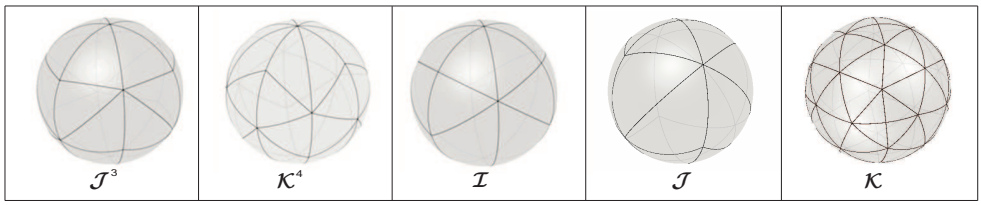

Figure 5.4: 3D representations of dihedral f-tilings of the sphere by two non congruent isosceles triangles with adjacency of type II.

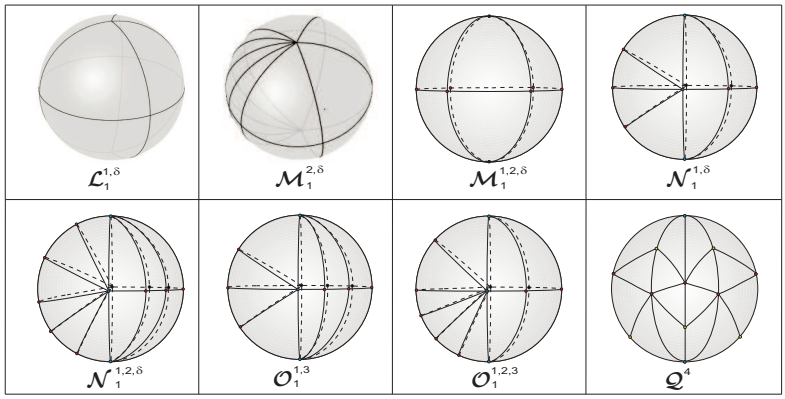

Figure 5.5: 3D representations of dihedral f-tilings of the sphere by two non congruent isosceles triangles with adjacency of type III a).

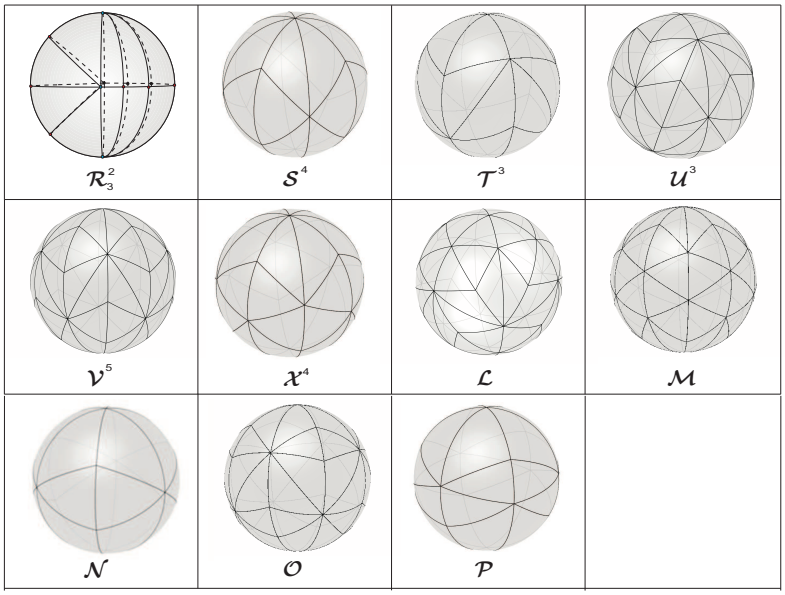

Figure 5.6: 3D representations of dihedral f-tilings of the sphere by two non congruent isosceles triangles with adjacency of type III b).

A. Santos in [14], in order to establish a relation between deformations of isometric foldings and deformations of its associated f-tilings, introduced a new metric in $\mathscr{T}(S^2)$ by giving to each face of a spherical f-tiling a convenient orientation.

In the last Section of each one of Chapters 2, 3 and 4, we provided deformations or insights toward deformations of each one of the produced f-tilings into the standard f-tiling, using this new metric.

One of the future research line will be the formal description of the insights given in some deformation sketches, which passes necessarily from the learning, among others, of the functionalities of the software *POV-Ray*.

We also intend to finish the study of all dihedral f-tilings of S^2, considering as prototiles, an isosceles and a scalene spherical triangle, and two non congruent scalene spherical triangles.

The study of toroidal f-tilings has just begun and our intention is to pursuit in this direction.

Bibliography

[1] Catarina P. Avelino and Altino F. Santos. Spherical f-tilings by triangles and r-sided regular polygons, $r \geq 5$. *Electronic Journal of Combinatorics*, 15(1), 2008.

[2] Ana Breda and Patrícia Ribeiro. Spherical f-tilings by two non congruent classes of isosceles triangles-I. *Mathematical Communications*, 17(1):127–149, 2012.

[3] Ana Breda, Patrícia Ribeiro, and Altino Santos. Dihedral f-tilings of the sphere by equilateral and scalene triangles-II. *Electronic Journal of Combinatorics*, 15(1), 2008.

[4] Ana Breda, Patrícia Ribeiro, and Altino Santos. Dihedral f-tilings of the sphere by equilateral and scalene triangles-III. *Electronic Journal of Combinatorics*, 15(1), 2008.

[5] Ana Breda, Patrícia Ribeiro, and Altino Santos. A class of spherical dihedral f-tilings. *European Journal of Combinatorics*, 30(1):119–132, 2009.

[6] Ana Breda, Patrícia Ribeiro, and Altino Santos. Dihedral f-tilings of the sphere by equilateral and scalene triangles-I. *Rendiconti del Seminario Matematico della Universit di Padova*, 124:1–23, 2010.

[7] Ana Breda and Altino Santos. Dihedral f-tilings of the sphere by spherical triangles and equiangular well-centered quadrangles. *Beiträge zur Algebra und Geometrie / Contributions to Algebra and Geometry*, 45(2):447–461, 2004.

[8] Ana Breda and Altino Santos. Dihedral f-tilings of the sphere by rhombi and triangles. *Discrete Mathematics and Theoretical Computer Science*, 7(1):123–140, 2005.

[9] Ana Breda and Altino Santos. Dihedral f-tilings of the sphere by triangles and well centered quadrangles. *Hiroshima Mathematical Journal*, 36(2):235–288, 2006.

[10] R. Dawson. Tilings of the sphere with isosceles triangles. *Discrete and Computational Geometry*, 30:467–487, 2003.

[11] R. Dawson and B. Doyle. Tilings of the sphere with right triangles I: The asymptotically right families. *Electronic Journal of Combinatorics*, 13, 2006.

[12] Ana M. d'Azevedo Breda. *Isometric Foldings*. PhD thesis, University of Southampton, U.K., 1989.

[13] Ana M. d'Azevedo Breda. A class of tilings of S^2. *Geometriae Dedicata*, 44:241–253, 1992.

[14] Altino Manuel Folgado dos Santos. *Spherical Folding Tilings*. PhD thesis, Universidade de Trás-os-Montes e Alto Douro, Vila Real, Portugal, 2005.

[15] B. Grünbaum and G. C. Shephard. Patterns on the 2-sphere. *Mathematika*, 28(2):1–35, 1981.

[16] B. Grünbaum and G. C. Shephard. *Tilings and Patterns*. W. H. Freeman and Company, 1986.

[17] S. A. Robertson. Isometric folding of riemannian manifolds. *Proc. R. Soc. Edinb. Sect. A 79*, pages 275–284, 1977.

[18] M. J. Sewell. *Complementary and Catastrophes*. University of Wiscosin - Madison Mathematics, Reserch Center, 1973.

[19] Yukako Ueno and Yoshio Agaoka. Tilings of the 2-dimensional sphere by congruent right triangles. *Memoirs of the Faculty of Integrated Arts and Sciences, Hiroshima University, Ser. IV*, 22:1–23, December 1996.

[20] Yukako Ueno and Yoshio Agaoka. Examples of spherical tilings by congruent quadrangles. Pre-print., 2001.

[21] Yukako Ueno and Yoshio Agaoka. Classification of tilings of the 2-dimensional sphere by congruent triangles. *Hiroshima Math. Journal*, 32(3):463–540, November 2002.